Precision Stretch Forming of Metal for Precision Assembly

by

Andrew Parris

B.S. Manufacturing Engineering, University of California at Berkeley, 1988
S.M. Technology and Policy, Massachusetts Institute of Technology, 1993

Submitted to the Department of Mechanical Engineering
in Partial Fulfillment of the Requirements for the Degree of

DOCTOR OF PHILOSOPHY
in Mechanical Engineering

at the

MASSACHUSETTS INSTITUTE OF TECHNOLOGY

May 1996

Signature of Author_____
Department of Mechanical Engineering
31 May, 1996

Certified by_____
David E. Hardt
Professor of Mechanical Engineering
Thesis Supervisor

Accepted by_____
Ain Sonin
Chairman, Department Committee on Graduate Students

Precision Stretch Forming of Metal for Precision Assembly

by
Andrew Parris

Submitted to the Department of Mechanical Engineering on 31 May, 1996
in partial fulfillment of the requirements for the degree of
Doctor of Philosophy in Mechanical Engineering

ABSTRACT

This thesis focuses on improving the precision of the stretch forming process. Economic changes and technological developments have created a need and an ability for companies to become more lean. Precision assembly, a relatively new and promising approach to lean aircraft assembly, is based on elimination or reduction of costly and inflexible assembly tooling through the use of part features to align parts relative to one another and through elimination of shimming, fitting, and rework. Precision assembly requires precision fabrication: the fabrication of detail parts that fit right in assembly, with key characteristics to tight enough tolerances that they can be used for alignment. While significant precision improvement has been made in machined parts, there is still much dimensional variation in sheet metal fabrication, it is considered an art, and it is ripe for improvement. Stretch forming was chosen as a representative process for which to develop and implement an approach to precision improvement that combines engineering and statistical investigations.

A two-dimensional analytical model of the stretch forming operation based on mechanics of solids was developed and used to predict stresses, strains, and springback. The model demonstrated that the operation is less sensitive to parameter variation under strain control than under force control. The model was also used to assess the effects of changes in material parameters, pre and post stretch, friction, chemical milling, cross-section, and routing. Model predictions compare well with experimental results and FEA predictions.

Studies were made to document variation and identify sources of variation in incoming material and the operations in the stretch forming process: heat treat, stretch form, chemical mill, and rout. The central study, on leading edges in the stretch forming operation, revealed significant variation of die table movement, force, strain, and separation of the part from the die, a measure of springback. Repeatably achieving optimized settings reduced leading edge variation 75%; this, combined with strain control instead of force control, reduced variation 92%.

The approach used is applicable to all precision improvement. Adherence to optimized settings and control of the operation based on part measurement apply to other fabrication operations as well.

Thesis supervisor: David E. Hardt
Title: Professor of Mechanical Engineering

Acknowledgments

People at Vought, where the studies were performed

Thanks to Joe Boivin, senior engineer, for help with implementing and testing strain measurement. Thanks to Jeff Shea and David Baxter, subsequent managers over the sheet stretch forming area, and to Wiley Matchett, William Wyatt, Jim Hale, Bubba Schafer, and Bill Carty, sheet stretch operators, for help and for making measurements and implementing improvements. Thanks to Mike Keller for having developed the strain measurement devices and setting up the measurement system. Thanks to Gary Hall, process engineer, for help with heat treat issues, incoming materials and specifications, and developing and coordinating the heat treat designed experiments, Robert Shook, statistician, for help in planning and preliminary statistical analysis, and Delbert Olson, technician, for tensile testing all the specimens. Thanks to Scott Taylor, inspection personnel, for performing all the extrusion stretch forming measurements. Thanks to Danny Hammontree, then manager in extrusion routing, for his help with planning the extrusion routing study and his overseeing it. Thanks to Greg Prince, Lead Engineer, for helping get me started with contacts and other helps. Thanks also to the many others at Vought (of whom there are too many to list individually) for y'all's helpfulness with my work and good ol' Suuuuthern Hospitaaaality.

People at Other Companies

Thanks to Brian Dieckman, general manager at Texas Aircraft Milling, for discussions on chem milling and measurements made in his facility. Thanks to all who participated in the phone interviews. Thanks to everyone on the Reconfigurable Tooling for Flexible Fabrication Project, for sharing ideas and information.

Thesis Committee

Thanks to my committee, professors David Hardt (chairman), Stan Weiss, and Tim Gutowski, for your guidance, feedback, and encouragement.

Lean Aircraft Initiative

Thanks to the Lean Aircraft Initiative for the opportunity to work on such an important project with such bright and interesting people, and for the funding.

Lab-mates

Thanks to my lab-mates, for your friendship, humor, and endurance of me.

House-mates

Thanks to my house-mates, too many to mention, except for Joel who's been a house-mate all these six years at MIT, for your friendship, your encouragement, bearing with me, and your good cooking.

Friends and Family

Thanks to my friends and Christian brothers and sisters whom I have had the pleasure and honor of knowing and with whom I've shared a part of the life God's given to each of us. You've encouraged me, challenged me, taught me, and helped me to enjoy life more, and for these things I am grateful. Thanks to my family—what you've given me is more and more valuable than I can express in a few words. Finally, thanks and praise to the LORD, who has given me new life and a hope, and to whom I have committed my life.

He has shown you, O man, what is good; and what does the LORD require of you but to do justly, to love mercy, and to walk humbly with your God?

(Micah 6:8, NKJV)

Dedication

In Memory of My Father

TABLE OF CONTENTS

1 INTRODUCTION

1.1 INTRODUCTION TO THE THESIS

Significant and fundamental changes have taken place in manufacturing capabilities and requirements over the past 20 to 30 years, yet accompanying fundamental changes in manufacturing practice often lag, especially in the aircraft industry. Earlier this century mass production was the production system accepted by nearly all of the developed world as the best system for producing large quantities of manufactured goods. The market was a seller's market—quality and delivery problems were tolerated, and customer satisfaction was not a high priority. However, today's market environment is fundamentally different from "the days of old," and even from a few years ago. Supply has increased and demand has slowed, leveled off, or even decreased; it is now a buyer's market—cost, quality, delivery, and customer satisfaction are increasingly important. Further, customers demand a greater variety of goods and a greater variety of features in these goods, and their preferences and needs change more quickly than ever. As a result, the external pressures on manufacturing practice require some fundamental changes within.

The Massachusetts Institute of Technology (MIT) *International Motor Vehicle Program* (IMVP) investigated the characteristics of successful automobile manufacturers around the world. It found that successful divisions shared in common a number of characteristics, and as a result required less time, less manpower, and fewer other resources, had less inventory, and produced a greater variety of higher quality automobiles than others. The findings of this study are documented by Womak et al [1990] in *The Machine That Changed the World*, in which the term *lean manufacturing* was coined to describe the manufacturing system in which more products of higher quality were produced in less time, with fewer resources and less inventory. To become lean has become the goal of many companies. The application of lean principles and practices has resulted in more efficient and effective companies with higher profits. Many attempted applications have also resulted in no benefit or even harm to the well being of the companies and their employees. Successful application requires a fundamental understanding of the underlying philosophy and principles and

the methods used to become lean. It also requires a commitment from all in the company to the philosophy and principles and to their application.

One of the US industries with the greatest opportunity (and need) for improving "leanness" is the military aircraft industry. In 1992, a joint project involving the US Air Force, MIT, and about 20 US aircraft industry companies was initiated in order to determine how to apply the lessons learned from the IMVP study to the military aircraft industry. The name of this project is the *Lean Aircraft Initiative* (LAI). Within the LAI, the sectors of the aircraft industry represented are airframe, engines, and avionics/others. A great deal of research has already been accomplished by the LAI in five (interrelated) focus areas: factory operations, human resources, product development, supplier relations, and policy/external environment. This thesis is part of LAI research in factory operations, and has been developed within the context of the airframe sector; however, the results are applicable to other sectors as well.

As will be discussed shortly, a new paradigm for aircraft assembly, often called *precision assembly* is being developed. It is based on dramatically reducing the amount of tooling used in assembly by having parts with precise dimensions, aligning parts relative to one another using features in the parts, and moving operations from assembly upstream, into fabrication. The first requirement of precision assembly, precision fabricated detail parts, is the topic of this thesis. A family of parts—stretch formed sheet metal and extrusions—was chosen as a case study to develop and apply an approach to precision improvement. The factory-related work of this thesis was performed at the Vought Center of the Commercial Aircraft Division of Northrop Grumman in Dallas, Texas.

In order to improve the precision of the stretch forming process,[1] theoretical and statistical investigations were made. A mechanics-based analytical model was derived and was used to determine the effects of various parameters and method of control on the stretch forming operation. In addition to the standard parameters—stress-strain relationship, radius of curvature, and pre and post stretch strain—the model takes into account varying radii of curvature, the effect of friction, chemical milling, cross-section

---

[1] Following Shigeo Shingo [1986], a *process* is the set of *operations* performed on a part. This terminology is discussed in more detail in Subsection 3.3.2.

shape (for modeling extrusions), and routing of extrusions. The model predicts stresses and strains within the material, springback, and final contour. The most significant finding is that the operation is much less sensitive to parameter variations under strain control than under force control.

A number of studies were made on the shop floor to determine the effect of parameters not captured in the model, the sources of variation, and the current level of variation. The most important study looked at the stretch forming operation and found significant variation in machine movement, force, strain, and contour deviation. The two most significant recommendations for precision improvement are: (1) repeatably achieve optimized settings and (2) use automatic, in-process strain measurement and control. Implementation of the proposed improvements resulted in a reduction in contour deviation of up to 92%.

In order to motivate the need for precision improvement, a brief introduction to the aircraft industry is now given.

1.2 INTRODUCTION TO THE AIRCRAFT INDUSTRY

The purpose of this introduction is to acquaint the reader with the characteristics of and recent changes in the aircraft industry, so that the need to become lean and the context in which it must be achieved are better understood.

1.2.1 Companies in the military aircraft industry

As already mentioned, the aircraft industry can be broken up into three sectors: airframe, engine, and avionics/other. All of the prime contractors are very large, generally with yearly revenues in billions of dollars. In the airframe sector, there are currently only a handful of prime domestic contractors that do both commercial and defense work. These are Northrop Grumman, Lockheed Martin, Boeing, Rockwell, and McDonnell Douglas. As the names indicate, there have been recent mergers in the aircraft industry.

The primary objective of a company in the aircraft industry, as in any industry, is to make a profit now and in the future. Generally this is accomplished by the objective: sell high quality aircraft (or components thereof) to airlines and the US and foreign military services, on time and at low cost, while making a profit. In order to do this in today's market, a company must be lean.

It is also important to remember the objectives of the US armed forces and how they view the defense industry. The US armed forces want the world's best military equipment at the least possible price. They also want the industry to be prepared to quickly ramp up production in response to military conflicts.

1.2.2 Characteristics of the aircraft industry

The product characteristics

An aircraft is a low volume, long life, high part count, and heavy product. Quantities built are generally from 20 to 200 per year, usually on the lower end. An aircraft may remain in production 20 or more years, and in service even longer, and spare parts must still be made during the time the plane is in service. There are generally 2 to 6 million parts on an aircraft. Commercial and military passenger and transport aircraft generally weigh between 100,000 and 400,000 pounds, while fighter aircraft generally weight between 20,000 and 35,000 pounds [Jackson, 1995].

Relationship to the government

The defense industry is characterized by heavy government involvement. Past cost overruns and quality problems have resulted in a significant amount of government involvement in the design and manufacture of military equipment. Not only have many military specifications and numerous other regulations been created, but military personnel also involve themselves directly in decisions made within the company. Although lower cost and higher quality are their objectives, it is not clear that these are always achieved.[2] Even in the commercial aircraft industry, the Federal Aviation Administration (FAA) has imposed significant requirements (for example, traceability of fracture critical parts and tooling certification) similar to many military requirements.

It appears that one of the things that hindered military contractors in the past was that an adequate profit motivation to improve manufacturing processes did not exist. While there were significant amounts of money available for new technology developments—generally for increased mission capabilities or related new manufacturing technologies—there was little money directed at improving current manufacturing processes or becoming leaner. In fact, incentives were often quite the opposite: the

---

[2] vanDer Muelen [1991] gives a very interesting history of government involvement in the aircraft industry.

government paid for inventory, the government paid for rework and scrap (these were included in contracts if the company could show data from past experience what the expected levels would be, and they could), the government paid for tooling. Since the amount of profit was proportional to the cost, there was often little financial incentive to reduce inefficient practices.

Finally, the certainty of significant and unpredictable changes in government demand and the short time horizons of government commitments have also had a detrimental effect on the ability to make more efficient long range plans.

Customers

Most aircraft companies produce for civilian airlines and military armed forces [Kelley and Watkins, 1995], including domestic and foreign customers (the US government acts as an intermediary for military sales to foreign governments).

Subcontracting

Generally one half or more of the cost of an aircraft or of the cost of military products is subcontracted to suppliers (the figure is 75% for the Lockheed Martin F-16 fighter aircraft) [Kelley and Watkins, 1995]. Thus, commercial sales and subcontracting are significant factors in this industry.

High investment, high cost, and high risk

For commercial aircraft, the price range is from $20 to $150 million, product development time is about four years, and development costs are about $4 billion [Kirkwood, 1992]. Development time for military aircraft nowadays is fifteen to twenty years, and fighter jets cost from $50 to $100 million apiece [Augustine, 1983].

The aircraft industry is also a very high risk industry. According to McAfee [1990, pg. 24], "It is difficult to overemphasize the intensity of the competition and degree of risk inherent in the commercial airframe industry. General breakeven requirements for a commercial transport include sales of 400-500 units, a 40 unit per year sales level, 5-6 years of negative cash flow, and 10-14 years to profitability."

Safety

Especially for the commercial sector, but for the military as well, possibly the most important requirement for an airplane is safety. An "unsafe" plane can do more to ruin a company's reputation—the airline or the manufacturer—than anything else.

Rapidly changing technology

There is constant pressure to develop and incorporate into aircraft (this is more true for military than for commercial aircraft) new materials, new methods of processing materials, and new components—for example, stealth technology, improvement in machining (especially high speed machining), use of composites and new alloys, and the ability to handle higher stresses (e.g., the F-16 fighter jet can pull a maximum of 9 G's, at which point the wing tips bend back 18"). The defense industry has a history of significant pressure from the government to include the latest design and manufacturing technologies, and this is expected to continue.

1.2.3 Recent changes and trends in the aircraft industry[3]

This very brief introduction to some of the more important factors influencing the aircraft industry would be incomplete without the following presentation of important recent changes and new trends.

Drop in demand, increased competition, and importance of customer satisfaction

Significant defense spending cutbacks (impacted somewhat by the collapse of the Soviet Union and somewhat by a significant budget deficit) have drastically reduced equipment purchases by the US armed forces. The aircraft industry has been hard hit by these cutbacks—employee layoffs, empty factories, and mergers are some of the results. These same cutbacks have also caused the military to demand "more for their money." Therefore, the military has put significant pressure on defense contractors to improve their operations. One response to the situation is that divisions engaged mostly in military work are searching for new, commercial markets and need to be able to compete with (often) more efficient commercial companies—in the US and abroad. It is expected that military demand will continue to be uncertain, lumpy, and low.

Quality improvement movements

There are many recent company-wide, industry-wide, national, and international initiatives and efforts aimed at improving quality and operational efficiency; for example,

---

[3] While the production volumes and many other factors differ, many of the same changes experienced by the aircraft industry have also been experienced by the automobile industry, as described by Sekine et al [1991] and Iizuka et al [1992]. As discussed by these authors, one of Nissan's crucial responses to the changes has been to improve flexibility. For Nissan, one of the primary means of accomplishing this is the Intelligent Body Assembly System (IBS). Note that assembly is a key area affecting flexibility.

total quality management, continuous improvement, worker empowerment, supplier certification, integrated process and product development teams, and lean manufacturing are representative of these initiatives. Aircraft companies have not been entirely left behind in these efforts, and some are making remarkable improvements in quality, cost, schedule, and the elimination of waste. Many exemplary cases have been studied and reported on by MIT researchers as part of LAI research. Further, a *Lean Enterprise Model* , a compilation of principles, metrics, and practices that a company can use to understand how lean it is and how to become leaner.[4]

Technological Improvements

Technologies available to companies have improved greatly, most importantly in information technology: communication, storage, and processing of information. For example: all new aircraft designs are made on computer aided design (CAD) systems (and some old designs are being digitized) and can be electronically analyzed for fit and interferences; numerical control (NC) codes are (nearly) automatically generated for most machining; scheduling and inventory practices are computer-controlled and can be simulated on computers; all of the above data can be communicated electronically, for example to the shop floor, or even to a subcontractor.

Two further technological improvements that have a great impact on manufacturing are in machine control and measurement systems. Closed loop and numerical control on newer machines have the capability to greatly improve the precision of fabricated parts. New developments in measurement systems, for example, the use of lasers and CCD cameras, permit faster and much more accurate and precise measurement of larger workpieces than in the past.

With regard to materials improvements, even though composites are gaining in importance, aluminum and other metals will continue to be very important in airframes for many years to come. It is likely that a good portion of future new aircraft will be upgrades of existing products (for example, the Boeing 737-700 aircraft, and possibly an upgraded Boeing 747 aircraft), which means that current manufacturing processes will continue to be used and composites will not make the inroads that they might in

---

[4] For further information, contact the Lean Aircraft Initiative at: Massachusetts Institute of Technology, Room 33-407, 77 Massachusetts Avenue, Cambridge, MA 02139. Also, check out the LAI Web page at http://web.mit.edu/ctpid/www/lai/index.html.

new aircraft designs. The high cost of composites and the improvements that can be gained from new metal alloys are two reasons that the increased use of composites on new designs may also be limited [Smith et al, 1994].

Decreasing government involvement

As the government and companies become leaner, it is expected that there will be less government involvement in the work performed at defense contractors. How and at what rate this will happen, only time will tell.

1.2.4 Summary and conclusions to introduction

The following summarizes the most important factors and trends in the aircraft industry:

- what was a seller's market is becoming a buyer's market,
- customer satisfaction is becoming increasingly important,
- costs were high and are going down, while quality was low and is going up,
- product variety and competition are increasing,
- demand decreased significantly, but is expected to stay steady for a while, and
- government involvement was high and is decreasing.

In order to succeed in this industry, companies must become lean. This thesis addresses one aspect of becoming lean which is applicable to the factory: precision improvement of detail part fabrication.

1.3 GUIDE TO THE REST OF THE THESIS

In Chapter 2, the concept of precision assembly is presented, and its requirements are discussed. In Chapter 3, the concept of precision fabrication is presented, and the approach to achieving it is discussed. In Chapter 4, an analytical model of the stretch forming operation is developed. In Chapter 5, the analytical model is used to assess the effects of various parameters and method of control on the stretch forming operation, and model predictions are compared to the results of finite element analysis (FEA) simulations and actual experiments. In Chapter 6 a practical understanding of the sheet metal stretch forming process is developed, sources of variation are identified, and approaches to precision improvement are recommended and evaluated. In Chapter 7 the same is done for the extrusion stretch forming process. In Chapter 8 lessons learned are considered, expansion of the approach to other processes is discussed, and the thesis is concluded. Since no thesis is complete without a bibliography and appendices, these are provided at the end.

2 PRECISION ASSEMBLY OF AIRCRAFT

This chapter begins with an introduction to aircraft assembly, discusses assembly tooling and the reasons it should be reduced, describes precision assembly, discusses the requirements for precision assembly, and concludes. Precision assembly is of fundamental importance to achieving lean assembly processes, and precision fabrication is one of the most important enablers of precision assembly.

2.1 AIRCRAFT ASSEMBLY

Aircraft assembly refers to the assembly of individual detail components as well as the joining of assemblies with other assemblies or individual components.[5] Others have described aircraft assembly and its inefficiencies in significant detail; in the following, a summary of their findings is combined with personal observation.[6]

Before making the upcoming sweeping generalizations, it is important to note two things: first, there is a wide range of practice, efficiency, and quality; second, significant improvements are being made, many of which have been initiated in the past few years—this is particularly true for new aircraft and new versions of existing aircraft.[7]

2.1.1 Characteristics of aircraft assembly

Aircraft assembly has not changed significantly since World War II. The primary advances in aircraft assembly since World War II have occurred in the development and application of automated fastening technology.[8]

---

[5] No distinction is made between subassembly and assembly. While the distinction is generally made, much of what is said about assembly refers equally well to both. Common terminology is given by Marschner [1942].

[6] A good, introductory text on aircraft structures and their relation to assemblies and detail parts is given by Cutler [1992].

[7] As mentioned already, many of these improvements have been studied and documented by LAI researchers at MIT.

[8] This technology was pioneered by Thomas H. Speller, Sr. Speller graduated from MIT in 1929 and started the General Engineering Co. in Buffalo, NY, (later re-named General-Electro Mechanical Corporation (GEMCOR). He was soon requested by Curtis Wright to develop an automated rivet squeezing machine for use in C-46 manufacturing. During World War II, Speller perfected his rivet squeezing equipment. His "Drivmatic" machine was capable of clamping the workpiece, drilling holes, inserting rivets, and squeezing the rivets. One major advantage was that no deburring of the holes was required before rivet insertion. This machine was first used at Douglas Aircraft in 1948. Subsequent milestones include the first NC riveter developed for

There is significant dimensional variation in detail parts and assemblies, and assembly tooling is always required. When, as is common, parts don't fit—either by design error or due to manufacturing variation—fitting, shimming, trimming, other rework, and/or scrap are necessary. These things significantly increase the cost and time involved in assembling an aircraft.

In the following, characteristics of aircraft assembly are given. All figures and references in this sub-section refer only to the aircraft industry.

Production control and work flow

Production volume is low, generally in the range from two to fifteen aircraft per month, while the number of parts going in to an aircraft is quite large, somewhere between two and six million for commercial aircraft [Kirkwood, 1992].

Work flow is generally slow and much longer than needed (including, for example, lead times of up to half a year or more and other planned delays) [Bartelson, 1993][9] and [Coleman, 1991].

Going hand in hand with the above, inventories are large, up to many times the value of the assembly [Bartelson, 1993]. According to Finan [1993, pp. 37-8], large inventories are the second major problem experienced in the production environment; the major root causes are ordering errors, engineering changes, ordering policy, scheduling policy, inventory accuracy, and manufacturing policy.[10]

Part shortages are common, even with large lead times [Coleman, 1991]. Finan [1993, p. 35] states that "Part shortages represent one of the major problems within the production environment." Also according to Finan, the major root causes of part shortages are ordering changes & errors, product quality, process flowtime variation, inventory accuracy, product configuration, and product configuration variation.

Boeing 727 production in 1961, first fuel tight fastening for Boeing 747 production in 1967, and the first CNC robotic fastening for 767 and 757 production, developed in the late 1970's. Since Speller's pioneering efforts, the use of automatic fastening has become widespread in the aircraft industry, and several equipment developers/manufacturers offer automatic fastening equipment. [GEMCOR, 1986]

[9] According to Bartelson [1993], one Boeing manager commented, "You can only get scolded for large inventories. You can get fired for part shortages."

[10] See also [Knight, 1992] for the benefits of and strategies for reducing inventory.

Lundstrom [1993] states that at the site he studied, over 70% of the assembly completions were late, and that employees at that location considered this normal.

There is a lot of fitting and rework. According to Coleman [1991], the percent of assembled units he studied requiring significant rework ranged from 12% to 35%. One of the major causes of rework, fitting, shimming, and the like is detail part variation.

As a result of all the extra time spent due to the above inefficiencies, including variation of detail parts, the assembly time of aircraft is much higher than it needs to be. For example, in one case the actual time required to complete assemblies was *five* times the nominal labor hours as calculated by an I.E. Methods/Standards engineer [Coleman, 1991].

Due to the long delays, quality feedback is delayed as well [Coleman, 1991], which makes it often ineffective and always difficult, and hinders quality improvement [Bartelson, 1993] and [Wenstrup, 1991].

Tooling was designed and is used to control the assembly geometry, to align parts within the assembly, and to accommodate detail part variation. Most aircraft currently manufactured were designed 10, 20, or even 30 years ago. As a result, designs are generally on paper, and design authority rests in the tooling. Because poor detail part precision was expected, the assembly process was designed to accommodate and tolerate significant amounts of variation in detail parts. An interesting study of variability in the assembly of sections 41 and 43 of the 757 which addresses some of these issues is given by Lee [1992].

Not only is there a great amount of tooling, it is generally dedicated to a specific task on a specific assembly. For example, for the Boeing 757 aircraft, "There are 18 lines, one for each door type. The lines are hard tooled so that only one type of door can be built in each line." [Bartelson, 1993, p.18]

This brief characterization reveals that typical aircraft assembly is anything but lean. Before addressing assembly tooling, a relatively recent term, *key characteristic*, useful in calling attention to the most important features of a part or assembly, is presented.

2.1.2 Key characteristics

The concept of a *key characteristic* (KC) was developed as a means of communicating the few most important characteristics of a product, assembly, or detail part. "KCs are

the critical features on the parts and assemblies that most affect the function, safety, or customer satisfaction of the product" [Cunningham et al, 1996]. Essentially, key characteristics are the things that must be right, which in this context means dimensionally correct to tight tolerances.

Key characteristics flow downstream. For example, key characteristics in an assembly determine the key characteristics of the detail parts that go into it. The starting point, or "top level," key characteristics come from the final assembly—the completed aircraft—and from there work their way down to the detail parts.

A more thorough treatment of key characteristics and their use in determining an optimal assembly process is given by Cunningham et al [1996]. Key characteristics are finding increasing use in the aircraft industry, for example, [Boeing, 1994].

2.2 ASSEMBLY TOOLING[11]

Assembly tooling dominates the aircraft assembly area, as a visit to any aircraft assembly site will immediately reveal. While assembly tooling serves many useful purposes, it is also a significant hindrance to lean.

2.2.1 Definition and benefits of assembly tooling

Assembly tooling is the set of all *things* used to assemble parts together. Specifically, assembly tooling is comprised of

- **workholding** devices for processing, inspection, transport, and, storage,
- the portion of processing or inspection equipment which **interacts** with the workpiece, and
- **shape** information storage devices used to determine assembly or detail part geometry.

Each piece of tooling can serve as workholding, interaction, and/or shape tooling. A certain amount of tooling is beneficial and necessary for support, efficiency, and quality (especially when there is significant part variation). The primary benefits of tooling are increased speed and improved repeatability of operations. Until recently, little research and little progress have been made in assembly tooling over the past half century.

---

[11] While the focus here is on assembly tooling, most of what is written here applies to fabrication tooling as well. The Reconfigurable Tooling for Flexible Fabrication (RTFF) project is working to develop flexible tooling for the stretch forming operation.

2.2.2 *Assembly tasks*

The wide variety of tasks that must be accomplished in order to assemble parts together can be organized the into eight categories given below.[12]

- Locate and align parts to one another
- Support parts under their own weight
- Define the shape of the assembly
- Locate and align an operation, e.g., drill, trim, rivet
- Support parts (or people) during an operation
- Perform an operation
- Inspect the assembly
- Move parts and the assembly

While tooling helps to accomplish many tasks, its service is not without cost.

2.2.3 *Assembly tooling as a barrier to lean manufacturing*

Typical assembly tooling in the aerospace industry has several salient characteristics:

- It is specific to a particular task on a particular assembly
- It must be transported to and from the location of use
- It must be stored and maintained when not in use[13]
- It is difficult (requiring large amounts of time and money) to create and alter[14]
- Changing assemblies (unloading one and loading the next) is time-consuming
- Changing tooling for different tasks is time-consuming
- It is the primary geometry information storage media

These characteristics impede leanness in several ways (there is not a one-to-one correspondence between the two lists):

- Non-value-added work related to transport, maintenance, repair, and storage of tooling is required
- Design changes are hindered
- New product introduction is delayed
- Significant amounts of capital are tied up in tooling

---

[12] See also [Marschner, 1942] for a discussion on aircraft assembly, including the tasks which tools perform.

[13] Tooling must be retained well after production has stopped—as long as the any of the planes still fly—in order to produce spares.

[14] According to Koonmen [1994], variation in detail parts is the primary cause for modifications of assembly tools. The high expense and time required to fabricate tooling is likely to lead to compromises in the quality of tooling.

- Tooling is a significant contributor to manufacturing cost (especially with low production volumes)
- Tooling problems are slow to get solved because of the cost and time involved
- Tooling breakdown will cause process delays

In addition to high cost, a common thread in all of these impedances is inflexibility. Current, hard tooling significantly impedes flexibility, which is central to becoming lean.

Possibly the most significant way in which tooling impedes leanness is one that is not directly obvious. In the same way that a young man whose parents always pay his credit card bills because they don't want him to go into debt will probably never learn to purchase only what he can afford, likewise, tooling, when used as a crutch for poor quality fabrication, will never encourage fabrication to achieve tighter tolerances. In both cases, there is a cost involved in this service.

2.2.4 Ideal assembly tooling

When considering the positive aspects of tooling with the lean manufacturing objective of minimizing waste, the following statements can be made about the ideal tooling (there is a close, but not one-to-one correspondence to the previous list):

- There is not much of it
- Tooling is flexible to more than one task or part
- Tooling is quickly and inexpensively created or altered
- Tool design time is short
- Tooling speeds operations
- Tooling helps operations to be repeatable
- Tooling promotes process optimization
- Tool transportation, storage, and maintenance are minimized

Tooling only adds value when it is in contact with the part. Everything else is non-value-added work and should be the focus of attention either for improvement or elimination. While some of these goals may be mutually contradictory, and their achievement may increase waste in another area, they represent goals which should be kept in mind when addressing tooling.

Becoming leaner in assembly necessitates elimination or significant reduction of the amount of tooling. However, assembly tasks must still be accomplished; they are generally accomplished by tooling, but this does not have to be so. If these tasks can be obviated—if the parts themselves are used to accomplish some of these tasks, or if

some of these tasks are performed in fabrication—the need for assembly tooling is reduced. This is the basis for the precision assembly philosophy discussed next.[15]

2.3 DESCRIPTION OF PRECISION ASSEMBLY

In essence, precision assembly is the assembly of parts with the minimum amount of tooling, where the alignment of parts relative to one another and the shape of the assembly are largely determined by the parts themselves; shims are avoided and, as much as possible, cutting operations are moved back into fabrication. James Koonmen [1994] defined precision assembly and reported on the successful application of precision assembly to the assembly of an aircraft floor grid structure.

Precision assembly is part of a paradigm shift from hard, fixed, tooling-based part and assembly definition to a more flexible, electronically-based definition. In the old paradigm, tooling often held precedence even over the drawings; in the new paradigm, the CAD definition is the final authority. In the old paradigm, tooling determined all alignment, gave the shape to the assembly, and was used to deal with the variation in detail parts; in the new paradigm, as much as possible, parts are self-aligning, the shape is determined by the parts themselves, and detail parts are fabricated to tight tolerances so that no shaping, fitting, or shimming of parts is necessary in assembly.

Precision assembly requires less tooling because (a) there are fewer tasks to be performed in assembly, (b) the parts themselves perform some of these tasks, and (c) remaining tooling can be more flexible (since it has less to do) and can be used for more than one operation, task, or assembly.

The amount of work in assembly—cutting, drilling, fitting, shimming, and rework—is reduced by requiring fabricated parts to be the right shape and have certain critical dimensions (key characteristics) adequately tight. Alignment of parts relative to one-another can be accomplished by precisely fabricating part features, for example, holes, slots, edges, and surfaces, for this purpose. Parts that come in the right shape eliminate the need for tooling to correct shape defects. Precision assembly is one of the primary motivating factors pushing precision fabrication.

---

[15] In the Appendix I of his thesis, Lindsay Anderson [1993] gives a brief overview of the history and future of Boeing's tooling philosophy. It is very much in line with what is being proposed here.

2.3.1 Dimensional requirements of precision assembly

Since fabrication requirements are driven by assembly requirements, it is necessary to determine tolerance requirements of precision assemblies and to compare them to tolerances of conventional assemblies. It is not within the scope of this research to delve deeply into the topics of what is or will be the optimal precision assembly strategy, or what are or will be the tolerances required of fabricated parts in order to make precision assembly feasible. These questions are being addressed by industry and academia, including research within the MIT Fast and Flexible Manufacturing Program (see, for example, [Cunningham et al, 1996]). This sub-section draws on the experience of people investigating precision assembly—how to make it happen, and how far it can be applied. It is not possible to make a definitive statement on precision assembly and its requirements because (a) all findings are preliminary, and (b) companies are not willing to share all they know about the topic, because of the highly competitive nature of the subject.

The first and most important thing to understand about precision assembly requirements is that tolerances vary according to the design philosophy and accompanying method of assembly, assembly sequence, and amount and variety of assembly tooling used. This means, for example, that there is no single "standard" tolerance for contour, or hole size, or hole location, but that tolerances vary, depending on, for example, whether or not a feature is used to align the part to another.

For sheet metal parts, critical contour tolerances may drop from a somewhat standard ± 0.030" down to about ± 0.010", while generally they don't change much due to the flexibility of sheet metal parts. Parts with strong contours, for example, leading edges, will have tighter contour requirements. Tolerances for the location of drilled holes and edges are generally tightened, often from the typical ± 0.030" down to between ± 0.005" and ± 0.010".

For extrusions, the key characteristics may be contour, leg angle, joggle depth, and/or flatness. Contour requirements may come down from around ± 0.015" or ± 0.030" to around ± 0.005 to ± 0.010" (external surface aerodynamics and a 'no shim' policy would lead to these tolerances). Leg angle requirements depend on whether the leg is free-standing or is connected to anything. If the leg is free-standing, the angle tolerances may be ± 2° to ± 4°, while if the angle is used as an attach point, the tolerances may be

± 1/4° to ± 1/2°. Location tolerances for features used to align parts are likely to drop from the common ± 0.030" down to about ± 0.005" and ± 0.010". Thickness tolerances probably need to be tightened as well.

Tolerances on features are tighter when the feature is used to locate the part relative to a fixture or another part or when the feature must meet up with another part. Although specified contour tolerances may not be tightened, some have found that the actual tolerances need to be tighter in order to achieve the required feature tolerances. Not all features on precision assembly parts, however, will have tight tolerances; some tolerances may be loosened, while many will remain the same. In order to achieve precision assembly feature tolerances requirements, some companies have gone to computer numerical control (CNC) routing and drilling. Sometimes, creation of precision features requires contour tolerances tighter than specified.

The precision of fabricated parts issue is much more involved than is presented here, and justice cannot be done to the subject so briefly, but anything that goes deeper than scratching the surface quickly becomes very complex and goes beyond the scope of this thesis. The sense one gets from discussions with people involved with precision assembly issues is that the current state of the development of precision assembly approaches is "work in process." Firm answers to questions are not forthcoming, and different individuals and companies differ in their opinions on how and to what extent to apply the precision assembly philosophy.

2.4 ENABLERS OF PRECISION ASSEMBLY

In order to accomplish precision assembly, a number of requirements must be satisfied. The most important are:[16]

- Design of parts, assembly, assembly methods, assembly tooling, etc.
- Precision fabrication: contour and features of detail parts
- Common, CAD definition
- Measurement technology
- Lean production system

---

[16] This list comes from consideration of many inputs, the most important of which is responses from LAI airframe companies to a questionnaire asking for the enablers of precision assembly (reduction of assembly tooling) and critical issues that need to be solved for it to happen. Hoppes [1995] has a similar list.

These are now discussed.

2.4.1 Design of parts, assemblies, assembly methods, and tooling

The two most important design issues are part and assembly design, and tolerancing. Often, owing to aerodynamic and strength requirements, it is difficult to have a great influence on design. However, it is not impossible. Alignment features can be included in designs to help coordinate the assemblies—existing holes can be used, for example. How the parts are to be made is also very important; for example, whether holes will be drilled in fabrication or in assembly, or whether a sheet metal buildup or a machined part will be used. Dimensioning of parts and assemblies and location of datums are very important as well. Finally, design of the assembly procedure has a significant impact on the ability to achieve precision assembly.

Tolerancing is a critical design issue for precision assembly. The two tasks of tolerancing are: determine which tolerances are necessary and allocate tolerances among the detail parts that constitute an assembly (which depends on detail part tolerances, assembly methods, and tools used in assembly). One of the tools used to assess the impact of detail part tolerances, assembly sequence, and assembly tooling is statistical preassembly [Koonmen, 1994]. Such a tool was used by Cunningham et al [1996] to simulate hundreds of assembly build processes. A number of references in the area of tolerances and tolerancing are given in the bibliography under the heading "Tolerances and tolerancing." Of particular interest, Anderson [1993] presents new development tools for tolerancing of aircraft assemblies.

One of the difficulties in going to precision assembly is that parts and assemblies, as well as assembly methods, have been designed to accommodate variation. Therefore, precision assembly is more difficult to apply on existing aircraft than on new aircraft. However, even if full-blown precision assembly is not advantageous for an existing aircraft, this doesn't mean that there is no opportunity or need for precision improvement; even if parts can't be used to determine contour or to align parts to one another, at least their contour and features can be correct so that fitting or shimming are not required. There is great room for improvement in assembly even without reducing assembly tooling.

The most flexible assembly tooling is *no* tooling, which should remain an objective. Next to that, flexible tooling can be flexible in terms of the variety of tasks or operations

that it performs (or supports) or in terms of the number of assemblies on which it can be used. If there are fewer assembly tasks to perform, it is only natural that the total amount of tooling will be less and that the remaining tooling can be more flexible. The following paragraphs cite a few examples of increased flexibility in assembly tooling.

Under a contract from MANTECH (Manufacturing Technology Directorate at Wright-Patterson Air Force Base), Rohr developed a flexible robotic workcell for the assembly of aircraft components. Key features of their system were two robots, a flexible fixture, automatic fastening, a metrology system, and specially designed end effectors. Typical assemblies that could be assembled in this system consist of a mildly contoured sheet and a number of parts such as chords, stiffeners, and brackets [Olsen, 1990], [Braun and Zanella, 1986], and [Braun and Zanella, 1988].

McDonnell Douglas and Texas Instruments' Manufacturing Automation Systems Group co-developed a flexible assembly cell to replace a family of 250 fixed tools, priced at $10,000 each. In addition to the flexibility gained by the elimination of hard tooling, assembly and inspection times were dramatically reduced, by up to a factor of 15, as reported by Goodman [1990a and 1990b].

Two large, automated assembly systems developed by Ingersoll Milling Machine Company are described by Hawthorne [1989]. The first is the Automated Spar Assembly Tool (ASAT); the second, called Masterhead™, can trim panels to final dimension, machine part location holes and perform the necessary drilling and fastening. Electromagnetic riveting (EMR) is used to obtain a very high, very controllable force with negligible reaction force; blind fasteners can also be installed.

A five axis, CNC riveting system for Airbus skin panels is described by Maskow [1986].

However, not all flexible assembly tooling has to involve automation and CNC control.

McDonnell Douglas has pursued less and more flexible assembly tooling (that is, less tooling which is more flexible) for the forward fuselage of the F/A-18E/F. One mainframe tool and 18 assembly jig accessories (AJAs) replace 27 separate assembly jigs. The plane is no longer moved from one jig to another, but remains in the mainframe tool and the AJAs are brought to the plane as they are needed. A reduction in initial assembly and bond jig tooling costs of 28% is expected [Kandebo, 1994].

Another interesting and flexible technique utilized by Airbus to move fuselage sections on air pillows is reported by Barrie [1992].

Other flexible assembly and material locating systems of interest are given in the bibliography under the heading "Vision systems and flexible and automated assembly."

2.4.2 Precision fabrication: contour and features of detail parts

As discussed already, in order to transfer the coordination task from tooling to the detail parts, the parts must contain precisely located features; for example, coordination holes and edges. In order to transfer the shape-defining function of tooling to parts, the parts themselves must arrive in the assembly area with the proper contours. In order to reduce assembly operations, parts need to be fabricated with the operations normally performed in assembly already performed; for example, drilling of certain holes and trimming. Finally, in order to eliminate assembly tasks such as shimming, fitting, strapping, hammering, and the like, parts need to be fabricated to high precision.

Precision fabrication is of fundamental importance to precision assembly because detail parts are literally and figuratively the building blocks of an aircraft. If detail parts have excessive variation (which they currently do), then assembly is burdened with fixing and accommodating this variation, resulting in significant waste. If detail parts are fabricated precisely, then assembly can be more efficient. Fabricating precision detail parts requires a new level of understanding of the processes and operations involved in fabrication, a thorough investigation of variation and the causes of variation in fabrication, and a comprehensive approach to precision improvement. This is the topic of the rest of the thesis, after the next few points

2.4.3 Common, CAD definition of parts

A common, electronic, CAD definition eliminates interpretation and is up-to-date. Incorrect interpretation and lack of currency appear to be the two most common causes of errors from the design side. CAD drawings replace tooling as the ultimate authority on dimensions. Since information is stored electronically, it is much more flexible, and it is accurate. Further, a CAD definition is necessary to accomplish the tasks of automatically checking for interferences and tolerance analysis. CAD definitions aid both assembly and fabrication by providing up-to-the-minute, electronic design specifications which can be printed, viewed on a computer monitor, or electronically transferred to an automatic processing device.

While not an easy task, on existing designs where no CAD drawings exist, a CAD definition can be created from paper or mylar drawings, measurement of parts, and other sources of information.

2.4.4 Measurement techniques

Since reduction of tooling is a primary objective of precision assembly, and because some measurements must still be made, measurement techniques must be able to make high precision measurements flexibly.[17] Measurement is necessary for the purposes of part alignment and inspection. Because of the requirements on accuracy, precision, and flexibility, new measurement techniques that can be used in assembly are based on optics: CCD cameras, lasers, and the like. They can be used to measure contours, features, and feature location (including gaps). A couple of recent and interesting measurement techniques are now discussed briefly.

Leica, a Swiss metrology company, has developed a contour measuring system based on a laser tracking, which uses a single laser and a reflective prism centered in a metal ball which can be moved along the contour of a tool or part.

Metronor, a Norwegian metrology company, created a "real time" photo-grammetry system. Their system, Metrology Norway System (MNS) uses two cameras to determine the spatial coordinates of a point-sized light source. As well, they feature a "Light Pen," which can be used to measure the location of surfaces or edges simply by touching the point of the pen to the desired feature; it is like a portable, hand-held coordinate measuring machine (CMM), they say.

Gordon [1987] presents, among other things, the author's development of "a fast and accurate six degree-of-freedom position sensor based on a light-stripe vision technique...." Gordon [1989] also presents a 3D vision system that can be used to eliminate alignment errors which is to be used "in a flexible assembly environment

---

[17] Lee [1992] states that inspection of assemblies has not been developed because: "1) there has not been a measurement system capable of measuring the product efficiently and effectively, and 2) there is a paradigm in aircraft manufacturing which states that accurate tools build accurate parts. ...However, ...good tools do not necessarily translate to good products. The effect of process variations (unplanned dimensional variations in parts and assemblies) have significant impact on the conformance of the product. With accurate tooling and parts with low variation, accurate assemblies can be produced." (p. 51)

(which) reduces the system's dependence of high-precision, expensive assembly fixtures and near perfect parts."

Other measurement devices or systems are given in the bibliography under the heading "Vision systems and flexible and automated assembly."

2.4.5 Lean production system

The production system in which precision assembly is undertaken is important because it determines the ability to make, and affects the motivation for making, improvements. The current production system (with its long lead times, large inventories, late completions, quality problems, and rework) leads to significant waste and an inability to improve—not only an inability, but also a lack of motivation to improve.[18] Precision assembly is most effective only in a lean production environment.

Some of the more important aspects of lean for precision assembly are material flow (inventory levels, lead time, cycle time, time on tool), detail parts quality, workforce skills, motivation, and flexibility, and how quality problems are dealt with (tolerated, or forced to improve).

2.5 SUMMARY AND CONCLUSIONS TO PRECISION ASSEMBLY OF AIRCRAFT

Aircraft assembly is laden with inefficiencies and quality problems. It is an area ripe for significant improvement. Precision assembly is a promising approach based on detail parts with tighter tolerances, using features in parts to align parts relative to one another, and moving machining operations from assembly to fabrication. Critical tolerances on parts for precision assemblies are significantly tighter than current tolerances; generally being tightened from a somewhat standard 0.030" to between 0.005" and 0.010". Even if there's no opportunity for self aligning of parts, there is a significant opportunity to improve assembly by fabricating parts with precise dimensions. Enablers of precision assembly are design of parts, assembly, assembly sequence, and assembly tooling), precision fabrication of detail parts, common CAD definition, measurement technology, and a lean production system. Of these, probably the most important is precision fabrication, because fabricated parts are the building blocks of an aircraft. This is the subject of the rest of the thesis.

---

[18] See [Lundstrom, 1993] for some good reading on this issue for aircraft assembly and recommended improvements.

3 PRECISION FABRICATION OF AIRCRAFT DETAIL PARTS

This chapter begins with a brief introduction to detail fabrication, the reasons for choosing stretch forming, and a brief introduction to the stretch forming process. After this, the state of the stretch forming industry is discussed based on interviews with personnel at about a dozen stretch forming facilities. Next, precision fabrication is described and discussed. Finally, the approach taken and frameworks used in the pursuit of precision fabrication for the stretch forming process are presented.

3.1 AIRCRAFT DETAIL PART FABRICATION

3.1.1 General

Fabrication of most metal parts can be categorized into machined, sheet metal, or cast parts, with some overlap. Aircraft detail part fabrication is similar in many respects to aircraft assembly, for example, in lead times, quality problems, number of parts, old designs, and practices. Lot sizes are generally 10-15 parts, and cycle times and set up times are long (1-10 minutes, and 20-30 minutes, respectively).

Significant progress has been made in machining in recent years, especially with the use of electronic data storage, manipulation, and communication, and NC control of operation; for example, one of the most significant recent developments in machining for the aircraft industry is high speed machining, which is capable of machining very thin walls because the low forces exerted during cutting are very low. Casting, along with machining, is more frequently used due to the ability combine a number of parts into a single part. However, apart from high temperature forming, such as super plastic forming, and the use of NC controls for some operations, sheet metal fabrication has not changed significantly in the past 50 or so years.

3.1.2 Sheet metal fabrication

The current situation in aerospace sheet metal fabrication can be described as follows: there are significant amounts of output variation (resulting in check & straighten, rework, scrap); sources of variation are significant and unknown; operations are not well understood; operations are not well controlled; fabrication is generally viewed as an art (not as a science). One of the most significant blemishes in every fabrication

shop is the *check and straighten* area, where many hours are spent inspecting parts and bending or hammering them so that they meet the specifications.

Sheet metal fabrication is composed of a wide variety of manufacturing operations such as bending, rolling, routing, hydroforming, and stretch forming.

3.1.3 Selection of stretch forming as the sample process

Machined parts were not chosen because much work has already been done on developing an understanding of machining and on improving the precision of machined parts. Currently achievable tolerances on machined parts are generally adequate for precision assembly, and if not, the ability to achieve tighter tolerances exists, if the money is available. On the other hand, sheet metal fabrication is ripe for significant improvement. Simple bending and matched die forming of sheet metal have received the lion's share of research and attention because they are ubiquitous in metal forming. However, stretch forming, while it is a significant process within the aircraft industry (most sheet metal skins on an aircraft are stretch formed, as are nearly all contoured extrusions), hasn't received as much attention, either theoretically or practically. Therefore, stretch forming provides an opportunity to make a unique, yet significant, contribution to the achievement of precision fabrication in the aircraft industry (which is sponsoring this research).

Two other practical reasons for the choice of stretch forming were the willingness of people at Vought, and particularly those in stretch forming, to let me spend time there, to learn their process, to work with them to develop and test (on the sheet stretch forming operation) an approach to precision improvement, and the ability to work very closely with another research project between MIT, Cyril Bath (a leading manufacturer of stretch forming equipment), and Northrop Grumman, which is developing a reconfigurable tool for the stretch forming operation.

While stretch forming was selected to serve as an example process of how precision might be improved, other processes can be improved based on the approach taken and the work done in this thesis.

3.1.4 Introduction to stretch forming

Because of the uneven stress distribution (through the thickness of the part) induced during sheet metal forming, the final part shape will vary from the shape imposed by

the forming tool—this change in shape is called springback. Stretching a part after forming reduces the unevenness of the stresses and thus reduces springback, so that the part shape more closely matches that of the die. The effect of springback is shown in the following diagram.

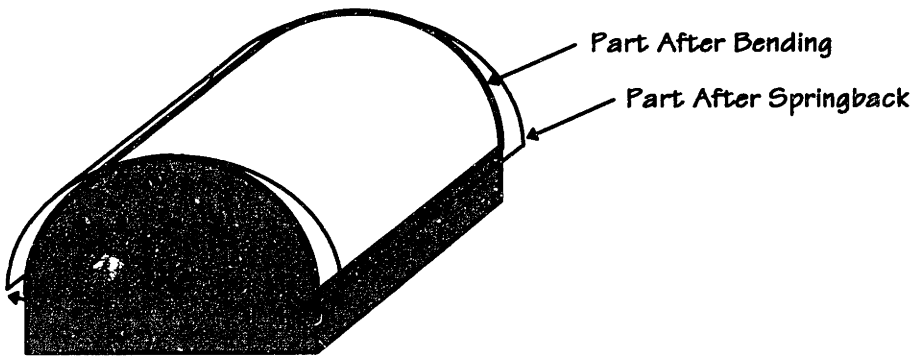

Figure 3.1 Effect of springback

A part formed to a contour (dark lines) springs back (light lines) toward its original shape. The following diagram shows the tensile and compressive stresses and strains that develop in a bent part, in order to show the orientation of the diagrams in Figures 3.3 and 3.4. The dashed line represents strain, while the solid line represents stress. Stress and strain are positive to the right and negative to the left. The strain after bending is directly proportional to how much the part is bent and the distance from the middle of the thickness. The stress is a function of the strain.

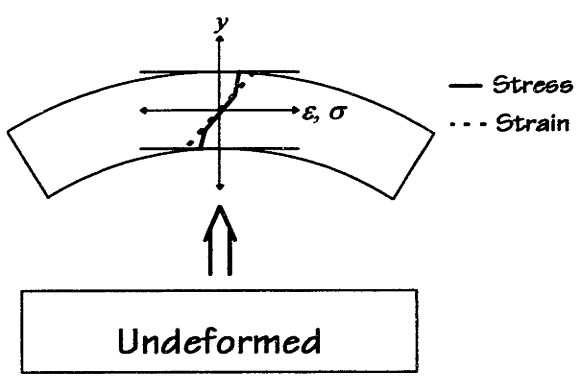

Figure 3.2 Stresses and strains in a part from bending

The stresses and strains after bending and after springback are shown in the following diagram. After bending, a moment exists within the part that reduces to zero when the part is released, causing springback, an unbending of the part

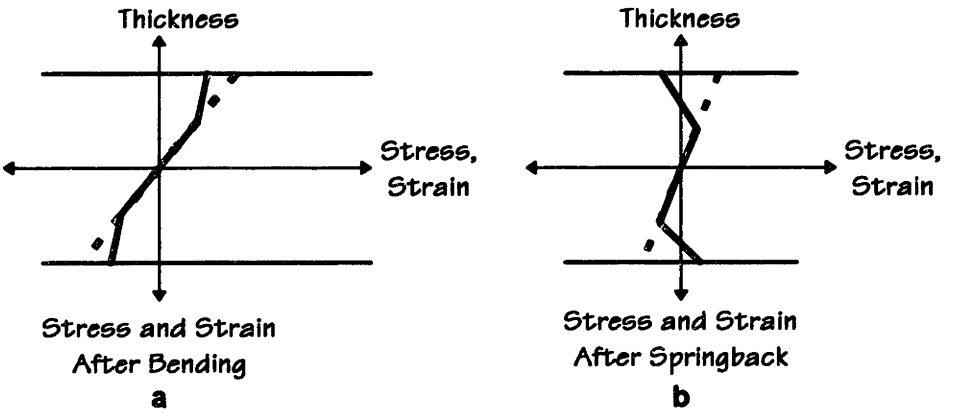

Figure 3.3 Stresses and strains in a part from bending and springback

Stretching a part after it has been bent results in a more even stress distribution in the part and less springback. Referring to Figure 3.1, the part would be stretched by holding the left and right edges of the part fixed and moving the die up into the part. Changes in the stresses and strains are shown in the following diagram. In Figure 3.4a, the stress and strain distributions after stretching have been added. In Figure 3.4b, the reduction in springback is evident in the fact that the slope of the strain line after springback changed only slightly from the slope after stretching. The final stress is zero according to this simple model.

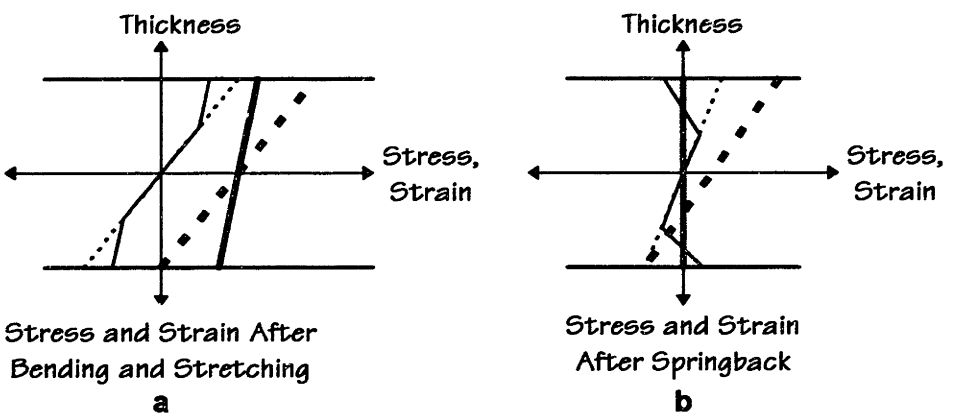

Figure 3.4 Stresses and strains in a part from bending, stretching and springback

Springback is greatest in parts with slight curvature, such as nearly all aircraft skins. Cook [1966] states, "Stretch forming was developed in World War II as a means for producing large accurately contoured sheets for aircraft wing and fuselage parts."

Two types of parts are commonly stretch formed: sheet metal and extrusions. As just mentioned, stretch formed sheet metal parts are generally skins, for example, leading

edges. Curvatures of such parts are not very tight, which makes these parts ideal for stretch forming. In the stretch forming operation used for sheet metal, called *drape forming*, the part is first bent over the die and then stretched. Extrusions are stretch formed to make parts such as chords, stiffeners, and brake rings. In the stretch forming operation used for extrusions, called *stretch wrap forming*, an initial stretch (pre stretch) is imposed on the part and the part is bent around the die under tension (wrap); an additional stretch is imposed after the part has been wrapped (post stretch). Other variations of the stretch forming operation exist, but these two are the most common.

3.1.5 Aircraft stretch forming industry survey

In order to get a sense of the state of the aircraft stretch forming industry in this country, an informal phone survey was made of people, mostly engineers, at prime contractors and subcontractors who are involved with stretch forming. Information was gathered from phone calls to over a dozen companies. As well, a factory visit was made to K-T Corporation in Shelbyville, Indiana, a major and well-respected supplier of stretch formed parts to the aircraft industry. While companies were generally willing to share information, the proprietary nature of much of the information requires that many specific data cannot be given here, and that generalizations are made. Thus, specific examples or company names are often omitted.

The equipment

The age of machines in this industry is mixed, with many older machines still in use (including some of WWII vintage). However, many older machines have been retrofitted with new, CNC controllers. The new controllers permit electronic storage of NC programs and control of the operation based on force (actually hydraulic pressure) or position. CNC controllers significantly increase the repeatability of the machine and the process. However, even with newer machines and newer controllers, operator experience is necessary to produce good parts, and the way one operator does something is likely to be different from the way another operator does it, and is likely to get different results.

Difference between old and new machines and more

SPC data taken in the early part of 1995 at Vought reveal that the average range of strain imposed on a lot of parts (measured by a strain measurement device) was almost three times as high for the older manually controlled machines than it was for the newer

CNC controlled machines. The average strain range for a number of lot of parts stretch formed on the newer machine was 0.11%, while the average for the old machine was 0.31%. A closer examination of about 20 lots revealed some more interesting information for these parts: an average range of 0.33%, an average standard deviation of 0.29%, an average total range per lot of 0.90%, and an average lot-to-lot difference between left- and right-handed parts (which should be the most the same) of 0.24%. These parts were formed on an old, manual, pressure-controlled press.

Given the significant difference between the old and new machines, one may conclude that much of the variation can be attributed to the improved control of the new machines. A closer look at the data reveals that the average range for the newer machine could be reduced to about 0.07% if three outlier lots were not included. Newer machines are run on position control, which, as discussed next, nearly eliminates sensitivity of the operation to material geometry and property variations.

Control of the operation

On older machines, the operation is controlled either visually or according to hydraulic pressure. Visual control of an operation means watching for visual cues in the part to know when to stop the operation. For example, in sheet metal stretch forming this may mean stopping the operation when all of the material is touching the die, or when all of the wrinkles are out, or when the part Lüders or "flashes." In extrusion stretch forming this may mean putting a mark on the part and seeing how far it moves. These are basically manual forms of strain control. If the stretch is controlled by hydraulic pressure, the desired pressure is manually set, and the part is stretched until as far the machine can stretch with the set hydraulic pressure.

On newer machines, the operation is generally controlled by position and/or force (which is generally estimated from hydraulic pressure). Most sheet metal parts are formed by drape forming, in which the part is "draped" over the die and then stretched, while most extrusions are formed by stretch wrap forming, in which the part is pre stretched, wrapped around the die under a tensile force, and then given a post stretch. Pre stretch is generally controlled by force, while post stretch is generally controlled by position. The wrap on NC machines is "learned" by the machine in a constant force or constant elongation mode, and then the positions are repeated for production parts; on older machines, the wrap is made under constant force. Some newer extrusion stretch

forming machines have a "yield point detector" function which senses when the material goes into plastic deformation during pre stretch.

Strain control by measuring the amount of strain in a part is rarely used. Strain measurements are sometimes made on a post-process basis, for example, to ensure that strain in the part is in accordance with specifications. The two most common methods of measuring strain are to use a tattle tale (a paper strain measurement device), and to scribe the part or mark it with a grid and then measure how much the lines separate. The resolution of these methods is generally between ± 0.1% and ± 1%. No one has used automatic in-process strain measurements to control the operation.

Measurements

The few studies that have been made of machine repeatability have shown NC controlled movement to be very repeatable. On the other hand, it has also been reported that some NC machines have an intermittent problem of "zero shifting" in which the zero position changes unexpectedly. In this case, operator input and adjustment are necessary.

Contour measurements are not made on most stretch formed sheet metal parts, apart from looking at the part on the die and seeing that it seems to fit, generally for the reason that contour is not a key characteristic because of the flexibility of sheet metal parts. While all customers specify how to measure the contour of sheet metal parts, especially the force allowed to get the part to contour for the measurement, nearly everyone agrees that these specifications are difficult to follow precisely. Often, conformance to contour is qualitatively measured by placing the part on a die and pressing the part to the die, to determine the gap between the part and the die. In a few cases, more advanced means are used to measure contour, such as a measurement of the contour by a CMM.

The key characteristics of stretch formed extrusions can include contour, leg angles, joggle depths, and flatness. Every company admits to having a "check and straighten" or "hand forming" area in which parts that do not meet the specifications are hand worked to bring them into tolerance. A consistent response to how much hand work is required on average and its cause was not found, but for difficult parts it could range

between half an hour and half a day per part.[19] For some, hand work appears to be the exception rather than the rule, while for others, the reverse is true. There is a split in opinion as to whether hand work is necessary more because of poor accuracy or because of poor precision, i.e., because a batch of parts is consistently the same shape, but off on average, instead of on average the right shape, but with significant variation about the average. When the average is off, it is not clear whether the deviation is on a lot-by-lot basis (i.e., a P/N fabricated in two lots is likely to come out different, for example, because of machine set up), or is consistent among lots of one P/N (i.e., a P/N fabricated in two lots is likely have the same deviation, for example, because of the die).

On the whole, very little SPC (control charting) is performed on stretch formed parts. For some combination of reasons, stretch forming receives a low priority for the implementation of SPC. An obvious difficulty with implementing SPC (which applies to nearly everything done in the aircraft industry) is that the volumes are very low.

Sources of variation

The most commonly mentioned sources of variation are incoming material properties, warpage from heat treat, dies, setup, machine movement, differences between operators, and routing. However, no one has investigated the contributions of each of these sources to the final part geometry.

Theoretical understanding of the stretch forming operation

There is a great deal of practical, experience-based knowledge in this industry, but hardly any theoretical understanding of what's going on in the material and why things happen. Alternately stated, there's a lot of *know-how*, but not a lot of *know-why*.

Summary and conclusions of informal survey

The equipment used in the stretch forming industry is a mixed bag of old and new machines; many of the older machines and nearly all of the newer machines have CNC control, which makes them more repeatable. Manually controlled machines generally rely on visual control (manual forms of strain control) and/or hydraulic pressure control, while NC controlled machines are controlled by position and force. SPC is not very

---

[19] Ewert et al [1991] claim that "Reworking the workpiece to mitigate the effects of springback have been known to increase the unit cost of production by 50%."

common in stretch forming, especially with sheet metal. Hand work of stretch formed extrusions is common, though it is not clear whether the primary cause is a lack of accuracy or a lack of precision. There are numerous sources of variation, but their relative contribution to the final part geometry has not been studied in depth. This is in part due to the lack of theoretical understanding of the stretch forming operation.

It is clear that stretch forming is still very much an art and that there is great opportunity to significantly improve the precision of stretch formed parts. This is the next topic.

3.2 PRECISION FABRICATION

Precision fabrication is the fabrication of detail parts, the critical dimensions (key characteristics) of which are to tight enough tolerances that

- the part fits just right in assembly, and
- some part features may be used to align parts in the assembly.

This implies accomplishing the above *without* hand work.

As already discussed in the previous chapter, precision assembly requirements may tighten tolerances to somewhere between a third and a sixth of current tolerances. This is not a small increment. The required precision depends on the needs of assembly. Tolerances should be only as tight as necessary to achieve a precision assembly or to make parts fit in current assemblies. The most important tolerances should be highlighted as key characteristics.

The task of improving the precision of a fabrication process is not a simple one, and therefore the rest of the thesis addresses this single issue. A quick summary of what is required and the approach taken is now given.

As already mentioned, precision fabrication refers to the fabrication of parts with accurate and precise contour and feature location *without* hand work. The necessary improvement in precision requires the transition of sheet metal forming from an art to a science. This requires a fundamental understanding of what is going on in each operation and in the entire process. This understanding is best acquired through both engineering and statistical approaches. Sources of variation must be identified and part variation must be reduced or eliminated, by some combination of eliminating sources of variation, reducing sensitivity to sources of variation, or compensating to offset the effects of sources of variation. Each operation within the process and the

process as a whole must be addressed, because the final part geometry and properties are impacted by every operation in the process and because the output from one operation is an input to the next.

3.3 Approach and Frameworks for Accomplishing Precision Fabrication

In order to achieve significant precision improvements, the approach taken must be both comprehensive, in order to capture and address all relevant factors, and detailed, in order to have the understanding of things necessary to make innovative improvements. The approach outlined next satisfies both of these requirements. After this, two frameworks for helping to think about the manufacturing operations and about how to deal with sources of variation are presented.

3.3.1 Combined engineering and TQM approaches

The approach taken in this thesis to improve fabrication precision was developed in order combine the best of what are often two somewhat exclusive, yet complementary, approaches to process improvement. These are called the engineering and TQM approaches. Although not true in all cases, there are generally significant differences in emphasis between engineering and TQM approaches. The engineering approach is characterized by an in-depth study of process or operation in which proactive, step improvement is sought, using a theoretically based, deterministic model of the process or operation. Further, much of the work is done on an individual basis. Often, some form of automatic control is part of the proposed solution. The TQM approach tends to strive for incremental improvement by creating an empirically based, statistical model which looks at the operation or process from the outside. Much of the work is done in teams, and root cause elimination is the ideal method of improvement. These characteristics are summarized in the following table.

Characteristic	Engineering Approach	TQM Approach
Modeling	theoretically based, deterministic	empirically based, statistical
Improvement method	improved control	root cause elimination
Work unit	individual	team
Improvement emphasis	step, proactive	incremental, responsive
Perspective	inside looking out	outside looking in

Table 3.1 Characteristics of the engineering and TQM approaches

Each approach, isolated from the other, has significant weaknesses. These are given in the following table.

Weakness	Engineering Approach	TQM Approach
Lack of emphasis	human factors	technical
Lack of skills	statistical	engineering
Lack of understanding	practical, shop-floor level knowledge	theoretical, what's happening & why

Table 3.2 Weaknesses of the engineering and TQM approaches

As should be evident from the above, a combination of the engineering and TQM approaches would be most effective because the strengths of one are matched to the weaknesses of the other. The approach to precision improvement in this thesis has been to integrate the somewhat standard seven step process improvement approach presented by Shiba et al [1993] with a more typical engineering approach. How this has been done for each of the seven steps and the work accomplished in each step are now briefly described.

Step 1: Select a theme

Theme selection is based on a prioritization of the needs of the "customer"—in this case, assembly.

As mentioned and discussed already, the theme chosen is precision improvement of fabricated parts. The characteristics of fabricated parts for which precision is required are material geometry and properties (while improved precision of properties is not directly pursued in this thesis, it stands to reason, since they are an input to geometry

and a process output, that if geometry is to be more precise, the precision of properties must increase as well). For stretch formed parts, these may include

- Geometry: contour, thickness, twist, bow, length, width, and angle
- Properties: strength, residual stress, and corrosion resistance

How much, if any, precision improvement is required of each characteristic is determined by the needs of assembly (some requirements may be loosened). This issue was addressed in the previous chapter.

Steps 2 & 3: Create a model, collect and analyze data, and assign causality

This stage is based on (a) developing a fundamental understanding of the process and its operations through an appropriate model and various other means, and (b) documenting variation and identifying sources of variation (and their magnitude and effect) through both engineering and statistical methods.[20]

Operations having the greatest effect on the precision of stretch formed parts—heat treatment, stretch forming, routing, chemical milling, and incoming material have been investigated. Although it can have a significant effect on precision, in order to narrow the focus, shot peening of extrusions was not investigated because many extrusions are not shot peened.

An analytical (engineering) model was developed for this step in order to gain a fundamental understanding of what is going on in the stretch forming operation and to assess the affect of various parameters and the method of control on the operation. The other means of gaining a theoretical understanding of what's going on was to perform a literature review. As a matter of focus and based on expected importance and benefit, development of a detailed, theoretical understanding of an operation was only undertaken for the stretch forming operation.

In order to develop a practical and statistical understanding of the operations that constitute the stretch forming process, measurements were made on the heat treat, stretch forming, chem mill and rout operations, and a designed experiment was

---

[20] According to Koonmen [1994, p. 15], "The key to precision assembly is continuous improvement in all fabrication areas, achieved primarily through a process of identifying and removing the causes of variation." This recent need for improved precision also exists in the automobile industry [Umehara, 1990].

performed to help understand output variation, which parameters vary, and how their variation affects the individual operations and the process.

Step 4: Plan and implement solution

This step is based on (a) the combined theoretical and statistical understanding of the process developed in steps 2 and 3, and (b) a general understanding of the causes of variation and the possible methods of eliminating and reducing output variation which are described shortly. The combination of theoretical and statistical knowledge led to a synergistic increase in the ability to come up with innovative and promising improvements and to justify their implementation *a priori*.

Recommended improvements to the current stretch forming processes have been formulated and presented. The most significant of these is automatic, in-process strain measurement for feedback to optimize and control the stretch forming operation. For various reasons, full implementation has not been possible, and testing has been difficult as well.

Steps 5 & 6: Evaluate effects & standardize solution steps

This step involves learning by evaluating the effects of changes made and standardizing the solution to similar situations. Limited tests have demonstrated significant reduction in variation from implemented improvements. Due to slowness of implementation and testing, standardization has not been accomplished.

Steps 7: Reflect on process, build understanding, and select next problem

In this step, reflection on the improvement process *and* on the manufacturing process has been undertaken in order to refine the approach to precision improvement , so that further improvement efforts will be better directed and more effective. The approach developed and lessons learned have been generalized to other manufacturing processes. Further research has been proposed.

3.3.2 Manufacturing model

The manufacturing model described below is presented in order to have a structured approach to understanding manufacturing operations. This structured approach promotes a consistent and complete understanding of each operation and is useful in deciding how to improve the operation. By going through the model, each thing that can affect an operation is listed systematically (kind of like a specialized fishbone diagram) and interactions are better understood. An earlier version of this model is

presented in [Parris, 1993]. Other models with similar approaches and objectives have been developed by Alting [1982], Kobayashi et al [1989], and Moore and Kibbey [1965].

Introduction of the model begins with terminology.

Terminology

In the following, each term is defined, and examples from one or more operations in the stretch forming process are given.

Material—the workpiece; for example, a sheet of metal or an extrusion.

Machine—the piece of equipment that provides movement and energy to the material and/or the interaction media; for example, the stretch forming press or the vat containing molten salt for solution heat treating.

Location tooling (fixturing)—what the machine uses to hold onto the material; this determines the boundary conditions for the material, and may or may not be stationary; for example, jaws on a stretch press or the basket used in chemical milling.

Interaction media (fabrication tooling)—what the machine uses to transform the material; for example, the die in stretch forming, the molten salt in solution heat treating, or the router bit used in routing.

Interaction—what happens between the interaction media and the material; it involves a transfer of energy; for example, the normal and frictional forces between tool and workpiece during stretch forming or the heat transfer between salt and workpiece during solution heat treating.

Transformation—what happens to the material; for example, stretching and bending of metal in stretch forming or the movement of precipitates into solution during solution heat treating.

Parameters—the constitutive relationships among states and fixed things affecting them, including initial material geometry and properties; for example, the stress-strain relationship, chemical composition and microstructure, or thickness of the workpiece, surface finish or contour of the die, stiffness of the machine's mechanical parts, and size and conductivity of the solution heat treating vat walls. Note also that at times, the

term *parameters* is used in a more general sense to indicate all things that affect an operation, including states and settings.

States—the energy and movement/location variables; for example, quenchant temperature and quench rate for quenching, the stress and strain distribution in the material during stretching, or the RPM of the router bit used in routing.

Settings—the desired states and parameters, changeable from one part to the next or one setup to the next; these are like the inputs to an operation; the dividing line between settings and parameters is difficult to place; for example, the desired temperature of and time in salt for solution heat treating, the initial jaw positions and final die position or final force exerted on the part for stretch forming.

Output—the geometry and properties of the material; for example, contour and residual stresses of the part after stretch forming, heat treat state of the material after quenching, or thickness after chemical milling.

Operation[21]—one step in the manufacturing process; for example, solution heat treating, stretch forming, or routing.

Process—the entire set of operations needed to produce a fabricated part; for example, the stretch forming process (note that the term *stretch forming* is used for both the operation and the process; note as well that the term *process control* is commonly used to apply to control of an operation, and that the term *in-process* describes something that happens during an operation).

Serial and parallel—these distinctions refer to the spatial progression of an operation over time; serial refers to the transformation occurring in a local area and sequentially, while parallel refers to the transformation occurring globally and simultaneously; operations are generally neither entirely serial nor entirely parallel, but lie somewhere in the spectrum between the two extremes; for example, routing occurs more serially and stretch forming occurs more in parallel.

Control—the system of feedback and adjustment used to achieve desired settings or states; open loop control is predictive and uses no feedback, while closed loop control uses some function of the difference between the desired and actual values of a state

---

[21] A very good presentation of the terms operation and process is given by Shingo [1986].

to drive the operation; for example, how the salt temperature is maintained, and how the position of a tension cylinder on the stretch press is achieved.

Operator—the person who (a) sets up tooling and the machine, (b) puts the part into the location tooling, (c) selects and adjusts settings, and (d) controls the operation (the extent of operator control depends on extent of automation); for example, the sheet stretch press operator or the routing operator.

Procedure—the set of tasks used by the operators to perform an operation and how the tasks are accomplished; this may vary from the officially documented operating procedures; for example, how the operator loads the material into a fixture or how the operator controls the amount of stretch in the stretch forming operation.

Environment—everything else that affects some aspect of the operation; for example, air temperature and humidity, the first of which affects natural aging of -W condition aluminum, and the second of which, when combined with high levels of the first, adversely affects operators.

A schematic diagram of the manufacturing model

The following schematic diagram illustrates the manufacturing model and helps to understand the relationships between its components.

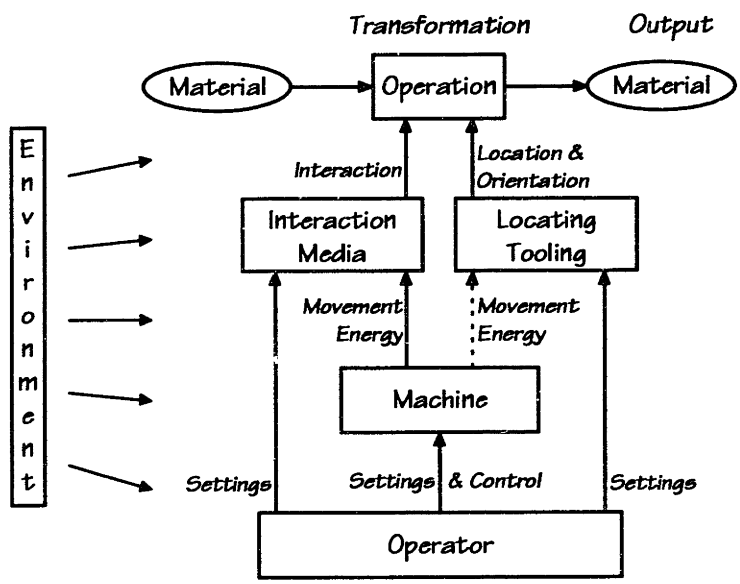

Figure 3.5 Schematic of the manufacturing model

There are a couple of important things to note from this schematic. The output of an operation is the material—its geometry and properties. The operator only influences

the operation through the machine (its settings and control), interaction media, and location tooling. The machine gives movement and/or energy to the location tooling and interaction media in order to achieve the transformation. The transformation is influenced by the material, the interaction (which is affected by the interaction media), and the location given by the location tooling. Though not shown, more automation results in the operator giving up control of the machine in the form of more settings for the machine.

Another useful thing to understand about a manufacturing operation is the frequency with which things are done—in particular measurements and control actions. The following diagram shows the possibilities.

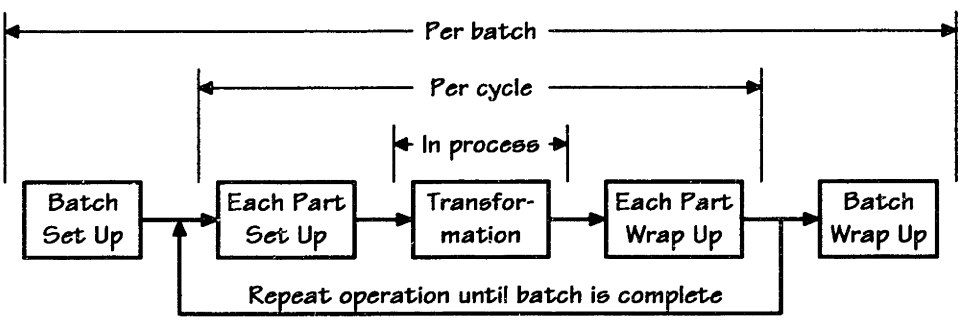

Figure 3.6 Frequency of occurrence in batch manufacturing

The following diagram shows the progression of operations in a process.

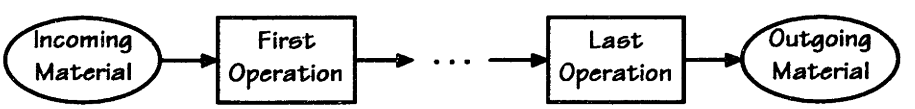

Figure 3.7 Progression of operations in a process

This diagram clearly shows that the output of one operation—material geometry and properties—is an input to the next operation, and, thus, that the output at the end of the process is affected by each of the operations. This is why precision improvement must be comprehensive.

Sources of variation are in the material, machine, location tooling, interaction media, settings, procedure, or environment. These combine to affect the interaction and transformation and, as a result, the output.

If the operation is well understood and adequately modeled, it is possible to predict some of the desired states during the operation—or at least at the end of the operation.

There are a few states, key states,[22] which give an indication of the entire operation and which, if controlled, will generally ensure the success of the entire operation.

Further, how the operation is controlled determines which sources of variation significantly affect an operation. Therefore, it may be possible to *choose* which set of parameters have influence on the operation by the choice of control strategy.

Three approaches to dealing with sources of variation are described next.

3.3.3 Variational model

The variational model [Parris, 1993] is used to provide a structure for thinking about variation and how to deal with it. The variational model is based on the following simple functional model of an operation:

$$Y = Y(P,U), \tag{3.1}$$

in which Y = outputs, P = parameters (some varying, perhaps randomly), and U = inputs (a subset of parameters which are known and manipulable). A first-order differentiation gives

$$\Delta Y = \frac{\partial Y}{\partial P}\Delta P + \frac{\partial Y}{\partial U}\Delta U. \tag{3.2}$$

Using this simple model, it is apparent that output changes are affected by parameter changes, sensitivity to these changes, adjustment of inputs, and sensitivity to input changes. Thus, output variation (a measure of the change in output) can be reduced by:

- elimination—reduce or eliminate sources of variation,
- optimization—reduce sensitivity to sources of variation, and
- compensation—adjust inputs when outputs vary.

Next, each approach is discussed briefly.

Elimination refers to eliminating the *source* of variation. Elimination means, for example, specifying and purchasing material of higher quality, fixing or replacing things that break or wear, correcting things that have been wrong all along (including design), and specifying or changing procedures. Strengths of elimination include: it is applicable to all sorts of causes of variation, it doesn't require a model, and it is a

---

[22] Key is used in the same sense as in *Key Characteristics*. As well, Taylor [1991] uses similar terminology, *key input variables*.

permanent fix (ideally). Weaknesses of elimination include: it may be too expensive or inherently not possible.

Optimization refers primarily to reducing the *sensitivity* of the output to sources of variation. Optimization can be accomplished theoretically or experimentally. Optimization can be used to find optimal settings, lubrication, or tool geometry, as well as incoming material geometry and properties. Strengths of optimization include: it makes optimal use of what one already has. Weaknesses of optimization include: the achievable benefit may be limited and it is generally experimentally intensive.

Compensation refers to compensating for the *effect* of sources of variation on the output. Compensation can be characterized by the state measured, the input adjusted, the process model, the control algorithm used, the time interval of measurement and adjustment, and whether it is performed manually or automatically. Strengths of compensation include: it can operate on a very small time scale, it can overcome a wide variety of variation sources, and it is useful when sources of variation can't be eliminated (to eliminate their effect). Weaknesses of compensation include: adjustable inputs may not exist, its implementation may be expensive, the necessary measurements may not be feasible, and an adequate model may not exist.

In order to demonstrate the difference in method of reducing output variation among the three different approaches, a simple example is given. The operation is sheet metal stretch forming. The problem is that variation of the contour is unacceptable. Assume that variation in strength of the material is identified as the primary cause. Specifically, assume that it varies unpredictably ± 10% from lot to lot. An elimination approach would be to specify and purchase material whose strength varies less, maybe ± 1%. An optimization approach would be to find the machine settings at which the output is least sensitive to strength variations. Compensation approaches would be to adjust the force used based on *a priori* knowledge of material properties or to control the operation based on displacement instead of force.

3.4 SUMMARY AND CONCLUSIONS TO PRECISION FABRICATION OF AIRCRAFT DETAIL PARTS

Aircraft detail fabrication, similar to assembly, has many inefficiencies and quality problems, particularly in sheet metal fabrication. Stretch forming was chosen as a sample detail part manufacturing process to use for the development, implementation,

and evaluation of an approach to precision improvement. Precision improvement is defined as the producing of detail parts with correct contours and precisely located features. The most important of these are indicated as key characteristics. The approach taken to achieve precision improvement is a combined engineering and statistical approach based on the 7 step improvement process. Finally, two frameworks useful in understanding manufacturing operations and how to deal with sources of variation were presented.

At this stage, the foundation for a thorough investigation into the stretch forming process has been laid. The next step is to gain a deep understanding of the process. This accomplished first by the development of an analytical model of the stretch forming operation, the topic of the next chapter.

4 ANALYTICAL MODEL OF METAL STRETCH FORMING

4.1 INTRODUCTION

4.1.1 Purpose of this chapter and the next

The primary purpose of the next two chapters is to develop a better understanding of the stretch forming operation with the ultimate objective of improving the precision of the stretch forming process. The model developed in this chapter is used in the next chapter to determine the effect of parameters and parameter changes on the stresses and strains within the part and the springback. The theoretical knowledge helps one to better understand, interpret, and act upon the statistical and other findings on the shop floor. The secondary purpose of the next two chapters is to contribute to the scientific knowledge and theoretical understanding of the stretch forming operation.

4.1.2 Outline

Equations are developed to predict—as a function of material parameters, die geometry, and applied strain or force—stresses and strains in stretch formed metal and springback. The equations are based on mechanics of solids and simple plasticity concepts. While these equations are essentially two-dimensional and do not capture various material anisotropies, they are adequate for the purpose of understanding the stretch forming operation and determining process sensitivities, and they are simple to use and straightforward to understand. The equations have been implemented in an Excel® spreadsheet. The following diagram summarizes inputs, outputs, and flow of the analytical model.

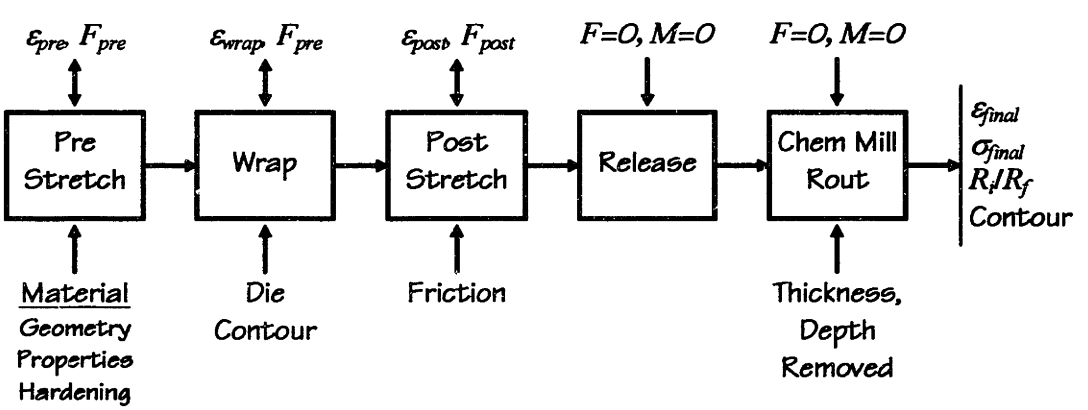

Figure 4.8 Diagram of analytical model inputs and outputs

Below each block are the parameters that are fed into the block, while above each block are the requirements imposed on the block. For the first three blocks, either strain or force is imposed, and the other is complementary to it. Forces, moments, and non-cylindrical contours are determined by numerical summation. The model outputs are the final stress, strain, springback ratio, and contour.

The next section reviews relevant literature on stretch forming. Next, preliminaries such as the geometry, nomenclature, and assumptions are given, after which the power law strain hardening stress-strain relationship is presented and modification is made for plane strain conditions.

Development of the model begins with a derivation of the equations for modeling drape forming (bend plus post stretch) using the no initial plastic deformation (No IPD) hardening model. After this, drape forming equations are derived with the Isotropic, Bauschinger, and Kinematic hardening models. Then, the equations are enhanced to model stretch wrap forming (pre stretch plus bend plus post stretch). The next four sections further enhance the model to account for the effect of chemical milling, non-rectangular cross-sections (extrusions), routing of extrusions, and friction and a varying radius of curvature along the length of the part (the last two are done together because the incremental approach needed to model these is the same). Finally, the yield surface method, a simpler method to determining stresses, is presented. The formulas derived with the yield surface method give exactly the same result as the previously derived formulas, are more flexible, and can more easily model additional steps.

In the following chapter, (a) the model is used to assess the effect of parameter changes and the method of control, (b) the effects of other non-ideal conditions are discussed, (c) and comparisons are made to actual experiments and FEA simulations.

4.2 LITERATURE REVIEW

Springback equations for bending are common in textbooks, but these normally use simple material models and don't include stretching. Most articles found in the literature that address bending and stretch forming are very limited in their focus and, therefore, in their ability to model the breadth of parameters needed to gain an understanding of the stretch forming operation that is useful to precision improvement. Specifically, the literature on bending and stretch forming generally suffers from most of the following limitations:

- The model doesn't include pre and/or post stretch
- The material model is too simple to capture actual material behavior
- The no initial plastic deformation model is assumed
- Different hardening models are not investigated
- Extrusion cross-sections cannot be modeled
- Chemical milling and routing cannot be modeled
- The equations are too complex to be readily understood and/or easily solved
- Friction is not modeled
- A changing radius of curvature cannot be modeled
- Variation and method of control are not addressed
- The relevance of the findings to the shop floor is hard to determine

In the following paragraphs, the most significant and relevant works relating to bending and stretch forming are briefly described, to show what has been done so far, to report the results of others, and to demonstrate that the existing literature falls short of serving the needs of this work. The works are categorized in order to give some structure to the many references. Further references are given in the second half of the bibliography, in which references are organized by topic.

4.2.1 The most relevant textbooks that address stretch forming

Hill [1950] develops fundamental equations for three dimensional plasticity, plane strain conditions, bending of beams and thick sheet, and bending with tension, but in the latter does not address the issue of springback. Hosford and Caddell [1983] delve into the mechanics of a large variety of metal forming operations, including stretch forming and plane strain bending. However, the authors use the standard no initial plastic deformation assumption. Lange [1985] briefly describes the stretch forming operation, discusses quality and other related issues, states the importance of lubrication and the effect that friction has of reducing the amount of strain, and shows the simple additive no initial plastic deformation model with elastic, perfectly plastic material.

4.2.2 The most relevant articles on bending and stretch forming

About 40 articles were found that address bending and stretch forming. The few that stand out from the rest are discussed here.

Baba and Tozawa [1964] have probably the most detailed look at the effect of the stretch profile—the amount of tension applied to the part before and after the wrap. The authors found that stretching after wrapping reduces springback more than

stretching before. The analysis is performed in three dimensions with strain hardening material and typical plasticity equations. It is not clear how the complex integrals were solved. The influence of the Bauschinger effect was also studied. Their conclusions are very similar to some of those arrived at in the next chapter. Control of the operation and the effect of changes in other parameters were not studied.

Duncan and Bird [1978] address springback in drawing. Linear strain hardening is assumed; however, this assumption eliminates residual stresses and doesn't show the benefit of stretching the part further than getting it all plastic. The authors note that the effect of friction over shallow curves is negligible compared to the effect of friction over the edges of the die, where radii of curvature are small. They also investigate the effect of various parameters.

El-Domiaty and Shabaik [1984] develop equations for springback for the stretch forming operation using the power law strain hardening material model. The no initial plastic deformation approach is used. Non-dimensional parameters are used, which make the results difficult to relate to actual forming situations.

El-Domiaty [1990] develops equations for stretch forming of beams with a T cross-section. This work extends equations developed by [El-Domiaty and Shabaik, 1984] for power law strain hardening sheet. Non-dimensional parameters are used.

Ewert et al [1991] patented a strategy for determining the stretch profile and die springback compensation to achieve the desired part shape after springback. However, some of the equations they use don't seem to spring from any physical basis.

Hessami and Yuen [1988] use a three dimensional numerical technique to predict stresses and strains after bending and stretching. They use non-dimensional parameters and an elastic, perfectly plastic stress-strain curve; pre and post stretches are modeled.

Ju [1985] uses a simplified thin shell theory to predict stresses, strains, and springback for three pre and post strain cases of stretch forming; some of his findings are similar to those in this thesis.

Queener and De Angelis [1968] wrote a foundational work on springback from sheet metal bending (no stretch). The authors make plane strain and plane stress adjustments to stress-strain curve parameters that are similar to those made in this

chapter. They demonstrate a very close relationship between their analytical model and experimental results. They use a modified technique developed by Treuting and Read [1951] to experimentally derive the residual stress-strain curve, and find close correlation to predictions. This method is similar to the one use to calculate springback changes for chemically milled material in this thesis.

Swift [1948] is one of the first authors addressing plastic bending under tension. The author uses linear strain hardening, included the effect of friction, and focuses on thinning as the primary contributor to the discrepancy between theory and practice.

Tozawa [1977] (in Japanese) used an analytical model (the method of solution was described in [Tozawa, 1965], also in Japanese, which this author did not look at) to predict the effect of changing various parameters. Tozawa used beam theory (including radial stresses), power law strain hardening, and takes into account plane strain conditions and Bauschinger effect. However, he does not consider friction, chem mill, or cross-sections, and does all calculations as a function of force, not strain. While he models both pre and post stretch, he does not model them together, although he cites Itoh [1968], who did (also in Japanese, which this author did not look at). Most of his results are similar to those found in this thesis.

Tozawa [1990] wrote one of the few articles on formed sheet metal directly aimed at improving accuracy. Stretch forming is addressed and an evaluation, based on results from other articles, is made of the effectiveness of the application of stretch before and after bending.

Ueda, Ueno, and Kobayashi [1981] investigate the effect of pre and post stretches in the stretch forming of channels and conclude that post stretch is more effective than pre stretch in reducing springback. The authors conclude that variation in springback can be reduced by determining the initial stretch by displacement instead of force.[23]

4.2.3 Soviet articles on stretch forming

A number articles on various aspects of stretch forming have been published in Soviet research journals, some of which have been translated into English. The following is a brief review of the more interesting and relevant of these articles.

Bodunov et al [1994a] propose an interesting method for reducing springback in a stretch formed T cross-section part: applying radial compression to the outside of the part at the end of the operation. Three dimensional plasticity equations are developed, and a solution procedure is given. Bodunov et al [1994b] further this work and show theoretical results that demonstrate the feasibility of this approach to reducing or eliminating springback.

Lysov et al [1985] and Lysov et al [1987] present a technique for calculating the tensile force in the stretch forming operation with account for the curvature of the free segment of the profile, located between the stretcher chuck and the point of profile contact with the bending die. According to the authors, calculations not accounting for curvature in the free segment of the profile can underestimate actual forces by as much as 20%.

[Oding, 1987a] describes a method for calculating parameters for a control program of a double curvature sheet stretch forming operation. The author defines the current boundary of contact between blank and punch surface and blank elongation and the stresses and strains of the sheet in the free area out of contact with the punch. The solution is constructed step-by-step, using the method of perturbations at each time step. One conclusion is that double curvature shapes are formed mainly by uneven stretching of the blank. One useful finding is that the transverse and shear strains that arise in the blank are of the same order of magnitude as the tensile strains.

It is interesting to note the emphasis in the Soviet literature on CNC-controlled stretch forming; hence, the articles address geometry and kinematics of the stretch forming operation outside of the material in contact with the die. As well, and this may be attributable to the recent vintage of this literature and the narrow scope of the literature search, there is much less emphasis on analytical modeling of the material and springback on the die than is found in the West. While Soviet authors have touched on a few areas into which this thesis goes into great detail, their treatment of these areas is more a side issue than the focus.

---

[23] It is an interesting side note that the articles that address variation and deal with issues relevant to the shop floor are all from Japan.

4.2.4 Books on aluminum

Since nearly all stretch formed parts are aluminum, some understanding of this alloy and its behavior (especially during the heat treat operation) is vital to understanding the stretch forming process. There are a few very good books which focus on aluminum alone. These include, for example, *Aluminum and Aluminum Alloys* (an ASM Specialty Handbook), edited by Davis [1993], and *Aluminum: Properties and Physical Metallurgy* (also published by ASM), edited by Hatch [1984]. Further, general books on metals and engineering materials will contain useful summary information. These include, for example, *Fundamentals of Engineering Materials* by Thornton and Colangelo [1985].

4.2.5 The need for a simple yet comprehensive model of stretch forming

The literature review demonstrated that there is still a need for the development of a simple yet accurate and comprehensive analytical model of the stretch forming operation that can be used to: predict the output of the operation, determine the sensitivity of the operation to parameter changes, and to evaluate the method of control. Equations developed in this chapter are not merely for theoretical knowledge, but are used to help understand and improve the stretch forming process—and they can be used by others for this same purpose. Therefore, for example, parameter ranges are focused to what is actually found in a stretch forming operation used to produce real parts, and the complete derivation of most equations is presented in a way that is easy to understand and follow. Basic concepts necessary to understand the more complex material are given, so that an individual with little prior knowledge of mechanics of solids can follow the points made and apply the lessons learned from this thesis to his or her own factory.

The analytical model developed in this thesis overcomes all of the limitations listed above. No other work has done this.

4.3 INTRODUCTION TO THE STRETCH FORMING OPERATION IN PRACTICE

For those unfamiliar with the stretch forming operation in practice, brief descriptions are given in Chapters 6 and 7. An introduction to the equipment and steps in the sheet stretch forming operation (drape forming) is given at the start of Section 6.2. A similar introduction to the extrusion stretch forming operation (stretch wrap forming) is given at the start of Section 7.4.

4.4 PRELIMINARIES

4.4.1 Units

While nearly all American companies in the aircraft industry still uses English units, much of the scientific community uses Metric units. Metric units are used in this chapter and the next. A conversion table is given in Appendix 6.

4.4.2 Model geometry and nomenclature

The detailed geometry of the model is shown in the following diagram.

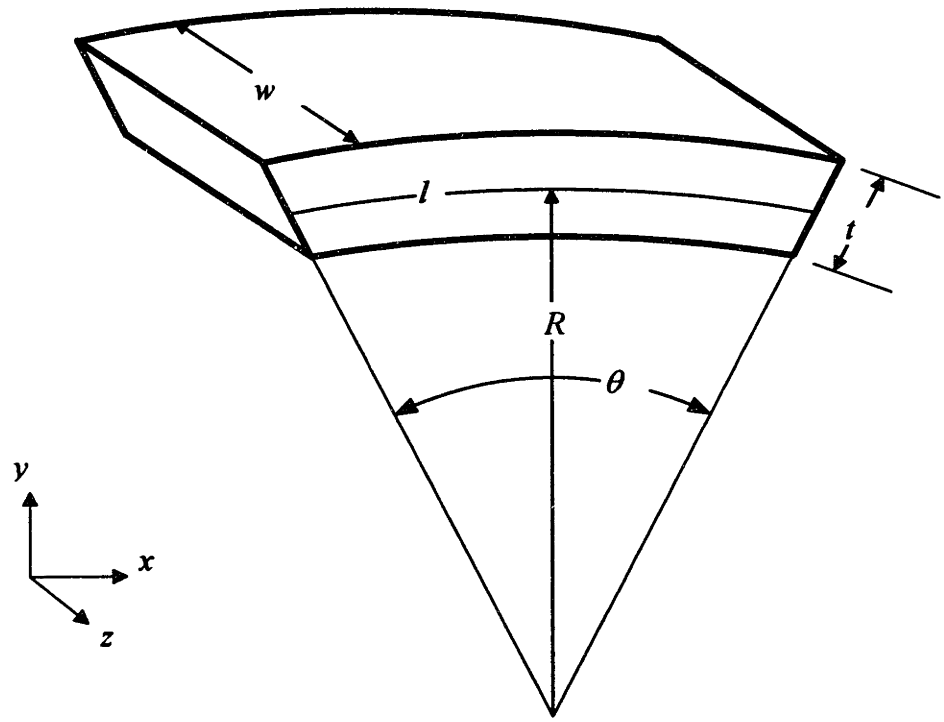

Figure 4.9 Detailed geometry of sheet used in analytical model

The following nomenclature, most of which is shown in the above drawing, is used. The initial workpiece thickness is t, width is w, and length is L. Note that the length direction is always in the direction of stretch. Regarding the bent workpiece, the bend angle of the workpiece is θ, the radius of curvature of the bend is R, and the length of the workpiece over the length of the bend is l. The midplane is located in the middle of the thickness of the part; it does not move, and it is used as a zero reference for the y dimension (which is always normal to the part surface). The term neutral axis is not used to refer to the midplane, because, while it applies during bending, when the part is

stretched, the neutral axis moves, while the midplane does not.[24] When the part takes the form of the die, the die radius is $R_d = R - t/2$; this negligible difference is ignored.

The following figure shows the radii of curvature and angles used to determine the springback ratio. The dark line represents the formed part, while the lighter line represents the part with springback.

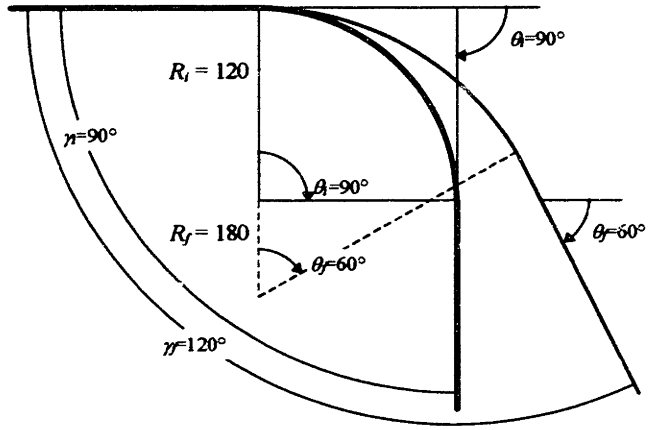

Figure 4.10 Radii of curvature and angles used to determine the springback ratio

If the initial bend geometry is given by $R_i = 120$ and $\theta_i = 90°$, and the final radius of curvature and angle are $R_f = 180$ and $\theta_f = 60°$, then the *springback ratio* is $R_i/R_f = 2/3$. The radii of curvature and bend angles are related by the geometric identity

$$\frac{R_i}{R_f} = \frac{\theta_f}{\theta_i}. \tag{4.1}$$

Note that the bend angle θ on the inside is the same as the angle θ on the outside. The enclosed angle γ is not used when discussing springback and angles; only the bend angle θ is used.

4.4.3 Simplifying assumptions

In order to achieve useful analytical results, some common simplifying assumptions are made. The radius of curvature,[25] width, and thickness[26] of the part are constant

---

[24] While a number of stretch forming models derive equations in which the neutral axis moves, it is simpler, more intuitive, and more informative to deal with a midplane that stretches.

[25] Since the radius of curvature is constant, there is no bending or unbending—which may affect stresses and strains—as the part is stretched.

throughout the length of the curved portion of the part and remain so during the operation. The length of the workpiece centerline l_o (at the midplane) remains unchanged when it is subject to bending only (which is reasonable given the large radius of curvature [Wang, 1993]). Relevant material properties are isotropic. Initial residual stresses and strains are zero. Plane sections remain plane. Strain contributed by stretching is simply additive to the bending strain. The effect of friction is negligible.

The effects of relaxing some of these assumptions are examined later.

4.4.4 Power law stress-strain relationship

The simple elastic, perfectly plastic approximation of material behavior is inadequate to capture the form of the actual stress-strain behavior. The constant slope, linear approximation of plastic deformation is better, but cannot be used because it does not capture the diminishing hardening as strain increases, and this has a profound effect on the stretch forming operation and how it is controlled. A very common, and quite accurate for aluminum, approximation of material stress-strain behavior is the "power law" approximation, and it captures strain hardening very well. The power law stress-strain relationship is now presented.

For small strains, deformation is purely elastic; that is, the stress is linearly proportional (the proportionality constant E is called the elastic modulus) to the strain ε. For larger strains, deformation is both elastic and plastic, and the stress σ is proportional to the strain to the power n, the strain hardening exponent. Mathematically, this is written as

$$\begin{aligned} \sigma &= E\varepsilon && \text{for } |\varepsilon| < \varepsilon_Y \\ \sigma &= K\varepsilon^n && \text{for } \varepsilon > \varepsilon_Y \\ \sigma &= -K|\varepsilon|^n && \text{for } \varepsilon < -\varepsilon_Y \end{aligned} \quad . \tag{4.2}$$

The variable K is generally called the strength coefficient. When the material has been plastically deformed, and the strain changes direction, the magnitude of the stress decreases at the slope of the elastic portion of the stress-strain curve until it begins to further strain harden.

---

[26] While constant thickness is not an assumption by intent, it is a fact that the model does not take into consideration material thinning; the model holds the material thickness constant.

While there is a distinction between engineering stress and strain and true stress and strain, the difference between them at the small strains seen in stretch forming is relatively insignificant. For example, when engineering strain is 5%, true strain is 4.88%, and the difference is about 2.5% of the engineering strain. At 10% engineering strain, the true strain is overestimated by about 5%. When using strain to calculate stresses in the elastic range, the error is quite small, since elastic strains are quite small. For example, at 0.2% strain, the actual stress is overestimated by only 0.1%. When using strain to calculate stresses in the plastic range, the error in stress is also small due to the slow increase of stress. For example, at 5.0% strain, the actual stress is overestimated by only 0.5% (for a strain hardening exponent of n = 0.21). Therefore, the use of engineering strain as a surrogate for true strain when calculating stresses is acceptable because of the small magnitude of the error introduced by this simplification. In all following calculations, engineering strain is used to approximate true strain because it is mathematically much simpler. The symbol ε is used.

This model assumes that the stress-strain parameters are independent of the amount of strain and that the material is not strain rate sensitive. Strain independence is a safe assumption because strains are generally quite low—under 5% for sheet and under 10% for extrusions—relative to strains of up to 50% or 100%, which are common ranges over which material stress-strain parameters may vary. Strain rate independence is a good assumption because strain rates are very low (generally $\dot{\varepsilon} < 0.02$), the m value for aluminum is generally less than 0.02 [Wagoner, 1985], and strain rate sensitivity, when low, generally becomes important only after necking [Wagoner, 1985], which (hopefully) does not occur in stretch forming.

The following chart contains a plot of an experimentally determined stress-strain curve for a specimen of Al 2024-O[27] along with an estimated curve based on the power law stress-strain relationship with parameters yield strength σ_Y = 77 MPa, elastic modulus E = 68947 MPa, and strain hardening exponent n = 0.210 to a maximum strain of

[27] The data are from standard tensile tests performed by the Structural Materials Group of the Corporate Research Center at the Grumman Corporation in 1991.

ε = 0.05 (5.00%).[28] The approximation is reasonably accurate. However, what is important for the model is not so much the absolute accuracy of the estimation to a particular alloy, but rather the general shape of the stress-strain curve—in particular, the decreasing slope of the stress-strain curve in the plastic region. The values of the parameters above are the standard parameters for all calculations, unless noted otherwise.

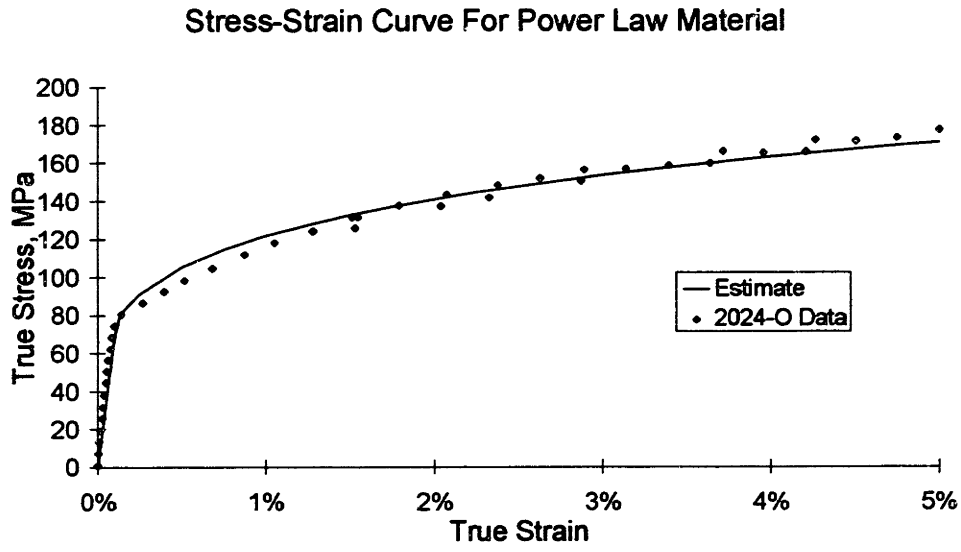

Figure 4.11 Actual and estimated power law stress-strain curves

The stress-strain relationship is completely characterized by the yield strength σ_Y, the elastic modulus E, and the strain-hardening exponent n. The value of K is determined by these parameters according to the following equation

$$\sigma_Y = K\varepsilon_Y{}^n = K\left(\frac{\sigma_Y}{E}\right)^n \Rightarrow K = E^n\sigma_Y{}^{1-n}. \tag{4.3}$$

For the standard properties, K = 320.9 MPa (46.5 ksi).

All equations are derived using the power law stress-strain relationship, which serves as a relatively accurate approximation to the actual material behavior.

---

[28] These parameters are given in metric units. Conversion to English units is straightforward: 1 ksi = 6.9847 MPa or, conversely 1 MPa = 145 psi. Therefore, the standard parameters in English units are σ_Y = 11.2 ksi and E = 10 ksi; n doesn't change.

4.4.5 Adjusting uniaxial properties to plane strain properties

Sheet metal stress-strain properties σ_y, E, and n are generally determined by a standardized "dog-bone" tensile test [ASTM B557, 1994]. Consequently, the properties reflect material behavior in uniaxial stress and triaxial strain conditions. When stretch forming sheet metal, however, the stresses and strains are assumed to be plane (biaxial). Therefore, a translation of properties from uniaxial to plane strain and plane stress may be necessary. This is done in Appendix 3, and the results are given below. (Similar results can also be found in [Hosford and Caddell, 1983], in [Queener and De Angelis, 1968], and in [Ju, 1985].)

It is possible to simply scale the values of σ_Y, ε_Y, E and K in order to transform uniaxial tensile test stress-strain curve properties to plane strain and plane stress conditions exhibited in sheet metal stretch forming. The following equations summarize the necessary changes. The plane strain stress-strain curve is given by

$$\begin{aligned} \sigma' = E'\varepsilon &= \frac{E}{\left(1-\nu^2\right)}\varepsilon \qquad \sigma' \le \sigma'_Y \\ \sigma' = K'\varepsilon^n &= \left(\frac{4}{3}\right)^{\frac{n+1}{2}} K\varepsilon^n \quad \sigma' \ge \sigma'_Y \end{aligned} \quad , \tag{4.4}$$

in which σ' is the adjusted stress. The adjusted yield strain and yield stress are given by

$$\varepsilon'_Y = \left(\frac{K'}{E'}\right)^{\frac{1}{1-n}} = \left(\frac{\left(1-\nu^2\right)K}{E}\left(\frac{4}{3}\right)^{\frac{n+1}{2}}\right)^{\frac{1}{1-n}} \quad \text{and} \quad \sigma'_Y = E'\varepsilon'_Y = \frac{E}{\left(1-\nu^2\right)}\varepsilon'_Y . \tag{4.5}$$

The following table gives an example of the changes involved, for the standard stress-strain curve parameters used in this thesis.

Property	Uniaxial, x	Plane Strain, x
E	68947 MPa	75766 MPa
K	320.9 MPa	381.2 MPa
n	0.21	0.21
ε_Y	0.112%	0.123%
σ_Y	77.0 MPa	84.8 MPa

Table 4.3 Uniaxial and plane strain stress-strain curve parameters

The uniaxial and plane strain curves are shown in the following chart.

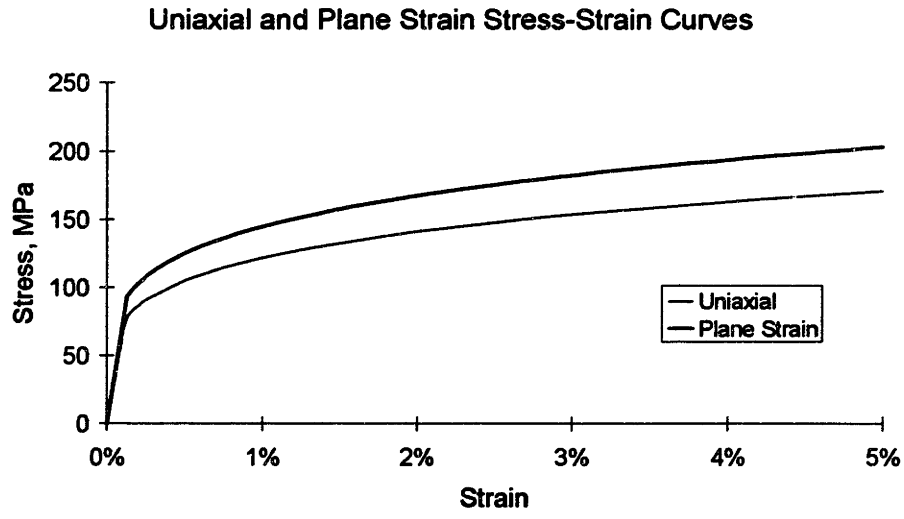

Figure 4.12 Uniaxial and plane strain stress-strain curves

Probably the most important thing to note about the change is that the material is effectively stronger under plane strain conditions than it is under uniaxial conditions.

Even though equivalent plane strain stress-strain curve parameters have been found, the original uniaxial parameters will generally continue to be used in this chapter for the sake of simplicity, since the qualitative behavior is more important than the quantitative.

Having gone through all the necessary preliminaries, the drape forming operation is now modeled.

4.5 MODELING DRAPE FORMING: BEND PLUS STRETCH

For the reader who is unfamiliar with the basic concepts of the mechanics of bending and springback, a brief introduction to bending and springback is given in Appendix 2. Most of what is written there can be found in basic mechanics texts. In this section, equations for predicting stresses, strains, forces, and springback for drape forming (bend plus stretch) are derived for the drape forming operation using the no initial plastic deformation (No IPD) strain hardening model.

4.5.1 Introduction

The stress curves in this chapter and the next have the orientation shown in the following diagram.

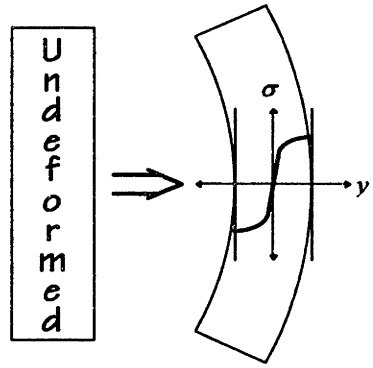

Figure 4.13 Stress as a function of distance from the midplane for pure bending

Stress, on the vertical axis, is shown as a function of distance from the midplane, on the horizontal axis. Thus, the bottom (or inside) of the part is at the left end of the diagram, while the top (or outside) of the part is at the right end.

The drape forming operation consists of two subsequent steps—bend and stretch. The bend is accomplished without significant stretching. The stage of the operation after the material has been bent is called the "initial" stage and is denoted by the subscript i. The initial stress distribution in a part that has been bent more than enough to cause initial plastic deformation is shown in the following diagram. The yield stress, σ_Y, and the distance from the midplane at which plastic yielding begins, y_Y, are indicated.

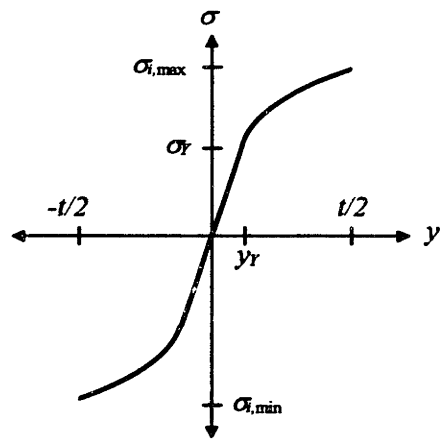

Figure 4.14 Stress as a function of distance from the midplane for pure bending

An important thing to note, as addressed in some detail in the Appendix 2, is that a significant moment exists within the part, which means that a significant amount of springback will result in order to reduce the moment.

To "set" the contour (to reduce springback), the bent part is stretched—this stretch is called the *post stretch*. The strain at the end of the post stretch stage, ε_I, is identified by the subscript I to indicate "intermediate strain." Calculation of the intermediate strain relies on the assumption that the stretch is uniform throughout the thickness (plane sections remain plane). Equations are now developed for the stress distribution and the springback ratio after the post stretch.

4.5.2 Development of equations with no initial plastic deformation

When the part is bent before any significant stretching occurs, the bending is likely cause some initial plastic deformation. This initial plastic deformation affects the development of stresses and strains in the part when it is post stretched. In some cases, when the material has a high yield strength and/or the die has a large radius of curvature, bending does not cause initial plastic deformation. Even though it is not correct, it can be assumed that the material does not initially plastically deform, in order to simplify the analytical equations. This is termed the no initial plastic deformation (No IPD) model or assumption. This is the common and simple approach assumed in nearly all textbooks when explaining stretch forming and why it is used. Derivation of the stress and springback equations according to the No IPD is now presented.

The following two diagrams show the path followed by an arbitrary point which undergoes plastic deformation first in compression as a result of bending and then in tension as a result of the post stretch. This point may be, for example, on the inner surface of the part as shown in Figure 4.14. The point moves along the stress-strain curve first to initial compressive plastic deformation, starting at the solid circle and ending at the **X**, as shown in the following diagram.

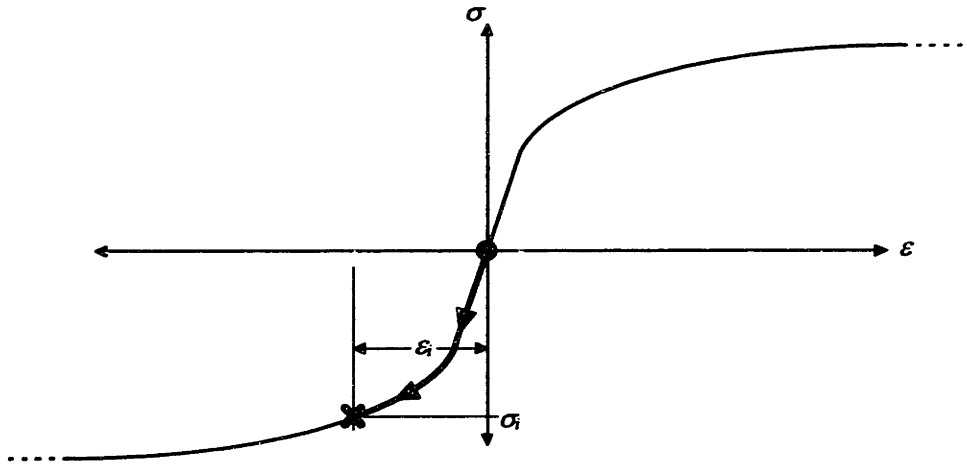

Figure 4.15 Development of stress and strain for a point on the inside of the material undergoing initial compressive plastic deformation as a result of bending

When the post stretch is added (ε_T is the post stretch strain), the stresses and strains move to the intermediate stage as shown in the second chart, again starting at the solid circle and moving to the **X**.

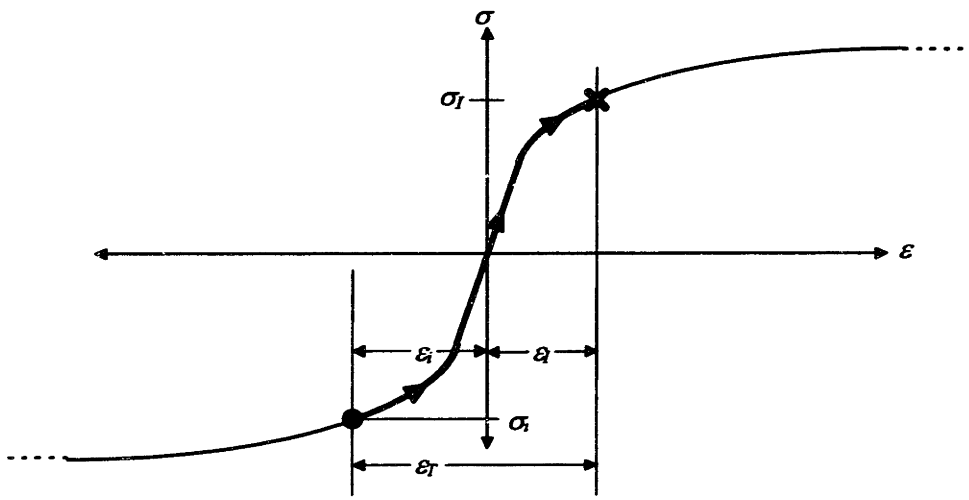

Figure 4.16 Development of stress and strain for a point on the inside of the material from post stretch after bending into compressive plastic deformation; No IPD model

Based on the above diagrams, the intermediate stress distribution is given by

$$\sigma_I = \begin{cases} -K|\varepsilon_I|^n = -K\left(\left|\frac{y}{R_i}+\varepsilon_T\right|\right)^n & \text{for } \varepsilon_I \le -\sigma_Y/E \\ E\varepsilon_I = E\left(\frac{y}{R_i}+\varepsilon_T\right) & \text{for } -\sigma_Y/E < \varepsilon_I < \sigma_Y/E \\ K\varepsilon_I{}^n = K\left(\frac{y}{R_i}+\varepsilon_T\right)^n & \text{for } \varepsilon_I \ge \sigma_Y/E \end{cases}, \tag{4.6}$$

If the post stretch strain, ε_T, is large enough that all of the intermediate stresses are tensile plastic, the intermediate stress distribution is given by

$$\sigma_I = K\varepsilon_I{}^n = K\left(\frac{y}{R_i}+\varepsilon_T\right)^n. \tag{4.7}$$

In order to simplify calculations and develop an analytical equation to predict springback, it is assumed that the post stretch is adequate to pull all the material into tensile plastic deformation. This is accomplished with less than 0.5% strain, and nearly all post stretch strains are greater than 1.0%, so the assumption is generally valid.

Calculation of moment and force

When the post stretch is large enough that all of the intermediate stress is tensile plastic, the intermediate moment is given by

$$M_I = \int_{-t/2}^{t/2} y\sigma_I dA = \int_{-t/2}^{t/2} yK\varepsilon_I{}^n w dy = \int_{-t/2}^{t/2} yK\left(\frac{y}{R_i}+\varepsilon_T\right)^n w dy. \tag{4.8}$$

Integration by parts,

$$\int u dv = uv - \int v du, \tag{4.9}$$

in which

$$u = y; \quad dv = \left(\frac{y}{R_i}+\varepsilon_T\right)^n dy; \quad du = dy; \quad v = \frac{R_i}{n+1}\left(\frac{y}{R_i}+\varepsilon_T\right)^{n+1}, \tag{4.10}$$

leads to

$$M_I = Kw\left[\frac{yR_i}{n+1}\left(\frac{y}{R_i}+\varepsilon_T\right)^{n+1}\Bigg|_{-t/2}^{t/2} - \int_{-t/2}^{t/2}\frac{R_i}{n+1}\left(\frac{y}{R_i}+\varepsilon_T\right)^{n+1}dy\right]$$

$$= Kw\left[\frac{yR_i}{n+1}\left(\frac{y}{R_i}+\varepsilon_T\right)^{n+1} - \frac{R_i^2}{(n+1)(n+2)}\left(\frac{y}{R_i}+\varepsilon_T\right)^{n+2}\Bigg|_{-t/2}^{t/2}\right], \qquad (4.11)$$

$$= \frac{KwR_i}{(n+1)}\left[y\left(\frac{y}{R_i}+\varepsilon_T\right)^{n+1} - \frac{R_i}{(n+2)}\left(\frac{y}{R_i}+\varepsilon_T\right)^{n+2}\Bigg|_{-t/2}^{t/2}\right]$$

which finally gives

$$M_I = \frac{KwR_i}{(n+1)}\left[t/2\left(\frac{t/2}{R_i}+\varepsilon_T\right)^{n+1} + t/2\left(\frac{-t/2}{R_i}+\varepsilon_T\right)^{n+1}\right.$$
$$\left. - \frac{R_i}{(n+2)}\left(\frac{t/2}{R_i}+\varepsilon_T\right)^{n+2} + \frac{R_i}{(n+2)}\left(\frac{-t/2}{R_i}+\varepsilon_T\right)^{n+2}\right]. \qquad (4.12)$$

The force on each end of the part required to achieve the intermediate tensile stress distribution is

$$F_I = \int_{-t/2}^{t/2}\sigma_I w dy = \int_{-t/2}^{t/2} K\varepsilon_I{}^n w dy$$
$$= \int_{-t/2}^{t/2} K\left(\frac{y}{R_i}+\varepsilon_T\right)^n w dy = \left[\frac{KwR_i}{n+1}\left(\frac{y}{R_i}+\varepsilon_T\right)^{n+1}\right]_{-t/2}^{t/2}, \qquad (4.13)$$

which gives

$$F_I = \frac{KwR_i}{n+1}\left[\left(\frac{t/2}{R_i}+\varepsilon_T\right)^{n+1} - \left(-\frac{t/2}{R_i}+\varepsilon_T\right)^{n+1}\right]. \qquad (4.14)$$

The force determined by this last equation is well approximated by using the post stretch strain to calculate an average stress according to $\sigma_T = K\varepsilon_T{}^n$, to give

$$F_I \approx wt\sigma_T = wtK\varepsilon_T{}^n. \qquad (4.15)$$

Determining springback

In order to determine the springback, the final moment M_f and the final force F_f are set to zero. This is accomplished by satisfying the following two integrals

$$M_f = \int_{-t/2}^{t/2} y\sigma_f dA = 0 \tag{4.16}$$

and

$$F_f = \int_{-t/2}^{t/2} \sigma_f dA = 0, \tag{4.17}$$

in which σ_f is the final stress distribution; it is given by

$$\sigma_f = \sigma_I + E\varepsilon_R + E\varepsilon_{SB}, \tag{4.18}$$

in which σ_I is the intermediate stress distribution (immediately after the post stretch and before release), ε_R, the relaxation strain, is the elastic strain recovery due to the release of the tensile force on the sheet (this will have a negative value), and ε_{SB} is the elastic strain induced by springback (a change in the radius of curvature). This equation holds when the combination of relaxation and springback strains causes only elastic deformation, which is always the case in drape forming.

The equation for σ_I is already known. ε_R is assumed to be uniform throughout the thickness of the material, and thus is independent of y. The springback strain, ε_{SB}, is given by

$$\varepsilon_{SB} = \frac{y}{R_i}\left(\frac{R_i}{R_f} - 1\right). \tag{4.19}$$

Combining the above into the final moment equation gives

$$\begin{aligned} 0 &= \int_{-t/2}^{t/2} y\left[K\varepsilon_I{}^n + E\varepsilon_R + E\varepsilon_{SB}\right]dA \\ &= \int_{-t/2}^{t/2} y\left[K\left(\frac{y}{R_i} + \varepsilon_T\right)^n + E\varepsilon_R + y\frac{E}{R_i}\left(\frac{R_i}{R_f} - 1\right)\right]wdy \end{aligned}, \tag{4.20}$$

which, rearranging, gives

$$\int_{-t/2}^{t/2} yK\left(\frac{y}{R_i} + \varepsilon_T\right)^n wdy = -\int_{-t/2}^{t/2} y\left[+E\varepsilon_R + y\frac{E}{R_i}\left(\frac{R_i}{R_f} - 1\right)\right]wdy. \tag{4.21}$$

The left hand side is the equation for the intermediate moment M_I, which has already been solved. Substituting M_I for the left hand side and integrating the right hand side gives

$$\begin{aligned} M_I &= -\int_{-t/2}^{t/2}\left[E\varepsilon_R y + y^2\frac{E}{R_i}\left(\frac{R_i}{R_f}-1\right)\right]w dy \\ &= -w\left[\frac{E\varepsilon_R y^2}{2} + y^3\frac{E}{3R_i}\left(\frac{R_i}{R_f}-1\right)\right]_{-t/2}^{t/2} \\ &= -\frac{2wE}{3R_i}\left(\frac{R_i}{R_f}-1\right)(t/2)^3 \end{aligned} \quad . \tag{4.22}$$

Due to symmetry, the elastic strain recovery, ε_R, drops out of the equation.

Rearranging gives

$$\frac{R_i}{R_f} = 1 - \frac{3M_I R_i}{2wE(t/2)^3} \quad . \tag{4.23}$$

Combined with the moment equation, this gives the springback ratio equation

$$\begin{aligned} \frac{R_i}{R_f} = 1 - \frac{3KR_i^2}{2E(n+1)(t/2)^3}\Bigg[&(t/2)\left(\frac{t/2}{R_i}+\varepsilon_T\right)^{n+1} + (t/2)\left(\frac{-t/2}{R_i}+\varepsilon_T\right)^{n+1} \\ &- \frac{R_i}{(n+2)}\left(\frac{t/2}{R_i}+\varepsilon_T\right)^{n+2} + \frac{R_i}{(n+2)}\left(\frac{-t/2}{R_i}+\varepsilon_T\right)^{n+2}\Bigg] \end{aligned} \quad . \tag{4.24}$$

The final force equilibrium equation is

$$F_f = 0 = \int_{-t/2}^{t/2}\sigma dA = \int_{-t/2}^{t/2}\sigma w dy = \int_{-t/2}^{t/2}\left[K\varepsilon_I{}^n + E\varepsilon_R + E\varepsilon_{SB}\right]dy \quad . \tag{4.25}$$

The width w can be dropped because it is a constant. Integrating gives

$$\begin{aligned} 0 &= \int_{-t/2}^{t/2}\left[K\varepsilon_I{}^n + E\varepsilon_R + E\varepsilon_{SB}\right]dy = \int_{-t/2}^{t/2}\left[K\left(\frac{y}{R_i}+\varepsilon_T\right) + E\varepsilon_R + Ey\left(\frac{1}{R_f}-\frac{1}{R_i}\right)\right]dy \\ &= \left[\frac{KR_i}{n+1}\left(\frac{y}{R_i}+\varepsilon_T\right)^{n+1} + E\varepsilon_R y + E\left(\frac{1}{R_f}-\frac{1}{R_i}\right)\frac{y^2}{2}\right]_{-t/2}^{t/2} \\ &= \frac{KR_i}{n+1}\left[\left(\frac{t/2}{R_i}+\varepsilon_T\right)^{n+1} - \left(\frac{-t/2}{R_i}+\varepsilon_T\right)^{n+1}\right] + 2E\varepsilon_R\, t/2 \end{aligned} \quad . \tag{4.26}$$

Due to symmetry, the springback terms fall out. Rearranging gives

$$\varepsilon_R = -\frac{KR_i}{2E(t/2)(n+1)}\left[\left(\frac{t/2}{R_i}+\varepsilon_T\right)^{n+1} - \left(\frac{-t/2}{R_i}+\varepsilon_T\right)^{n+1}\right] = -\frac{F_I}{wtE}, \tag{4.27}$$

the elastic strain recovery due to the release of the tensile force on the sheet. The elastic strain recovery is well approximated by $K\varepsilon_T^n/E$.

If the contour (radius of curvature) of the die varied or if friction had to be taken into account, the next step would be to integrate the results of the above equation integrate the above equation along the length of the part (this is done in Section 4.11). However, this analysis continues with the assumption of a cylindrical die and negligible friction. Thus, the final angle is simply given by

$$\theta_f = \theta_i \frac{R_i}{R_f}. \tag{4.28}$$

Final stress distribution

At this point, the final residual stress distribution in the part can be calculated. The final stress distribution is

$$\sigma_f = \sigma_I + E\varepsilon_R + E\varepsilon_{SB}. \tag{4.29}$$

Equations for σ_I, $E\varepsilon_R$, and $E\varepsilon_{SB}$ can be inserted to get the final stress distribution and are restated here. The intermediate stress is given by

$$\sigma_I = K\left(\frac{y}{R_i}+\varepsilon_T\right)^n, \tag{4.30}$$

the stress change due to elastic stretch recovery is given by

$$E\varepsilon_R = -\frac{KR_i}{2(t/2)(n+1)}\left[\left(\frac{t/2}{R_i}+\varepsilon_T\right)^{n+1} - \left(\frac{-t/2}{R_i}+\varepsilon_T\right)^{n+1}\right], \tag{4.31}$$

and the stress change due to springback is given by

$$\varepsilon_{SB} = \frac{y}{R_i}\left(\frac{R_i}{R_f}-1\right) \tag{4.32}$$

Example

The following series of charts demonstrates the effect of the post stretch. The standard parameters are used, and the post stretch strain ε_T is 0.50%. The horizontal axis

variable is y, the distance from the midplane, while the vertical axis is stress. The leftmost part of the chart represents the inside of the part, and the rightmost part of the chart represents the outside of the part (as shown by Figure 4.13). The first chart shows the stress distribution in the part from bending only.

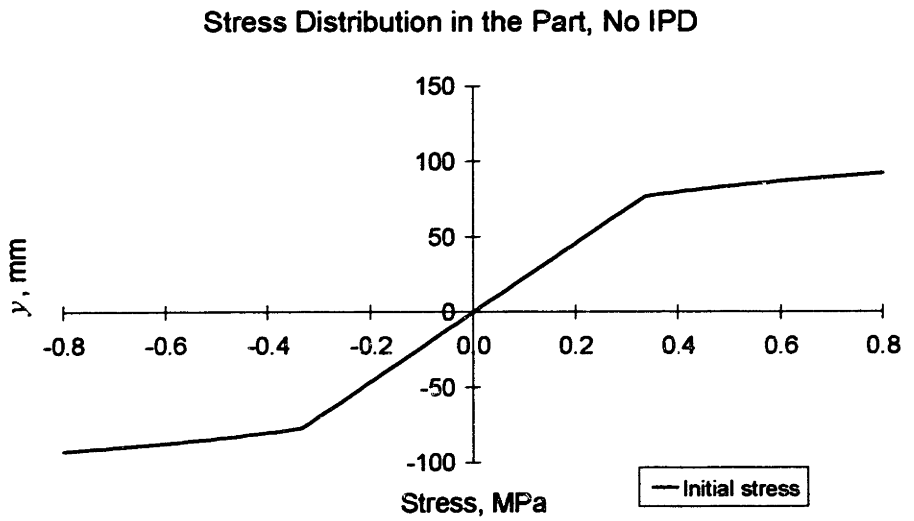

Figure 4.17 Initial stresses within a part; No IPD model; standard parameters; 0.5% post stretch

The intermediate stress distribution, at the end of post stretch, is added in the following chart and is shown by the long dashed line.

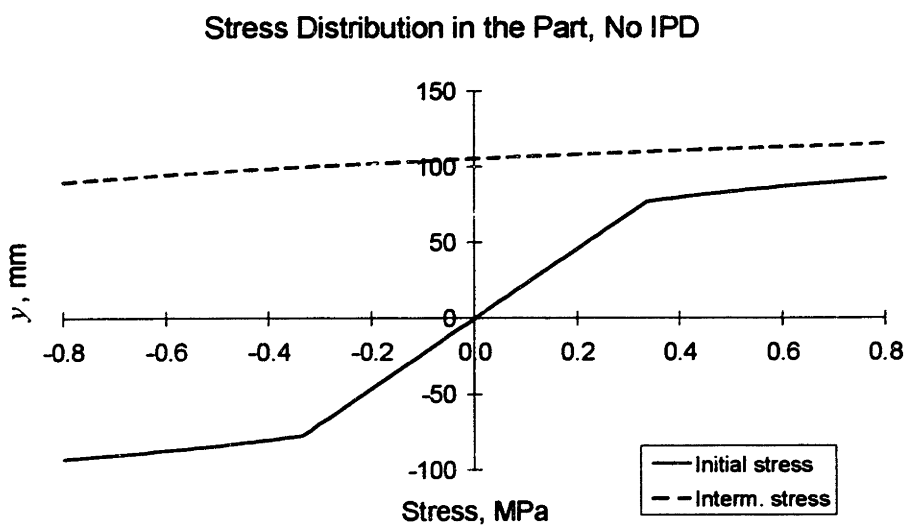

Figure 4.18 Initial and intermediate stresses within a part; No IPD model; standard parameters; 0.5% post stretch

After the part is released, it springs back and relaxes, to give the residual stress distribution added in the following chart. Because of its small magnitude, the residual stress distribution has been multiplied by a factor of 10; it is represented by the short dashed line. The change in stress due to springback is shown by the gray line.

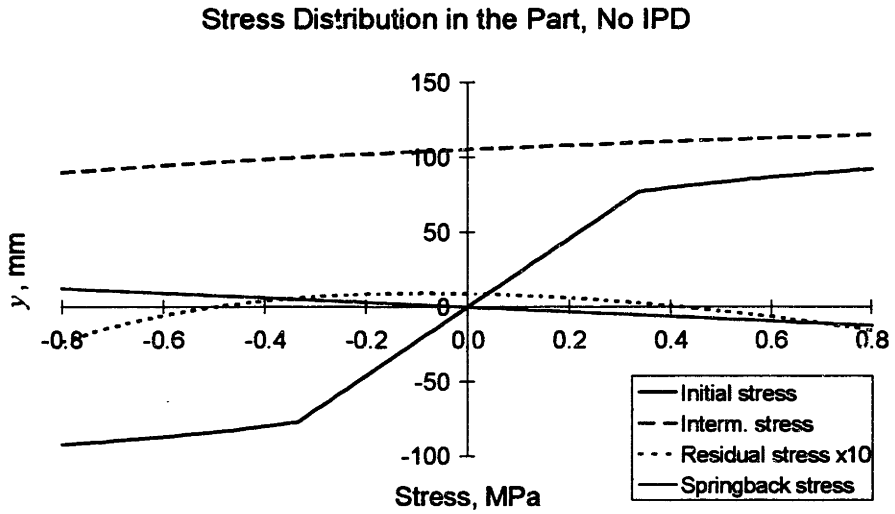

Figure 4.19 Initial, intermediate, springback, and residual stresses within a part; No IPD model; standard parameters; 0.5% post stretch

The springback ratio is R_i/R_f = 0.9328. If the initial angle of the bend θ_i were 90°, the final bend angle θ_f would be 83.95°. Without stretching, the springback ratio is R_i/R_f = 0.3437, and the final angle θ_f is 30.94°—this demonstrates the significant effect of the post stretch. Stresses are shown in the following chart.

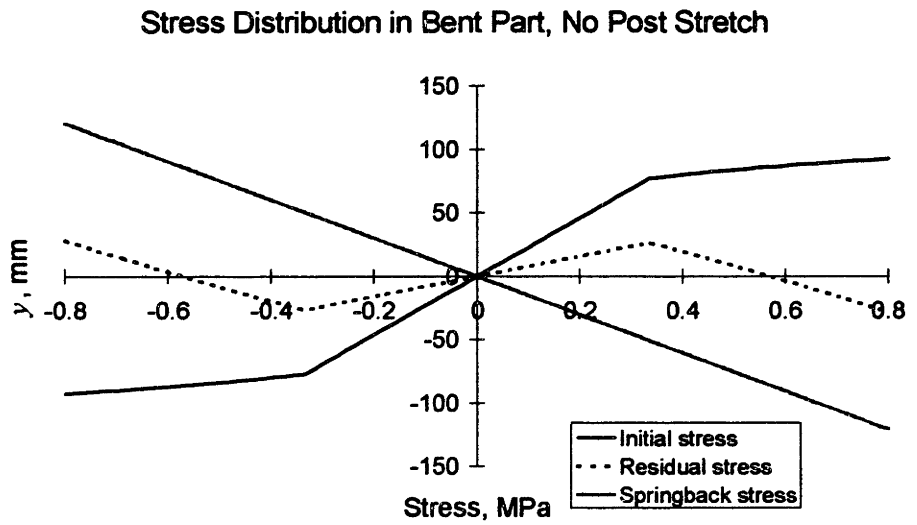

Figure 4.20 Initial, springback, and residual stresses within a part; standard parameters; no post stretch

Note that in the above chart the residual stresses are *not* multiplied by 10, and the springback stress is much greater than in the previous chart. Clearly, stretching significantly reduces the springback so that the operation produces a part with final geometry much closer to that of the die than the unstretched part. The following chart shows how the springback ratio changes as a function of the post stretch strain.

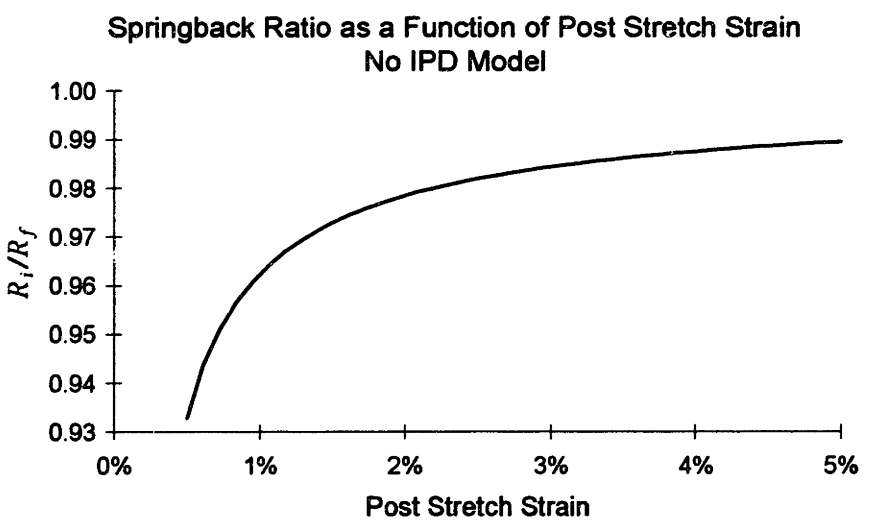

Figure 4.21 Springback ratio as a function of post stretch strain; No IPD model; standard parameters

The increase in springback ratio is significant at lower strains and decreases with increasing strain.

How stretching reduces springback

It is important to reiterate *how* the stretch reduces the springback. Stretching reduces springback by reducing the moment. In a strain hardening material, the moment is reduced as the part is stretched because the differences in stress through the part thickness decrease as strain increases. This is because of the decreasing slope of the stress-strain curve.

4.5.3 Approximation of integral with numerical summation

For the hardening models still to be developed, and for the No IPD model for any amount of post stretch strain, the integrals for the final moment and force cannot be solved analytically in the general case. The most practical means of overcoming this inability to perform integrals analytically is to approximate the integrals by numerical summation—that is, to calculate stresses at discrete intervals through the thickness of the part and to perform a summation of the force and moment at these points. Mathematically, these equations are written as

$$M_f = \sum_{-t/2}^{t/2} y\sigma_f \Delta A = \sum_{-t/2}^{t/2} y\left[K\varepsilon_I{}^n + E\varepsilon_R + E\varepsilon_{SB}\right]w\Delta y = 0 \qquad (4.33)$$

and

$$F_f = \sum_{-t/2}^{t/2} \sigma_f \Delta A = \sum_{-t/2}^{t/2}\left[K\varepsilon_I{}^n + E\varepsilon_R + E\varepsilon_{SB}\right]w\Delta y = 0\,. \qquad (4.34)$$

The above numerical summations were implemented in an Excel spreadsheet using 101 increments and a slight modification, that the stresses at the inside and outside of the part are given only 1/2 of their weight (this gives more accurate results).

Using the numerical summation method, the springback ratio can be determined in one of two ways. First, it can be determined by adjusting the springback ratio and relaxation strain so that both the final moment and force summations are equal to zero. This is done with relative ease with the solver function in Excel, and it is quite fast for purely elastic springback because in this case the springback ratio and relaxation force are independent of one-another. This independence was shown to hold for the no initial plastic deformation model, and always holds when there is no pre stretch (drape forming), or with pre stretch (stretch wrap forming) when the post stretch is large

enough to bring all of the part into plastic tensile deformation. The second and faster approach is to sum the intermediate moment and plug it into the following equation

$$\frac{R_i}{R_f} = 1 - \frac{3M_I R_i}{2wE(t/2)^3}. \tag{4.35}$$

Similarly, the relaxation strain can be determined by adjusting the relaxation strain or by determining it from the summed force at the end of the post stretch, if everything that happens after the post stretch is elastic. The relaxation strain is then given by

$$\varepsilon_R = -\frac{F_I}{Etw}. \tag{4.36}$$

Implementation of both methods in the spreadsheet have shown the two methods to be equivalent to four significant figures. As well, implementation in the spreadsheet has shown that the analytical equations for the No IPD model give the same results as the summation, to four significant figures. Therefore, the numerical summation method has adequate resolution.[29]

Another advantage of the numerical summation method is that it is simple to plug in new equations in order to test the effect of different stress-strain equations, without having to attempt a different integral.

As the amount of plastic deformation increases, the No IPD assumption is less and less valid, and the equations developed above become less accurate. In order to better model what actually goes on in the material and to more accurately predict springback, other material strain hardening models must be used. Equations for three material models with varying levels of the Bauschinger effect are now developed.

4.6 MODELING DRAPE FORMING WITH DIFFERENT MATERIAL HARDENING MODELS

Equations for three material models are now developed: the Isotropic, Bauschinger, and Kinematic hardening models.

---

[29] Only at very low post stretch strains is there a difference, but this is attributed to the fact the analytical equation is unstable below very low strains (0.27%), and as it approaches this point, its numerical accuracy is poor. Therefore, it can be safely assumed that for the other models as well the numerical summation method gives a more than adequate approximation to the integral.

4.6.1 Development of equations with Isotropic model

In this sub-section, all the equations are developed for modeling what goes on in the material during the sheet metal stretch forming operation, according to the Isotropic hardening model. According to the Isotropic hardening model, the hardening that results from plastic deformation is isotropic in the sense that it is independent of the direction of the plastic deformation. The Isotropic hardening model is generally a good model for reverse bending of aluminum if it doesn't have much of a stress-strain history [Tozawa, 1978].

Determining the effective strain and stress

The initial compressive plastic deformation at the inside of the material makes the stress-strain equations more complex. If strain is increased in magnitude without a change in direction from the initial to the intermediate stage, the resulting *effective* strain is simply the sum of the original strain and the strain increment. However, if the direction of strain is changed and the original strain caused plastic deformation, an *effective* strain must be calculated which takes into account the initial hardening.

To understand how this is done, consider the material at the innermost surface, $y = -t/2$, which has undergone initial compressive plastic deformation. Its stress-strain path is shown in the following chart. As a positive strain from the post stretch is induced, the stress increases at the slope if E until it reaches a stress that is the positive value of the initial compressive stress. At this point, further strain causes the material to continue to strain harden as it would if there were additional negative strain imposed on the initial condition causing further plastic deformation, except that the stress is now positive. The effective strain in the intermediate stage for such material, ε_{eff}, is larger than the sum of the initial and imposed strains, $\varepsilon_i + \varepsilon_T$. The following diagram shows how the effective strain is calculated in this case. Note that the initial strain, ε_i, is a negative number in the region of the part below the midplane, and for this reason when shown in the diagram is given a negative sign to indicate a positive dimension. ε_T is the post stretch strain; ε_E and ε_P are the elastic and plastic portions thereof, respectively.

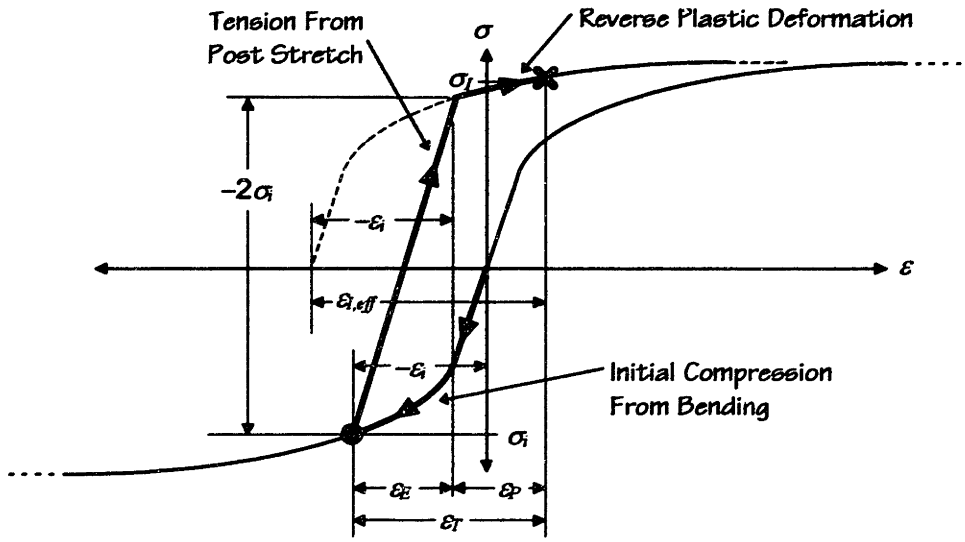

Figure 4.22 Evolution of stress and strain within a part; bend plus post stretch; isotropic model

As shown in the above diagram, the effective strain for that portion of the material which has undergone compressive plastic deformation and is brought into tensile plastic deformation is given by

$$\varepsilon_{I,eff} = -\varepsilon_i + \varepsilon_P = -\varepsilon_i + (\varepsilon_T - \varepsilon_E) = -\varepsilon_i + \left(\varepsilon_T + \frac{2\sigma_i}{E}\right), \tag{4.37}$$

in which

$$\varepsilon_T = \varepsilon_E + \varepsilon_P . \tag{4.38}$$

The effective strain for the portion of the material on the inside of the part subjected to initial plastic deformation and then stretched is given by

$$\varepsilon_{I,eff} = \begin{Bmatrix} \sigma_i/E + \varepsilon_T & \text{for} \quad \varepsilon_T < 2|\sigma_i|/E \\ -\varepsilon_i + \left(\varepsilon_T + \dfrac{2\sigma_i}{E}\right) & \text{for} \quad \varepsilon_T \geq 2|\sigma_i|/E \end{Bmatrix}, \tag{4.39}$$

For the rest of the material it is

$$\varepsilon_{I,eff} = \varepsilon_o + \varepsilon_T , \tag{4.40}$$

The intermediate stresses, then, are given by

$$\sigma_I = \begin{Bmatrix} E\varepsilon_{I,eff} & \text{for} \quad \sigma_i < -\sigma_Y \quad \text{and} \quad \varepsilon_T < 2|\sigma_i|/E \\ K\varepsilon_{I,eff}^{\,n} & \text{for} \quad \sigma_i < -\sigma_Y \quad \text{and} \quad \varepsilon_T \geq 2|\sigma_i|/E \\ E\varepsilon_{I,eff} & \text{for} \quad \sigma_i > -\sigma_Y \quad \text{and} \quad \varepsilon_{I,eff} < \sigma_Y/E \\ K\varepsilon_{I,eff}^{\,n} & \text{for} \quad \sigma_i > -\sigma_Y \quad \text{and} \quad \varepsilon_{I,eff} \geq \sigma_Y/E \end{Bmatrix}. \tag{4.41}$$

These equations are good for any amount of non-negative post stretch strain.

Determining springback and the residual stress distribution

The final stress state, as before, is given by

$$\sigma_f = \sigma_I + E\varepsilon_R + E\varepsilon_{SB}. \tag{4.42}$$

The intermediate stress, σ_I, is just above. Determination of the springback ratio and elastic recovery has already been discussed.

Examples

The following chart shows the stresses for a stretch formed part using the Isotropic model, the standard parameters, and a post stretch of 0.5%.

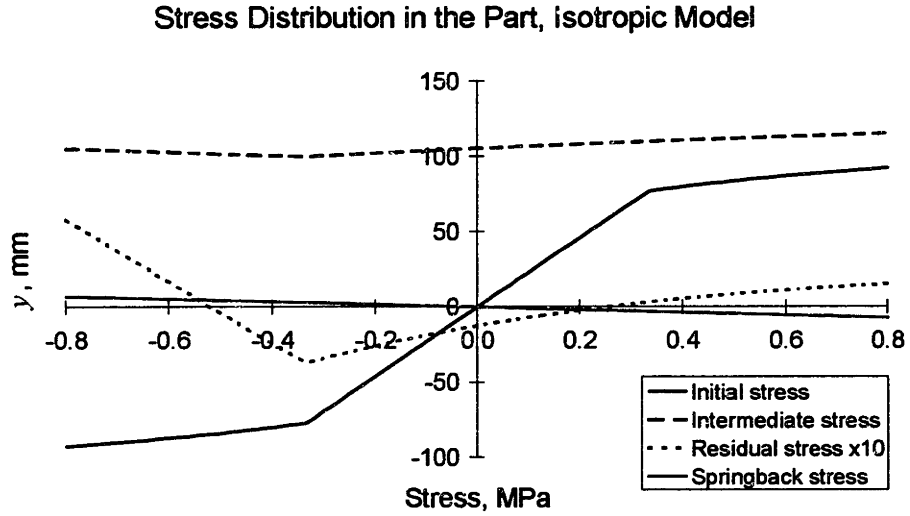

Figure 4.23 Initial, intermediate, springback, and residual stresses in a part; Isotropic model; standard parameters; post stretch strain = 0.5%

Note that the stress is not strictly increasing between the bottom and top. Because of plastic strain hardening in compression, the actual intermediate stress distribution exhibits a dip towards the middle of the part because the middle of the part did not experience the strain hardening that the bottom of the part experienced. The next chart shows the results for the same material parameters, with the post stretch increased from 0.50% to 5.00%. Notice that the intermediate and residual stresses are now nearly constant.

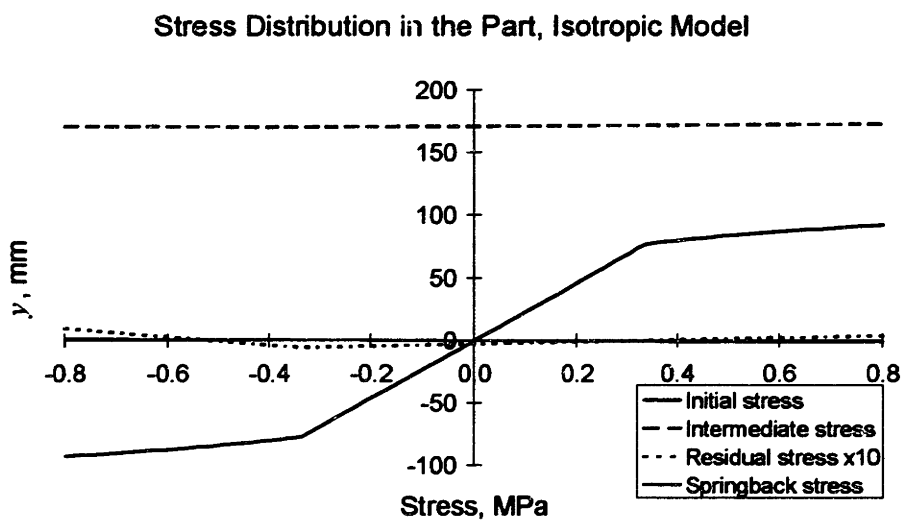

Figure 4.24 Initial, intermediate, springback, and residual stresses in a part; Isotropic model; standard parameters; post stretch strain = 5.0%

The increase of post stretch strain from 0.5% to 5.0% increased the springback ratio from 0.9613 to 0.9932.

Next, the equations for the Kinematic hardening model are developed.

4.6.2 Development of drape forming equations with the Kinematic model

Determining the effective strain and stress

In the Kinematic hardening model, when material goes into compressive plastic deformation and then into tensile plastic deformation, the stress at which the tensile plastic deformation begins is $2\sigma_Y$ above the compressive stress. It then continues in tension along the stress-strain curve starting at the same slope at which it left off in compression. While this is not exactly what happens—a more gentle entry into plastic deformation would probably occur—taking this into account either results in a discontinuity or is too complicated to model mathematically; so for the sake of continuity and ease, the model is as stated. The stress and strain progression for a point on the inside of the part which undergoes first plastic compression and then plastic tension are shown in the following diagram.

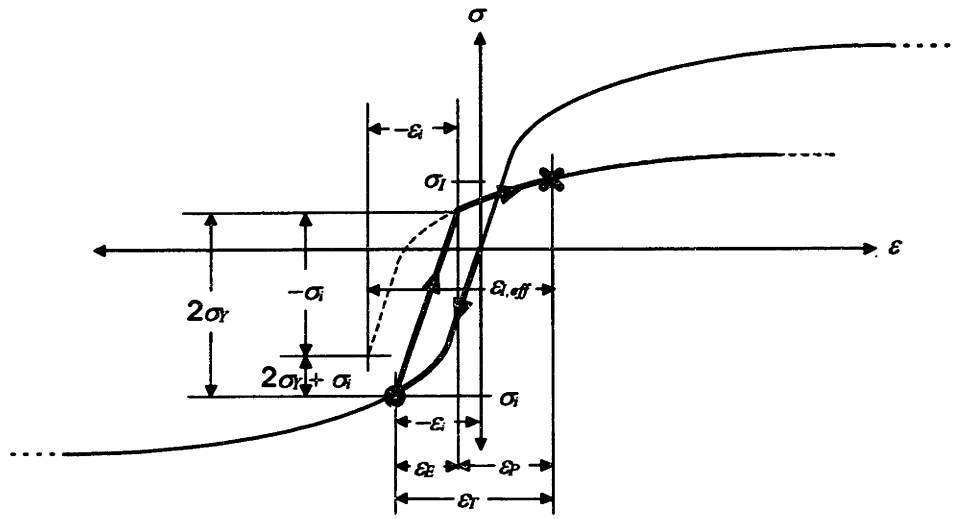

Figure 4.25 Development of stresses and strains within the part; Kinematic model

The above diagram shows that the effective strain for the portion of the material on the inside of the part subjected to initial plastic deformation, after post stretch, is given by

$$\varepsilon_{I,eff} = \begin{Bmatrix} \varepsilon_T & \text{for} \quad \varepsilon_T < 2\sigma_Y/E \\ -\varepsilon_i + \varepsilon_T - 2\sigma_Y/E & \text{for} \quad \varepsilon_T \geq 2\sigma_Y/E \end{Bmatrix}. \tag{4.43}$$

For the rest of the material,

$$\varepsilon_{I,eff} = \varepsilon_i + \varepsilon_T, \tag{4.44}$$

The intermediate stress distribution, then, are given by

$$\sigma_I = \begin{Bmatrix} \sigma_i + E\varepsilon_{I,eff} & \text{for} \quad \sigma_i < -\sigma_Y \quad \text{and} \quad \varepsilon_T < 2\sigma_Y/E \\ 2\sigma_i + 2\sigma_Y + K\varepsilon_{I,eff}{}^n & \text{for} \quad \sigma_i < -\sigma_Y \quad \text{and} \quad \varepsilon_T \geq 2\sigma_Y/E \\ E\varepsilon_{I,eff} & \text{for} \quad \sigma_i > -\sigma_Y \quad \text{and} \quad \varepsilon_{I,eff} < \sigma_Y/E \\ K\varepsilon_{I,eff}{}^n & \text{for} \quad \sigma_i > -\sigma_Y \quad \text{and} \quad \varepsilon_{I,eff} \geq \sigma_Y/E \end{Bmatrix}. \tag{4.45}$$

These equations are good for any amount of non-negative post stretch strain.

Examples

The following chart shows the initial, intermediate, and residual stresses within a part according to the Kinematic model, with the standard material parameters and a post stretch strain of ε_T = 0.5%.

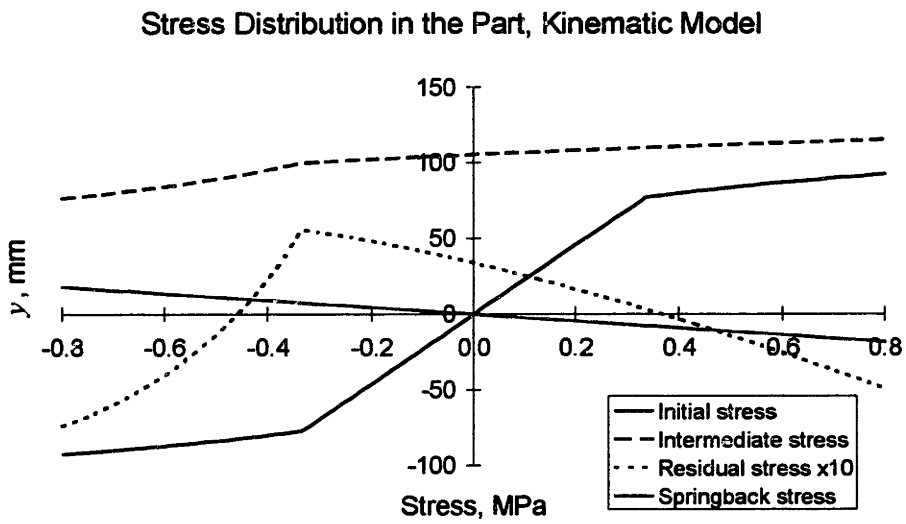

Figure 4.26 Initial, intermediate, residual, and springback stresses within a part; Kinematic model; standard parameters; post stretch strain = 0.5%

Note that the residual stress distribution is opposite in form to that given by the Isotropic hardening model. This is because with Isotropic model, initial compressive plastic deformation increases stresses after the material is brought into tensile plastic deformation, while with the Kinematic model the stresses are lower.

The springback ratio with the Kinematic model and 0.5% post stretch strain is R_i/R_f = 0.9008. When the post stretch strain is increased to 5.0%, the springback ratio is reduced to R_i/R_f = 0.9291. The stresses for 5.0% post stretch strain are shown in the following chart.

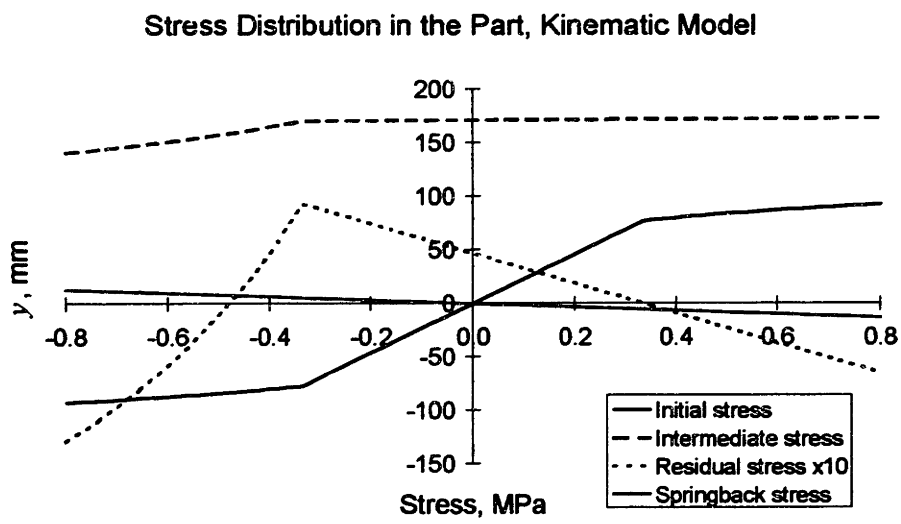

Figure 4.27 Initial, intermediate, residual, and springback stresses within a part; Kinematic model; standard parameters; post stretch strain = 5.0%

4.6.3 Development of equations with Bauschinger model

A middle case between the Isotropic and Kinematic models, termed the Bauschinger model, is now addressed. It is called the Bauschinger model because is models the Bauschinger effect, but not as severely as the Kinematic model.

Determining the effective strain and stress

In this model, the stress level at which plastic deformation begins in compression or tension is only affected by plastic deformation in that direction. Therefore, for example, if the material is first stretched to σ_o, and then compressed, compressive plastic deformation will begin at $-\sigma_Y$. If the part is then stretched, tensile plastic deformation will begin at σ_o. As with the Isotropic and Kinematic models (and for the reason already stated), it enters plastic deformation in tension at the same slope at which it was when undergoing plastic deformation in compression. The stress and strain path for a point on the inner surface of a stretch formed part first undergoing initial compressive plastic deformation due to bending and then undergoing tensile plastic deformation due to stretching is shown in the following diagram.

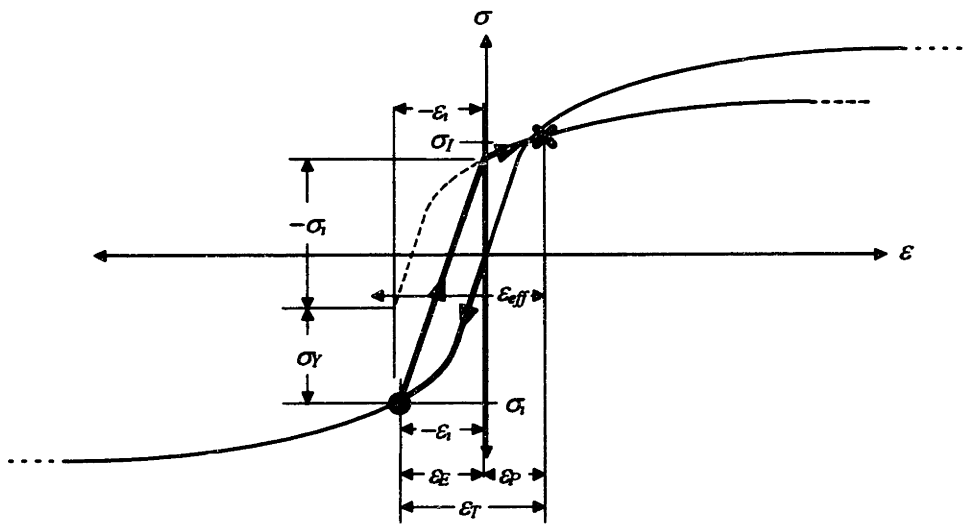

Figure 4.28 Development of stresses and strains within part; Bauschinger model

The above diagram shows that the effective strain for the portion of the material on the inside of the part subjected to initial plastic deformation, after post stretch, is given by

$$\varepsilon_{I,eff} = \begin{cases} \varepsilon_T & \text{for } \varepsilon_T < (\sigma_Y - \sigma_i)/E \\ -\varepsilon_i + \varepsilon_T - (\sigma_Y - \sigma_i)/E & \text{for } \varepsilon_T \geq (\sigma_Y - \sigma_i)/E \end{cases}. \tag{4.46}$$

For the rest of the material,

$$\varepsilon_{I,eff} = \varepsilon_i + \varepsilon_T, \tag{4.47}$$

The intermediate stresses, then, are given by

$$\sigma_I = \begin{cases} \sigma_i + E\varepsilon_{I,eff} & \text{for } \sigma_i < -\sigma_Y \text{ and } \varepsilon_T < (\sigma_Y - \sigma_i)/E \\ \sigma_i + \sigma_Y + K\varepsilon_{I,eff}{}^n & \text{for } \sigma_i < -\sigma_Y \text{ and } \varepsilon_T \geq (\sigma_Y - \sigma_i)/E \\ E\varepsilon_{I,eff} & \text{for } \sigma_i > -\sigma_Y \text{ and } \varepsilon_{I,eff} < \sigma_Y/E \\ K\varepsilon_{I,eff}{}^n & \text{for } \sigma_i > -\sigma_Y \text{ and } \varepsilon_{I,eff} \geq \sigma_Y/E \end{cases}. \tag{4.48}$$

These equations are good for any amount of non-negative post stretch strain.

Examples

The following chart shows the initial, intermediate, residual, and springback stresses within a part according to the Bauschinger hardening model, with the same material parameters as used in the other models and with a post stretch strain of ε_T = 0.5%.

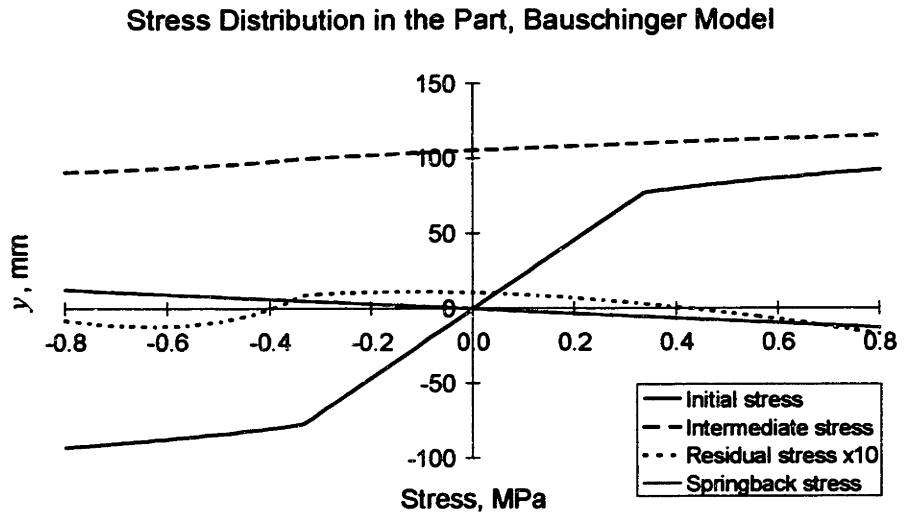

Figure 4.29 Initial, intermediate, residual, and springback stresses within a part; Bauschinger model; standard parameters; post stretch strain = 0.5%

In this case, the springback ratio is R_i / R_f = 0.9310. When the stretch is increased to 5.0%, the springback ratio becomes R_i / R_f = 0.9612. The stresses in this case are shown in the following diagram.

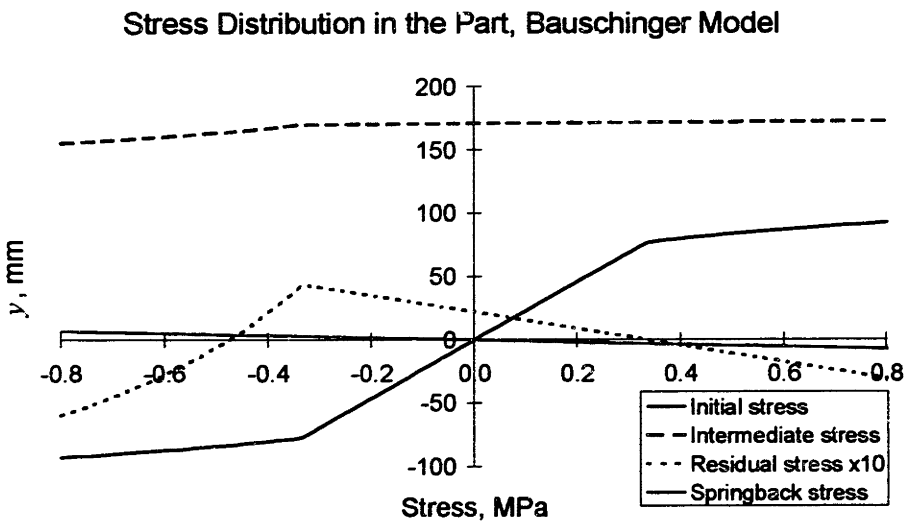

Figure 4.30 Initial, intermediate, residual, and springback stresses within a part; Bauschinger model; standard parameters; post stretch strain = 5.0%

Next, equations are developed to model the stretch wrap forming operation.

4.7 MODELING STRETCH WRAP FORMING

Some parts—mostly extrusions—are pre stretched before they are bent. In this operation, called stretch wrap forming, the part is pre stretched to a specified strain or force, the part is then wrapped (bent under constant force), after which a post stretch of a specified additional strain or force may be added.

As demonstrated in this section, pre stretching to a given force or strain and wrapping has a significant and somewhat unexpected effect on the stretch of the material: the material elongates somewhat during the wrap. This effect increases with increasing material thickness. The springback ratio is also affected: if the stretch is imposed before instead of after bending, springback increases significantly; however, if the part is pre stretched and post stretched, the springback goes back down.

4.7.1 Development of equations for pre stretch and constant force wrap

The derivations below are for a sheet, but, as shown later, they are easily modified to model extrusions as well.

Pre stretch

At the end of the pre stretch, the stress and strain are uniform throughout the part. The pre-stretch stress is:

$$\sigma_o = \begin{Bmatrix} E\varepsilon_o & \text{for } \varepsilon_o \le \sigma_Y / E \\ K{\varepsilon_o}^n & \text{for } \varepsilon_o > \sigma_Y / E \end{Bmatrix}, \tag{4.49}$$

in which ε_o is the pre stretch strain—the subscript o is used to denote the state of the material immediately after pre stretch. This is shown in the following diagram, for the case in which the pre stretch brings the material into tensile plastic deformation.

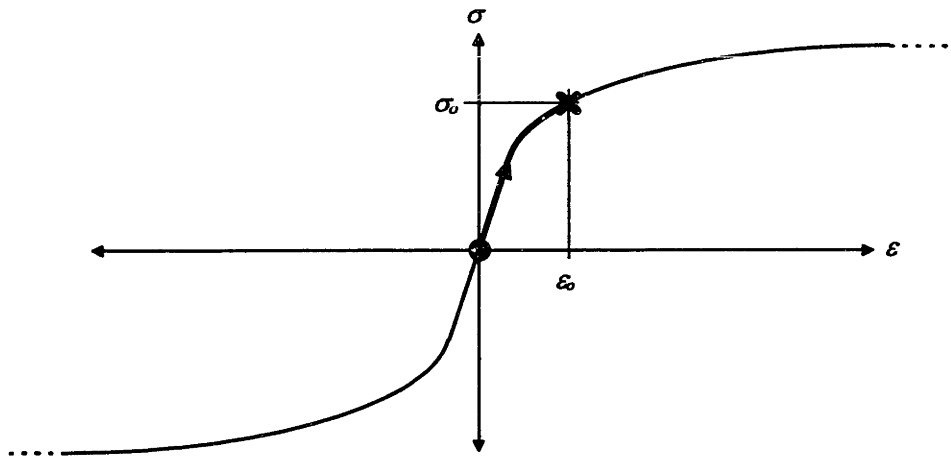

Figure 4.31 Development of stress and strain from pre stretch

The force required to accomplish the pre stretch is

$$F_o = tw\sigma_o, \tag{4.50}$$

in which t and w are the thickness and width of the sheet, respectively.

Wrap

At this point, the equations depend on the material model. The Isotropic model is the primary one developed. When the equations of other models differ from the Isotropic model equations, they are developed separately. The No IPD model is no longer considered because it no longer makes sense.

All models

Wrapping (bending the sheet at the constant pre stretch force) causes strains to increase on the outside of the part and to decrease on the inside of the part. The midplane is permitted to elongate. For all three models, if the pre stretch did *not* cause any plastic deformation, the stress distribution at the end of the wrap is given by

$$\sigma_i = \begin{Bmatrix} \text{A: } -K\left|\varepsilon_o + \varepsilon_B + \varepsilon_{ST}\right|^n & \text{for } \varepsilon_o + \varepsilon_B + \varepsilon_{ST} < -\sigma_Y/E \\ \text{B: } E\left(\varepsilon_o + \varepsilon_B + \varepsilon_{ST}\right) & \text{for } \left|\varepsilon_o + \varepsilon_B + \varepsilon_{ST}\right| < \sigma_Y/E \\ \text{C: } K\left(\varepsilon_o + \varepsilon_B + \varepsilon_{ST}\right)^n & \text{for } \varepsilon_o + \varepsilon_B + \varepsilon_{ST} > \sigma_Y/E \end{Bmatrix}, \tag{4.51}$$

in which ε_B is the strain induced by bending during the constant force wrap ($\varepsilon_B = y/R_i$), ε_{ST} is the elongation of the midplane due to wrapping, and σ_i is the initial stress at the end of the constant force wrap.

This stress distribution is shown in the following diagram. Note that in this and some of the following diagrams, the entire stress distribution within the part is being shown. In this case, the leftmost darkened portion of the stress-strain curve represents the inside of the part, and the rightmost portion represents the outside of the part. Further, in this case, the variable y is also shown as a horizontal axis label. The solid circle indicates the state of the material at the end of pre stretch. The hollow circle indicates the stress and strain state of the midplane at the end of the wrap.

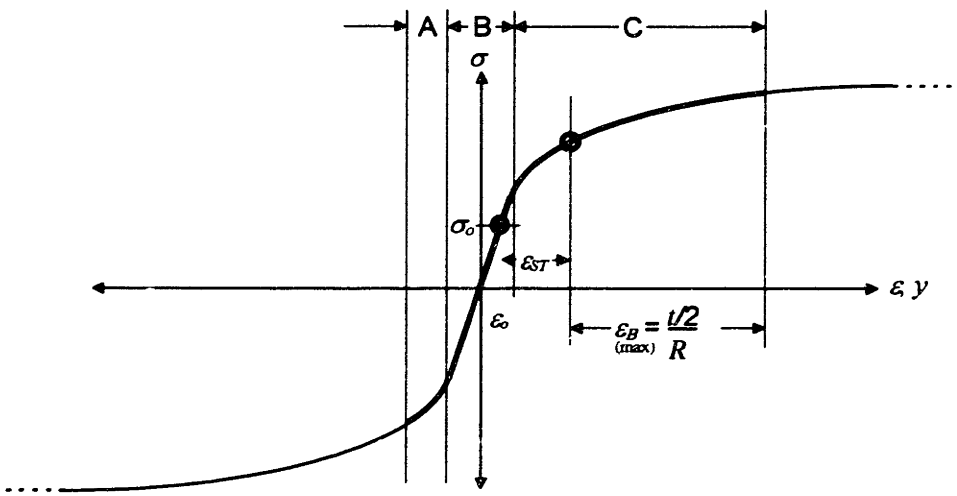

Figure 4.32 Development of stress and strain for wrap for the entire part; elastic pre stretch strain

The material can be divided up into three regions. In the first case, A, the material goes into compressive plastic deformation (on the inside); in the second case, B, the material is elastically compressed or stretched; in the third case, C, the material goes into tensile plastic deformation (on the outside).

Isotropic model

For the isotropic model, if the pre stretch *did* bring the part into plastic tensile deformation, then the stress distribution at the end of wrap is given by

$$\sigma_i = \begin{Bmatrix} \text{A:} & -K\left(\varepsilon_o - 2\sigma_o/E - \left(\varepsilon_B + \varepsilon_{ST}\right)\right)^n & \text{for } \varepsilon_B + \varepsilon_{ST} < -2\sigma_o/E \\ \text{B:} & E\left(\sigma_o/E + \varepsilon_B + \varepsilon_{ST}\right) & \text{for } -2\sigma_o/E < \varepsilon_B + \varepsilon_{ST} < 0 \\ \text{C:} & K\left(\varepsilon_o + \varepsilon_B + \varepsilon_{ST}\right)^n & \text{for } \varepsilon_B + \varepsilon_{ST} \geq 0 \end{Bmatrix}. \quad (4.52)$$

This is shown for the Isotropic model in the following diagram.

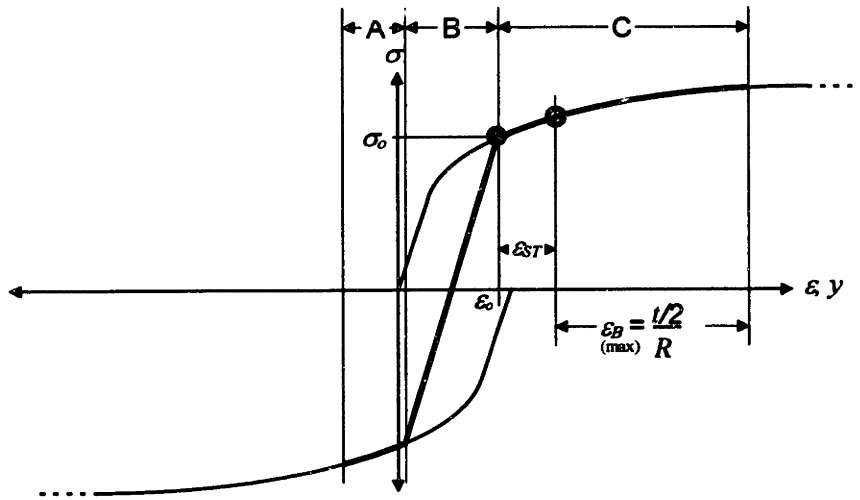

Figure 4.33 Development of stresses and strains in wrap; Isotropic model

In the first case, A, the material goes into compressive plastic deformation at the stress level that is the negative of the pre stretch stress; in the second case, B, the material is elastically compressed; in the third case, C, the material is stretched further, plastically in tension. Cases B and C always occur, while case A occurs only with thick sheet over small radii of curvature, or nearly always with extrusions.

Bauschinger model

For the Bauschinger model, if the pre stretch *did* bring the part into plastic deformation, the effective strain distribution at the end of wrap is given by

$$\varepsilon_{i,eff} = \begin{Bmatrix} \text{A: } \varepsilon_o - (\sigma_o + \sigma_Y)/E - (\varepsilon_B + \varepsilon_{ST}) & \text{for } \varepsilon_B + \varepsilon_{ST} < -(\sigma_o + \sigma_Y)/E \\ \text{B: } \varepsilon_B + \varepsilon_{ST} & \text{for } -(\sigma_o + \sigma_Y)/E < \varepsilon_B + \varepsilon_{ST} < 0 \\ \text{C: } \varepsilon_o + \varepsilon_B + \varepsilon_{ST} & \text{for } \varepsilon_B + \varepsilon_{ST} \geq 0 \end{Bmatrix}. \quad (4.53)$$

the stress distribution at the end of wrap is given by

$$\sigma_i = \begin{Bmatrix} \text{A: } \sigma_o - \sigma_Y - K(\varepsilon_{i,eff})^n & \text{for } \varepsilon_B + \varepsilon_{ST} < -(\sigma_o + \sigma_Y)/E \\ \text{B: } \sigma_o + E\varepsilon_{i,eff} & \text{for } -(\sigma_o + \sigma_Y)/E < \varepsilon_B + \varepsilon_{ST} < 0 \\ \text{C: } K(\varepsilon_{i,eff})^n & \text{for } \varepsilon_B + \varepsilon_{ST} \geq 0 \end{Bmatrix}. \quad (4.54)$$

This is shown for the Bauschinger model in the following diagram.

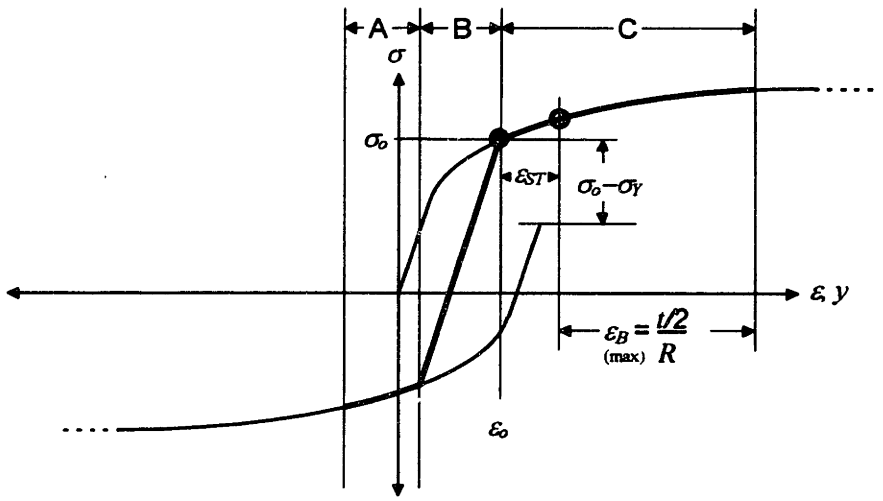

Figure 4.34 Development of stresses and strains, wrap; Bauschinger model

The primary difference from the Isotropic model is that the plastic deformation in compression now starts at a stress of $-\sigma_Y$.

Kinematic model

For the Kinematic model, if the pre stretch *did* bring the part into plastic deformation, the effective strain distribution at the end of wrap is given by

$$\varepsilon_{i,eff} = \begin{Bmatrix} \text{A: } \varepsilon_o - 2\sigma_Y/E - (\varepsilon_B + \varepsilon_{ST}) & \text{for } \varepsilon_B + \varepsilon_{ST} < -2\sigma_Y/E \\ \text{B: } \varepsilon_B + \varepsilon_{ST} & \text{for } -2\sigma_Y/E < \varepsilon_B + \varepsilon_{ST} < 0 \\ \text{C: } \varepsilon_o + \varepsilon_B + \varepsilon_{ST} & \text{for } \varepsilon_B + \varepsilon_{ST} \geq 0 \end{Bmatrix}. \qquad (4.55)$$

the stress distribution at the end of wrap is given by

$$\sigma_i = \begin{Bmatrix} \text{A: } 2\sigma_o - 2\sigma_Y - K(\varepsilon_{i,eff})^n & \text{for } \varepsilon_B + \varepsilon_{ST} < -2\sigma_Y/E \\ \text{B: } \sigma_o + E\varepsilon_{i,eff} & \text{for } -2\sigma_Y/E < \varepsilon_B + \varepsilon_{ST} < 0 \\ \text{C: } K(\varepsilon_{i,eff})^n & \text{for } \varepsilon_B + \varepsilon_{ST} \geq 0 \end{Bmatrix}. \qquad (4.56)$$

This is shown for the Kinematic model in the following diagram.

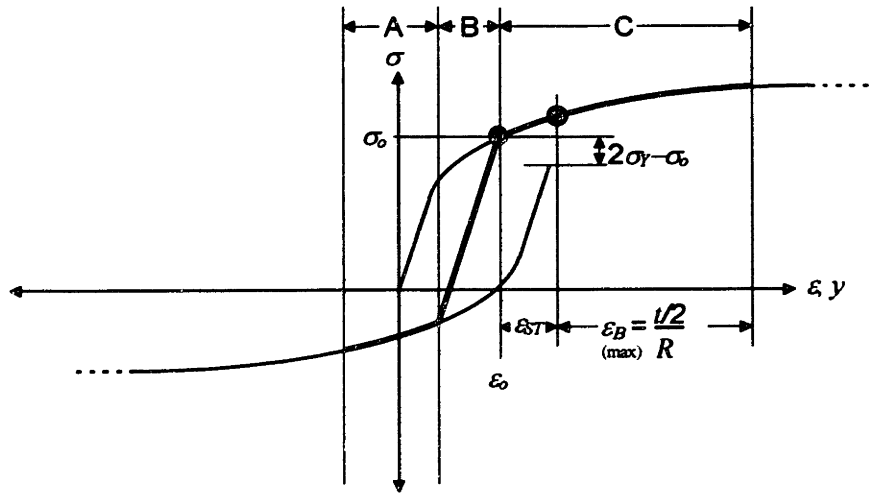

Figure 4.35 Development of stresses and strains for wrap; Kinematic model

The primary difference from the Isotropic model is that the plastic deformation in compression now starts at a stress of σ_o - $2\sigma_Y$.

Post stretch

If the part is given a post stretch, ε_T, the stress at the end of the post stretch but before relaxation (the intermediate stress) depends on the initial stress state (A, B, or C) and the amount of strain added, as given in the following set of equations, which work with both pre stretch conditions (stretched to less than or greater than plastic yielding).

Isotropic model, region A

For material initially in region A, the effective strain is given by

$$\varepsilon_{I,eff} = \begin{Bmatrix} \text{a: } \varepsilon_T & \text{for } \varepsilon_T < -2\sigma_i/E \\ \text{b: } \varepsilon_{i,eff} + 2\sigma_i/E + \varepsilon_T & \text{for } \varepsilon_T \geq -2\sigma_i/E \end{Bmatrix}. \tag{4.57}$$

The stress is given by

$$\sigma_I = \begin{Bmatrix} \text{a: } \sigma_i + E\varepsilon_{I,eff} & \text{for } \varepsilon_T < -2\sigma_i/E \\ \text{b: } K\varepsilon_{I,eff}{}^n & \text{for } \varepsilon_T \geq -2\sigma_i/E \end{Bmatrix}. \tag{4.58}$$

In this case, the material moves from an initial stress marked by a solid circle to a stress somewhere along the thick curve, such as the point indicated by the **X**. This is shown in the following diagram for a particular point initially in region A.

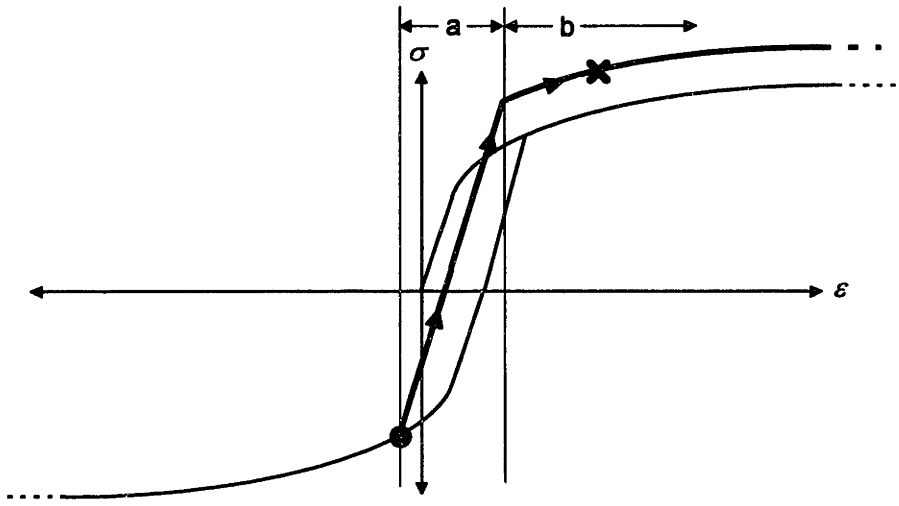

Figure 4.36 Development of stresses for post stretch; Isotropic model

For the point in region A, if the post stretch is not very large, the material will only be stretched elastically, and will lie somewhere along the thick line in region a; if the post stretch is large enough, the part will be brought into tensile plastic deformation, and will lie somewhere along the thick line in region b, with previous strain hardening contributing to the material strength.

Bauschinger model, region A

For material initially in region A, the effective strain is given by

$$\varepsilon_{I,eff} = \begin{cases} \text{a: } \varepsilon_T & \text{for } \varepsilon_T < (\sigma_o - \sigma_i)/E \\ \text{b: } \varepsilon_{i,eff} - (\sigma_o - \sigma_i)/E + \varepsilon_T & \text{for } \varepsilon_T \geq (\sigma_o - \sigma_i)/E \end{cases}. \tag{4.59}$$

The stress is given by

$$\sigma_I = \begin{cases} \text{a: } \sigma_i + E\varepsilon_{I,eff} & \text{for } \varepsilon_T < (\sigma_o - \sigma_i)/E \\ \text{b: } \sigma_o - K\varepsilon_{i,eff}{}^n + K\varepsilon_{I,eff}{}^n & \text{for } \varepsilon_T \geq (\sigma_o - \sigma_i)/E \end{cases}. \tag{4.60}$$

If the pre stretch did not bring the part into plastic deformation, σ_o is replaced by σ_Y.

This is shown for a particular point in region A, in the following diagram.

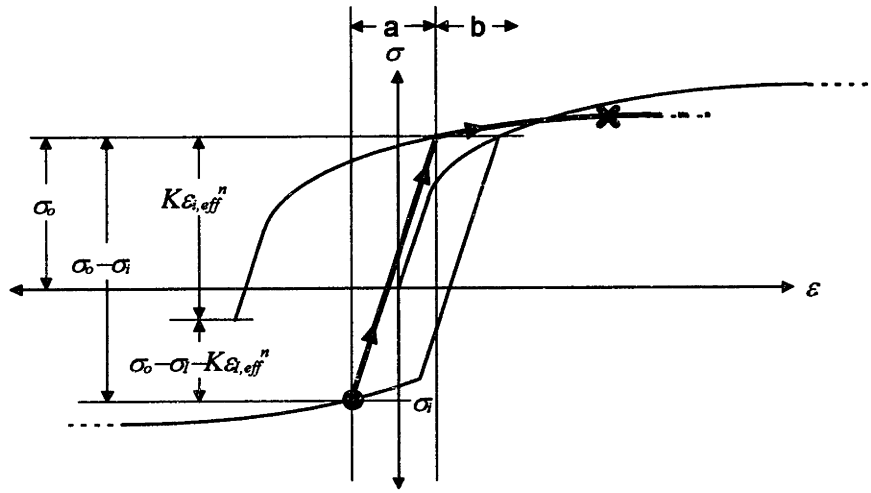

Figure 4.37 Development of stresses for post stretch; region A; Bauschinger

In this case, plastic deformation in tension begins at a stress of σ_o.

Kinematic model, region A

For material initially in region A, the effective strain is given by

$$\varepsilon_{I,eff} = \begin{cases} \text{a: } \varepsilon_T & \text{for } \varepsilon_T < 2\sigma_Y/E \\ \text{b: } \varepsilon_{i,eff} - 2\sigma_Y/E + \varepsilon_T & \text{for } \varepsilon_T \geq 2\sigma_Y/E \end{cases}. \tag{4.61}$$

The stress is given by

$$\sigma_I = \begin{cases} \text{a: } \sigma_i + E\varepsilon_{I,eff} & \text{for } \varepsilon_T < -2\sigma_Y/E \\ \text{b: } \sigma_i + 2\sigma_Y - K\varepsilon_{i,eff}{}^n + K\varepsilon_{I,eff}{}^n & \text{for } \varepsilon_T \geq -2\sigma_Y/E \end{cases}. \tag{4.62}$$

This is shown for a particular point in region A, in the following diagram.

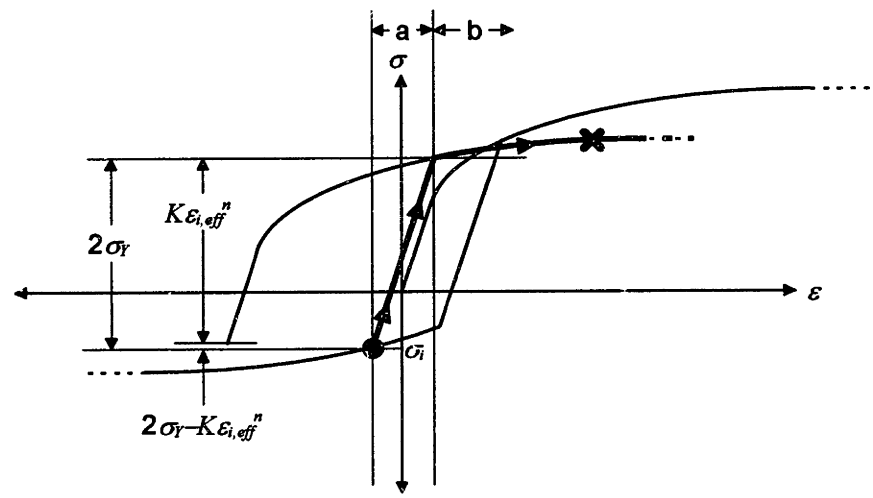

Figure 4.38 Development of stresses for post stretch; region A; Kinematic model

In this case, plastic deformation in tension begins at a stress of $\sigma_i + 2\sigma_Y$.

All models, region B

For material initially (at the end of wrap) in region B, in which the initial strain caused only elastic deformation,

$$\sigma_I = \begin{cases} \text{a: } \sigma_i + E\varepsilon_T & \text{for } \sigma_i + E\varepsilon_T < \sigma_o \\ \text{b: } K\left(\varepsilon_o + \varepsilon_B + \varepsilon_{ST} + \varepsilon_T\right)^n & \text{for } \sigma_i + E\varepsilon_T \geq \sigma_o \end{cases}. \tag{4.63}$$

This set of equations holds for all three material models. For material in which the pre stretch did not bring the part into plastic tensile deformation, σ_o is replaced by σ_Y.

This is shown for a particular point in region B, in the following diagram.

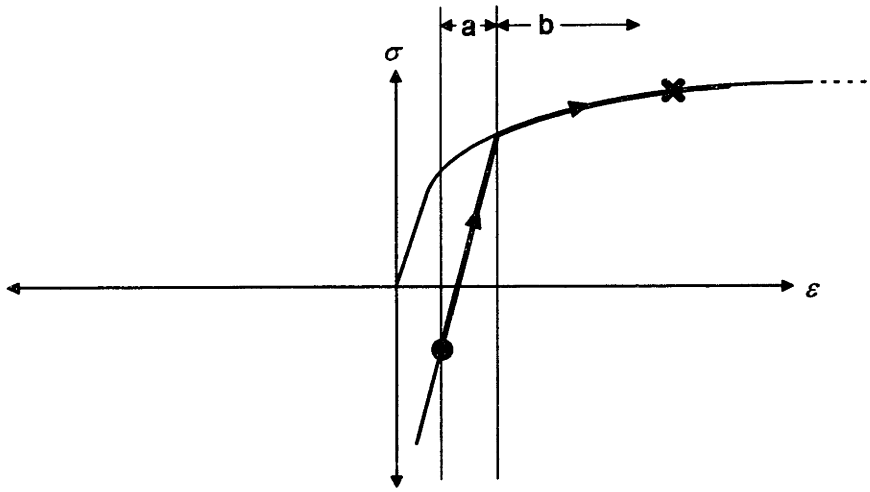

Figure 4.39 Development of stresses for post stretch; region B; all models

If the post stretch doesn't bring the point in region B to tensile plastic deformation, that point is only stretched elastically, and its stress lies somewhere along the thick line in region a; if the post stretch is large enough, that point is brought into tensile plastic deformation, and its stress somewhere along the thick line in region b, with previous strain hardening contributing to the material strength.

All models, region C

For material initially in region C, the intermediate stress is given by

$$\sigma_I = K\left(\varepsilon_o + \varepsilon_B + \varepsilon_{ST} + \varepsilon_T\right)^n. \tag{4.64}$$

This is shown for a particular point in region C, in the following diagram.

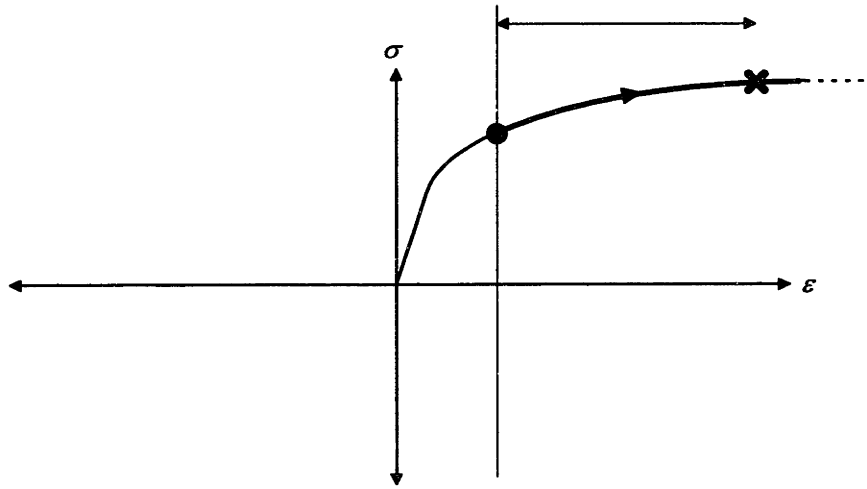

Figure 4.40 Development of stresses in part; region C; all models

Any amount of post stretch will simply move this portion of the material further to the right along the stress-strain curve.

Springback ratio and relaxation

In order to determine the residual stresses in the part and the springback ratio, the same equation for the final stress as before is used, namely,

$$\sigma_f = \sigma_I + E\varepsilon_R + E\varepsilon_{SB}, \tag{4.65}$$

and the springback ratio and relaxation strain are determined in the same manner as before. However, this equation assumes that the combination of relaxation and springback strains causes only elastic deformation.

In almost all extrusions and some rare cases of thick parts with pre stretch and little or no post stretch, the springback strain and relaxation strain combine to cause plastic deformation in compression on the inner side of the part as it relaxes. Therefore, the equations for this possibility are now derived.

Plastic compression on relaxation

The negative strain caused by the relaxation may cause some of the material in region b at the end of the post stretch to go into compressive plastic deformation. Material brought into tensile plastic deformation could not (practically) go into plastic compressive deformation, so in the following, consideration is only given to compressive plastic deformation of material in region b.

Material in region b at the end of post stretch was either in region A or in region B at the end of wrap. These two cases are now considered, without further diagrams.

For a point in region A at the end of wrap, compressive plastic deformation after relaxation and springback requires that

$$\varepsilon_R + \varepsilon_{SB} + \varepsilon_T < 0 . \tag{4.66}$$

The effective strain in this case is

$$\varepsilon_{f,eff} = \varepsilon_{I,eff} - \left(\varepsilon_R + \varepsilon_{SB} + \varepsilon_T\right). \tag{4.67}$$

The stress equations are the same as were used for the stress at the end of wrap for a point in region A, only that $\varepsilon_{f,eff}$ is substituted for $\varepsilon_{i,eff}$.

For a point in region B at the end of wrap, compressive plastic deformation after relaxation and springback requires that

$$\left\{\begin{array}{ll} \sigma_I + E\left(\varepsilon_R + \varepsilon_{SB} + \varepsilon_T\right) < -\sigma_o & \text{for the Isotropic model} \\ \sigma_I + E\left(\varepsilon_R + \varepsilon_{SB} + \varepsilon_T\right) < -\sigma_Y & \text{for the Bauschinger model} \\ \sigma_I + E\left(\varepsilon_R + \varepsilon_{SB} + \varepsilon_T\right) < \sigma_o - 2\sigma_Y & \text{for the Kinematic model} \end{array}\right\}. \tag{4.68}$$

For the case of no tensile plastic deformation from the pre stretch, $\sigma_o = \sigma_Y$. The effective strain is the same as it would be at the end of wrap for a point in region A, except that $\varepsilon_R + \varepsilon_{SB} + \varepsilon_T$ is used instead of $\varepsilon_B + \varepsilon_{ST}$. The effective stress is also the same as it would be at the end of wrap for a point in region A, with $\varepsilon_{f,eff}$ substituted for $\varepsilon_{i,eff}$.

It may sometimes happen that, due to the bottom of the yield surface moving up in the Kinematic model, material at the outside of the part may go plastic due to the combination of relaxation and springback strains. However, practically this does not make sense, so it is not included in this version of the Kinematic model.

When the possibility of plastic compressive deformation upon release of the material exists, the order of which strain change can be important. In the above, it is assumed that the relaxation and springback strains occur simultaneously, so that their sum is used to calculate stresses. In theory, it would be possible to allow the part to relax first and then spring back, or spring back first and then relax.

Example

Using the standard parameters (with noted changes), a few examples are now given in order to show the results of the above calculations. If the pre stretch is made at 70.0 kN, the pre stretch strain is 1.04%. As the pre stretched sheet is wrapped (bent around the die at constant force), the midplane elongates 0.19%. Finally, a post stretch of 1.40% (to 85.0 kN) brings the total stretch at the neutral axis to 2.63%. If there were

no post-stretch, the springback ratio would be R_i/R_f = 0.9075. With post-stretch, the springback ratio is increased to R_i/R_f = 0.9826.

The following chart shows the constant stress distribution in the part after pre stretch.

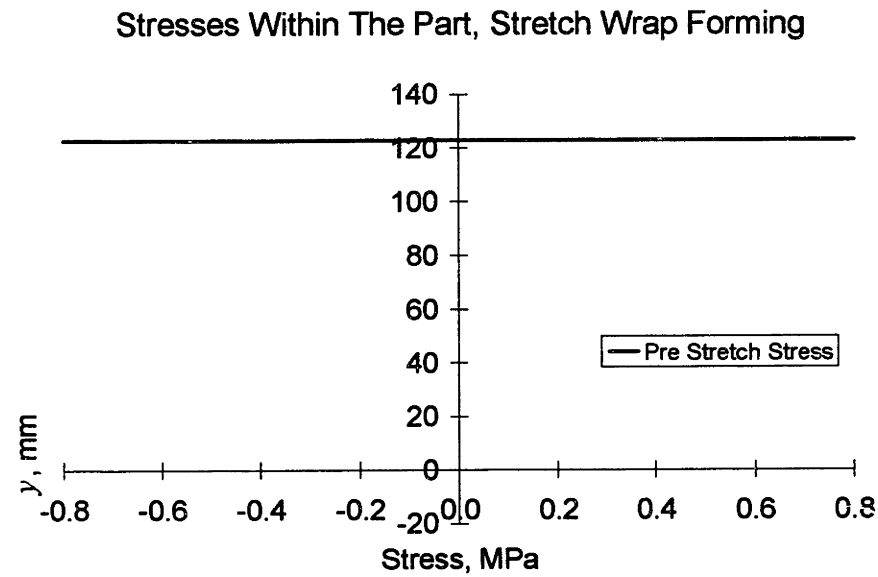

Figure 4.41 Pre stretch stress within part; standard parameters; 1.04% pre stretch strain (70kN pre stretch force)

In the next chart, the stress distribution after wrap is included.

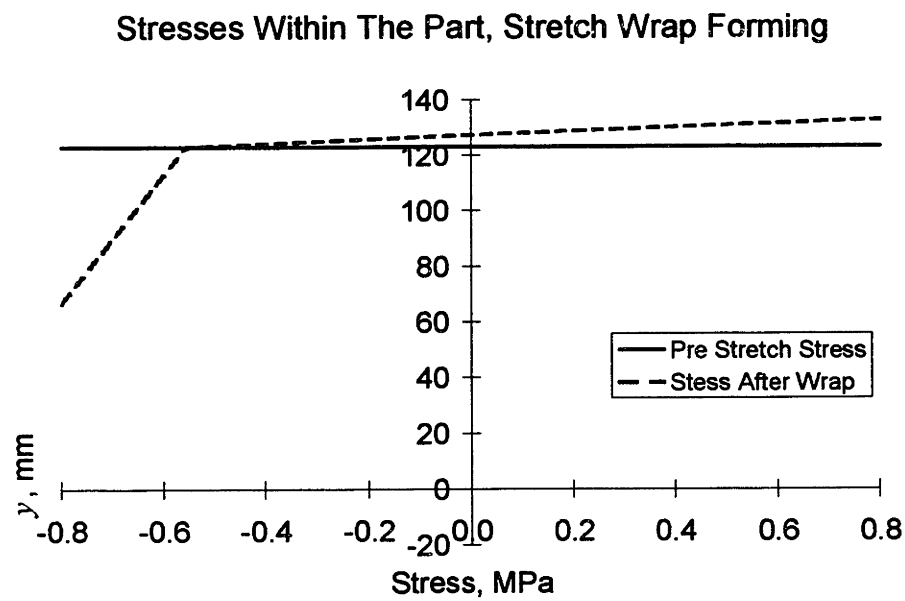

Figure 4.42 Pre stretch and wrap stresses within part; standard parameters; 1.04% pre stretch strain (70kN pre stretch force)

The stretch of the midplane as a result of wrapping under constant force is indicated by the fact that the stress at the midplane increases. In the next chart, the stress distribution obtained after post stretch is added.

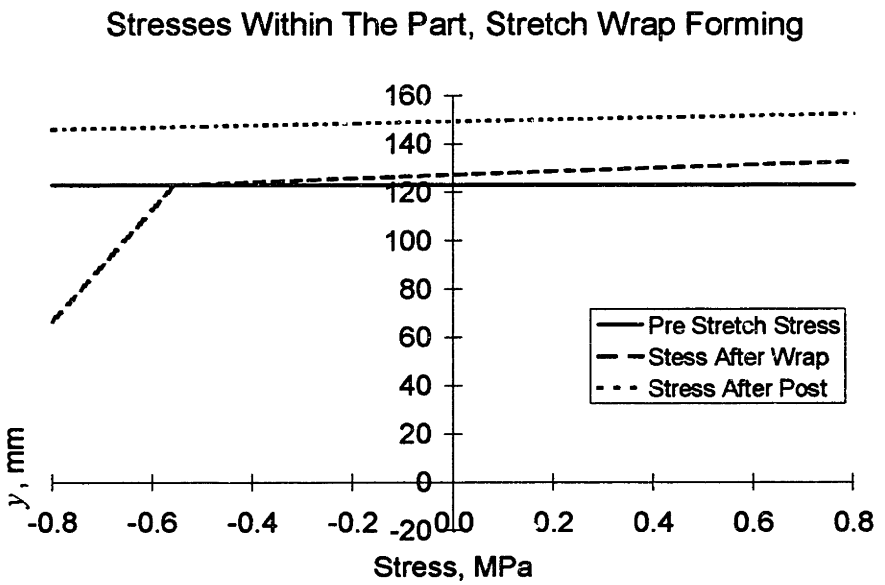

Figure 4.43 Pre stretch, wrap, and post stretch stresses within part; standard parameters; 1.04% pre stretch strain; 1.40% post stretch strain (85kN force)

Finally, the residual and springback stress distributions are added in the following chart. The springback stress is the change in stress due to springback. The change in stress from relaxation can be estimated from the average stress at the end of the post stretch.

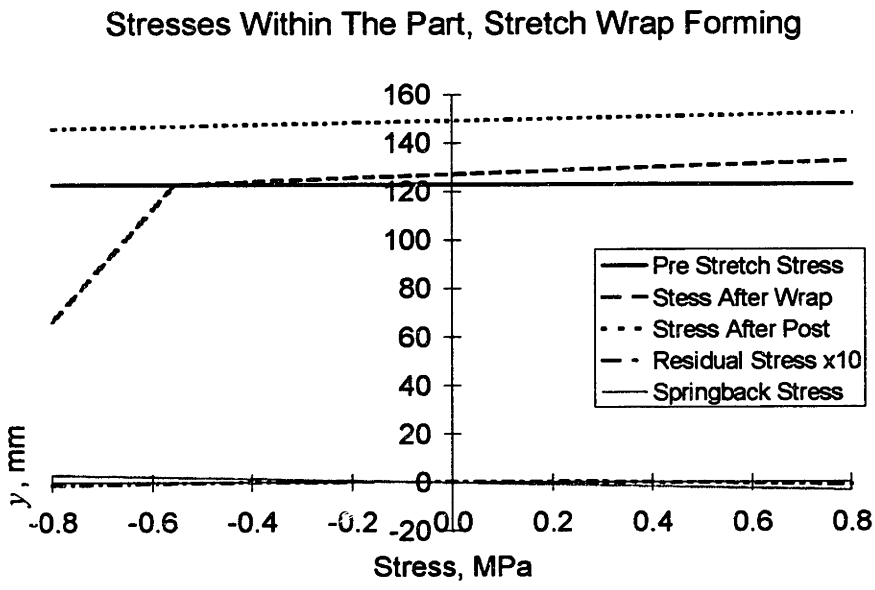

Figure 4.44 All stresses within part after release; standard parameters; pre stretch strain = 1.04%; post stretch strain = 1.40%

While the Isotropic model has been used, the result for the parameters and stretch profile used above is the same as that for the Bauschinger and Kinematic models since there is no initial compressive plastic deformation.

If the material thickness were increased and/or the radius of curvature were decreased, the effects of constant force stretch would be more pronounced, as shown in the following chart in which the radius of curvature is only 100 mm, and all other parameters the same. In this case, the midplane elongation from bending is 0.57% (with R_i = 300 mm, it was only 0.19%). The post stretch stain of 1.40% requires a post stretch force of 87.3 kN (instead of 85.0 kN) and achieves a total midplane stretch of 3.01%. The springback ratio just after pre stretch plus bend is R_i/R_f = 0.9201, while adding the post stretch increases it to R_i/R_f = 0.9843.

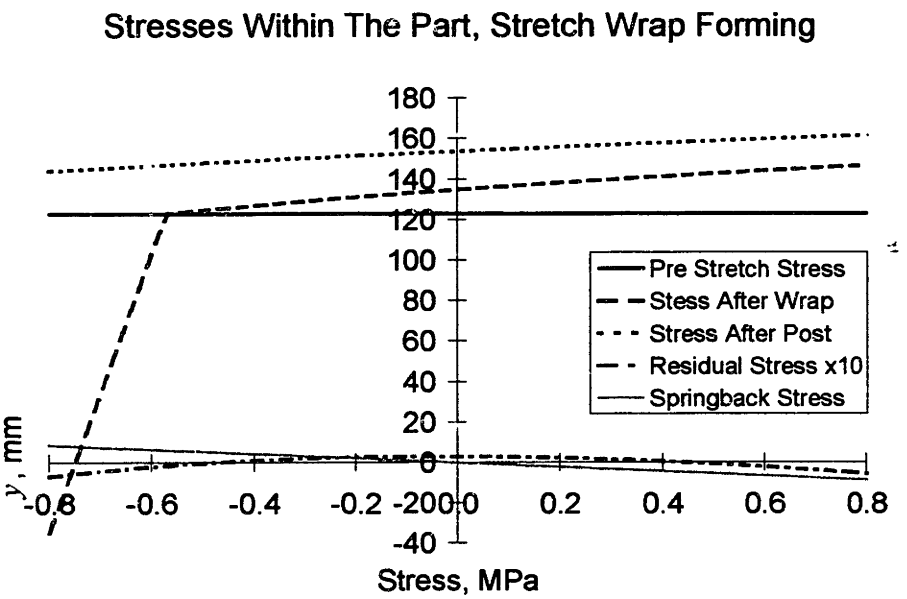

Figure 4.45 All stresses within the part; die radius of curvature = 100mm; pre stretch strain = 1.04%; post stretch strain = 1.40% (87.3 kN)

A smaller radius of curvature or a thicker part would cause compressive plastic deformation on the bottom (inside) of the part during the wrap (at this point the models would begin do diverge, starting with the Kinematic model). This is shown in the following two chart for the Isotropic model, with a die radius of only 30mm. In this case, the midplane elongation from wrap is 1.91%, the post stretch force needed to achieve 1.40% strain is 93.7kN, and the springback ratio after wrap is R_i/R_f = 0.9494, while after post stretch it is R_i/R_f = 0.9883.

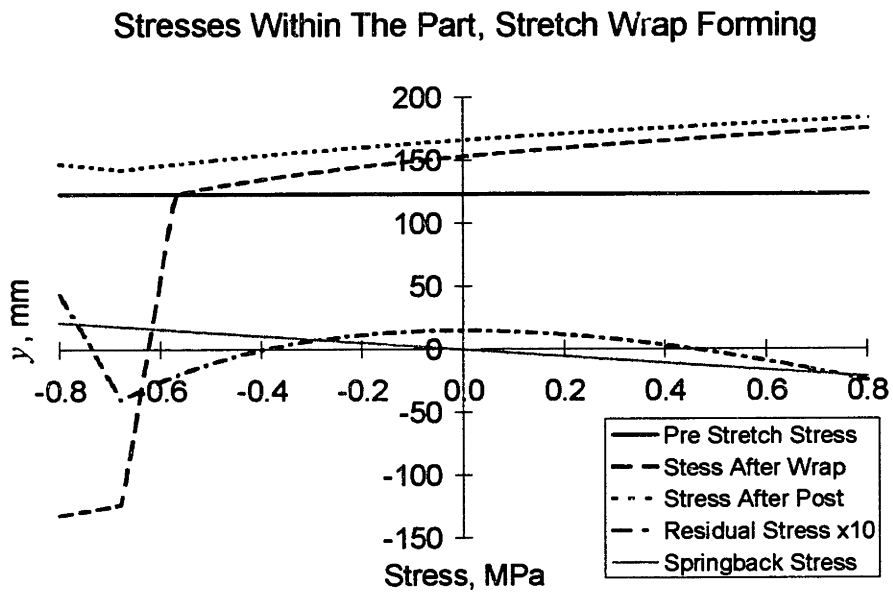

Figure 4.46 All stresses within the part; die radius of curvature = 30mm; pre stretch strain = 1.04%; post stretch strain = 1.40% (93.7 kN); Isotropic model

Summary and conclusions to modeling stretch wrap forming

The above equations in this section can be used to model the stretch wrap forming operation for any amount of pre stretch and any amount of post stretch. Thus, these models can be used to model drape forming by setting the pre stretch equal to zero. For most stretch wrap forming of sheet metal, the results for Isotropic, Kinematic, and Bauschinger models will be exactly the same since the wrap does not induce compressive plastic deformation, and their differences lie in what happens when plastic stresses are reversed. However, with extrusions, or when the part is thick enough or the die radius of curvature is small enough, compressive plastic deformation will occur.

4.8 MODELING CHEMICAL MILLING

In chemical milling, a layer of thickness t_{cm} is removed from the inside radius of the part after the part has been stretch formed. Because the removed material has a stress distribution different from that of the rest of the part, its removal affects springback.

Derivation of a single analytical equation for springback after chemical milling for the No IPD model is given in Appendix 4. Since a single equation is not possible for the other hardening models (because of the integral involved), a different approach is used for the Isotropic, Bauschinger, and Kinematic hardening models. To model the effect of chem mill with the other material models, and to permit any amount of post stretch, the

approach taken with the numerical summation method is actually quite simple: the increments of force and moment that fall in the portion of the material removed by the chemical milling are set to zero.[30] An iterative solution scheme is used to find the relaxation stress and springback ratio which result in zero final force and moment. The approach must be iterative because force and moment are no longer independent, as was demonstrated with the analytical solution in the appendix.

Examples

The following chart demonstrates the effect of chem milling a stretch formed part under the No IPD assumption. The standard parameters are used, and the post stretch is ε_T = 0.50%. Without chem mill, the springback ratio is R_i/R_f = 0.9328, and if the initial angle of the bend were 90°, the final bend angle θ_f would be 83.95°. When 0.20 mm is chem milled from the inside if the sheet, the springback ratio is R_i/R_f = 0.9372, and the final bend angle θ_f is 84.38°. This increases the bend angle 0.46%, but corresponds to a closing of the enclosed angle (the part "closing up"). The part closes up because material which is removed by the chem mill operation is in compression, and its removal allows the inside of the part to compress further. This is shown in the following chart. The residual stress distribution after chem mill is shown as solid dots.

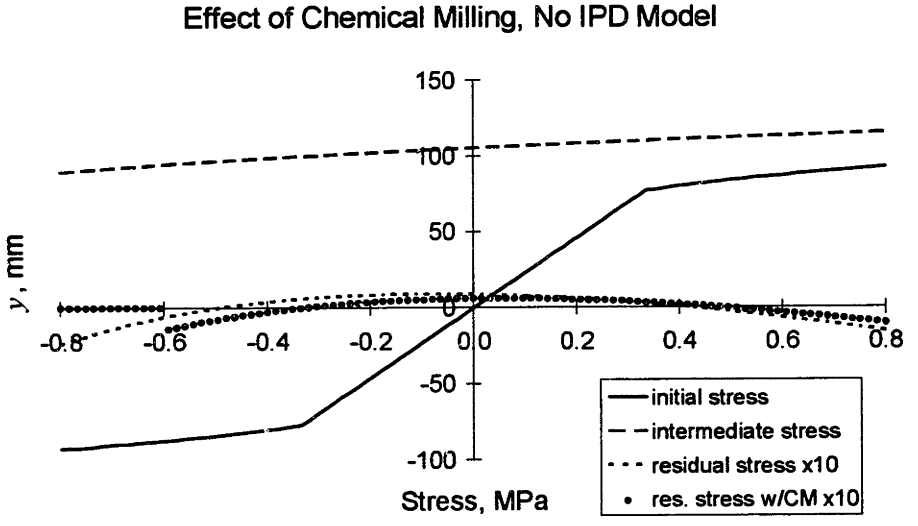

Figure 4.47 All stresses after chemical milling; drape forming; standard parameters; No IPD model; 0.5% post stretch strain, 0.2 mm removed

[30] This approach was suggested by professor Mary Boyce at MIT.

If the Isotropic model is used with everything else the same, the results turn out differently from the No IPD model. The Isotropic model predicts tensile residual stress at the inside of the part for this set of conditions, so the angle actually increases. The springback ratio before chem mill predicted by the Isotropic model is R_i/R_f = 0.9613, but after chem mill it is R_i/R_f = 0.9496. Hence, a final bend angle of 86.51° from springback after stretch forming decreases to a bend angle of 85.46° after chem mill. This is a change of 1.21%, a more significant change than for the No IPD model. Further, the change is in the opposite direction—the part opens up—because the portion of the material removed by chem mill was in tension. The following chart shows the residual stress distributions.

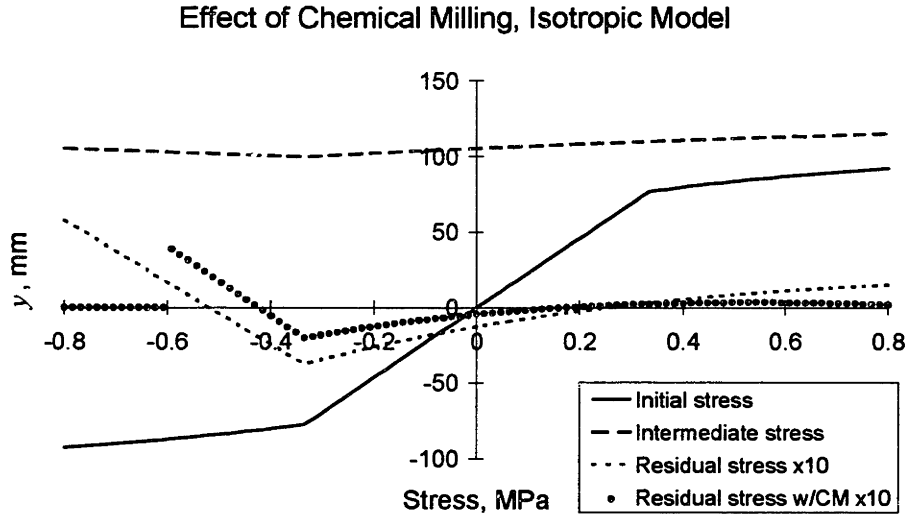

Figure 4.48 All stresses after chemical milling; drape forming; standard parameters; Isotropic model; 0.5% post stretch strain, 0.2 mm removed

These examples demonstrate the effect of the hardening model on change in contour from chem mill.

4.9 Modeling Stretch Wrap Forming of Extrusions

All of the above discretized equations are very easily extended to apply to a simple two-dimensional analysis of springback in extrusions as well. While the stress and strains that develop in extrusions as they are stretch formed can be quite complex, for the purposes of predicting springback and because the deformation of extrusions is not permitted to be out-of-plane (due to the die and clamps) it is possible to ignore things such as lateral movements and shear stresses that may develop at corners. Since

lateral movement of the cross-section are prohibited, even asymmetric (with respect to the y axis) cross-sections can be modeled for the purposes of predicting longitudinal stresses and strains, and springback.

To begin the extrusion stretch forming operation, the ends of the part are clamped in jaws and tension is applied to the part through the movement of the tension cylinders, to a pre-determined force or displacement. The arms on which the jaws are located are then rotated back simultaneously and the part is wrapped around the die under constant force (the tension cylinders extend during wrapping in order to achieve constant force). At a pre-determined wrap angle (of the arm), the part is given a post stretch either to a pre-determined displacement or to a pre-determined force.

Generic extrusion stretch forming cross-section geometry

The generic geometry shown in the following diagram is capable of modeling almost any simple extrusion cross-section: C, L, T, I, Z, U, +, H, and square.

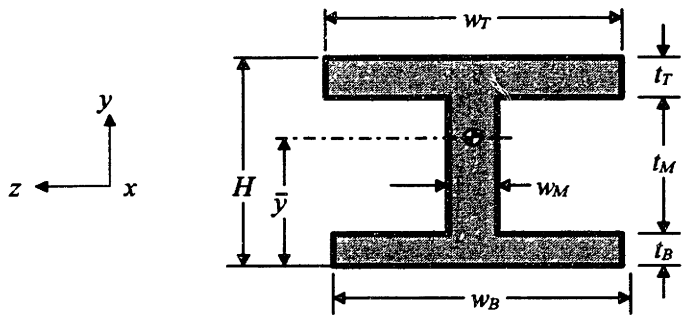

Figure 4.49 Extrusion cross-section geometry

Since the model is being used only to estimate longitudinal stresses and strains, the horizontal location of the parts of the cross-section is not important—only the total widths and heights. For a T cross-section part, t_B is set to zero.[31] For an H cross-section part, w_T is the sum of the widths of the legs above the middle bar, w_M is the total width of the middle bar plus legs, and w_B is the sum of the widths of the legs below the middle bar.

[31] And w_B is set equal to w_M because of how the spreadsheet equations are set up.

The midplane of an extrusion is located vertically at a distance $\bar{y}$ from the bottom of the part (this is also called the vertical location of the centroid of the cross-sectional area). For an extrusion with the dimensions shown above, $\bar{y}$ is given by

$$\bar{y} = \frac{\sum_i \bar{y}_i A_i}{\sum_i A_i} = \frac{\left(H - \frac{t_T}{2}\right)(t_T w_T) + \frac{t_B}{2}(t_B w_B) + \left(\frac{t_M}{2} + t_B\right) t_M w_M}{t_T w_T + t_B w_B + t_M w_M}. \tag{4.69}$$

Note that the denominator is the equation for the total cross-sectional area of the part.

For pure bending, and not allowing for a change in the length of the midplane, the strain is assumed to be linearly proportional to the distance from the midplane. That is,

$$\varepsilon = \frac{y}{R_i}, \tag{4.70}$$

in which y is measured from the midplane of the cross-section and R_i is the radius of curvature at the midplane. Often, the radius of curvature of the part R_i is specified at some distance from the midplane (for example, it may be defined at a distance t_T from the top of the part—a location which can be defined by the die). In this case, an adjustment needs to be made to the radius of curvature. Let H_R be defined as the distance from the bottom of the cross-section of the part to the location at which the radius of curvature of the die R_i is defined, and R_y be the radius of curvature at the midplane. The following equation is used to get from R_i to R_y

$$R_y = R_i - \Delta R = R_i - \left(H_R - \bar{y}\right). \tag{4.71}$$

These are shown in the following figure.

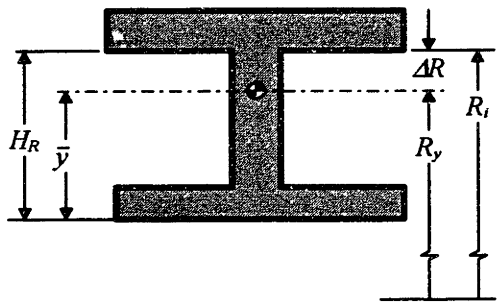

Figure 4.50 Radius of curvature adjustment for extrusions

At this point, the radius of curvature used for equations is R_y. Unless specifically mentioned, it is assumed that the radius of curvature is specified at the midplane of the part cross-section, so that $R_i = R_y$.

4.9.2 Adaptation of equations

While a single analytical equation is not achievable, it is possible, as before, to adapt the numerical summation approach to the changing cross-section width of an extrusion. All of the stress and strain equations are exactly the same for extrusions as they are for sheet metal, and the uniaxial tensile test material properties can be used. Only the incremental force and moment equations change because of the change in width of the parts. The incremental force is simply the stress for that increment times the incremental height times the width of that increment, and the width changes according to the vertical location in the part, and is given by the part geometry. The incremental moment is simply the incremental force multiplied by the distance from the midplane (in fact, the moment is independent of the location of the midplane).

Once the intermediate strains, stresses, forces, and moments are calculated, if the strains caused by springback and relaxation are entirely elastic (which is often the case), the springback ratio is given by

$$\frac{R_i}{R_f} = 1 - \frac{R_i M}{E I_{zz}}, \tag{4.72}$$

in which I_{zz} is the moment of inertia of the entire cross-section. Determination of the moment of inertia is shown in Appendix 5. When springback and relaxation cause plastic deformation after the part is released, ε_R and R_i/R_f must be adjusted to achieve zero final force and moment.

Example

One set of calculations is now made to show one possible result from the above equations. The part is an I cross-section with the geometry: H = 50 mm, $t_B = t_T$ = 5 mm (t_M = 40 mm), $w_B = w_T$ = 50 mm, w_M = 5 mm. The die radius of curvature is 500 mm. The part is given a pre stretch strain of 0.5% (which gives an initial force of 73.84 kN), and a post stretch strain of 3.0% (to a force of 108.1 kN). The springback ratio is R_i/R_f = 0.9922.

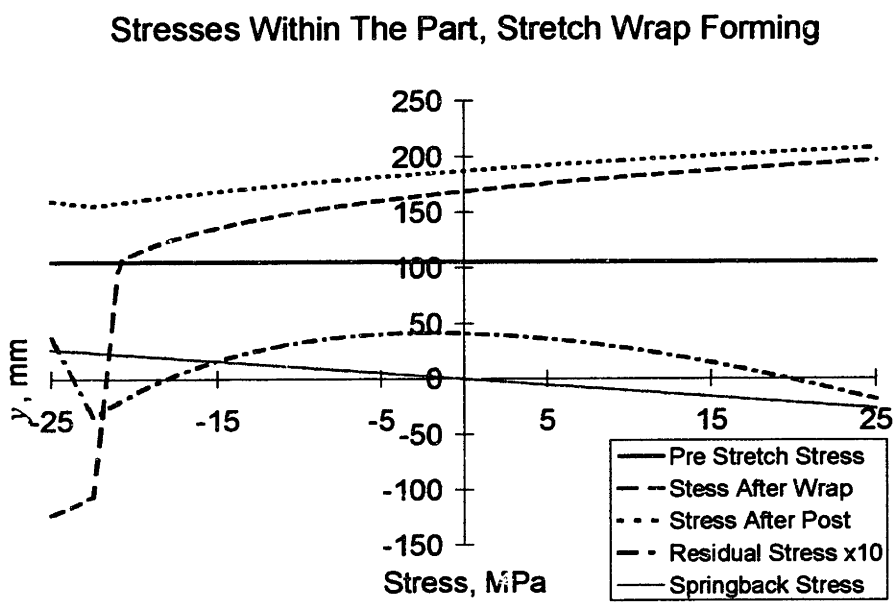

Figure 4.51 Stresses within the part; I cross-section; standard parameters; isotropic hardening; pre stretch strain of 0.5%; post stretch strain of 3.0%

The amazing thing that happens with this part is that in order to keep the force constant while wrapping, the midplane of the part stretches 4.19%! As mentioned previously, this is because upon bending the stresses decrease in compression much more quickly than they increase in tension, so that the part must stretch a significant amount in order to keep the force constant. The shape of this part (with a very thick bottom and top and a thin web) exaggerates this effect, but elongation during wrap is present in all stretch wrapped parts.

The next section deals with adjustments to the equations for routing of extrusions.

4.10 MODELING ROUTING OF STRETCH WRAP FORMED EXTRUSIONS

The approach to modeling the effect of routing of extrusions on springback is the same as that used to model the effect of chemical milling on sheet with the numerical summation method. It is assumed that material is routed from the inside of the part, since the outside of the part generally meets up against the inside of a skin and for this reason is not routed. Incremental forces in the part of the material routed are set to zero, so that they no longer contribute to the force or moment. The springback ratio and relaxation strain are adjusted in order to achieve zero net force and moment. Since release of extrusions often results in compressive plastic deformation, it may be necessary to model routing as an additional step after the part is released.

4.11 MODELING THE EFFECT OF FRICTION AND VARYING RADIUS OF CURVATURE

So far, friction has been ignored or assumed to be negligible, and the radius of curvature has been assumed to be constant over the length of the part. In this section, both of these assumptions are relaxed and the equations for modeling these two changes are derived. The following diagram shows the effect of friction on a die with varying radius of curvature.

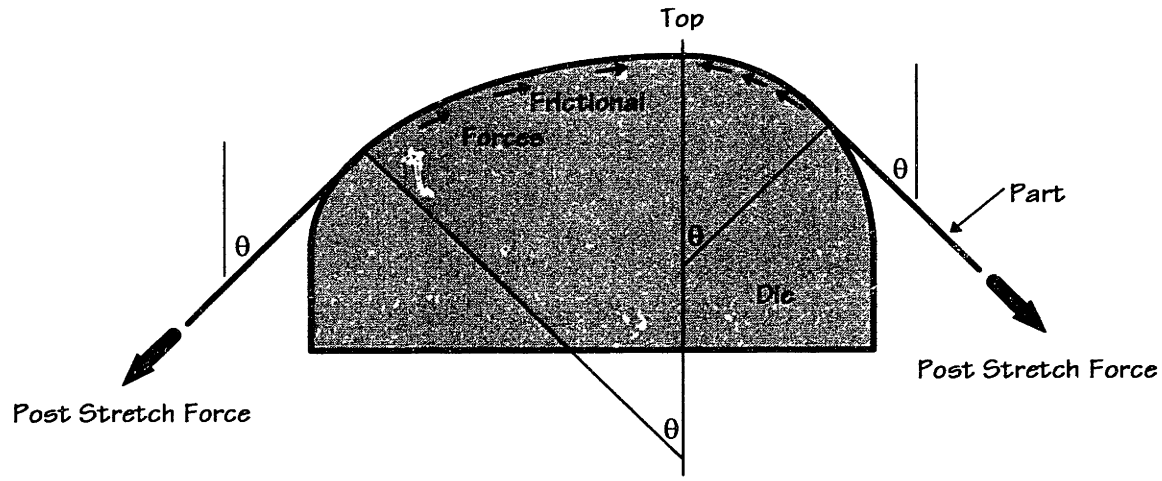

Figure 4.52 Diagram of a die and part with changing radius of curvature, showing the direction of frictional force

Friction acts in the direction opposite to the applied force and motion and reduces the force and strain along the length of the part during post stretch. Friction increases springback and causes the final part contour to be further away from the die than it would be without friction.

If the bend angles θ on both sides of the part are the same (this can be accomplished for analysis purposes by rotating the die if they are not the same), the part can be divided into two halves (left and right) at the top, where the part is horizontal. Friction reduces the force along the length of the part according to the formula

$$F = F^* e^{-\mu\beta}, \tag{4.73}$$

where β is the angle from the point of contact, μ is the coefficient of friction, and F^* is the force at the free end of the part. Since the bend angles are even for the left and right hand sides, the force at the top will be the same at the top for both sides, given that the forces are the same on both sides.

In drape forming, friction has no effect during bending, because there is no longitudinal force during bending. In stretch wrap forming friction has no effect during the pre stretch because the part is not in contact with the die. The effect of friction during wrap is negligible because bending is likely to occur before the part touches the die, and the normal forces are very low at this point because the part is being pulled tangentially off the die at the point of contact. Friction affects the post stretch for both drape forming and stretch wrap forming. Friction reduces the force and strain along the length of the part, from the point of contact to the top. In stretch wrap forming, the part cannot experience less force than the force at the end of the wrap. Therefore, in stretch wrap forming, while Equation 4.73 is used, the post stretch force is not permitted to fall below the wrap force.

A varying radius of curvature means that the amount of bending in the part varies along the length of the part, and as a result springback will also vary along the part.

4.11.1 Determining contour

The method used to determine the final contour of a stretch formed part with friction is the same as that used to model the effect of a varying radius of curvature along the length of the part. Because of the inability to determine the final contour by integration, numerical summation is used to approximate the final part contour. Only the right half of the part is modeled—the left half of the part can be modeled as the right half of a part and then flipped horizontally. The length of the part in contact with the die L is broken up into a sufficient number of segments, each of length ΔL_i and radius of curvature R_i (the i in this case indicating the i^{th} segment, not i for initial). If the length of each segment is the same, it is given by

$$\Delta L_i = L/N. \tag{4.74}$$

The incremental angle change from one segment to the next is given by

$$\Delta\theta i = \Delta L_i/R_i. \tag{4.75}$$

Then the angle of segment i is given by

$$\theta_i = \sum_{j=1}^{i} \Delta\theta_j \,. \tag{4.76}$$

Finally the change in contour from the segment is given by

$$\Delta X_i = \Delta L_i \cos\left(\theta_{i-1} + 0.5\Delta\theta_i\right) \quad \text{and} \quad \Delta Y_i = -\Delta L_i \sin\left(\theta_{i-1} + 0.5\Delta\theta_i\right). \tag{4.77}$$

The contour is given by the endpoints of the segments according to

$$X_i = \sum_{j=1}^{i} \Delta X_i \quad \text{and} \quad Y_i = \sum_{j=1}^{i} \Delta Y_i \,. \tag{4.78}$$

This assumes that the topmost point of the part is taken as the origin. The following diagram shows two segments, and associated geometry and equations.

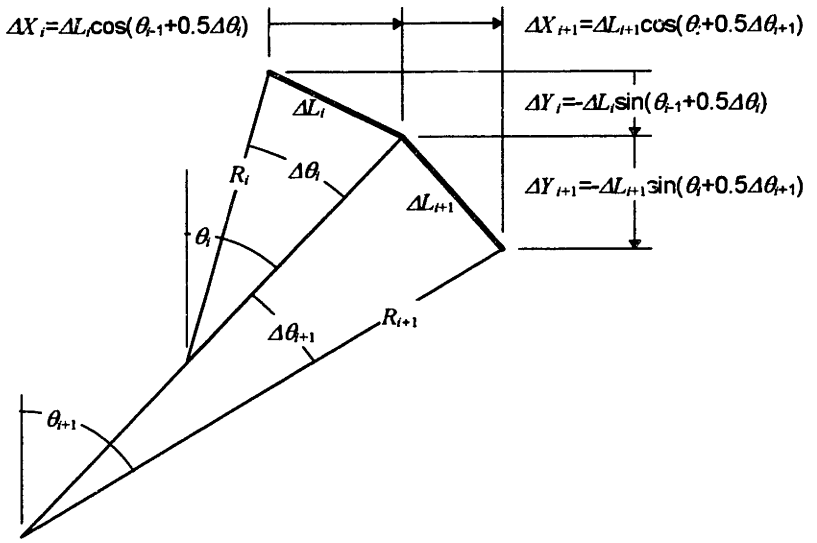

Figure 4.53 Incremental geometry calculations

The above equations permit the modeling the effect of friction and varying radii of curvature on the final contour of a part. The amount of midplane strain, relaxation, and springback ratio are calculated for each segment. Then the equations just above are used to calculate the actual initial and final contour for the whole part, so that they can be compared. This approach can be used to model only friction, only varying radius of curvature, or both. A simplifying assumption made for the case of varying radius of curvature is that the effect of the change in radius of curvature due to sliding during post stretch is negligible.

Implementation in a spreadsheet used N = 50 segments. In order to evaluate the magnitude of the magnitude of the error introduced by use of the numerical summation approach, the contour achieved by this method was compared to the contour achieved by an analytically smooth curve. For a part with R = 300 mm and L = 300 mm, the difference between the position of the end of the part using the numerical summation method was the same as that of the analytically smooth curve to 4 or 5 significant figures—very accurate.

4.11.2 Examples

For the standard material and die parameters (with constant radius of curvature), the effect of friction on the drape forming operation is shown in the following chart. The die shape, the final part shape (with and without friction), and the shape error, the distance between the die and final part shape (with and without friction) are shown.

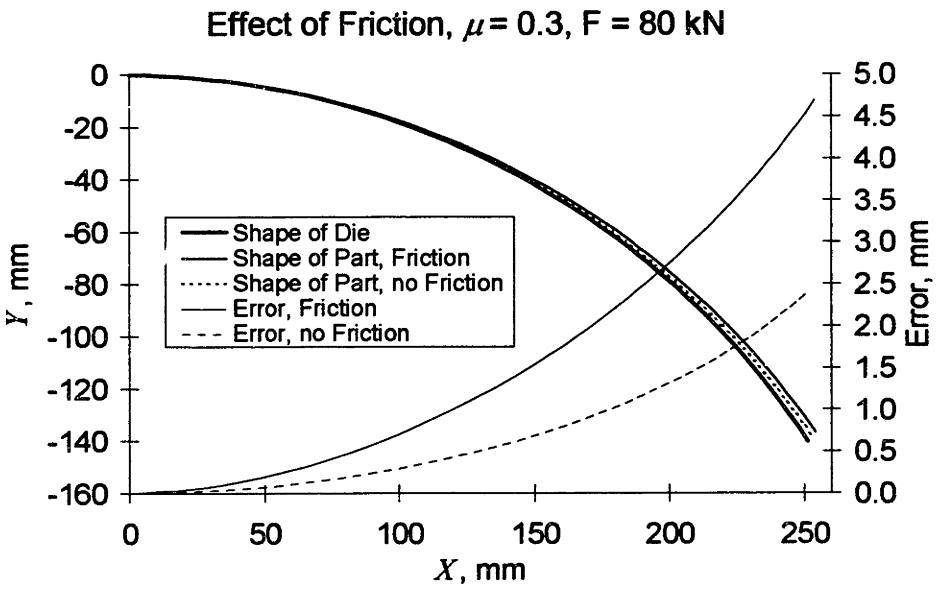

Figure 4.54 Effect of friction on contour; standard parameters; Isotropic hardening; drape forming; post stretch force = 80 kN; $\mu = 0.3$

The coefficient of friction in this example is $\mu = 0.3$. The length of part contacting the die is 300 mm, so that the initial bend angle is $\theta = 57.30°$. The post stretch force is 80 kN. The maximum post stretch strain, 1.96%, occurs at the point of contact between the die and part, while the minimum post stretch strain, 0.45%, occurs at the top of the part. Friction doubled the shape error at the end of the part—from about 2.4 mm (0.094") to about 4.7 mm (0.19").

The following chart demonstrates the ability to vary the radius of curvature and model the effect of friction on a leading edge-shaped part. The X axis scale is adjusted so that the X and Y axes are to roughly the same scale (to give some semblance of a leading edge).

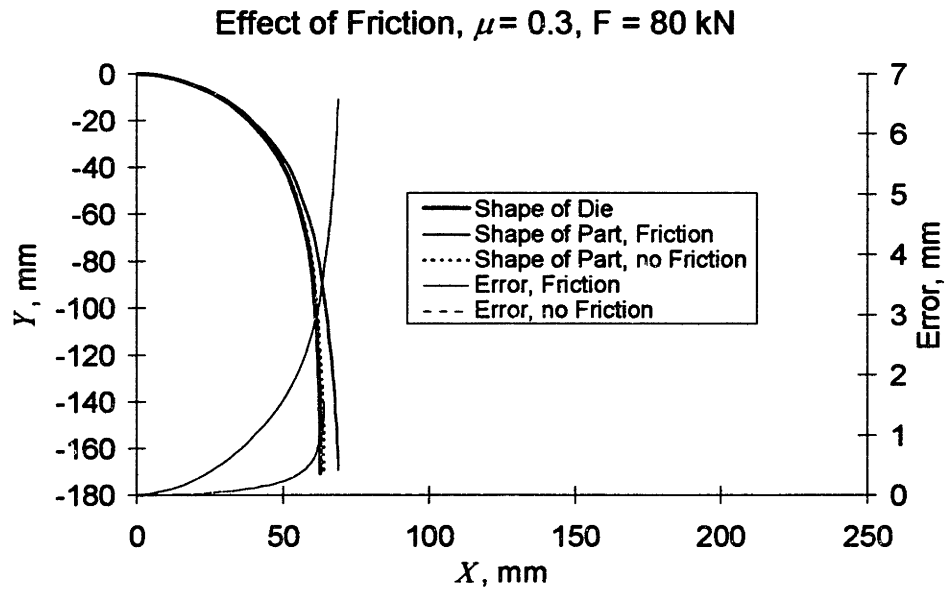

Figure 4.55 Effect of friction; leading edge; drape forming; isotropic hardening; post stretch force = 80 kN; μ = 0.3

The total length of part in contact with the die is 200 mm, and each segments is 4 mm long. The first 10 segments have a radius of curvature of R_i = 50 mm, the next 10 have R_i = 80 mm, the next 10 have R_i = 200 mm, and the last 20 have R_i = 1000 mm. The initial bend angle is θ = 90.53°. With friction, the post stretch strain at the point of contact with the die is 1.97%, while at the top of the die it is only 0.25%. Without friction, the post stretch strain at the point of contact with the die is 1.97%, while at the top of the die, it is only 1.37% (the reason for the decrease in strain at the top without friction is that the increased initial plastic deformation at the top caused by bending at a smaller radius of curvature hardened the part). The shape error at the end of the part for the no friction case is 1.54 mm (0.061"), while with friction it is 6.58 mm (0.259")—contour deviation is increased by a factor of four.

4.12 A SIMPLER METHOD TO CALCULATE STRESSES

Very late in this thesis, another, simpler approach to keeping track of the actual and effective stresses and strains within the material was found.[32] This approach, using the concept of a yield surface is now described.

---

[32] The term "found" is used because the idea is old hat to those knowledgeable in plasticity, and others have worked out some form of the equations set forth in the following. Even so, it does

4.12.1 The yield surface approach

It is possible to perform all of the above stress and strain calculations in a simpler way using a circle to represent the yield surface [Mroz, 1967].[33] The yield surface is the locus of stresses that lie on the boundary between elastic and plastic deformation. The stress state in the material, in the plane stress condition, is given by the stress σ_1 in the x direction and σ_2 in the z direction.

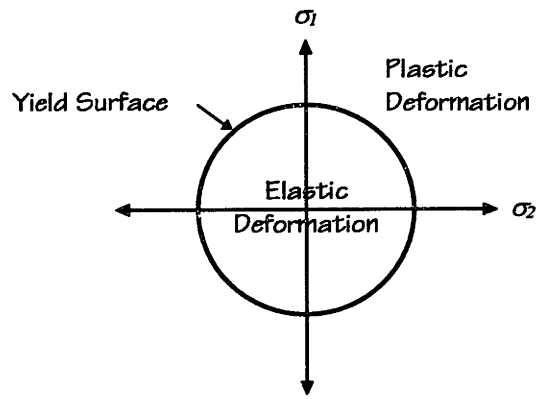

Figure 4.56 Yield Surface: demarcation between elastic and plastic deformation

If the stresses change so that they remain inside the yield surface, only elastic deformation occurs; if the stresses change so that they reach the yield surface, then plastic deformation begins and continues as long as the stresses move in such a way as to "push" on the yield surface, causing some combination of enlargement and movement of the surface.

In two dimensions it can be assumed that the yield surface is represented by a circle, according to the von Mises yield criterion. If uniaxial stress is assumed (which it is in this case), the stress state of the material is represented by the position of the current stress on the vertical, x, axis.[34] When plastic deformation occurs, the stress state of the material lies on the yield surface. The first two important circle parameters are its size

---

not appear that this approach has been used by anyone in direct application to stretch forming in an analytical model as is done here.

[33] It was by reading through and trying to understand Mroz's approach—which was different than this one, because he was dealing with cyclical stresses and used a piece-wise linear approximation to a curved stress-strain curve—that the idea came to try this approach.

[34] When plane strain is assumed, since the relationship between stress in the x and z directions is fixed, this method can still be used with an appropriate scaling of material properties as was shown earlier in this chapter.

and location. For uniaxial stress conditions, the circle can only move up and down and change in size. How the size and location change depends on the material strain hardening model. Elastic strain (movement within the circle) has no effect on the location or size of the yield surface.

Changes in radius and location of the circle for the Isotropic, Kinematic, and Bauschinger models are now given. In each case, the starting conditions are the same with the circle centered at zero and the radius equal to the yield stress.

Isotropic model

For the Isotropic model, the yield surface expands the full amount of the change in plastic stress, while the center does not move. This is shown in the following set of diagrams. The dark **X** denotes the stress at the end of a particular step, the dark line with an arrow at the tip shows how the stress changed in the step, and the yield surface from the last step is shown lightly. The radius and vertical location of the center of the circle are denoted by R_i and C_i; the subscript i indicates the stage.

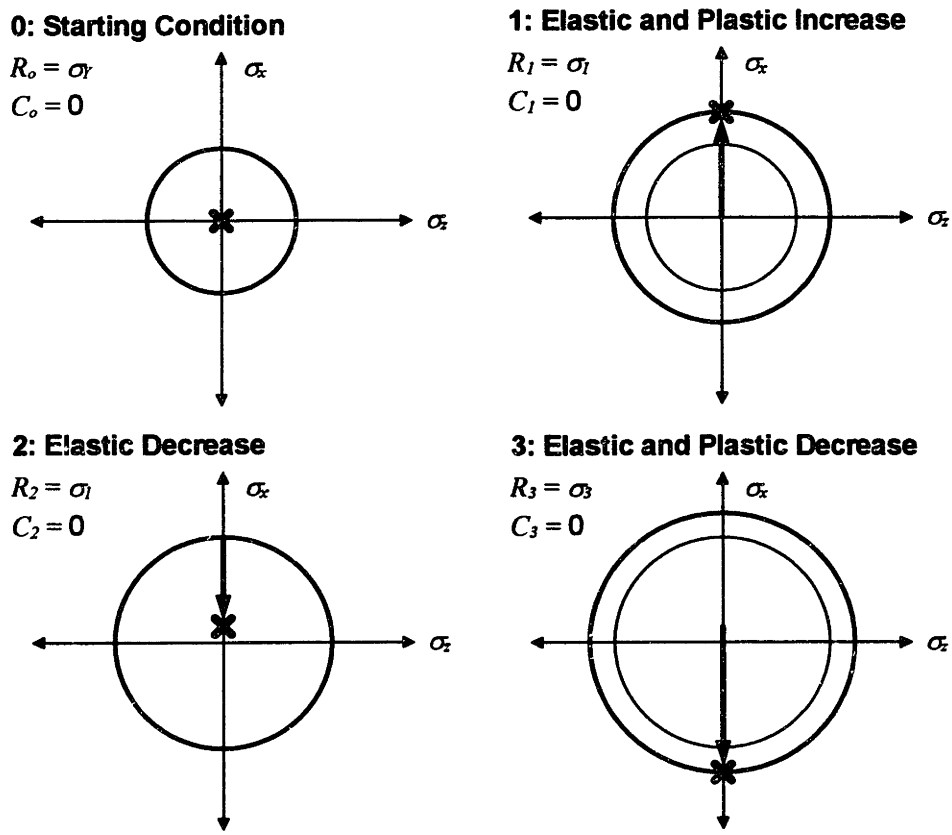

Figure 4.57 Change in yield surface for Isotropic hardening with change in direction of elastic and plastic strains

Kinematic model

As the material plastically deforms and strain hardens, the Kinematic model yield surface does not increase in size, but the center moves the distance of the change of plastic stress. This is shown in the following set of diagrams is for a set of strains similar to what was used in Figure 4.57.

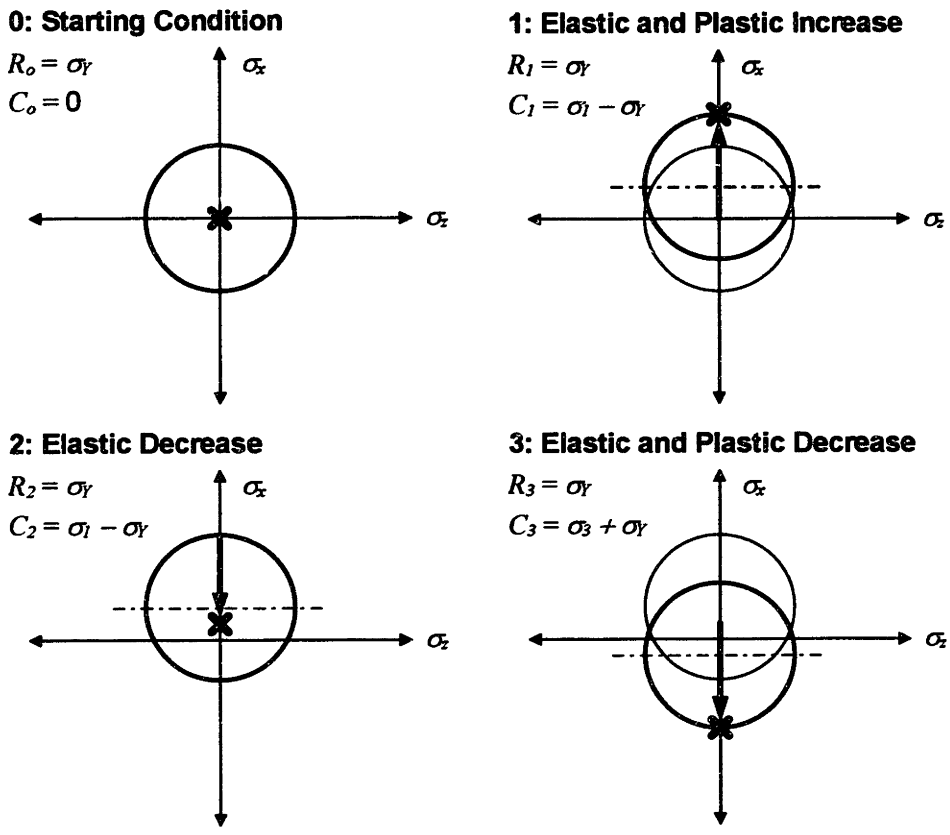

Figure 4.58 Change in yield surface for Kinematic hardening with change in direction of elastic and plastic strains

Bauschinger Model

For the Bauschinger model, the yield surface radius expands at 1/2 of the change in plastic stress, and the center moves also at 1/2 of the change in plastic stress. This is shown in the following set of diagrams for a set of strains similar to those used in Figure 4.57.

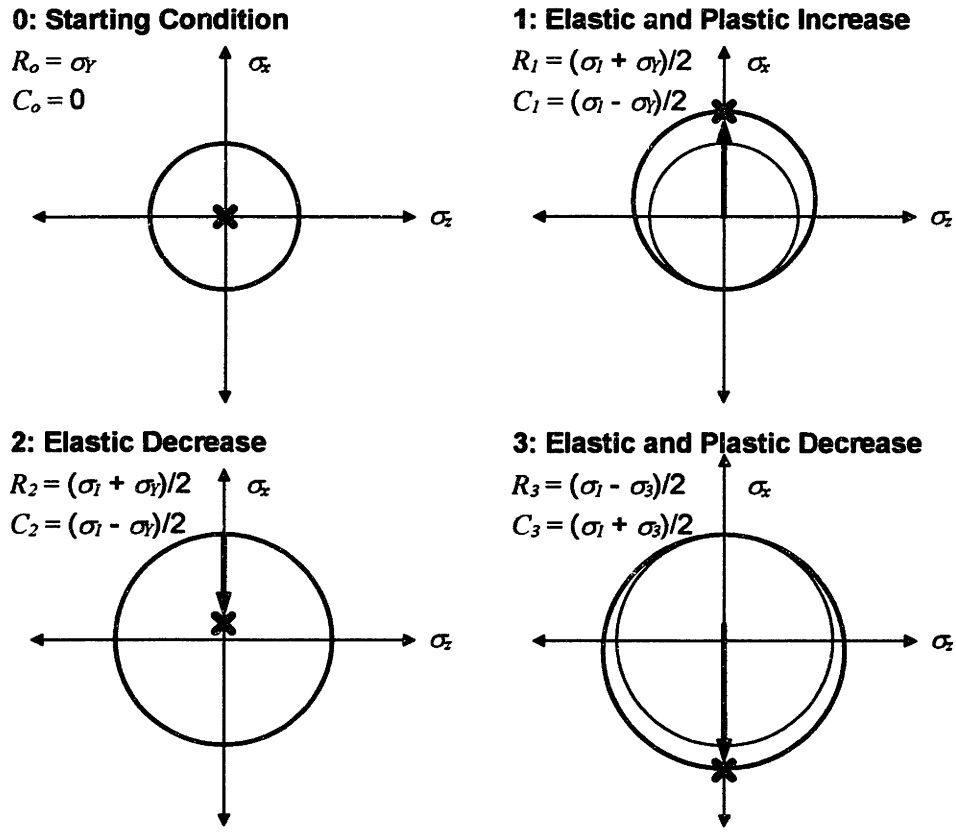

Figure 4.59 Change in yield surface for Bauschinger hardening with change in direction of elastic and plastic strains

4.12.2 Development of equations

The above diagrams do not reveal hardening. In order to model a material, the total amount of hardening and the instantaneous rate of hardening must be known. It is possible to write a set generic equations that can be used to determine hardening and yield surface size and location as strains are imposed on the material. In fact, this one set of equations can be used to model all three material models, Isotropic, Kinematic, and Bauschinger, as well as any model between the Isotropic and Kinematic models (of which the Bauschinger model is just one), simply by adjusting one parameter. This is done now.

To go from the current stress-strain state, k, to the next, k+1, the following variables must be known: the yield surface radius R_k and vertical location of the center C_k of the yield surface, the stress σ_k and the current amount of strain hardening $\sigma_{k,eff}$, the last of which is calculated from the effective strain $\varepsilon_{k,eff}$. Of course, the material stress-strain

curve parameters, σ_Y, E, n, and K, must be known. Here, as earlier in this work, an elastic, power law plastic stress-strain curve is assumed.

The generic state k shown in the following diagram.

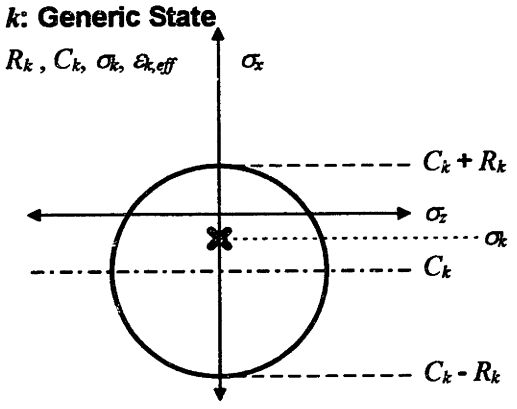

Figure 4.60 Generic state yield surface characterization

The current, k, stress-strain state is generic, in that it covers all possible combinations of the four variables. The current stress lies somewhere between the maximum and minimum stresses given by the location and size of the circle. In order to find out what happens next, in step k+1, the amount of strain imposed $\Delta\varepsilon_{k+1}$ must be known. From this, a test stress $\sigma_{k+1,test}$ is calculated by

$$\sigma_{k+1,test} = \sigma_k + E\Delta\varepsilon_{k+1}. \tag{4.79}$$

A test is made to determine if the imposed strain causes compressive plastic, elastic, or tensile plastic deformation, by checking if the test stress falls below, inside, or above the current yield surface. The test is in the following equation

$$\begin{aligned} &\text{if} && \sigma_{k+1,test} < C_k - R_k && \Rightarrow \text{compressive plastic} \\ &\text{else, if} && \sigma_{k+1,test} < C_k + R_k && \Rightarrow \text{elastic} \\ &\text{else} && \left(\sigma_{k+1,test} \geq C_k + R_k\right) && \Rightarrow \text{tensile plastic} \end{aligned} \quad . \tag{4.80}$$

Next, the amount of strain hardening resulting from any plastic deformation is determined. In order to do this, the amount of elastic strain is subtracted from $\Delta\varepsilon_{k+1}$. The amount of elastic strain is the amount of strain taken up in going from the point inside the circle to the perimeter in the direction it is going. Then, in exactly the same manner as for equations derived earlier, the next total effective strain $\varepsilon_{k+1,eff}$ is the current effective strain $\varepsilon_{k,eff}$ plus the next change in strain $\Delta\varepsilon_{k+1}$, minus the next elastic

strain. If the strain is entirely elastic, the effective strain doesn't change at all. The equation for the next effective strain is

$$\begin{aligned} &\text{if compressive plastic} && \Rightarrow \varepsilon_{k+1,eff} = \varepsilon_{k,eff} - \Delta\varepsilon_{k+1} - \left(\sigma_k - \left(C_k - R_k\right)\right)/E \\ &\text{else, if elastic} && \Rightarrow \varepsilon_{k+1,eff} = \varepsilon_{k,eff} \\ &\text{else (tensile plastic)} && \Rightarrow \varepsilon_{k+1,eff} = \varepsilon_{k,eff} + \Delta\varepsilon_{k+1} - \left(\left(C_k + R_k\right) - \sigma_k\right)/E \end{aligned} \quad . \tag{4.81}$$

Note that if the stress in the current step is on the yield surface in the same direction of the next strain increment, the elastic strain is zero. Next, according to the power law strain hardening rule, the new effective stress is calculated as

$$\begin{aligned} &\text{if plastic} && \Rightarrow \sigma_{k+1,eff} = K\left(\varepsilon_{k+1,eff}\right)^n \\ &\text{else, (elastic)} && \Rightarrow \sigma_{k+1,eff} = \sigma_{k,eff} \end{aligned} \quad . \tag{4.82}$$

The increase in stress due to strain hardening, H_{k+1}, is given by

$$H_{k+1} = \sigma_{k+1,eff} - \sigma_{k,eff} \, . \tag{4.83}$$

The new stress is then given by

$$\begin{aligned} &\text{if compressive plastic} && \Rightarrow \sigma_{k+1} = C_k - R_k - H_{k+1} \\ &\text{else, if elastic} && \Rightarrow \sigma_{k+1} = \sigma_{k+1,test} \\ &\text{else (tensile plastic)} && \Rightarrow \sigma_{k+1} = C_k + R_k + H_{k+1} \end{aligned} \tag{4.84}$$

At this point, the change in the position and size of the yield surface must be calculated. If the strain is entirely elastic, the yield surface does not change. As already mentioned, when there is plastic strain, for the Isotropic hardening model, the center stays at zero and the radius increases by the amount of hardening; for the Kinematic hardening model, the center moves by the amount of hardening and the radius doesn't change. Between these two lies a whole range of intermediate possibilities. It is possible to capture them all with the following equation

$$R_{k+1} = R_k + AH_{k+1}, \tag{4.85}$$

in which A = 1 for the Isotropic hardening model, A = 0 for the Kinematic hardening model, and 0 < A < 1 for everything else in-between. The Bauschinger model is achieved when A = 1/2. The new position of the center is given by

$$\begin{aligned} &\text{if compressive plastic} && \Rightarrow C_{k+1} = \sigma_{k+1} + R_{k+1} \\ &\text{else, if elastic} && \Rightarrow C_{k+1} = C_k \\ &\text{else (tensile plastic)} && \Rightarrow C_{k+1} = \sigma_{k+1} - R_{k+1} \end{aligned} \tag{4.86}$$

This concludes all of the calculations for the new state k+1. If another strain increment is imposed, the calculations are performed anew. The values of the four variables which characterize the initial stress-strain state of the material are

$$R_o = \sigma_Y \qquad C_o = 0 \qquad \sigma_o = 0 \qquad \varepsilon_{o,eff} = \sigma_Y / E \tag{4.87}$$

The results obtained from Equations (4.79) through (4.87) are exactly the same as those obtained through the earlier equations for the Isotropic, Kinematic, and Bauschinger models.

4.12.3 Advantages and disadvantages of this method

There are a number of advantages to using the equations just developed instead of earlier equations. A few of these are now addressed.

Only four current states and the strain increment are required to calculate the new state, regardless of the direction or magnitude of the strain. The four state variables retain all the necessary strain history for the next iteration. Because of this, it very easy to tack onto the last state another strain increment in order to model another step. As a result, the equations presented above are much faster to work with.[35]

By simply changing one parameter, A, it is possible to model both Isotropic and Kinematic hardening models and the whole range in-between.

It is possible, but has not been done, to give the material an initial strain hardening and residual stress distribution by appropriately specifying the four initial variables. This would be useful for investigating the influence of initial residual stresses (such as those caused by quenching in the heat treat operation) on the stretch forming operation.

There are some minor disadvantages to using the above equations as well. Most importantly, the relationship between the above and a stress-strain curve is not intuitively obvious to the casual observer (for this reason all of the previous development is still included in this thesis). Further, a simple, one-equation analytical solution is not possible from this method.

---

[35] To give an indication of the time difference, the above equations were essentially derived in one evening and night—altogether not more than six hours. The equations for the other method were developed over weeks, and required excruciating amounts of error-proofing and then more time-consuming adjustments (enhancements) in order to increase their ability to model things. Of course, the great amount of learning that occurred with the earlier method also had a lot to do with being able to derive these equations so quickly.

4.12.4 Summary and conclusions to yield surface method

An alternate, easier to use, and more elegant method for calculating stresses as a function of strains in the sheet metal stretch forming operation was developed (it is acknowledged that others have developed these or something similar to these equations before). While not as intuitively enlightening as the equations developed earlier in this chapter, ease of use makes this method the preferred one in some cases.

4.13 SUMMARY AND CONCLUSIONS TO ANALYTICAL MODEL CHAPTER

Equations were developed to model the stretch forming of metal over a cylindrical die. Model parameters are material geometry and properties, die radius of curvature, and the forces or strain imposed on the part. Model outputs are stresses and strains in the material at stages in the operation, and the springback ratio. The two outputs of greatest interest are residual stresses and the springback ratio. Stretch forming of sheet metal and extrusions has been modeled. Adjustments for plane strain and plane stress conditions have been made. The effect of chemical milling of sheet metal and routing of extrusions has also been modeled. Four different material models—Isotropic, Bauschinger, Kinematic, and No IPD—were presented, and any model between the Isotropic and Kinematic can be modeled using the yield surface concept. Finally, the ability to model friction and a varying radius of curvature along the length of the part have been developed. Numerical summation has been used instead of integration to determine moments and net forces within the material.

A very important difference between the equations developed here and those developed by others is that these equations are simpler and easier to implement in order to make predictions. Further, the method of presentation of the results and the focus on the area of the concern to a real stretch forming operation make this approach more useful to the stretch forming practitioner.

The charts in this chapter have been presented to demonstrate the use of the equations. In the next chapter, the equations are used to better understand the stretch forming operation and its sensitivities to changes in parameters, and output from the equations is compared with published data, experiments, and FEA simulations.

A further, significant benefit of the knowledge gained in this chapter and the next is the increased ability to understand and interpret the statistical data collected from the actual manufacturing process, and to know where to look for precision improvement.

5 ANALYTICAL MODEL: FINDINGS AND COMPARISONS

In this chapter, the analytical model developed in the previous chapter is used to determine the effect of changes in parameters and the difference between strain control and force control on the operation. Then, a couple of non-ideal conditions are addressed. Finally, in order to validate the model, analytical model predictions are compared with experimental and finite element analysis simulation (FEA) results.

The reader should recall that a higher springback ratio implies less springback and a lower springback ratio implies more springback.

Since the effect of changes is generally assessed by how the changes affect the springback ratio, the first section in this chapter investigates the effect of a change in radius of curvature on the contour.

5.1 THE EFFECT OF SPRINGBACK RATIO ON PART CONTOUR

The following diagram shows how part contour deviates from a check fixture (CF) or contour template (CT) when its final radius of curvature is different that of CF or CT (i.e., it is different from what is expected). The part radius of curvature is less than the CF radius of curvature, but the math holds for the other way around as well.

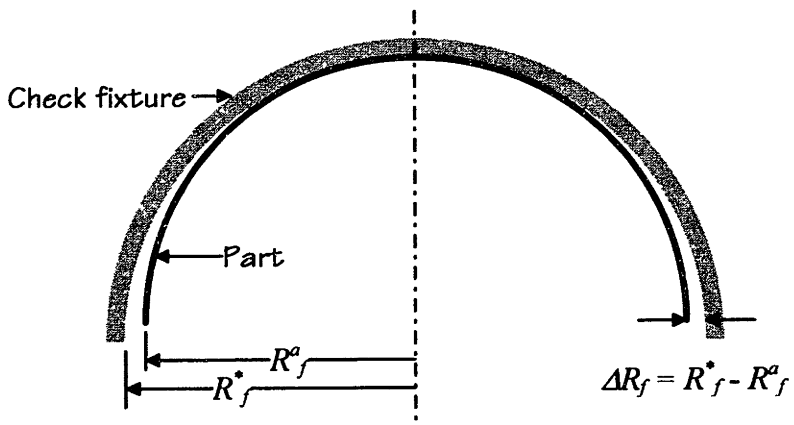

Figure 5.61 Part and check fixture with different radii of curvature

As the diagram shows, if a circular part is located at the center of the check fixture and is at that point tangent to the fixture, then if the part's actual radius of curvature is R^a_f and the inside radius of the check fixture is the desired radius of curvature, R^*_f, the horizontal separation between the part and fixture 90° from the point of tangency is

$R_f^* - R_f^a$. Due to offsets required for the thickness of the part and a slight vertical change in position of the end of the part due to springback, this formula is not entirely exact, but as a first order approximation it captures the essence of the point very well, and simply. The springback ratio is R_i / R_f. The desired or reference final radius of curvature R_f^* is equal to $R_i / (R_i/R_f)^*$, and the actual radius of curvature R_f^a is equal to $R_i/(R_i/R_f)^a$, in which the desired or reference springback ratio is $(R_i/R_f)^*$, and the actual springback ratio is $(R_i/R_f)^a$. The percent change in final radius of curvature is given by

$$\Delta R_f\,\% = 100 \times \frac{R_f^{\,a} - R_f^{\,*}}{R_f^{\,*}} = 100 \times \frac{\dfrac{R_i}{(R_i/R_f)^a} - \dfrac{R_i}{(R_i/R_f)^*}}{R_f^{\,*}} = 100 \times \left(\frac{(R_i/R_f)^*}{(R_i/R_f)^a} - 1 \right). \quad (5.1)$$

The percent change in springback ratio is given by

$$\Delta R_i/R_f\,\% = 100 \times \frac{(R_i/R_f)^a - (R_i/R_f)^*}{(R_i/R_f)^*} = 100 \times \left(\frac{(R_i/R_f)^a}{(R_i/R_f)^*} - 1 \right). \quad (5.2)$$

Calculating the percent change in R_f from the percent change in R_i/R_f, is accomplished by the following equation:

$$\Delta R_f\,\% = -\Delta R_i/R_f\,\% \times \frac{(R_i/R_f)^*}{(R_i/R_f)^a}. \quad (5.3)$$

And, of course, the magnitude of the change in mm or inches is given by

$$\Delta R_f = R_f \times \Delta R_f\,\%/100. \quad (5.4)$$

The above equations can also be used for deviation of one part from another, with the first part having the * superscript and the second having the a superscript.

5.1.1 Example

As an example, for a part made with R_i = 300 mm (11.81") and a total bend angle of 180°, if the springback ratio was expected to be 0.950, but turned out to be 0.960 (the part in this case not springing back as much as expected, roughly a 1% change in the springback ratio), the amount of separation between the part and the CF (if it were springback compensated for a springback ratio of 0.950) as defined above would be

$$\Delta R_f = 300 \times \left(\frac{0.95}{0.96} - 1\right) = \text{-3.125 mm } (= \text{-0.123"}). \quad (5.5)$$

The percent change of radius of curvature is -1.04%, while the percent change of springback ratio is 1.05% (when the two springback ratios are within a few percent of one-another, the percent changes are almost the same magnitude). For a change in springback ratio of about 0.1%, from 0.950 to 0.951, the separation would be 0.315 mm, which is 0.012". If the part were larger, say, with R_i = 1000 mm (39.4"), a 0.1% change in springback ratio would create a separation of 1.05 mm, which is 0.041".

The above demonstrates that a small change in springback ratio can have a significant effect that on contour. With a bend angle of less than 180°, the contour deviation will be roughly proportional to the bend angle, so that, for example, with a bend angle of 90°, contour deviation would be half the difference between the reference and actual radii.

5.2 EVALUATING THE EFFECT OF PARAMETER CHANGES

In this section, the analytical model, implemented in Excel© spreadsheets, is used to show how changes in various parameters affect springback and part contour. Unless otherwise noted, the Isotropic hardening model and standard parameters (σ_Y = 77 MPa, E = 68947 MPa, n = 0.210, {K = 320.9 MPa}, t = 1.60 mm, R_i = 300 mm) are used in the equations, and the effect of friction is assumed to be negligible. As mentioned in the previous chapter, the Isotropic hardening model is the default because it best represents the behavior of aluminum [Tozawa, 1978]. The results are often specific to the parameters and hardening model used, so care must be taken when generalizing results for a particular set of parameters. Changes in material stress-strain curve parameters are defined next.

5.2.1 Effect of changing material parameters on the stress-strain curve

A change of the elastic modulus does not affect the rest of the curve, i.e., n and K do not change. In order to accomplish this, the yield strength is adjusted so that the plastic and elastic portions of the curve meet. The adjusted yield strength is given by

$$\sigma^*_Y = E^* \left(\frac{E^*}{K}\right)^{\frac{1}{n-1}}, \quad (5.6)$$

in which the E^* is the changed elastic modulus.

Ideally, a change of the yield strength would just move the plastic portion of the curve up or down. This is *almost* accomplished simply by changing the yield strength and adjusting K according to the equation in the previous chapter. The slope of the plastic portion of the curve changes slightly, but moving the curve without changing the slope at all would require a different stress-strain relationship.

Changing the strain hardening coefficient is accompanied by adjusting K.

The effects of a 10% increase in the elastic modulus, yield strength, and strain hardening ratio on the stress-strain curve are shown in the following chart.

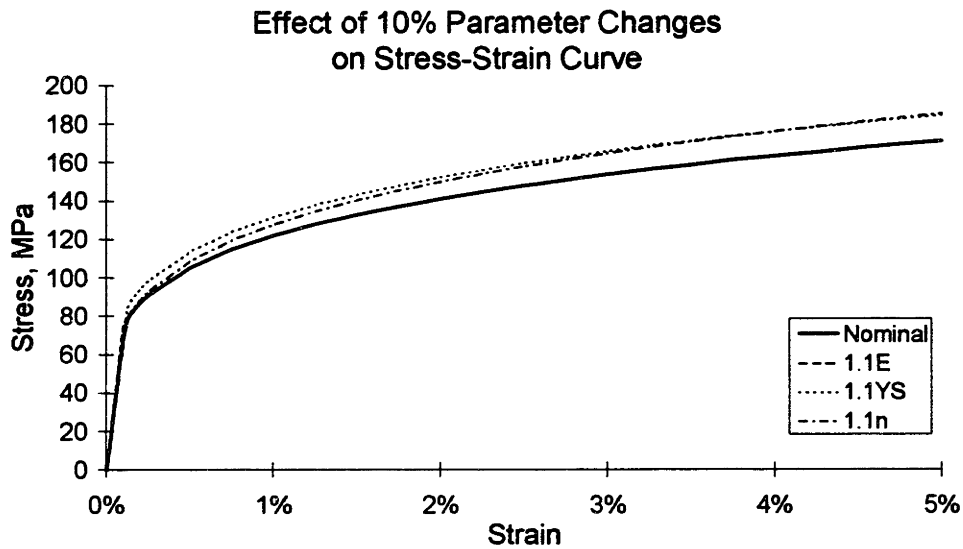

Figure 5.62 Effect of parameter changes on the stress-strain curve; nominal curve is of standard parameters

Note that at higher strains the effect of increasing the strain hardening coefficient surpasses the effect of increasing the yield strength.

The effect of control method on the drape forming operation is investigated first.

5.2.2 Effect of control method on drape forming

Introduction to force, displacement, and strain control

To control the stretch forming operation by a variable is to measure that variable, compare it to a target value, and adjust the movement of the machine based on the difference between the actual and target values. The stretch forming operation is

generally controlled by force, displacement, or strain. To the analytical model, there is no difference between displacement and strain control, except in the friction case.

Force control is accomplished by controlling the forces exerted by the die or the jaws. Forces may be measured directly by a force transducer, but often hydraulic pressure is used as a surrogate. Due to the temperature dependence of hydraulic oil viscosity and the change in pressure caused by moving oil (as cylinders move), this is not a very reliable measure of force. Even if force were reliably measured, things such as changes in material properties reduce the ability to predict strain from the force. Displacement control is accomplished by controlling the displacement of the die or the jaws. Displacement is a surrogate for strain, and may not be reliable due to setup changes, machine compliance at high forces, slippage, or other reasons. Even if it is repeatable, the actual strain is not known if only displacement is measured. Strain control is accomplished by controlling the strain in the part. Strain may be measured by marking the parts and seeing how the marks move, or more qualitatively by watching how the part forms on the die or how its surface texture changes. In both displacement and strain control, forces will vary as the material stress-strain relationship changes.

As is now demonstrated, the sensitivity of the stretch forming operation to changes in parameters—both the controlled parameter and material parameters—depends on how the operation is controlled. The two methods now considered are force control and strain control, since displacement control is essentially the same as strain control, except that it is a surrogate. Currently, force control is used on the machine on which leading edges are stretch formed at Vought.

Sensitivity to parameter variation

The control method of choice should be the one that is most robust to changes in parameters; that is, its sensitivity to parameter variation should be small. Analytically this is best measured by the change in the springback ratio as a function of changes in parameters. The following chart shows the effect of a 10% change in elastic modulus, yield strength, strain hardening exponent, thickness, and radius of curvature on the springback ratio under force control.

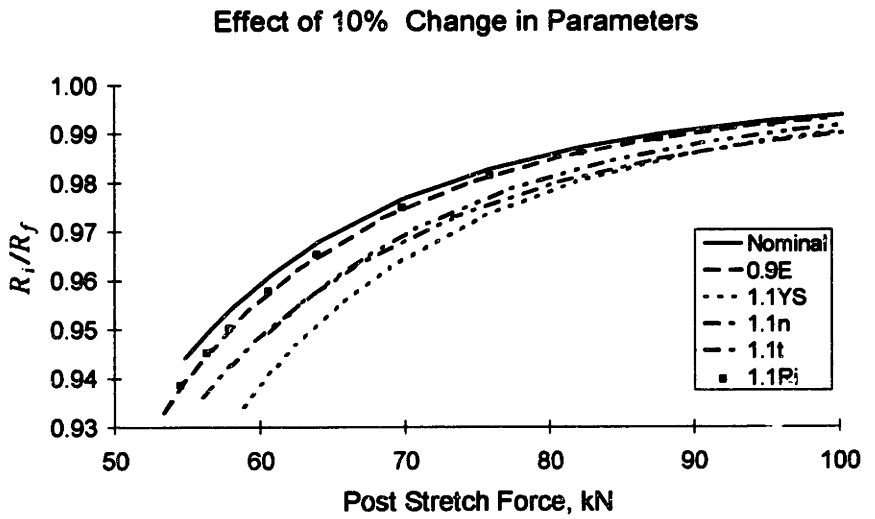

Figure 5.63 Effect of 10% change in parameters on springback ratio; drape forming; force control

The following chart shows the effect of a 10% change in these same parameters on the springback ratio under strain control.

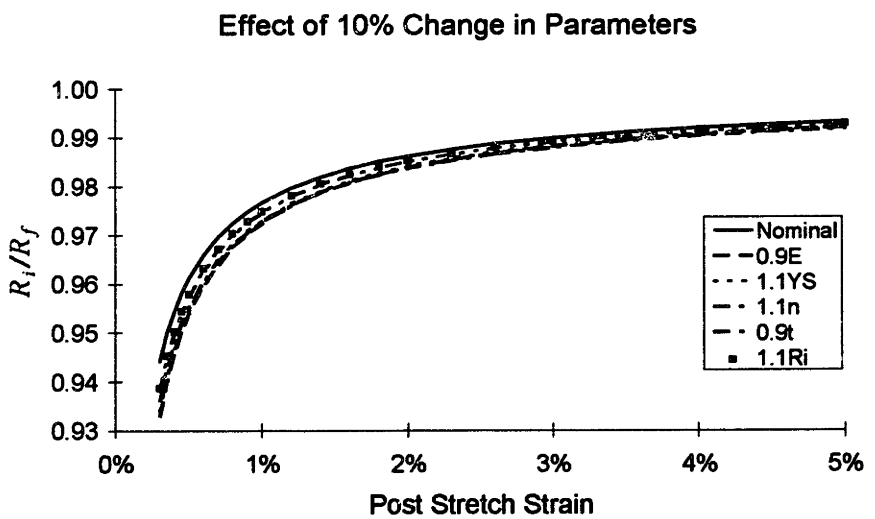

Figure 5.64 Effect of 10% change in parameters on springback ratio; drape forming; strain control

The spread in the curves is much less under strain control than under force control, demonstrating that of the two control methods strain control is more robust to changes in material parameters. The sensitivities are now investigated quantitatively.

The following table shows the change in springback ratio for a 10% change in parameter under strain and force control, at a nominal post stretch strain of 1%.

Parameter	Change in Springback Ratio	
	Strain Control	Force Control
Yield Strength +10%	-0.38%	-1.27%
Strain hardening exp. +10%	-0.40%	-0.90%
Thickness -10%	-0.21%	+0.62%
Elastic modulus -10%	-0.42%	-0.22%
Radius of curvature +10%	-0.19%	-0.17%

Table 5.1 Change in springback ratio for 10% change in parameters for strain and force control at 1% post stretch strain

The springback ratio under force control is two to three times more sensitive to changes in the three parameters that are most likely to change—yield strength, strain hardening exponent, and thickness—than under strain control. Interestingly, the direction of the effect of a decrease in thickness is different under force control than it is under strain control. The changes are greater at higher post stretch strains.

Sensitivity to changes in force or strain

The next chart shows sensitivity of the springback ratio to changes in post stretch strain and force.

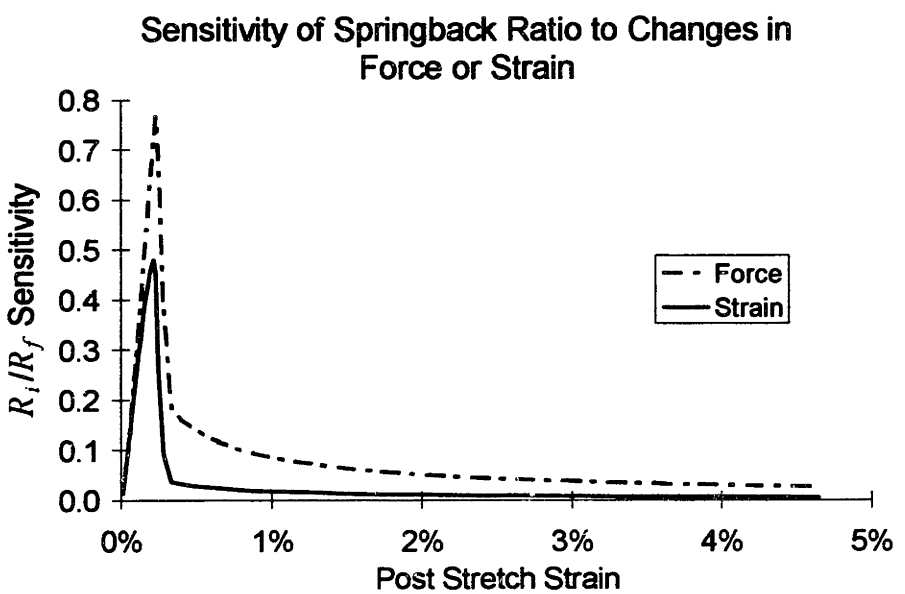

Figure 5.65 Sensitivity of springback ratio to changes in force or strain; drape forming

The springback ratio sensitivity to force is calculated according to the following formula

$$\text{Force sensitivity} = \frac{\Delta\left(R_i/R_f\right)}{\Delta\left(F\right)/F} \quad . \tag{5.7}$$

The sensitivity to strain is calculated in the same manner. The chart shows that the sensitivity of the springback ratio to changes in force is higher than its sensitivity to changes in strain. At 80 kN (1.93%), the sensitivity to changes in force is 0.053, while the sensitivity to changes in strain is 0.011, almost a five-fold difference. At 93 kN (4.0%), the sensitivities are 0.030 and 0 .006, respectively, again a five-fold difference.

A change in the yield strength affects more than just the springback ratio. Under force control a 10% increase in yield strength reduces the strain in the part by 30%, while a 10% decrease in yield strength increases the strain by 50%—which is likely to cause the part to break. If the operation is controlled according to strain, the strain is insensitive to changes in yield strength.

The relationship between post stretch force and strain

The reason for the difference between the sensitivity of the operation to changes under force and strain control is explained by the relationship between post stretch force and strain. This is shown in the following chart.

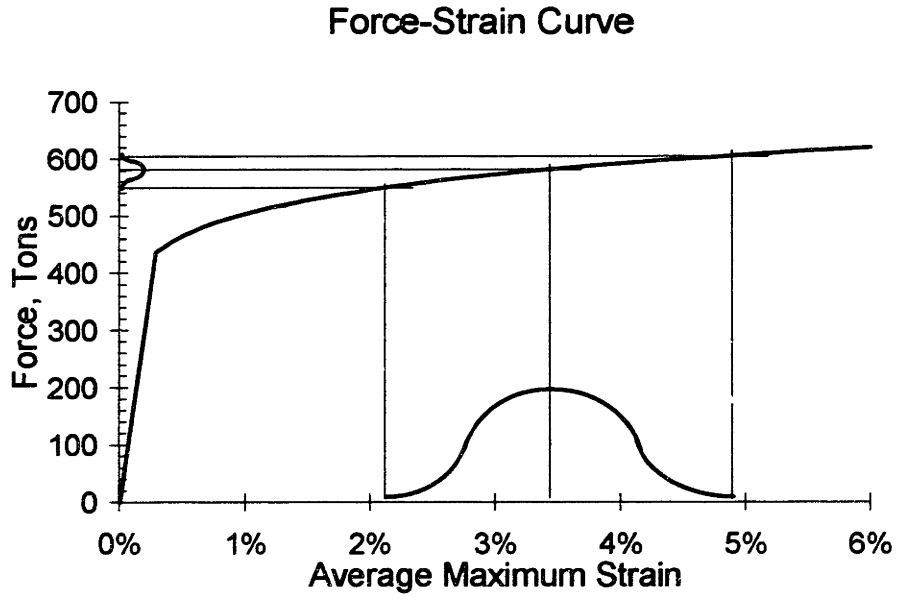

Figure 5.66 Force-strain curve for drape forming

The chart demonstrates the shallow and decreasing slope of the force-strain curve at strains above plastic yielding. The two bell curves superimposed on the chart show

that small changes in the force translate into large changes in strain. Further, it can be seen that as the curve moves up and down slightly, a constant force results in a wide range of strains. This effect is exaggerated at higher strains (and with harder materials) where the slope of the curve is shallower, making it easy to stretch a part much less or much more, even to break a part, under force control if the force or the material properties vary slightly. However, if a part is stretch formed under strain control, the strain does not change when material properties change. Further, under strain control small changes in strain result in small changes in strain and smaller changes in force. Since springback depends on the strain in the material, not the force, it is clear that strain control is superior to force control.

Summary and conclusions to effect of control method on drape forming

The following two pairs of graphs summarize the points made above regarding the sensitivity of the stretch forming operation to changes under strain and force control. The first pair shows the changes in strain, force, and springback ratio for a 10% change in controlled parameter. Figure 5.67a shows changes for a 10% change in strain under strain control, while Figure 5.67b shows changes for a 10% change in force under force control.

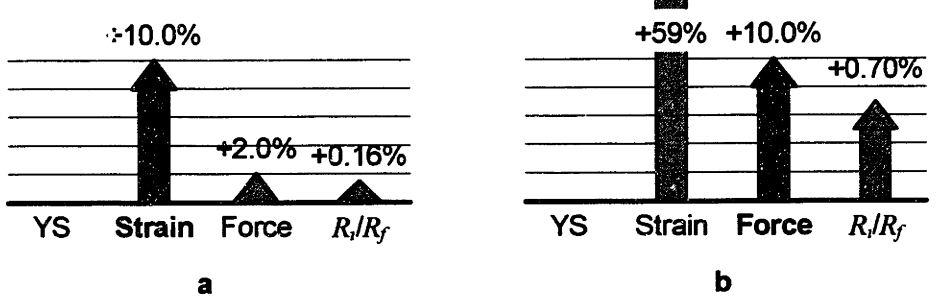

Figure 5.67 Sensitivity of drape forming to a 10% change in strain or force; drape forming; nominal post stretch strain is 1.0%

The difference in sensitivity to changes in the controlled parameter is evident. Changes are about five times greater under force control than under strain control.

The following pair of graphs shows the changes in strain, force, and springback ratio for a 10% increase in yield strength. Figure 5.68a shows the changes under strain control, while Figure 5.68b shows the changes under force control.

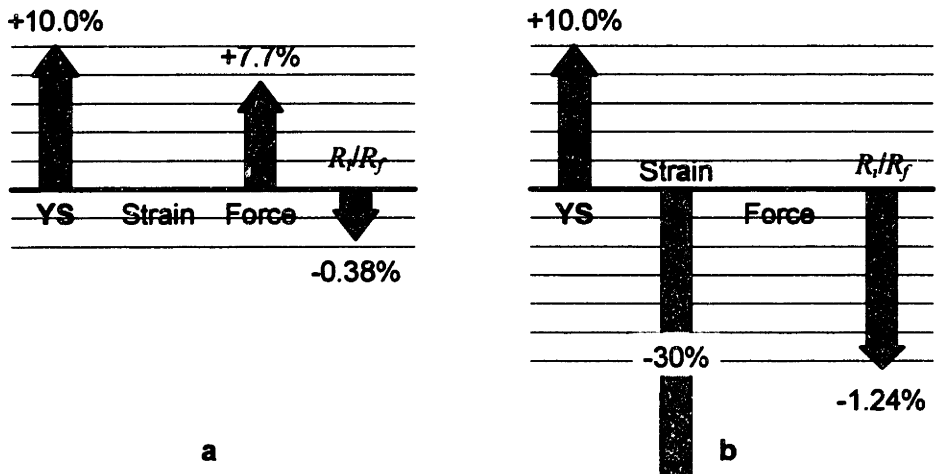

Figure 5.68 Sensitivity of drape forming to a 10% change in yield strength; drape forming; nominal post stretch strain is 1.0%

In this case, the springback ratio is over three times as sensitive to changes in yield strength under force control than under strain control. Further, the strain changes much more under force control than the force changes under strain control. These graphs demonstrate that it is desirable to control the stretch forming operation by strain or displacement, instead of by force. As discussed in the next chapter, the leading edges studied at Vought are formed under force control, not strain control. Therefore, one of the recommendations for improving the stretch forming operation will be to control the operation by strain instead of force.

Given the superiority of strain control over force control, the comparisons made in the rest of this chapter are generally made on the basis of post stretch strain, not force.

5.2.3 Effect of hardening model on drape forming

The strain hardening model used also has a significant impact on the results. In the previous chapter, equations to model four strain hardening models were developed: No IPD, Isotropic, Bauschinger, and Kinematic. As mentioned already, these models differ in how they deal with material that reverses the direction of plastic deformation, and the Isotropic model best represents aluminum.

The following chart shows the difference in springback ratio for the four models.

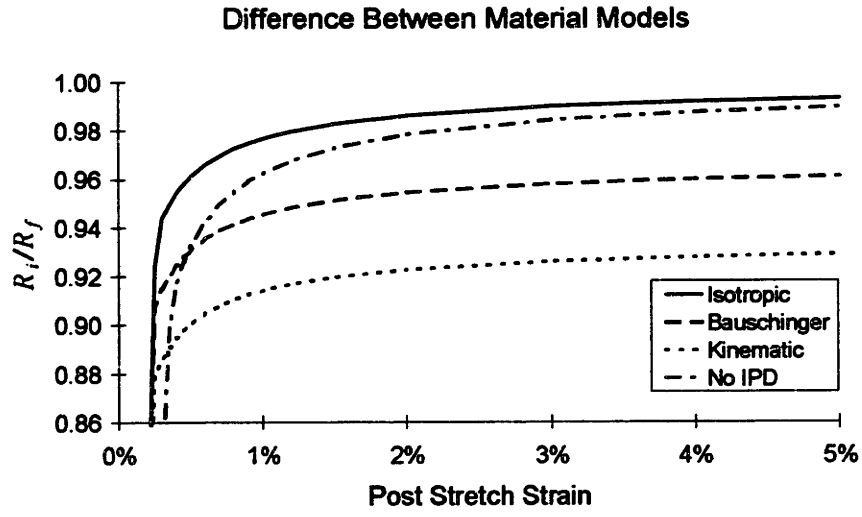

Figure 5.69 Effect of material model on springback ratio as a function of post stretch strain; drape forming

The Isotropic, Bauschinger, and Kinematic models give the same result up to about 0.2% post stretch strain. This is the strain at which the material on the inside of the part that undergoes initial compressive plastic deformation begins to go into tensile plastic deformation, starting with the Kinematic model. The initial compressive plastic deformation reduces the plastic tensile stresses in the Bauschinger and Kinematic models relative to the No IPD model, while the tensile stresses are increased in the Isotropic model. This is the reason for the difference in springback ratio between the models.

The difference between models decreases for thinner material, because with thinner material there is less initial compressive plastic deformation, which is the cause of the differences among the models. If the material is thin enough so that bending causes no plastic deformation, all four curves will be the same (the Isotropic, Bauschinger, and Kinematic models will converge to the No IPD model).

The following chart shows the intermediate stresses predicted by the four models with a post stretch of 0.5%. The initial stress is also shown.

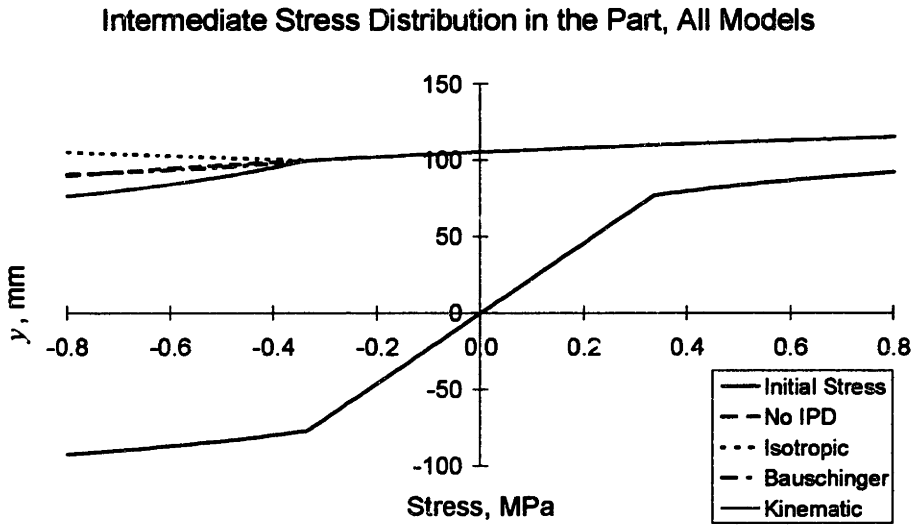

Figure 5.70 Difference in intermediate stress distribution due to hardening model; post stretch strain = 0.5%; drape forming

The effect of the initial compressive plastic deformation is clearly seen. The following chart shows the predicted residual stresses, multiplied by a factor of 10.

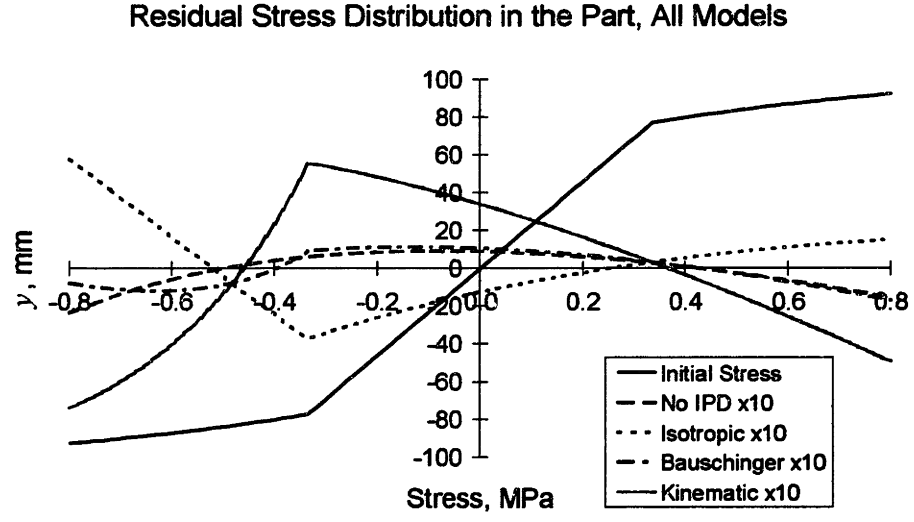

Figure 5.71 Difference in residual stress distribution due to hardening model; post stretch strain = 0.5%; drape forming

The residual stresses differ significantly from one-another. The isotropic model predicts tensile residual stresses at the outside of the part and compressive residual stresses on the inside, which is opposite of what is predicted by the other models. The differences in residual stresses will cause different responses to chemical milling and routing.

Summary and conclusions to effect of strain hardening model

The strain hardening model affects the residual stresses and the springback ratio. What happens to the material initially in compressive plastic deformation as it is brought into tensile plastic deformation is the source of difference between the models. The cumulative strain hardening for this material is the greatest with the Isotropic model, and results in the highest springback ratio and in tensile residual stresses on the outside of the part. The Isotropic model is the default model in this chapter.

5.2.4 Effect of plane strain parameter adjustment on drape forming

As presented in the previous chapter, the standard uniaxial and plane strain material parameters are

Property	Uniaxial, x	Plane Strain, x
E	68947 MPa	75766 MPa
K	320.9 MPa	381.2 MPa
n	0.21	0.21
ε_Y	0.112%	0.123%
σ_Y	77.0 MPa	84.8 MPa

Table 5.2 Uniaxial tensile test and plane strain stress-strain curve parameters

The following chart shows the change in springback ratio as a function of post stretch strain when plane strain parameters are used.

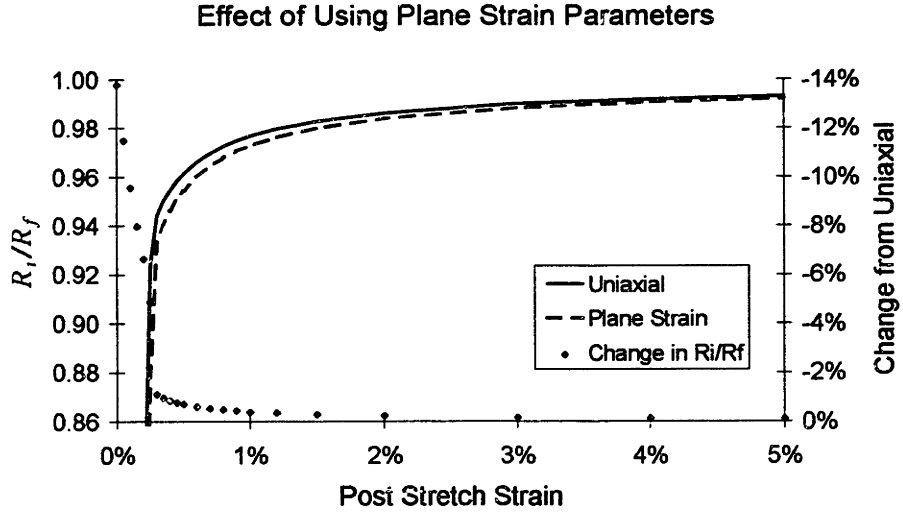

Figure 5.72 Effect of plane strain parameters on springback ratio; drape forming; strain control

With no post stretch, use of plane strain parameters decreases the springback ratio by 14%, increasing the predicted springback. At post stretch strains over 1%, the change in springback ratio is small—about 0.1% to 0.2%. Therefore, it may not be necessary to use the plane strain parameters when predicting springback at post stretch strains over 1% and as a function of post stretch strain. However, the difference would be much greater if the predictions were a function of post stretch force rather than strain.

The strain conditions of most parts are somewhere between plane strain uniaxial strain when the parts are being stretched. Stretch of leading edges will be nearly plane strain because the width is much greater than the length (direction of pull).

5.2.5 Effect of chemical milling on drape forming

As mentioned in the previous chapter, chemical milling is assumed to take material off the *inside* of the part, and the only changes in stress are those that occur as the strains change to bring the moment and force to zero after the material has been removed, and these changes are entirely elastic.

The following chart shows how the springback ratio changes as the amount of material removed is increased from nothing to half (0.8 mm) of the original part thickness. The amount of post stretch strain was 0.5%, and the isotropic model was used.

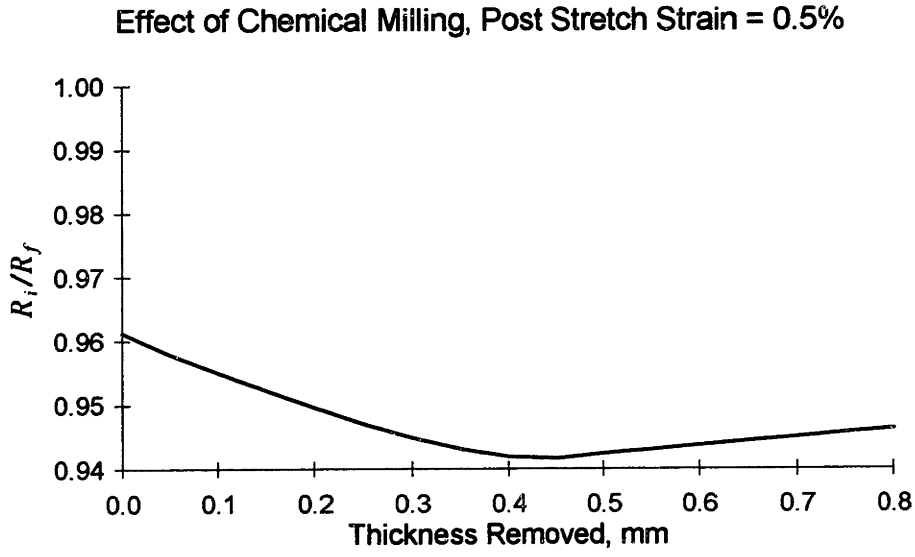

Figure 5.73 Effect of chem mill on springback ratio as a function of thickness removed ; post stretch strain = 0.5%

The chart reveals that (with the Isotropic model), removing up to half of the material always increases the springback, with the largest change in springback at just over 25% (0.4 mm) of the material removed. The effect of chem mill on the springback ratio decreases with increasing post stretch strain. At 1% post stretch strain, the change in springback ratio is -0.70% for 0.2 mm removed and -1.16% for 0.6 mm removed. At 3% strain, the changes are -0.30% and -0.52%, respectively.

The strain hardening model used significantly impacts the magnitude and direction of the change in springback ratio due to chem milling, because of the different residual stresses in the material.

Changes in the springback ratio for the four material models are shown in the following chart. The significant changes for and differences between the Isotropic and Kinematic models can be seen. The model predictions converge at about t_{cm} = 0.43 mm because all of the material that went into initial compressive deformation is removed at this point, and, therefore, so is the only difference between the models.

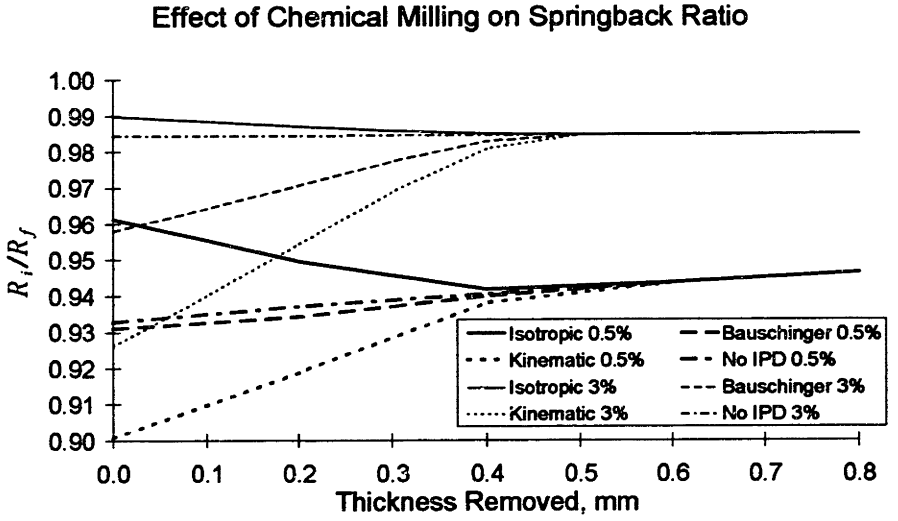

Figure 5.74 Effect of chem mill thickness removed on springback ratio for all strain hardening models; post stretch strain = 0.5% and 3.0%; drape forming

This chart shows some expected and some unexpected results. For the Isotropic model, the change in springback is less at higher post stretch strains. For the No IPD model, the effect of chemical milling is slight and decreases to almost nothing at 3% strain. For the Bauschinger and Kinematic, the change in springback is greater at higher strains for thicknesses of material removed less than 0.5 mm. This is because

according to these models the residual stress distribution in the part is greater at higher post stretch strains than at lower strains.

Summary and conclusions to effect of chemical milling

The effect of chemical milling on springback depends on the amount of material moved, the amount of post stretch strain, and which strain hardening model best represents the material. For the Isotropic and No IPD models, the change in springback ratio reduces as post stretch strain increases, while for the Bauschinger and Kinematic models, the change in springback ratio increases. Up to a little over 0.43 mm (the border between elastic and plastic compression on the inside), the springback ratio decreases for the Isotropic model and increases for the No IPD, Bauschinger, and Kinematic models as the amount of material removed increases; after this, the springback ratio increases as more material is removed and all the models converge because there is no longer any difference among the models since all the material initially compressively plastically deformed is removed at this point.

Although aluminum hardening is better represented by the Isotropic hardening model than other models, it may be more accurate with an A value slightly less than 1. In this case, the effect of chemical mill is probably negligible for post stretch strains over 1-2%.

5.2.6 Effect of parameters on stretch wrap forming sheet

In this subsection, the effects of changing parameters in the stretch wrap forming operation are evaluated.

Effect of pre stretch strain on springback ratio

The following chart shows the effect of changing the pre stretch strain on the springback ratio. The parameters are standard, except that the radius of curvature has been reduced from 300 mm to 160 mm to more strongly capture the effect of bending.

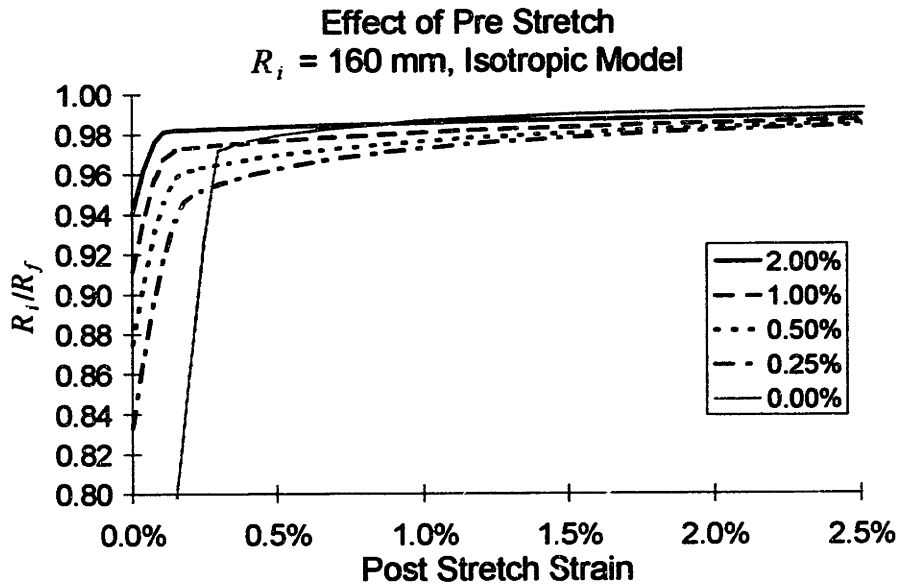

Figure 5.75 Effect of pre stretch on springback ratio; R_i = 160 mm; Isotropic model

Except for the no pre stretch curve, the results are as expected: a higher pre stretch strain means a higher total strain when the post stretch strain is added to it, and so increasing pre stretch strain reduces springback. However, as the chart shows, the no pre stretch part has more springback at first, but after about 1.1% post has less springback than all of the pre stretched parts. This is because for these parameters the pre stretch eliminates initial compressive plastic deformation, which strain hardens the material and reduces springback. In fact, if the springback ratio is shown as a function of total strain (pre stretch, midplane elongation during wrap, and post stretch), this is more clearly seen, as shown in the following chart.

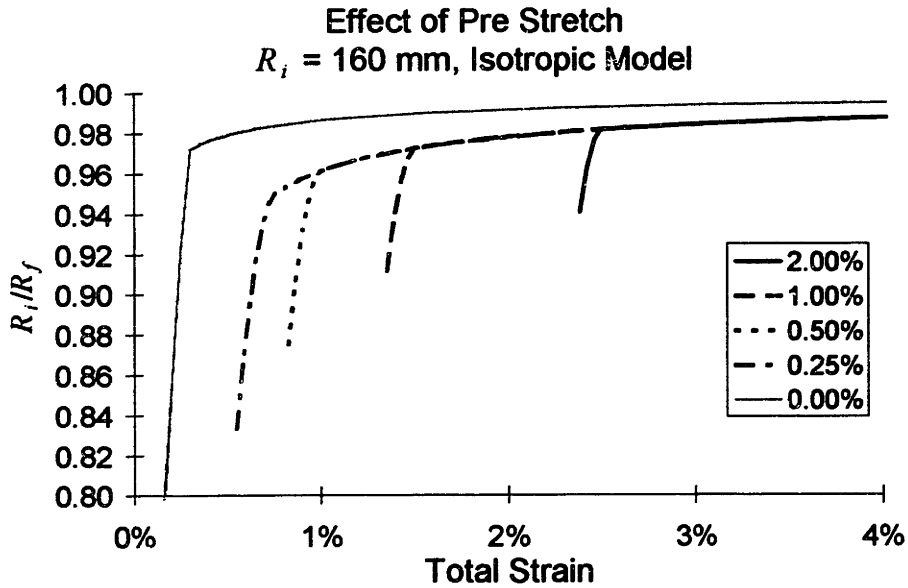

Figure 5.76 Effect of pre stretch on springback ratio; R_i = 160 mm; Isotropic model

The first interesting insight from the above chart is that the reduction in springback from the no pre stretch case is much stronger when viewed as a function of total strain. The second is that after a small amount of post stretch strain, all of the different pre stretch curves lie on the same curve as a function of total strain. This second point makes sense in retrospect, because since there is no initial plastic deformation, the important parameter is the total amount of strain.

Elongation from wrap

Based on this last observation, it becomes apparent that when there is no compressive plastic deformation in the wrap (when the pre stretch is large enough and t/R_i is small enough), it is possible to use the No IPD model to predict the springback ratio if there is enough post stretch strain to pull the entire part into tensile plastic deformation. This is shown in the following chart where the springback ratio is plotted as a function of the total strain for No IPD drape forming (total strain is simply the post stretch strain) and for pre stretch forming to various strains (total strain is the pre stretch strain plus the elongation during wrap plus the post stretch).

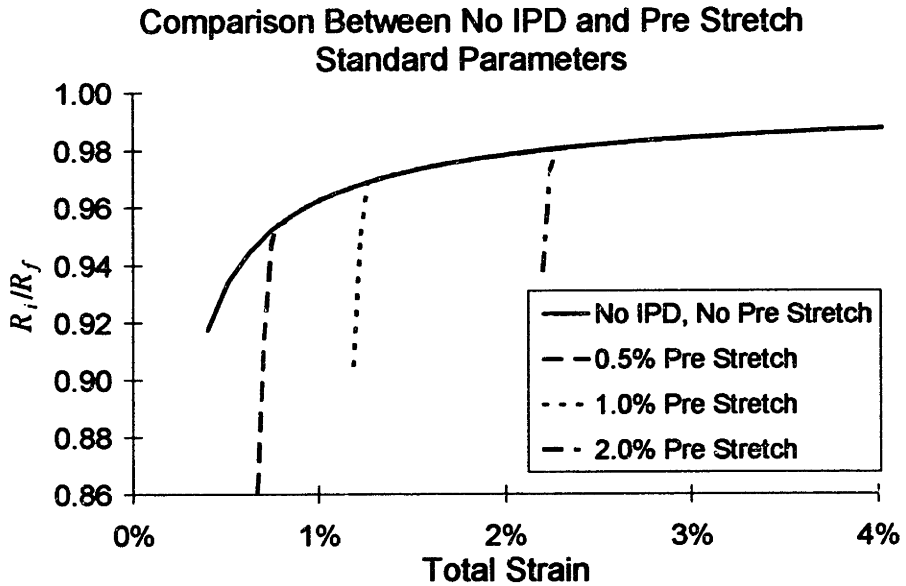

Figure 5.77 Comparison of springback ratios for No IPD model and pre stretch

As predicted, the curves are exactly the same after the parts are brought completely into tensile plastic deformation. This is because in no case is there compressive plastic deformation. Therefore, the No IPD analytical equation has another use, because it is much simpler and faster to use the single equation than to perform a numerical summation. However, this can't be used for most extrusions because they are high enough (tall in the thickness direction) that they have a significant amount of compressive plastic deformation even with pre stretch.

Effect of timing of strain on springback ratio

An interesting question to ask is: what is the effect on springback of dividing up the combined pre and post stretch strain? The following chart shows how the springback ratio changes for a combined pre plus post stretch of 3.0% as its timing varies from all in the post stretch to all in the pre stretch. Pre stretch and post stretch forces are also shown.

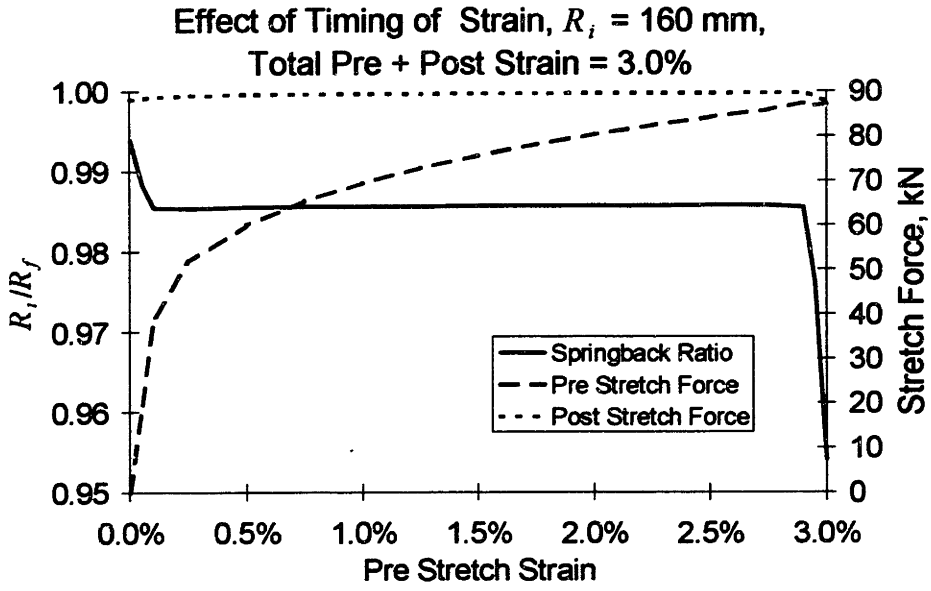

Figure 5.78 Effect of timing of 3% pre plus post stretch strain on springback ratio; R_i = 160 mm

The chart reveals that springback is lowest when all of the strain is in the post stretch; then it remains essentially level until it drops dramatically when almost all of the strain is in the pre stretch. At very low pre stretch strain, the same effect is seen as in Figures 5.75 and 5.76: initial compressive plastic deformation caused by pure bending reduces springback. At the highest pre stretch strain, when almost no post stretch is given, the springback ratio is reduced because the material on the inside has a significantly reduced stress due to the elastic reduction in strain caused by bending under constant force, which is not brought back into the plastic range due to the low post stretch strain. Even though the pre stretch and post stretch strains sum to 3.0%, the midplane elongates as the part is wrapped around the die; it elongates 0.39% at 3% pre strain.

As already mentioned, the strain hardening model strongly affects springback when there is initial compressive plastic deformation. As the hardening parameter A decreases from 1 (at which it represents Isotropic hardening), the springback ratio in the no pre stretch case decreases, and if A is decrease far enough (the Bauschinger effect is strong enough), the initial compressive plastic deformation increases springback relative to the pre stretch cases.

Effect of pre stretch strain on midplane elongation

The midplane elongates because as the part is wrapped around the die at constant force, the stresses decrease elastically and increase plastically. Since elastic decreases in stress are much faster than plastic increases, the midplane elongates to maintain a constant force. If the part is thick enough and the pre stretch strain small enough, the inside will go into compressive plastic deformation. The following chart shows how the midplane strain increases as a function of the pre stretch strain for a part that has compressive plastic deformation on the inside at low pre stretch strains.

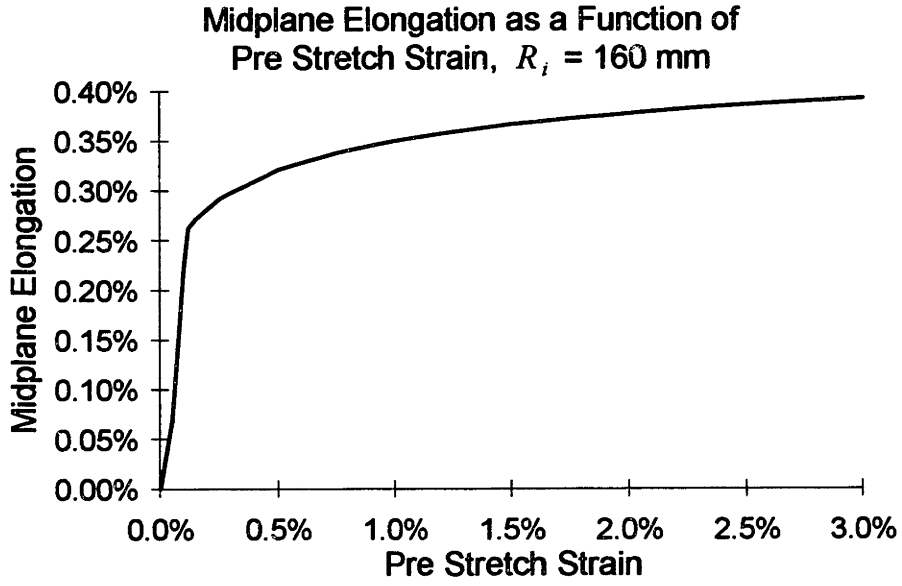

Figure 5.79 Effect of pre stretch strain on midplane elongation; R_i = 160 mm

At pre stretch strains below about 0.2% the inside of the part goes into compressive plastic deformation. At pre stretch strains above about 0.2%, the inside of the part no longer goes into compressive plastic deformation. The elongation increases roughly in proportion to the pre stretch force.

Summary and conclusions to effect of parameters on stretch wrap forming sheet

Pre stretch reduces the amount of initial compressive plastic deformation, thus increasing springback over the no pre stretch case. As a function of total strain (pre stretch, wrap elongation, and post stretch), the amount of pre stretch has no effect on springback after the first about 0.1% or 0.2% post stretch strain, when the pre stretch eliminates all initial compressive plastic deformation.

If a total amount of pre stretch plus post stretch strain is specified, there is a wide range of combinations of the two which give essentially the same springback. However, near all pre strain, springback increases, while near all post strain, springback decreases. Elongation due to wrapping increases quickly at low pre stretch strains, and continues to increase at roughly the rate of increase in pre stretch force.

A significant but unaccounted-for (by the model developed in this thesis) benefit of pre stretch is that the compressive strains on the inside of the part are greatly reduced. Reduction of compressive strains is very important for extrusions, which may buckle on the inside if they were subjected to pure bending. For this reason, extrusions are nearly always pre stretched. Stretch wrap forming of extrusions is the next topic.

5.2.7 Effect of parameters on stretch wrap forming extrusions

As mentioned in the previous chapter, lateral and shear strains are ignored in this model. Although these are likely to affect the part shape, especially angle and flatness, they should not have much of an effect on contour and springback.

Geometry

The following geometries will be used for four cross-sectional shapes, I, L, T, and H. They all have the same cross-sectional area, 700 mm^2. The Isotropic model is used in all cases, except when the effect of the material model is being investigated. All dimensions are in mm. Nomenclature was presented in the previous chapter.

I geometry: $H = 50$, $t_B = t_T = 5$, $t_M = 40$, $w_B = w_T = 50$, $w_M = 5$

L geometry: $H = 50$, $t_B = 5$, $w_M = w_T = 10$, $t_T = 0$, $t_M = 45$, $w_B = 50$

T geometry: $H = 50$, $t_T = 5$, $w_M = w_B = 10$, $t_B = 0$, $t_M = 45$, $w_T = 50$

H geometry: $H = 50$, $t_B = t_T = 20$, $t_M = 5$, $w_B = w_T = 5$, $w_M = 50$

These geometries are shown in the following diagram.

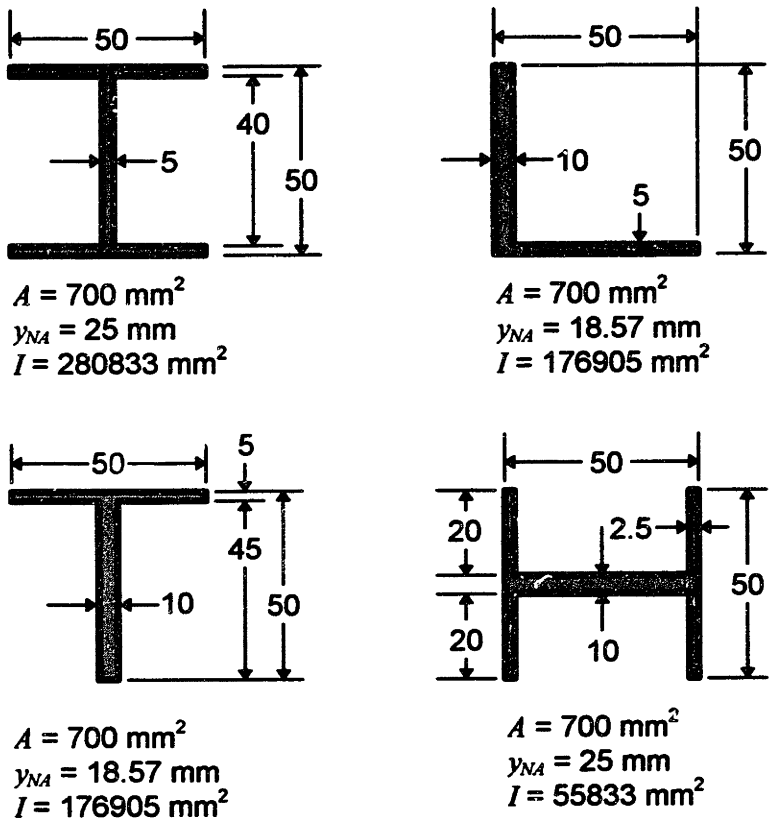

Figure 5.80 Extrusion cross-section geometries; all dimensions in mm

The radius of curvature is always defined at, and it is assumed that all extrusions are bent around, y_{NA}, the vertical centroid of the cross-sectional area. Note that this location varies from part to part, even though all have the same height and width. Due to vertical asymmetry in the T and L cross-sections, this point does not remain the neutral axis in pure bending.

Comparisons

Different cross-sections have different amounts of springback even in pure bending. If each part is bent to an initial radius of curvature of 300 mm and released, the springback ratios are 0.9624 for I, 0.9578 for T and L, and 0.9476 for H. Springback increases when there is less material at the outside, primarily because the moment is decreased much more quickly when more material is at the outside. Therefore, an I cross-section has the least springback, and an H cross-section has the most.

The following chart shows the effect of the cross-section on the springback ratio as a function of post stretch strain with 1% pre stretch strain.

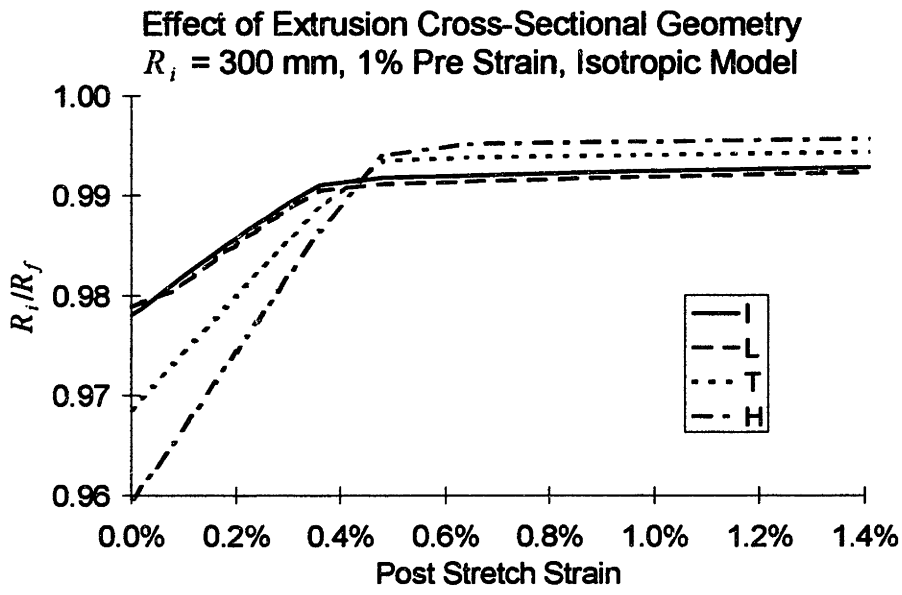

Figure 5.81 Effect of cross-section geometry on springback ratio; pre stretch strain = 1%

The first conclusion to draw from this chart is that the springback of a stretch formed extrusion is much less than the springback of a sheet. At lower strains, the difference is the greatest: the springback ratio of the standard sheet under the same conditions is 0.9053. Above about 0.4% post stretch strain, all geometries have a springback ratio of over 0.99, while at 1% post stretch strain, the springback ratio for the standard sheet is 0.98. For small post stretch strains, less than about 0.5%, T and H cross-sections have more springback than I and L cross-sections, while for larger amounts of strain, the reverse is true.

The following chart shows the stress after a 1.0% pre stretch (thick, horizontal line), after wrap (medium lines), and after a 1.0% post stretch (thin lines) for the four cross-sections.

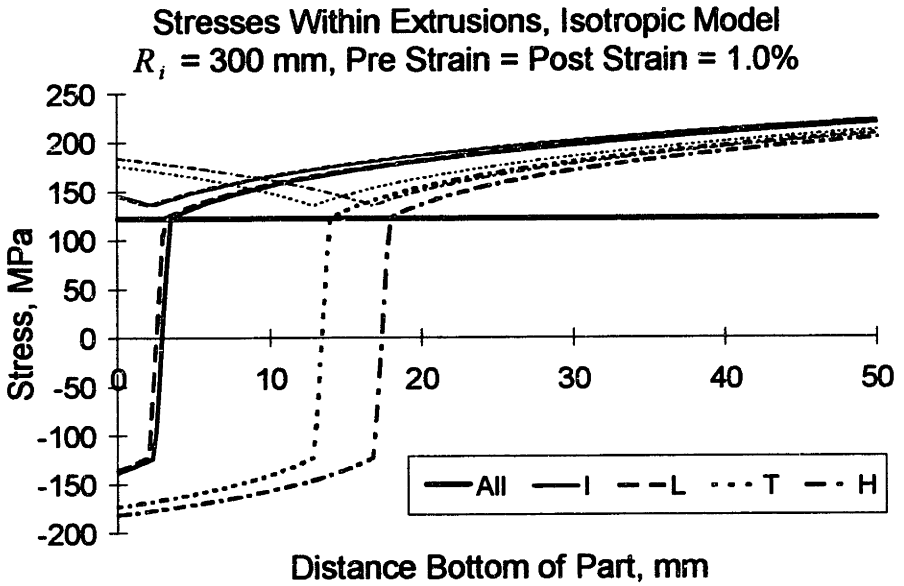

Figure 5.82 Effect of cross-section geometry on stresses within the part; pre stretch strain = post stretch strain = 1.0%

Because they have very wide sections at the inside of the part, both the I and the L extrusions have very little plastic deformation on the inside of the part; instead, the midplane of these parts elongates about 7.2% during the wrap. This is why they have less springback at very low post stretch strains. The T and H extrusions elongate less during wrap and have more compressive plastic deformation on the inside. This is why without a post stretch they have more springback, while a higher post stretch strains they have less springback (because the initial compressive plastic deformation hardens the material, causing higher stresses once tensile plastic deformation is achieved).

As expected, the analytical model predicts that a smaller radius of curvature reduces the springback.

At a radius of curvature of 600 mm, the effect of pre stretch on springback of extrusions is of the same form as it is for sheet metal: as a function of total strain, a higher pre stretch strain increases springback. This is shown in the next chart for a T extrusion.

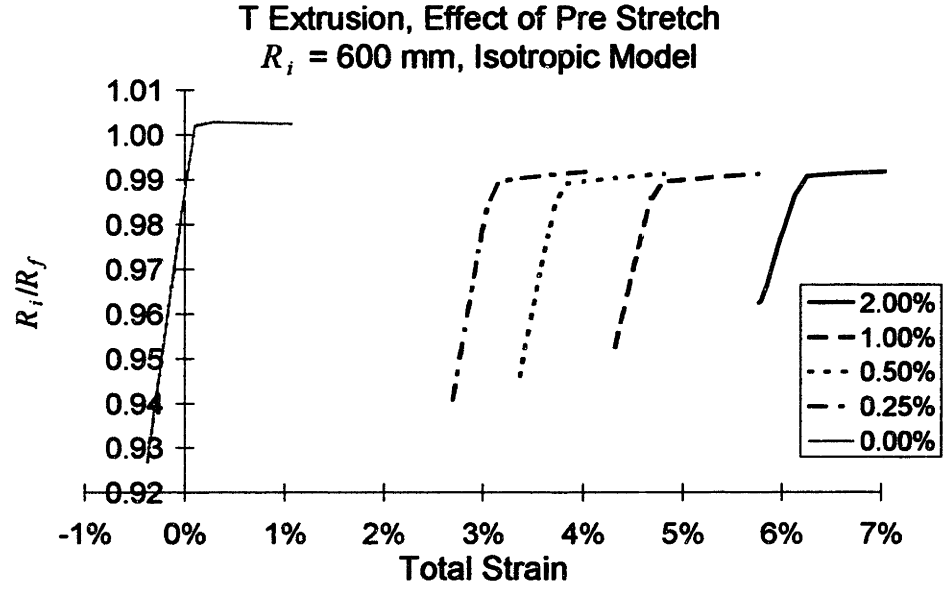

Figure 5.83 Effect of cross-section geometry on stresses within the part; pre stretch strain = post stretch strain = 1.0%

Each part received between zero and 1.4% post stretch strain. This chart also demonstrates that midplane elongation is significant for extrusions and that when considering strain control of extrusions, the amount of elongation that occurs during the wrap must be included in a total strain measure.

Summary and conclusions to effect of parameters on stretch wrap forming extrusions

Extrusions spring back less than sheet. The cross-sectional shape of an extrusion has a significant effect on the springback. A tighter radius of curvature reduces springback. As a function of total strain, pre stretch increases springback because it reduces the amount of initial compressive plastic deformation.

5.2.8 Effect of routing on extrusions

In this sub-section, the effect of routing on springback of extrusions is examined. Only the T-shaped extrusion is considered (an upside-down L-shaped extrusion would give the same predictions), because this is the most likely cross-section to be routed on the inner side. The isotropic hardening model is used; results will be different for other hardening models. Routing is modeled as a separate step after stretch forming.

The following chart shows the effect of increasing the amount of routing on total springback. R_R is the radius of curvature after routing.

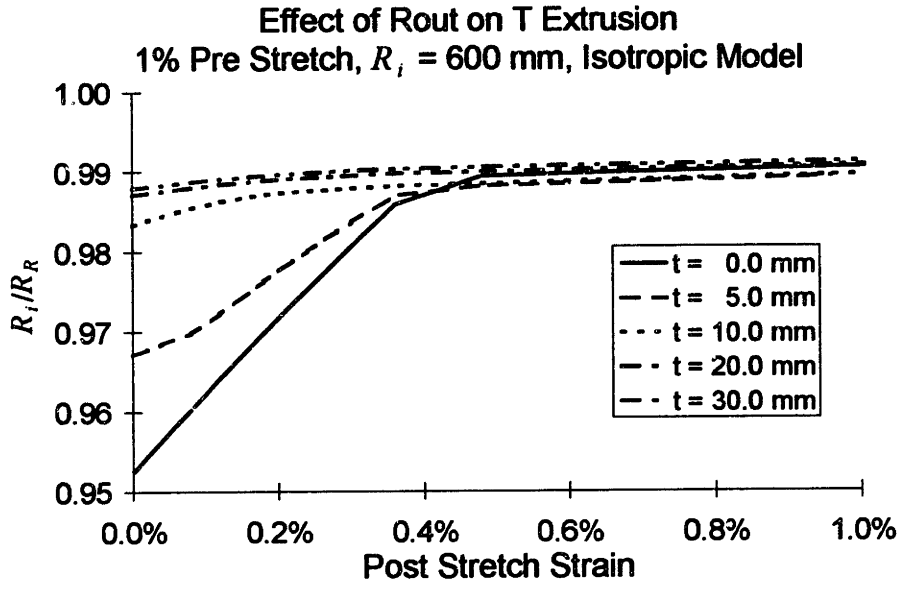

Figure 5.84 Effect of routing on T extrusion springback ratio; R_i = 600 mm; pre stretch strain = 1.0%

The chart shows that at low post stretch strains the springback ratio increases significantly as more material is removed, by causing the contour to close. At higher strains, the direction of contour change depends on the amount of material removed. For 5 mm and 10 mm removed, the contour opens, while for 20 mm and 30 mm removed, the contour closes. The following two charts investigates these phenomenona. The first chart is for no post stretch and 20 mm removed.

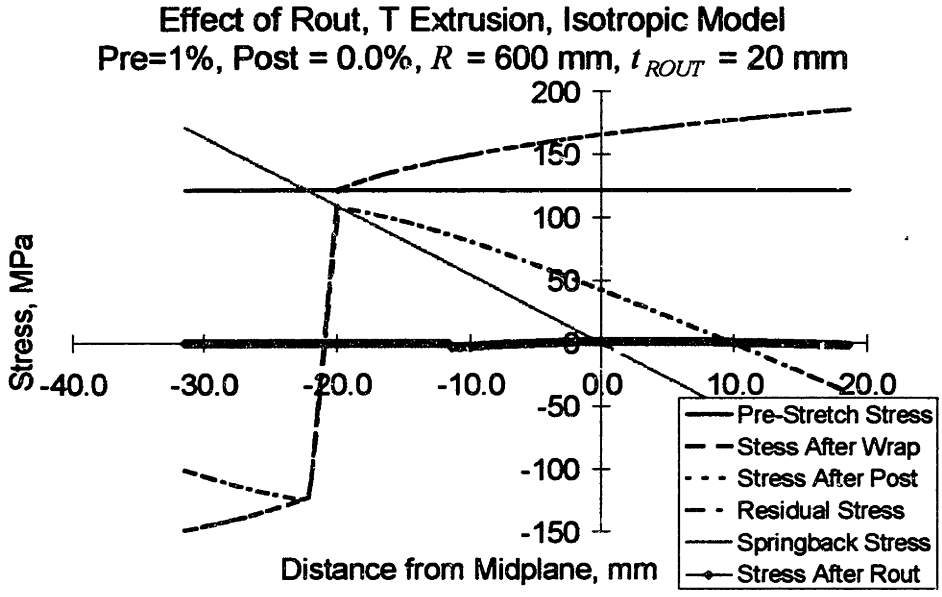

Figure 5.85 Effect of routing on stresses in a part; R_i = 600 mm; pre stretch strain = 1.0%; no post stretch strain; thickness removed = 20 mm

The chart shows that the part closes up because much of the material removed was in compression. Removal of the portion of the part that went into initial compressive plastic deformation significantly affects the springback ratio.

The following chart shows the same case, but with a post stretch of 1.0%.

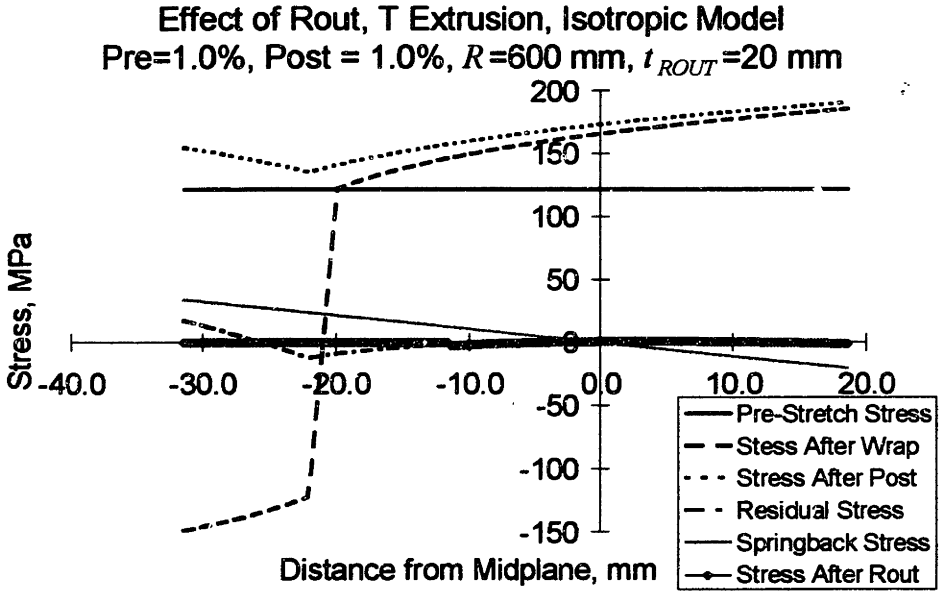

Figure 5.86 Effect of routing on stresses in a part; R_i = 600 mm; pre stretch strain = 1.0%; post stretch strain = 1.0%; thickness removed = 20 mm

In this case, the residual stresses are much lower, and the moment contributed by the removed portion of the part was essentially zero, so the part exhibited almost no opening up at all.

The following chart shows the effects of routing and cross-section on springback.

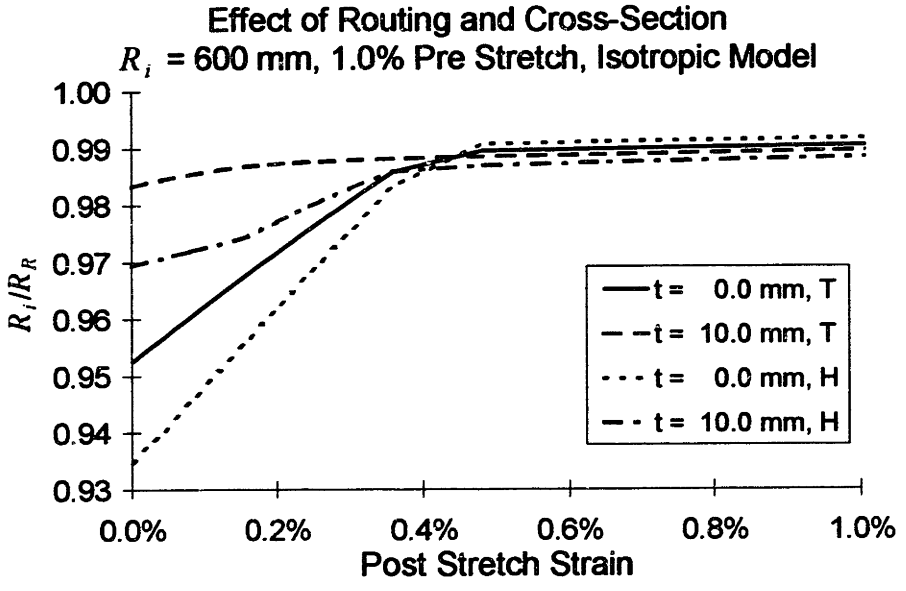

Figure 5.87 Effect of routing and cross-section on springback ratio; R_i = 600 mm; pre stretch strain = 1.0%

For a radius of curvature of 600 mm and 1.0% pre stretch, while the H cross-section springback ratio is increased by routing for small post stretch strains, it is decreased for larger strains, and the difference at large strains remains significant. This is the same behavior as that of a T cross-section, except that the effect is greater for the H cross-section part at higher strains.

The following chart shows the effect of routing with everything exactly the same, except that the Bauschinger model is used instead of the Isotropic model.

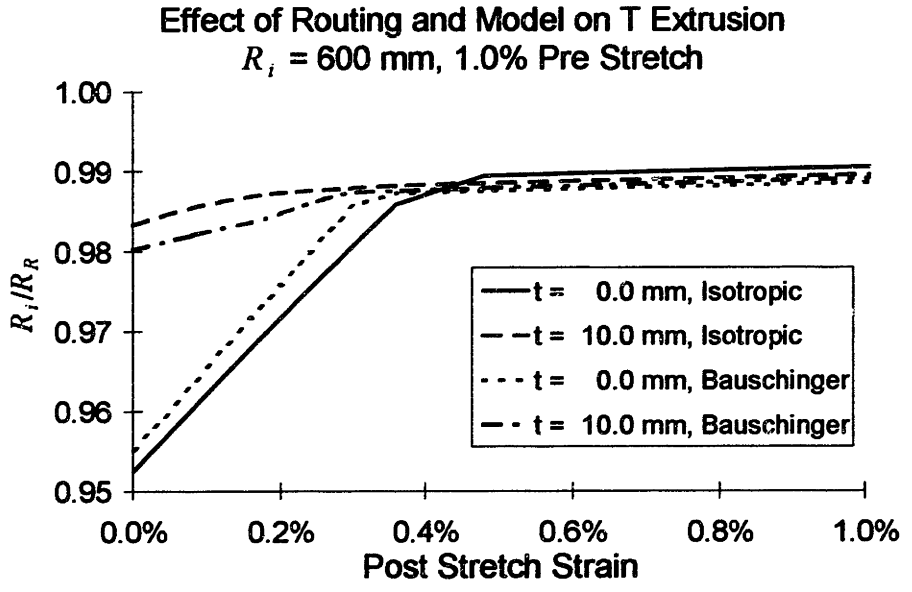

Figure 5.88 Effect of routing and strain hardening model on T cross-section springback ratio; R_i = 600 mm; pre stretch strain = 1.0%

The chart reveals that for the Bauschinger model the part always closes when 10 mm are routed from the inside, the amount of closing being great for small amounts of post strain and little for larger amounts. The part always closes because the residual stress is always compressive on the inside for the Bauschinger model, even at higher post stretch strains.

The following chart shows the effect of pre stretch strain on the change in springback caused by routing.

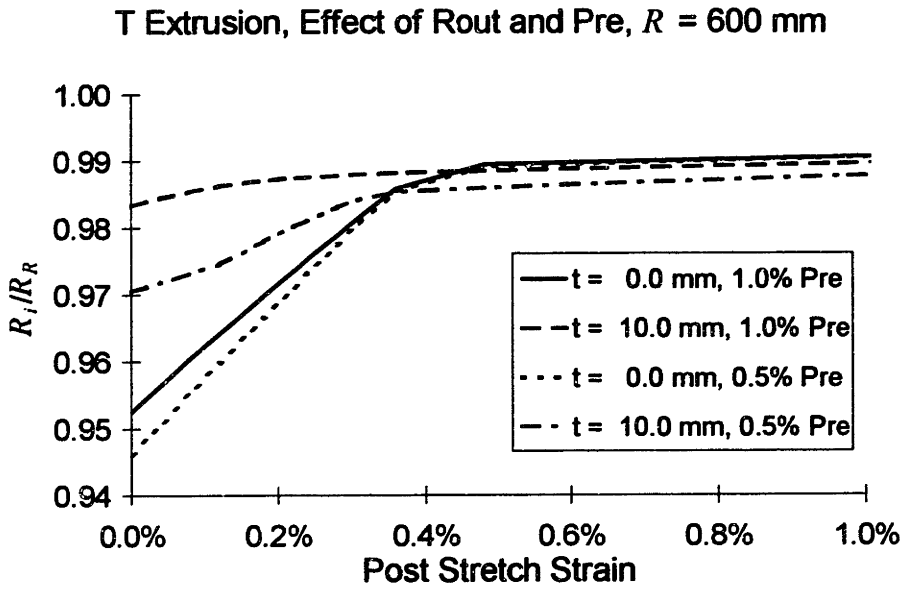

Figure 5.89 Effect of routing and pre stretch on T cross-section springback ratio; R_i = 600 mm

The chart shows that below about 0.4% post stretch strain, routing 10 mm off the inside of a T cross-section extrusion significantly increases springback, and above about 0.4% post stretch strain it slightly decreases it. The change in springback ratio at higher post stretch strains is less for a higher pre stretch. Although not shown, the results are essentially the same if the total strain is used instead of post stretch strain.

Summary and conclusions to effect of routing on extrusions

Routing has a significant effect on springback. This effect depends upon the extrusion cross-section, the amount of pre and post stretch, the amount of material removed, and the strain hardening behavior.

5.2.9 Effect of friction

The significant effect that friction can have on the stretch forming operation is now investigated. Friction affects the stretch forming operation by reducing the longitudinal forces, and therefore the strains, in the part during the post stretch. Friction does not affect pre stretch, because the part does not touch the die in pre stretch. Since normal forces are very low as the material is brought into contact with the die during wrap, friction is assumed to be negligible during wrap.

Drape forming calculations

The effect of friction is first investigated with drape forming. In this case, the material is wrapped around the die 45° on each side (for a total bend angle of 90°) and then post stretched with a force at the free end of the part of F^* = 80.0 kN. The coefficient of friction μ is varied from 0.0 to 0.3. The coefficient of friction for lubricated metal on a solid metal die is generally between 0.1 and 0.2. Numerical summation is used to approximate the geometry. The results are shown in the following charts and discussed subsequently. As described in the last chapter, only the right half of the part is modeled, from the point of contact to where the part is horizontal (the top). The following chart shows the stretch force as a function of the angle β from the point of contact. Since θ is 45°, β = 0 represents the free end of the part and β = 45° represents the top of the part.

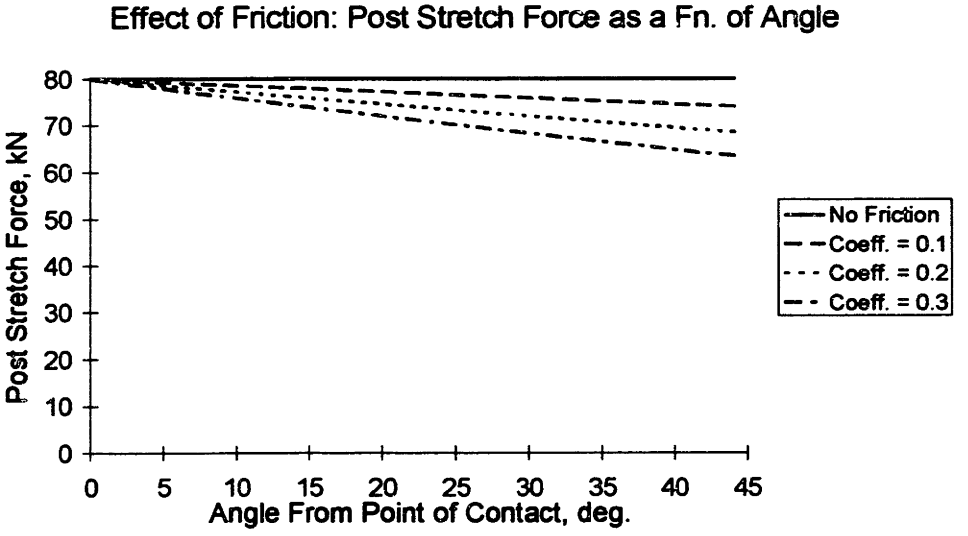

Figure 5.90 Effect of friction on post stretch force in part; No IPD model

The chart shows that the stretch force decreases roughly linearly with increasing angle from point of contact, and roughly linearly with increasing coefficient of friction. For μ = 0.3, the stretch force at the top is decreased by 21%. Because the force decreases, so does the strain, as shown in the following chart.

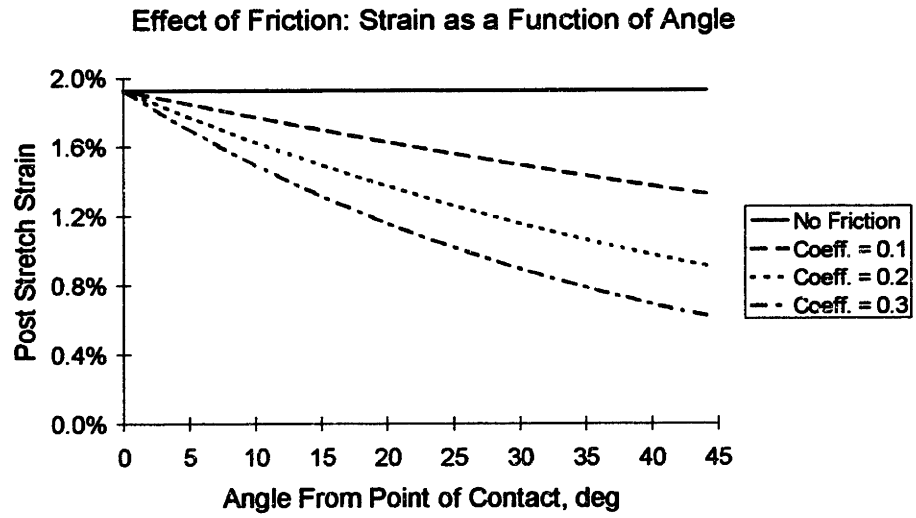

Figure 5.91 Effect of friction on post stretch strain in material; No IPD model

Strain is much more sensitive to friction than force. For $\mu = 0.3$, the strain at the top is 32% of what it is at the ends (which is also what it is at the top without friction). The springback ratio is a function of the strain and is shown in the next chart.

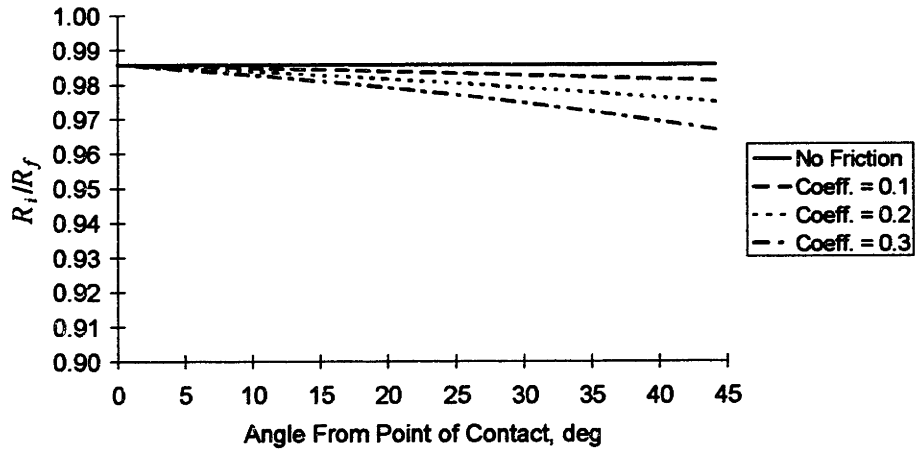

Figure 5.92 Effect of friction on springback ratio in material; No IPD model

The springback ratio is not as sensitive to the decrease in force as is the strain. For $\mu = 0.3$, the springback ratio is 1.9% lower at the top than at the point of contact. The effect of the increase in springback can be measured by the change in angle and the contour deviation at the point of contact (POC), as shown in the following chart.

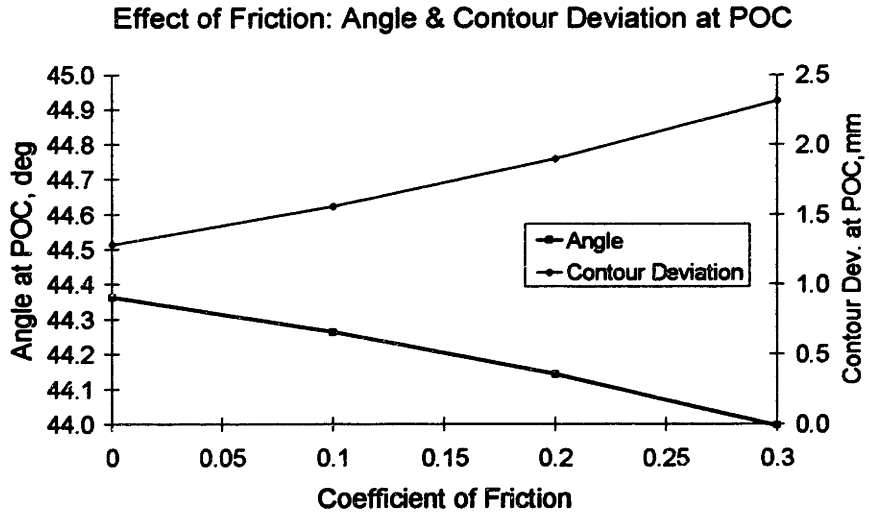

Figure 5.93 Effect of friction on final total angle; No IPD model

As expected, the final angle θ_f decreases (there is more springback) with increasing friction. Lastly, the amount of elastic recovery along the length of the part is also affected by friction because as the coefficient of friction increases, the part is stretched less. However, the difference in change in length is insignificant—about 0.05 mm (0.002"), which, over the length of the part initially in contact with the die, 235.62 mm, is only a change of 0.04%.

The following table summarizes the effect of friction from the above charts.

	At top	At top	At top	At end	At end
μ	Force	Strain	R_i/R_f	Angle	Contour Dev
0.0	100% (=80 kN)	100% (=1.93%)	100% (=0.9859)	100% (=44.36°)	100% (=1.29 mm)
Chg 0.1	- 7.4%	-21.2%	-0.5%	-0.2%	+21%
Chg 0.2	-14.3%	-52.8%	-1.1%	-0.5%	+48%
Chg 0.3	-20.6%	-67.7%	-1.9%	-0.8%	+80%

Table 5.3 Effect of friction on force, strain, springback ratio, angle, and contour deviation

The most important thing to note from this table is that while friction has a very significant effect on the force and even more on the strain, its effect on the springback ratio is much less, and its effect on the final angle at the free end is even less. However, the effect on contour is significant, increasing the contour deviation at the

end of the part by 80% (1 mm) at $\mu = 0.3$. As will be noted shortly, as the post stretch strain is reduced to low levels, the effect of friction on the springback ratio and contour increases significantly.

Effect of friction on stretch wrap forming

The effect of friction on stretch wrap forming is now investigated. Standard parameters are used, except that the radius of curvature is 160 mm. The length of the part in contact with the die is 160 mm, so that the bend angle from the top of the die is 57.3°. The pre stretch strain is 1.5%. The coefficient of friction is $\mu = 0.2$. The first chart shows the force and post stretch strain as a function of the length of the part form the top.

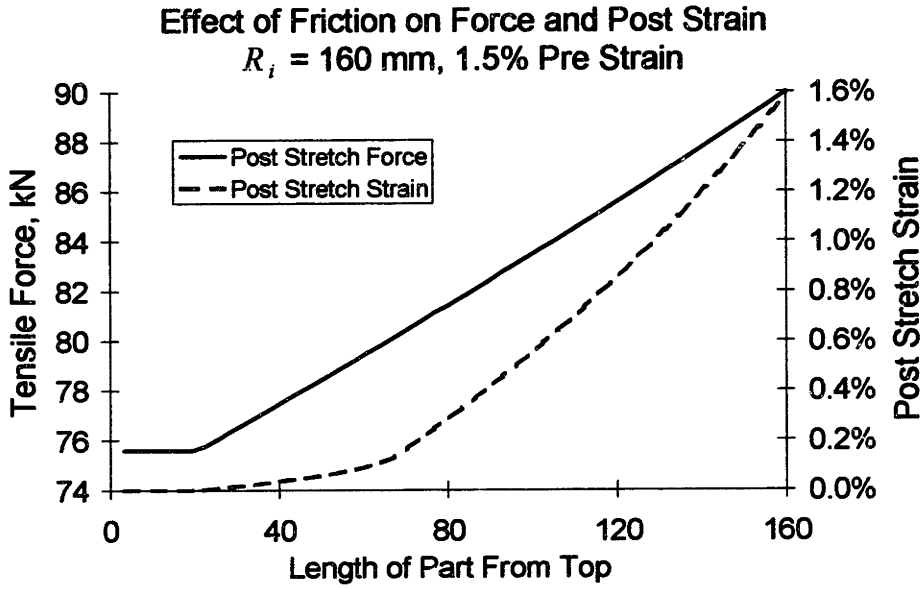

Figure 5.94 Effect of friction on post stretch force and strain; R_i = 160 mm; $\mu = 0.2$; pre stretch strain = 1.5%; post stretch force = 90 kN

The very top of the part did not receive any post stretch due to the effect of friction. Since the part is already at 75.6 kN of force at the end of wrap, this is the minimum force that the part sees during the post stretch. The post stretch strain varies significantly within the part, from zero at the top up to 1.6% at the point of contact. The following chart shows the post stretch force and springback ratio in the part.

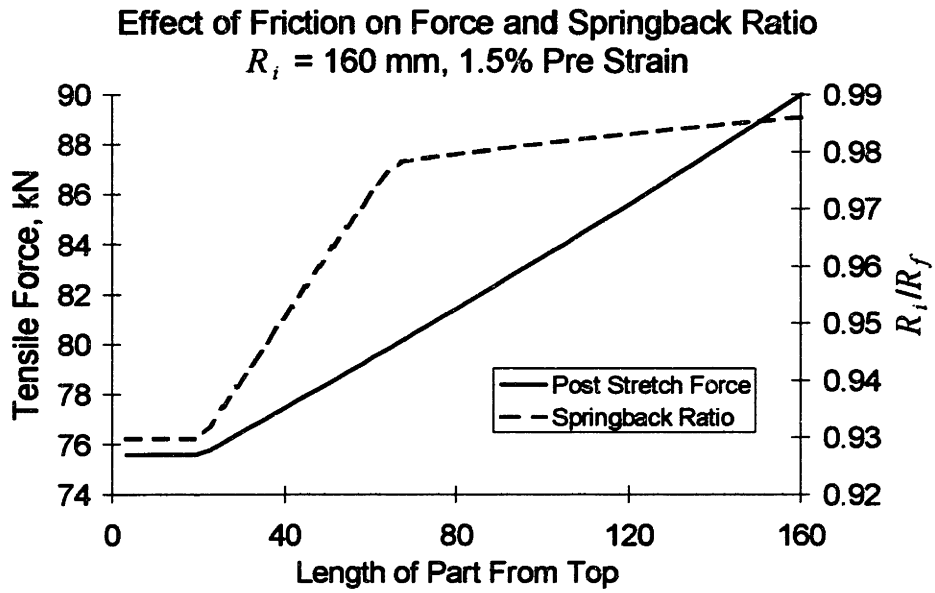

Figure 5.95 Effect of friction on post stretch force and springback ratio; μ = 0.2; R_i = 160 mm; pre stretch strain = 1.5%; post stretch force = 90 kN

The effect friction on the springback ratio is significant, because much of the part is not getting enough force (or strain) to bring the springback ratio over the "shoulder" in the springback ratio curve that occurs at a force of around 80 kN (about 0.2% strain). The following chart shows the die and part contours with and without friction.

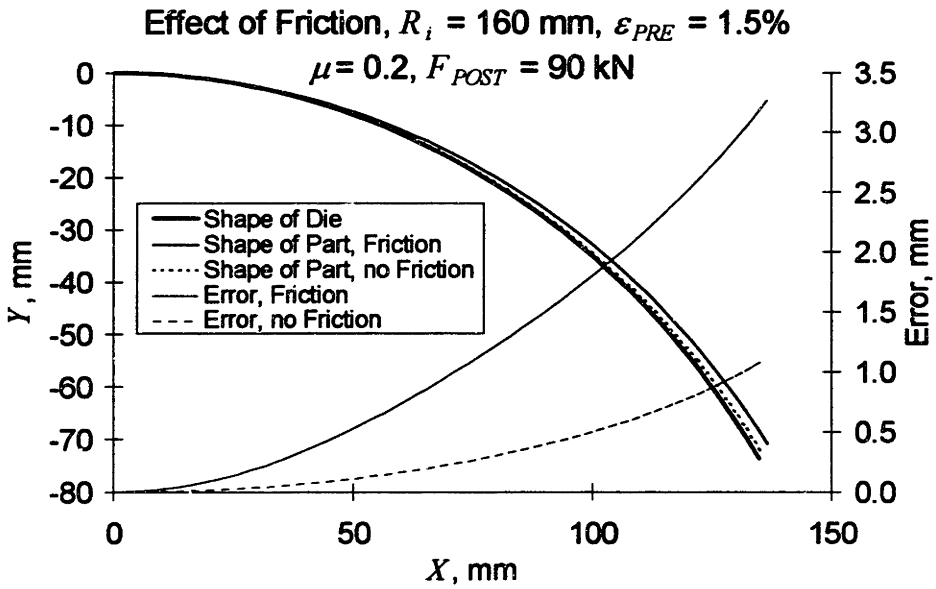

Figure 5.96 Effect of friction on part contour; R_i = 160 mm; μ = 0 and 0.2; pre stretch strain = 1.5%; post stretch force = 90 kN

The significant effect of friction on part shape can be seen in this chart. Friction causes the contour deviation at the end of the part to increase from 1.09 mm to 3.07 mm. The angle at the end of the part, which is 57.3° when the part is touching the die, is 56.49° without friction and 55.48° with friction, giving effective springback ratios of $\theta_f/\theta_i = R_i/R_f$ = 0.9860 without friction and 0.9683 with friction, a decrease of 1.8%. The average post stretch strain in the material on the die without friction is 1.59%, while with friction it is 0.49%—a three-fold difference!

The following table summarizes the effect of friction on this part.

	At top	At top	At top	At end	At end
μ	Post Force	Post Strain	R_i/R_f	θ	*Contour D.*
0.0	90.0 kN	1.76%	0.9860	56.49°	1.09 mm
0.1	81.6 kN	0.31%	0.9797	56.32°	1.40 mm
0.2	75.6 kN	0.0%	0.9298	55.48°	3.07 mm
Chg. 0.1	- 9.3%	- 82%	-0.6%	+0.3%	+ 28%
Chg. 0.2	-16.0%	-100%	-5.7%	+1.8%	+182%

Table 5.4 Effect of friction on force, strain, springback ratio, angle, and contour deviation; post stretch force = 90 kN; R_i = 160 mm; pre stretch strain = 1.5%

The following table summarizes the same statistics for a post stretch of 95 kN.

	At top	At top	At top	At end	At end
μ	Post Force	Post Strain	R_i/R_f	θ	*Contour D.*
0.0	95.0 kN	2.59%	0.9886	56.64°	0.89 mm
0.2	78.1 kN	0.05%	0.9582	56.25°	1.66 mm
Chg. 0.2	-16.0%	-98.1%	-3.1%	+1.7%	+87%

Table 5.5 Effect of friction on force, strain, springback ratio, angle, and contour deviation; post stretch force = 95 kN; R_i = 160 mm; pre stretch strain = 1.5%

A higher post stretch force reduced the effect of friction.

The effect of friction is higher in stretch wrap forming than in drape forming due to the lower limit on force. This effect can also be seen in leading edges, the next topic.

Effect of friction on leading edges

Since leading edges were the part of study in the practical understanding section of the thesis, they are studied now in order to better understand how friction and stretch force

affect the final part contour. This analysis uses the geometry for the leading edge described in the last chapter. The radius of curvature varied incrementally from the top of the part to the end, the first 40 mm having R_i = 50mm, the next 40 mm having R_i = 80 mm, the next 40 mm having R_i = 200 mm, and the last 80 mm having R_i = 1000 mm. The part length in contact with the die is 200 mm, and the total bend angle is 90.53° (this is only the right half of the part). The amount of excess material (between the end of the die and the jaws) is 50 mm. The part is modeled for no pre stretch (drape forming) with post stretch forces of 85 kN, 90 kN, and 95 kN. The part is also modeled for a pre stretch of 1.0% with post stretches of 90 kN and 95 kN. The coefficient of friction takes the values μ = 0.0, 0.1, 0.2, and 0 .3. The overall springback ratio is determined from the final angle, that is, $R_i/R_f = \theta_f/\theta_i$, and θ_f is determined by numerical summation of the contour as described in the previous chapter. The post stretch strain is determined by averaging the strain through the entire part, including the excess; this is what would be sensed by a position-controlled operation.

The first chart shows the overall springback ratio and contour deviation (end error) as a function of post stretch force for the four levels of friction.

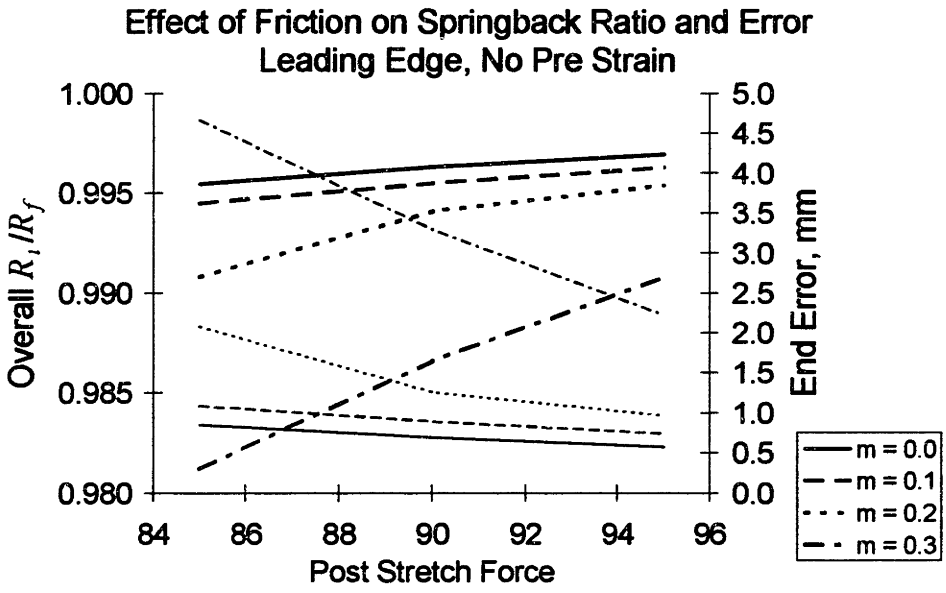

Figure 5.97 Effect of friction on overall springback ratio and contour deviation at end of part for leading edge; no pre stretch; force control

This chart shows the powerful effect friction can have on increasing springback and contour deviation. As long as the coefficient of friction is small ($\mu \leq 0.1$), it does not

have much effect: the contour deviation at the end increases about 0.24 mm (0.009") at 85 kN and 0.17 mm (0.007") at 95 kN when μ changes from 0 to 0.1. At larger values of μ, the springback ratio is significantly affected: the contour deviation increases by about 1.0 mm (0.039") at 85 kN and 0.23 mm (0.009") at 95 kN when μ changes from 0.1 to 0.2. The effect is even greater when going to $\mu = 0.3$.

The next chart shows the same information but as a function of post stretch strain.

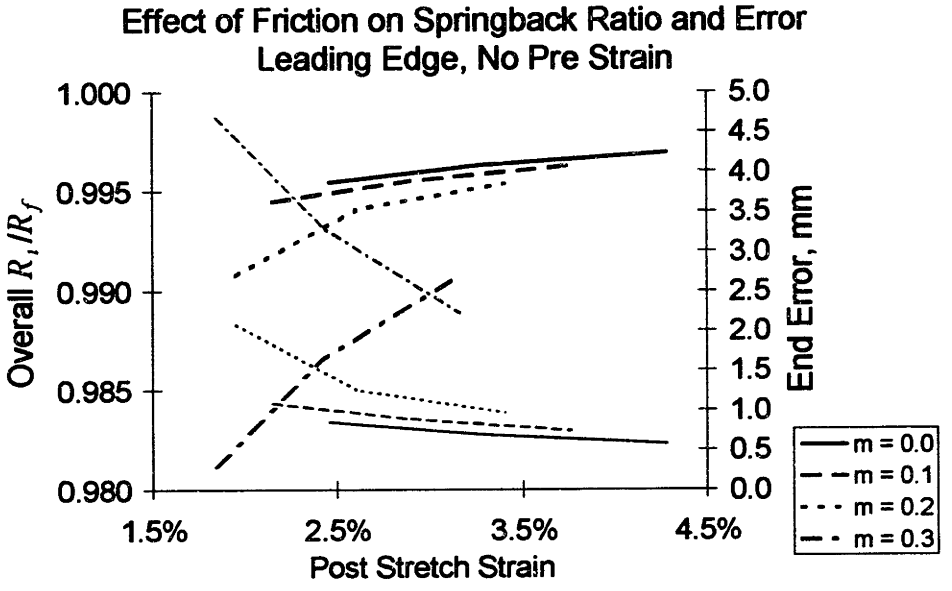

Figure 5.98 Effect of friction on overall springback ratio and contour deviation at end of part for leading edge; no pre stretch; strain control

While the chart appears to imply that springback and contour deviation are slightly more sensitive to post stretch strain than then are to post stretch force, this is not so, because the range of the strain, with respect to its average is about 100%, while the range of the force, with respect to its average is about 13%. Therefore, the operation is much more sensitive to normalized changes in force than normalized changes in strain.

The following chart shows the changes in springback ratio and contour deviation as a function of post stretch force with a 1.0% pre stretch strain (to 69.42 kN).

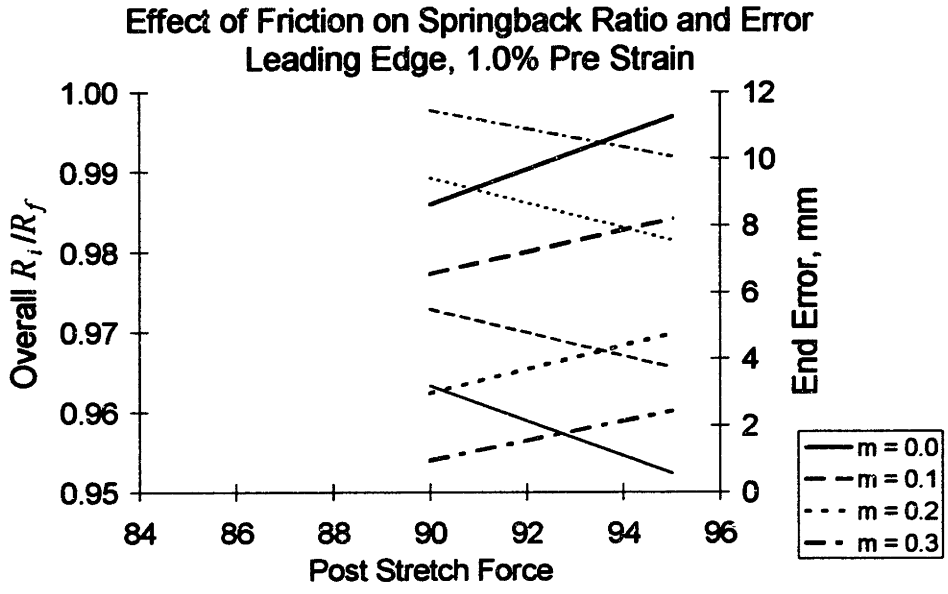

Figure 5.99 Effect of friction on overall springback ratio and contour deviation at end of part for leading edge; pre stretch strain = 1.0%; force control

Except at the high post stretch force of 95 kN without friction, the overall springback ratio is significantly lower and the contour deviation significantly higher with pre stretch than without pre stretch. Therefore, a pre stretch does not help reduce springback, but actually increases springback when there is friction. This is partly because without the pre stretch, the part undergoes compressive plastic deformation on the inside when it is bent over the die, which significantly reduces springback. The other reason is that the post stretch strain is greater without pre stretch because the initial force is zero and the part stretches at lower forces. These effects can be seen in the following two charts, the first of which shows the springback ratio and post stretch strain in the part along its length with a coefficient of friction of $\mu = 0.1$.

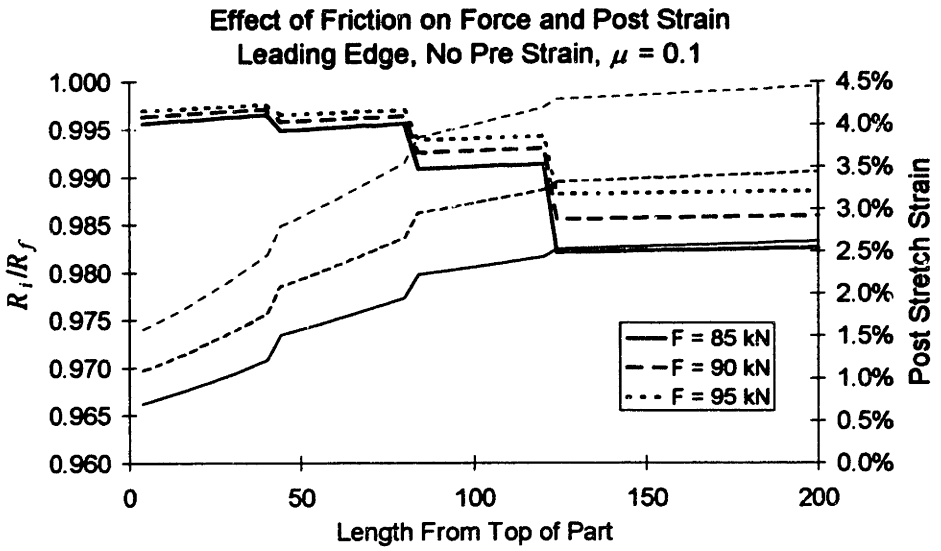

Figure 5.100 Effect of friction on springback ratio and post stretch strain within a leading edge; no pre stretch; $\mu = 0.1$

In spite of the fact that the post stretch strain at the top of the part is roughly only 1/3 of what it is at the bottom (end) of the part, the springback ratio is higher at the top than at the end. This is due to the compressive plastic deformation caused by bending the part around such a tight radius of curvature. The following chart shows the same information for the part with a 1.0% pre stretch.

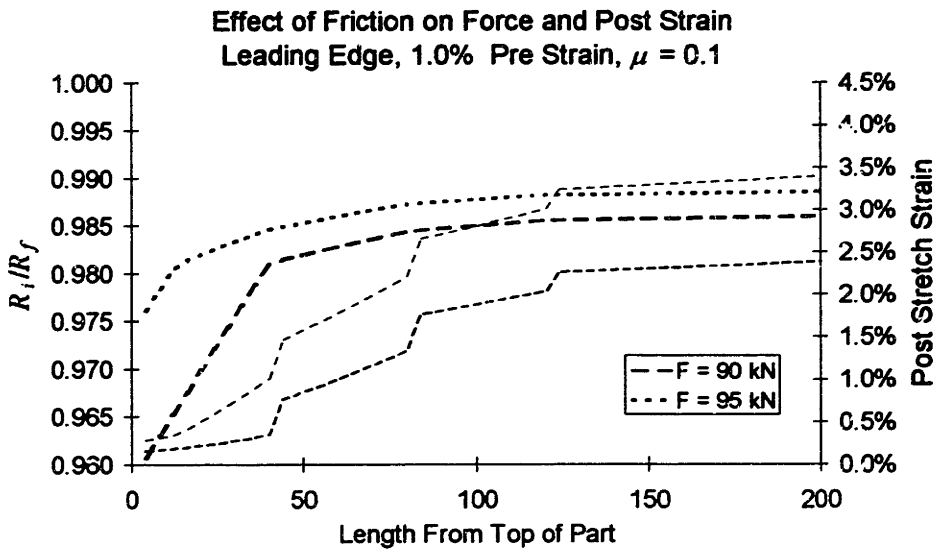

Figure 5.101 Effect of friction on springback ratio and post stretch strain within a leading edge; pre stretch strain = 1.0%; $\mu = 0.1$

The springback ratio is lower throughout the material because the initial compressive plastic deformation is greatly reduced or altogether avoided (there's just a very small bit of compressive plastic deformation on the inside of the part at R_i = 50 mm), and the post stretch strain is reduced from the no pre stretch case.

Without post stretch, the springback ratio at the top with no pre stretch is 0.8344 and with pre stretch it is 0.9369. However, the small amount of strain that reached the top of the no pre stretch part reduced the springback much more than the smaller amount of strain that reached the top of the pre stretch part. The following chart shows this point more clearly.

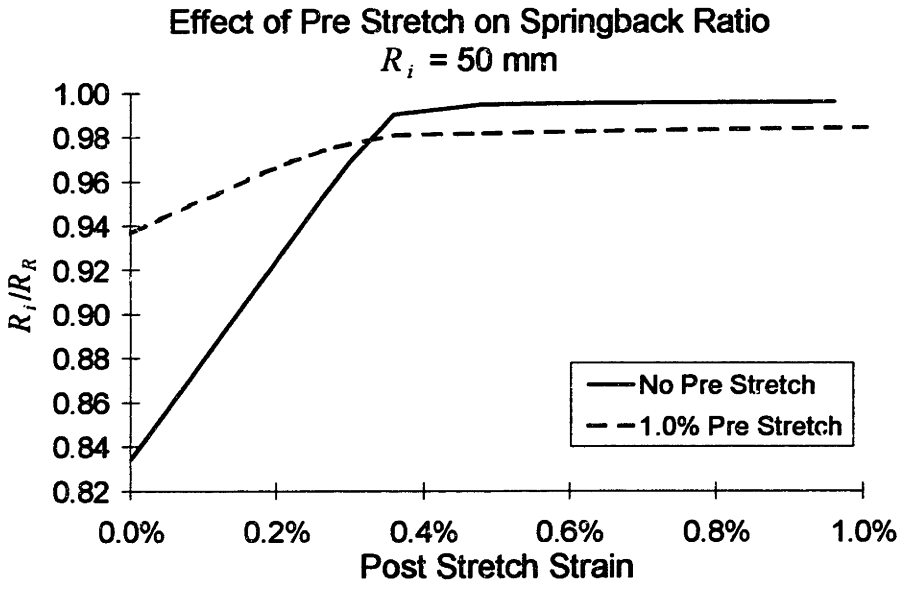

Figure 5.102 Effect of pre stretch on springback ratio; R_i = 50 mm; strain control

The chart shows that after about 0.35% post stretch strain, the springback ratio without pre stretch surpasses the springback ratio with pre stretch. But this tells less than half the story. The following chart shows the same two curves, this time as a function of post stretch force.

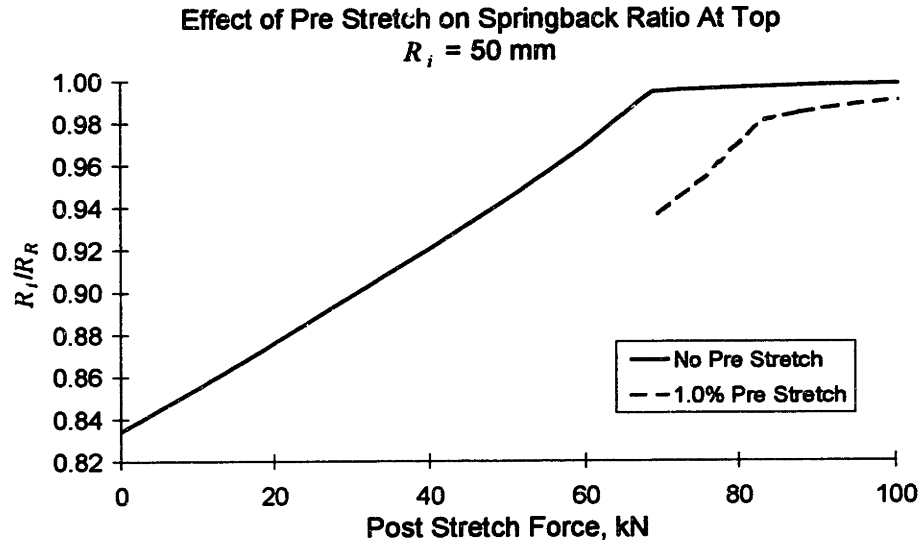

Figure 5.103 Effect of pre stretch on springback ratio; R_i = 50 mm; force control

This chart reveals that at the top, for any post stretch force over about 50 kN, the no pre stretch part has a higher springback ratio at the top. The curve for the pre stretched part only goes down to 69.42 kN, because this is the force required for the 1.0% pre stretch. However, such a low post stretch force is unlikely to occur; it doesn't occur in this part even with a coefficient of friction of 0.3 and the low post stretch force of 85 kN. Therefore, pre stretch generally increases springback, and the increase is greater with friction.

Summary and conclusions to effect of friction

Friction can have a significant effect on the stretch forming operation. Friction reduces the post stretch force along the length of the part from the point of contact to the "top" of the die. The reduction in force in turn reduces the strain, which in turn reduces the springback ratio. With the cylindrical die example used for drape forming, in which the bend angle (for the right side of the part) is 45°, a no-friction strain at the top of the part decreased 21%, 53%, and 68%, and a no-friction contour deviation of 1.29 mm (for a part length of 235.6 mm) increased 21%, 48%, and 80% with coefficients of friction μ = 0.1, 0.2, and 0.3, respectively.

Because of the high initial force which reduces the post stretch strain, and because of the elimination or reduction of initial compressive plastic deformation, the effect of friction on stretch wrap forming is greater than the effect of friction on drape forming.

The effect of friction on a leading edge part is significant, except at very low coefficients of friction, around $\mu = 0.1$. The operation is less sensitive to friction under strain or position control than under force control. This is more evident when springback is viewed as a function of post stretch force.

5.3 CONSIDERING NON-IDEAL CONDITIONS

The analytical model makes many simplifying assumptions. While the model is very useful for developing a deeper understanding of the operation, seldom are all the assumptions completely valid. As well, some parameters which affect the operation are not included in the model. The effects of a few non-ideal conditions are now addressed qualitatively.

5.3.1 Thinning of the part due to stretching

As mentioned in the assumptions, thinning is not considered in this model. Since the part would actually thin under imposed longitudinal strain or forces, forces due to stretching would be overestimated if a strain was imposed (although stresses would be accurate), and both stresses and strains due to stretching would be underestimated if a force was imposed. Overestimation of force under strain control would have no effect on the springback ratio, while underestimation of stretching stresses and strains would result in an overestimation of the springback ratio (and underestimation of springback). Due to thinning, changes in stress due to bending and unbending would be overestimated, and moment arms would be overestimated. Overestimation of the changes in stress due to bending and unbending and of the moment arms would probably have almost no effect on the springback ratio because these effects would cancel one-another out.

Under assumptions of plasticity and plane strain (no strain in the width direction), the thickness strain would have to be the negative of the stretching strain in the length direction, that is, $\varepsilon_y = -\varepsilon_x$. It is possible to adjust the model to account for this change. This is done for one case, just to see how it would impact things. The standard parameters, the Isotropic model, and drape forming are used. For a 0.5% post stretch, without thinning adjustment, $R_i/R_f = 0.9613$, and the required force is 52.061 kN; with thinning adjustment, $R_i/R_f = 0.9609$, and the required force is 52.043 kN. For a 2.0% post stretch, without thinning adjustment, $R_i/R_f = 0.9862$, and the required force is

69.091 kN; with thinning adjustment, R_i/R_f = 0.9858, and the required force is 69.065 kN. For a 5.0% post stretch, without thinning adjustment, R_i/R_f = 0.9932, and the required force is 83.571 kN; with thinning adjustment, R_i/R_f = 0.9927, and the required force is 83.541 kN. As is evident, the springback ratio is consistently overestimated by about 0.05%, and the required force is overestimated by about the same amount. Because they are in the fourth decimal place, these differences are clearly insignificant. Therefore, it can be safely concluded that not including thinning is not a significant source of model error.

5.3.2 Initial residual stress and anisotropy

Residual stresses are imparted to the material through plastic yielding, which at the same time work hardens the part.

All incoming sheet that has undergone deformation since annealing has some residual stresses from a variety of possible sources, the most significant being the rolling process used to make the sheet, heat treat quench, the extrusion operation used to make extrusions, and bending and unbending subsequent to the rolling operation (for example, from coiling sheet).

Residual stresses from the rolling process used to make sheet, through the thickness of the part, are generally compressive on the outside and tensile in the middle. They are generally repeatable. Residual stresses from the heat treat quench are generally unpredictable and very significant. Residual stresses from the extrusion operation are generally repeatable and significant. Residual stresses from bending and unbending are somewhat complex and depend on how the material is bent and unbent.

The sum of these and other sources create in the part a somewhat unknown and unpredictable initial stress state. These (and the associated strain hardening) affect the operation by causing the effective strains and the actual stresses to differ from those predicted in the model. These result in unpredictable variation in stresses and springback, which can lead to contour variation. As stretch forming strains are increased, the effect of initial anisotropy diminishes.

It is possible to include initial strain hardening and residual stresses in the model based on yield surfaces. However, to do so is beyond the scope of this research.

According to Sa [1989], the strain hardening behavior (represented by the strain hardening exponent n) has a much greater impact on stretching metal than does anisotropy (represented by R). For this reason it is safe to ignore anisotropy.

5.3.3 Non-cylindrical dies for sheet stretch forming

Few stretch forming dies are cylindrical in shape, an assumption that has been made in the analytical model. Many other possibilities exist, though they can be roughly categorized as some combination of varying the radius of curvature along the length of the part (which has been modeled) and having curvature in the plane orthogonal to the plane in which curvature already exists and to the initial sheet surface; this condition is called compound curvature. Compound curvature necessitates three-dimensional stress and strain analysis, and is beyond the scope of this work.

Determination of shear strains has been addressed by others, for example Aryshenskii [1983], Lysov and Komarova [1987], and Oding [1987a, 1987b]. Determination of secondary bending strains has been addressed by Johnson and Yu [1981], Oding [1987a, 1987b], and others. However, numerical results from such calculations are generally only good for very little curvature (large radii of curvature). Oding [1987a, 1987b] resents very interesting results as he addresses both shear strain and secondary bending strain, in addition to primary bending strain, for a compound contour part. His most significant and relevant result is that shear and secondary bending strains can be on the same order of magnitude as the bending strains. However, he does not address the impact of these additional strains on the shape of the part.

The simplest conclusion to draw regarding the effect of compound curvature is that it causes an uneven strain distribution (longitudinal, width, and shear strains) within the part, which will cause uneven springback, and possibly some undesirable warpage. As with stretch forming over a cylindrical die, the greater the stretch—or in this case, the greater the minimum stretch—the more evenly strains will be distributed, and the more even will the springback be distributed. However, too great a stretch may cause the part to fail. Because of the large amount of strain some portions of the part must undergo before other portions begin to stretch, compound curvature may also require multiple pulls with annealing in-between. In addition to allowing larger strains, annealing also reduces the effective strain differences.

Another approach to reduce an uneven strain distribution due to compound curvature is to change the shape or movement of the jaws. For example, segmented jaws could vary the amount of stretch given the material. Jaws could also be curved (varying in height) in the shape of the contour—some sheet stretch forming presses have this capability. Finally, the part perimeter could also be contoured, either simply angled on the cut ends or more fully contoured. The jaws of the stretch forming press would have to be able to accommodate the contoured perimeter. Complex contouring of the part would probably require FEA to determine the optimal contour and pull sequence.

5.4 Comparison of Results with Others' Work

In this section, analytical model predictions are compared with results obtained from experiments and finite element analysis (FEA) simulations in order to validate that the model accurately predicts stresses, strains, springback, and contour.

Validation through comparison with experiment or another model is difficult for a couple of reasons. If the results are experimental, material properties and other relevant parameters may be difficult to determined, and accuracy is uncertain when there is significant variation. If the results are from a model, unknown model parameters throw the predictions into questions. Further, different model assumptions are likely to produce different results, and the model may not accurate. With that said, some comparisons are now attempted.

5.4.1 Springback for pure bending of aluminum from handbook

In the most recent ASM specialty handbook on aluminum, edited by Davis [1993], two springback compensation tables, one for 2024-O and one for 2024-T3, are given for pure bending. The following chart shows the springback ratios calculated from the handbook data and predicted by the analytical model for 2024-O. No material properties were given for the material used to determine the compensation tables, so the standard material properties were used in the analytical model, without adjustment for plane strain.

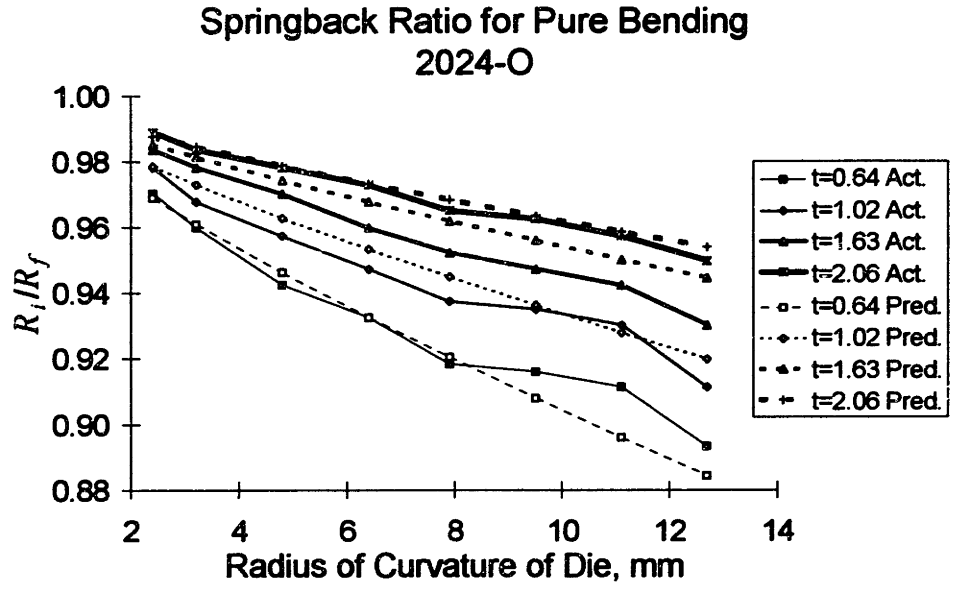

Figure 5.104 Comparison of predicted springback ratio for pure bending with springback compensation tables for 2024-O aluminum

The agreement between the handbook data and the analytical model is quite good. The analytical model results are smoother than the handbook data, which is probably due to the statistical variation in the experimentally derived handbook data.

The next chart shows the handbook data and analytical model results for 2024-T3.

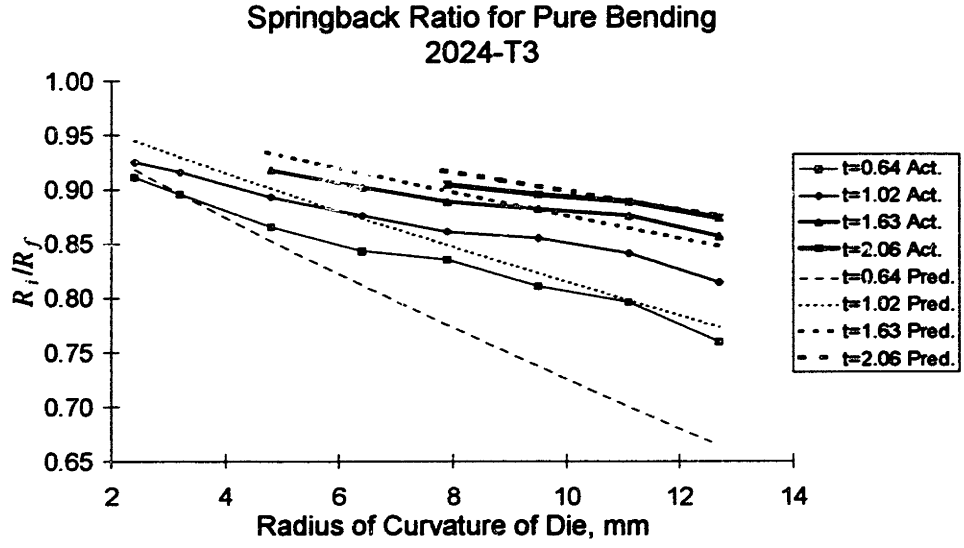

Figure 5.105 Comparison of predicted springback ratio for pure bending with springback compensation tables for 2024-T3 aluminum

The agreement is not very good, in that there appears to be a consistent difference in slope between the experimental data and the predictions. The material parameters used to model the 2024-T3 material are: E = 72000 MPa (10,443 ksi), σ_Y = 345 MPa (50 ksi), and n = 0.120 (estimates of the elastic modulus and of the strain hardening exponent are based on experiments performed at Northrop Grumman [Papazian, 1991]). In order to achieve a better fit between the data and model predictions, the following parameters were arrived at by trial and error, with the guiding thought that in order to change the slope the material would have to be more strain hardening in the plastic regime (i.e., that the strain hardening coefficient would have to be higher): E = 90000 MPa, σ_Y = 150 MPa, and n = 0.4. The experimental results and new predictions are shown in the following chart.

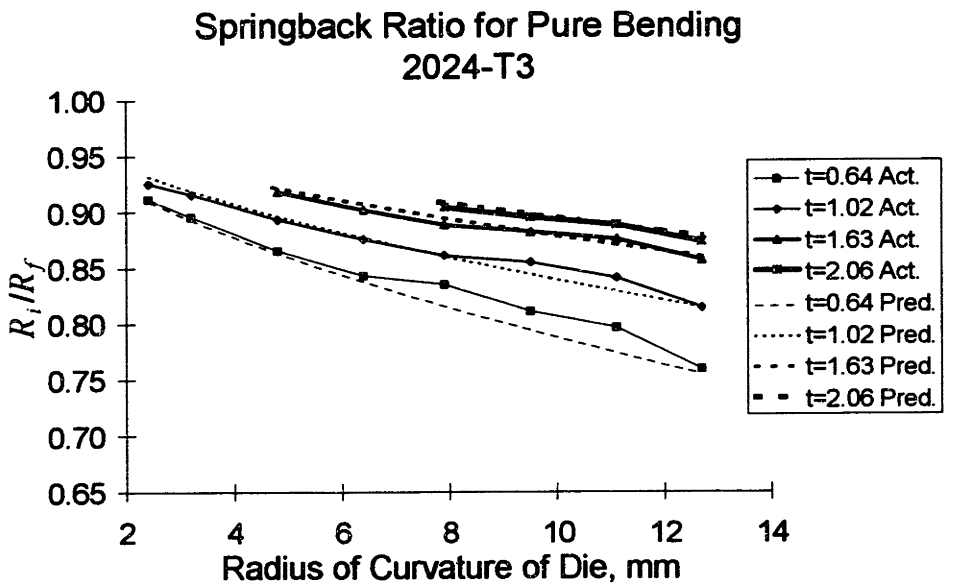

Figure 5.106 Comparison of predicted springback ratio for pure bending with springback compensation tables for 2024-T3 aluminum; adjusted parameters

The agreement between the experimental results and analytical model predictions with the new parameters is quite good. The modifications made to the material properties indicate that the material begins plastic deformation much sooner than expected (just over a third of the common yield strength), and that the rate of strain hardening is much higher than expected (over three times that found experimentally with a tensile test). The source of the unexpected material behavior is not certain.

Summary and conclusions to springback for pure bending of aluminum from handbook

Springback ratios calculated from experimentally determined handbook data compared very well with analytical model predictions for 2024-O aluminum. However, for 2024-T3 the predictions were way off with somewhat standard material properties for this material. Only with significant parameter adjustments did the predictions compare well with the handbook data. The source of this error is uncertain.

5.4.2 Sheet stretch wrap forming experiments and FEA simulations

A number of experiments were performed by Jerry Nardiello and Robert Schwartz at the Northrop Grumman Advanced Technology Development Center (ATDC) in Bethpage, NY as part of the research for the ARPA-funded Reconfigurable Tool for Flexible Forming (RTFF) project. FEA simulations of these experiments were performed at the same facility by Lembit Kutt. The experimental and FEA results are presented in the proprietary report [Northrop Grumman, 1996].

Description of test specifics

The materials used were 0.032" (0.8128 mm) and 0.063" (1.6 mm) thick sheets of aluminum alloy 2024-O. The unformed parts were 6" wide and there was 24" of material between the jaws. Parts were formed without lubrication around cylindrically-shaped Richlite© dies, with radii of curvature of 5" and 10".

The parts were stretch wrap formed on a Cyril Bath V-30 stretch wrap forming press with a recently upgraded controller. Both jaws were attached to very precise (resolution to $\pm$ 20 lbs) load cells. All the parts were snugged at 800lbs (except a handful which were snugged at 200lbs, but this was found to be too low). The 0.032" parts were pre stretched to either 800 lbs or 2000 lbs, while the 0.063" parts were pre stretched to either 800 lbs or 4000 lbs (except the handful snugged at 200 lbs). The wrap angle for most of the 5" radius parts was 37° (the wrap angle as defined by Northrop Grumman people is half of the bend angle as defined by me), and for all of the 10" radius parts was 17.5°.

Springback ratios from the experiments were calculated by determining (from the geometry of the setup) the angle to which the parts were pulled, θ_i, and by measuring the final angle of the part, θ_f. Knowing these two values, the springback angle is given by $R_i/R_f = \theta_f/\theta_i$.

The FEA simulation and the analytical model stress-strain curves are shown in the following chart along with the data from which they were derived.

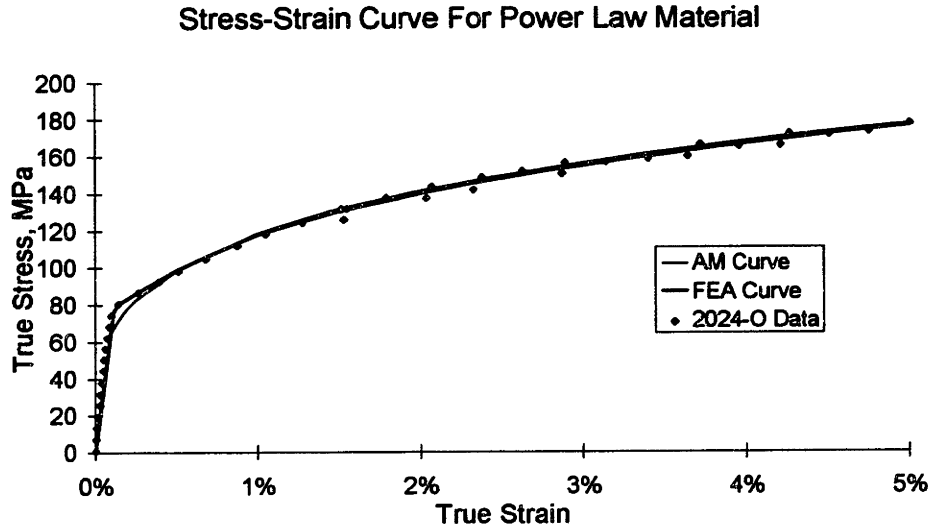

Figure 5.107 Actual and estimated stress-strain curves for aluminum alloy 2024-O

The analytical model parameters were K = 375.3 MPa and n = 0.2523. In order to keep the standard elastic modulus of E = 68947 MPa, the yield strength had to be adjusted to σ_Y = 64.62 MPa. The FEA model used discrete points, not the power law equation, to define the plastic portion of the stress-strain curve, which is the reason for the slight difference in curves around the yield point. Other than that, the agreement among the models and experimental data is excellent. Plane strain conversions of these properties were also made for the analytical model, and they are: E = 75766 MPa, σ_Y = 79.65 MPa, and K = 449.4 MPa (n doesn't change). While no friction was generally assumed for the analytical model, two cases were calculated with a friction coefficient of μ = 0.2 in order to get a sense of the magnitude of the effect of friction on the analytical model.

The FEA simulation used ABAQUS© explicit code for the pre stretch, wrap, and post stretch, and ABAQUS© standard code to determine the springback. Isotropic material hardening was assumed. A coefficient of friction of 0.2 was used in the simulation.

Results

The following charts show the three results together. The curves are from the analytical model developed in this thesis; the solid triangles and diamonds are

experimental results; the hollow triangles and diamonds are FEA simulation results. In the first chart, the + and x are the analytical model calculations with friction.

The first chart shows the springback ratio as a function of the post stretch force for 0.063" thick material and a die radius of 5".

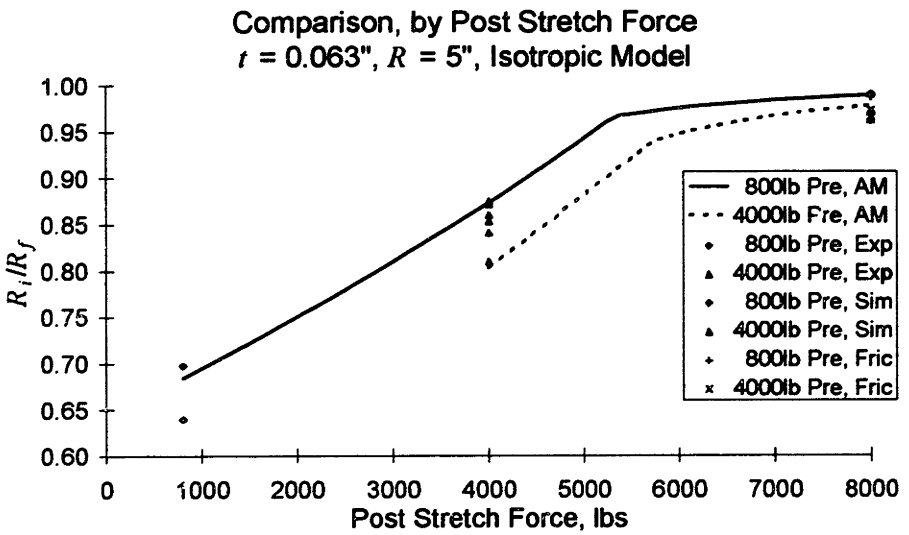

Figure 5.108 Comparison of springback ratio predictions and experimental results; analytical model, FEA simulation, and experiment; t = 0.063"; R_i = 5.0"; by force

A number of things can be gleaned from this chart. A higher pre stretch force reduces the springback ratio as a function of post stretch force, resulting in more springback for a given post stretch force. This is because of the increased strain hardening that occurs in the material when it is wrapped at only 800 lbs. The experimental data are relatively close to the analytical model predictions. The FEA predictions are sometimes closer. As well, in the two post stretch cases in which the effect of friction was accounted for, its effect on the springback ratio (approximated by θ_f/θ_i) is negligible. Therefore, no friction is assumed for the rest of comparisons.

The next chart shows the springback ratio as a function of post stretch. While the predictions for the curves is same as in the above chart, the experimental data are different, except for four points for which both post load and post stretch strain were recorded (generally, only one or the other was recorded).

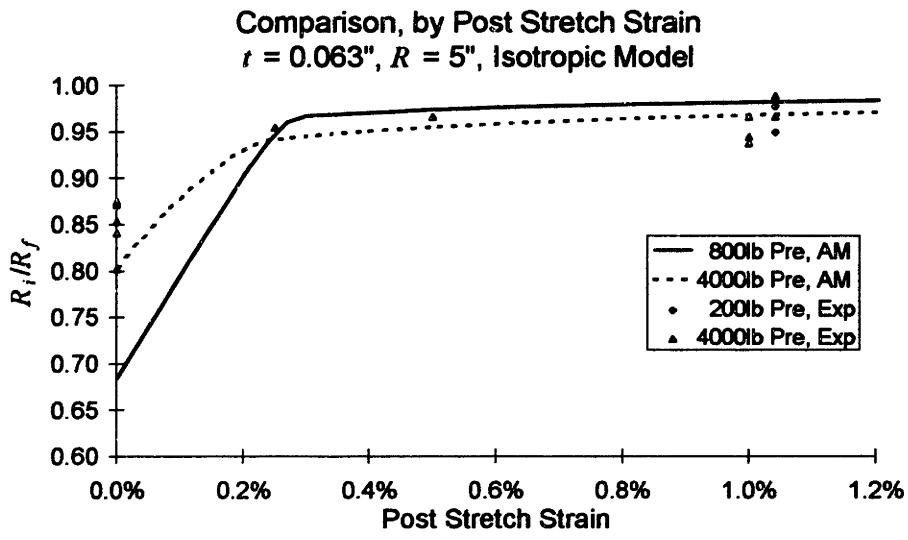

Figure 5.109 Comparison of springback ratio predictions and experimental results; analytical model, FEA simulation, and experiment; t = 0.063"; R_i = 5.0"; by strain

In this chart, the agreement between the experimental results and analytical model predictions looks better. However, as in the previous chart, in the no post stretch zone, the experimental data show less springback than the model. This may be due to the inability of the machine to hold a constant force during the wrap (higher forces would reduce springback). At strains over 0.2%, the agreement looks better, although it can be seen again that the experimental data have significant variation. A lower pre stretch force results in more springback at very low post stretch strains, but above about 0.25% post stretch strain, the lower pre stretch force part has less springback.

The following chart shows the predictions and experimental results for 0.032" thick material stretch wrapped around a 5" radius die.

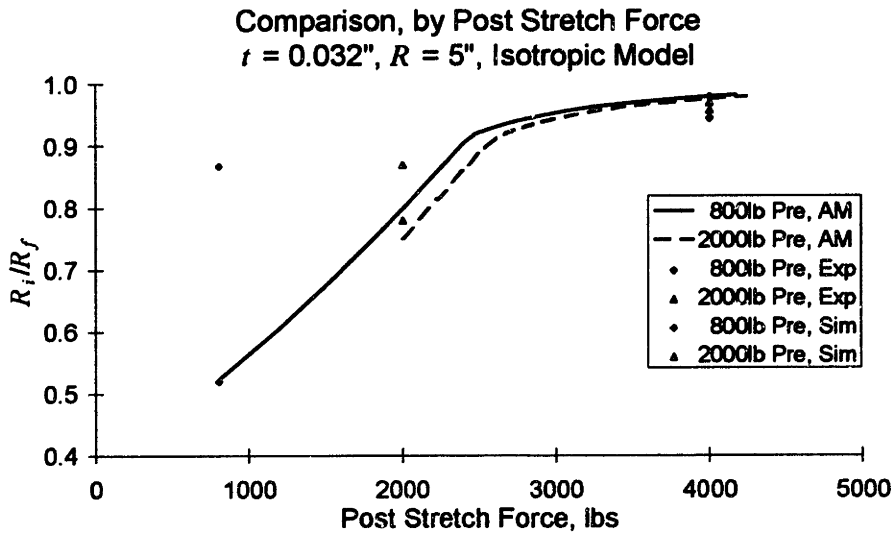

Figure 5.110 Comparison of springback ratio predictions and experimental results; analytical model, FEA simulation, and experiment; t = 0.032"; R_i = 5.0"; by force

The no post stretch experimental results are far above the expected results. However, it was noted by the experimentalists that with the 0.032" material, machine control was difficult, and the parts were very flimsy. As in the previous charts, the experimental results at the high post loads are lower than the theoretical predictions. The agreement between the analytical model and simulation is quite good.

Results from experiments and simulations performed with a 10" radius die are about the same as for the 5" die.

One possible explanation for the fact that at higher post stretches the experimental data nearly always lie just a little bit under the curves is that the Isotropic hardening model overestimates the amount of hardening that the material experiences. The following chart is the first chart redrawn with the Bauschinger hardening model curve drawn in as well.

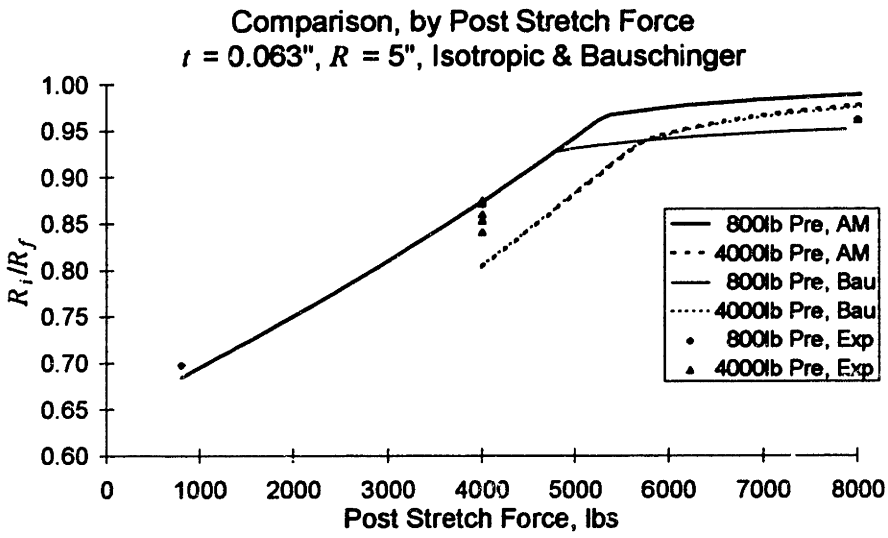

Figure 5.111 Comparison of springback ratio predictions and experimental results; analytical model Isotropic and Bauschinger strain hardening models, and experiment; t = 0.063"; R_i = 5.0"; by force

At high forces there is now a significant difference between the springback ratio for the Isotropic and Bauschinger models with the 800 lb pre stretch force. The Bauschinger model hits just below the data. The factor A in the yield surface method model could be adjusted to reflect the value that best fits the actual behavior of aluminum. Concerning the 4000 lb pre load, there is almost no difference between the two curves because there is almost no initial compressive plastic deformation, which is the source of difference between the two models.

Finally, plane strain properties are tried to see if they bring the analytical model predictions any closer to the experimental results. The following chart shows the results, for the same stretch profiles as above.

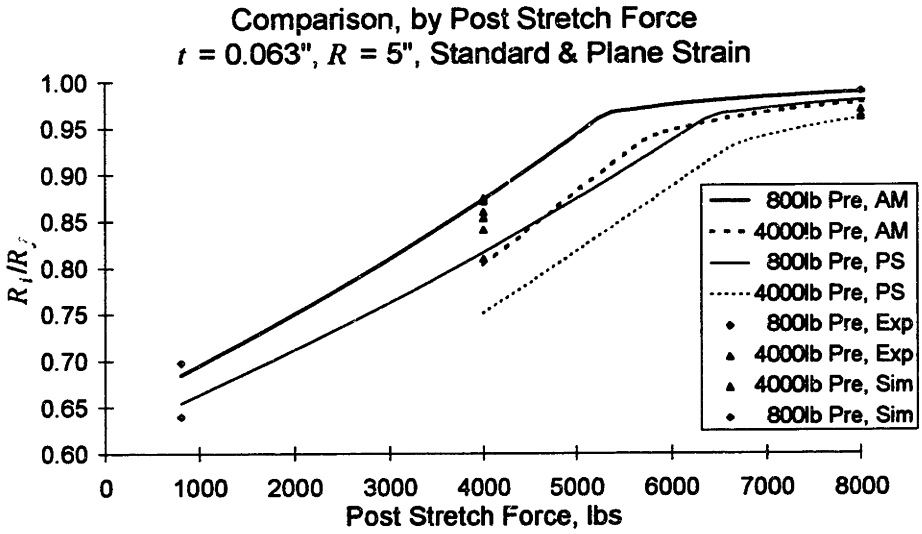

Figure 5.112 Comparison of springback ratio predictions and experimental results; analytical model standard and plane strain parameters, and experiment; t = 0.063"; R_i = 5.0"; by force

Unfortunately, the direction of change without post stretch moves the predictions further away from the experimental results. However, at high post stretch forces, the direction of change brings the predictions closer to the actual data. The analytical model prediction is closer to the FEA prediction for the 800 lb pre stretch force without post stretch, but moves away with post stretch. The analytical model prediction moves away from the FEA prediction for the 4000 lb pre stretch case without post, and moves to the other side (roughly the same distance) with post stretch.

Summary and conclusions to stretch wrap forming experiments and FEA simulations

The analytical model predictions compare well with experimental results and FEA simulations of these experiments. Use of less than Isotropic hardening may give better results. Use of plane strain properties had a mixed benefit in that predictions at low forces moved away from experimental results, while at high forces they came closer.

5.4.3 Other FEA simulations

Some FEA analyses were also performed at MIT for the RTFF project, which are now used in order to compare with the predictions of the analytical model developed. The parameters are essentially the same as the above parameters, except that only 0.063" thick material stretch wrapped around a 5" die was modeled, and the wrap angle was

37.12° (half of the bend angle). The stress-strain curve parameters did not change. The FEA model used a coefficient of friction of $\mu = 0.2$.

An attempted comparison of springback ratios for stretch wrap formed parts without post stretch did not work out because two sets of FEA predictions with (at least) different convergence criteria gave conflicting results. While the FEA predictions were not very far off from the analytical model predictions, the comparison was not useful.

However, a look at the stresses within the parts, shows that the agreement between the two models is actually quite good. The following chart shows the stresses within the part for a 1000 lb pre stretch force without post. The dark lines are the analytical model predictions using uniaxial tensile test properties, while the lighter lines are the predictions using plane strain properties. The points are FEA simulation predictions.

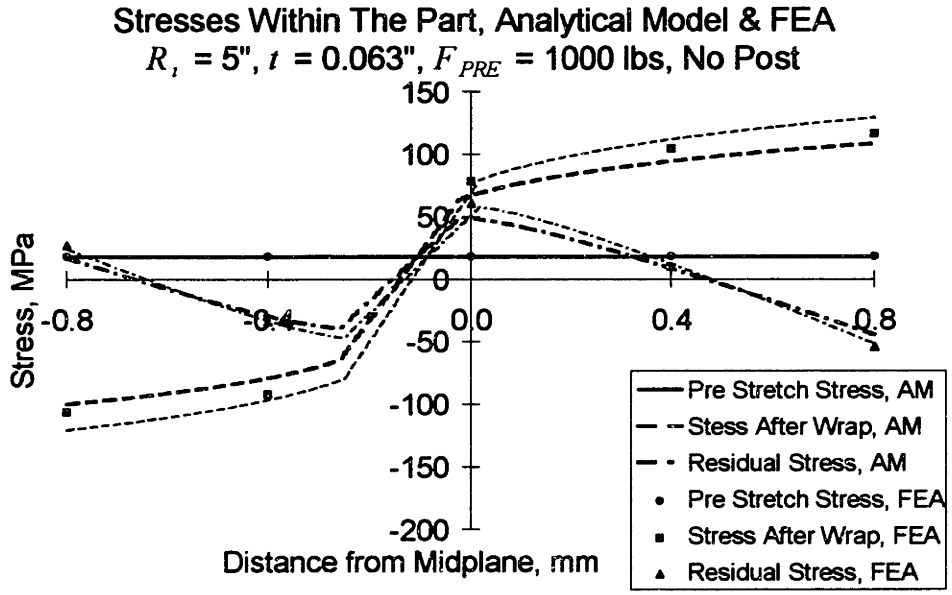

Figure 5.113 Comparison of stresses within a part; analytical model and FEA; t = 0.063"; R_i = 5.0"; pre stretch force = 1000 lbs; no post stretch

The correlation between the FEA and analytical model predictions is very good. It is difficult to tell whether the uniaxial tensile test or plane strain parameters match the FEA data better. Both the analytical model and the FEA models capture the midplane elongation, the compressive and tensile plastic deformations, and the effect of springback and relaxation. The following chart shows the same information for a pre stretch force of 4,000 lbs without post stretch.

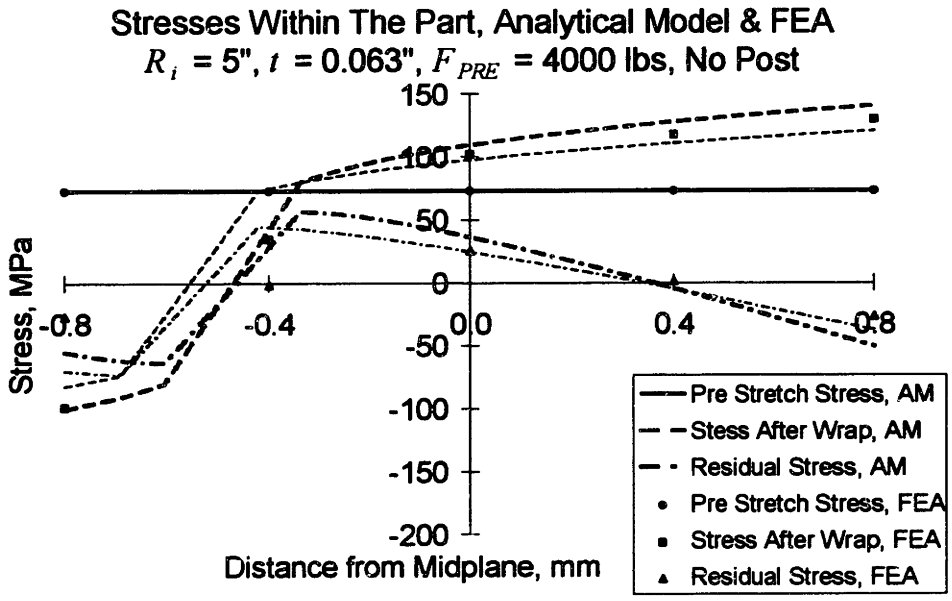

Figure 5.114 Comparison of stresses within a part; analytical model and FEA; t = 0.063"; R_i = 5.0"; pre stretch force = 4000 lbs; no post stretch

Again, the correlation is quite good, and it is hard to say if the uniaxial or plane strain parameters give a prediction closer to the FEA prediction. The next chart shows the same information for a pre stretch force of 8,000 lbs without post stretch.

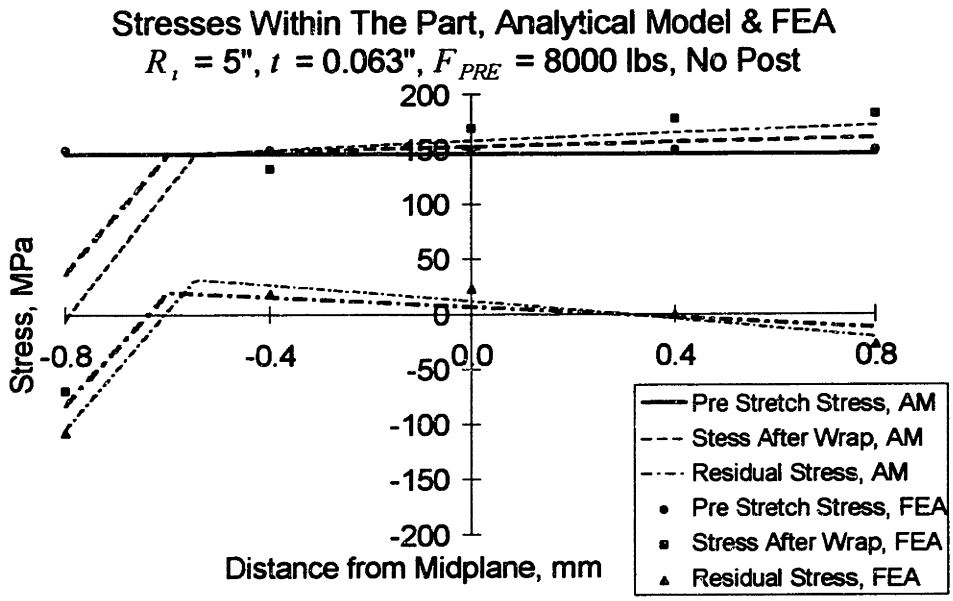

Figure 5.115 Comparison of stresses within a part; analytical model and FEA; t = 0.063"; R_i = 5.0"; pre stretch force = 8000 lbs; no post stretch

Again, the agreement is quite good. The stress after wrap at the inside, however is significantly different between the two models; it appears that the "shoulder" predicted by the FEA model is further towards the middle of the part than predicted by the analytical model due to the apparently steeper slope of the plastic region. Finally, in the last case, shown in the following chart, the pre stretch force is 1,000 lbs and the post stretch force is 8,000 lbs.

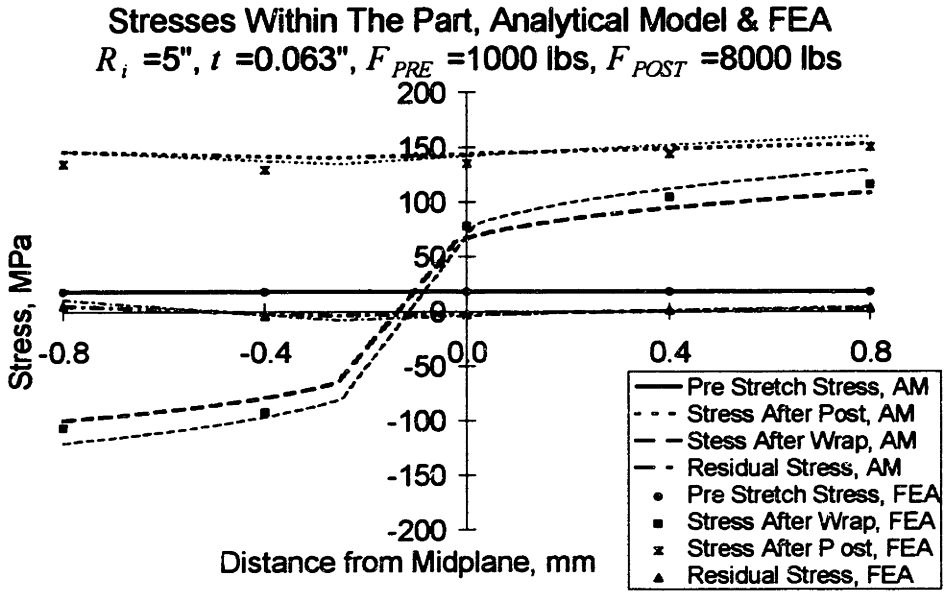

Figure 5.116 Comparison of stresses within a part; analytical model and FEA; t = 0.063"; R_i = 5.0"; pre stretch force = 1000 lbs; post stretch force = 8000 lbs

Again, the agreement is quite good. It is interesting to note that while the analytical model uniaxial and plane strain stresses look nearly the same for the post stretch, the strains tell a very different story. Since plane strain conditions effectively make the material harder, the predicted post stretch strain to reach 8,000 lbs is only 0.96% with plane strain parameters, while it is 2.14% standard parameters. The FEA model predicted springback ratio is 0.9486, while the analytical model prediction is 0.9881 for the standard parameters and 0.9788 for the plane strain parameters. This is a significant difference.

If the effect of friction is taken into account in the analytical model, the force at the top is 7,046 lbs, for the wrap angle of 37.12° (half of the bend angle) and μ = 0.2. The post stretch stresses are, as a result, a lower (lower than the FEA model predictions), and the dip in the residual stresses is very slightly exaggerated. The springback ratio

predicted by the analytical model with friction will still be higher than that predicted by the FEA model, because the springback ratio at the top of the part (where it is minimum) is 0.9829 for uniaxial parameters and 0.9699 for plane strain parameters.

Summary and conclusions to other FEA simulations

Comparison between stresses and strains in the part predicted by the analytical model and FEA simulation showed the two to be in very close agreement. It is not clear from the charts whether uniaxial tensile test properties or adjusted plane strain properties in the analytical model give better agreement.

5.5 SUMMARY AND CONCLUSIONS TO ANALYTICAL MODEL FINDINGS AND COMPARISONS

In this chapter, the analytical model developed in the previous chapter was used to predict stresses, strains, and springback as a function of the various parameters that affect the operation. Analytical model predictions were used to understand how the operation is affected by changes in parameters and to demonstrate the superiority of strain control over force control. A few non-ideal conditions were qualitatively discussed. Finally, analytical model predictions were compared with experimental results and FEA simulation predictions.

5.5.1 Analytical model results

The most significant findings from use of the analytical model are highlighted here. It must be kept in mind that these findings are based upon a certain set of parameters, and that they may not hold for other sets of parameters; generally they hold qualitatively, but not always. Many of the results are dependent on the Isotropic hardening assumption.

Effect of springback ratio on part shape

A simple analysis showed that even small changes in the springback ratio, on the order of 0.1%, can have a significant effect on part contour. For example, on a 180° bend angle part with a radius of curvature of 1 meter (39.37"), a 0.1% change in springback ratio gives contour deviations at both ends of 1.05 mm (0.41").

Effect of parameter changes on drape forming as a function of post stretch strain

The effects of parameters changes on the springback ratio were predicted for drape forming. The most significant result is that the springback is less sensitive the changes under strain control than under force control. The stretch forming operation was also

shown to be much less sensitive to changes in strain than to changes in force (changes were normalized by dividing by the nominal value). Therefore, strain (or displacement, if strain measurement is not feasible) control is the preferred method of control.

Effect of material models

Predictions of the four material models were compared. The models differ in the behavior of material that changes direction of plastic deformation. In drape forming with initial plastic deformation, the Isotropic, Bauschinger, and Kinematic models give the same result for very small post stretch strains, but predictions diverge as the portion of the material initially in compressive plastic deformation goes into tensile plastic deformation. Past about 0.5% post stretch strain, the Isotropic model gives the highest springback ratio, followed by the No IPD, Bauschinger, and Kinematic models. Residual stress distributions predicted also differ; the Isotropic model predicts tension on the outside and compression in the middle, the opposite of the other models.

Effect of plane strain parameters

The effect of using plane strain parameters instead of standard, uniaxial tensile test parameters has very little impact—about 0.1% to 0.2% change—on the springback prediction, as a function of strain at post stretch strains over 1%. The effect would be much more significant for springback as a function of post stretch strain.

Effect of chemical milling of sheet metal

The effect of chem milling on sheet metal depends most on the thickness of material removed, the hardening model, and the amount of post stretch strain. The difference between form of the residual stress distribution predicted by the Isotropic model and that predicted by the other models results in parts opening up when material is chem milled from the inside of a sheet according the Isotropic model, and parts closing up with the other models.

Effect of parameter changes on stretch wrap forming sheet

Above a very small amount of pre stretch force (or strain), increasing pre stretch force reduces springback as a function of post stretch strain. Increasing pre stretch strain increases springback as a function of total strain. This is because the increased pre stretch reduces the initial compressive plastic deformation. If a part is to be given a fixed amount of pre plus post stretch strain, the mix has little effect on the springback, except when it's nearly all in the post stretch (springback reduces) and when it's nearly

all in the pre stretch (springback increases). When sheet is pre stretched, the model differences diminish to the extent that initial compressive plastic stresses are diminished. If initial compressive plastic stresses are eliminated, it is possible to use the No IPD model with total strain to predict stresses, strains, and springback.

Effect of parameter changes on stretch wrap forming extrusions

Four extrusion cross-section shapes were studied: I, L, T, and H. Springback from pure bending is highest for the H cross-section and lowest for the I cross-section. With a pre stretch strain of 1% and with post stretch strains over about 0.5%, H and T cross-sections have less springback than I and L cross-sections.

Effect of routing on extrusions

Routing extrusions on the inside causes them to open up, according to the Isotropic model. The effect is greater for greater amounts of material removed and varies according cross-section and the amount of pre and post stretch strain.

Effect of friction

Friction can significantly affect the stretch forming operation by reducing the force, strain, and springback ratio along the length of the part during the post stretch. The effect of friction increases dramatically for larger bend angles and larger coefficients of friction. Friction can significantly affect force and strain when a part is post stretched. The effect of friction on the springback ratio and final bend angle is much less than its effect on force and strain. For low coefficients of friction and not very large bend angles, the effect of friction on contour is small, but for parts such as leading edges the effect of friction is significant, depending on the value of the coefficient of friction. The effect of friction increases significantly for lower post stretch forces.

When friction acts on a part that has been pre stretched, it is possible that the increased force of the post stretch will not reach the top of the part. If this happens, the springback ratio remains at the (low) value determined only by the pre stretch for that portion of the material. Contrary to common perception, the model predicts that springback is increased as a result of pre stretch on a part such as a leading edge, because of the initial compressive plastic deformation during pure bending and because of the greater penetration of strain into the part without pre stretch. Extrusions generally must be pre stretched because they are likely to buckle without the reduction in compressive stresses achieved by pre stretch.

The operation is less sensitive to changes in the coefficient of friction when controlled by strain than when controlled by force.

5.5.2 Non-ideal conditions

The effect of the model not including material thinning was investigated and found to be negligible. While it would be possible to model the effect of varying residual stress patterns in the incoming material, this was deemed to be outside the bounds of this thesis. The effect of double curvature, based on a brief literature review, is significant due to the shear strains and non-uniformity of the strains and stresses resulting in the part. Again, detailed analysis is out of the bounds of this thesis.

5.5.3 Comparison with experiments and simulation

Comparisons were made between the predictions of the analytical model and experimental results and FEA simulation predictions to validate the analytical model.

The analytical model predictions agree well with springback calculations made from springback compensation tables for pure bending of 2024-O aluminum. However, the predictions are significantly off for pure bending of 2024-T3 aluminum.

Comparison with experiments and FEA simulations of stretch forming 0.032" and 0.063" thick, 6" wide 2024-O aluminum sheets over 5" and 10" radius dies showed relatively good correlation for the prediction of springback ratio. Comparison with FEA simulation prediction of stresses within the part showed a very close correlation, and in most cases stresses differed only by a few percent.

While more a more thorough set of experiments and FEA simulations would be needed to validate the model for different geometries (especially extrusions), material parameters, and stretch profiles, the comparisons given have generally shown that the analytical model gives predictions that are relatively well correlated with the experimental and FEA simulation results.

5.5.4 Final note

Having gained the theoretical insights from this chapter into how parameters affect the operation and how the operation should be controlled (by strain, instead of force), the next two chapters focus on developing a practical, shop floor level understanding of the stretch forming process and how parameters affect the operation, on documenting variation and sources of variation, and on improvements to reduce variation.

6 SHEET STRETCH FORMING: PRACTICAL UNDERSTANDING

6.1 INTRODUCTION

In the previous two chapters, a theoretical understanding of the stretch forming operation was developed through the derivation of an analytical model of the operation and its use to determine what occurs inside the material, to determine how changes in parameters affect the operation, and to evaluate the difference between force and strain (displacement) control. With this background, the next step towards precision improvement is to gain a thorough, practical understanding of the entire stretch forming process at the shop floor level, after which improvements can be proposed, implemented, and evaluated. The objectives of the studies performed in this chapter are to understand things not captured in the model, to identify and characterize the sources of variation, and to document current variation. Based on the results of the studies, process improvements are recommended, and evaluated when possible.

All of the measurements presented in this chapter were performed at the Vought Center of the Commercial Aircraft Division of Northrop Grumman in Dallas, Texas, except for the chem mill study which was performed at Texas Aircraft Milling, Inc., in Dallas, Texas. Without spending time at the other stretch forming locations, it is difficult to know how the practice at Vought compares with that of others. The informal telephone survey seemed to indicate a good deal of similarity, with some companies faring better and some worse. The reader must relate the findings in this chapter (and in all of this thesis) to his or her own facility in order to determine what next steps to take to improve precision in the fabrication processes at his or her facility.

Since the American aircraft industry works in English units, these are used in the following two chapters. A conversion table to Metric units is given in Appendix 6.

6.1.1 Chapter outline

First, the sheet stretch forming process is described. The chapter is then divided into five sections and a conclusion. Each section presents a study of a portion of the stretch forming process.

The most important and largest study focuses on the stretch forming operation. Machine and material parameters were measured for over 25 lots of leading edges.

The study documents significant variation within a part, from part to part, and from lot to lot. Machine settings appear to contribute the most to the variation. Two improvements are recommended: repeatably achieve optimized settings and implementing automatic, in-process strain control. Strain control is addressed in some depth, and preliminary results from the recommended improvements are presented which indicate the significant improvements possible—up to 92% reduction in contour variation compared to current practice.

The second study is on incoming material property and geometry variations. Incoming yield strength, ultimate tensile strength, and elongation are found to vary significantly.

The third study is a designed experiment performed on the heat treat operation to determine the effect of material thickness, quench delay, and time at room temperature on various material properties. Time at room temperature affects nearly all measured outputs for aluminum alloy 2024. A combination of material thickness and cladding affect nearly all of the material outputs for aluminum alloy 7075, and time at room temperature also has a significant effect.

The fourth study looks at racking and time and temperatures in the heat treat operation. Good racking is critical to reducing warpage. Times and temperatures are well controlled, except for in the quench step.

The fifth study looks at the chemical milling operation, which has minimal effect on variation of contour and thickness. Etch rate is most sensitive to temperature and alloy.

The primary conclusion on sources of variation from this chapter is that while incoming material property variations are significant, most of the variation in the stretch forming operation is caused by varying initial conditions for the stretch forming operation and force control of the operation (instead of strain control). Determining and achieving optimal initial conditions and control of the operation by strain instead of force are recommended, and tests show great promise for precision improvement.

6.1.2 Description of process and operations

The purpose of the sheet stretch forming process is to manufacture precision contoured skins. Skins, the exterior of an aircraft, vary greatly in size and shape. The following diagram shows the stretch forming process flow.

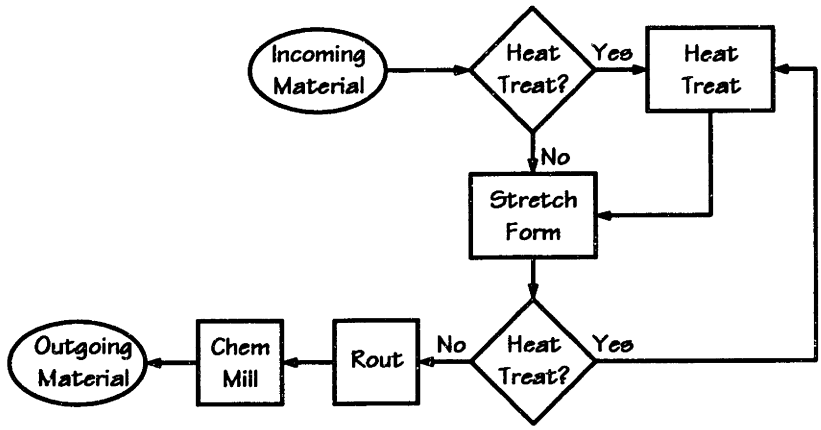

Figure 6.1 Process flow diagram of sheet stretch forming

Each operation is now described in the order in which it occurs in the process flow.

Incoming material and heat treatment[36]

Sheet metal arrives as stacked sheet (though it may have been previously rolled). Some parts are received and stretch formed in the -T condition (generally, 2024-T3), and are not heat treated in house. Most parts are received in the -O (annealed) condition and are stretch formed either in the -O condition or in the -W (unstable, after solution heat treatment) condition. If the material is stretch formed more than once in the -O condition, it is annealed between stretches, except for the final stretch. The heat treatment before the final stretch is always solution heat treatment. Parts may be stretch formed more than once because (a) a single stretch would impose too great a strain on the material, causing surface blemishes (Lüder lines and/or orange peel) or failure, (b) a single stretch would result in too much springback, (c) it is more efficient to heat treat bent parts (more formed parts can be loaded per rack than flat parts), and/or (d) formed parts warp less in heat treat than flat parts.

Aluminum is solution heat treated in order to create a high strength part (through age hardening) which can be formed while it is relatively soft and ductile (while it is in the -W condition). Material is heated up to slightly below its melting temperature, either in an oven or a vat of molten salt, and kept at that temperature for a period of time in order to allow precipitates to be absorbed into solution. Then, the material is quickly cooled to room temperature by quenching it in a vat of water, creating an unstable,

---

[36]A brief introduction to aluminum alloys, the heat treat operation, and relevant terminology, extracted from [Davis, 1993], is given in Appendix 1. See also [Hatch, 1984].

supersaturated state. The part strengthens as precipitates form over time either at room temperature (natural aging) or at an elevated temperature (artificial aging).

Stretch forming (drape forming)

The purpose of the stretch forming operation is to form a sheet of metal to the contour of a die through a combination of bending and stretching. In the drape forming operation, a part is placed on a die and its ends are clamped, after which the part is bent and then stretched in order to "set" the contour. Generally, the jaws are stationary and the die moves in order to impart the stretch; this is how it is done at Vought.

Routing

The purpose of the routing operation is to remove excess material needed for the stretch forming operation. After being placed between upper and lower contoured fixture halves, excess material is removed by routing, using the fixture as a guide. Holes are also drilled at this time. Generally, there is, intentionally, still excess left after routing. No study was made of the routing operation in sheet stretch forming.

Chemical milling

The objective of the chemical milling operation is to remove a layer of metal from the surface the stretch formed part through a chemical reaction between the metal and chemicals in a solution into which the metal is placed. A protective mask is applied to the entire surface of the part and the mask is dried. Then the borders of the sections of masking that are to be removed are scribed using a template for guidance. The masking over the part of the material to be thinned the most is removed. The part is dipped into a vat of chemicals until the desired thickness is achieved. After this, either the part is finished or another section of masking is removed and more material is removed. This cycle is repeated to create the desired surface profile.

Next

Because of the importance of the sheet stretch forming operation study and improvement suggestions, this study is presented first, while the other studies are presented according to the process flow.

6.2 SHEET STRETCH FORMING OPERATION STUDY

6.2.1 Description of the operation

The following diagram shows simplified top and front views of a typical sheet stretch forming press and possible movement of the jaws and die table. Each end of each jaw can move independently, and the jaw mechanism can rotate, as shown in the diagram. The angle of jaw rotation shown in the front view is called the *yoke swing angle*; it is zero when the jaw is vertical as shown in the diagram. The difference between the horizontal positions of a jaw is set by the *jaw angle*. Although not shown, the die table can have a difference in height between the East and West ends; this angle is the *die table angle*.

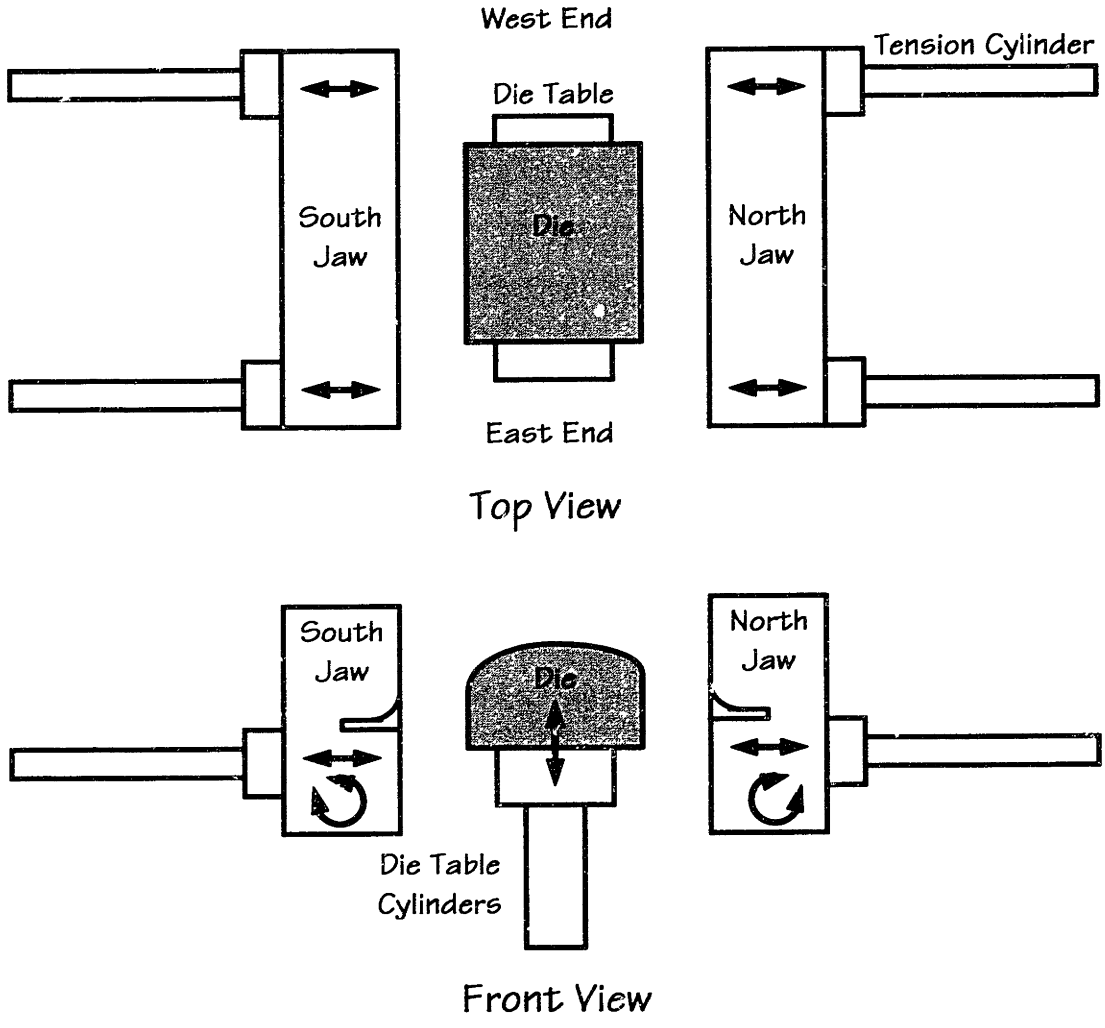

Figure 6.2 Schematic of sheet stretch forming equipment

The steps in the sheet stretch forming operation (drape forming) are shown in the following diagram and described briefly in the following paragraphs.

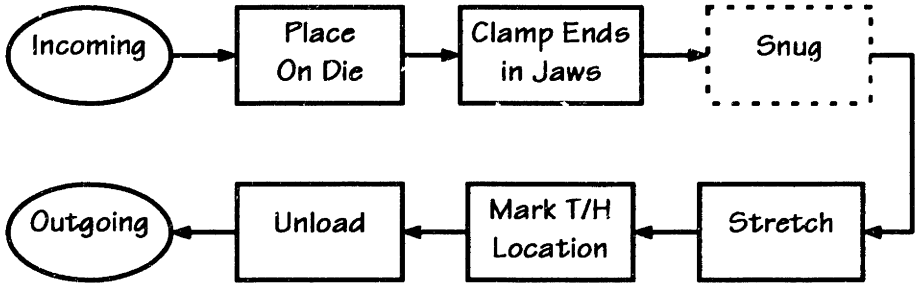

Figure 6.3 Drape forming process flow diagram

Incoming material

Sheet metal geometry and properties are addressed in the next section. Thickness and yield strength appear to vary the most.

If the material has been solution heat treated in house, the quench will induce stresses and strains in the material that cause it to warp and contribute to uneven stresses and strains in the material; further, leaving -W condition material at room temperature causes it to age harden, which significantly affects material properties. If the material has been stretch formed already, then variation in the previous stretch operation will be a source of variation to subsequent stretches.

To achieve a desired contour, the most important material properties are yield strength, elastic modulus, and the strain hardening behavior of the material. The extent of the influence of material properties depends on how the operation is controlled. The most important initial geometry characteristics are contour and thickness.

The following diagram shows the next three steps in the drape forming operation.

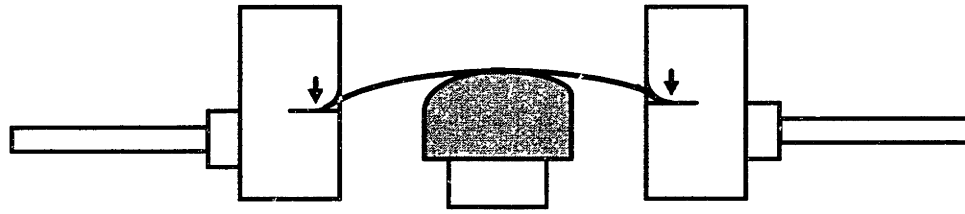

Material on die, and ends clamped in jaws

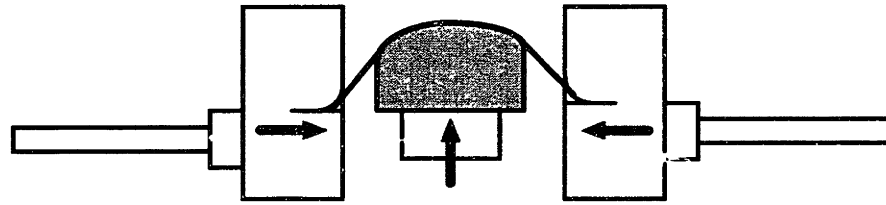

Snug
(jaws are moved in and table is raised to make the part taught)

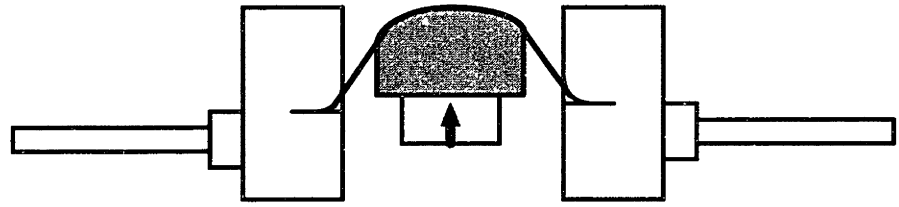

Stretch
(die table is raised to impart stretch)

Figure 6.4 Steps of sheet stretch forming operation

Place on die and clamp ends in jaws

The operators take the workpiece from the stack of incoming sheet and place it on the lubricated die. Next, the operators align the workpiece relative to the jaws and the die, and clamp the jaws. The important settings in this step are the location of the material in the jaws, the location of the die, and the location of the jaws. The two most important material location issues are the position of the material widthwise with respect to the die and the position of the material in the clamps lengthwise. If the snug step is avoided, the jaw positions are those used for the stretch.

Snug

In the snug step, the jaws are brought to the positions at which they will stay during rest of the operation and the die table is raised until the part fits snugly over the die.

The important settings are the location of the jaws and the forces or displacements (plural since the die table rests on two cylinders) of the die table at snug.

Stretch

In the stretch step, the die table is raised until the part is stretched far enough.

Machine

Die table movement is very important as it determines the amount of stretch. How it is controlled—by force or by position—is very important. The tilt of the die table affects the difference in stretch from one end of the part to the other.

The other important machine movement (ideally, in this case there would be no other movement) is that of the jaws and their supporting structure. Compliance in the machine may be important at high forces.

The ability of the machine to repeatably achieve the desired starting position and angle of the jaws, to keep the jaws from moving during the stretch operation, and to repeatably achieve the desired end of stretch condition are the most important machine contributions.

Die

In this step, the die contour and surface characteristics are important. It is common to create kirksite dies by CNC milling a block of kirksite, a zinc-based alloy (earlier tools were made off of a splash from the master shape tool). Due to springback, the die shape is sometimes modified based on the part shape achieved from stretching some sample parts. Inability to get the die shape "just right" may result in a consistent source of contour error from the die. Generally, kirksite dies are sanded as part of the set up procedure. Dies are lubricated using a paint roller to apply the lubricant.

Control system

The most important control issue is how the movement of the die is controlled and how the end of this step is determined—whether by force, position, or some other means. The analytical model demonstrated that the amount of stretch is more sensitive to changes in force than changes in strain or displacement. Further, the operation is less sensitive to material strength variations under strain (or displacement) control than under force control. Die table movement is at times also controlled visually—that is, the operator watches the deformation in the part and knows by experience when it has been pulled far enough. For example, the part may be pulled until it "flashes" or begins to form Lüder lines (both visible phenomena). While visual control is a form of strain

control, it is qualitative rather than quantitative and does not give an accurate idea of the actual strain in a part.

Mark tooling hole location

At the end of the last stretch, the tooling hole locations are marked on the part. Tooling hole locators are in the die. The locations are marked either with a mallet (by hitting the material over the locator to get an imprint) or with an indentor which has been aligned to the locator. Part geometry is not affected, but geometry measurement is affected, because the part is aligned using the tooling holes that will be drilled in the part based on the tooling hole location mark. Thus, correct contour may appear to be off.

6.2.2 Measurements and calculations

A number of measurements were made in the stretch forming operation (and also at points in the stretch forming process) in order to better understand variation, the sources of variation, and the effects of changes in parameters in this process. The measurements also provide a basis for process improvement and evaluation of the effectiveness of proposed improvements. Most of the measurements were made on 2024-T3 leading edges, which are not solution heat treated at Vought. All leading edges are formed on a GEC Alsthom Cyril Bath VTL-750 sheet stretch forming press. Contour measurements made after rout and after chem mill are included here to determine how the contour changes throughout the stretch forming process.

Leading edges were chosen for two primary reasons: first, they are among the most difficult sheet metal parts to form because of their demanding contour requirements; second, they are stiff enough and the bend is tight enough that it is possible to get a useful and accurate measure of springback. In order to get an indication of the effect of heat treat on variation, a lot of solution heat treated leading edges was also measured. A few non-leading edge parts were also measured.

Each part number (P/N) was given a letter of the alphabet (A, B, C, ...) as a simpler means of identification. Within a lot of a given P/N, parts were numerically identified (1, 2, 3, ...) in order of stretch; subsequent operation steps were not performed in order according to identification number, but the number was still used for identification.

Description of measurements

A variety of measurements were made. Data taken changed over time as it was learned that some data were not useful and others would be useful.

Separation from die

In order to give an indication of springback, separation of the material from the die at the end of the part (EOP) was recorded. Separation is used as a measurement for three reasons: (1) it is relatively easy to measure, (2) it is a good indicator of the fit of the part in assembly, and (3) it is a good indicator of what's happening in the operation. Separation was measured with a straight-edge ruler and no hand pressure. This measure represents how close the part contour is to the die surface, which is very important in assembly. Finally, separation is primarily influenced by springback, a function of strain, and it gives a good idea of what's actually going on in the part.

The following diagram shows how the material sits on the die after the stretch forming operation, with the final part outlined lightly. The separation of the part from the die on the diagram is exaggerated from what is normally found. Note the taper from the big end to the small end.

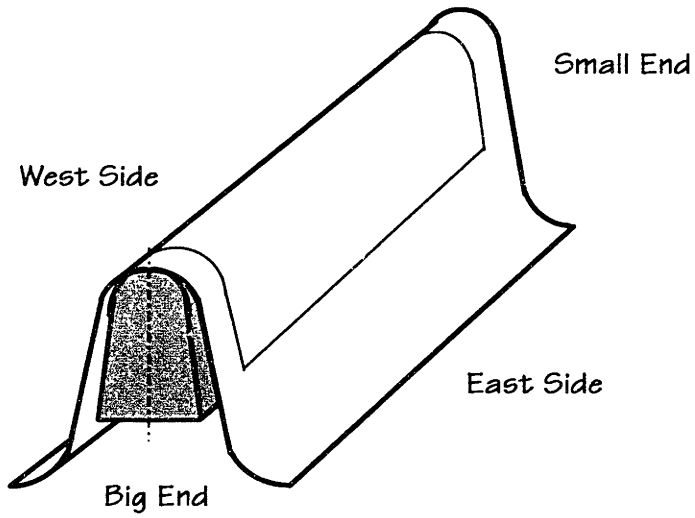

Figure 6.5 Leading edge part on die with separation

The following diagram shows where the measurements were made—in line with the EOP at the ends of the material. Separation was measured with no effort made to seat the material on the die in any particular manner. In order to eliminate the effect of seating, separation is averaged at each end.

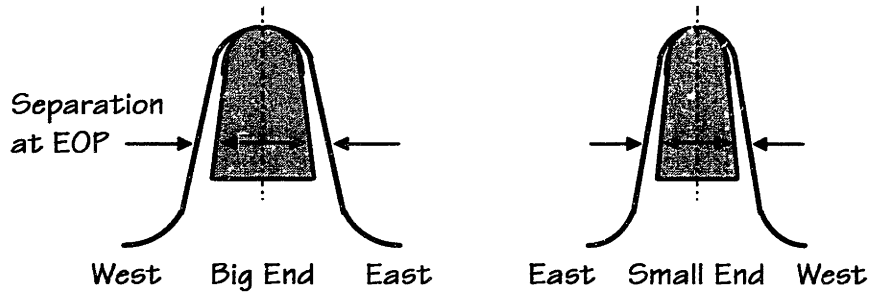

Figure 6.6 Separation of leading edge part from die at EOP

Separation measurements were made immediately after the stretch, after rout, and after chem mill. After routing and chem mill, parts were set one at a time on the stretch forming die to make the measurements.

Strain

Strain was measured in order to assess the amount of strain imposed on the part, and to determine the correlation between strain and springback. Scribe marks were made at the edge of the flat part in the six locations shown in the following diagram. The outer four pairs of scribe marks were made with 5" separation, while the middle two sets were made with 3" separation.

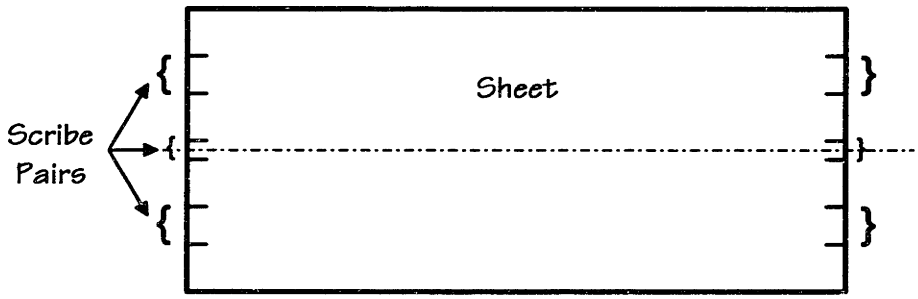

Figure 6.7 Location of scribe pairs used for strain measurement

The four outer sets of strain measurements were only started in lot H. The two middle sets were started in lot I.

Machine measurements

All leading edges are stretched on a Cyril Bath VTL 750 stretch press, a relatively modern CNC machine. The following data were recorded from the control panel:

- Die table position at snug
- Die table position at end of operation (at maximum load)
- Maximum die table force in tons
- Left and right start and stop yoke swing angles (only until lot G)

- Die table rate
- Die table angle (starting with lot H)
- Die table force at snug (starting with lot K)
- Jaw positions and angles (only for testing improvements)

Material information

The following material information was recorded for each lot (up to lot G) from the certification sheets: P/N, material type, material size (length, width, and thickness), lot number, and supplier-measured yield strength.

Calculations

A number of calculations are made from the measurements described above. Calculations which might need explanation are described here.

The amount of die table movement is calculated by subtracting the table start position from the table stop position. Normalized die table movement is calculated by the following equation:

$$\text{Normalized Movement} = \frac{\text{Table Movement}}{(1/2\ \text{Length of Material} - \text{Length in Jaws})}. \qquad (6.1)$$

This normalization takes into consideration of the effect of the original length of the sheet on the strain. Length is in the stretching direction; thus, since leading edges are stretched in the short direction, this is considered the length direction.

Strain is calculated from the distance between the scribe marks before and after the stretch operation. The distance between the 5" scribe marks was measured with calipers, while the distance between the 3" scribe marks was measured with a tape measure because it was over a curve.

The *maximum* strain is calculated by adding the amount of strain relaxation expected at the measured load to the strain calculated from measurement of the scribe marks. The purpose of the maximum strain is to have a strain measure that corresponds to the strain imposed on the part at maximum load.

The maximum average stress in the material is given by

$$\text{Stress} = \frac{\text{Maximum Force (tons)} \times 2}{2 \times \text{Thickness (in)} \times \text{Width (in)}}\ (\text{ksi}). \qquad (6.2)$$

The maximum average stress is maximum because it occurs at maximum force; it is average because it is averaged over the whole area of the sheet carrying the load. The 2 in the numerator is because there are 2,000 lbs per ton. The 2 in the denominator is because the total tonnage is carried by two sides of the part.

Intercepts and slopes are calculated according to the standard least squares regression method. The r^2 regression coefficient is used to give an indication of the strength of linear correlation between two sets of data; a value of zero implies no correlation and a value of one implies perfect linear correlation—strong correlations have a value of over 0.7. While the r^2 value is not the best indicator of correlation between two sets of data, it is reasonably good and its use is quite simple.

6.2.3 Presentation and discussion of the data

Individual part data

Following are the run charts for P/Ns A and D. Variations are typical of those of other parts as well. The vertical scales are the same on both charts. The variables plotted are normalized table movement multiplied by a factor of 10, the average big and small end separations, and the maximum average stress.

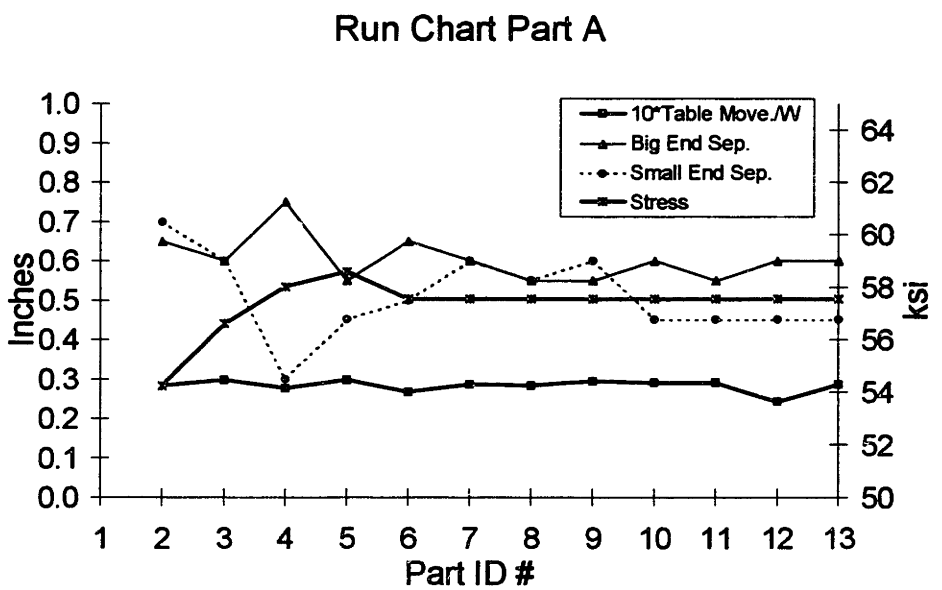

Figure 6.8 Run chart, P/N A

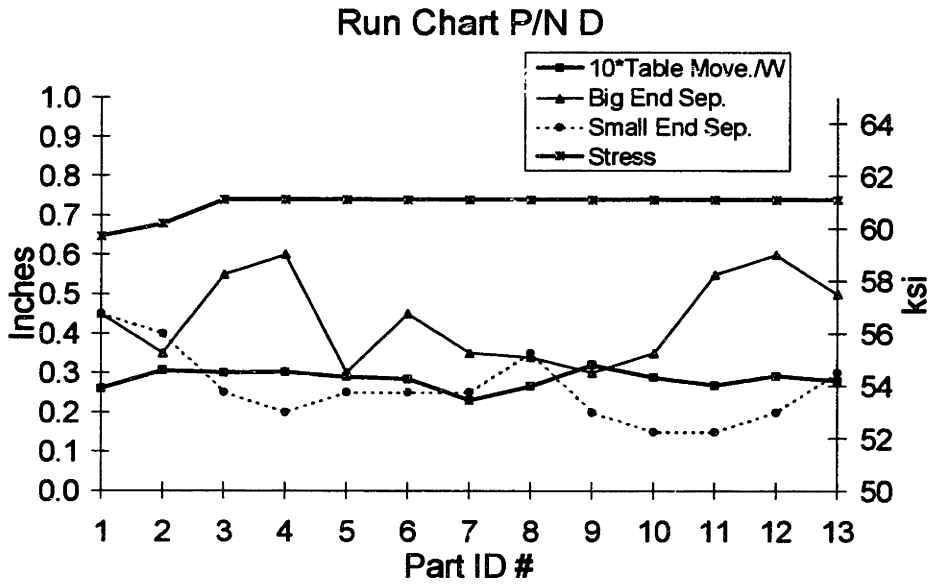

Figure 6.9 Run chart, P/N D

A few insights can be gleaned from these two charts (and other charts not shown).

First, it appears that it takes the operators a few parts to arrive at the desired maximum force. This is because records are not kept, or not used, which indicate the desired force and other settings for each P/N. The parts are generally controlled manually by force, as opposed to by position. The most important reason that this machine is not run in the automatic mode is that, due to flooding a while back, the automatic control system does not work.

Second, the separation differs between the ends. In fact, an inverse relationship is evident—if one end has more springback, the other has less. This is because with a fixed force, if one end has more of it (resulting in more strain and less springback), the other end must have less (resulting in less strain and more springback). Further, separation varies significantly from part to part within a lot and from lot to lot.

Third, there is significant variation in the separation. Further, comparison of the two charts reveals that average separation is inversely related to the average stress.

Fourth, even though the force is constant, die table movement and separation vary significantly. This indicates that there are other significant sources of variation.

Run chart for 2024-T3 material

The next chart shows the average table movement, separation, and stress for P/Ns A to G and I, all 2024-T3 parts.

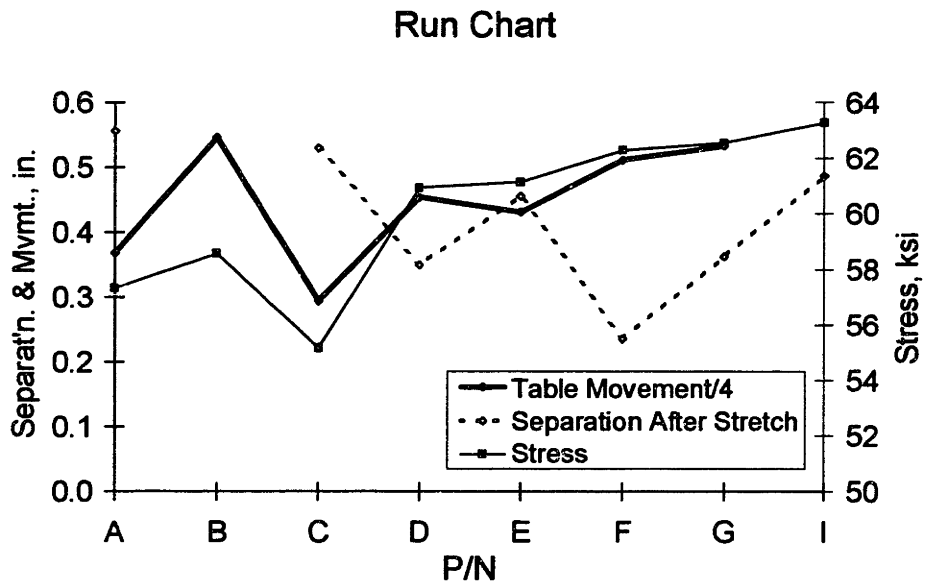

Figure 6.10 Run chart of average table movement, separation, and stress

This chart shows how the three parameters vary among lots. As expected, table movement and stress rise and fall together, while separation is generally inversely related to these two. This chart also shows the significant differences in table movement and stress among the different lots.

Average stress and separation

The following chart shows the relationship between average stress and springback for 2024-T3 P/Ns A and C to G. P/N B was excluded because the significant difference in separation between the two ends adversely affected the data.

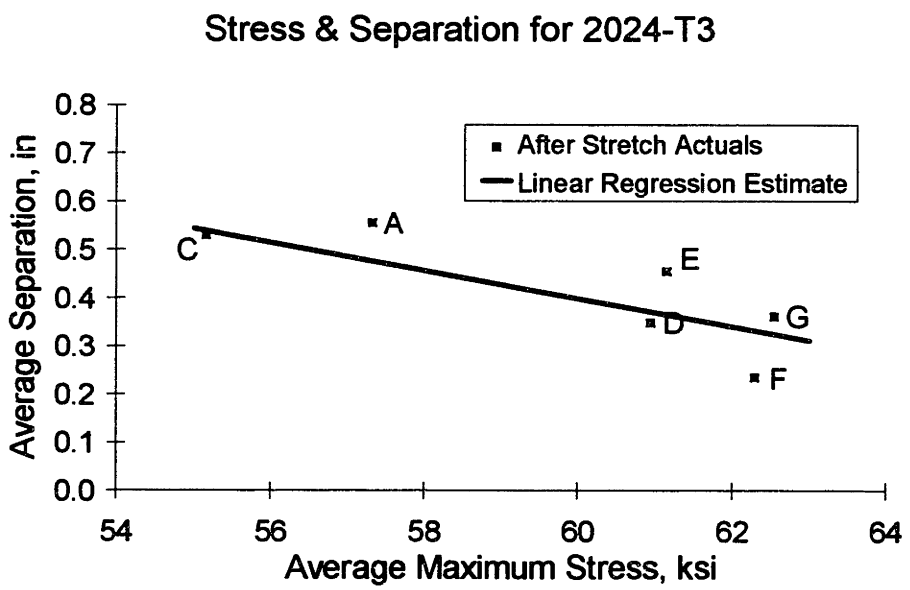

Figure 6.11 Average separation as a function of average maximum stress, after stretch forming

This chart clearly shows the expected result that as parts are stretched further (as the average stress increases), springback decreases. Thus, in order to reduce springback, an adequately high stress could be estimated and parts should be pulled to that stress. For 2024-T3 leading edges, 62 ksi looks like it would be a good force. The ultimate tensile strength for 2024-T3 obtained from tensile tests is around 62 ksi. However, leading edges are stretch formed in conditions which approach plane strain, so that the effective ultimate tensile strength is around 72 ksi, and 62 ksi gives about 3% post stretch strain (this has been verified analytically).

The next chart shows the separation after routing and after chem mill as well.

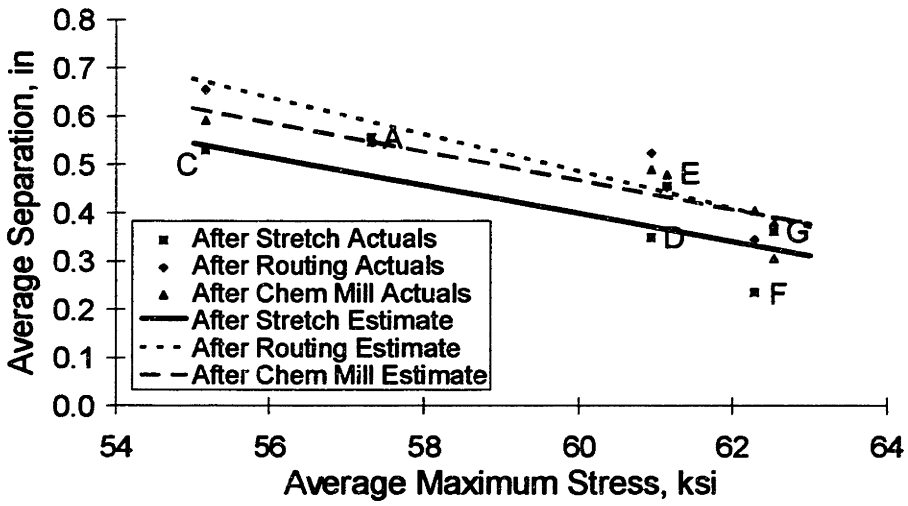

Figure 6.12 Average separation as a function of average maximum stress, after stretch forming, routing, and chem mill

There is little difference between the slopes of the lines apart from statistical variation. The r^2 values for the relationship between maximum average stress and average separation are shown in the following table

	r^2
After Stretch	0.612
After Rout	0.856
After Chem Mill	0.725

Table 6.6 Strength of correlation between stress and separation

The r^2 values indicate a relatively good correlation. While the correlation between stress and springback can be used to estimate springback from stress, the data used here are averages, and the variation within each lot is too great to do this within a lot.

Data analysis using a the Student's t distribution on the difference in separation of each lot shows that the change in separation between after stretch and after rout is significant at between 80% and 90%—close to the border line of what is commonly accepted as statistically significant. Separation after stretch and after rout may not be directly comparable because (a) material is cut off the ends of the part, and there is likely to be some end effect, and (b) removal of the weight of the excess material may

result in increased separation. The change in separation between after rout and after chem mill is not significant.

Die table movement and separation

The relationship between die table movement and separation looks the same as the relationship between stress and separation. The r^2 value for the correlation between die table movement and separation is 0.697, and between normalized die table movement and separation is 0.624. These are essentially the same as the 0.612 r^2 value for the correlation between stress and separation. In theory (as shown in Chapter 5), die table movement (a substitute measure of strain) should correlate better with separation than force. However, the above results indicate that there is no statistical difference. This leads to the conclusion that there are some significant, unaccounted-for sources of variation that make die table movement a poor predictor of springback.

One of the sources of variation in die table movement is the load at which the part is snugged. As the snug force is increased, the die table movement decreases because more movement occurs before snug at higher snug forces, but this pre-snug movement is not counted in die table movement. The following run chart shows the correlation between forces and die table position for P/N LO.

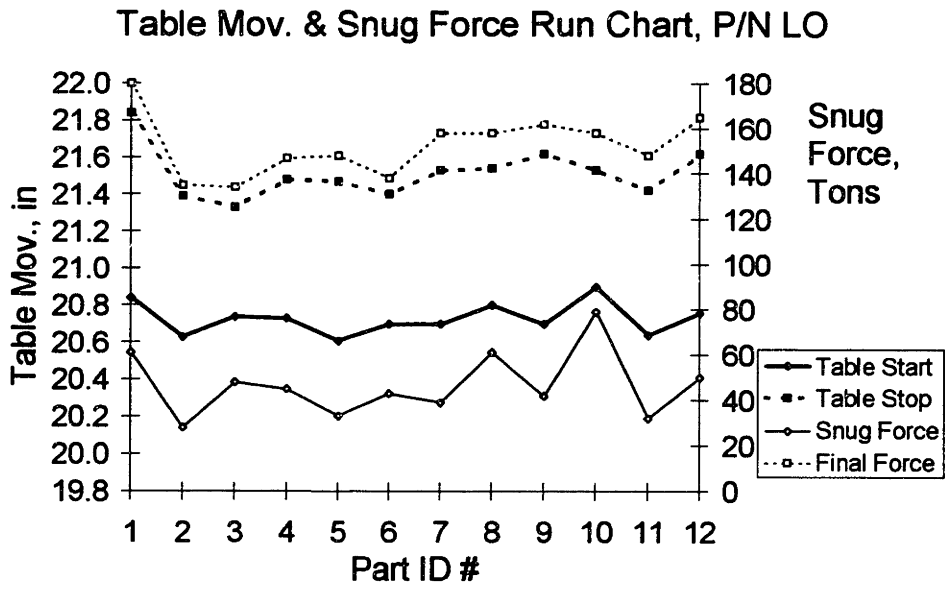

Figure 6.13 Run chart of start and stop table positions and forces, P/N LO

The correlations between snug force and die table start position and final force and die table stop position are clearly evident. However, the data for all the lots do not show a significant difference between the correlations between die table movement and separation versus die table stop position and separation. In order to improve predictions based on table movement, it is necessary to snug the part to the same force each time. Force should be used for snugging, instead of displacement, because the stress-strain curve in the elastic region—where snugging occurs—is very steep, and displacement (or strain) is very small, making the operation more sensitive to force.

Separation by end

The following chart shows the relationship between average separation from the die at both ends of the part after stretch, after rout, and after chem mill for P/Ns A to G.

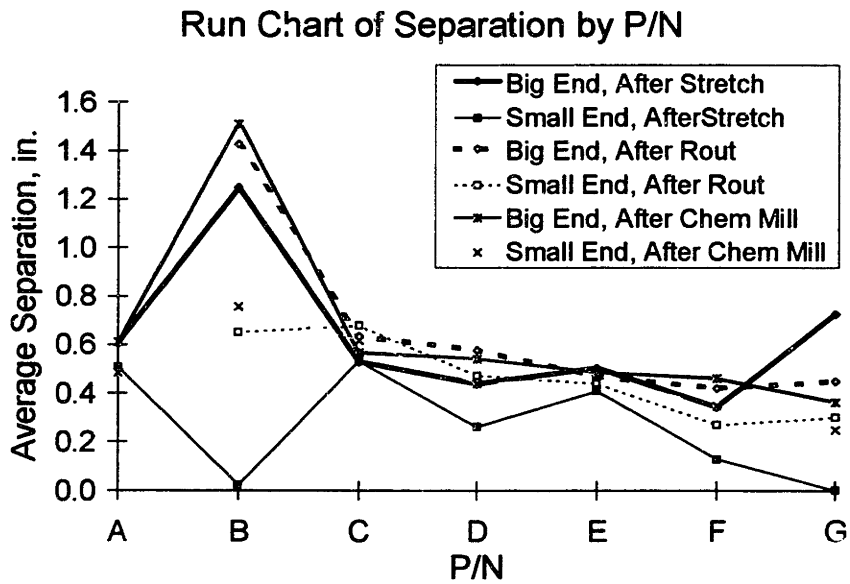

Figure 6.14 Run chart of separation, P/Ns A to G

This chart reveals that the average separation is not always the same at both ends of the part, and that the big end generally has a larger separation—in two lots B and G the difference is very significant. Since more stretch produces less separation (less springback), it may be deduced that in general the stretch is greater at the small end than at the big end. Further, the data indicate that in the cases where there is a big difference between separations directly after stretch—P/Ns B and G—the difference decreases after rout and chem mill. This may be because as excess material is removed at rout, the part adjusts somewhat to a more equal separation.

The following chart shows the relationship between cylinder forces and strains at each end for P/N M.

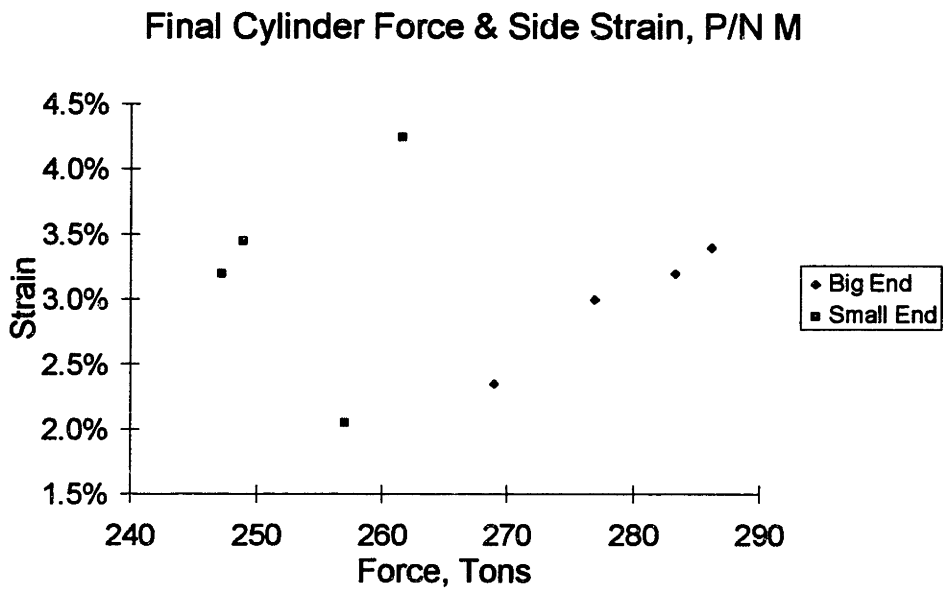

Figure 6.15 Strain as a function of final force by cylinder, P/N M

The chart shows a 25-30 ton difference in forces between the small and big ends at the end of the stretch. Further, except for the low strain point on the small end, there is a strong, positive correlation between force and strain at each end. However, there is also a puzzling element: the higher force end has lower strains than the lower force end. Although the cause is uncertain, it may be attributable to the die not being centered between the two cylinders or to differences in the jaw positions and angles.

Correlation between separation and other measured states

The correlation between measurable states and separation is generally not very strong within a lot of parts, but it is stronger by some measures than by others. The following table shows the r^2 values for the correlation between table stop position, table movement, and maximum force and average separation.

	Table Stop Position	Table Movement	Maximum Force
A	0.013	0.004	***0.712***
B	0.000	0.027	0.222
C	0.258	0.330	0.086
D	***0.498***	0.009	0.229
E	0.008	0.019	0.030
F	0.260	0.027	***0.674***
G	0.051	***1.000***	0.250
H	0.139	0.118	0.008
I			0.029
J	0.141 (***0.625***)	0.298 (***0.675***)	0.398
K	0.136	0.073	0.016
M	0.207	***0.959***	0.190
AVERAGE	0.155 (0.199)	0.260 (0.295)	0.237

Table 6.7 Correlation strengths between strain and table stop position, table movement, and force; bold and italicized values have r^2 values higher than 0.4

It is immediately evident that the correlations vary sporadically, and that there is very little ability to predict separation by any of these measures. Because the variation is so great, the differences among the average r^2 values are not statistically significant.

The correlation between strain and separation is stronger than the correlation between force or either die table state and separation. While average strain (the average of all four strain measurements on a part) is poorly correlated to average separation, the average strain at each end has a higher correlation to the separation at each end. The following table shows the values for the correlations between separation and table stop, table movement, force, overall average strain, and average strain at each end, for those parts in which strain was measured. All r^2 values higher than 0.4 are bold and italicized. Because of the poor correlations, the linear regression estimate sometimes gives the wrong sign for the slope of the line (separation should decrease with increasing strain, and the slope should be negative, but the predicted value is positive). Elements in the table with the wrong sign slope are shaded, and their r^2 values are not included in the average.

Correlation between ...	H	I	K	M	Avg.
Table Stop-Separation	0.139		0.136	0.207	0.139
Table Movement-Separation	0.118		0.073	0.016	0.067
Force-Separation	0.008	0.398	0.016	0.190	0.147
Average: Strain-Separation	0.038	0.182	0.076	0.017	0.057
Big End: Strain-Separation	***0.481***	0.130	0.067	***0.401***	0.316
Small End: Strain-Separation	***0.439***	***0.892***	0.350	0.379	***0.540***

Table 6.8 Correlation strengths between strain and table stop, table movement, force and separation; bold and italicized values have r^2 values higher than 0.4

The first conclusion to draw from this table is that although there is a lot of variation and the correlations are almost never strong, it appears that strain by end has a better correlation to separation by end than table stop position, table movement, force, or average strain have to average separation. The second is that, in order to have any chance at predicting separation from strain, it must be done on an end-by-end basis.

For P/N H, the two sets with the highest correlation are the average strains at the big and small ends compared with the average separation at the big and small ends. The following chart shows the average strain and separation measurements at each end for P/N H.

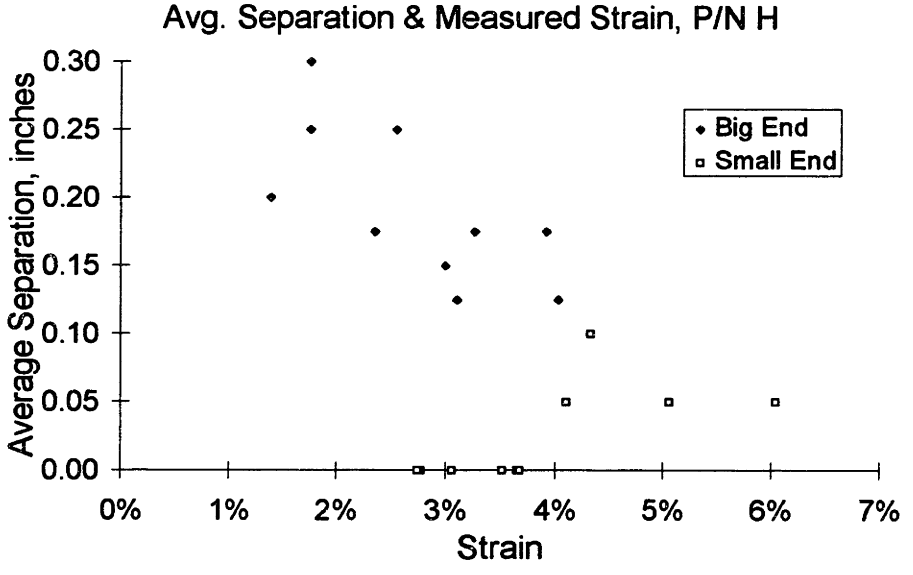

Figure 6.16 Average separation as a function of strain, P/N H

While the big end separation data show a strong correlation to big end strain and decrease with increasing strain, as expected according to theory, the data at the small end are not consistent with theory. The zero separation data for lower strains at the small end are anomalous, and can possibly be attributed to measurement error—the separations were recorded as zero, while all indications are that these values are incorrect. This is the reason that the correlation between the average strain and separation at the small end is not valid.

Force-strain curve

Given the mechanical properties and dimensions of the sheet of metal being stretched, it is possible predict the expected relationship between maximum strain and maximum force of the die table with a force-strain curve. This is simple and relatively accurate for leading edges because the sheet is pulled down essentially vertically off the die. Actual strain and force data can be plotted on the same chart in order to make a comparison. This is done in the following chart for part H, the first part to have strain measurements made. The stress-strain parameters used for the force-strain curve were estimated from the data.

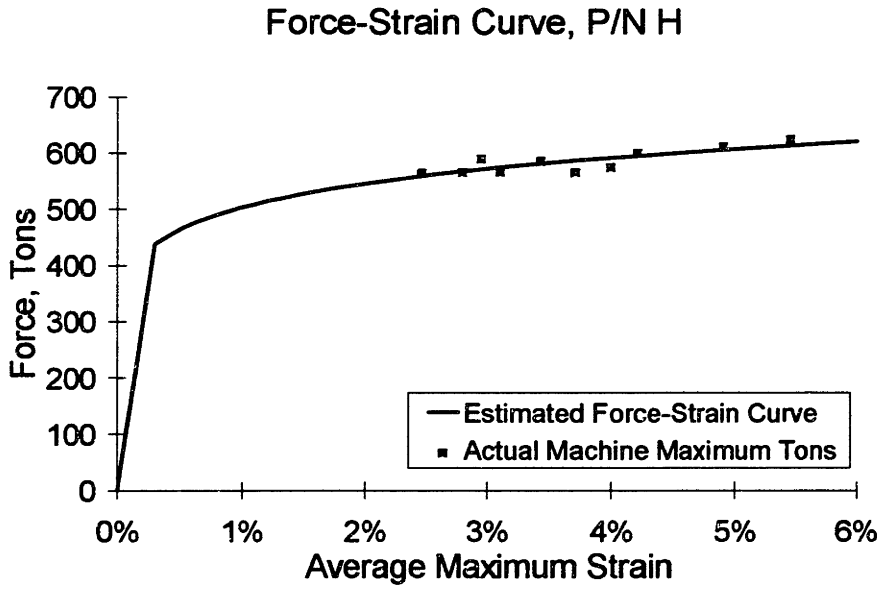

Figure 6.17 Force-strain curve, P/N H

The important thing to notice is that while the spread of force is maybe only 10% of the average, the spread of strain is almost 100% of the average. This argues for control based on strain (or position if it's a good predictor of strain), as opposed to force.

Table movement and strain

There is a significant difference in the amount of strain expected in the material based on die movement and the measured strain. This difference is evident in all lots. The next chart shows the relationship between strain and die table movement for P/N H.

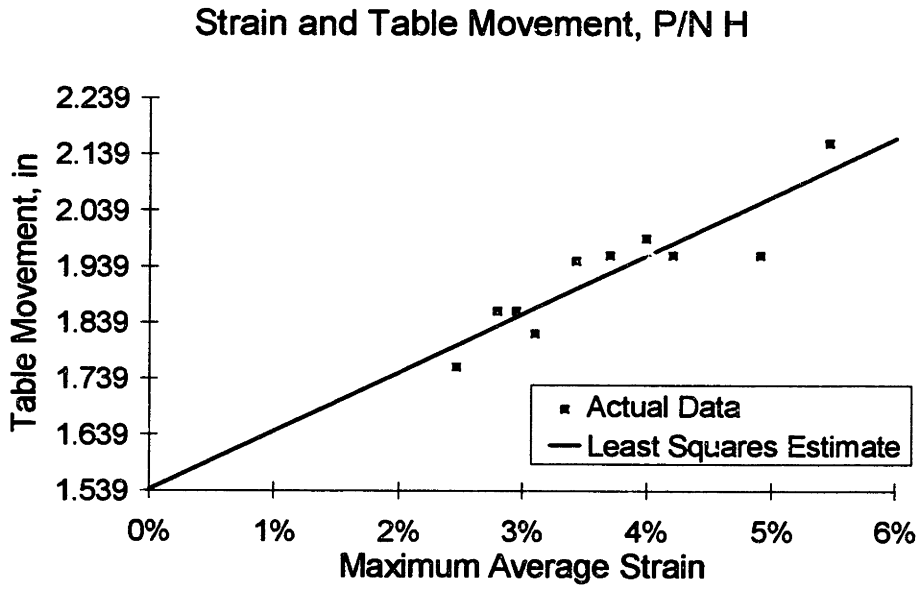

Figure 6.18 Table movement as a function of strain, P/N H

Based on a least squares regression analysis, the amount of table movement that did not contribute to strain in the material was 1.539 inches. For an average table movement of 1.93 inches, this is nearly 3/4 of the total table movement. Apparently, there is significant compliance somewhere in the machine. This compliance is probably either in the jaws or in the fact that the part is not fully taught at snug. The yoke swing angle consistently increased from the start to the end of the pull, usually on the left side from 0.1° to 0.9° and on the right side from 0.5° to 1.5°.[37] This is likely the cause of most of the compliance. Regardless of the cause or magnitude of the "offset," a strong correlation between table movement and average strain exists in this lot, which is evidenced by an r^2 value of 0.815.

[37] According to the stretch press manufacturer, the yoke swing angle should not change, and it was suggested that maintenance take a look at this problem.

Effect of material properties on the operation

As established earlier in this chapter, incoming material properties are a potential source of variation. It was found, for example, that the yield strength of 2024-T3 can vary up to 4% or 8% of the average. Since yield strength is assumed to be most indicative of material behavior in the first five percent of strain, it is used to find out if incoming material properties have any significant effect on the operation. However, no correlation was found between yield strength and average stress, average separation, or die table movement, for P/Ns A to G. This lack of effect of yield strength on the operation can be explained by one or both of the two following points. First, yield strength may not be as good an indicator of material strength variations as assumed. Secondly, and more likely, variations of other parameters are so large that they overshadow any effect that material strength may have on the operation. When the process is better controlled and other sources of variation and their effects have been reduced, variation of material properties will likely become significant.

Effect of natural aging

The effect of natural aging on material properties was measured in the heat treat designed experiment. Now, the impact of aging (strengthening) on the stretch forming operation is studied in P/N J. The time between when each part was taken out of the freezer and when it was stretch formed was recorded (parts were placed in the freezer within a few minutes after coming out of quench). The following run chart shows separation at the big and small ends, scaled normalized die table movement and time at room temperature, and average stress calculated from tonnage.

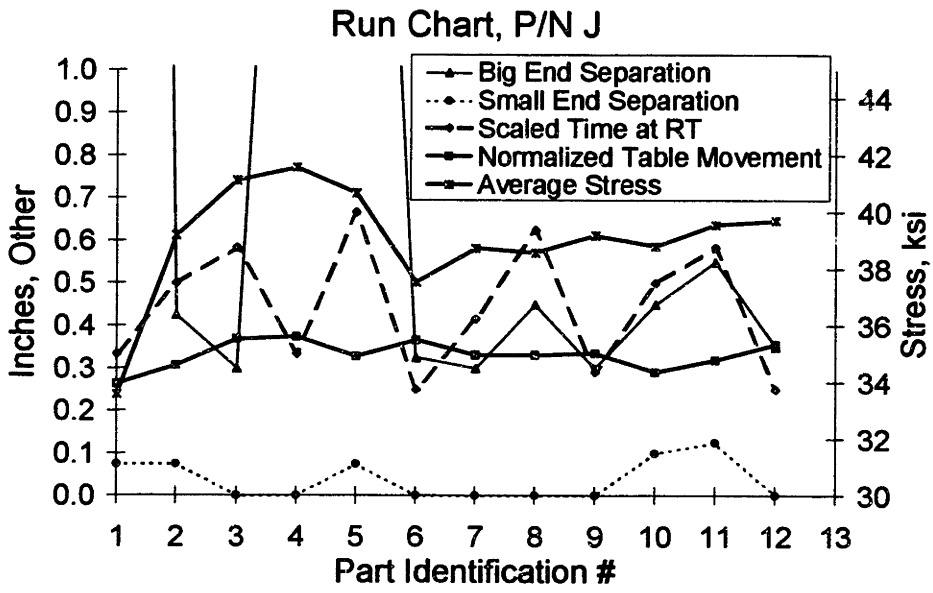

Figure 6.19 Run chart of P/N J, showing effect of time at room temperature

While there are other significant causes of variation in the first few parts, there appears to be a significant correlation between time at room temperature and separation at the big end for parts 6 to 12. This correlation is expected because with the stretch forming press under force control, as the material hardens at room temperature it is stretched less for the same amount of force, and the lower stretch causes more springback (a greater separation of the part from the die). The following chart demonstrates the effect more clearly. Separation, normalized die table movement, and average stress are plotted as a function of time at room temperature for the 9 parts which had average separations less than 1 inch. Two parts were at room temperature for 30 minutes, two for 60 minutes, and two for 70 minutes.

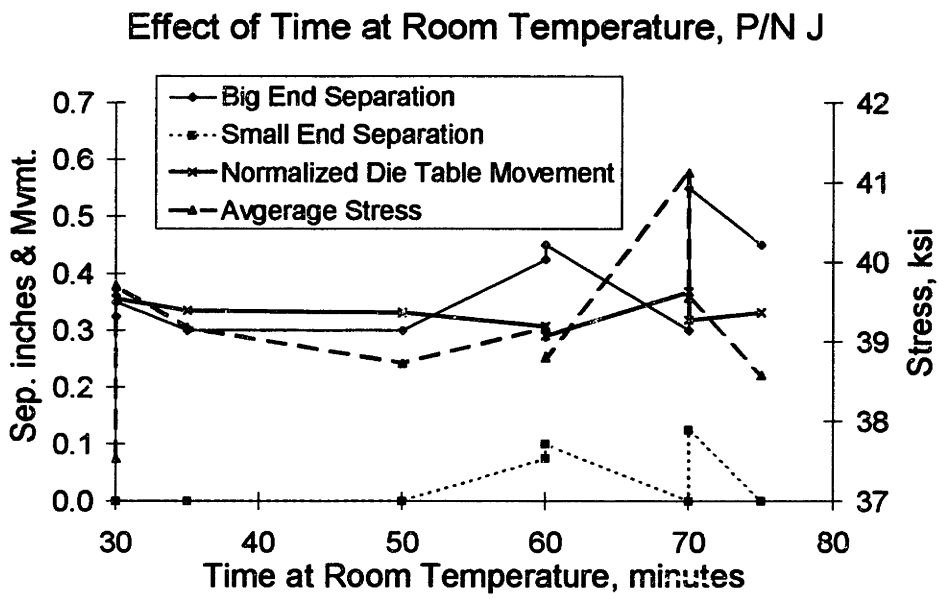

Figure 6.20 Effect of time at room temperature, P/N J

A number of correlations are evident in this chart. As the time at room temperature increases, the average separation increases and the normalized die table movement decreases, even though the average stress remains relatively unchanged (the operation was force-controlled). Excluding the part at 70 minutes which was formed under exceptionally high force and the three parts with very large separation, the lot can be divided into two groups of parts: those left at room temperature 30 to 50 minutes and those left at room temperature 60 to 80 minutes. From the 30-50 minute parts to the 60-80 minute parts, the average time at room temperature increased by 82.8%, the average big end separation increased 27.5%, the average small end separation moved away from zero, and the average normalized die table movement decreased 6.5%, while the average stress stayed essentially constant (it increased 1.6%). These results are expected as the material age hardens.

For some reason, one the two 70 minute parts was formed at an exceptionally high force (41.1 ksi). This increased the normalized die table movement and decreased both of the separations relative to the other 70 minute part. This demonstrates the ability to compensate for the effect of natural aging on material strengthening.

Variation quantified

Variation in the states of the operation is quantified in the following table. In the first three columns, one standard deviation of the listed state is divided by the nominal

value for each lot. In the last two columns, one standard deviation of the average separation at each end is shown for each lot. Column averages are given in the last row. For P/N J, the standard deviation of the separation at the big end in parentheses is without the three outliers.

P/N	Standard Deviation / Average			Standard Deviation	
	Table Stop	Table Movement	Maximum Force	Avg. Big End Separation	Avg. Small E Separation
A	2%	5%	2%	0.06"	0.11"
B	5%	7%	1%	0.07"	0.04"
C	5%	11%	2%	0.11"	0.14"
D	3%	8%	1%	0.11"	0.09"
E	2%	6%	1%	0.24"	0.14"
F	4%	9%	3%	0.13"	0.17"
G	2%	8%	0%	0.04"	0.00"
H	4%	6%	4%	0.06"	0.04"
I			1%	0.25"	0.17"
J	10%	10%	5%	2.40" (0.09")	0.05"
K	6%	8%	0%	0.04"	0.04"
LO	17%	15%	9%		
LW	22%	25%	7%		
M	1%	6%	0%	0.02"	0.04"
Avg.	6%	10%	3%	0.30" (0.10")	0.09"

Table 6.9 Averages and standard deviations of table stop position, table movement, and maximum force, and standard deviations of separation by end

The above values reflect only one standard deviation; a range of six standard deviations is needed to include 99% of the population. These variations are significant. Three further useful insights can be readily gleaned from this table.

First, the final table position (table stop) is more consistent than the amount of distance that the table moved between snug and stop (table movement). The likely reason for this is that parts are not snugged consistently, as already mentioned.

Second, the maximum tonnage has a standard deviation over average ratio of only three percent, while table stop and table movement have ratios of six and ten percent —twice as much. This is expected because the operation is force-controlled. Since the average stress is calculated from the maximum tonnage, its variation is the same as that of maximum tonnage, and so it is not shown.

Third, and most interesting, the average separation at the big end and small end have standard deviations of 0.30" and 0.09", respectively. (However, if three parts in P/N J, which had enormous amounts of springback are excluded from the calculations, the big end average standard deviation becomes 0.10".) This means that at three standard deviations (3σ), the parts can be expected to vary within a lot $\pm$ 0.590". The standard deviations among lots (the standard deviation of the set composed of the average separations at each end for each lot) are 0.28" for the big end and 0.20" for the small end (without the three P/N J parts), giving $\pm 3\sigma$ limits between lots of $\pm$ 0.840" and $\pm$ 0.600". This is significant part contour variation.

While not shown above, the average strain variation for those parts on which strain was measured was 29%. This is almost ten times greater than the 3% force variation!

While it would be reasonable to expect that at higher average stresses separation varies less, the data do not reveal a change in variation as a function of average stress in the range of stresses used for these parts.

Relationship between strain on the sides of the part and strain at the top

Comparisons of correlations indicated that, of all the measured states, strain correlates best with separation (though the correlation is not very strong), when average strain at each end is correlated to average separation at each end. Based on this finding, one may hypothesize that a stronger correlation might be found between strain around the top (nose) of the leading edge and separation, because, according to theory, strain at the top has the greatest effect on springback.

However, analysis of data from P/N K and P/N M, the only two lots in which strain at the top was measured, showed that correlations between strains at the top and separation by end were on average worse than the correlations between strains at the sides and separation by end. Further, analysis showed no significant correlation between strains at the top and sides by end. The cause of this is probably the inaccuracy of the strain

measurement method. The initial distance between scribe marks is 3"; thus, each 0.030" represents 1% strain. However, the resolution of the measuring device (a tape measure) is 0.015", and at best it can be read to 0.0075", which is 0.25% strain. Further, there is variation in the initial scribe distance. Tattle tails[38] were also used at one point, but their repeatability is no better than the scribe method.

6.2.4 Other measurements and findings

Measurements separate from the above are now presented and discussed along with relevant findings from observation and conversations with operators.

Strain measurements on non-leading edge parts

Tattle tails were used to measure strain in the direction of stretch on three parts in order to get an idea of how strains vary from one area of a part to another, and from one part to another. The following diagram shows, roughly, the shape of the die at each end.

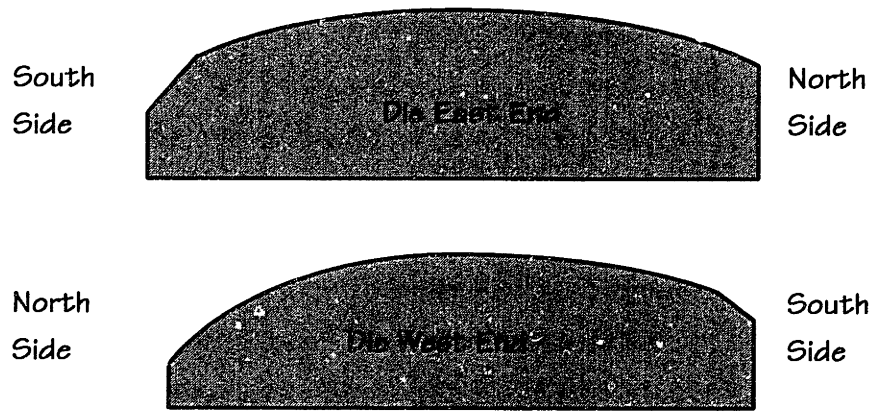

Figure 6.21 Die shape

The following diagram shows top views of the positions of the tattle tails and the strains measured at these locations for three parts. These parts had already been pre formed in the -O condition, had most of the final contour in them already, and were measured as they were being pulled in the -W condition. These parts were pulled on an older, manually controlled machine. The arrows on part #3 indicate the direction of stretch.

---

[38] A *tattle tale* is a simple, single-use device used to measure positive strain along one axis.

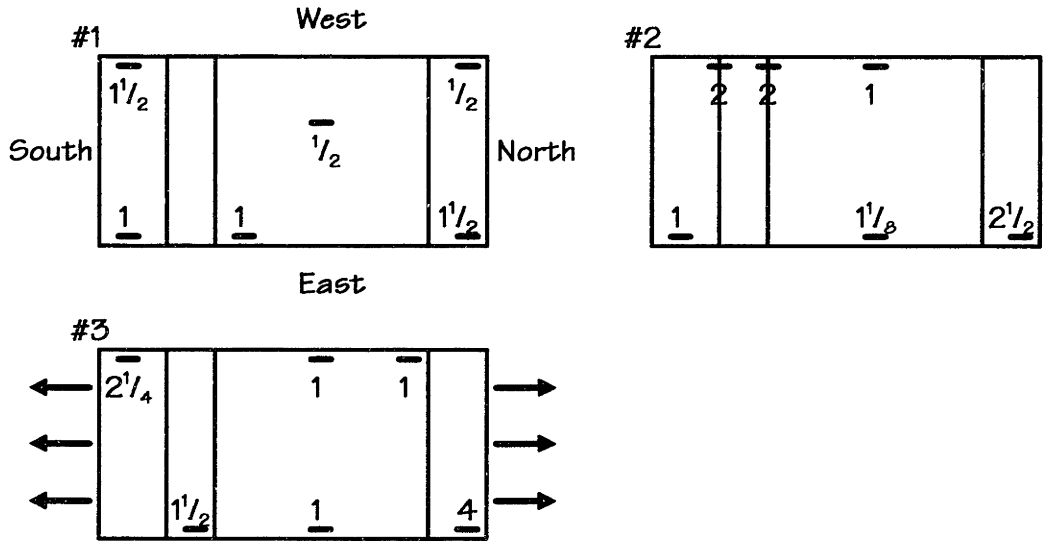

Figure 6.22 Strain measurement locations and readings

Two parts of another lot, of 7075-O aluminum, 0.100" thick with and initially 81" x 92", had the following strains. These parts were also pulled in the North-South direction.

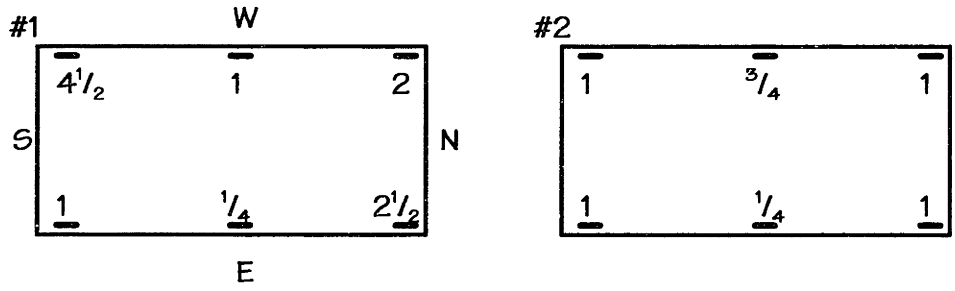

Figure 6.23 Strain measurement locations and readings

Two observations immediately jump out from the above measurements.

- strains vary significantly within a part, and
- strains vary significantly from one part to another within a lot.

There is insufficient data to determine the exact amount of variation, and it is impossible to generalize from this small amount of data to all stretch-formed parts, but it is likely that similar variations are found with other parts as well. Likely sources for these variations are jaw position and angle, jaw movement (undesired, during the operation), material location relative to jaws and die, and die angle and movement. The effect of friction—lower strains in the middle than at the ends—can also be seen in the above diagrams.

Jaw movement measurements

The jaws of one of the older sheet metal stretch presses were moved from "home" position to the "out" location repeatedly, and the out location was measured each time. The following figure is a simple schematic of the stretch press, the positions, and the location of the measurements made at each end of each jaw.

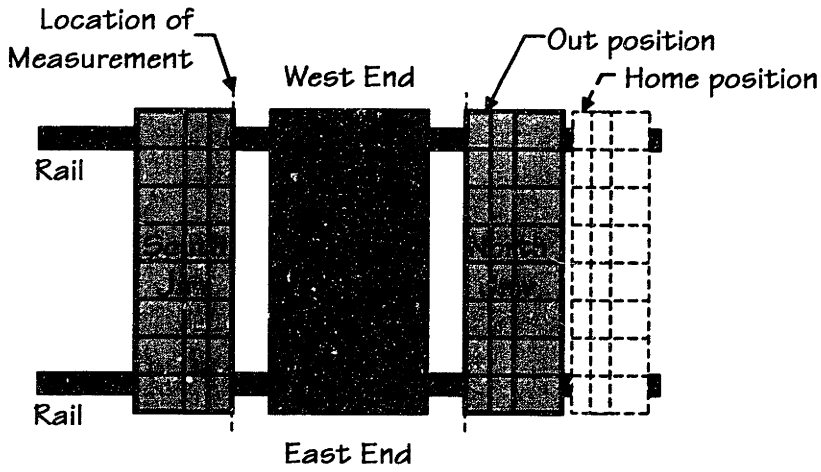

Figure 6.24 Schematic of stretch press showing jaws and measurement locations

Movement of each end of each jaw is controlled automatically and independently (position is set by turning a knob) and is hydraulically powered; each position is measured by a linear to rotary position transducer. The following chart shows the measured distances from the first out position at each end of each jaw.

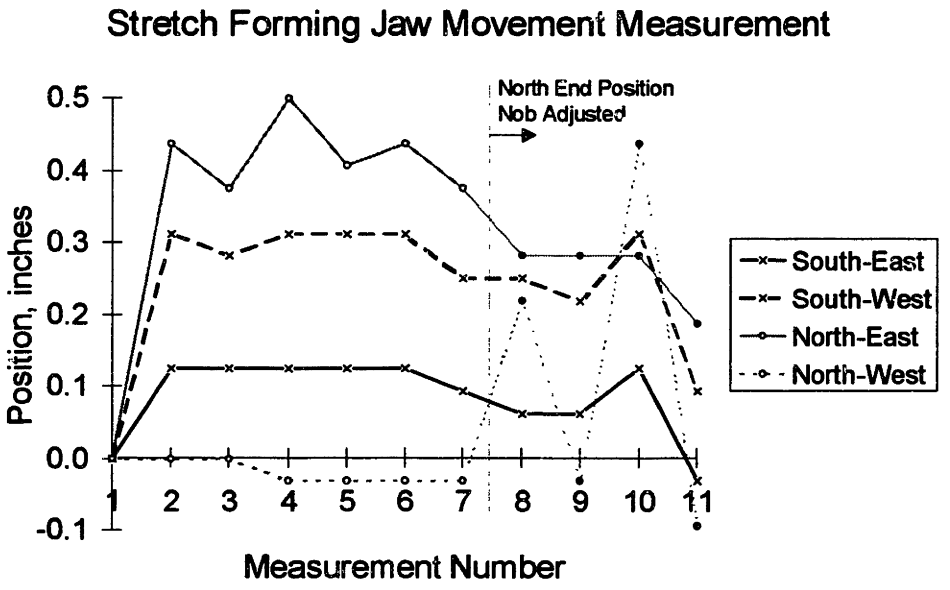

Figure 6.25 Run chart of jaw positions

The variation is significant. Positions of the ends of the south jaw appear to be strongly correlated to one-another, while the north jaw end positions show no correlation. Measurements 1 and 11 were taken after the jaws were sitting in the out position for an extended period of time; these measurements indicate significant and varying amounts of drift. Movements 8 through 11 on the north jaw were achieved by changing the position knob and returning it to same setting as before; these measurements indicate that the variation increases when the position knob is changed. Measurements of the table height repeatability were attempted, but the drift was so significant—about 1/2" in one to two minutes—that repeatable readings could not be made.

The jaw position measurements were made without any load on the machine; it is almost certain that positional variations is greater under loaded conditions and that loads cause the jaw positions to change over time. Further, the machine operators noted, and this author observed, that the jaws of this machine (which are supposed to hold the edges of the part in a fixed location as the die is raised) lifted up off the rails an inch or more during the stretch forming operation. Such sources of variation have a significant effect on the strain imparted to a part. As a side note, the lifting up of the jaws off of the rails is one of the ways the operators judge how far the part is being stretched—there must be a better way.

Another significant source of variation on one of the older machines is that the two cylinders under the die table do not always start their upward motion at the same time, even though they are commanded to do so. This causes an at least one or two inch height difference between the cylinders and will result in one end of the part being stretched more than another if the operator does not stop and start over. Although not measured, it is likely that die table movement also varies between cylinders, even if they start together.

Even on newer machines, positions of the die table and jaws sometimes jump out of calibration slightly, so that from one day or one week to the next, there are slight changes in where the jaws or die table think they are. Existence of this problem outside of Vought was confirmed in the phone interviews with stretch formers.

Measurement of slop on tooling hole indentors

Most dies have at least two tooling hole locators built into the die as shown in the following diagram.

Die With Tooling Hole Locators

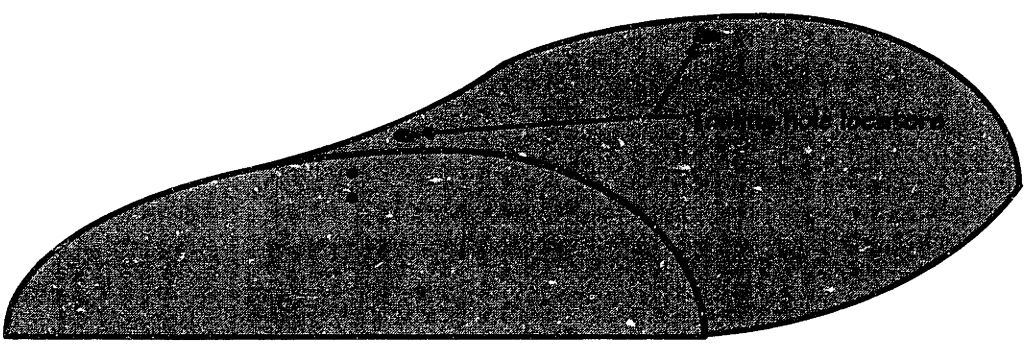

Figure 6.26 Die with tooling hole locators

A tooling hole locator is drawn roughly to scale in the following diagram.

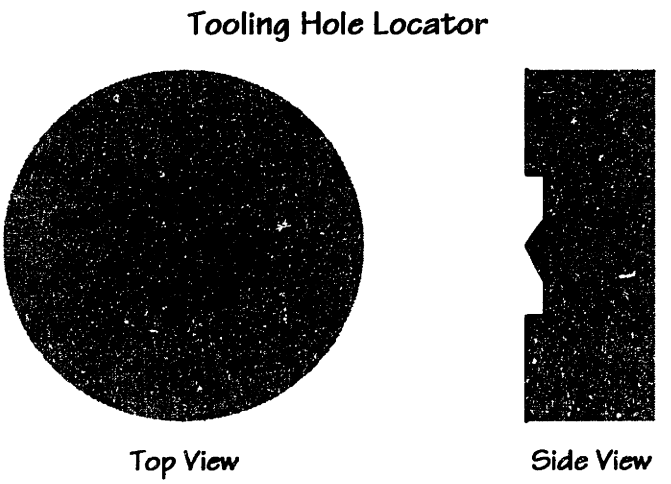

Figure 6.27 Close-up of tooling hole locator

An indentation is made in the part over these locators by one of two methods. In the first method, a soft mallet is used to hit the part directly over the locator, causing the locator to indent the part. This method is highly accurate (in imprinting the location of the tooling hole locator) and repeatable. In the second method, a tooling hole indentor is used to indent the part from the top. This tool is shown in the following diagram.[39]

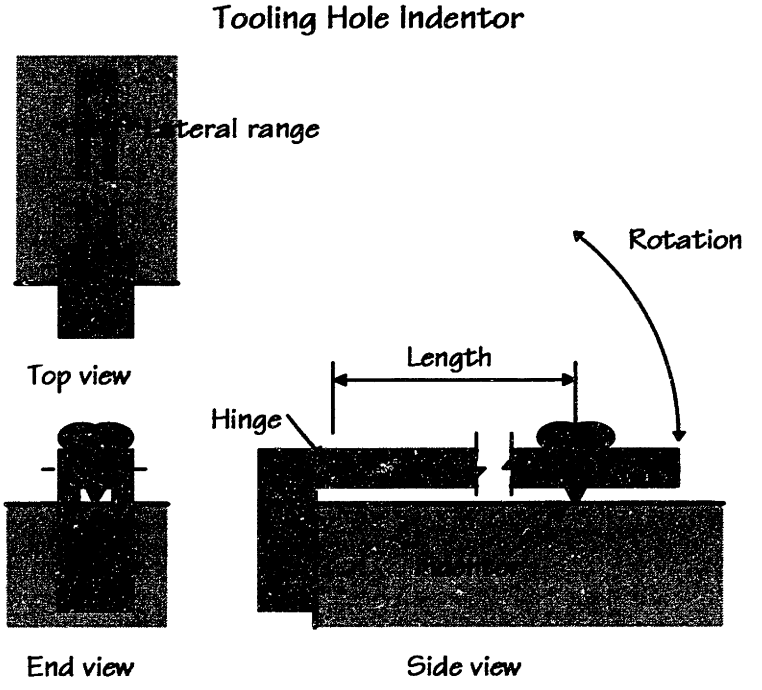

Figure 6.28 Tooling hole indentor

[39] Different companies use other designs, but the concept is similar.

The tooling hole indentor plugs into two holes on the side of the die. The length between the hinge and the indentor is set by the operator, who tries to adjust it so that the indentor is directly over the center of the tooling hole locator. In addition to the longitudinal variation caused by the manual adjustment method, the indentors have a significant lateral range because the hinge is often loose, which it sometimes has to be if the lateral location is off when the tooling hole indentor is plugged in. As a result, the operator knows to push the indentor arm to one side or the other in order to mark the tooling hole location in the right place. The following table shows rough measurements of the distance from the hinge to the indentor and the lateral range of four indentors.

Device #	Distance to Indentor	Lateral Range
1	8.5"	0.17"
2	10.0"	0.69"
3	9.0"	0.11"
4	n/a	0.00"

Table 6.10 Tooling hole indentor lengths and ranges

Device #1, which was on a die, also had a roughly 0.050" length error between the center of the tooling hole and the tip of the indentor. The lateral range on device #4 was zero because the joint was tight. These data confirm the validity of operator complaints that this method has significant variation.

Another source of variation for the location of tooling holes is the ability to locate a drill bit on the indentation made by either method. Since this is a manual operation, and drill bits have a tendency to wander, this is sure to add a significant amount of variation. Measurement of differences between tooling hole locations and tooling pins at the chem mill vendor showed significant variation in the location of tooling holes.

Measurements were made at chem mill on three lots, all stretch formed sheet, to give an idea of the variation. On the first lot, out of twelve parts, three pieces pinned properly (i.e., tooling holes on the part and tooling pins on the template lined up properly), while the tooling hole locations were off between 0.030" and 0.070" on the other nine. On the second lot, all eight parts were off between 0.125" and 0.180". On the third lot, all thirteen parts were off approximately 0.050" to 0.080". The data show that the errors are both accuracy errors (the average location is off) and precision errors (there is variation about the average).

Die

Since die location is only changed from one lot to the next, it was not studied as a source of variation. Location of the die on the table is generally set using a tape measure, and is probably repeatable to within 1/4 inch. Die location is adequately repeatable when setup sheets are used to determine the correct location. Die geometry as a source of variation was not studied. Because all dies at Vought are kirksite, and thus are very stiff and wear-resistant, change in their geometry is not an issue. Since die surfaces are sanded before each setup and generously greased before stretch forming each part, friction does not appear to be a source of variation.

Material location

The part is located relative to the die in the width direction by eyesight, and by marking the edge of the part on the jaws with a felt tip marker; this is probably repeatable to within 1/4 inch as well. The part is always pushed to the back of the jaws, which makes the lengthwise location of the material very repeatable.

Force measurement using hydraulic pressure

Force measurement based on hydraulic pressure is in error due to movement of the hydraulic fluid during the operation. Forces are overestimated by about 10 (30) tons, at 300 (600) tons, which is a 3.3% (5.0%) error due to die table movement. Die table speed, how long a machine has been running, and the ambient temperature will cause hydraulic fluid flow and pressure to vary.

6.2.5 Summary of findings from the measurements and observations

Incoming material

The most significant finding from this study regarding material properties is the effect of aging on the amount of stretch. Because -W condition material strengthens while sitting at room temperature, material left out longer stretches less, and as a result springs back more. While incoming material properties vary significantly, they do not have a noticeable effect on the operation.

Machine

While CNC control of machine movement makes it relatively repeatable, there are still some significant sources of variation in machine movement. Most significant is the difference between the two cylinders, which results in a difference in strain, force, and separation between the ends of a leading edge. The compliance in the press is also a

source of error, as shown by the amount of die table movement that does not contribute to strain in the part. Occasional "jumps" in calibration contribute to variation over longer periods of time. Deterioration of machines (especially leaks and sensor degradation) over time causes them to be less repeatable. While the newer Cyril Bath stretch press is quite reliable, older machines are incapable of achieving tight control on machine movement.

Die

Within a lot, the die does not appear to be a significant source of variation.

Jaws and material location

The location and angle of the jaws were not measured for P/Ns A to M. However, it is hypothesized that they are a significant source of the variation found in these parts. The data gathered during the improvement implementation phase demonstrate that changing jaw location and angle has a very significant impact on the operation—on strains, displacements, and separation. It is unclear whether location of the material in the jaws is a significant source of variation.

Settings

Settings are generally determined by experience—what "works." Sometimes, documented setup cards are not kept or are not consulted. When this is the case, re-finding the right settings adds variation because of the trial and error process, and because what works differs from one time to another and from one operator to another. Settings for manually controlled machines generally vary more than settings for CNC controlled machines because of the improved repeatability of CNC control.

Snug

Measurements show that the die table force and position at snug vary significantly. If the stretch forming operation is controlled by die displacement (movement of the die from snug), variation in the snug will significantly affect the displacement. Further, force and position generally differ from one end of the part to the other at snug. These depend on the die table angle, which is difficult to set so that both ends are stretched the same amount.

The jaw position and angle at snug have a very significant effect on (and are likely much of the reason for variation in) the strain distribution within the part, springback, and contour.

Stretch

The current setting for the amount of stretch—force—is not consistently achieved. The force set and achieved varies within a part (from one end to the other), from one part to the next, and from one lot to the next. Correlations between force and displacement are not very strong, and correlations between these two and strain and separation are generally weak as well.

Tooling hole location

Measurements taken at chem mill demonstrate that tooling hole locations vary significantly. Part of the cause lies in the imprecision of the tooling hole indentor method of marking tooling hole location. This will throw the part contour off when tooling holes are used for alignment.

Control

The most important control issue is control of die movement—whether by force, position, or other measure. Confirming predictions from the analytical model, the data show that while the maximum force varies only slightly, strain variation is almost a factor of 10 greater than force variation.

slight changes in tonnage result in significant changes in strain, that the operation is much more sensitive to changes in force than changes in displacement. The data also reveal that the force setting is not consistent.

States

The objective of the stretch forming operation is to repeatably achieve the desired output—material properties and geometry. However, neither force nor die table movement correlate strongly with separation, the primary indicator of part contour. When each end is considered individually, strain has a higher, but still weak, correlation with separation. The correlations are much stronger when comparing lot averages. Since theory dictates a strong correlation among parameters, one must conclude that other parameters significantly affect the operation and its output, part contour. Measurements also show significant variation in all states, including strain and separation, within a part, within a lot of parts, and from one lot to another.

There appears to be a significant potential benefit in controlling the operation by measuring what's actually happening in the material—that is, by measuring strain. This and other proposed improvements are addressed shortly.

Environment

The most significant environmental source of variation is ambient temperature, because it affects the rate of natural age hardening, as well as machine movement and hydraulic pressure.

Material output

Strain and contour vary significantly within a part, within a lot, and from one lot to the next. Specifically, three standard deviations of the average separation by end, found for each lot and averaged over all the lots are about 0.57" (excluding three parts with very high separation in P/N J would bring this down to 0.28"). Change in separation from before to after routing was borderline significant, while change in separation from before to after chem mill was statistically insignificant.

Summary and conclusion to summary of findings

The findings summarized above indicate significant variation in the stretch forming operation. It appears that variation in settings and machine movement are the source of most of the variation. At Vought, leading edges are stretched to a desired force, but under force control the operation is more sensitive to sources of variation, and strain and die table movement vary more than they would under strain or displacement control. While this in-depth study was performed on leading edges, other measurements indicate significant variations in other parts as well. In light of these findings, improvements are now recommended to improve the precision of the stretch forming operation.

6.2.6 Proposed improvements

The proposed improvements to the sheet metal stretch forming operation (with focus on leading edges) fall into two categories.

1. Repeatably achieve optimized settings
2. Use automatic strain control

These are now addressed.

Repeatably achieve optimized settings

Many settings affect the operation. The optimal value of each should be determined, recorded, and consulted, and the desired settings should be repeatably achieved. The settings that most need to be optimized and repeatably achieved are:

- Jaw positions and angles

- Die table angle
- Snug force
- Final force, displacement, position, or strain

Each setting is now discussed.

Jaw positions

Jaw positions and angles should be exactly the same for each part within a lot. If the jaws are moved out to load and unload parts (as is done for leading edges), they must be brought back repeatably to the same position and angle at snug for each part. On CNC machines, jaw position and angle can be automatically controlled to achieve the exact same settings each time, thus eliminating jaw position and angle as a source of variation. If the machine does not have CNC control, use of a tape measure would probably be adequate, and if the machine is prone to jump out of calibration, manual measurement may be necessary to ensure the desired settings are achieved.

Further, the optimal jaw position needs to be determined and agreed upon. A consistent approach, developed from operator experience, could be used to find optimal jaw positions. As with the other settings, optimization should be aided by strain measurement to determine what's going on in the material. Once found, these and all other settings should be recorded and adhered to for all subsequent setups, and any changes should be noted along with an explanation of any changes.

Die table angle

The data show an often significant difference in the amount of strain between the near and far ends of a part. This is mostly attributable to the die table angle (and somewhat to jaw position). The die table angle must be optimally set and controlled; a couple of possibilities exist, ranging easiest (and least effective) to most difficult (and most effective) to implement. First, the die table angle could be adjusted after a few parts based on average separation or strain measurements. Second, the die table angle could be automatically adjusted to equalize cylinder pressures at snug. Third, equal cylinder pressure could be a requirement throughout the stretch. Finally, if strain control is used, the cylinders could be controlled independently so that the average part strain is equal at both ends throughout the operation. These compensation approaches use measurements to adjust machine movement, thereby eliminating a source of variation.

Snug force

The snug force should be the same each time if snug is used for the start of displacement or strain control. In the elastic range, the force-strain curve is very steep, due to the high elastic modulus. Therefore, the snug step should be force-controlled. The force should be significantly less than the force needed to cause the material to yield.[40] Displacement or strain control require a repeatable snug to make the operation less sensitive to variations, whereas a force- or final die table position-controlled snug makes the operation insensitive to changes in the snug. Under displacement or strain control, snugging to a pre-determined force compensates for variations in initial conditions, making the process insensitive to these sources of variation.

Final force, displacement, position, or strain

Determining the desired die table force, displacement, or position, or strain at the end of stretch can be performed both on the shop floor and theoretically. Shop floor data show that for aluminum alloy 2024-T3 62 ksi is a good stress within the free material to shoot for at the end of stretch, and it should give a strain of about 2.0 to 2.5%, under plane strain conditions. The most important thing for improving precision is that the setting is repeatably achieved. Use of load cells or load pins would effectively eliminate force measurement error, but would be expensive.

Die table displacement control should significantly improve repeatability over force control, because displacement is essentially a surrogate for strain, and so is much more closely tied to strain than force. However, with machine compliance it is not possible to directly calculate strain (although strain measurements can be made on the part and correlated to table movement). If the snug is repeatable, table movement from a force-controlled snug is probably the best measure for displacement control. Final die table position control is similar to displacement control, except that no indication of strain is given at all, and initial condition variations will affect this form of control more than snugging repeatably. Part of the reason that displacement and position control are not expected to be as repeatable as strain control is that they affect the average strain, but are not easily used to control the strain in the part from end to the other.

---

[40] Thirty tons seemed to work well for parts that were stretched to between 450 and 700 tons.

If strain control is to be implemented, of course the optimal strain needs to be determined. Probably between two and three percent strain, preferably towards the higher end, should be used. In theory, a higher strain should lead to less springback, which should also lead to less variation of springback. The data collected before testing the improvements do not indicate a significant reduction in variation with less springback. However, one lot pulled under displacement control with repeatably achieved optimized settings that had on average 1/25th the springback of the other displacement-controlled lot had about 1/3rd the variation of the other lot. This issue deserves more attention.

Use automatic strain control

Strain control is likely to provide the most repeatability. Essentially, strain control is measuring what's going on in the part itself and using this to control the operation.

The "old" way of determining when a part has been stretched enough, by watching to see how the material moves on the die is, actually, a method of strain control as well. The difficulty it suffers, however, is that it gives no indication of the actual strains in the part. Further, when the material is all against the die, it is difficult to gage further movement, and so the stretching is often stopped at this point, even though the part could actually use more strain.

Because strain control is such a major topic, it is discussed separately, next.

6.2.7 Strain measurement and strain control

Strain control of the stretch forming operation is proposed because both force and displacement control have inherent variation. Strain control means measuring part strain in-process with one or more strain measurement devices and adjusting machine movement to achieve a desired strain trajectory. In-process strain measurement and control eliminates prediction of strain based on material properties or the geometry of the setup and machine movement, all of which are likely to change and have significant variation. Strain control makes the process insensitive to most sources of variation.[41]

---

[41] Part measurement has been found to be the best indicator of process health in stamping [Allen, 1989] and [Keeler, 1985], and it is a fundamental principle in control that the closer one gets to measuring the desired output, the more effective is the control system (since springback is only something that happens at the end of the operation, it is not possible to use springback for in-process control of the operation).

Strain control is already used to some extent in stretch forming, because experience has shown it is often the best predictor of the state of the operation. The most common current strain measurement and control methods are: watching the part to see how it deforms on the die, watching for Lüdering or "flashing" of the part, marking the part and seeing how far the mark moves, measuring strain with a tattle tale, measuring strain with a grid (a set of lines) or scribe marks. Each method can give a useful measure of part strain, but suffers from one or more of the following weaknesses: actual strain is not indicated, there is significant variation inherent in the method, it permanently marks the part, and it is manually performed. This thesis proposes to go a step further than these through the use of an accurate and precise, automatic, in-process strain measurement device with real-time electronic reading of the strain measurements, ultimately for the purpose of controlling the operation by strain. The strain measurement devices used in this research were developed by Vought, and because of the proprietary nature of this technology, the actual design cannot be discussed.

6.2.8 How to implement automatic strain control

Before going on to the results of implementing the recommendations, the issue of how to implement automatic strain control is addressed. A number of questions must be answered in order to decide on how to best control the stretch forming operation by automatic strain control.

When should strain measurement initiated?

When strain measurement is initiated is very important to the success of strain control. This has to do with when the strain measurement devices are placed on the part and when they are zeroed (initialized). Obviously, the former may occur before the latter, but the latter may not occur before the former. The following table shows the possible points at which strain measurement can be started, which strains are included or excluded with each option, and each option's primary advantage and disadvantage.

Measurement started	Strains included	Strains excluded	Primary advantage	Primary disadvantage
In flat	All	None	Repeatable	Difficult to move part
After loading	Some bending, all stretch	Bending at loading		Strains change before forming
After snugging	Almost all stretch	Most bending	Measures only stretch	Noisy if snug is not repeatable
After forming	None	All	Repeatable	Gives no useful info.

Table 6.11 Possible stages of stretch forming to start strain measurement

Based on this table, it appears most reasonable to initiate measurement after snugging, as long as snug is repeatable. The strain measurement devices should not be placed on the part in the flat due the difficulty of moving a sheet of metal with wires attached to it. Whether the devices are put on after loading or after snug depends on convenience.

Where should the strain measurement device(s) be placed?

This question can be answered by answering four sub-questions: (1) how many strain measurement devices should be used? (2) where, according to the amount of strain, should the device(s) be placed? (3) where, along the length of the part, should the device(s) be placed? and (4) what measurement method and method of attachment is being used?

The answer to the first question depends on (a) the degrees of freedom on the machine that can be adjusted in response to strain measurement, (b) the number of measurements needed to represent what's going on per degree of freedom, and (c) ease of use. The number of degrees of freedom represented by the strain measurements should exceed the number of degrees of freedom that can be independently adjusted on the machine. Ideally, only one strain measurement device is adequate to represent the strain, but more than one device may be needed to create an average strain measurement for a given degree of freedom if for some reason a single measurement would not accurately represent what's going on. Finally, ease of use requires use of as few strain measurement devices as possible.

To answer the second question, the two cases of where the most or the least amount of strain are expected are addressed. The strain measurement device should be placed in a location that best characterizes the strain state of the material. If the strain

measurement device is located where the most strain is expected, this should serve to represent what's going on in the rest of the part. On the other hand, if the portion of the part that is strained the least (strained last, but still strained) is measured, this may serve as a better indicator, to ensure that all of the part has been stretched. However, since this strain will only change at the end of the operation, it cannot be used for machine control, and it may not give a good indication of maximum strain elsewhere in the part. Even though the point of least strain can't be used for control, measuring strain there in addition to the point of greatest strain will certainly give a good indication of changes in the operation. Again, ease of use will significantly affect the best location.

To answer the third question, three cases are considered: placing the strain measurement device in the excess off the die, just on the die, or in the middle of the part. In the excess, the strain measured is unaffected by friction or changes in radius of curvature. However, due to friction and complex contours, strain in the excess differs from strain in the part. Just on the die, the strain is more representative of the part. In the middle of the die, due to friction, the strain is representative of the least amount of strain. The ability of the strain measurement device to measure strains on a contour will influence the ideal location. Further, if the material where the strain is measured is in an area of changing radius of curvature, material movement will affect the strain reading. Again, ease of use will influence the best location, e.g., the middle of the die may be hard to reach.

A number of measurement devices and technologies can be used or created to measure strain. If the device is mechanically-based, the issue of attachment to the part is important. If it is optically-based, where the optical measuring device (for example, CCD camera or laser) can be located is important. If the measurement technique affects the surface finish on a skin quality sheet, its use will be limited to material in the excess. The technique's ability to measure strain over different and varying curvatures is also important.

As is evident from the above, the ideal strain measurement device locations depend on the die and the machine used, must be considered specially for each situation, and must be easy to reach. Due to changing strains throughout the part, the strain measurement device must be placed in the same location each time.

When should the operation be stopped?

At what strain should the operation be stopped? This value must be strategically placed between the maximum allowable strain (either due to thinning, fracture, or surface blemishes) and the minimum strain required to hold contour. To minimize springback and other shape distortion, all of the part should see at least 1% strain if this doesn't impose too great a strain elsewhere in the part. A good, average strain to shoot for is about 3%. This will vary from part to part.

What resolution and gage length are needed?

The appropriate gage length must be selected based on (a) the smallest strain increment that needs to be measured, (b) the resolution attainable, and (c) the amount of space (gage length) available on the part. These are now discussed.

The strain at which plastic yielding of aluminum begins is between 0.1% and 0.4%, depending on the strength of the alloy. To measure strain accurately and repeatably below the yield point, gage resolution would have to be very small. However, that may not be necessary. The following table shows the minimum required resolution for a given gage length as a function of the smallest strain increment measured.

Smallest Strain Increment Measured	Minimum Required Resolution		
	1" Gage	3" Gage	5" Gage
1.0%	0.010"	0.030"	0.050"
0.1%	0.001"	0.003"	0.005"
0.03%	0.0003"	0.0009"	0.0015"
0.01%	0.0001"	0.0003"	0.0005"

Table 6.12 Strain gage resolution requirements

If one is not attempting to measure fractions of elastic strains, the smallest strain increment that needs to be repeatably measured is probably 0.1%. In order to measure to 0.1% strain repeatably, the smallest strain increment measured of 0.03% is probably adequate. However, automatic control is likely to require finer strain increments. Achievable resolution depends on the device and technology used. The amount of space available on the part depends on part geometry, the measurement method and method of attachment used, and the configuration and movement of the tooling.

What are the requirements of an automatic strain measurement system?

Ideally, an automatic strain measurement system would have the following features:

- Be simple, fast, and easy to use.
- Accept 1 to 4 strain measurement devices.
- Sample the strain measurement devices and update measurements on a display at least 3 to 4 times per second (a higher rate is needed for automatic strain control).
- Permit averaging of measurements.
- Allow zeroing of strains at any time.
- Allow setting of limits at which the system audibly or otherwise alerts the operator that a pre-determined amount of strain has been achieved.
- Store the strain readouts in a file so they can be analyzed later.
- Have output of devices capable of being used as a control input to the machine controller.

Summary and conclusions to how to implement automatic strain control

In order to implement automatic strain control, one of the most important factors is ease of use. Strain measurement should generally be initiated after snug, if snug is repeatable. Ideally, one strain measurement device should be used per degree of freedom of movement during the stretch. Location of strain measurement devices depends on the part shape. If strain in the part is uniform, 3% is a good target strain. Resolution of the strain measurement device depends on the smallest strain increment that needs to be measured, which is likely to be around 0.03%, but may be smaller for automatic control. Automatic strain measurement system requirements are listed directly above. Under automatic strain control, outputs from the measurement devices feed back into the machine controller.

Plots of strain measurements

In order to give an idea of the capability of the strain measurement devices used for the research performed in this thesis, the following charts show the strains measured on three leading edge parts, of P/N N.

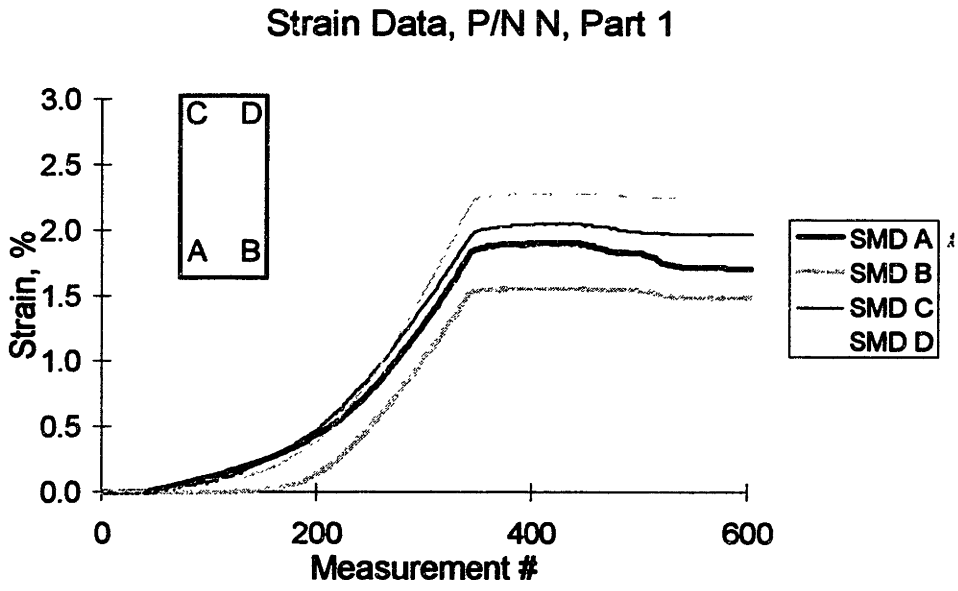

Figure 6.29 Strains measured on part 1 of P/N N

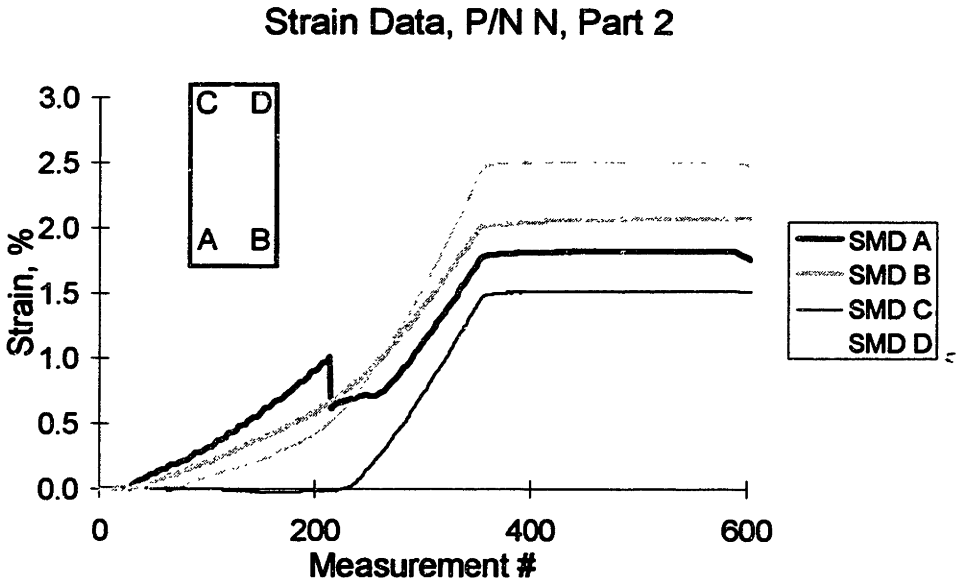

Figure 6.30 Strains measured on part 2 of P/N N

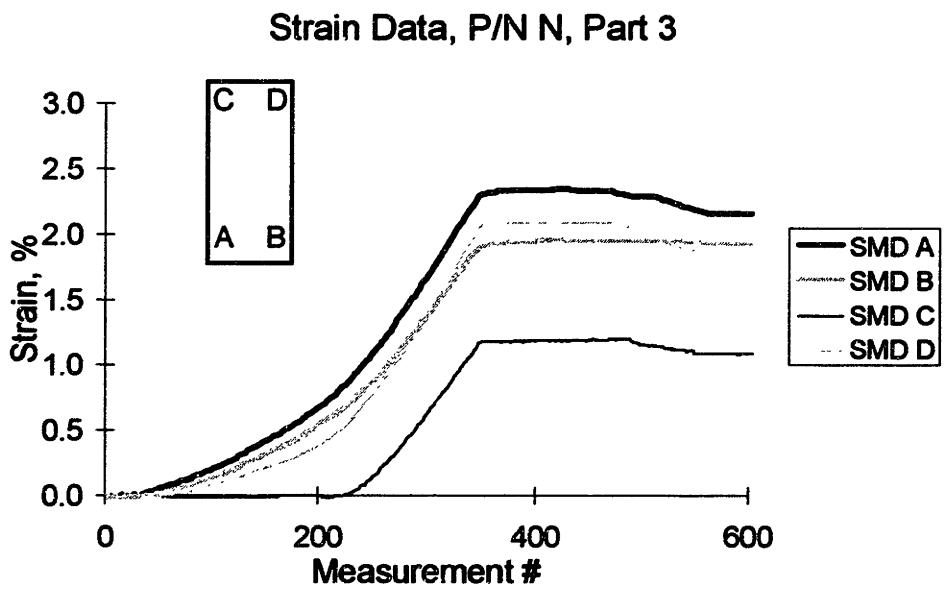

Figure 6.31 Strains measured on part 3 of P/N N

In-process strain measurement reveals how the strains change during the operation. This is useful in helping the operators to determine the optimal machine setup, or to determine if a previously optimal set is still optimal, and if not why. For example, on part 2, the measurements show that somehow the part shifted, causing the strain at location A to drop suddenly. Further, in parts 2 and 3, the measurements show that the reason location C has less strain than the other locations is that it doesn't begin to get stretched until about 1/3 of the way through the stretch. The charts also show machine compliance. If there were no compliance, the slope of the increasing strain curves would be constant, because the die table moves at a constant rate. Instead, strain increases slowly at first while most of the compliance is being pulled out of the machine, and quickly at the end, when it is mostly the part stretching.

It appears that the resolution of the strain measurement devices (somewhere around 0.01% strain) is good enough for use in automatic control.

6.2.9 Implementation of recommended improvements

Three sets of recommended improvements were made and tested on leading edges: force control, displacement control, and strain control, each with repeatably achieved optimized settings. Preliminary data gathered from the tests demonstrate significant precision improvement, with a promise for more.

How recommendations were implemented

Optimization of settings was done partly by theory and partly by operator experience. The maximum die table force was predicted to give an average stress of 62 ksi, and the snug force was set to 30 tons (initially 100 tons was suggested, but this was found to be too high). The die optimal table angle and jaw locations and angles were found through operator experience combined with strain measurements when available. Once the optimal settings were determined, they were repeatably achieved by the operators manually ensuring the same initial conditions each time (recall, the automatic control on this machine is not working). Only the parts after the first one or two parts, when changes were made to settings, were used to determine the statistical variation of these methods. This is because it is assumed that operators would refer to setup sheets for future lots, and there would be no need to re-optimize the settings each time a lot is run.

Force control was implemented by repeatably achieving the same maximum force for each part. Displacement control was implemented by snugging the part to 30 tons and repeatably achieving the same movement to final position one each part. Strain control was implemented by measuring the strain in the part, starting at a 30 ton snug, and stopping the operation when the average strain at the big end reached a predetermined value.

The strain measurement system met all of the requirements described above. Strain measurement device outputs went into a portable computer and the measurements were displayed on its screen in real time at a sample rate of about 4 times per second (which was fast enough for testing purposes). Four strain measurement devices were used; one on each side of each end of the part, as shown in the following diagram.

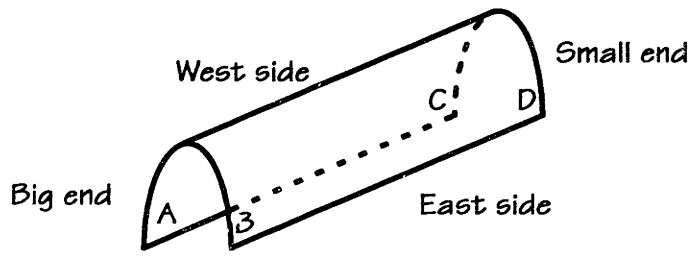

Figure 6.32 Locations of thickness measurements on formed leading edge

The devices were attached either in the excess or on the part just on the die. They were attached after the material was clamped in the jaws, and sometimes even after

the part was snug (since the jaws are very close to the die for leading edges, this was difficult at best).

6.2.10 Results of improvement implementation

Implementation of the recommended improvements resulted in a significant reduction in variation.

Reduction in variation of strain

Before implementing strain control on 0.090" and 0.100" thick leading edges, strain control was tested on two other parts: P/N O, a 0.016" thick 2024-T3 leading edge, formed two at a time, and P/N P, a cowling, a double-curvature part which is stretched and annealed a number of times because of the significant amount of strain required to achieve the final shape. In both parts, statistically significant reduction of strain variation was achieved. In both P/N O and P/N P, strain variation, measured by the standard deviation of strain, was reduced by around 70%.

Results of implementing recommendations for stretch forming leading edges

Six lots of leading edges were tested with the proposed improvements, and the results show significant reduction in contour variation and other variables compared with current practice.

The settings were optimized and repeatably achieved in each of the six lots. The following table shows how each lot was controlled, the variation in table stop position, table movement, maximum force, and strain (one standard deviation over the average), and variation of the separation at each end (one standard deviation). If cells are blank it is because those data were not gathered.

P/N	Control Method	Standard Dev./ Average				Standard Deviation
		Table Stop	Table Move.	Max. Force	Strain	Averaged at Ends Separation
Current	Force	6%	10%	3%	29%	0.190"
Q	Disp.					0.009"
R	Strain	5%	4%	1%	14%	0.009"
S	Strain	2%	5%	1%	7%	0.014"
S2	Force	1%	5%	0%		0.047"
T	Disp.	2%	2%	1%		0.027"
U	Strain	1%	3%	2%	14%	0.023"
Average	Force	1%	5%	0%		0.047"
Average	Disp.	2%	2%	1%		0.027"
Average	Strain	3%	4%	2%	12%	0.015"

Table 6.13 Standard deviations over averages of table stop position, table movement, maximum force, and strain, and standard deviations of separation for three control methods and repeatably achieved optimized settings

The table shows that in addition to reducing the variation in table stop position, table movement, maximum force, and strain, implementation of the proposed improvements significantly reduced the contour variation.

P/N Q, run under displacement control, was run at such a high force that the average separation was only 0.016" at the big end and 0.021" at the small end. Because of this, the P/N Q standard deviation is artificially low compared to the rest, and hence is not included in the average for displacement control separation. However, the significantly lower variation demonstrates another method of decreasing springback: increasing the stretch. Operators are generally very hesitant to increase force or strain beyond what their experience tells them is reasonable. However, strain measurement can be used to know exactly what's going on in the part and more tightly control the operation. This tighter control and assurance that the part is not being stretched too far will permit higher strains and reduced springback. Without strain measurement, this could not be done.

The data in the last column of Table 6.13 are shown in the following chart to visually demonstrate the significance of the precision improvement.

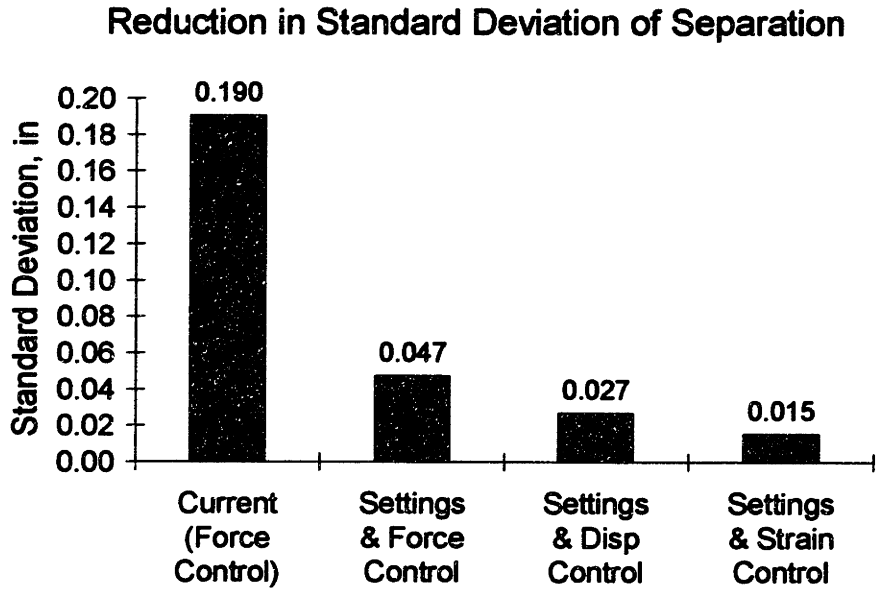

Figure 6.33 Reduction of standard deviation of separation for repeatably achieved optimized settings and three control methods

While the results are based on limited data, they correspond with expectation. Current practice for leading edges is force control with little control on achieving settings. Simply by achieving the same initial and final settings, the variation (as measured by the standard deviation of average separation at each end) is reduced to about 1/4 of the current variation. Further reduction by almost 1/2 is accomplished by using displacement control. Still further reduction of almost 1/2 is accomplished by using strain control. Repeatably achieving optimized settings and strain control reduced variation to 8% of the current level!

There is an even more promising aspect to this data. The improvement achieved through strain control was by manual strain control—the operator was given verbal instruction on when stop the operation. This method is in the *prototype* stage, not far up along the learning curve, as demonstrated in part by the still significant variation in strain of 12% under strain control. Even with this significant variation, it is the best of the three control methods. After the strain measurement method is refined and automatic strain control is implemented on the machine, one can expect further variation reduction. For example, as mentioned already, automatic strain control can be used to equalize the average strains at both ends of a leading edge. Further, a

heuristic could be developed to adjust die table angle, and jaw positions and angles based on strain measurements and separation at the four corners of the leading edge.

Benefit of knowing what's going on in the material

Strain measurement is of fundamental importance to improving precision because it monitors what's going on in the material. Force and displacement measurement and control are too removed from strain and are net measurements. Force measurement relies on a model of the operation to predict what's actually going on in the material. Displacement is one step closer to strain than force, but still requires a model to predict what's going on in the material. Further, force and displacement are net measurements averaged over the whole part, and thus cannot capture variations within a part. For example, both force and displacement methods require a material model, an understanding of the effects of friction, and the geometry of the setup in order to predict strain in the part, which is then used to predict springback.

Strain measurement directly measures the material state which most influences springback. Effective optimization of the stretch forming operation requires a knowledge of the strains in the material. For example, knowing whether to adjust the die table angle or the jaw position or angle requires knowledge of strains. Effective trouble-shooting also requires a knowledge of the strains. For example, when a part breaks as the part is being stretch formed, knowledge of the strains can immediately be used to determine if the part was overstretched or it failed prematurely due to a gripping problem or defect in the material (for example, a nick in the edge).

Why not springback control?

If it is true that controlling the operation by a state that is closer to the output, then why not, one may conclude, control the operation by the separation? While separation can (and should) be used with strain measurements in determining optimal settings, it can't be used to control the operation as it's happening, because springback occurs after the operation is complete (and it is not possible, for a number of reasons, to stop the operation and measure springback part of the way through the operation). Further, at this point there seems to be too much variation in springback to use it for control of the operation.

6.2.11 Summary and conclusions to sheet stretch forming operation

Study of the variation in the stretch forming operation revealed significant variation of part strain and contour deviation (measured by separation between the part and the die at four locations) within a part, from one part to the next, and from one lot of parts to the next. Study of the sources of variation revealed that the few most important sources of variation to the stretch forming operation (for 2024-T3 leading edges) are

- die table angle
- initial jaw position and angle
- maximum die table force, displacement, or position

Correlation between measured variables was generally not very strong, which confirms the finding that there are numerous sources of variation affecting the operation.

Initial material yield strength was not found to correlate with any measured variables. For parts that are solution heat treated, room temperature aging was found to have a significant effect on the operation. Although not studied quantitatively, operator experience is unanimous on the points that quenching causes warpage, and that racking, quenchant temperature, quench delay, and quench entry rate significantly affect warpage, which contributes to variation in final part geometry.

The change in contour from routing was borderline significant and is likely different because of edge effects. The change in contour deviation from chem mill was not significant.

Two recommendations were suggested to improve the precision of the stretch forming operation:

1. Repeatably achieve optimized settings
2. Use automatic strain control

Implementation of the recommendations on leading edges yielded a significant reduction in variation as measured by the standard deviation of the contour deviation. Repeatably achieving optimized settings was accomplished by having the machine operators (a) determine what they believed to be the optimal settings according to their experience and aided by strain measurements and (b) repeatably achieving these settings for each part. Strain control was accomplished by attaching strain measurement devices to the part and stopping the operation when the strain reached a desired level.

In the baseline (current) case, no special effort was made to optimize and repeatably achieve settings, and the operation was force-controlled. The baseline standard deviation was $\sigma = 0.190$". Improvements for repeatably achieved optimized settings with three different methods of control are:

- Force control: variation reduced to 25%, $\sigma = 0.047$"
- Displacement control: variation reduced to 14%, $\sigma = 0.027$"
- Strain control: variation reduced to 8%, $\sigma = 0.015$"

The results indicate that significant variation reduction (precision improvement) is possible with existing technology and techniques simply by repeatably achieving optimized settings and controlling the operation by force (the current method). Also with current technology, using displacement control instead of force control almost halves the variation again. Further reduction in variation, by a total of 92%, was achieved with strain control. Variation was also reduced in one lot by increasing the stretch. As variation is reduced, other sources of variation are likely to become important, for example, material property variation.

Even with the significant reduction of variation achieved with optimized and repeatably achieved settings under strain control, further reduction in variation is expected. The method of strain control was manual and still in the learning stages; ultimately strain control would be performed automatically by a machine and will be refined, both of which will further improve achievable precision. Finally, regardless of the control method used, strain measurement is necessary to find out what's going on in the material and to optimize the operation.

6.3 INCOMING MATERIAL STUDY

Incoming material geometry and properties can have a significant effect on the stretch forming process. Therefore, an attempt is now made to analyze variation of incoming material geometry and properties. First, specifications are summarized and discussed, and second, measurements of material properties are presented and discussed.

6.3.1 Specifications used to purchase sheet metal

Aluminum specifications, created by the U.S. government and industry-wide organizations (e.g., ANSI), are used in all acquisition of aluminum for the aircraft industry. These give an indication of the potential variation in material geometries and properties. However, it should be expected that, given the age of these documents,

material suppliers are able to produce material to significantly tighter tolerances than those specified—and this is generally the case, as is demonstrated later.

Material Geometry

Length and width specifications for sheet aluminum used for stretch forming are: ± 0.125" (ANSI-H35.2.1985). On a 50" dimension, this would be 0.125/50, or 0.25%, which is very little. The specifications also note that tolerances are applicable at ambient mill temperatures, and that a change in length of 0.013 inches per 100 inches per 10° F (6° C) must be recognized; this is also very little.

Bilateral thickness tolerances for sheet metal used are specified at about ± 0.0031" (ANSI-H35.2.1985). For a 0.062" thick part, this would be 0.0031/0.062, or 5%, which is very significant.

Flatness tolerances (maximum deviation from flat) are specified to be mostly between 1/4" and 1/2", depending on material thickness and the distance between buckles or edge wrinkles. Flatness tolerances are not applicable to -O material.

Material Properties

Mechanical property specifications for alclad[42] 2024-O sheet 0.063"-0.499" thick are: yield strength (σ_Y) ≤ 14 ksi, ultimate tensile strength (σ_{UTS}) ≤ 32 ksi, and elongation ≥ 12%; for alclad 2024-T3 sheet 0.063"-0.128" thick, the specifications are: σ_Y ≥ 39 ksi, σ_{UTS} ≥ 61 ksi, and elongation ≥ 15% [QQ-A-250/5F].

Mechanical property specifications for alclad 7075-O sheet 0.063"-0.187" thick are: σ_Y ≤ 20 ksi, σ_{UTS} ≤ 36 ksi, and elongation ≥ 10% [QQ-A-250/13E].

Grain size is a significant determinant of strength, hardening characteristics, and surface texture. Alloys can be specified according to special microstructure requirements, for example, to minimize Lüdering, or with minimum residual stresses.

Chemical composition is also specified and influences the material's mechanical properties, response to heat treat, and corrosion properties. Chemical composition limits are given in the above specifications as well. Tolerance ranges on various elements are generally around 10% to 30% of the nominal.

Summary and conclusions to material specifications

Specified length and width tolerances ensure that these are minimal sources of variation. On the other hand, specified thickness tolerances permit the thickness to be a very significant source of variation. Mechanical property specifications permit significant variation, because only maximum or minimum limits are given. Chemical composition specifications are generally quite wide, too, but it is unclear how these affect material properties and the solution heat treat operation.

6.3.2 Other sources of information about incoming sheet metal

Measurements from the heat treat designed experiment reveal an average deviation from nominal thickness for the four lots measured of 0.9%. This value is in line with an estimate of material thickness variation of 1% by someone working at an aluminum supplier.

Measurements on a few selected incoming sheets indicate that variation of length and width is much less than the specifications, on the order of up to ± 0.020". However, on a batch parts cut in-house that had been diffusion bonded, the difference in width was up to about 0.5" on a dimension of roughly 50", which is about 1%.

The rolling process used to make sheet out of ingots and from heat treating causes residual stresses in the material. Even annealed (-O condition) material is generally reduced in thickness another 50% or so after the last anneal, so that it will have varying residual stresses in the thickness direction. Further, the straightening operation after uncoiling will induce further residual stresses varying through the thickness.

Evidence of variation of mechanical properties from lot to lot comes from Michael Nolan [1993, pg. 49] who reported findings by Jovanovski that mechanical properties did not vary significantly within coils, but among different coils.

A study was made of the sheet metal properties as reported by a supplier of sheet metal to Vought. This study and its results are addressed next.

---

[42] In order to retard corrosion, most aluminum skins are clad on one or both sides with a layer of aluminum alloy purer than the base alloy. The term *alclad* denotes this.

6.3.3 Certification data analysis

Analysis of data from incoming material certification sheets, which accompany each package of material delivered by any supplier, shows significant variation of incoming material properties for a given alloy and temper. However, this variation is greatly reduced if material properties are segregated according to material thickness.

How the tests are performed

Tensile tests are performed in the long transverse direction (perpendicular to the rolling direction). Engineering stresses are given, and the elongation is of the gage length of the tensile specimen after fracture. Two measurements are made for each lot of material; the maximum and minimum yield strength (σ_Y), ultimate tensile strength (σ_{UTS}), and elongation are reported.

Analysis of 7075-O alclad sheet data

The statistics for 7075-O alclad sheet are based on 13 supplier lots.

The average incoming yield stress is 13.9 ksi. The standard deviation of the 26 values is 0.65 ksi. This gives a 3σ (three standard deviations; if the data are normally distributed, the average $\pm 3\sigma$ should contain 99.7% of the population) of 2.0 ksi, which is 14% of the average. This represents very significant variation. However, if the sheets are segregated according to thickness, the average yield stresses are 15.2 ksi for 0.060" thick sheet (n = 2, i.e., two parts were 0.060" thick) and 13.6 ksi for 0.090" to 0.100" thick sheet (n = 10), with corresponding standard deviations of 0.21 ksi and 0.18 ksi. For both of these, 3σ represents 4.1% of the average yield strength.

The average incoming ultimate tensile strength is 29.4 ksi. The standard deviation of the 26 values is 0.53 ksi. This gives a 3σ of 1.59 ksi, which is 5.4% of the average. This represents significant variation. However, if the sheets are segregated according to thickness, the average ultimate tensile stresses are 29.7 ksi for 0.063" thick sheet (n = 2) and 29.4 ksi for 0.090" to 0.100" thick sheet (n = 10), with corresponding standard deviations of 0.21 ksi and 0.62 ksi. Respectively, 3σ for these represent 2.1% and 6.4% of the average ultimate tensile strength.

The average incoming elongation is 17.4%. The standard deviation of the 26 values is 1.36%. This gives a 3σ of , which is 24% of the average. This represents very significant variation. However, if the sheets are segregated by thickness, the average

elongations are 18.4% for 0.060" thick sheet (n = 2) and 17.6% for 0.090" to 0.100" thick sheet (n = 10), with corresponding standard deviations of 1.25 ksi and 1.20 ksi. Respectively, 3σ for these represent 20.4% and 20.5% of the average elongation. This still represents very significant variation. However, if elongation is measured according to material type, mill finish material has an average of 18.1% with a standard deviation of 0.83% (3σ = 13.8% of the average), and another microstructure specification has an average of 16.8% with a standard deviation of 1.46% (3σ = 26.2% of the average). The higher standard deviation for the other microstructure is probably because it contains a variety of thicknesses, while the mill finish has only 0.100" thick parts. It appears that differences in strengths among types of sheet, e.g., mill finish or other microstructure, are overshadowed by the differences among thicknesses.

Analysis of -T62 condition properties (provided on the certification sheet as evidence that the material will respond properly to heat treating) shows general increases in the magnitude and variation of the yield and tensile strengths and decreases in the magnitude and variation of the elongation.

There are few statistically significant correlations among material properties. One of these is the positive correlation between yield strength and ultimate tensile strength in the -O condition, though this relationship is different between mill finish and other types of material, as seen in the following chart.

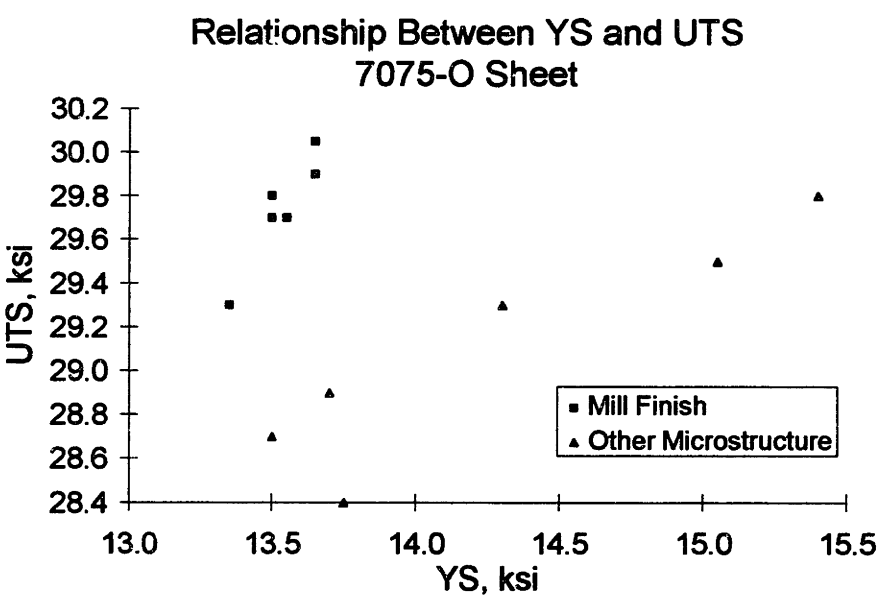

Figure 6.34 Ultimate tensile strength as a function of yield strength for 7075-O

Such a positive correlation indicates that as the yield strength changes, the whole curve stress-strain curve moves up or down.

There appears to be no correlation between properties in the -O and -T62 temper. There is a positive correlation between ultimate tensile strength and elongation for 7075-O, while there is no correlation between the two for 7075-T62.

For the sake of comparison of properties from another vendor, data from seven alclad 7075-O certification sheets for 0.063" thick mill finish material give average yield strength, ultimate tensile strength, and elongation of 13.7 ksi, 29.6 ksi, and 16.3%, respectively. The standard deviations are 0.74 ksi, 0.79 ksi, and 1.22%, which give 3σ of 2.22 ksi, 2.37 ksi, and 3.66%, which are 7.5%, 17.44%, and 22.5% of the averages, respectively. In each case, these represent significant variations. The variation of the yield stress and ultimate tensile stress values given for -T62 material increase in absolute terms, but decrease as a percent of the average. The variation of the elongation decreases in absolute terms and as a percent of the average. The average properties compare well with the average properties from the first vendor for the mill finish 7075-O material (13.9 ksi, 29.4 ksi, and 17.4%), but the variation in this material is larger than for the first vendor (3σ of 3.5%, 2.5%, and 13.7%).

For the seven lots from the other vendor, there are, however, strong correlations between yield strength and tensile strength in the -O and in the -T62 conditions. Further, the slope of the least squares regression estimate is almost 1, indicating, again, movement of the whole yield curved up or down with changes in yield strength. There is also a relatively strong correlation between yield strengths in the -O and -T62 conditions, and between ultimate tensile strengths in the -O and -T62 conditions.

Analysis of 2024-O alclad sheet data

The statistics for 2024-O alclad sheet are based on 4 lots.

The average incoming yield stress is 11.7 ksi. The standard deviation of the 8 values is 0.95 ksi. This gives a 3σ of 2.85 ksi, which is 24% of the average. This represents very significant variation. However, if the sheets are segregated by thickness, the average yield stresses are 13.3 ksi for 0.080" thick sheet (n = 1) and 11.2 ksi for 0.090" to 0.100" thick sheet (n = 3), with corresponding standard deviations of 0.07 ksi and 0.06 ksi. For both, 3σ represents 1.6% of the average yield strengths.

The average incoming ultimate tensile stress is 25.4 ksi. The standard deviation of the 8 values is 0.43 ksi. This gives a 3σ of 1.29 ksi, which is 5.1% of the average. This represents significant variation. However, if the sheets are segregated according to thickness, the average ultimate tensile stresses are 26.1 ksi for 0.080" thick sheet (n = 1) and 25.2 ksi for 0.090" thick sheet (n = 3), with corresponding standard deviations of 0.07 ksi and 0.20 ksi. Respectively, 3σ for these represent 0.8% and 2.4% of the average ultimate tensile strength.

The average incoming elongation is 19.8%. The standard deviation of the 8 values is 0.80%. This gives a 3σ of 2.4%, which is 12.1% of the average. This represents very significant variation. However, if the sheets are segregated by thickness, the average elongations are 20.3% for 0.080" thick sheet (n = 1) and 19.7% for 0.090" to 0.100" thick sheet (n = 3), with corresponding standard deviations of 0.35 ksi and 0.88 ksi. Respectively, 3σ for these represent 5.2% and 13.4% of the average elongations.

Due to the small sample size, it is difficult to determine other significant differences between thicknesses, or between the types of material. Heat treating to -T42 increases average yield strength, ultimate tensile strength, and elongation; standard deviations of the ultimate tensile strength and elongation are increased, while the standard deviation of yield strength is decreased. Heat treating to -T62 increases the average yield strength and ultimate tensile strength and reduces the average elongation; the standard deviation of the ultimate tensile strength is increased, while the standard deviations of the yield strength and elongation are increased.

The correlations between properties of the material in the -O condition and properties of the material in the -T42 and -T62 conditions are marginal. The correlation between yield strength and ultimate tensile strength in the -O and -T42 conditions is quite strong, while it is weak in the -T62 condition.

Analysis of 2024-T3 alclad sheet data

The statistics for 2024-T3 alclad sheet are based on 9 lots.

The average incoming yield stress is 45.0 ksi. The standard deviation of the 18 values is 1.18 ksi. This gives a 3σ of 3.54 ksi, which is 7.9% of the average. This represents significant variation. However, if the sheets are segregated by thickness, the average yield stresses are 44.5 ksi for 0.090" thick sheet (n = 5) and 45.6 ksi for 0.100" thick

sheet (n = 4), with corresponding standard deviations of 1.34 ksi and 0.53 ksi. Respectively, 3σ for these represent 9.0% and 3.5% of the average yield strength.

The average ultimate tensile strength is 64.1 ksi, with a 3σ of 2.04 ksi, which is 3.2% of the average. The average elongation is 17.5%, with a 3σ of 2.85%, which is 16.3% of the average. Neither ultimate tensile strength nor elongation are strongly correlated to thickness.

There is a negative correlation between elongation and ultimate tensile strength, independent of thickness. There is a positive, thickness-dependent, correlation between yield strength and ultimate tensile strength for aluminum alloy 2024-T3.

Sources of variation in the testing

Some of the variation in the above data, especially elongation, can be attributed to the test equipment and test procedure. ASTM B 557 reports the findings of an inter-laboratory repeatability and reproducibility test program involving six labs. For testing of sheet aluminum alloy 2024-T351 within each lab, averaged from yield strength measurements within the six labs, 3σ was 4.2% of the average yield strength measured (as determined by the 0.2% offset method). For ultimate tensile strength, 3σ was 2.7% of the average. For elongation, 3σ was 9.0% of the average. While these numbers are significant, the data above demonstrate that the capability within the aluminum supplier far exceeded the capabilities of the labs in the inter-laboratory program. This is reasonable to expect, since an aluminum supplier should have a fine-tuned testing process, and the test in the specification is probably dated.

Material thickness variations will add variation to the mechanical property measurements if they are not accounted for in the stress calculations.

Summary and conclusions to certification data study

Incoming mechanical material properties vary significantly. When segregated according to thickness, three standard deviations of the yield strength divided by the average were 4.1%, 1.6%, and 6.0%, for 7075-O, 2024-O, and 2024-T3, respectively. However, when not segregated according to thickness, these increased to 14%, 24%, and 8%, respectively. Variation in ultimate tensile strength is similar. Of the three properties, elongation had the largest variation—on average 3σ was around 15% or more of the average elongation, even when segregated according to thickness.

Yield strength and ultimate tensile strength are positively correlated with one-another, and the slope of the least squares regression line between them is about 1. This indicates that as the yield strength increases, the stress-strain curve moves up and down, without a great effect on the strain hardening coefficient. Some correlation exists between properties in the -O condition and in the -T condition.

Most of the analysis was performed on -O condition material, while parts are often formed in the -W condition. It is unclear whether variation is increased or decreased in the -W condition relative to the -O condition, or whether there is any correlation between -O and -W condition properties. Lastly, the certification sheet properties reported are for only two points in an entire lot, and this says nothing about variation from part to part in a lot or within a part.

6.3.4 Analysis of tensile test data from a major aerospace metal supplier

A large set of data was collected by a major aerospace metal supplier in order to assess the variation of material properties. Tensile test data—yield strength, ultimate tensile strength, and elongation—were gathered over a half year period for the aluminum alloy 2024-T3. Tensile test direction is long transverse—perpendicular to the rolling direction. Sample sizes range from around 30 to well over 1000. The data include four thickness ranges: 0.030-0.040", 0.041-0.063", 0.064-0.080", and 0.081-0.125". The data also include four categories of description: bare, alclad, alclad minimum Lüdering (ML), and alclad minimum residual stress (MRS). Summary data are shown in the following table. The standard deviations shown are averages of standard deviations within the samples in the specified categories.

Special	Thickness Range, in	σ_Y, ksi		σ_{UTS}, ksi		Elongation, %	
		Average	St. Dev.	Average	St. Dev.	Average	St. Dev.
ALL	ALL	44.48	1.30	65.25	1.22	18.50	1.56
BARE		46.57	1.20	68.15	1.23	17.73	1.27
ALCLAD		43.94	1.45	64.34	1.28	18.63	1.76
ALCL, ML		43.00	1.08	64.19	1.05	19.50	1.50
ALCL, MRS		44.42	1.48	64.32	1.31	18.15	1.73
	0.030-0.040	43.10	1.09	63.84	1.07	18.01	1.19
	0.041-0.063	44.93	1.34	65.94	1.66	18.27	1.46
	0.064-0.080	44.73	1.13	65.71	1.11	18.89	1.69
	0.081-0.125	45.17	1.65	65.52	1.04	18.83	1.92

Table 6.1 Material property variations from major aluminum supplier

The data reveal a number of interesting things about the material categories. Bare material is consistently stronger than alclad material. This is expected, because the aluminum cladding is a purer alloy than the base material, and so it is softer, making an alclad part not as strong as a bare part. MRS material has a higher yield strength and lower elongation than the other alclad material. This is also expected, because the residual stress is minimized by stretching the material into the plastic region, therefore increasing the yield strength and using up some of the elongation, but not affecting the ultimate tensile strength. ML material has a higher elongation than the others. This has something to do with the microstructure modifications that minimize Lüdering.

The data reveal one statistically significant effect of material thickness: the thinnest material has significantly lower yield strength, ultimate tensile strength, and elongation.

The data also reveal significant variation of material properties. The average of all the standard deviations give 3σ of 8.8% of the average yield strength, 5.6% of the average ultimate tensile strength, and 25.4% of the average elongation. The 3σ values of yield strength are lower for the bare and alclad ML materials (~8%) than they are for the alclad and alclad MRS materials (~10%).

Summary and conclusions to study of tensile test data from major supplier

In addition to finding expected differences among material types, the data confirm that significant variation of yield strength, ultimate tensile strength, and elongation can be expected.

6.3.5 Summary and conclusions to incoming material study

While specified geometry and property tolerances are much greater than actual variation, there is still significant variation. The most significant geometry variation is in thickness. While the specification tolerance is about 5% of the specified thickness, limited data showed a variation of 1% of the specified thickness. Specifications for yield and ultimate tensile strengths are unilateral, which permits a lot of variation. Material certification sheet data indicate that, when grouped properly, yield strength and ultimate tensile strength generally vary between 2% and 6% of the average, while elongation generally varies between 15% and 25% of the average. Variation of the yield stress divided by the average tends to decrease from -O to -T condition material, while the changes in variation of ultimate tensile stress and elongation divided by the average are mixed. Correlations between yield strength and ultimate tensile strength are strong, while correlations between strengths in the -O and -T conditions are of mixed strength.

The above data and analyses address material properties as the *source* of variation. While experiments have not been made to determine the effect of this variation, the use of analytical model in Chapter 5 and all stretch forming operators attest to changes in incoming material properties as having a significant effect on the operation and the part geometry as well.

6.4 HEAT TREAT DESIGNED EXPERIMENT

6.4.1 Introduction

A designed experiment was performed in order to better understand the effect of changes in parameter levels on material properties in the solution heat treat operation, and to determine the effect of parameter levels on variation. The experiment was run with three factors—quench delay, material thickness, and time at room temperature from quench—each at two levels, for two aluminum alloys, 2024 and 7075, both initially in the -O (annealed) condition. The following material property outputs were measured:

yield strength, ultimate tensile strength, elongation, conductivity, hardness, and stress at the onset of Lüdering or Orange Peel (both surface phenomena).

Analysis revealed that the most significant factor affecting the outputs was the time from quench at room temperature. Cladding had a significant affect on the output measurements.

6.4.2 Description of the test

The designed experiment and data analysis were accomplished according to standard practice as found in [Phadke, 1989] and [Montgomery, 1985]. The process flow for the designed experiment is given in the following diagram, which also shows when the factor levels were varied.

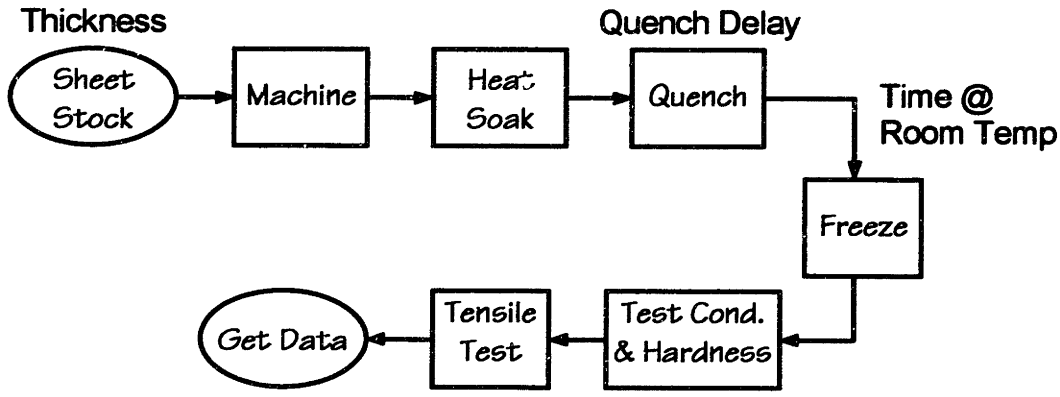

Figure 6.35 Process flow diagram for heat treat designed experiment

Material, factors, and factor levels

The plan was to perform the experiments on bare sheet; however, although bare material was requested, it turns out that the 0.040" thick 7075 sheet was alclad. The initial condition of the metal was annealed (-O). Before the material was solution heat treated, tensile test specimens were cut from sheet stock according to ASTM B557 (gage length of 2.000" and width of 0.500"). Specimens were sheared and machined so that the stretch was in the long transverse direction—property tests performed for the material certification sheets are also in the long transverse direction. Each specimen was labeled with a *specimen number* (which is different from the *number*).

The three factors and their levels for each alloy are given in the following table.

Factor #	Factor	Level 1	Level 2
1	Thickness	0.040"	0.080"
2	Quench Delay	5 seconds	10 seconds
3	Time From Quench at Room Temp	20 minutes	53 minutes

Table 6.2 Factors and levels for heat treat designed experiment

Both quench delay times are within the 10 second allowable quench delay specified for these thicknesses.

Two repetitions were made of each set of tests, and the experiment was run once for 2024 and once for 7075. This gives $2^5 = 32$ tests (two full factorial tests). The designed experiment matrix is given below. As shown in the last column, the testing order was randomized.

Number	Material	Thickness	Quench Delay	Time From Quench	Test Order
1, 17	2024, 7075	0.040"	5	20	7, 23
2, 18	2024, 7075	0.040"	5	20	5, 21
3, 19	2024, 7075	0.080"	5	20	8, 24
4, 20	2024, 7075	0.080"	5	20	14, 30
5, 21	2024, 7075	0.040"	10	20	6, 22
6, 22	2024, 7075	0.040"	10	20	12, 28
7, 23	2024, 7075	0.080"	10	20	1, 17
8, 24	2024, 7075	0.080"	10	20	15, 31
9, 25	2024, 7075	0.040"	5	53	10, 26
10, 26	2024, 7075	0.040"	5	53	16, 32
11, 27	2024, 7075	0.080"	5	53	11, 27
12, 28	2024, 7075	0.080"	5	53	2, 18
13, 29	2024, 7075	0.040"	10	53	4, 20
14, 30	2024, 7075	0.040"	10	53	9, 25
15, 31	2024, 7075	0.080"	10	53	3, 19
16, 32	2024, 7075	0.080"	10	53	13, 29

Table 6.3 Experiment matrix for heat treat designed experiment

Eight extra specimens, of material, thickness, and quench delay were made just in case any of the tests ran into difficulty. Eight tests were also performed on parts in the annealed (-O) condition, two each of each material and each thickness. Four of the eight "just in case" specimens were tested up to about 3% strain to get a better idea of the shape of the stress-strain curve (which, for all the other tensile tests, was not generated beyond what was needed to determine the yield strength).

Output and method of measurement

What was measured and how the measurements were performed are now described. All measuring instruments are involved in a rigorous calibration program.

Initial width and thickness were measured with an electronic Starrett 1 inch micrometer which is accurate to ± 0.0001".

Two hardness measurements were made, one at each end of the specimen. The Rockwell superficial hardness scale 15T was used with a 1/16" ball indentor on a Wilson series 500 hardness tester, with 3 kg minor and 15 kg major loads.

Two conductivity measurements were made, one at each end of the specimen. Electrical conductivity was measured with a Nortec model NDT 5α conductivity meter, on the % IACS (Percent International Annealed Copper Standard) scale.

Yield strength was determined by dividing the load at yield (read from the stress-stain curve according to the 0.2% offset rule) by the original area, and ultimate tensile strength was calculated by dividing the load at failure by the original area. The tensile tests were run on a Tineus Olsen Electromatic V universal testing machine with 30,000 lbs capacity and an accuracy of about 1% of the reading. This machine is about 9 years old and is calibrated every 6 months. The tests were performed at a pull rate of between 30 and 70 ksi/minute. The actual tensile test time experienced by most of the specimens was between 10 and 12 minutes.

To determine elongation, the two parts of the fractured specimen were put together and the final gage length was measured.

The load at onset of either Lüdering and/or orange peeling was recorded. When both Lüdering and orange peel occurred, which started first was not recorded.

Further test details

The tensile specimens were cut out of sheet stock and machined in the long transverse direction in accordance with ASTM B557. Each specimen was deburred individually with emery cloth. At this point each specimen was marked with a specimen number and its thickness and width were measured.

The specimens were heat soaked in a molten salt bath for 30 minutes at a temperature of 920°F ± 5°. The specimens were quenched with either a 5 or 10 second quench delay. The quenchant (water) temperature was 80°F. The specimens were carried to the lab directly after quench and placed in a freezer at a temperature of -5°F for three days. The 20 minute at room temperature specimens were at room temperature for about 12 minutes before being placed in the freezer, while the 53 minute specimens were at room temperature for 45 minutes before being placed in the freezer. The room temperature was 73°F in the lab where the parts naturally aged and the experiments were performed. Shortly before the tensile test was to be made, each specimen was taken out of the freezer and allowed to warm up to room temperature, at which point hardness and conductivity were measured. Then the tensile test was run until fracture. The time between taking specimen out of the freezer and beginning the tensile test was 7 or 8 minutes. All of the tests were performed three days after the heat treat, within a 24 hour period.

6.4.3 A note on the statistical variation of tensile test data

The caveat regarding testing accuracy and repeatability given in the sub-section on the certification sheet data analysis also applies to the results from these tests.

6.4.4 Comparison of initial properties

Four different combinations of alloy and sheet thickness were used in this designed experiment—2024 and 7075 aluminum at thicknesses of 0.040" and 0.080". As mentioned already, all of the 2024 sheet and the 0.080" thick 7075 sheet were bare, while the 0.040" thick 7075 sheet was alclad. The properties reported by the company who manufactured these sheets are:

Alloy, Thickness		YS	UTS	% Elongation
2024-O bare, 0.040"	Max.	13.8	29.2	13.5
2024-O bare, 0.040"	Min.	13.5	29.0	13.0
2024-O bare, 0.080"	Max.	*	*	*
2024-O bare, 0.080"	Min.	*	*	*
7075-O alclad, 0.040"	Max.	14.6	29.3	16.5
7075-O alclad, 0.040"	Min.	14.6	29.0	14.0
7075-O bare, 0.080"	Max.	15.4	30.4	17.0
7075-O bare, 0.080"	Min.	15.2	30.2	16.5

Table 6.4 Certification sheet tensile test results of initial material * not available

The initial material properties measured at Vought are:

Alloy, Thickness		YS	UTS	% Elongation
2024-O bare, 0.040"	Max.	14.71	29.02	14.0
2024-O bare, 0.040"	Min.	14.11	27.21	13.5
2024-O bare, 0.080"	Max.	13.42	28.08	15.5
2024-O bare, 0.080"	Min.	12.51	26.95	14.0
7075-O alclad, 0.040"	Max.	14.93	30.55	17.0
7075-O alclad, 0.040"	Min.	14.55	30.00	16.0
7075-O bare, 0.080"	Max.	14.52	29.38	18.0
7075-O bare, 0.080"	Min.	13.42	28.33	15.0

Table 6.5 Vought-measured tensile test results of initial material

The difference in properties measured by Vought from those measured by the supplier, as a percent of the values reported by the supplier are given in the following table.

Alloy, Thickness		YS Difference	UTS Difference	% Elongation Difference
2024-O bare, 0.040"	Max.	6.59%	-0.62%	3.70%
2024-O bare, 0.040"	Min.	4.52%	-6.17%	3.85%
2024-O bare, 0.080"	Max.	*	*	*
2024-O bare, 0.080"	Min.	*	*	*
7075-O alclad, 0.040"	Max.	2.26%	4.27%	3.03%
7075-O alclad, 0.040"	Min.	-0.34%	3.45%	14.29%
7075-O bare, 0.080"	Max.	-5.71%	-3.36%	5.88%
7075-O bare, 0.080"	Min.	-11.71	-6.19%	-9.09%

Table 6.6 Change in measured properties from supplier to Vought * not available

The differences between the supplier and Vought's measurements are significant. It is not clear whether the differences reflect the fact that the location of the specimens used at Vought were from a different location in the lot, or whether the differences reflect the differences in measurement accuracy and precision.

All of the measurements are within the property specifications.

Incoming material thickness

Statistics for the specimen thickness and width measurements are given in the following table.

			Average	St. Dev.
Thickness	2024-O	0.040"	0.0405	0.00000
		0.080"	0.0812	0.00012
	7075-O	0.040"	0.0400	0.00005
		0.080"	0.0807	0.00033
Width	2024-O	0.040"	0.5041	0.00081
		0.080"	0.5032	0.00149
	7075-O	0.040"	0.5030	0.00174
		0.080"	0.5037	0.00200

Table 6.7 Thickness measurement averages and standard deviations

These data indicate that the 0.040" thick material has less thickness variation than the 0.080" thick material and that the average thickness of the 0.080" thick 2024-O material is statistically different from the nominal. The variations are very small. The

differences of the average thicknesses from nominal (specified) thicknesses of the four lots are 1.25%, 1.50%, 0%, and 0.88%. Though not a large sampling, this gives an idea of variation in part thickness among lots. Widths vary more than thicknesses, which is expected because the thickness is determined by the rolling process, while width is determined by a manual machining operation in which a number of specimens were stacked and machined.

6.4.5 Presentation and statistical analysis of designed experiment results

Alloy 2024 main effects

The following chart shows the main effects of the factors on yield strength, ultimate tensile strength, conductivity, hardness, elongation, and onset load for the 2024 aluminum. The main effect of a factor is the effect of that factor on the output.

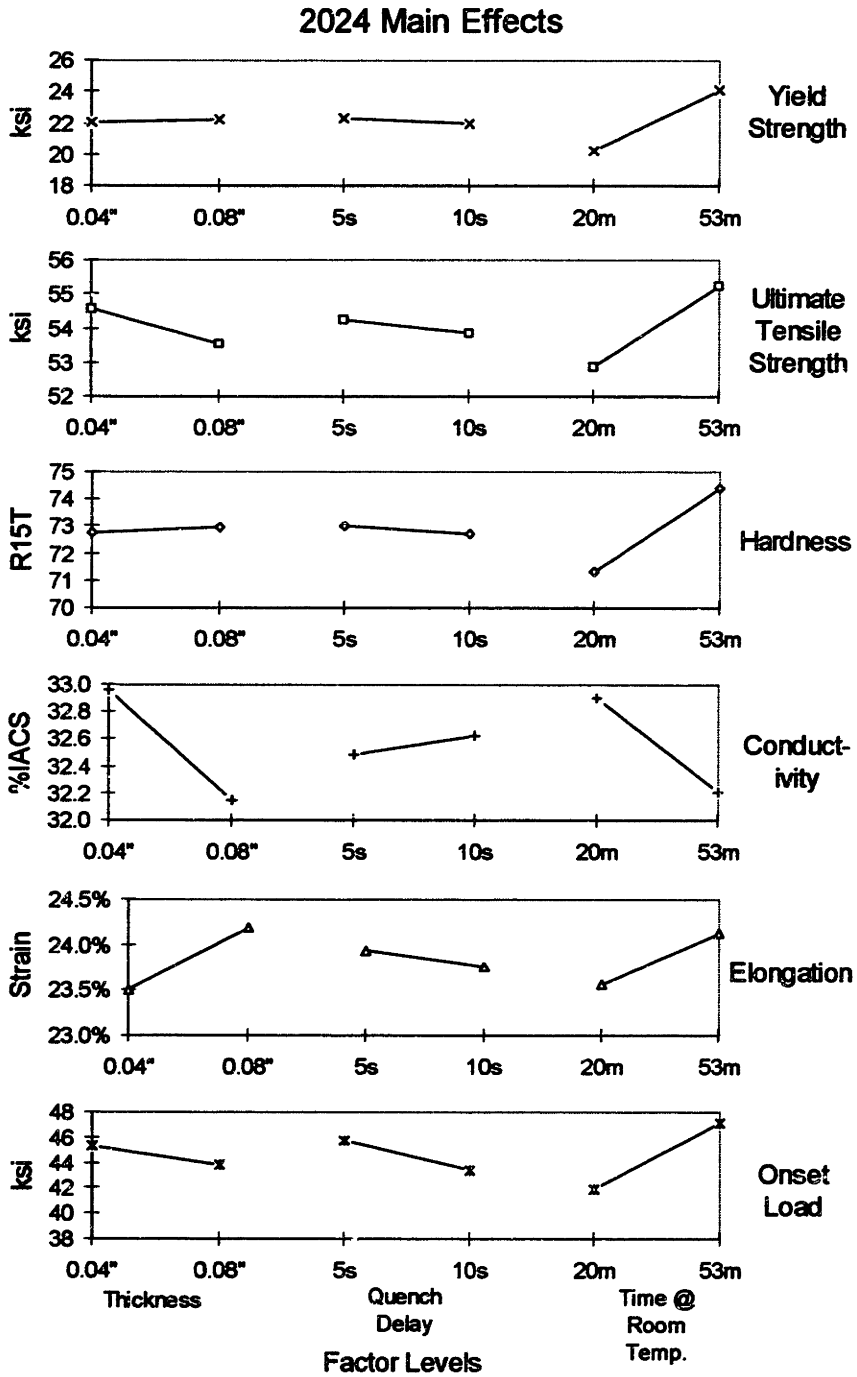

Figure 6.36 Alloy 2024 main effects: yield strength, ultimate tensile strength, hardness, conductivity, elongation, and onset load

The chart shows the effects of the three factor levels on each output. However, because there is no indication of statistical variation, it is not possible to determine which effects are statistically significant just by looking at the chart.

The following table indicates the statistical significance of the effects and highlights the statistically significant effects (greater than 99% confidence). The statistic shown, the F ratio, gives an indication of the statistical significance of the difference between two sets of data. In this case, the F ratio indicates the statistical significance of the effect of the various factor level combinations on the output. Factor A is thickness, factor B is quench delay, and factor C is time at room temperature. Multiple-factor levels indicate interaction among those factors; for example, AB indicates the interaction between factors A and B. For this designed experiment, the minimum F ratio for the 99% confidence level is 11.26. F ratios under 3.46 are under the 90% significance level, and are therefore considered insignificant.

	F Ratio						
Levels	**A**	**B**	**C**	**AB**	**AC**	**BC**	**ABC**
Yield Strength	0.57	1.34	**174.60**	0.02	0.43	1.58	0.74
Ult. Tens. Str.	**18.32**	2.99	**100.65**	0.02	0.02	2.05	0.01
Hardness	0.50	1.27	**166.59**	**12.12**	0.36	0.75	1.27
Conductivity	**19.02**	0.60	**14.08**	0.50	2.52	0.06	1.56
Elongation	0.91	0.07	0.61	0.07	0.61	0.61	0.37
Onset Load	1.31	3.49	**16.89**	0.05	0.02	0.00	0.65

Table 6.8 Alloy 2024 F ratios for each factor and output; 99%+ significant effects are bold

This table reveals that time at room temperature has a significant effect on all the outputs in the table except for elongation with over 99% confidence. The other over 99% significant effects are of thickness on conductivity and ultimate tensile strength, and the interaction between thickness and quench delay on hardness. Increasing thickness is known to reduce conductivity, apart from any effect it may have on the heat treat operation. There is a 90% significant effect of quench delay on the onset load for Lüdering/orange peel.

Alloy 2024 main effect equations

It is possible to predict the value of an output for a given combination of factor levels by using the estimated effects of each factor and each combination of factors. The following table shows the overall average of each output and each of the effects for the 2024 aluminum.

Output	Avg.	A	B	C	AB	AC	BC	ABC
Yield Strength	22.14	0.22	-0.34	3.85	-0.04	-0.19	-0.37	0.25
Ult. Tens. Str.	54.06	-1.01	-0.41	2.36	0.03	-0.03	-0.34	-0.03
Hardness	72.87	0.17	-0.27	3.08	-0.83	0.14	0.21	0.27
Conductivity	32.55	-0.81	0.14	-0.69	0.13	0.29	0.04	0.23
Elongation	23.8%	0.7%	-0.2%	0.6%	-0.2%	0.6%	-0.6%	0.4%
Onset Load	44.57	-1.44	-2.35	5.17	-0.28	0.16	0.08	-1.01

Table 6.9 Alloy 2024 effect of factor levels on output

The generic equation for an output is:

$$\text{Output} = \text{Average} + \frac{1}{2}A + \frac{1}{2}B + \frac{1}{2}C + \frac{1}{2}AB + \frac{1}{2}AC + \frac{1}{2}BC + \frac{1}{2}ABC. \qquad (6.3)$$

The sign of the variable is changed if the factor is at its low level. For interactions, the sign is changed if the multiplication of the signs yields a negative sign, e.g., for variable AB, if A is low and B is high, then multiplication of the signs is (-1)x(+1) = -1, and the sign of the variable must be changed. In the case of yield strength, the general predictive equation is:

$$YS = 22.14 + 0.11A - 0.17B + 1.925C - 0.02AB - 0.095AC - 0.185BC + 0.125ABC. \quad (6.4)$$

The equation tc predict yield strength of 0.040" thick (A low), 5 second (B low), 53 minute (C high) 2024 alloy is:

$$YS = 22.14 - 0.11 + 0.17 + 1.925 - 0.02 + 0.095 + 0.185 + 0.125 = 24.51. \qquad (6.5)$$

If only the statistically significant effects are considered, which for yield strength is only the time at room temperature, the predicted yield strength is 24.065 ksi.

Note that the above table indicates that the initiation of surface roughening differs by about 5 ksi between material at room temperature for 20 minutes and material at room temperature for 53 minutes. As expected, surface roughening, most likely Lüdering, occurs earlier in material that has age hardened less.

Alloy 2024 main effect variation

The following chart shows the standard deviations of the main effects at the various factor levels. It gives an indication of the effect of factor levels on output variation.

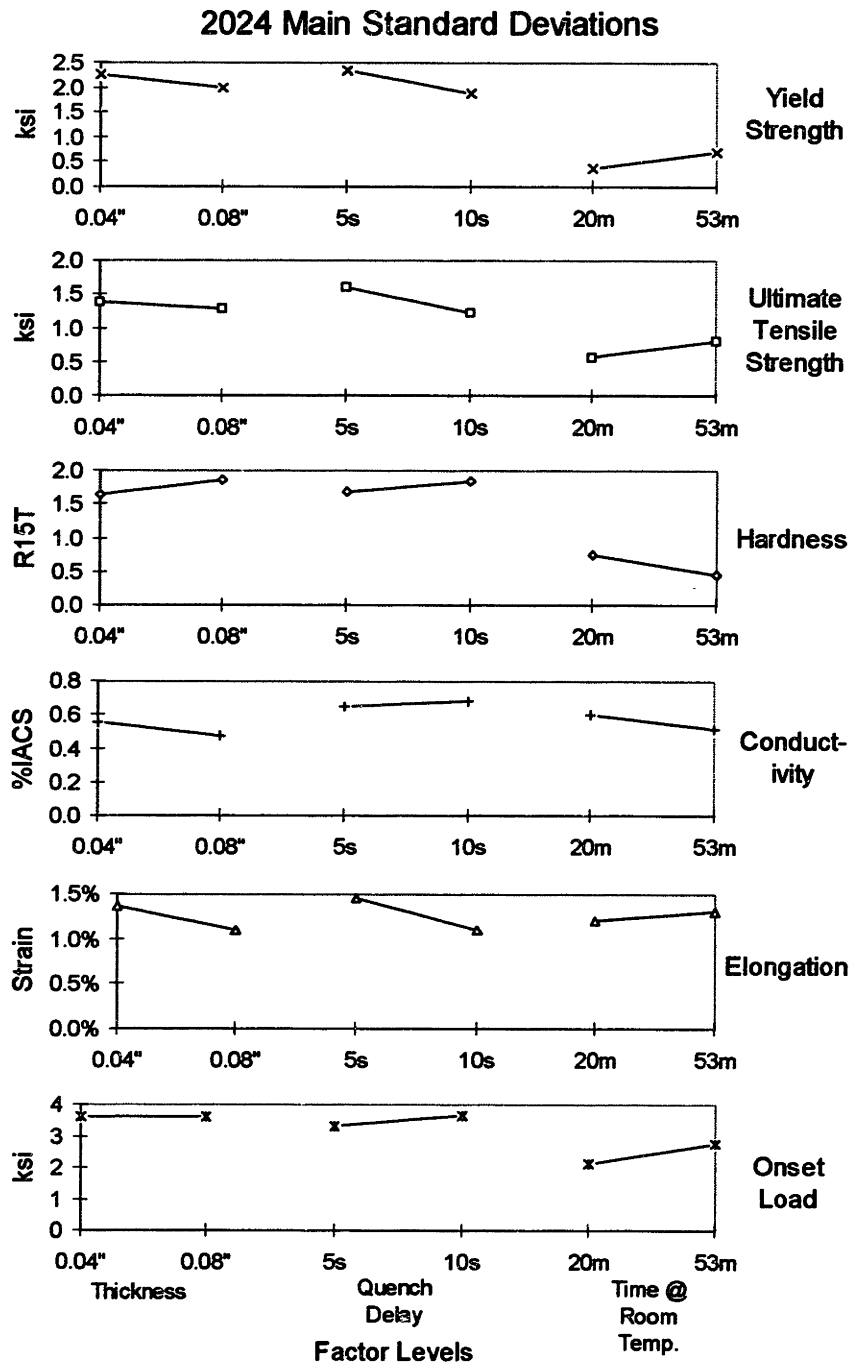

Figure 6.37 Alloy 2024 main standard deviations: yield strength, hardness, conductivity, ultimate tensile strength, and elongation

The chart shows that standard deviations are generally reduced when the data are grouped according to the time at room temperature. This indicates that for the effects for which this is the case, most of the variation is attributable to the change in time at room temperature. The chart also shows, for example, that the yield strength standard

deviation is lower for the 10 second quench delay than for the 5 second quench delay. This indicates that the yield strength is less sensitive to change in other factors at 10 seconds than at 5 seconds. Further, and very importantly, the variation of the yield strength, ultimate tensile strength, and elongation are less at 20 minutes than at 53 minutes, leading to the conclusion that not only is the material strength increased, but these properties become more sensitive to change in the other factors as the parts sit out at room temperature longer.

Alloy 2024 correlation among outputs

In addition to the ability to assess the significance of the effect of factors on the output, the data also permit assessment of the correlations among effects, for example, the correlation between yield strength and hardness. Some of the significant correlations are now addressed.

The following chart shows the relationship among yield strength, hardness, and conductivity. The conductivity points are segregated according to thickness because the main effect F ratio revealed that thickness has a significant effect on conductivity. Note that the conductivity scale increases from top to bottom.

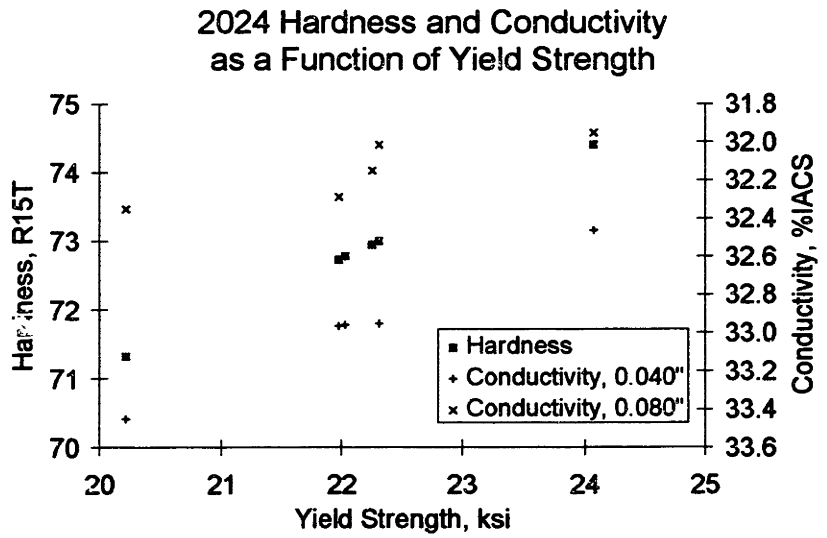

Figure 6.38 Alloy 2024 hardness and conductivity as a function of yield strength

The chart shows a strong correlation among yield strength, hardness, and conductivity.

The following chart shows the relationship among yield strength, ultimate tensile strength, and elongation. The data are segregated according to thickness, because the main effect F ratio revealed that thickness has a significant effect on these outputs.

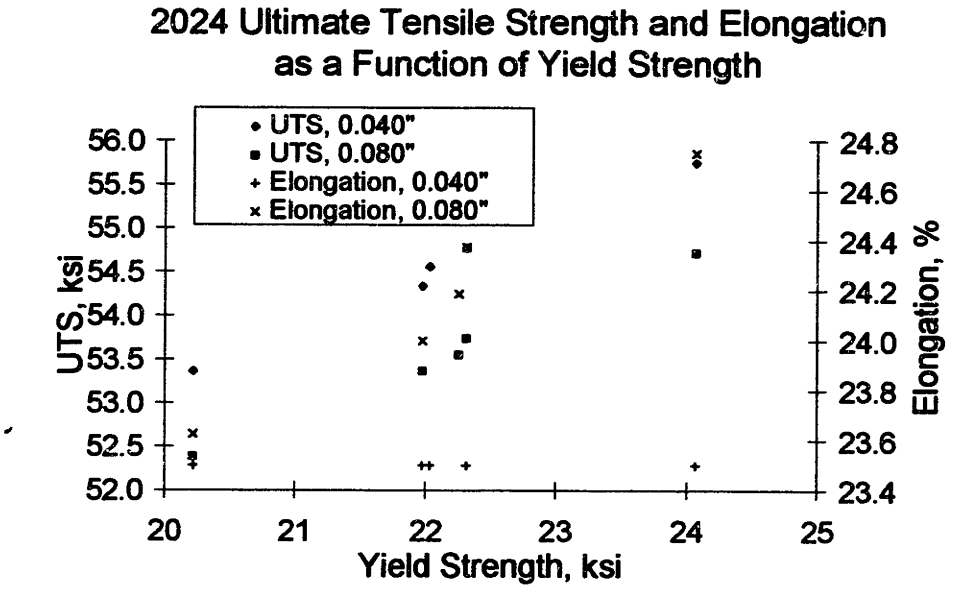

Figure 6.39 Alloy 2024 ultimate tensile strength and elongation as a function of yield strength

The chart shows a strong correlation between yield strength and ultimate tensile strength. Values for the 0.040" thick material are slightly lower than values for the 0.080" thick material. A strong correlation between yield strength and elongation exists for the 0.080" thick material, but there is almost no correlation for the 0.040" thick material.

Alloy 7075 main effects

The following chart shows the main effects on yield strength, ultimate tensile strength, conductivity, hardness, and elongation for 7075 aluminum.

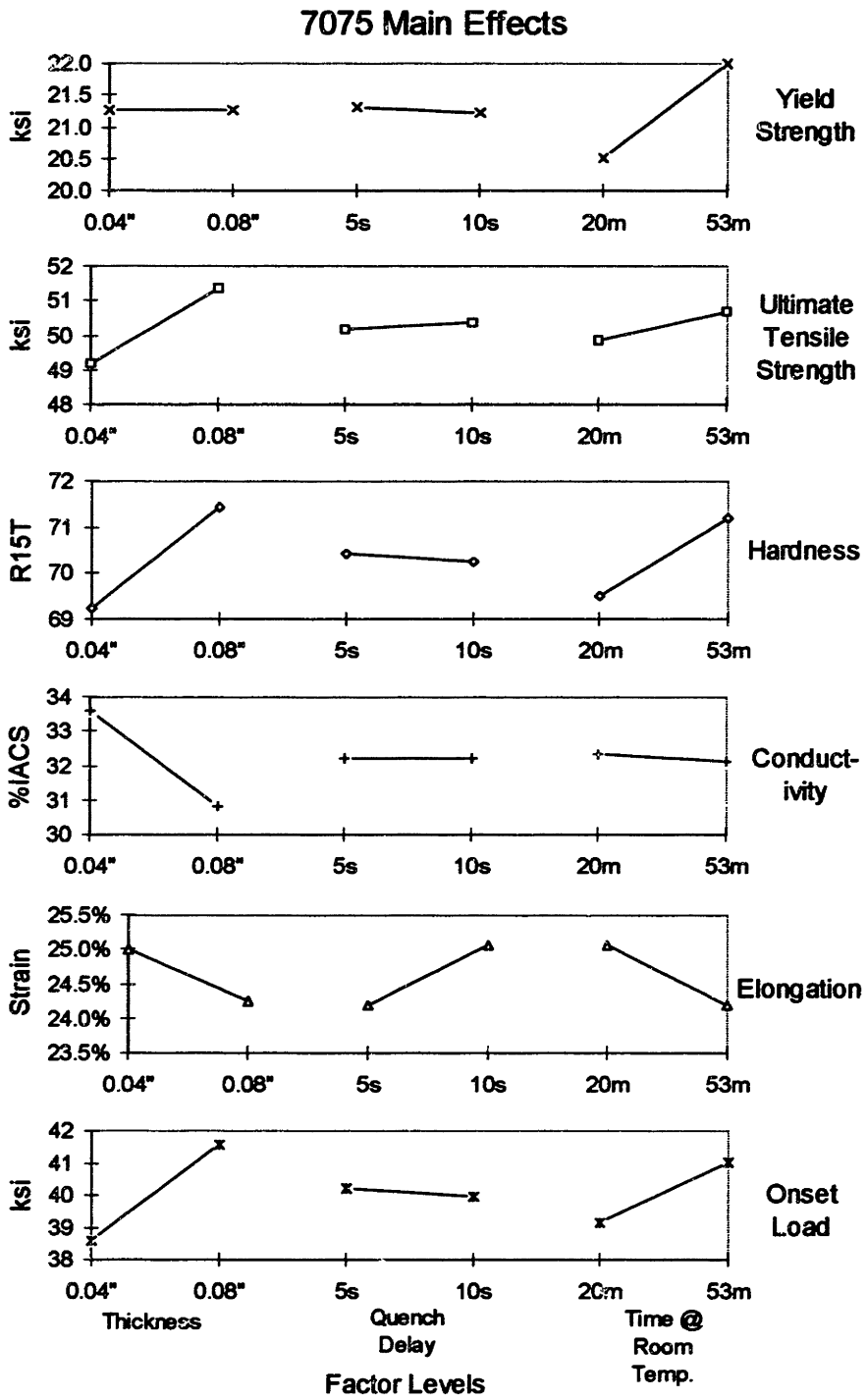

Figure 6.40 Alloy 7075 main effects: yield strength, hardness, conductivity, elongation, and ultimate tensile strength

The table below indicates the statistical significance of the effects and highlights the statistically significant effects. Factor A is thickness, factor B is quench delay, and

factor C is time at room temperature. An F ratio greater than or equal to 11.26 indicates that the probability that the factor has an effect on the output is over 99%. F ratios over 5.32% indicate over 95% confidence.

	F Ratio						
Levels	**A**	**B**	**C**	**AB**	**AC**	**BC**	**ABC**
Yield Strength	0.00	0.17	**49.21**	0.66	3.37	0.49	2.14
Ult. Tens. Str.	**114.3**	0.69	**17.52**	0.688	1.248	0.142	0.703
Hardness	**38.28**	0.28	**22.78**	0.03	0.03	0.78	0.28
Conduct.	**196.94**	0.00	0.91	0.49	0.00	0.00	0.02
Elongation	1.71	2.33	2.33	0.05	0.05	0.00	0.19
Onset Load	**24.99**	0.188	*10.27*	0.805	3.15	3.464	*8.203*

Table 6.10 Alloy 7075 F ratios for each factor and output; 99%+ significant effects are bold, 95%-99% significant effects are italicized

Time at room temperature has a statistically significant effect on yield strength, ultimate tensile strength, hardness, and onset load. Material thickness and cladding have a statistically significant effect on hardness, conductivity, ultimate tensile strength, and onset load. The cladding is probably the reason for the significant difference in hardness and conductivity.

Alloy 7075 main effect equations

The following table shows the overall average of each output and each of the effects for the 7075 aluminum.

Output	Avg.	A	B	C	AB	AC	BC	ABC
Yield Strength	21.26	0.00	-0.09	1.49	-0.17	0.39	0.15	-0.31
Ult. Tens. Str.	50.28	2.18	0.17	0.85	0.17	0.23	0.08	-0.17
Hardness	70.34	2.19	-0.19	1.69	0.06	-0.06	0.31	-0.19
Conductivity	32.23	-2.76	0.00	-0.19	0.14	0.00	-0.01	-0.02
Elongation	24.6%	-0.8%	0.9%	-0.9%	-0.1%	-0.1%	0.0%	0.2%
Onset Load	40.08	2.97	-0.26	1.90	0.53	1.05	-1.11	1.70

Table 6.11 Alloy 7075 effect of factor levels on output

Use of this table to predict the output for a set of factor levels has already been explained and demonstrated.

Alloy 7075 main effect variation

The following chart shows the standard deviations of the main effects at the various factor levels. It gives an indication of the effect of factor levels on output variation.

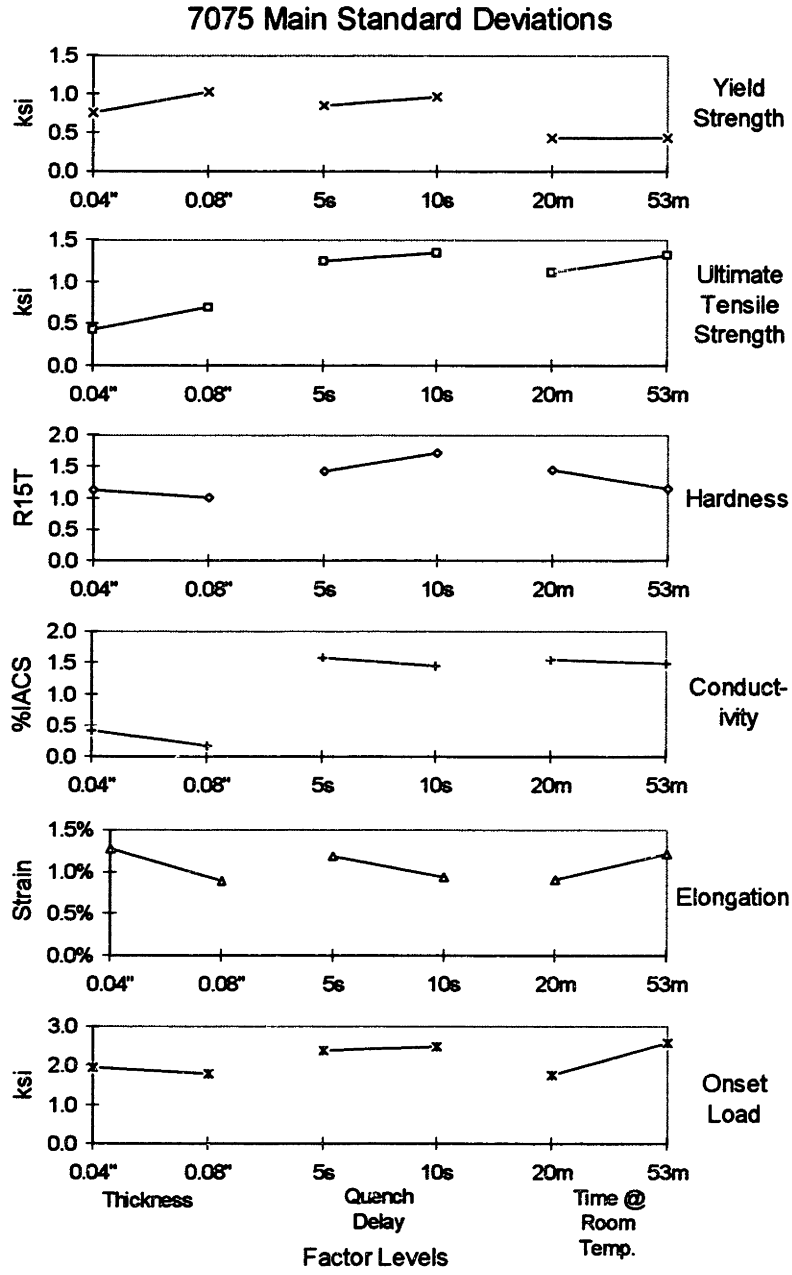

Figure 6.41 Alloy 7075 main standard deviations: yield strength, hardness, conductivity, elongation, and ultimate tensile strength

The chart shows that standard deviations of ultimate tensile strength, hardness, and conductivity are lower when the data are grouped according to material thickness. This

indicates that for these effects, most of the variation is explained by the thickness. The chart also shows, for example, that the hardness variation is higher for the 10 second quench delay than for the 5 second quench delay. Therefore, the hardness is more sensitive to change in other factors at 10 seconds than at 5 seconds. Further, ultimate tensile strength, elongation, and onset load are more sensitive to changes in other factors when material is left out at room temperature for longer periods of time.

Alloy 7075 correlation between effects

The following chart shows the relationship among yield strength, hardness, and conductivity. Hardness and conductivity are segregated according to material thickness because the main effect F ratios revealed that thickness has a significant effect on these outputs. Note that the conductivity scale increases from top to bottom.

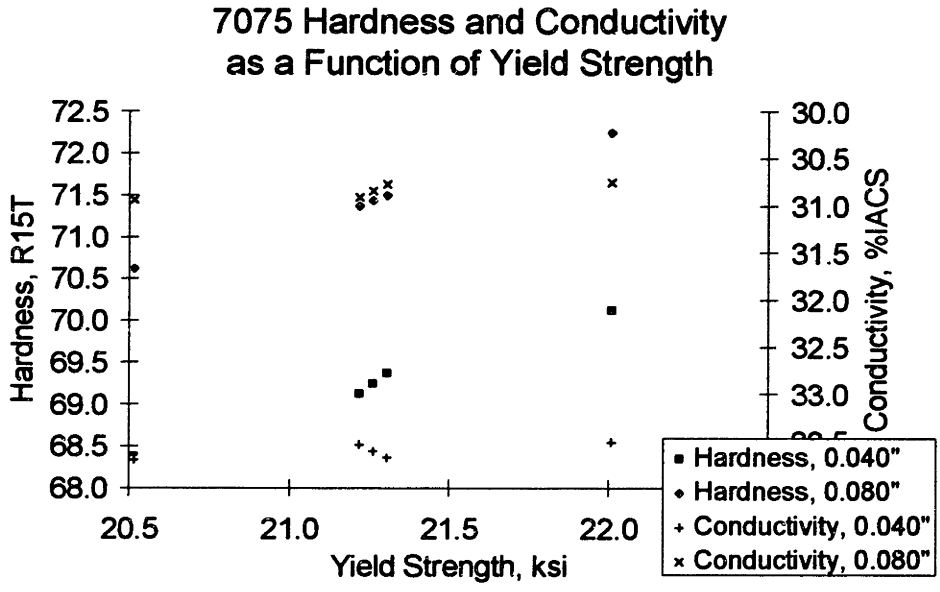

Figure 6.42 Alloy 7075 hardness and conductivity as a function of yield strength

The chart shows a correlation between yield strength and hardness when these are segregated according to thickness. There appears to be no correlation between yield strength and conductivity. Further analysis reveals insignificant correlation between hardness and conductivity, and positive correlations between yield strength and ultimate tensile strength or elongation, when segregated according to thickness.

6.4.6 Effect of aging on yield strength

The following chart is based on natural (room temperature) aging charts found in [Davis, 1993, pp. 309-310] and [ALCOA, 1974]. Because the data for this chart were

generated by estimating the value of the curves found in the above references at intervals of 1/2 hour, this chart and predictions based on these values cannot be expected to be very accurate.

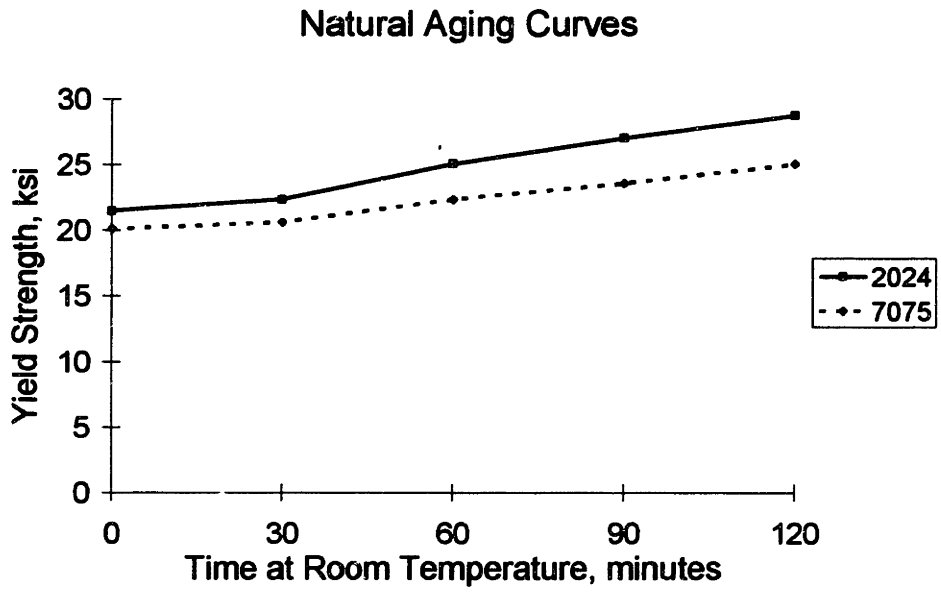

Figure 6.43 Natural aging curves for aluminum alloys 2024 and 7075 from Davis [1993] and ALCOA [1974]

The following table summarizes the actual (found in this experiment) and expected (from the references) yield strengths.

Alloy	Time @ RT	Actual	Expected
2024	20	20.2 ksi	22.0 ksi
2024	53	24.1 ksi	24.3 ksi
7075	20	20.5 ksi	20.5 ksi
7075	53	22.0 ksi	22.0 ksi

Table 6.12 Comparison between actual and expected yield strengths

The agreement is exceptionally (and surprisingly) good. The only significant difference is for 2024 at room temperature for 20 minutes.

6.4.7 Surface phenomena

The heat treat condition affects the development of the surface phenomena Lüder lines and Orange Peel.

Lüder lines are slip planes that appear on the surface of the part. Wilson [1988] states that macroscopic shear bands in aluminum (Lüder lines) are due to the development of micro-bands within individual grains which promote the formation of micro-bands in neighboring grains, and explains the effect of age hardening on the formation of shear bands. Hatch [1984] confirms that Lüder line formation is more likely in the freshly quenched condition.

Orange Peel is a roughening of the surface due to the movement of grains at a free surface. Guangnan et al [1990, p. 34] investigate surface roughening of sheet metal during stretch forming. The authors conclude that "In all strain states, the grain rotation is still the main source which causes surface roughening." For the aluminum alloys studied by Guangnan et al, the roughness increment was found to be almost independent of the initial roughness.

Grain size also affects the development of Lüder lines and Orange Peel. Lüder lines are more likely to occur with smaller grain sizes. The Orange Peel effect becomes noticeable and increases with larger grains. Formation of Lüder lines and Orange Peel is also influenced by the strain, the microstructure of the alloy, and the strain rate.

The designed experiment revealed that Lüder lines and Orange Peel started later for material that sat out longer at room temperature. For aluminum alloy 2024, the onset stress increased 5.2 ksi, from 42.0 ksi to 47.2 ksi, while for 7075, the onset stress increased 1.9 ksi, from 39.1 ksi to 41.0 ksi. In terms of strain, these increases are somewhat offset by increases in yield strength of 3.85 ksi and 1.49 ksi for 2024 and 7075, respectively. For 2024, thick specimens exhibited only orange peel while thin specimens exhibited both Orange Peel and Lüder lines. For 7075, thick specimens exhibited only Orange Peel, while thin specimens exhibited only Lüder lines.

Given the age hardening time sensitivity of these surface phenomena, using them as a guide to how much strain is in the part may not be a good strategy.

6.4.8 Summary and conclusions to heat treat designed experiment

For 2024 aluminum, time at room temperature has a significant effect on all of the outputs except elongation. The difference in yield strength between the 20 and 53 minute levels of time at room temperature for 2024 aluminum was found to be 3.85 ksi. For example, a part of 2024-W sheet metal formed 20 minutes after heat treat would

have a yield strength of 20.2 ksi, while a part formed half an hour later would have a yield strength of 24.1 ksi, an increase of almost 20%. The ultimate tensile strength increases 2.36 ksi, which is 4.4%. This indicates that natural aging raises the stress-strain curve and also reduces the strain hardening coefficient slightly. As demonstrated by the analytical model, such changes have a significant impact on the stretch forming operation and part contour, especially if operation is force-controlled. Thickness only has an effect on conductivity and ultimate tensile strength.

For 7075 aluminum, time at room temperature has a significant effect on all of the output except conductivity and elongation. The combination of thickness and cladding has a significant effect every output except yield strength and elongation, but this is probably more attributable to the cladding than the thickness. The difference in yield strength between the 20 and 53 minute levels of time at room temperature or 7075 aluminum was found to be 1.49 ksi. For example, a 7075 part formed 20 minutes after heat treat would have a yield strength of 20.5 ksi, while a part formed half an hour later would have a yield strength of 22.0 ksi, an increase of 7.3%. Ultimate tensile strength increases about half as much as yield strength in absolute terms.

2024 aluminum properties change more significantly as a function of time at room temperature than 7075 properties. A positive correlation between yield strength and ultimate tensile strength was found for 2024 aluminum, but not for 7075. For both alloys, yield strength (for 2024 only), ultimate tensile strength, and elongation were less sensitive to changes in other parameters if they were at room temperature for a shorter period of time. Quench delay had no statistically significant effect on any output, except a 90% significant effect on onset load for 2024 aluminum.

As parts sit at room temperature after solution heat treating, their properties change significantly over time due to natural aging. If not accounted for, these changes will add significant variation to the manufacturing process. Further, sensitivity to changes in other factors increased as parts were left at room temperature for a longer time, which indicates that it would be better to form parts earlier rather than later.

The main effect equations can be used to predict outputs as a function of the factors.

6.5 HEAT TREAT OPERATION STUDY[43]

6.5.1 Description of steps

The heat treat operation flow is shown in the following diagram. While aging is not explicitly shown, it occurs naturally between heat soak and form, except when frozen.

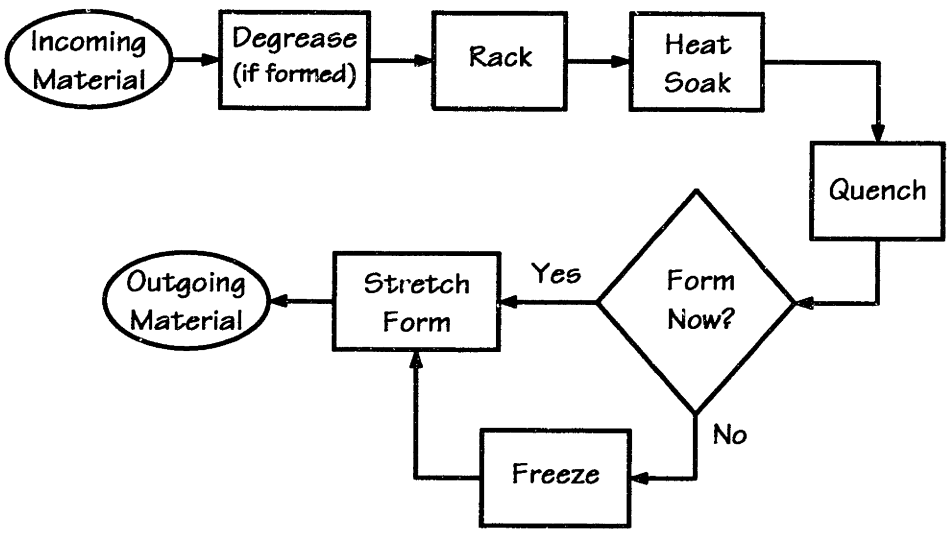

Figure 6.44 Solution heat treat operation flow diagram

Each step is now described.

Incoming material

The sheet metal is generally aluminum alloys 2024-O and 7075-O, clad on one or both sides.

For multiple pull parts, the solution heat treat operation is used only before the last pull (in-between other pulls, the part is annealed). If the part has already been stretch formed, it has a contour and a non-uniform stretch history, whereas before stretch forming, material has no contour and has a relatively uniform stretch history.

The two most important material properties affecting the response of the material to the heat treat operation are its chemical composition and its microstructure, because these determine the material's response to the heat treat process. The two most important material geometry characteristics are thickness, because of its effect on the rate of

---

[43] While this study has been performed on sheet metal heat treating, nearly everything applies equally well to heat treating of extrusions.

heating or cooling and because thinner parts warp more readily, and contour, because less contoured parts warp more readily.

Both 2024-W and 7075-W spontaneously age at room temperature, although the rate of aging of 2024-W is higher than that of 7075-W.

Degrease

If parts have been formed already, they are degreased before being placed into the molten salt bath. Before the end of 1995, parts were degreased in a vapor degreaser containing trichlorethylene after racking. Currently, a water soluble oil is used in forming, and the parts are degreased using hot water and soap before racking. This step does not affect the output, except that parts may be blackened if not all the grease is removed.

Rack

Parts are racked by placing them in a basket and tying down the edges of the parts with aluminum wire to prevent motion. Holes are drilled in the excess sheet metal to attach wire to the part. Preventing motion is important for two reasons: to prevent the whole part from moving due to currents or agitation in the fluid (this is particularly important for skin quality parts), and to reduce warpage caused by thermal gradients in the material during the first few seconds of quench. Since racking has a very significant effect on warpage, setup sheets which describe proper racking procedure are generally created. Some sheets are bent (or bent more if they've already been formed) in order to reduce warpage—this has been shown by experience to work. Movement of the rack is accomplished by a manually controlled hoist system that is pneumatically powered in the vertical direction.

The important characteristics of the basket are its structure and rigidity. The settings are how rack is configured and how the part is attached to it.

Heat soak

In heat soak, the basket is lowered into a molten salt bath (the interaction media) at 920° F and sits there (soaks) for a specified amount of time which depends on the alloy, thickness, and cladding. During this time, soluble hardening elements are dissolved into the solid solution of the aluminum matrix. Some grain growth and annealing may also take place, and in clad material diffusion occurs between the base metal and the cladding. The salt temperature must be between 910° and 930° F. Since

the soak temperature is slightly below the eutectic melting temperature, overheating is likely to cause some melting and result unacceptable material properties. Underheating will reduce the effectiveness of the heat treating operation.

Minimum (maximum) soak times in salt are between 10 (15) and 35 (45) minutes—longer times are for thicker parts. The maximum times are specified for clad material, but adhered to for all sheet. The middle of the range is used as the nominal.

Sometimes the operator will hang the rack with parts over the open salt bath for a few minutes to ensure that it is completely dry; this also gives a slight preheat to the material and reduces the thermal shock to the material and to the salt bath.

The machine parameters are: shape and volume of the vat (oven), heating capability, thermal characteristics of the vat (oven) walls, and salt (air) mixing ability. The interaction media properties are the thermal characteristics of the salt. None of these are expected to change. Ambient temperature is the significant environmental factor.

The settings are the time in the salt bath and the temperature of the salt bath. The most important states are the actual temperature distribution of the part and the salt and the location of the basket.

Quench

To quench a part heated in the salt bath, the operator lifts the basket out of the salt bath, manually pulls the lift mechanism (from which the basket is being held by two hooks) over the quench tank, and lowers the basket into the quench tank. This requires skill and strength, as the masses are heavy and the basket hangs from the lift mechanism and swings when the lift mechanism is moved.

It is vitally important to get the material from the salt to the quenchant in a short time. Too long a quench delay allows excessive precipitation, which, at such high temperatures, reduces final material strength and corrosion resistance. Maximum quench delays, generally between 7 and 10 seconds, are specified.

The function of the quench is to bring the material to room temperature as quickly as possible. The rate of entry into the quenchant affects the quench delay and significantly affects the warpage caused by thermal gradients. A faster rate of entry causes higher thermal gradients and, thus, more warpage.

Water is the generally specified quenchant. Its temperature immediately prior to quenching must be less than 90° F, and it may not exceed 100° F at any time during the quench. No lower limit is placed on quenchant temperature, although 32° F would seem to be a practical lower limit for water. Quenchant temperature is affected by ambient temperature and the load intensity. The quenchant can be cooled or heated, but temperature control is manual. Parts are to remain in the quenchant for not less than two minutes. They are to remain in the quenchant not more than four minutes if they require cold storage.

Important machine parameters are the shape and volume of the tank, heating or cooling capability, thermal characteristics of the tank walls, thermal control algorithm, and water mixing ability. States of the quench tank are the wall temperature distribution, heater or cooler temperature, and mixer speed. Ambient temperature is a significant environmental factor. Settings are the desired quenchant temperature and desired mixer speed. Quenchant states are its temperature and flow.

Age

The state of the material between quenching and aging is denoted as -W and is unstable in the sense that the material spontaneously ages—that is, precipitates form and its strength increases. This may occur either at room temperature (natural aging) or at an elevated temperature (artificial aging). Solution heat treated parts are normaily stretch formed as soon as possible after quench. A delay between 10 and 15 minutes can be expected if parts are heat treated one-at-a-time, due to the time it takes to remove the part from the basket and get it ready in the stretch forming press. If multiple parts are heat treated at the same time, an additional delay of 10 to 15 minutes can be expected for each subsequent part from the same heat treat batch. If there is a significant delay between heat treat and stretch forming, the parts are immediately refrigerated and are generally pulled out one-by-one just before stretch forming. The rate of natural aging increases with the ambient temperature, so that parts at room temperature age slower in winter and faster in the summer.

The likelihood of Lüder lines developing as the material is stretched decreases as the material ages. Lüder lines in the part portion of the material are cause for failure for skin quality parts. If it is likely that parts will Lüder, they are often left to sit for a period of time (for example, twenty to thirty minutes) before being stretch formed.

Aging does not stop until the part has reached a stable state, which occurs well after the part has been formed.

6.5.2 Information, tests, and experiments to assess sources of variation

A number of observations and measurements were made in order to assess the contribution of the heat treat operation to the variation of material geometry and properties. These are discussed below.

Racking

Racking mostly affects part warpage. Potential sources of variation in the racking step are how a part is oriented and how it is fixed to the basket, and bending of the part.

Although generally specified in setup sheets, racking practices vary slightly from operator to operator. Bending flat sheet, or even pre-formed parts, reduces warpage, but may also affect part contour. Since bending is done by hand, it may be somewhat inconsistent.

Salt bath

Observations of the heat treat operation and records in the heat treat log indicate that the amount of time a part spends in heat soak is not a source of variation; this time is very carefully monitored and the nominal times are closely adhered to.

Monthly temperature uniformity surveys are performed on all heat treat furnaces and vats. Results and insights from some of the Salt Vat #14 (used to solution heat treat all the sheet stretch forming metal that is heat treated) survey results are given here.

Test description

Temperatures are measured with 10 thermocouples (T/Cs). Two tests made are the overshoot test and the recurrent high and low test. The overshoot test is performed by placing a large part (the *load*) into the salt bath and measuring the temperature response within the salt bath. This test is performed in order to ensure that the temperature control system doesn't cause the salt temperature to exceed a critical temperature after a load is put in. When the overshoot test is complete, the temperatures are monitored to determine the recurrent low and high temperatures.

Overshoot test and daily temperature variations

In addition to giving the maximum temperature, the overshoot test gives an indication of temperature changes in the salt bath from the load. Partial results of the overshoot test

on 10 March, 1995 are shown in the following chart, which demonstrates effect of putting a load into the salt bath on the salt bath temperature at five locations. The thickest line (SV14 C) represents the temperature readings at the control T/C. The medium thick lines (SV14 M4 and M7) represent the temperature readings at the two monitor T/Cs. The thin lines (Low and High) represent the temperature readings at the low and high T/Cs in the recurrent low and high temperature test.

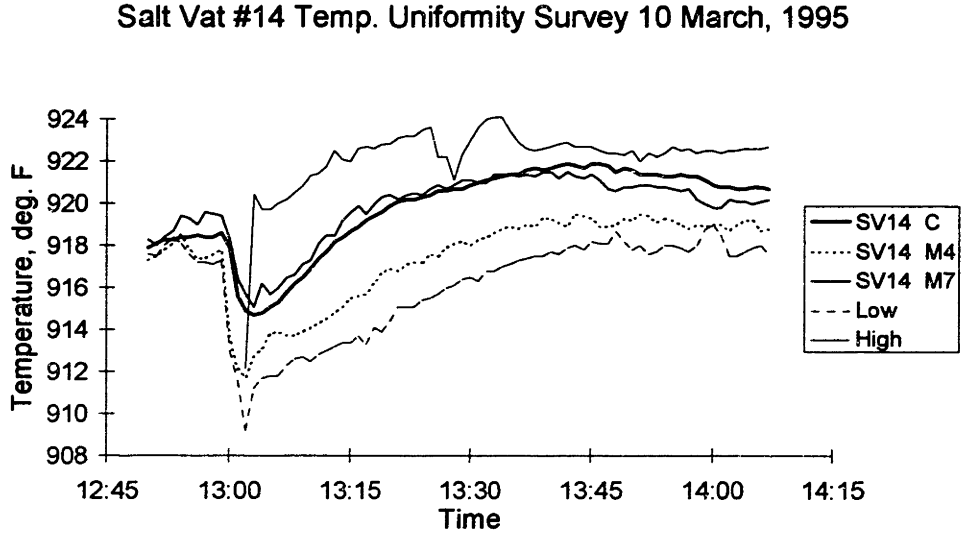

Figure 6.45 Salt vat #14 temperature uniformity survey, 10 March, 1995; five T/C readings are shown: control, monitors 4 and 7, and the recurrent low and high

The temperature variations in the salt bath are at least 2 to 3 times greater than those recorded by the control and monitor T/Cs shortly after the load has been put in. Further, the average salt temperature changes over time, first decreasing about 4 degrees and then increasing to about 3 degrees above the starting temperature.

The following chart shows temperatures of the control and two monitor thermocouples throughout one day. The vertical lines indicate when loads were put in and taken out.

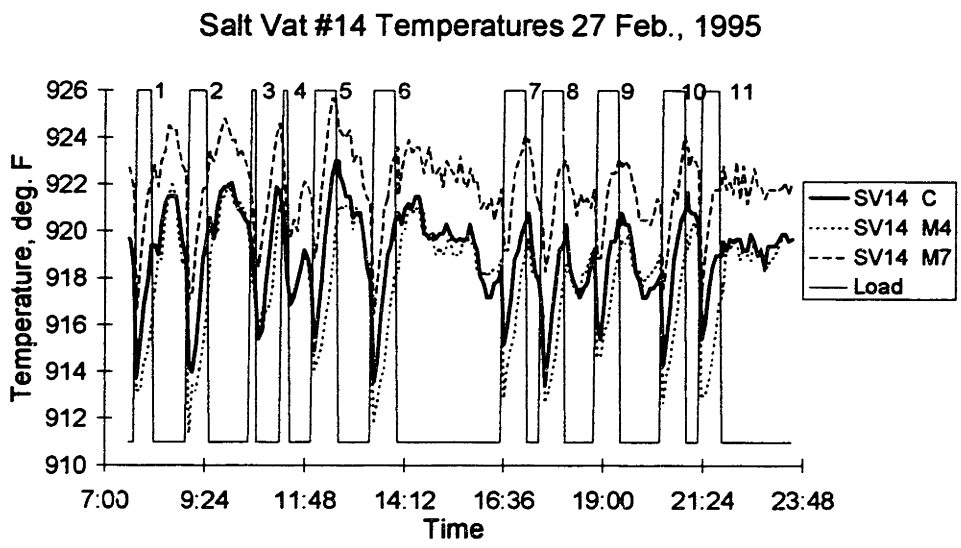

Figure 6.46 Salt vat #14 temperature and loads, 27 Feb., 1995

The same trends as found in the overshoot test are present, validating that it is representative of what normally goes on. Note as well that the average temperature does not change in the long run.

The temperature of the part being heat treated is not measured. However, since molten salt and aluminum are good heat conductors, and since sheet metal by nature is very thin, it is a good assumption that the metal is at essentially the same temperature as that of the immediately surrounding salt within a few seconds.

Recurrent low and high temperature test

The recurrent low and high temperature test determines the low and high temperature readings after the temperatures have reached a relatively steady state following the overshoot test. The following table shows the relevant information for this test for the months of January through July, 1995.

Month	Low T/C #	High T/C #	Low Temp	High Temp	Difference
Jan.	9	5	917.9°	919.8°	1.9°
Feb.	9	6	917.6°	920.8°	3.2°
March	9	3	917.1°	922.7°	5.6°
April	9	1	918.1°	920.2°	1.9°
May	3	5	920.0°	921.8°	1.8°
June	4	5	919.3°	920.8°	1.5°
July	4	5	920.0°	921.9°	1.9°

Table 6.13 Recurrent high and low T/C results, January to July, 1995

The table shows that the maximum steady state temperature differences are relatively small most of the time, at least 1.5° and at most 5.6° (it appears that a change was made between the March and April tests). As the charts for the overshoot test demonstrate, temperature variations during the transient portion of the test vary much more than this, and are much more relevant to understanding temperature variation. Parts are never left in the tank long enough for the salt to reach a steady temperature.

Summary and conclusions to heat soak sources of variation

Heat soak appears to be a very small source of variation, because the salt bath remains well within the allowed temperature window, and the metal temperature is essentially at the salt temperature.

Quenchant temperature

Potential sources of variation in the quench operation are quench delay, rate of entry into quenchant, and quenchant temperature.

The quench delay and rate of entry into the quenchant may vary from one load to the next largely because of the human operator involved. Operator skill, in addition to sheer physical strength, is required to achieve the desired delay time and rate of entry repeatably. The quench delay time doesn't exceed the maximum allowed time. Even so, there is a difference between the time that the top and bottom of the material spend between exiting the salt bath and entering the quenchant. The designed experiment from the previous section demonstrated that this has a negligible effect on material properties.

Quench delay time and quench entry rate affect material warpage through the intensity of the stresses caused by thermal gradients within the part. According to operators, quenching a part a few seconds sooner can significantly increase warpage, and a faster quench entry rate also increases warpage. This effect has not been quantified.

The quenchant temperature varies according to the ambient temperature and the load intensity (the amount of heat introduced to the quenchant from quenching per unit of time). Ambient temperatures vary according to the time of day (warmer in the afternoon) and the time of year (warmer in the summer). As a day progresses, the average temperature of the quenchant increases from the ambient temperature and, more significantly, from the load intensity (that is, from the heat contained in the parts that are quenched in it). The following data give an indication of the combined effect of load intensity and ambient temperature.

Quenchant temperatures on February 27, 1995 are shown in the following diagram. The vertical lines show when loads were put into and taken out of the salt vat, so that the falling edge indicates when parts were quenched.

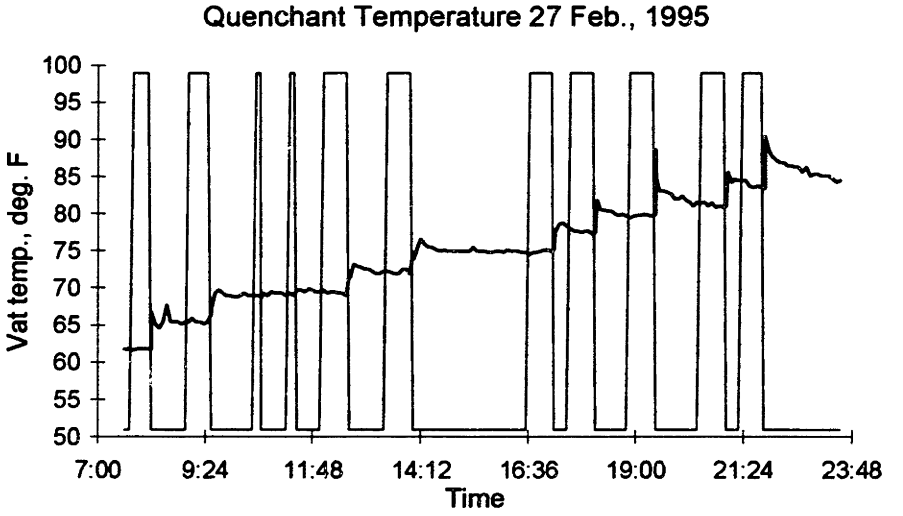

Figure 6.47 Quenchant temperature and loads, 27 February, 1995

Loads 3 and 4 were exactly the same, as were loads 5 through 10. Between loads 5 through 10, the initial quenchant temperature increased just over 12°, from 69.0° to 81.1°. The increases in temperature from start to end of quench (neglecting momentary peaks) ranged from 2.9° to 4.7°, with an average of 3.6°. The increase in quenchant temperature between the beginning and end of the day was about 20°.

Probable effects of changes in quenchant temperature

Although measurements haven't been made, it is possible to state two likely effects of varying the quenchant temperature. One effect mentioned by operators is that a colder quenchant will induce greater warpage in the part. This occurs because a colder temperature creates greater thermal gradients which cause greater strains and stresses in the part. The other effect is that higher temperatures would lead to (a) slightly slower cooling of the part and, therefore, slightly more aging as the part cools to the quenchant temperature and (b) slightly faster aging during the time that the part is in the quenchant and until it reaches room temperature after it is taken out. Perhaps there is a temperature at which some combined measure of warpage and cooling is optimized.

Summary and conclusions to quenchant temperature

Quenchant temperature changes from one point in time to another, depending mostly on the loading intensity and ambient temperatures. Heat treat data (for more than one quench tank) at various times of the year show that initial quench temperatures vary from a low of about 60° F (in the morning in winter) to a high of about 90° F (in the late afternoon in the summer). This trend is also seen in the extrusion quench tanks. The effect of this source of variation has not been measured in this study, but it may be beneficial to do so. Operators report that a shorter quench delay and a faster quench rate both increase part warpage.

Age

The things that affect aging are material composition and microstructure, time and temperature between quench and stretch, refrigeration time and temperature, and artificial aging time and temperature.

The time between quench and stretch forming can vary significantly, because often a group of parts is heat treated at once, but they can only be stretched one-at-a-time. Thus, if a group of 4 parts comes out of the quench at the same time, and each part requires 5 (10) minutes to stretch, the time difference between the first and last stretch will be at least 15 (30) minutes. Parts are also intentionally left to sit out at room temperature to minimize Lüdering. The designed experiment in the previous section demonstrated that room temperature aging significantly affects material properties.

Refrigerator temperature is well controlled, and with the low temperature and short time a part is in there, it is unlikely to be a significant source fo variation. Some parts stress relieve and change shape during artificial aging, but artificial aging was not studied.

6.5.3 Summary of sources of variation and suggested improvements for heat treat

Based on the above, sources of variation are listed according to the step in the operation and recommendations for improvement are made.

Material

Chemical composition and microstructure are the two material properties that can effect the output of the operation. These have not been studied. In order to eliminate this potential source of variation, chemical composition and microstructure could be more tightly specified. While tighter control is achievable with today's technologies, the cost of this option is not certain. Not much can be done to further optimize the operation to make it less sensitive to composition and microstructure variations, because it has already been optimized. Compensation for the effect of changes in composition or microstructure is not feasible in the heat treat operation because measurement is not easy, and no readily usable model exists. However, as shown by the analytical model and the sheet stretch forming study and improvements, strain control of the operation can be used to minimize the effect of material property changes on the operation.

Thickness, doesn't vary enough from nominal to affect the heat treat operation.

Racking

Racking has a very significant effect on part warpage, but little on heating or cooling. Racking is not so much a source of variation itself as it is a way of reducing a source of variation—warpage. In order to minimize warpage, racking should be performed the same, optimal way each time, and the part should be securely attached to the rack. The optimal racking method for each part should be agreed to by the operators and documented.

Heat soak

Heat soak time and temperature are tightly controlled due to corrosion resistance requirements; they are very repeatable and not significant sources of variation.

Quench

Quench delay, rate of entry into quenchant, and quenchant temperature can each have an effect on the material geometry and properties. None of these was studied. Less warpage occurs with a longer quench delay, a slower rate of entry into quenchant, and a warmer quenchant. On the other hand, less precipitation occurs with a shorter quench delay, a faster rate of entry, and a cooler quenchant. Given that upper limits are specified for quench delay and quenchant temperature, it may be optimal to try and quench at some point under these limits. In order to get times more repeatable, manual control of quench may need to be replaced by automatic control, although the operators are quite skilled. Quenchant temperature could be kept at a constant temperature. More investigation into this topic is needed.

Age

Aluminum ages at room temperature, and thus natural aging is a source of variation if parts are left out at room temperature for varying amounts of time. This source of variation could be eliminated by placing limits on the total amount of time a part may spend at room temperature before stretch forming. However, this is probably not feasible, because parts sometimes need to sit out in order to inhibit Lüdering. If parts are left out, then each part should be left out for the same amount of time. Finally, it is possible to predict the amount of strengthening of the material based on how long it sits out, and to adjust the amount of strain or force used in the stretch forming operation to compensate for the effect of aging.

6.5.4 Summary and conclusions to heat treat operation study

Part warpage due to quenching and change of material properties due to aging are the two most important sources of variation from the heat treat operation. No study was made of warpage, largely because it is very difficult to quantify. Leaving solution heat treated aluminum at room temperature causes natural aging, which strengthens the material. The effect of aging on material properties was the topic of the previous section, and the effect of material properties on the stretch forming operation was addressed in the previous chapter.

6.6 CHEM MILL OPERATION STUDY

The chemical milling operation is used to remove material over large surface areas of a part. Chem mill primarily affects part thickness, but may also affect part contour.

6.6.1 Description of the chem mill operation

The steps of the chem mill operation are shown schematically in the following diagram.

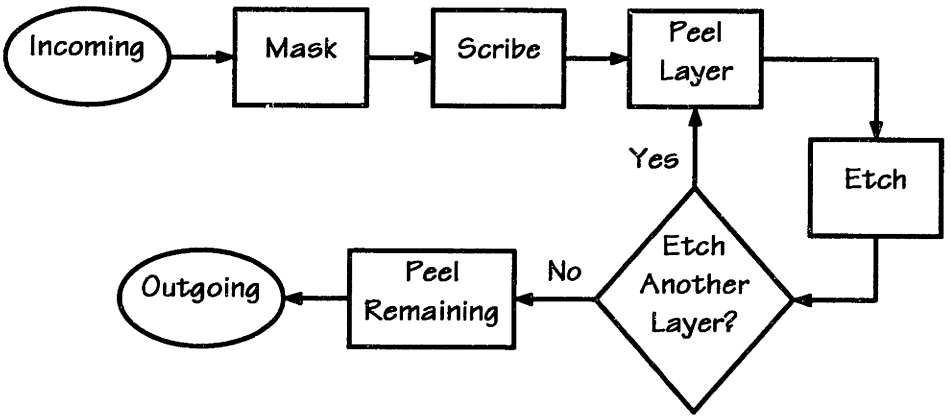

Figure 6.48 Flow diagram of steps in the chem mill operation

Each step or group of steps is briefly discussed next.

Incoming Material

The material for chem milling is generally contoured, stretch formed sheet of 2024 or 7075 aluminum, varying in initial thickness from 0.040" to somewhat over 0.100", and clad on one or both sides. The most relevant material properties are likely to be chemical composition, microstructure, and residual stresses. The most important material geometry parameter is thickness.

Mask, scribe, and peel

The purpose of the mask is to prevent etching of the material. Surface cleanliness is very important, because the mask does not properly adhere to a dirty or even moist surface, and poor adhesion allows etchant to infiltrate between the mask and material. The accuracy of the scribing template and the locations of the tooling holes and pins are critical to properly locating the perimeter of the etch area. Operator skill is important in accurately tracing the template contour and not penetrating into the part too far. During peeling, care must be taken to not disturb the remaining mask, and, for thin parts, to not distort the part due to forces applied.

Etch

Machine

The two machines are a large vat containing a chemical solution and a material movement mechanism, the latter of which may be, for example, a crane or gantry. A typical vat and basket are shown in the following diagram.

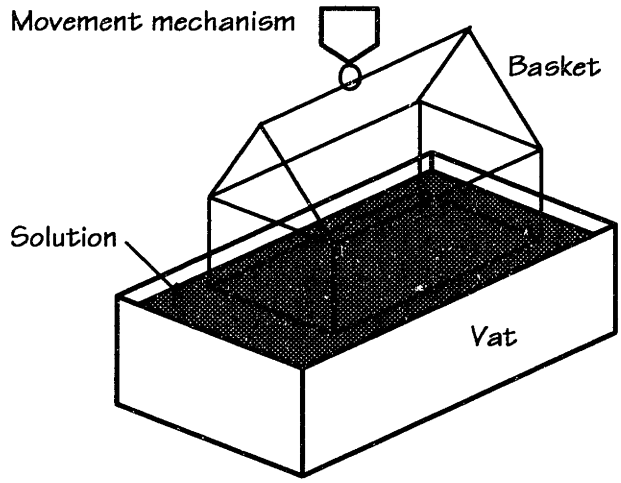

Figure 6.49 Chem mill vat, movement mechanism, and basket

The function of the vat is to control the temperature and flow of the chemical solution. The important machine parameters are the vat geometry and thermal characteristics, the temperature control system, and the flow control system. The states are: temperature of the walls and heating/cooling elements, activity of the flow control system.

The function of the material movement mechanism is to move the basket into and out of the solution, and to and from a loading and unloading station. The state of interest of the material movement mechanism is the location of the rack holding device.

Location tooling

The location tooling is very simple. It is the basket or other rigid structure used to hold and support the part. Parts are generally attached to the basket at their tabs.

Interaction media

The interaction media is the chemical etching solution. Its base is water; the etchant is caustic soda: NaOH + Na_2S. The surface finish generally achievable from this etchant is R_a 2.5-4.0 μm. When finer surface needed, triethanolamine (TEA) is added, so that surface finishes of R_a 1.0-1.5 μm are achievable [Davis, 1993].

While specified chemical content ranges are quite wide, the contractor keeps the chemicals within a much tighter set of limits, e.g., ± 1 oz/gallon instead of ± 4 oz/gallon. Temperatures are kept at around 175-185° F. The states of interest of the solution are its temperature, chemical composition, and flow.

Output

Material properties, except for a change in residual stresses, are not affected by the chem mill operation.

Chem mill reduces the thickness of the exposed portion of the part. If there are significant residual stresses in the part, the contour may change. The surface finish is also affected.

Settings and states

The most important settings, the first two of which are also states, are: chemical composition of the solution, solution temperature, and time in solution. Part thickness is the most important material state.

Control

Chemical composition, temperature, and time in solution are the three most important states to control.

Temperature can be continuously monitored (electronically or mechanically), and, depending on the whether compensation is automatic or manual, it can be more or less tightly controlled.

It appears that composition is only checked daily, due to the time-consuming nature of the measurement process, the work involved to add caustic and other chemicals, and the slow change in composition over time.

Control of part thickness is often achieved by pulling the part out a minute or two before the expected amount of material is to be removed, and measuring its thickness. If needed, the part is put back into the solution to remove the full amount of material.

6.6.2 Measurements of the chem mill operation

Measurements made of the chem mill operation are now presented and discussed.

What was measured

Basically, two sets of measurements were made. The first focuses on the change in material thickness through a number of dips; the second focuses on things affecting the etch rate. These were felt to be the most important areas deserving attention.

Thickness measurements were made on three lots at six locations on each part, initially and after each etch dip. In order to determine what affects the etch rate, time in

solution, thickness, temperature, and concentrations of chemicals in the etching tanks recorded daily were analyzed. The parts for nearly all the measurements were 2024-T3 aluminum leading edges with initial thicknesses of 0.100". One set of measurements used non-leading edge parts. The following diagram shows the location of the thickness measurements on the leading edges. Measurement locations 2 and 5 were on the tabs, and these locations were measured with a hand micrometer to the nearest 0.001", while the other measurements were measured to the nearest 0.0001".

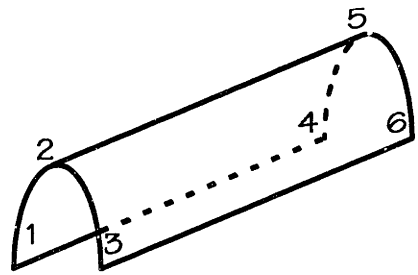

Figure 6.50 Locations of thickness measurements on formed leading edge

Change in thickness at a location

Thickness changes were measured on lot P/Ns B, E, and F of the sheet metal stretch forming measurements. The following chart shows the ratio of the actual thickness over the desired thickness at location 1 for each part in lot P/N B, initially (M0) and after each dip (M1, M2, and M3). P/N B was etched in three batches, in sizes of four, four, and five parts.

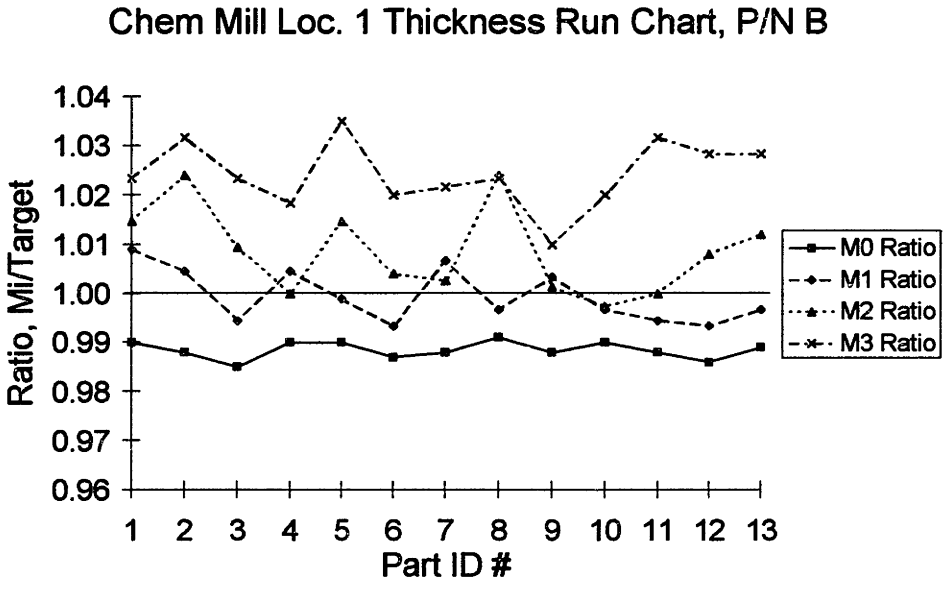

Figure 6.51 Thickness ratios at location 1 for four dips, P/N B

The chart shows that part-to-part thickness variation increases from the initial value. While the increase in variation is exaggerated by the fact that the denominator is shrinking as the dips proceed, it is still present.

The following table indicates the change in variation from the initial thickness to the final thickness. Only locations 1, 3, 4, and 6 were used, because only these were measured after each etch dip. The "Average" value is the average thickness of all the measurements of all the parts after each dip. The "St. Dev." value is the average of the standard deviations at each of the four locations for all of the parts in a lot.

		Measurement			
		M0	**M1**	**M2**	**M3**
P/N B	**Average**	98.82	90.30	76.38	61.89
	St. Dev.	0.15	0.57	0.61	0.50
P/N E	**Average**	99.04	89.85	75.37	61.83
	St. Dev.	0.22	1.10	0.93	0.59
P/N F	**Average**	89.17	78.2	*	*
	St. Dev.	0.39	0.46	*	*

Table 6.14 Average thickness and part to part standard deviations; units are thousandths of an inch * P/N F had only one chem mill step

The table reveals that the part to part variation within a lot changes from dip to dip (ANOVA analysis shows these changes to be significant to well over 99% confidence), and that the trend appears to be an increase in variation followed by a decrease, though the final variation is still higher than the initial variation.

The following table shows how variation changes within a part as the part is chem milled. Each value in the table is the average of the standard deviations within each part initially and after each etch step. Again, only locations 1, 3, 4, and 6 are included.

		Measurement			
		M0	**M1**	**M2**	**M3**
P/N B	**St. Dev.**	0.15	0.43	0.79	0.43
P/N E	**St. Dev.**	0.31	0.39	0.79	0.37
P/N F	**St. Dev.**	0.25	0.32	*	*

Table 6.15 Within part thickness standard deviations; units are thousandths of an inch * P/N F had only one chem mill step

Again, the variation changes from batch to batch (for P/Ns B and E, ANOVA analysis showed the changes to be significant to well of 99% confidence), but the direction of change is uncertain.

So far, the effect of chemical milling on the variation of part thickness is somewhat ambiguous. Further insight can be gained from the following charts which show the progression of measurements for P/N E. Note that the vertical scale on each chart is the same, and that this lot was divided into two batches of five and eight parts. There is no record of which parts were in which batch, although one can guess from looking at the charts that parts 1,2,3,5, and 8 were in one batch and the rest in another batch.

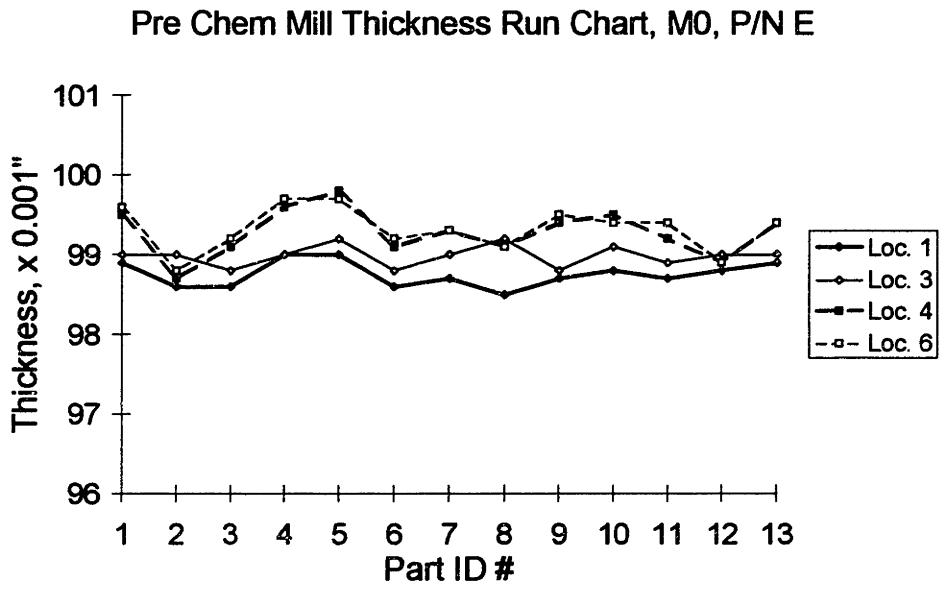

Figure 6.52 Sheet thickness measurements before chem mill, P/N E

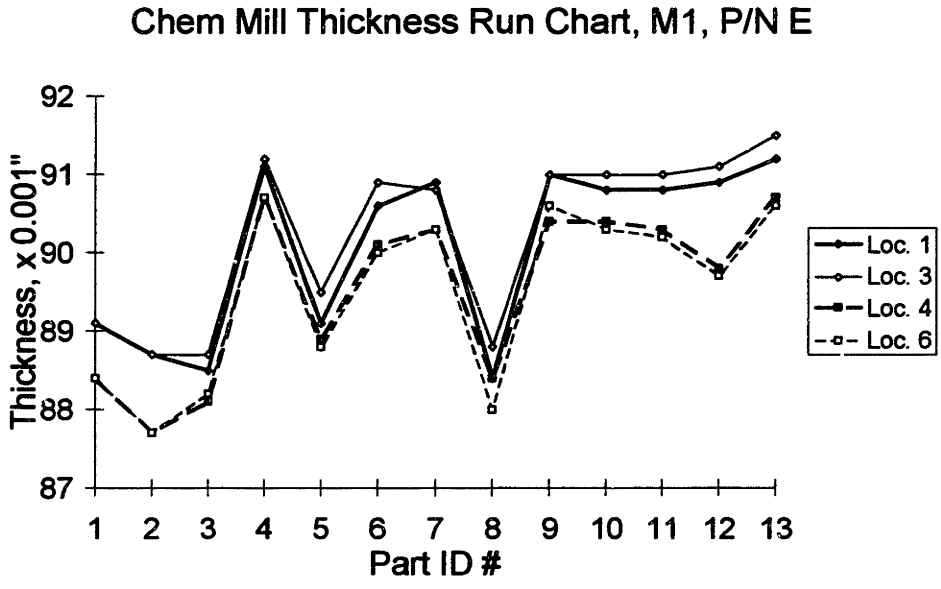

Figure 6.53 Sheet thickness measurements after first dip, P/N E

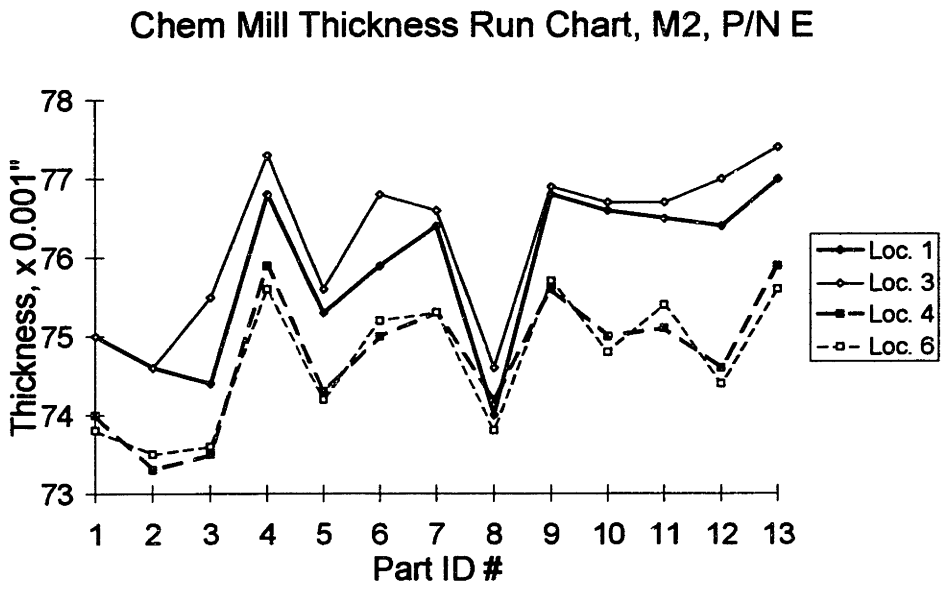

Figure 6.54 Sheet thickness measurements after second dip, P/N E

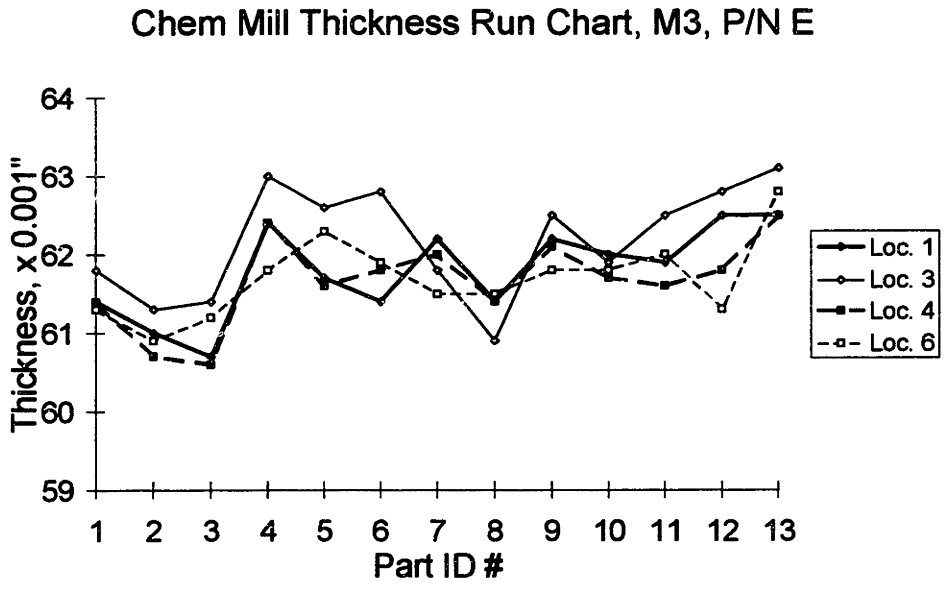

Figure 6.55 Sheet thickness measurements after third dip, P/N E

Measurements from the first dip clearly demonstrate that differences between batches can be significant. However, as is evident in the measurements from the last dip, it is possible to compensate for these differences, generally by leaving the part in for less time in following dips. Measurements after the first and second dip show a significant difference between thickness at the ends, because one end is in the solution longer than the other during the time the parts are lowered into and raised out of the solution.

The difference is gone after the third dip, probably due to the common practice of alternating which end is up if there is more than one dip.

Etch rate and temperature

The following figure shows the solution temperature and etch rate for 35 batches of leading edge parts.

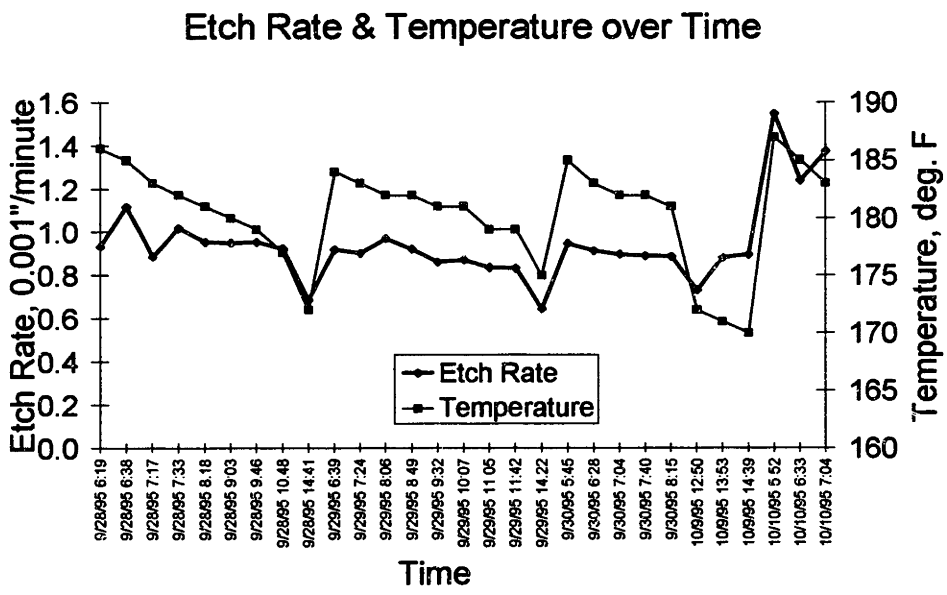

Figure 6.56 Etch rate and temperature over time

A strong correlation between temperature and etch rate is seen. As well, an interesting cycle in temperature is evident: temperature generally decreases slowly after jumping up. A look at the date and time of day at the bottom of the chart indicates that the temperature of the solution generally starts off high and cools as the day progresses. This decreasing temperature trend is somewhat confusing because (a) the etching reaction is exothermic and increases the temperature of the solution, which would tend to heat up the solution throughout the day and (b) ambient temperatures normally increase as the day progresses, and one might thus expect the solution temperature to increase throughout the day as well. The data show no significant effect of caustic content on the etch rate. This is probably because the caustic content is kept within a relatively tight range.

Analysis of the data for each P/N reveals differences in the correlations between etch rate and temperature. The cause of this is not known, but it does not appear to be solution composition. Another set of measurements in which different materials were

etched was analyzed. The following chart shows etch rate as a function of temperature for the two different alloys—2024-T*X* and 7075-T6—along with the predictions based on least squares regression.

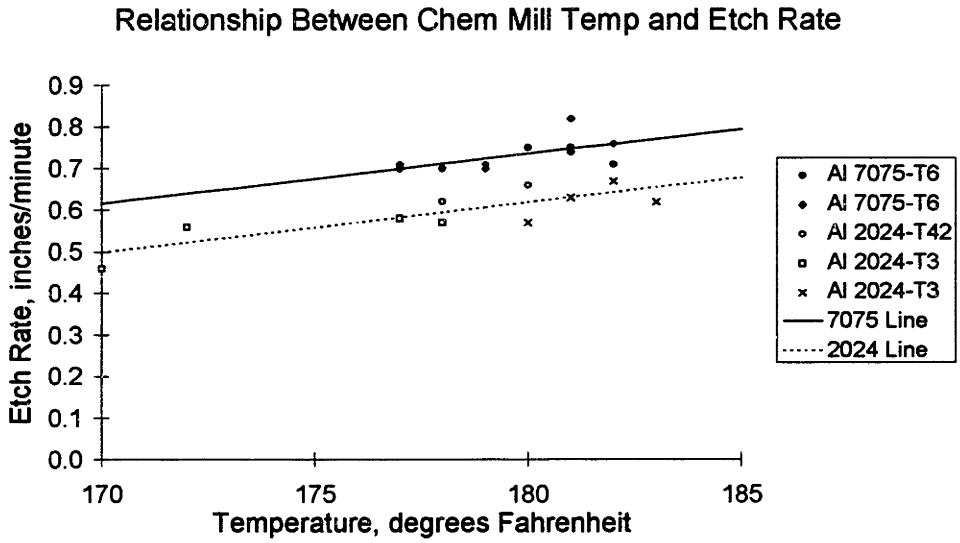

Figure 6.57 Etch rate as a function of temperature, for alloys 2024 and 7075

This chart reveals that etch rate is influenced not only by temperature, but also by alloy. The predictive equations for etch rate as a function of temperature are:

$$\text{For 2024-T}X\text{:}\quad ER = 0.0119 \times T - 1.41 \tag{6.6}$$

$$\text{For 7075-T6:}\quad ER = 0.0120 \times T - 1.55, \tag{6.7}$$

in which T is temperature in °F and ER is the etch rate in inches per minute.

Accurate prediction of etch rate will permit better timed removal of the parts from the solution and smaller deviation of actual thickness from desired when parts are removed. Further, it may be possible to eliminate the practice of checking parts shortly before they are expected to be finished, which can be a source of variation due to the longer time that the bottom of the part spends in solution as a result of dipping and removing the parts twice.

Tooling hole locations

As reported in Section 6.2, tooling hole locations are often significantly off, on average and around the average, by 0.050" to 0.150". Such large variations will significantly affect the ability to properly align the chemical milling scribe template, resulting in deviation of the location of the milled pockets from their desired location. Further, even

though the part may be the correct shape, if its tooling hole locations are off, it will appear as though the part shape is off as well. However, according to the chem mill supplier, misalignment of the etch perimeter is not a significant problem.

6.6.3 Other sources of variation

The material geometry can be a source of variation for etch rate. It is commonly held that thinner sections etch faster than thick sections, and the center of a pocket etches faster than the outside. Analysis of the data does not show a significant effect of thickness on etch rate.

The effect of chemical milling on the contour depends on the residual stresses in the part. Change in contour for a given amount of material removed is related to the residual stresses in the removed material. More equal residual stresses in the part will lead to less change in contour. This point has already been addressed, and the data did not show a change in contour from chem milling.

If parts are pulled out of the solution too quickly, the forces generated by fluid drag are great enough to plastically deform the part. Thus, this must be done slowly.

6.6.4 Summary of chem mill variation and sources of variation

Scribing and tooling hole locations

No measurements were made on scribe locations, since these were from the start deemed not to be important—they had been a negligible cause of quality problems. However, based on the findings that tooling hole locations can vary significantly, and given that the scribe location can only be as good as the location of the template, it is clear that these will vary somewhat.

Etch rate

Solution temperature has the greatest effect on the etch rate. Solution content was not found to significantly affect the etch rate. Aluminum alloy 7075 etches faster than 2024.

Effect on contour

As determined in Section 6.2, change in springback from after rout to after chem mill is statistically insignificant.

Thickness variation

Analysis showed that thickness variation within a part and from part to part changes from dip to dip, and increases between the first and last dips. The average thickness

was off from target thickness by about one to two thousandths of an inch. The average part to part standard deviation increased from an average of 0.25 thousandths of an inch to about 0.50 thousandths of an inch. The average within part standard deviation increased from an average of 0.24 thousandths of an inch to about 0.37 thousandths of an inch. These changes are insignificant relative to contour variations in the stretch forming operation.

6.6.5 Recommended chem mill improvements

Recommended changes for precision improvement are now given.

Incoming material and fixturing

Variation in tooling hole location should be reduced in order to better align parts with the template. While chem mill scribers have become skilled at accommodating misalignment between tooling holes and their templates, this is undesirable. Parts and the templates need to be fabricated (and some templates may need to be reworked) so that tooling pins and holes match up properly.

Settings and control

The two most important settings are temperature and time in solution. Solution temperature should be kept constant. A designed experiment could be performed to determine the temperature at which the operation produces the best results, or, more simply, the middle of the specified range could be used. Time in solution should be predicted based on temperature (which is easier with constant temperature) and alloy.

6.6.6 Summary and conclusions to chem mill operation

An investigation was made into the significant causes of variation in the chemical milling operation. The general conclusion is that chem mill contributes very little to part geometry variation. Variation in thickness is at most a few thousandths of an inch.

The two most important factors affecting the etch rate are the temperature of the solution and the alloy. No effect of solution composition on etch rate was found within the range used.

Misalignment between tooling hole locations and scribe templates is significant—from 0.030" to 0.180" on some parts. The impact of misalignment was not measured.

The major improvement recommended is to predict the time in solution based on solution temperature and alloy. Further, solution temperature should be held constant

(eliminated as a source of variation). This will enhance predictive capability and hopefully allow precise prediction of material thickness so that parts don't have to be taken out and measured shortly before target thickness is expected to be achieved.

Unfortunately, no quantitative indication was found to predict precision improvement based on the recommended improvements.

6.7 SUMMARY AND CONCLUSIONS TO SHEET STRETCH FORMING PRACTICAL UNDERSTANDING

A number of investigations have been made in the stretch forming process on the shop floor to develop a practical understanding of the sheet stretch forming operation—to determine which parameters affect which other parameters, to assess the current level of variation in the process, and to identify sources of variation. The investigations were guided by both input from the shop floor and a theoretical understanding of the operations that constitute the stretch forming process. Further, improvements were recommended and tested, the most significant of which are repeatably achieving optimized settings and automatic strain control of the stretch forming operation.

Most of the variation identified in the stretch forming process for 2024-T3 leading edges (the focus of most of the measurements) originates in the stretch forming operation. Variation was found to be significant within parts, between parts in a lot, and from one lot to another, as indicated by the following parameters: force, die table movement, strain in the material, and separation of the material from the die. Sources of variation identified by the study are changes in settings (most importantly the maximum force, the die table angle, and the initial positions and angles of the jaws) and control of the operation by force instead of strain. Proposed improvements are two-fold:

- repeatably achieve optimized settings
- use in-process, automatic strain measurement and control

Although based on limited data, implementation of the proposed improvements dramatically reduced contour variation. From a current contour variation of 0.190" (one standard deviation of the average separation at the ends) with force control and no special effort made to repeatably achieve the settings, the reductions in variation realized are as follow:

- force control with repeatably achieved optimized settings: 75% to 0.047"
- displacement control with repeatably achieved optimized settings: 86% to 0.027"

- strain control with repeatably achieved optimized settings: 92% to 0.015"

These results demonstrate the improvement attainable first from repeatably achieving optimized settings, and then from getting closer to strain control. Since the strain measurement technique and the control method (manual) were in the testing stage, further reduction in variation is expected as the strain measurement technique is refined and automatic strain control is implemented.

Investigation of material geometry and properties showed that the material stress-strain properties vary significantly for a given alloy, although variation is reduced when material is grouped according to thickness as well.

A designed experiment was performed to determine the effects of material thickness, quench delay, and time at room temperature on material properties. In accordance with expectations, material strengthens as it age hardens at room temperature, and the effect is stronger on 2024 than on 7075. Natural aging for 53 instead of 20 minutes increased the yield strength of 2024 by almost 20%, and of 7075 by about 7%. A combination of thickness and cladding had a significant effect on 7075 output. Quench delay was found to have no significant effect on any measured output.

Investigation into the heat treat operation revealed that temperatures and times in the operation are well controlled, with the exception of the quench. Although not measured, it was found that warpage is significant and is significantly affected by racking, quench delay, rate of entry into quench, and quenchant temperature. Optimal racking methods should be documented and adhered to. Further investigation is recommended to study the effect of the various quench parameters on warpage and to determine an optimal set of parameters at which warpage is minimized. Age hardening between quench and stretch forming affects material strength. All parts should spend the same amount of time at room temperature, but if this is not possible, it is possible to compensate for the effect of age hardening in the stretch forming operation.

Study of the chemical milling operation revealed that it has little effect on precision. Thickness variation is increase slightly, but remains relatively insignificant. Temperature of the chemical solution and alloy were found to have the most significant impact on etch rate. Maintenance of a constant etchant temperature is expected to enable better prediction of etch time, which will reduce the need to take a part out of the solution and measure it shortly before it is expected to be the correct thickness.

It was also found that tooling hole locations in the parts often varied significantly. This variation should be eliminated.

The next chapter is similar to this one, except that everything is done for the extrusion stretch forming process.

7 EXTRUSION STRETCH FORMING: PRACTICAL UNDERSTANDING

7.1 INTRODUCTION

The purpose, content, and flow of this chapter are the same as in the previous chapter.

7.1.1 Description of process and operations

The purpose of the extrusion stretch forming process is to manufacture precisely shaped extrusions. Stretch formed extrusions are used in a variety of places in an aircraft and include parts such as brake rings, chords, and stiffeners. Generally, they are designed to fit up to the skin of the aircraft.

The process flow for extrusion stretch forming is shown in the following diagram.

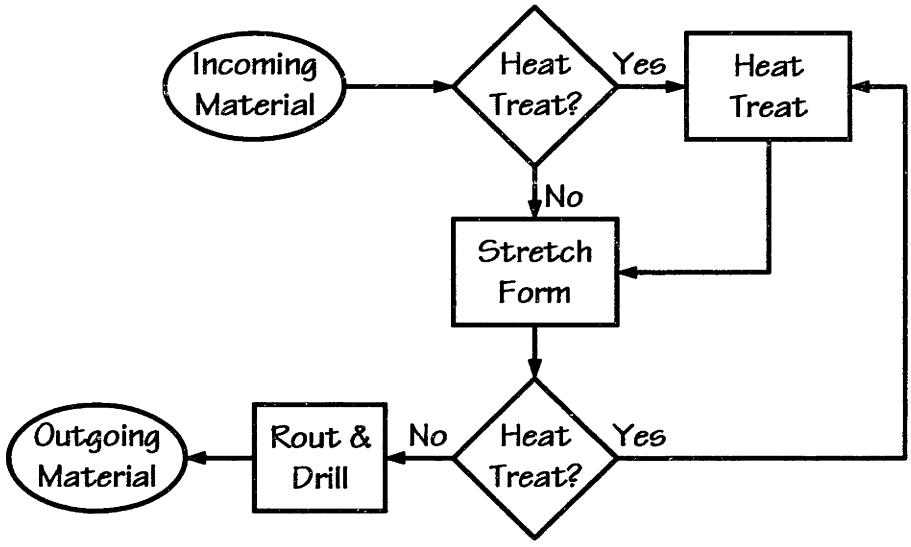

Figure 7.1 Extrusion stretch forming process flow diagram

Some parts are shot peened as well, but this is operation is not addressed. While not shown, a lot of hand work goes on in the check and straighten operation in order to bring parts into tolerance. Each operation is now briefly described.

Incoming

Extrusions purchased from suppliers may or may not be ordered to the exact length needed for each lot of parts. Therefore, parts are sometimes cut in-house. As well, angles are not always ordered to the exact angle needed for each lot of parts (for example, a 90 degree angle may be ordered when a 87 degree angle is needed). In this case, the needed angle is created by brake forming.

Heat treat

The heat treat operation is similar to that used in the sheet stretch forming process. Again, it's purpose is to put the material in the -W condition so that it can be formed while soft and then age hardened after forming. Heat treat is composed of the following steps:

1. Rack: one lot of parts (usually 10-15) is loaded into a basket; parts are appropriately spaced and then wired to the basket to reduce warpage.
2. Soak: the basket is lowered into a salt vat (or air furnace) and left there for a pre-determined amount of time.
3. Quench: the basket is pulled out of the salt and lowered into a vat of water within about 10 seconds in order to quickly bring down the temperature.
4. Unload: the parts are unloaded from the basket.
5. Freeze: the parts are then put into a freezer until they are stretch formed.

Stretch forming

The stretch forming operation imparts the contour to the part by stretching the part (pre stretch), bending it around the die under constant force (wrap), and further stretching the part (post stretch). This is the stretch wrap forming operation. The first stretch is composed of the following steps:

1. Load: the part ends are inserted into the jaws and the jaws are closed.
2. Pre stretch: the part is level stretched (straight).
3. Wrap: the part is wrapped around the die under the same force to which it was stretched in the pre stretch. Portions of the part may be forced against the die using clamps as the part is being wrapped.
4. Post stretch: the part is stretched further to reduce springback.
5. Joggle: some parts are joggled at this point.
6. Unload: the forces are relaxed, the jaws are opened, and the part is removed.

If the stretch forming operation is the second stretch, step 2 is performed with the part wrapped around the die as far as it was wrapped at the end of the first stretch.

Routing

The purpose of the routing operation is to cut out portions of the part which are not needed, to cut the part to the desired length, and to drill whatever holes may be needed. Manual routing is accomplished through the following steps:

1. Load: a part is loaded between two halves of a fixture, and the fixture is clamped.

2. Rout: using the fixture as a guide, the unneeded material is cut off and the ends are defined. Clamps generally are repositioned as the part is routed in order to access all of the part.
3. Drill: holes are drilled, again using the fixture as a guide.
4. Unload: the clamps are removed and the part is taken out.

Check and straighten

The purpose of this operation is to correct shape deviations. Skilled operators use various tools to bend and hammer parts into the desired shape. This operation is not investigated because part of the objective of this thesis is to eliminate it by making it unnecessary. Parts are check and straightened after routing, although if the part contours vary enough from nominal, they may be check and straightened before routing as well.

Next

Having briefly outlined the extrusion stretch forming process, each operation is now addressed in some detail.

7.2 INCOMING MATERIAL STUDY

Similar to sheet stretch forming, incoming material geometry and properties have a significant effect on the extrusion stretch forming process. Therefore, an attempt is now made to analyze variation in incoming material geometry and properties. First, specifications are summarized and discussed, and second, measurements of material properties are presented and discussed.

7.2.1 Material specifications

As in the sheet metal stretch forming chapter, the relevant portions of government and industry standards for extrusions are given here in order to get a sense of the possible ranges of material geometry and properties.

Material geometry

Length specifications require tolerances of ± 0.1875" for extrusions less than 12' long and ± 0.3125 for extrusions between 12' and 30' long (ANSI-H35.2.1985). For an 8' long part, this would be 0.1875/(12x8), or 0.20%, which is very little.

Thickness tolerances are specified to be ± 10%, but not less than ± 0.010" and not more than ± 0.060" (ANSI-H35.2.1985). This is very significant.

Angle tolerance specifications for leg thicknesses less than 0.187" are ± 2°, and for thicknesses 0.188-0.749" are ± 1.5° (ANSI-H35.2.1985). These are not applicable to material in the -O condition. This is significant.

Cross-sectional tolerances for dimensions which are at least 75% metal, for parts with a circumscribing circle diameter (CCD) of less than 10" are specified to be: ± 0.009" for 1/2-3/4" dimensions, ± 0.010" for 3/4-1" dimensions, ± 0.012" for 1-1 1/2" dimensions, ± 0.014" for 1 1/2-2" dimensions, and ± 0.024" for 2-3" dimensions (ANSI-H35.2.1985). For a part with a CCD of less than 10", a 1" dimension can vary 1%. This is borderline significant.

Flatness tolerances, the maximum deviation from a reference surface, are specified at 0.004" per inch of width, but not less than 0.004" (ANSI-H35.2.1985). These are not applicable to -O material.

Straightness tolerances, the allowable deviation from straight along length, are generally specified to be 0.0125" per foot length (ANSI-H35.2.1985). For a 10' long part, a bow of 0.125" at the middle would be acceptable.

Twist tolerances per foot are for the distance from the end to a flat surface, subtracting out deviation due to lack of straightness: for circumscribing circle diameter (CCD) < 1 1/2", 1" per foot in length, not to exceed 7" total; for 1 1/2" ≤ CCD < 3", 0.5" per foot in length, not to exceed 5" total ; for CCD ≥ 3", 0.25" per foot in length, not to exceed 3" total (ANSI-H35.2.1985). These are not applicable to -O material. For a 10' long extrusion with a CCD of 2", this would mean an allowable deviation at one end of 5" from twist alone. This is significant.

Material properties

Mechanical property specifications for all purchased 2024-O extrusions have been: YS ≤ 19 ksi, UTS ≤ 35 ksi, and elongation ≥ 12% (QQ-A-200/3F).

Mechanical property specifications for all purchased 7075-O extrusions have been: YS ≤ 24 ksi, UTS ≤ 40 ksi, and elongation ≥ 10% (QQ-A-200/11E).

Both of the above specifications canceled on April 21, 1995 and replaced by the American Society for Testing and Materials (ASTM) specification B221, "Aluminum and Aluminum Alloy Extruded Bars, Rods, Shapes and Tubes."

Grain size is a significant determinant of strength, hardening characteristics, and surface finish. Alloys can be specified according to special microstructure requirements. Chemical composition is also specified and can influence the material's mechanical properties, response to heat treat, and corrosion properties.

7.2.2 Other sources of information about incoming extrusions

Length measurements of a number of incoming extrusions were made as part of the extrusion measurements. These revealed that, while initial lengths were nearly always within 0.010" of the nominal dimension, there were some exceptions: a couple of parts in one lot differed from the nominal dimension in increments of inches—specifically, of 14 parts in the lot, 8 were at nominal, three were 1" too long, two were 2" too long, and one was 3" too long. The operator probably could reject the parts which were too long because they were out of specification.

Thickness measurements for two lots of part showed three standard deviations of thickness over nominal thickness ratios of 1.6% for a 0.200" thick part and 4.4% for a 0.076" thick part. Angle measurements on two lots showed no variation in angle.

Conversation with operators reveal that an important source of variation for thin extrusion-type parts made from brake formed or roll formed sheet are the widths, heights, and angles of the legs. These affect widths, angles, and flatness of the part.

Analysis of data from four lots of extrusion certification sheets for one extrusion P/N showed similar property variation to that found in sheet metal.

7.2.3 Summary and conclusions to incoming material study

Specifications permit significant variation in material thickness, angles, twist, and stress-strain properties. However, it appears that actual parts are manufactured to tighter tolerances than given in the specifications. Still, length and thickness variations are significant. Property variations are probably similar to those of sheet metal, with yield strength and ultimate tensile strength varying about 2-6% of the average.

7.3 HEAT TREAT OPERATION STUDY

The heat treat operation for extrusions is essentially the same as that for sheet, except that the racking is a bit different.

Proper racking of extrusions is necessary to avoid excessive warpage upon quench. Parts should be arranged, properly spaced, and fixed in location by wire in order to enable good flow of quenchant, allowing the parts to cool more evenly. Photographs of proper racking of typical parts are provided for the heat treat operators. Straight extrusions are racked so that they lie in the basket at roughly 30°. According to specifications, parts should be separated by no less than 1" from one another. Although better racking takes more time, the reduction in warpage that results warrants it due to the time saved not only in locating the part in the tooling during the subsequent stretch forming operation, but also in the amount of hand work required after stretch forming. Thinner parts warp more than thicker parts.

At Vought, extrusions that are too long for the salt vat and quench tank are solution heat treated in a "drop bottom" air furnace. Heating of the part in air is, of course, much slower than in molten salt, and it would be expected that it is also a bit less even. As a matter of focus, the drop bottom furnace was not investigated.

Since most extrusions formed are 7075, the effect of time at room temperature for -W material is less than for most sheet, which is mostly 2024. The reader is referred to the heat treat designed experiment and study in previous chapter for more information; most of what is said there about sheet metal applies equally well to extrusions.

7.4 EXTRUSION STRETCH FORMING OPERATION STUDY

The extrusion stretch forming operation addressed here is the stretch wrap operation, in which the material is first stretched and then wrapped around a die under generally constant tensile force. The following diagram shows the steps in this operation.

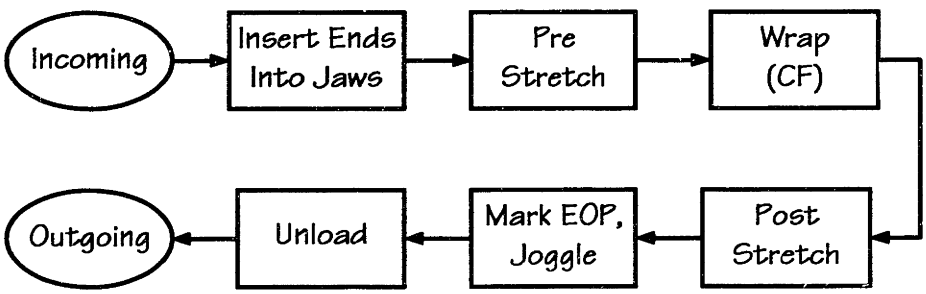

Figure 7.2 Extrusion stretch forming operation flow diagram

7.4.1 Description of the operation

Incoming material

Critical incoming dimensions of an extrusion are thickness, angles, and, to a lesser extent, length. The most important material property is its stress-strain relationship.

If the part has already been stretched once, then the amount of stretch and the contour imparted in the previous stretch-wrap operation are very important. Material that has been heat treated will be warped to some extent; this affects the effective strains and the stresses in the material. A more warped part must be stretched more in order to eliminate the warpage.

Stretch press diagram

The following diagram shows a top view of a typical "swing arm" extrusion stretch forming press.

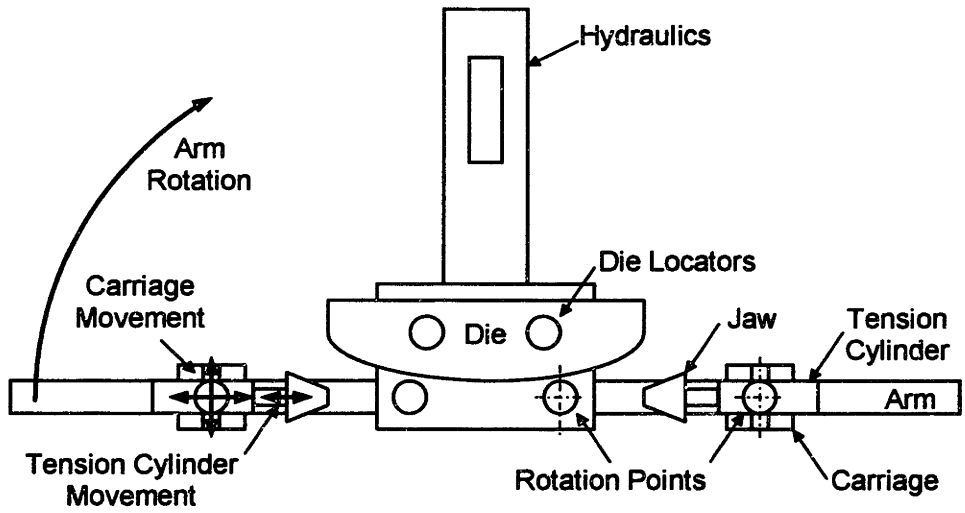

Figure 7.3 Typical swing arm extrusion stretch forming press

The following diagram shows top and front views of the die, part, and jaws at some point in the wrap.

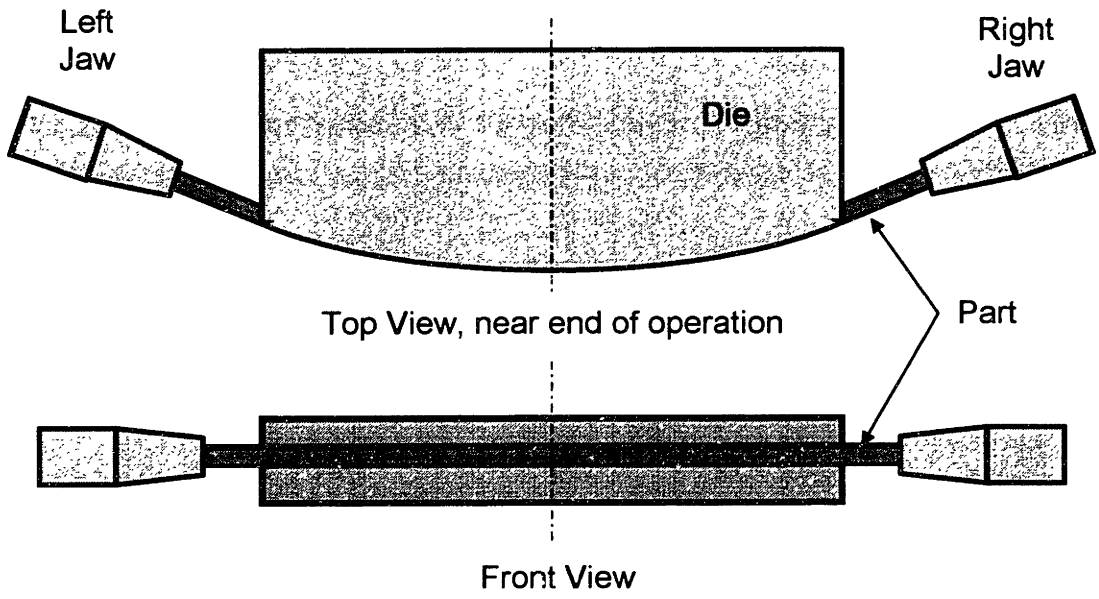

Figure 7.4 Top and front views of extrusion stretch forming die, part, and jaws

Insert into jaws

Inserting the ends of the extrusion into the jaws is straightforward. If the part has been solution heat treated in house, fitting the extrusion into the die and jaws may be difficult due to warpage.

Pre stretch

In this step, the part is given an initial stretch without (further) bending. The important setting, the amount of strain imposed on the part, is determined either by displacement, force or pressure, or sight (on some of the older machines). If there is any slippage in the jaws, most of it will occur at this point. The target pre stretch strain normally varies from just over yielding (the initiation of plastic deformation) to1% or 2%.

Wrap

Machine

In this step, the material is wrapped around the die. Depending on how the part is first "learned" by the machine, the wrap may be essentially under constant force control or the force may vary so that some line running along the length of the part undergoes no strain. Even when the constant force trajectory has been learned, subsequent parts are generally wrapped using a "lookup table" of swing arm angle and tension cylinder position, instead of in force control mode. Because it is at this point that the part comes into contact with the die, the alignment of the jaws horizontally and vertically relative to

the position of the die is very important at this stage. The carriage position, tension cylinders extension, and arm rotation are the critical machine movements. Often, in order to prevent leg angle changes or for other reasons, clamps or blocks are placed on the part and die as the part is being wrapped. These affect the frictional forces.

The ability of the operator to repeatably set and the ability of the machine to repeatably achieve the same ending wrap angle depend on the age of the machine. On older machines, the ending wrap angle is set by a screw mechanism (and the operator finds the correct angle visually), while on newer machines, the desired angle is stored electronically.

The ability of the machine to achieve a desired force when force control is used is also important. When hydraulic pressure is used to estimate force (which is generally the case) and the machine is moving, the movement will affect the estimate. Temperature, leakage, and machine movement friction also affects the estimate.

Die

The alignment of the die relative to the jaws and the point of rotation of the arms is very important. Die contour tolerances are around ± 0.005" on contour and ± 1/4° on angles—generally 1/3 of the part tolerances. Whether or not a die is springback compensated will have an effect on the part contour and on the amount of stretch needed to get the part contour within tolerances. Further, how well a die is springback compensated will have an effect on the nominal part shape.

Generally, the die is very liberally lubricated before each part is put on the die, so that there's never any lack of lubrication on the die. Lubrication is very important to reduce the effect of friction.

Dies wear. Given the age of some of the programs for which parts are built, dimensional changes over the years may be significant. Generally, die contour is not inspected unless there is a complaint that there may be a problem with it—thorough die inspection would take about a day. However, it is possible and probable that slow die shape changes are not noticed, and dies may be out of contour.

Post stretch

In this step, the tension cylinders are used to give the part a post stretch. The amount of stretch given is generally specified as either a displacement or a strain, which must be translated into a displacement.

On newer machines, the amount of post stretch force or displacement is entered and controlled electronically. On older machines, this is done visually. One method used is to mark the part with a felt tip marker and pull until the mark moves the desired distance. This is probably the easiest and an effective means of strain control.

Mark EOP and joggle

The end of the part (EOP) is scribed or marked in some other manner at this point, and a joggle may be made. This step was not studied.

Unload

The jaws are unclamped and the part is removed. Depending on how tightly the part is stuck in the die and how thin the part is, it may be possible to plastically deform the part while removing it from the die.

Outgoing material

The important material geometry outputs from this operation are contour, flatness, angles, and thickness.

Settings

Paper extrusion stretch setup sheets record the recommended machine settings. The machine hydraulic fluid pressures, low and high are given. If the stretches are force controlled, forces are given, while if they are displacement controlled, strains or displacements are given. Wrap angles are also specified. Some die setup instructions are included as well. Comments regarding the use of snakes, clamps, and blocks, and joggling are also given in the setup sheets. However, instructions on setup sheets are not always followed.

While numerical quantities for stretch are given, it is questionable whether these are in fact followed closely, since most operators make decisions according to their experience. How the numerical quantities were derived and agreed upon is also unclear. For example, specified post stretches for final wraps (both with a preform) range from a low of about 0.32% to a high of about 5.88%. Most post stretches are specified to be between 1.5% and 3.5%.

Assumedly, information contained in a machine program is more closely adhered to, although it may be changed by the operator.

Number of stretch-wraps

A little over half of the extrusions stretch formed at Vought are stretched only once, while a little under half are stretched twice, based on a survey of a little over 200 set up sheets.

7.4.2 Introduction to the extrusion stretch forming measurements

The objective of these measurements is to get a better understanding of variation, where it comes from, and which process parameters are correlated and how. For the most part, only the part (and not the machine) was measured.[44]

Part measurements were made initially (before any stretching), after pre stretch, after final stretch, and after rout on features that were thought to give an indication of the state of the part.

Measurements were performed on four lots. P/N A was a thick, T-shaped extrusion with a considerable amount of curvature imparted during the stretch forming operation; the top of the "T" was on the inside of the part. P/N B was a Z-shaped extrusion also with considerable curvature. P/N C was a T-shaped extrusion with very little curvature; the top of the "T" was on the inside. P/N D was a T-shaped extrusion with a very sharp bend in the middle, giving a bend angle of roughly 140°; the top of the "T" was on the outside. The part was given two pre forms, and the leg of the "T" was cut out at the bend between the first and second pre forms.

7.4.3 Measurements and calculations made

The measurements and the calculations made from them are now described. A generic part with a typical part contour is shown in the following diagram to indicate where the measurements were made.

---

[44] A more in-depth study was planned, but due to a number of complications and difficulty in getting data, this plan was not pursued.

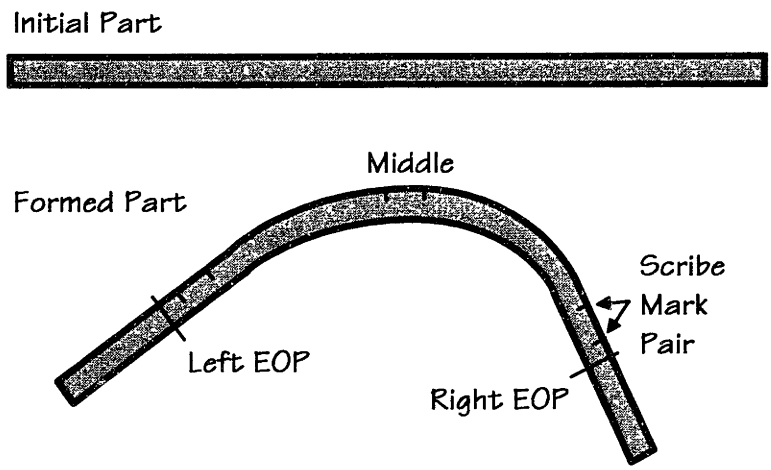

Figure 7.5 Diagram of extrusion before and after stretch wrap forming

As the diagram shows, scribe mark pairs were made in three locations, near each EOP and in the middle. According to the person who made the measurements, distances were measured to the nearest 0.010" and angles to the nearest 1/2°.

Contour deviation is defined as the deviation of the part contour from the template (used to measure part contour) at EOP. The middle of the part touches the template, and the equal distance between each EOP and the template is the contour deviation.

The following table lists the details of all the measurements made and what, if anything, they were used to calculate. Not all measurements were made on all parts.

What measured	Where measured	When measured: after ...	Used to calculate
Length	end to end	initial, pre, final	strain
Scribe marks	L&R EOP, middle	pre, final	strain
Thickness	L&R EOP, middle	initial, pre, final	strain
Conductivity	L&R EOP, middle	initial, pre, final	
Texture	overall	pre, final	
Contour deviation	L&R EOP	pre, final, rout	
Flatness	L&R EOP, middle	pre, final, rout	
Leg angle	L&R EOP, middle	initial, pre, final, rout	

Table 7.16 Location, timing, and use of measurements on extrusions

7.4.4 Presentation and discussion of data

Initial length

For P/N A, of 14 parts, 8 were 132" long, 3 were 133" long, 2 were 134" long, and 1 was 135" long. These varying initial lengths impacted subsequent strain and lengths. The following table summarizes the specified and actual initial part lengths.

P/N	Specified Length	Actual Length Average	Percent Off	Standard Deviation
A	121.2"	132.7"	9.5%	1.00"
B	119.0"	120.1"	0.9%	0.00"
C	39.0"	39.05"	0.1%	0.00"
D	48.0"	48.0"	0.0%	0.00"

Table 7.17 Specified and actual part lengths

Except for P/N A, there was no variation of part length within a lot, although the averages were slightly off.

Conductivity

Initial 2024-O conductivity for P/N A averaged 46.7% IACS; in the -W condition it averaged 30.0% IACS. Initial 7075-0 conductivity for P/N B averaged 47.9% IACS; in the -W condition it averaged 28.8% IACS. Conductivity before and after heat treat showed no correlation for individual pieces. Conductivity also showed no correlation to any other measured or calculated parameter.

Average strain

For P/Ns A and B, the two lots on which thickness measurements were made, thickness strain was not well correlated with longitudinal strain measured by scribe marks. However, there was a relatively good correlation between strain measured by length and by scribe marks, and between strain at the ends and strain in the middle measured by scribe marks, though they were not the same.

The following table shows the average strains as measured by overall part length, EOP scribe marks, and middle scribe mark(s), after pre and final stretches, for each lot. The numbers in parentheses for P/N A are without the one part that was pulled 11% in the pre stretch.

P/N Label	Method	After Pre	After Final	Additional
A	Length	3.90% (3.34%)	6.59% (6.04%)	2.53% (2.54%)
	EOP Scribe	4.21% (3.96)	6.92% (6.43%)	2.64% (2.38%)
	Middle Scribe	5.70% (5.38%)	8.41% (7.81%)	2.56% (2.30%)
B	Length	0.36%	1.30%	0.92%
	EOP Scribe	2.44%	3.58%	1.11%
	Middle Scribe	2.39%	2.90%	0.50%
C	Length	2.43%	3.33%	0.87%
	EOP Scribe	7.50%	10.00%	2.33%
	Middle Scribe	10.00%	12.25%	2.27%
D	Length	2.31%	3.75%	1.39%
	EOP Scribe	2.50%	3.48%	0.96%
	Middle Scribe	3.37%	6.73%	3.26%

Table 7.18 Average strain measurements for each lot of material

For all four P/Ns, the strains after pre measured by length are always less than those measured by the scribes. The probable reason for this is that the scribe strains are at the outside of the part and contain bending and stretching strains, while the length is measured on the inside for P/Ns A, B, and C. The additional strain for P/N A is roughly the same regardless of how it was measured, suggesting an even strain throughout the part. For P/N B, the additional length strain was between the EOP and middle scribes, suggesting that friction reduced strain in the middle. For P/N C the additional length strain was much less than the scribe strains, and it is unclear why, given that the part had little curvature. For P/N D, the additional middle scribe strain was the largest because the leg of the T was removed from this area, giving it a smaller cross-section.

The following table gives an indication of variation in the amount of stretch by giving the standard deviation of the strains within each lot, in the same manner as the averages were found for the above table. Again, the numbers in parentheses for P/N A are without the one part that was pulled 11% on the pre stretch.

P/N Label	Method	After Pre	After Final	Additional
A	Length	2.27% (0.96%)	2.08% (0.36%)	0.76% (0.79%)
	EOP Scribe	1.19% (0.75%)	2.07% (0.57%)	1.10% (0.57%)
	Middle Scribe	1.41% (0.81%)	2.35% (0.71%)	1.12% (0.63%)
B	Length	0.04%	0.29%	0.28%
	EOP Scribe	0.22%	0.47%	0.48%
	Middle Scribe	0.43%	0.26%	0.48%
C	Length	0.00%	0.00%	0.00%
	EOP Scribe	0.00%	0.00%	0.00%
	Middle Scribe	0.00%	0.00%	0.00%
D	Length	0.43%	0.42%	0.59%
	EOP Scribe	0.38%	0.32%	0.50%
	Middle Scribe	0.63%	0.75%	0.50%

Table 7.19 Variation in strain measurements for each lot of material

This table shows significant differences in variation among the parts; generally one standard deviation is between 10% and 20% of the average strain. Note that in the table the % sign indicates percent strain, not the standard deviation divided by the average (which would also have a percent sign).

Within part strain

The relationships between end and middle strains for P/N A are shown in the following chart.

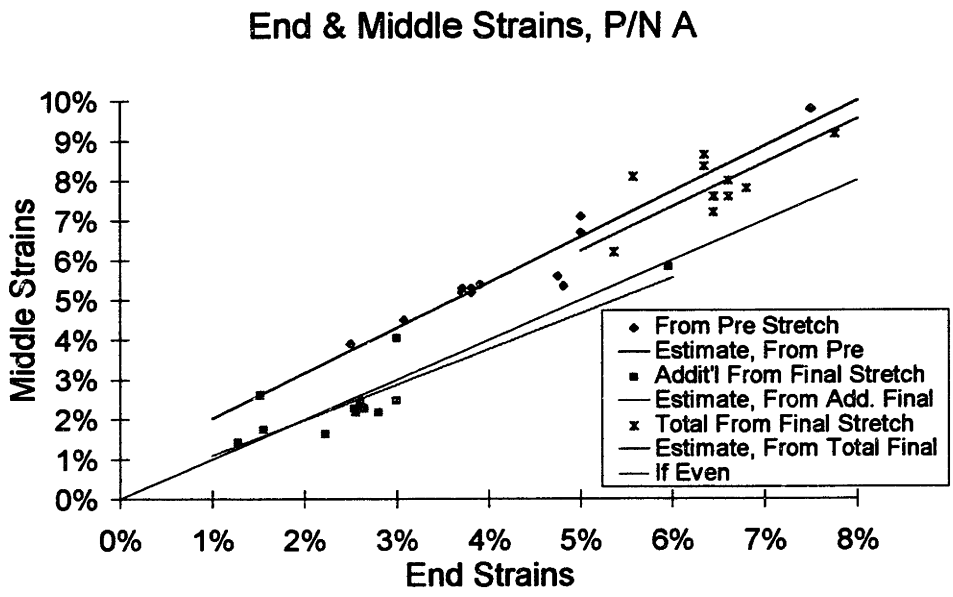

Figure 7.6 End and middle strains for P/N A

The chart shows that the middle strains are consistently higher than the EOP strains after pre stretch; this is due to there being more curvature in the middle than the ends. The amount of additional stretch given by the final stretch is essentially the same in the middle and at the ends; this is because no more curvature is added in the middle, and the effect of friction appears to be negligible.

The chart also shows relatively strong correlations between strain at EOP and strains in middle of the part. The r^2 values for the three correlations for which there are estimates in the chart are: $r^2 = 0.923$ for after pre, $r^2 = 0.945$ for after final, and $r^2 = 0.774$ for additional.

While not shown in the diagram, both of the EOP strains for each part in a given lot were always exactly the same, indicating that the part was stretched the same amount at both ends.

For P/N A, there is also a strong correlation between the amount of pre strain and additional strain: the greater the pre strain, the smaller the additional strain. This relationship is shown in the following chart.

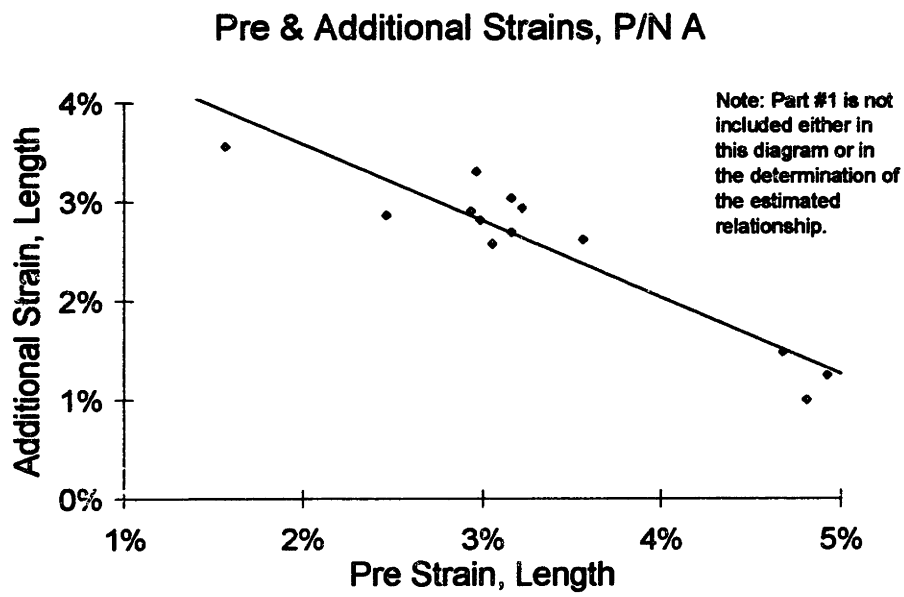

Figure 7.7 Pre and additional strain, P/N A

The r^2 value for this relationship is 0.877. The same trend is found in P/N D.

Texture

Surprisingly, except for the one part which was stretched about 11%, there appeared to be no correlation between strain after pre stretch and intensity of the surface texture (from Orange Peel and/or Lüdering) for P/N A. The surface texture didn't change noticeably after the initial stretch. The other lots had no noticeable surface texture.

Contour

Contour measurements on P/N A were not made in such a way that any useful information could be gained from them. Contour measurements for P/N C were the same from one part to the next. The after pre contour deviation was 0.50", the after final contour deviation was 0.05", and the after rout contour deviation was 0.06". Therefore, the part opened up 0.01" as a result of routing—this part was routed on the outside. Because P/N D received routing and hand work, its contour measurements don't provide any insight.

For P/N B, there appears to be no correlation between contour deviation and any of the strains. However, there is a very strong relationship between contour after final stretch and after rout, as shown in the following chart.

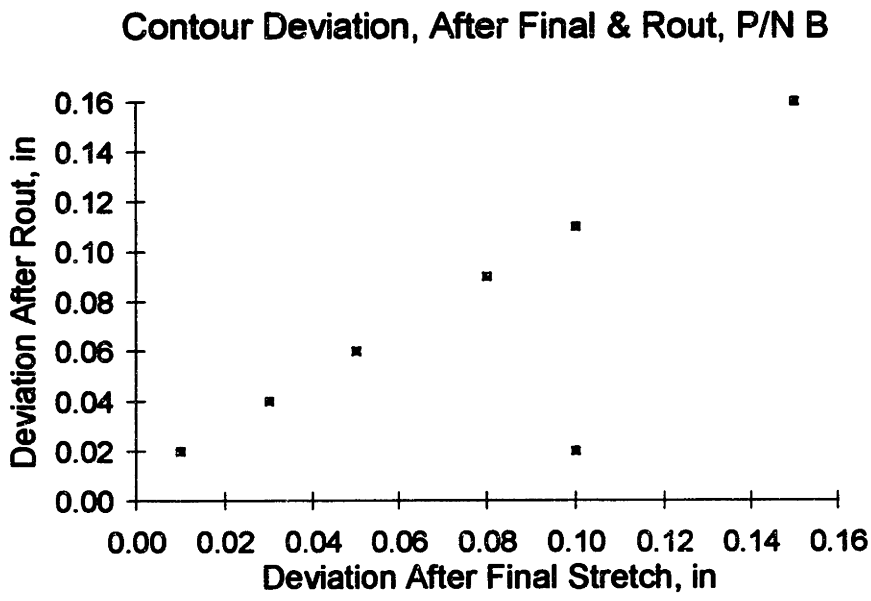

Figure 7.8 Contour deviation after final stretch and after rout, P/N B

Apart from one data point, the data lie on a line with a slope of 1 and an offset of 0.010", which means that the effect of the rout is to predictably increase the contour deviation by 0.010". It is very likely that the only reason the single data point is off is because of a decimal point mistake made by the person measuring the part: if the deviation after final stretch were 0.010" instead of 0.100", all the points would lie exactly on the same line. This will be assumed to be the case for further discussion of the data. For P/N B the pre stretches were all the same, except for the third part (not the one off above). This may be part of the reason these data are so well correlated.

The relationship between strain and final contour deviation for P/N B is somewhat enigmatic, as shown in the following diagram.

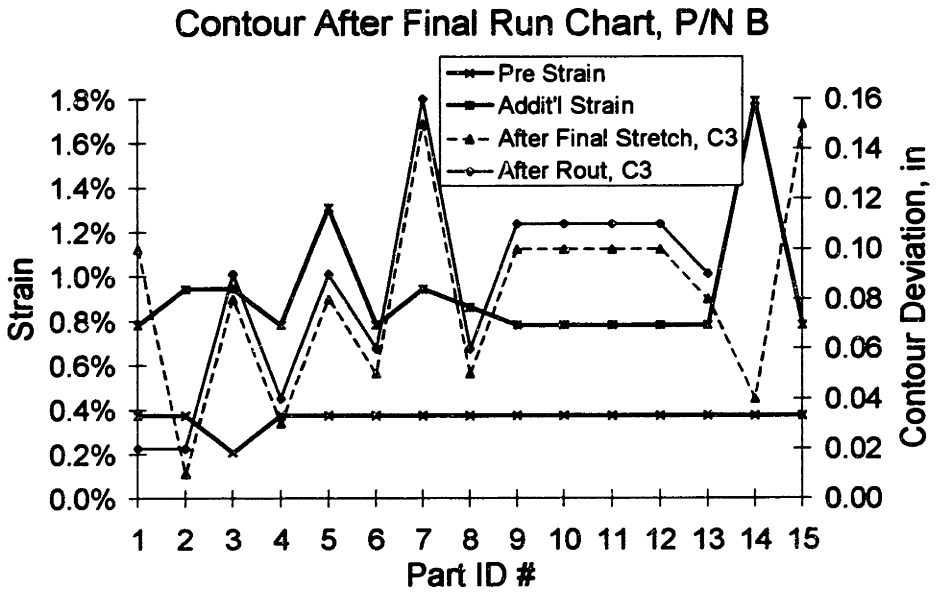

Figure 7.9 Run chart of strain and contour, P/N B

For part ID #s 1 to 9 (assuming, as already mentioned, that part ID #1 has an after final contour deviation of 0.010") there appears to be a positive correlation between additional strain and contour deviation, but the relationship seems to be the opposite for part ID #s 10 to 15. Evidently, other factors enter into the relationship which significantly affect the final contour. Since the contour deviation was exactly the same for all P/N B parts after pre stretch, it is impossible to assess the effect of initial contour on final contour.

Contour variation was also calculated. The following table gives the average and one standard deviation of the contour deviation after pre, after final, and after rout.

P/N Label	What	After Pre	After Final	After Rout
B	Average	0.85"	0.075"	0.082"
	Standard Dev.	0.00"	0.044"	0.041"
C	Average	0.50"	0.050"	0.06"
	Standard Dev.	0.00"	0.00"	0.00"
D	Average	2.40"	0.00"	
	Standard Dev.	0.00"	0.00"	

Table 7.20 One standard deviation of contour deviation after pre, final, and rout

For P/Ns B and C, the average contour deviation is reduced by about a factor of 10 between after pre and after final. According to the measurements, only P/N B had variation in the contour. For P/N D, contour deviation was eliminated, but this was with hand work. Unfortunately, variation in the date from one lot to the next is too great and there are too little data to draw any conclusions.

Angle

Angle was not measured on P/N A, and the angles on P/Ns C and D didn't change noticeably. For P/N B, although the angle varied from part to part, it was always the same within each part at all three measured points. Because the pre wrap stretch was so consistent, there was no opportunity to establish a relationship between strain and angle. There appears to be no correlation between the angle after pre stretch and after final stretch or rout (the angles didn't change between after final stretch and after rout). However, there appears to be a relationship between the final stretch and angle. The following chart shows the relationship between angle and the final strain for P/N B.

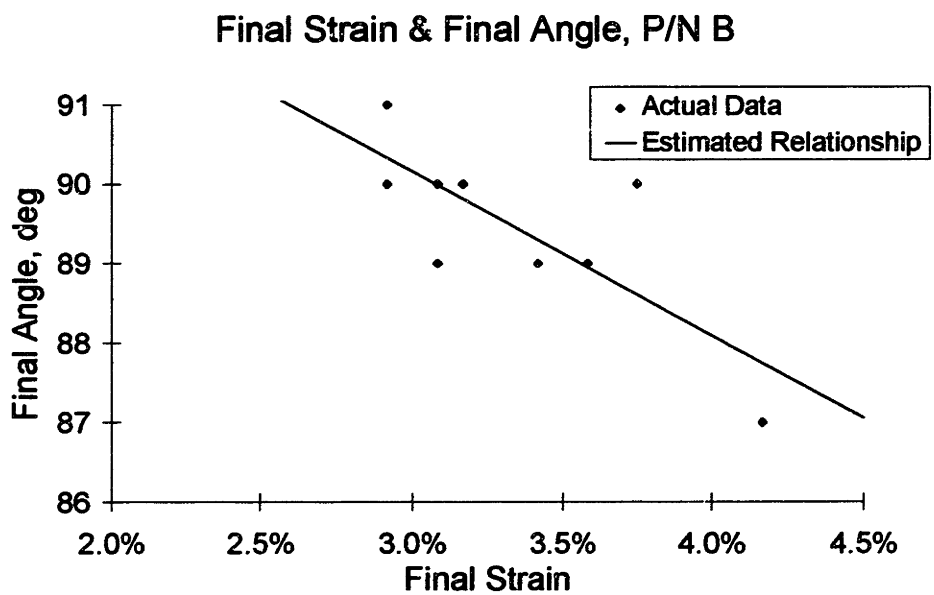

Figure 7.10 Correlation between final strain and angle, P/N B

The r^2 value for this relationship is 0.634—not too strong, due to other factors influencing the outcome. The equation for the line is:

$$\text{Angle} = -2.07 \times \text{Strain} + 96.37 \qquad (7.1)$$

The above equation could be used to select the strain needed to achieve a 90° angle. In this situation, a strain of 3.08% would give an expected angle of 90°.

There appears to be no correlation between contour deviation and angle, after final and after rout.

7.4.5 Part gripping

Variation of grip location

Extrusions are not always gripped repeatably, with regard to how much of the extrusion is in the jaw. In order to get an idea of this variation, the distance between the last gripper mark and the end of the part was measured on P/N A.

The following chart shows the distance between the last gripper mark closest to the end of the part and the end of the part for both the long and short ends, and a three level qualitative indication of the amount of slip at the long end (even the high level of slip was not very significant); there was no noticeable slip at the short end. Note that the terms long end and short end refer to the length of straight leg at either end of the part.

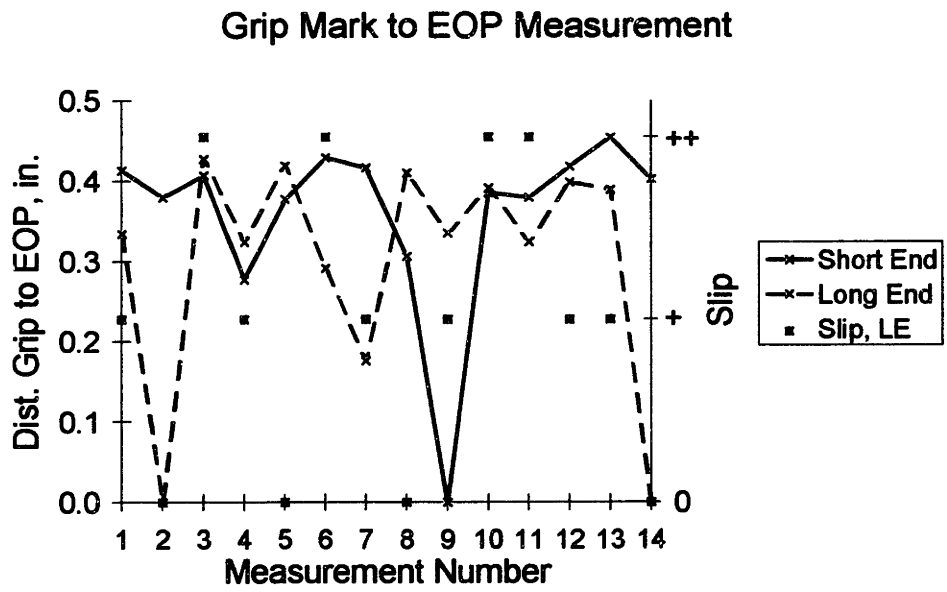

Figure 7.11 Distance between last gripper mark and end of part, P/N A

As is evident from the chart, there is no correlation between the distances at the ends; there is also no correlation between distance at the long end and slippage at the long end. The standard deviation of the distance at the short end was 0.11", while at the long end it was 0.14"—the sum has a standard deviation of 0.17". These give three

standard deviations of 0.33", 0.42", and 0.51", respectively. To have an idea of the effect that this would have on a part, a part ideally initially 25 inches long (between grips) stretched in theory 2.00% would only be stretched 1.96%, a decrease of only 0.04% strain, which is 2% of the desired strain. Clearly, this effect is insignificant.

Other gripper sources of variation

Material gripping can contribute in a number of ways to variation. Three additional sources of variation were identified when the author spent time working with a swing-arm type extrusion stretch forming machine at Northrop Grumman in Bethpage, New York. Four potential sources of variation were noticed:

1. As the jaws close on the material, they are pushed forward, maybe 1/2" to 1" per jaw; this may cause the part to bend some if the jaws don't move back.
2. As the jaws close, they may rotate in one or both of two ways as shown in the following diagram, causing twist or uneven strains from top to bottom in the part.

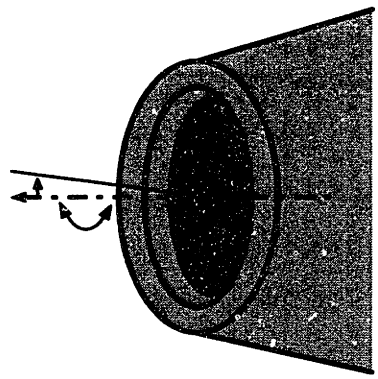

Figure 7.12 Diagram of jaw showing possible rotation caused by closing jaws

3. As tension is applied to the cylinders, the jaws slip out a little bit, together, possibly about 0.050". For a 25" long part, 0.050" on each jaw works out to 0.4%, which is significant at low strains, and which will impact the operation if it is displacement-controlled.

It's difficult to assess the effect of each of these potential sources of variation, but it is likely that each can cause some amount of variation. Note that gripping mechanisms are similar for most brands of extrusion (swing arm) stretch forming presses, so that these findings are applicable to most presses, especially older ones.

7.4.6 Observations on rework in check and straighten

The amount of time a lot of parts spends in check and straighten can vary from half an hour to a whole week. According to one source, the top three problems, in order, in check and straighten for stretch-formed extrusions are

1. Leg angle
2. Contour
3. Bow & twist (these have to do with flatness)

The three are somewhat interrelated. Changing bow and twist, probably won't affect the contour, but changing contour or leg angle will affect bow and twist.

As discussed in Chapter 3, there is no agreement on whether the primary cause of hand work is lack of precision or lack of accuracy. Both must be addressed.

Some parts are check and straightened beyond the specified requirements in order to make it easier for assembly to do their work.

7.4.7 Summary of extrusion variation and sources of variation

Unfortunately, the data set is quite small, and doesn't reflect all possible variations and sources of variation. With this caveat in mind, an effort is made to summarize what has been learned from the measurements and from discussions with people knowledgeable about the operation.

Incoming material geometry and properties

Incoming material thickness and angles were very consistent. The lengths of three out of four lots were very consistent, while in the fourth there was significant variation. While actual variation was not documented, both operators and engineers assert that incoming material properties vary significantly.

Changes in material properties due to aging do not appear to occur between pulling parts out of the freezer and stretching because parts are taken out one-at-a-time and placed directly on the machine for stretching.

The most significant source of variation in material geometry appears to be warpage caused by the heat treat operation. This source of variation was not measured, but it is universally agreed among those familiar with the stretch forming operation (and this has been confirmed by at least one study in the industry) that this is one of the primary sources of variation in the extrusion stretch forming operation.

Die alignment

While die alignment was not investigated, a passing comment made by a knowledgeable individual on the shop floor implied that tooling alignment is not well controlled. This was confirmed by casual observation. The variation added by tooling

alignment which would affect different lots of the same P/N formed at different times does not show up in the current study which concerns only variation within a lot.

Machine movement

On newer machines, machine movement is very repeatable, whereas on older machines it is much less repeatable and is likely to be a significant source of variation.

Die geometry

There is no clear agreement on how often die geometry is the cause of variation. Over the short term, die geometry does not wear significantly. Unless the die contour is perfectly adjusted to compensate for springback—this would require foreknowledge of parameters of the operation, in particular strain, and how they affect springback—it will always cause the part contour to differ from the desired contour.

Clamping and joggling

Clamping was not studied, but it can have a significant effect on the operation. How, when, where , and with what force an operator applies clamping initially or as the part is being stretch formed can significantly affect angles, flatness, and even contour (the latter by affecting frictional forces which affect the amount of strain in the part). Joggling significantly affects the contour, but was not studied.

Friction

Due to the small sample size, the effect of friction was difficult to separate out from other effects.

Settings

The most important settings are those specifying the alignment of the die and jaws, the positions and movements of the carriages, tension cylinders, the arm angles, and the stretch profile. None of these was studied, largely due to difficulty in getting this data.

Variation

The data are inconclusive about the variation in contour and angle. Strain was found to vary significantly within a part, within a lot, and from lot to another. While the correlation between stain and contour deviation could not be established, but there was evidence of a correlation between strain and angle on the one part where there was noticeable angle change. The change in contour resulting from routing appears to be consistent from part to part within a lot, and of a magnitude of 0.010".

7.4.8 Proposed improvements

Based on the above findings, some improvements are proposed. The improvements fall into the same two categories as the improvements for the stretch forming operation:

1. Repeatably achieve optimized settings
2. Control of the operation

These are now addressed.

Repeatably achieve optimized settings

Many settings affect the operation. The optimal value of each should be determined, recorded, and consulted, and the desired settings should be consistently achieved. The most important settings that need to be optimized and repeatably achieved are the die and machine settings.

Die

The die position needs to be consistent from one setup to the next. Setups must be optimized, specified, and repeated from lot to lot. Use of setup cards can help in this task. A scheme for quick, precise location of the die would be very useful.

Die contour optimization is a difficult issue, and requires further investigation. The question to be answered is: when the setup is repeatable, and the warpage from heat treat is minimized, what combination of die contour and stretch profile will give parts that are dimensionally correct on average and repeatable?

Machine settings

Optimal settings for the wrap angle and stretches should be determined by some combination of theory, experience, and measurement, including strain measurement. The critical machine settings are initial and final wrap angle, initial tension cylinder and carriage positions, and target displacements or forces. On older machines, hydraulic pressure is very important. If strain control is used, then the desired strain should be optimized.

Control of the operation

Control of the operation encompasses two issues. First, the type of controller (NC or manual), and second control of the stretches, including strain control.

Machine

Stretch wrap forming presses are either manually- or NC-controlled. Unless some form of visual strain control is used, the amount of stretch on manually controlled machines is controlled by hydraulic pressure, which is subject to significant uncertainty and is a poor form of force control, a poor form of control. A move towards NC control or strain control, which can be performed manually, is recommended. This is very important: a very simple, manual form of strain control, using the strain measurement devices can be used on old presses which does not necessitate NC control, but offers most of the benefit of NC control.

NC-controlled machines are likely to benefit from stain control, but this has not been tested. Jaw slippage will affect displacement control, but will not affect strain control, which makes strain control superior if jaw slippage is significant.

Strain control

The same strain control method suggested in the previous chapter for sheet stretch forming can also be of benefit to extrusion stretch forming. Since neither position (if it is even available) nor force (load) control is very good on older machines, the most significant improvement would be to apply strain control to the old machines. The most simple form of control would be to attach a strain measurement device to the part and have a large digital readout so that the operator can pull the part to a pre-determined strain. The points made in the previous chapter with regard to sheet stretch forming apply almost without change to extrusion stretch forming as well, and are not repeated.[45]

7.4.9 Summary and conclusions to extrusion stretch forming study

Measurements of four lots of parts revealed that while strain generally varied significantly within a part and a lot, almost no correlations between strain and angle or contour deviation existed. This leads to the conclusion that there are other, significant sources of variation. Contour deviation appears to be variable, and may be 0.120" (3σ) or more. Change in contour from rout appears to be consistent, around 0.010". The most significant sources of variation in the extrusion stretch forming operation are

---

[45] An interesting combination of force and displacement control is the yield point elongation method. During pre stretch, a stress-strain curve is generated, and when the yield point is detected, a displacement control is used to stretch the part a pre-determined amount after yield.

found among variation in the amount of strain imposed on the part, setup, warpage from heat treat, and machine movement (more for older machines). Precision could be improved by more consistent setups, reduction of warpage from heat treat, and more consistent stretching and wrapping, especially on older machines. Extrusion stretch forming is expected to benefit significantly from the use of strain or displacement control where force control is currently being used.

While the data are too limited to lead to any strong conclusions, they point to this as an area in which more investigation is warranted, and implementation of repeatably achieving optimized settings and strain control should be pursued.

7.5 ROUTING OPERATION STUDY

In this section, the routing operation is described, measurements made are described and reported, the findings are discussed, and sources of variation and suggested improvements are given.

7.5.1 Routing operation description

In the manual routing operation, excess material is cut off of the stretch formed extrusion using a Hand Router Fixture (HRF) to guide the routing tool. Lot sizes are usually 10 to 15 parts.

The following diagram shows the steps in the routing operation.

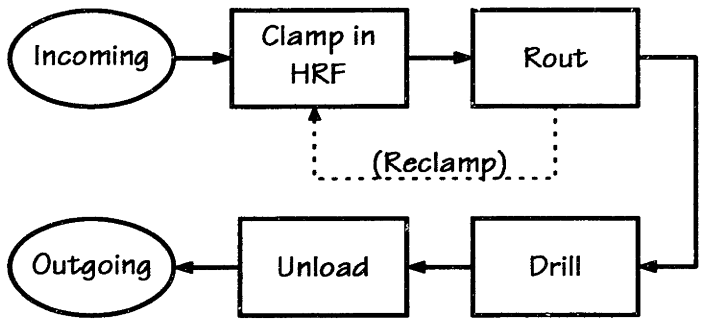

Figure 7.13 Routing operation flow diagram

The following diagram shows a cross-section view of a router in action.

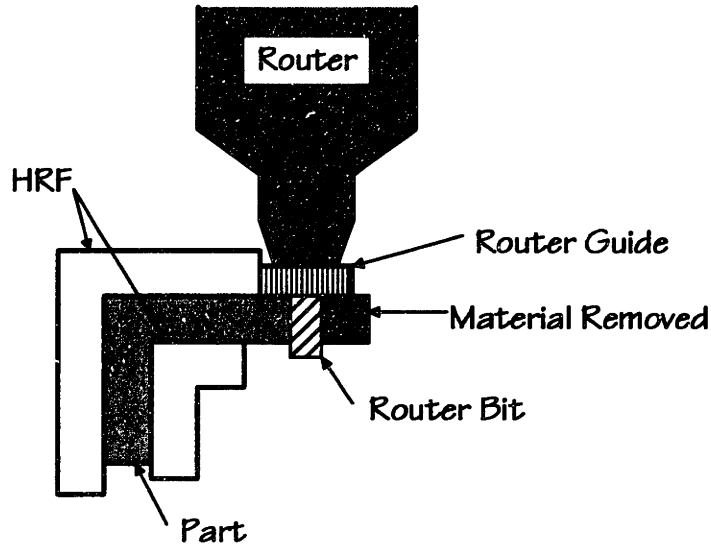

Figure 7.14 Router cutting material

Incoming material

The geometric key characteristics relevant to the routing operation are contour, leg angles, and possibly flatness. Other geometry characteristics can't vary enough to affect the routing operation. In order to fit better in the HRF, some parts are first check and straightened. The key property characteristic for routing is the residual stress distribution within the material. This determines how the contour changes in response to routing.

Clamp in HRF

A part is secured in the two halves of an HRF with clamps (for example, C clamps) positioned along the length of the part. Where and how strongly they are clamped, along with the deviation of the part contour from the HRF, will affect the seating of the part and the accuracy and precision of the operation.

Rout

Once the part is seated and clamped in the HRF, the three things that will affect the part dimension are (a) the router bit and router guide diameters, (b) the HRF dimension, (c) in-process re-clamping of the part, and (d) operator skill.

Drill

Once the part is seated and clamped in the HRF, the three things that will affect the part dimension are (a) the drill bit diameter, (b) the HRF—size and location of the hole, and whether or not it has a bushing, and (c) operator skill. Drilling was not studied.

Unclamp & remove

As the part is unclamped and removed, nothing significant can happen.

Outgoing

In addition to the incoming part characteristics, the important outputs of this operation are leg width, hole size and location, and EOP location. The contour will change because of the residual stresses in the removed material.

Settings

The only settings to speak of in this operation are for the router and the clamping. For the router, the router bit and guide diameters are specified, as is the router RPM. For the clamping, while it may be possible to specify clamping locations and sequence, specifying clamping force may be difficult.

Control

Since this is a manual operation, nearly all control is manual. Possibly the most significant opportunity for operator input is the angle at which the router is held, relative to the edge of the HRF; ideally, as shown in Figure 7.14, the cutter is parallel to the HRF edge.

7.5.2 Objective of the measurements

The objective of this set of measurements was to better understand variation and correlations in the manual routing operation, and to assess the effect of the operator.

7.5.3 What was measured

A number of measurements were made on the workpiece, routers, and templates used for the routing operation; other relevant information was also recorded. This was done for five lots, each of which was given a letter of the alphabet to represent its actual P/N. These parts are different from the parts measured in the previous section.

For each P/N, the 0.109" setback was measured at each end of part (EOP, L = left and R = right) and in the middle of the part for five parts. The offset is the distance between the edge of the HRF and the edge of the part, and it should be 0.109". As well, at both EOPs, detail measurements of the part and the Sample Part Template (SPT) were made for the same five parts. Router guides and cutter diameters were measured. In order to determine the effect of the operator, the 0.109" offset was measured at both

ends of two sets of three parts, each set routed by a different operator. The measurements made are shown in the following diagram.

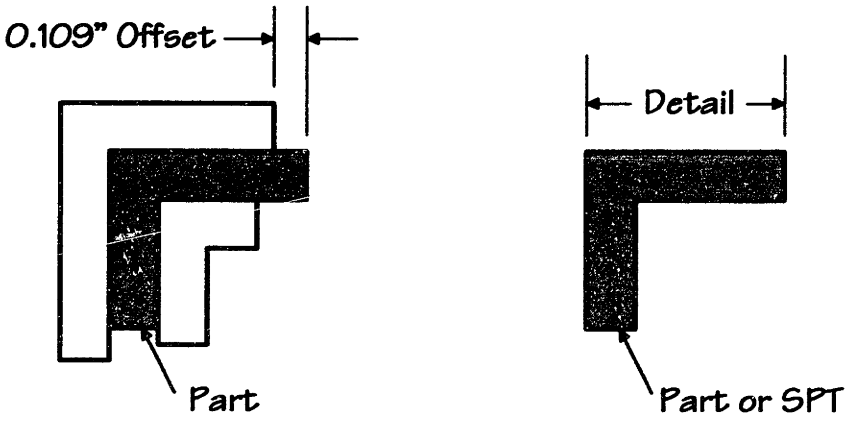

Figure 7.15 Offset and detail measurements

Averages of the measurements were made, and then the differences between these averages and the desired measurement were calculated in order to determine the error (since dimensions vary, error is used as a means of normalizing the data). For example,

$$\text{Error}(\text{offset L EOP}) = \text{Average}(\text{offset L EOP}) - 0.109. \qquad (7.2)$$

7.5.4 Results and discussion

Although limited in quantity and scope, the data gathered are quite revealing and suggest directions for further investigation.

Average errors and standard deviations

The following run chart shows the average errors for the five lots, according to what was measured and where.

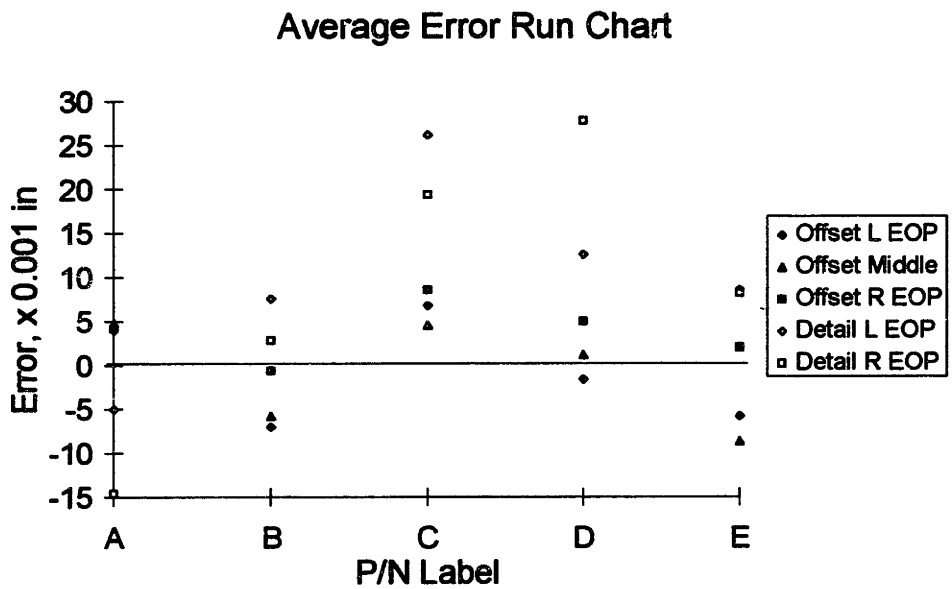

Figure 7.16 Average error run chart, for all lots

This chart shows a couple of interesting things. First, there appears to be a positive correlation between the average offsets errors and the detail part errors. It also shows that the offset errors are in the ± 0.010" range, while the detail errors are in the ± 0.030" range.

When all the sets of five offset measurements are taken together, the average error over all these measurements is 0.0008", which indicates that, regarding the offset, the operation is well centered. For the five sets of offset measurements: per location on each part, the average standard deviation is 0.0048" (that is, the standard deviation of the sample which consisted of a particular location on a particular P/N for each location on each of the five parts measured was found, and the standard deviations of each sample were averaged); for each part, the average standard deviation is 0.0055" (that is, the standard deviation of the sample which consisted of all locations on a particular P/N for each of the five parts measured was found, and the standard deviations of each sample were averaged), and for all measurements (the sample was all the measurements), the standard deviation is 0.0070". These numbers indicate the expected result that the variation increases as the amount of data considered increases—from each location on each part, to each part, to all parts.

When all the sets of five detail measurements are taken together, the average error over all these measurements is 0.0094", which indicates that on average the details

measure almost 0.010" more than desired. Since the offset is on target, the implication is that either the HRF, the sample part, or the location of the parts in the tool is adding about 0.0082" to the dimension. Again for the five sets of detail measurements: per location on each part, the average standard deviation is 0.0079"; for each part, the average standard deviation is 0.0088", and for all measurements, the standard deviation is 0.0094". These numbers also show the expected result that the variation increases as the amount of data considered increases. Further, the increase in variation from the offset measurements (of roughly 50%) is expected and indicates that variation is added between achieving the desired offset and achieving the desired detail dimension.

The following run chart shows the average standard deviations of the measurements by location on each part.

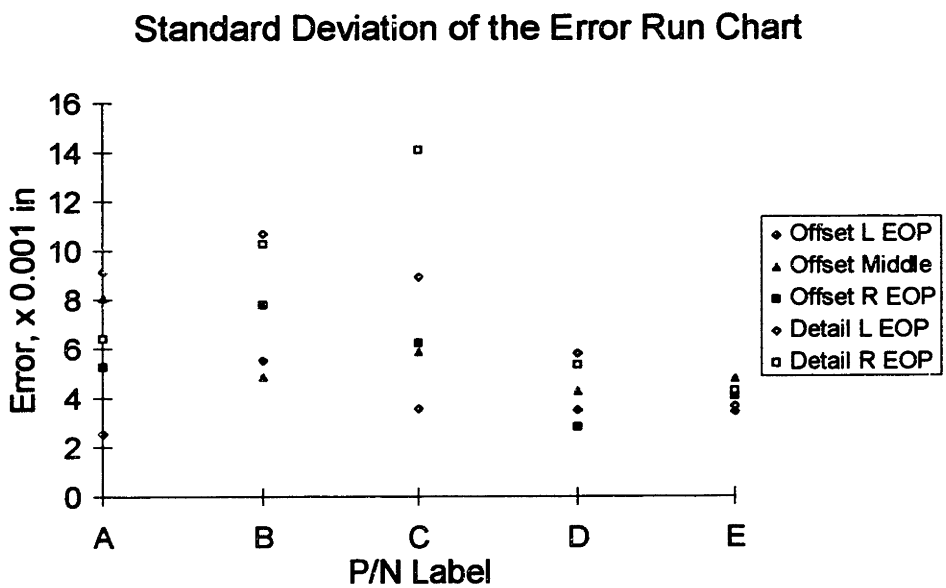

Figure 7.17 Standard deviation of the error run chart for all lots

The expected increase in standard deviation between the offset and the detail measurements is evident in this chart. As well, there appears to be no difference in standard deviation among the three offset locations measured and between the two detail locations measured.

Effect of operator

Two operators were used in this portion of the measurements. The same operator was Operator #1 each time, and the same operator was Operator #2 each time. The

supervisor remarked that he chose two of his best operators for these measurements in order to eliminate skill level as a source of variation.

The following run chart shows the averages of the offset errors by P/N, location, and operator.

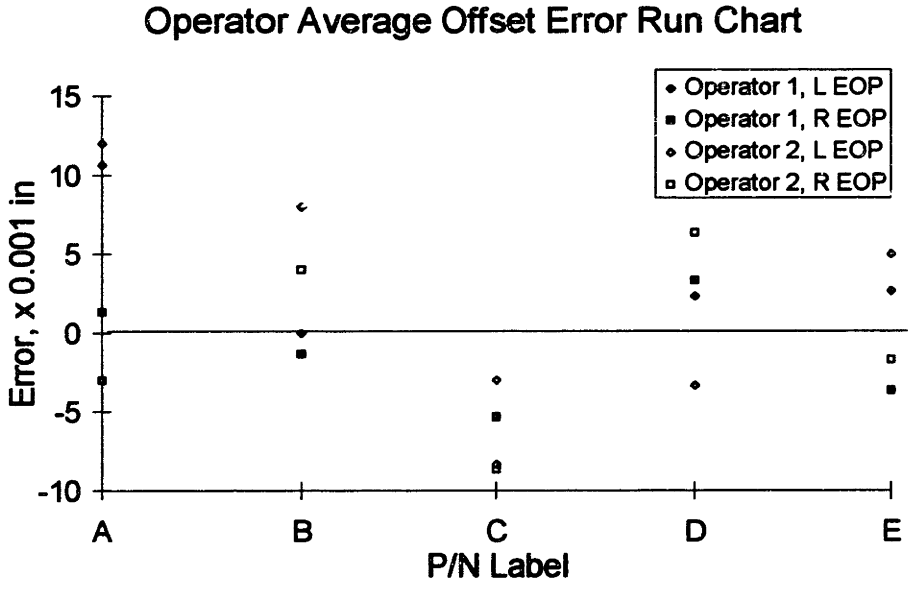

Figure 7.18 Operator average offset error run chart

The differences do not appear to be significant. No significant difference was found when comparing the standard deviations of the offset measurements either. It would be interesting to find out if the operator has an effect on the detail error, but these measurements were not made.

Relationship between offset error and detail error

There ought to be a relationship between the offset error and the detail error because the former significantly affects the latter. One would expect a positive correlation between the two. The following chart shows these errors for each P/N, plotting the detail error as a function of the offset error.

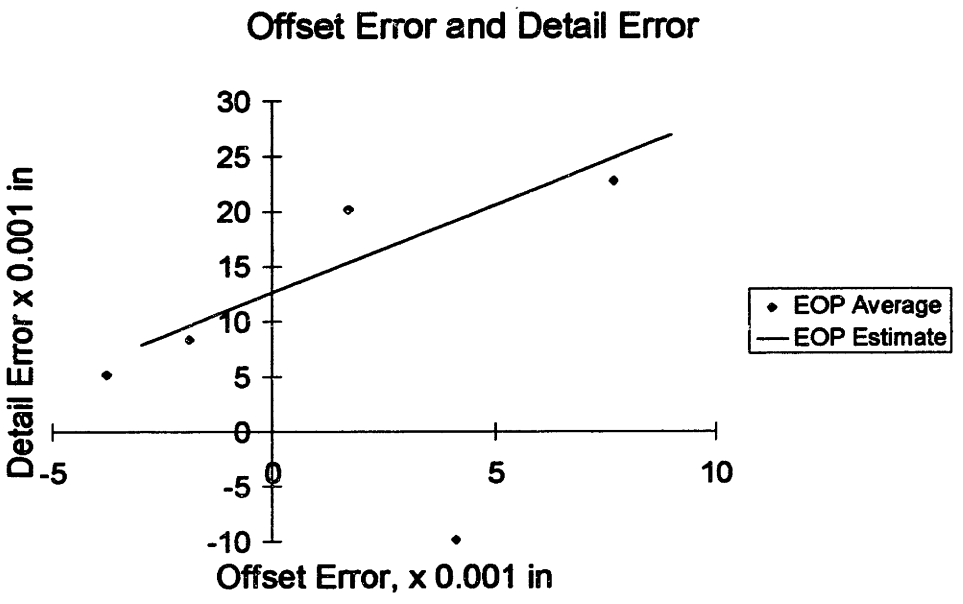

Figure 7.19 Offset error and detail error

While P/N A (at the bottom) is far off from the rest, there is a relatively strong correlation between the offset error and the detail error for P/Ns B through E. The r^2 value for these four P/Ns is 0.860. The offset is estimated to be at 0.0127", while the slope of the line is 1.6. One would expect a slope of 1.0 (because each additional unit offset error should result in an additional unit of detail error) and an offset of 0.0082" (because that is the difference between the offset and detail error averages calculated above). If P/N A is included in the calculations, the slope becomes 0.71, the offset comes out to be 0.0082", and the r^2 value is 0.064.

Clamping and errors

The number of clamps used *appears* to have an effect on the average detail dimension error, but not on the offset error. One would expect that the use of clamps would have an impact on the detail dimension and not on the offset error, because clamping affects the nesting of the part in the tool, which relates directly to the detail error and shouldn't affect the offset error. The following chart plots the offset and detail errors as a function of the number of clamps used on each lot.

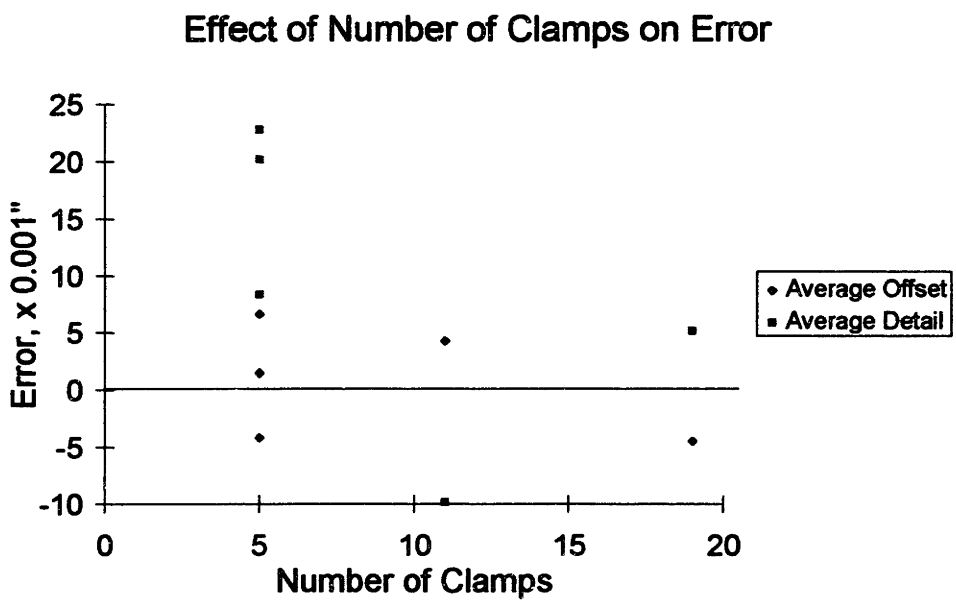

Figure 7.20 Number of clamps and error

The highest average detail errors were on two of the three the parts for which fewest number of clamps (5) were used. While this merits more investigation, it is not possible to jump to the conclusion that more clamps is the solution to improving detail dimensions, though it may be. First, the size of the part has not been taken into consideration—maybe it is the size of the part which is significant, or possibly the number of clamps per length. Second, detail measurements were only made at the EOP, and clamping at the EOP may somehow be different from clamping on the rest of the part. Third, the data are too few to be sure that a correlation even exists. Another possible explanation for the data in the chart is addressed next.

Direction of errors

An interesting phenomenon is evident in Figure 7.20: the magnitude of the detail error depends on whether or not the offset error and the detail-offset (caused by either the seating of the part in the tool or from the contour of the routing template) errors are both in the same direction or not. The detail-offset error is calculated by subtracting the offset error from the detail error. The following run chart shows these three errors.

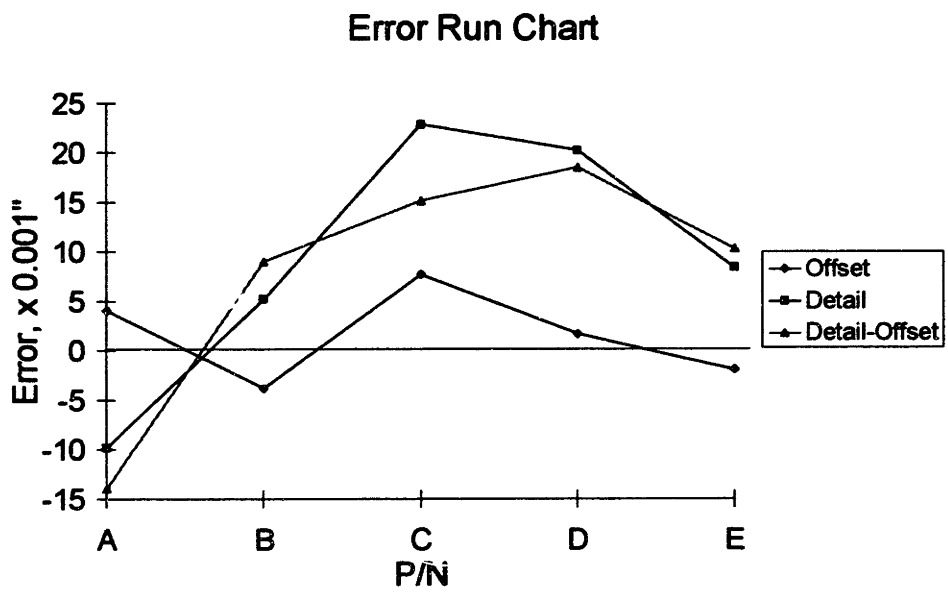

Figure 7.21 Error run chart, all lots

As the chart shows, for P/Ns A, B, and E, the offset and the detail-offset values are opposite in sign, so that there is some canceling effect. On the other hand, the offset and detail-offset values for P/Ns C and D are both in the same direction, resulting in the two highest detail errors.

Therefore, if the value of the detail-offset error were known before-hand, it seems possible that the offset could be adjusted in order to achieve the targeted detail dimension—if dimensional requirements were tight enough to require this. It is interesting to note that, except for P/N A, the detail-offset error is relatively consistent at around 0.013", as stated earlier.

Individual run charts

The individual run charts for each P/N show a combination of strikingly strong correlations right along with strikingly poor correlations. This may indicate that while it is possible to achieve much more repeatable results, there are intermittent sources of variation that disturb the operation. The five run charts are shown on the following pages.

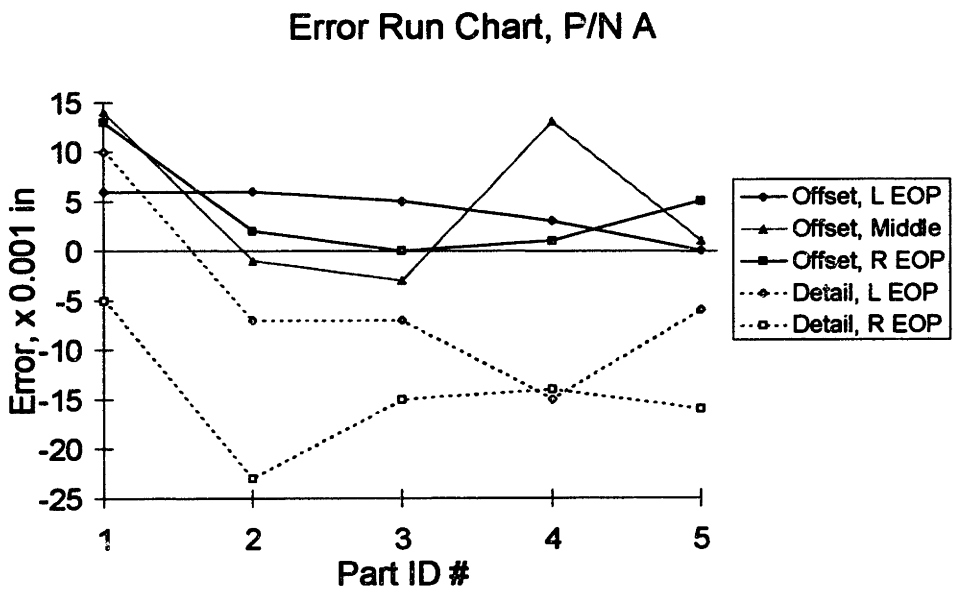

Figure 7.22 Error run chart, P/N A

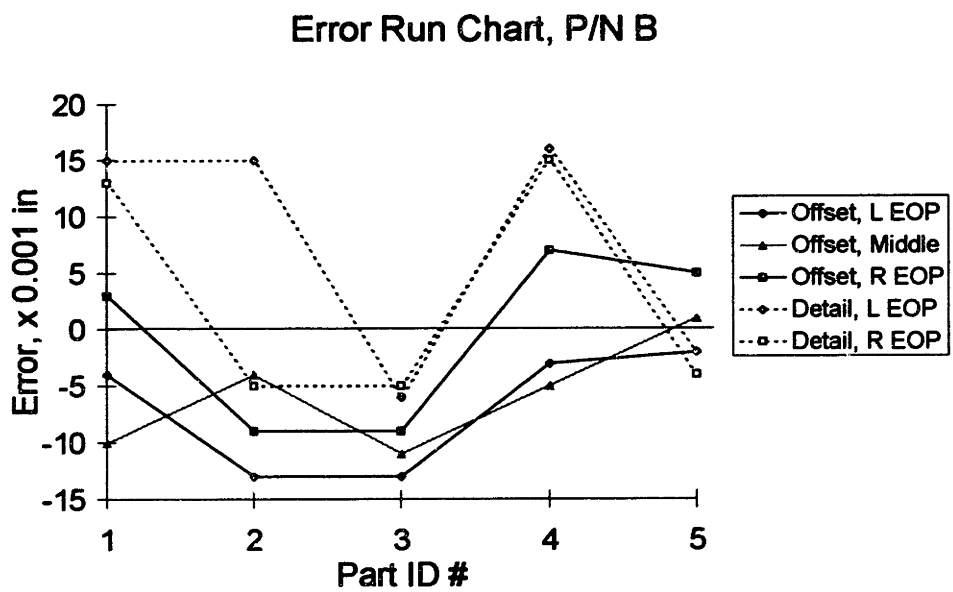

Figure 7.23 Error run chart, P/N B

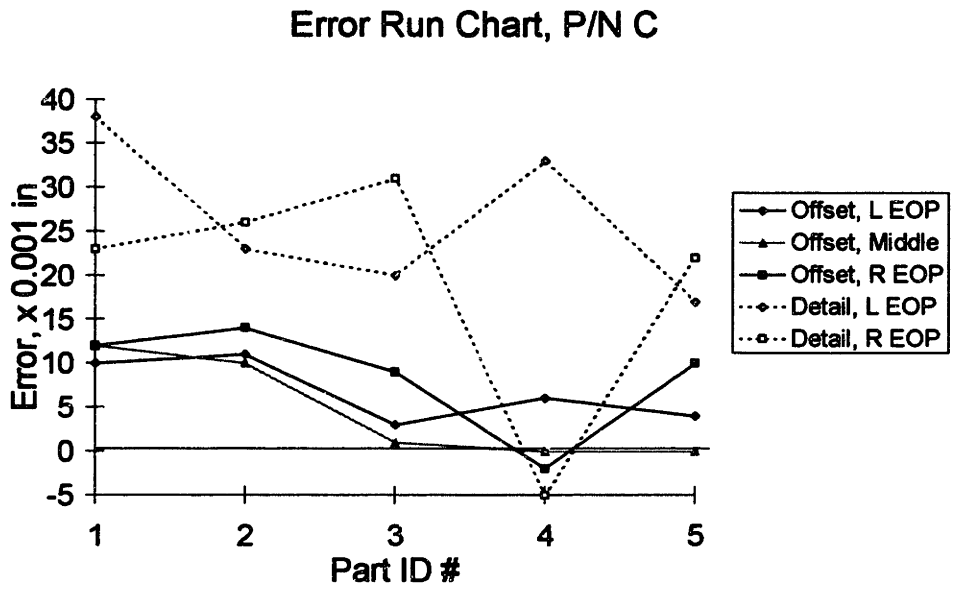

Figure 7.24 Error run chart, P/N C

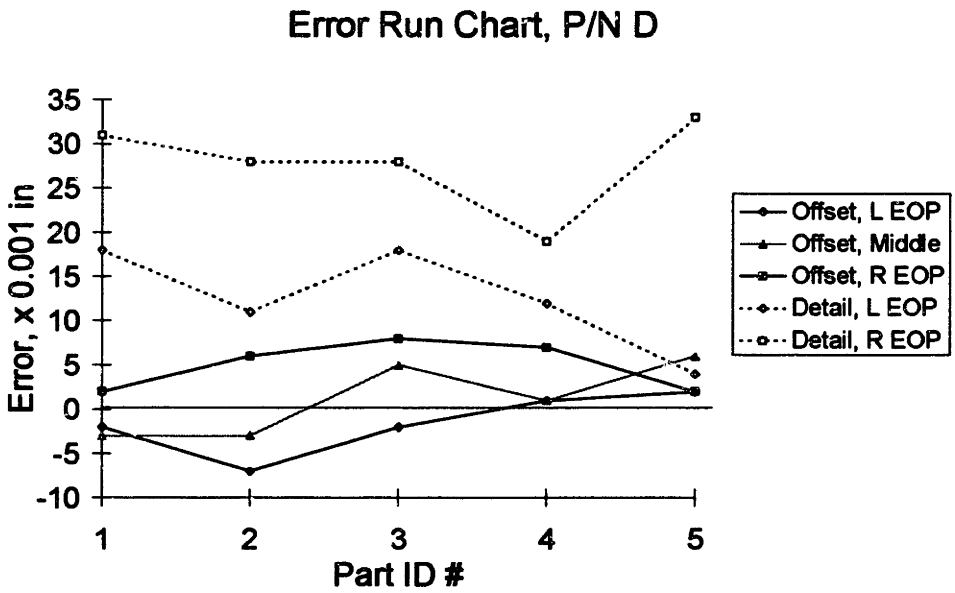

Figure 7.25 Error run chart, P/N D

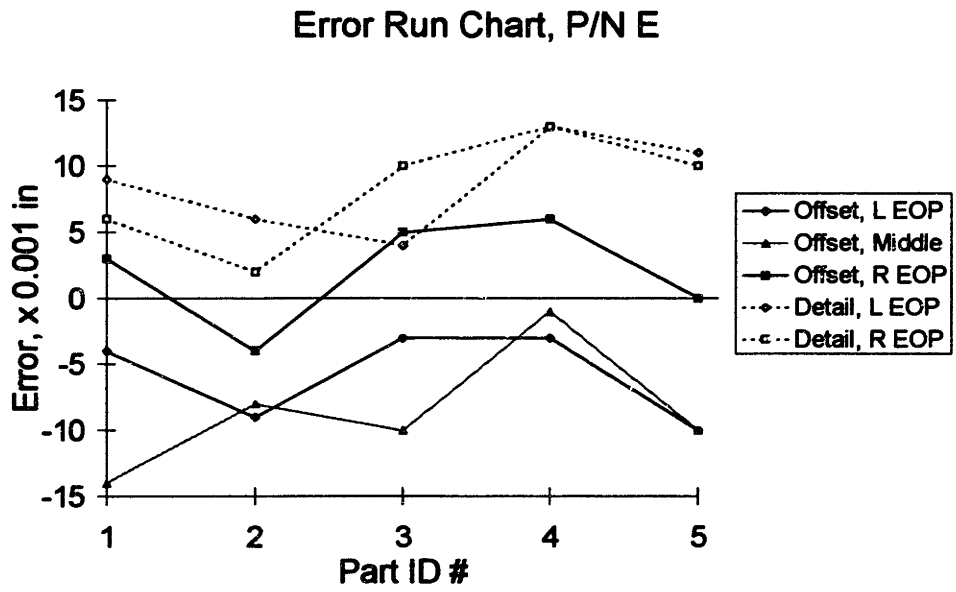

Figure 7.26 Error run chart, P/N E

As an example of this dichotomy of strong correlations and wide variations consider the following examples. The left and right EOP offset errors for P/Ns B, C, and E track very well, except for one part in P/N C. The middle offset error hardly ever appears well correlated with errors at the ends. The left and right detail errors track relatively well for P/Ns A, B, D, and E, except for one part on each lot. However, there appears to be a negative correlation between detail errors for P/N C.

Other parameters

Of the other information recorded, no other parameter seems to have a significant on output or its variation.

Whether parts were check and straightened first or not didn't make a significant difference—however, one should not conclude that check and straighten has no effect on the parts, because it is the parts that are the most bent out of shape that are sent to check and straighten. Thus it appears that after check and straighten, these parts fare just as well as those which didn't need it.

The router guide and cutter diameters never varied more than 0.001", so this couldn't be a significant source of variation. Router speeds were always set at 18,000 RPM. Four of the five P/Ns were located by scribe line; only one, P/N C, was joggle-nested, and its results weren't significantly different from the others.

7.5.5 Summary of routing variation and sources of variation

To begin with, it is important to note that most of the dimensions affected by the routing operation are not critical. Most of the cut edges do not mate up with anything; the legs serve mainly to give stiffness. However, the EOP location relative to the contour and joggles *is* important (even if the part contour is initially correct, a shift in the location of the EOP will cause the contour to be off). And the contour is very important.

The measurements have shown that the 0.109" offset from tool is centered to 0.001" and has $3\sigma = 0.021$". The average detail error was 0.009" and variation of the detail dimensions is indicated by $3\sigma = 0.027$". This satisfies the common $\pm$ 0.030" dimensional specification. There is no significant difference in offset error between roughly equally skilled operators. Clamping is likely to affect the error, but too few data prevent a conclusion. Detail errors are the largest when the direction of offset error and the detail - offset error are in the same direction. Finally, run charts reveal strikingly good and poor correlations among the measured output.

After having reviewed and discussed the above results, the routing supervisor, Danny Hammontree, suggested that the two most significant sources of variation in this operation are clamping and the part shape. Both of these affect how the part sits in the routing template, and both of these are likely to vary from part to part. The solution to the clamping problem may be to standardize clamping locations and technique among all operators for each lot. The solution to the part shape problem is either to stretch form parts more repeatably or to have them check and straightened before coming to routing—clearly, the first option is more desirable, and is in line with the objectives of this thesis.

Other possible sources of variation are the hand routing fixture (HRF), which locates the part and guides the cutter, and the sample part template (SPT), which is used as a reference. These were not measured. However, the specification that tooling (which includes HRFs and SPTs) tolerances are generally 1/3 of the part tolerances can be used as a guide to the (theoretically) maximum deviations in these, $\pm$ 0.010". While the HRF and SPT may contribute to the average of the measurements at a particular location on a part being off, they cannot account for the variation at a given location.

Another issue brought up by Mr. Hammontree which didn't enter into this study, but which affects final part contour, is springback that occurs as a result of material being

cut away (this is addressed in the previous section and in the analytical model chapters). While springback in the curvature is always an issue, additional springback results when material around a joggle is cut away, due to the increased residual strains that surround a joggle. Not only does the contour change, but joggle depth also changes. The change in contour from routing without joggles was consistent.

7.5.6 Proposed improvements

A few comments about precision improvement are now made.

The most significant source of variation affecting the measurements made appears to be the seating of the part in the HRF. The exact cause for this is not directly evident, but is probably a combination of clamping practice and part contour. Clamping could be improved by documenting the clamping arrangement for each part. Part contour could be improved by the recommendations in the previous section.

As suggested by Mr. Hammontree, predicting the changes in contour and joggle depth that result from the routing operation, and changing the targets so that the shapes after routing are the desired ones, is necessary to achieving the desired contour. Clearly, repeatable stretch forming and joggling operations are pre-requisites to this approach.

For very significant precision improvement, automation of the routing operation may be required. An interesting and novel design for an automated N/C machine to rout stretch formed extrusions has been proposed by Jeff Norris at Vought [Norris, 1993].

7.5.7 Summary and conclusions to extrusion routing study

Measurements were made on a number of parts after routing to get a better understanding of variation, correlations among parameters, and operator influence. While there is a lot of statistical uncertainty, some interesting and useful correlations have been found.

The routing operation appears to be just capable of achieving ± 0.030" tolerances on part dimensions. The 0.109" offset is achieved to the nearest 0.001", but the parts themselves are on average about 0.009" too big.

There appear to be significant opportunities for improvement, but with the limited amount of data gathered, it is difficult to know where to begin. It is likely that variations in clamping and part shape have a significant effect on after rout part dimensional

variation. As well, springback resulting from material removal will affect final part contour and joggles.

In order to get a better understanding of the sources of variation and their impact on the output, more—numerically and in scope (for example, also measuring sample part and HRF accuracy and further investigating clamping)—data should be gathered.

7.6 Summary and conclusions to Extrusion Stretch Forming: Practical Understanding

The extrusion stretch forming process, used to create parts such as brake rings, chords, and stiffeners, consists of the following operations: heat treat, stretch form, and rout & drill. The existence and busyness of the check and straighten operation testifies to significant deviation of part geometry from the specified tolerances.

In similar fashion to sheet metal, incoming material and geometry specifications permit significant variation of stress-strain properties, thickness, angle, twist, and flatness. While variations appear to be significantly less than the specifications permit, they are still significant. Incoming yield strength and ultimate tensile strength variations are probably similar to sheet metal variations, between 2% and 6% (3σ/average). Thickness within two lots varied 1.6% and 4.4%.

The heat treat operation was not studied, but experience revealed that racking and quenching have a very significant effect on part warpage. The reader is referred to the two sections addressing the heat treat operation in the previous chapter.

While a study was made of the extrusion stretch forming operation, firm conclusions are hard to draw from the limited data collected. Older machines with manual control (and which generally use force control based on pressure measurement) are less repeatable than newer, NC-controlled machines. Variation of up to 0.120" (3σ/average) was found in contour. Correlations among angles and contour (when they varied) and strain were not significant. Change in contour due to routing was found to be repeatable. Recommendations for improving the precision of the extrusion stretch forming operation are the same as for the sheet stretch forming operation: repeatably achieve optimized settings and control the operation by strain. No tests have been made of proposed improvements, but based on the reduction in variation found in

sheet metal stretch forming from essentially the same recommendations, this would be a worthwhile endeavor.

Routing measurements showed the operation to be capable of achieving ± 0.030" tolerances. Measurements showed a dichotomy of strikingly strong and strikingly poor correlations among detail errors and offset errors. Clamping and part contour not to tolerance are probably the main causes of variation, while averages being off may be attributable to hand router fixtures and sample part templates.

8 THESIS SUMMARY AND CONCLUSIONS

8.1 SUMMARY OF ACHIEVEMENTS AND RESULTS

This thesis focuses on precision stretch forming of metal for precision assembly of aircraft. The first three chapters laid necessary groundwork and demonstrated the need for precision fabrication. The next two chapters developed a theoretical understanding of the stretch forming operation. The following two chapters investigated the stretch forming process on the shop floor and demonstrated significant improvement in the precision of parts when recommended changes were made.

8.1.1 The need and opportunity for precision fabrication

Significant economic changes and technological advances over the past few years have created the need and the ability for companies to become lean—to reduce waste, improve quality, reduce inventory, reduce flow times, and respond more quickly to customers' changing needs. This research responds to the need of companies in the aircraft industry to become lean. Previous studies of airframe assembly revealed significant waste. Tooling is one of the most significant barriers to becoming lean in aircraft assembly, largely because of its significant cost and inflexibility.

A new philosophy of aircraft assembly, precision assembly, is emerging. Precision assembly aims to significantly reduce the waste associated with assembly tooling by eliminating or drastically reducing the amount of assembly tooling. Among other things, this requires precision fabrication—the fabrication of parts to tight enough tolerances that (a) part features can be used to align parts relative to one another and (b) fitting, shimming, trimming, and rework of features and contour are minimized or eliminated.

For precision fabrication parts, contour tolerances may drop to about 1/3rd of standard tolerances, from ± 0.030" to ± 0.010",[46] while locating feature tolerances may drop to about 1/5th to 1/10th of standard tolerances, from the range of ± 0.030" - 0.060" to the range of ± 0.003" - 0.010", and angle tolerances at attach points may drop from about ± 1° to about ± 1/4°. Not all features on precision fabrication parts need to have these tight tolerances; some tolerances may be loosened, while many will remain the same.

A combined engineering and statistical approach to precision improvement was demonstrated to be useful for the proactive improvement of precision in the stretch forming process due to a synergism between theory and practice. The seven step approach to quality improvement described by Shiba et al [1993] was used and enhanced by incorporating the development of a theoretical understanding of the stretch forming operation.

8.1.2 Theoretical understanding: analytical model

A two dimensional analytical model of the stretch forming operation was developed based on mechanics of solids and simple plasticity theory. The model assumes a single curvature die, isotropic material properties, and a power law strain hardening stress-strain relationship. The model is capable of incorporating the effects of a range of strain hardening models (Kinematic to Isotropic), any amount of pre stretch strain and post stretch strain, cross-section (for extrusions), chemical milling, routing, friction, and a changing radius of curvature along the length of stretch. The model was used to determine the operation's sensitivity to parameter changes and to compare strain and force control. The Isotropic hardening model was generally used because it best reflects the behavior of aluminum.

The most important findings from the analytical model are

- The operation is much less sensitive to changes in parameters under strain control than under force control
- Pre stretch increases springback
- Friction has a significant effect only at high coefficients of friction ($\mu \geq 0.2$) and large bend angles ($\theta \geq 45$)
- The effect of chem mill and routing on springback depends on the residual stresses after the stretch forming operation; the effect is reduced with greater post stretch strain
- Cross-section affects springback

Analytical model predictions compared well with experiments and FEA predictions.

---

[46] Contour requirements are driven not only by assembly requirements, but also by the need to repeatably achieve precision in locating features in fabrication.

8.1.3 Practical understanding: shop floor studies and improvements

In concert with the theoretical understanding gained from the model, a number of shop floor studies were made of the incoming material and the significant operations in the stretch forming process. The primary objectives of these studies were:

- Document variation
- Identify sources of variation

The first three studies—one on incoming material and two on the heat treat operation—investigate material geometry and properties prior to the stretch forming operation. Two studies investigate the stretch forming operation—one of sheet metal, one of extrusions. The two final studies investigate the chem mill and rout operations which occur after stretch forming. Based on the findings from these studies, improvements were recommended, some of which were implemented and evaluated. The most important points from each study are now reviewed.

The incoming material study

Investigation of incoming sheet and extrusion properties and geometry revealed that material specifications used in all purchases permit significant variation in material properties and in material thickness. For extrusions, angle and, flatness, and twist are also permitted to vary significantly. A study of sheet metal properties revealed significant variation in yield strength and ultimate tensile strength (2-6% of the average), and elongation (15-20%) of incoming sheet for a given alloy, temper, thickness, and microstructure specification. A smaller study of seven lots of one P/N showed a 17.4% variation in yield strength and a 7.5% variation in ultimate tensile strength. Correlation between material properties before and after solution heat treating ranged from non-existent to medium strength ($0.2 < r^2 < 0.7$), and correlation between yield strength and ultimate tensile strength was generally strong ($0.72 < r^2 < 0.92$). The latter correlation indicates a move of the entire stress-strain curve with a change in yield strength.

The heat treat designed experiment

A designed experiment was performed on the heat treat operation for aluminum alloys 2024 and 7075 to determine the effect of three factors—sheet thickness, quench delay, and time at room temperature. Measured outputs were yield strength, ultimate tensile strength, elongation, hardness, conductivity, and stress at which Lüdering and/or

Orange Peel initiated. For alloy 2024, the only significant factor was time at room temperature. Leaving the material at room temperature for 53 minutes instead of 20 minutes increased the yield strength 20% and ultimate tensile strength 4.4%. For alloy 7075, it turned out that the thinner material was alclad, while the thicker material was bare. The combination of thickness and cladding, and time at room temperature were significant factors.

The heat treat study

Since correct solution heat treating is crucial to achieving adequate corrosion resistance and final part strength, most of the heat treat operation is relatively well controlled and does not appear to cause variation in material properties. However, the heat treat operation has a significant impact on part contour because of the warpage that occurs as the part is quenched. Factors affecting warpage are racking, quench delay, quench entry rate, and quenchant temperature. Investigation of these factors is recommended. As is evident in the heat treat designed experiment findings, leaving material at room temperature for various amounts of time before forming significantly affects material properties and be a source of variation.

The sheet stretch forming operation study

The sheet stretch forming operation study is the most important study, because most of the contour variation is found in this operation, and the suggestions to improve precision were implemented and tested for this operation, resulting in a more than ten-fold reduction in contour variation. The study focused on 2024-T3 leading edges, a difficult part to fabricate precisely due to the strong contour, thickness, and length.

Contour variation (measured by the standard deviation of the average separation at each end), strain, force, and die table movement were found to be significant within parts, from one part to the next, and from one lot of parts to the next. The primary contributors to part variation are

- Changes in settings[47]
  - + die table angle

---

[47] Nolan [Nolan, 1993] concludes that for sheet stamping the most significant sources of variation are variability in properties of the incoming steel and changes in press line settings. The solution he proposes is to ensure consistent set ups and runs and then to optimize the settings. Kudo [1990] presents factors resulting in imprecision in formed parts, which overlap in areas with findings in this thesis. The author also describes requirements for precision improvement.

+ jaw positions and angles
+ final force

- Control of the operation by force instead of strain (or displacement)

Currently the operation is force-controlled, and no special effort is made to repeatably achieve settings. The recommended improvements are

- Repeatably achieve optimized settings
- Use automatic in-process strain control

Displacement control, a substitute for strain control, was also tested. Although the data are limited, significant precision improvement was achieved by implementation of the recommendations, as shown in the following chart (already shown in Chapter 6).

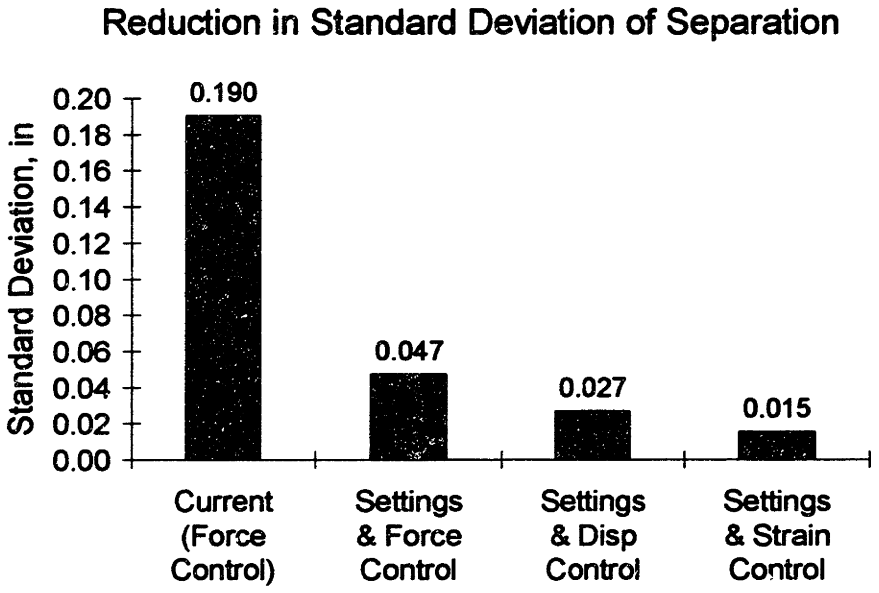

Figure 8.1 Reduction of standard deviation of separation for repeatably achieved optimized settings and three control methods

Optimization of settings was accomplished by the machine operators by experience, and it is enhanced by strain measurement. The important improvement in repeatably achieved optimized settings is the repeatability. Without changing the control method, repeatably achieving optimized settings reduced variation by 75%. With repeatably achieved optimized settings and using displacement control instead of force control, variation was reduced a total of 86%. Both of these improvements are achievable without modification or addition to the current equipment.

Strain control with repeatably achieved optimized settings reduced variation 92%. Since the strain control method was manual and in the testing phase of its development, further variation reduction is expected with further development of the strain measurement technique and the implementation of automatic strain control. Theoretically, strain control is the best form of control for three reasons:

- The operation is less sensitive to changes in strain than changes in force
- Under strain control, the operation is less sensitive to changes in the material
- Strain control measures and controls by what's actually happening in the part

The extrusion stretch forming study

Limited data were collected and no improvements were tested in the extrusion stretch forming study. Correlations among strain, contour, and angle were poor or non-existent, if the latter two changed at all (within the precision of the measurements). Contour was found to vary up to 0.120". Change in contour from routing was a consistent 0.01". Recommendations for improvements for the extrusion stretch forming operation are essentially the same as for the sheet stretch forming operation: repeatably achieve optimized settings and measure and control the operation by strain.

The chem mill study

The chem mill operation was not found to have a significant effect on variation in the stretch forming process. Etch rate depends mostly on etchant temperature and alloy. Fit problems between parts and scribe templates indicate significant variation in tooling hole locations in the parts.

The extrusion routing study

Offset and detail part measurements were made on five lots of five parts each. While the data are few, there were some interesting findings. The routing operation appears to be just capable of achieving ± 0.030" tolerances on part dimensions. The 0.109" offset is achieved to the nearest 0.001", but the parts themselves are on average about 0.009" too big. It is likely that variations in clamping and part shape have the most significant effect on dimensional variation of the routed dimensions. Further investigation is necessary to get a handle on variation and sources of variation.

Summary to shop floor studies and improvements

While significant variation was found in incoming material geometry and properties, repeatably achieving optimized settings and measuring and controlling the stretch

forming operation by strain reduced contour variation by 92%. The two operations following the stretch forming operation were not found to contribute to contour variation.

It is noteworthy that the two recommended improvements contain the three types of variation improvement suggested by the variational model. Repeatably achieving settings is elimination of a source of variation, optimization of settings is reducing sensitivity of the operation to sources of variation, and strain control is compensation.

8.2 WHAT SHOULD/COULD BE DONE NEXT

The findings in this thesis point to promising areas of practical application of lessons learned from this research and further research. A couple of these are now addressed.

8.2.1 Analytical model

While the ability of the analytical model to accurately predict stresses, strains, and springback was demonstrated to some extent, further comparison of the analytical model predictions with experimental results and FEA predictions under a wider range of parameters would be useful. In particular, the ability to predict output for extrusion stretch wrap forming and routing, and the ability to incorporate initial strain hardening and residual stresses varying through the thickness should be tested.

While the Isotropic hardening model has been used to model aluminum, it may be that the material is more accurately modeled by using a value of A of slightly less than 1 (in the yield surface approach). This and its effects should be investigated.

If the model is adequately accurate, it could be used to predict how to compensate dies for springback. Current springback compensation, when done, is almost without exception very much an art form, and may require numerous iterations, which significantly increase the cost of the die. Use of the analytical model to predict the appropriate die contour to compensate for springback would be very beneficial.

8.2.2 Shop floor

Based on the results of the studies and evaluation of the proposed changes that have been implemented so far, there are significant opportunities for precision improvement.

Heat treat and aging

Study of the heat treat operation revealed two areas which could use more study and some tighter control: racking and quenching. Experience has shown that both racking

and quenching have a significant effect on warpage, which affects the final part contour. While quantifying the effect of racking and quenching would be a difficult task, input from operators warrants tighter control of settings for both racking and quenching. Heat treat operators could agree on optimal racking for each part, document it, and then follow their instructions. Further, based on their experience, or even some simple experiments, it should be possible to agree on the optimal quench entry rate, quench delay, and quenchant temperature.

Time at room temperature should be tightly controlled. If it cannot be kept consistent, a simple algorithm to compensate for changes in material properties could be developed.

Repeatably achieve optimized settings

Initial and final settings should be optimized and repeatably achieved. For sheet and extrusion stretch forming, strain measurement can be used to help optimize settings. Each sheet metal P/N should have a setup sheet which documents the settings:

- Location of die on the die table
- Location of edge of part
- Location and angle of jaws
- Die table angle
- Die table rate
- Snug force
- Final force, die table position or displacement, or strain
- Target separation from the die
- Changes made to any of the above, and reason for the changes

Most operations have such setup sheets, but they are not always used and not always up-to-date. Use and currency of setup sheets should be required. Ideally, the actual value of each of the above parameters for each part should be recorded (if it can be accurately determined) in order to aid in trouble-shooting and understanding the contribution of each of these parameters to the operation.

Automatic strain measurement and control

Strain measurement is necessary to know what's going on in the part. The findings in this thesis demonstrate a potential for significant improvement in precision of contour through the use of strain control. More work is needed to refine the strain measurement technique and to implement automatic strain control. Further, on

machines which have no automatic control, it would be useful to develop a simple method to implement manual strain control.

Statistical process control

Statistical process control (SPC) through the use of control charts is not very common in stretch forming. SPC is most useful for detecting changes in an otherwise in-control, randomly varying operation. Study results have given an indication of the relative importance of the various parameters—a charted parameter should have a strong influence on the output and have a propensity to change (for example, strain), or be a strong indicator of the output (for example, separation). Because of the low production volume and small lot size for aircraft fabrication, it is recommended that data be taken on each part. This increases the operators' ability to respond to statistically significant changes. For each operation, the suggested parameters to chart are now given.

For heat treat, quench temperature should be charted if it is not well controlled.

For sheet and extrusion stretch forming, strain and separation (for an extrusion this may be from a contour template or check fixture) are the two most important parameters. For extrusions, angle and flatness are also very important. Die table movement (tension cylinder movement for extrusions) and maximum force could also be charted. What is measured and how will depend in part on the machine and the extent of automatic control.

For chem mill, etch rate and temperature could be charted together, segregated by alloy. Further, deviation of depth of cut from desired depth of cut could be charted.

In order to truly capture the entire manufacturing process, some measure of the part fit in assembly should be made as well. For example, contour deviation at attach points could be charted. However, due to the long (months, often) delay between fabrication and assembly the usefulness of this data may be largely lost.

8.2.3 Promoting a theoretical understanding of stretch forming

Interactions with individuals throughout the aircraft stretch forming industry indicate a significant lack of theoretical understanding of the stretch forming operation. For example, people commonly believe that aluminum yields at 2% - 3% strain, which is well beyond the strain at which aluminum actually yields (0.1-0.4%). Shop floor people do an amazing job with the equipment they have and with their limited understanding of

the mechanics of sheet metal forming. They have, over years of experience, developed a method for achieving acceptable parts. Even so, it would be useful to educate both engineers and operators in a proper understanding of the behavior of the material in stretch forming so that they could make more significant contributions to process improvement. Material could be developed to convey simple concepts necessary for understanding the stretch forming operation.

8.2.4 Precision assembly and precision fabrication

Due to the high level of interest and activity already existent, it probably doesn't need to be said that research in precision assembly and precision fabrication should continue and expand. Most of the focus on precision fabrication has been aimed at part features as opposed to part contour, even though part contour is critical to achieving precision assembly and to achieving precision part features. Determination of the precision requirements of fabricated parts for precision assembly is very important to the development of precision fabrication.

8.2.5 Process simplification

To eliminate the variation and additional processing caused by in-house solution heat treatment, it would be beneficial to eliminate the in-house solution heat treat operation. This operation is normally required because the parts cannot be stretched enough in one step. Aluminum suppliers are developing alloys with more formability in order to avoid heat treat.[48] Formability requirements should include surface texture requirements, e.g., no Lüdering or Orange Peel. Better repeatability of the operation through strain control and springback compensation of the dies would be necessary to eliminate in-house heat treat. This elimination would improve process flow and reduce variation.

8.2.6 New process development

A novel idea which would permit fuller control of strain within complex contour parts is suggested by Wilson [1988]. The author suggests the use of controlled temperature gradients in warm sheet forming to control the distribution of flow strength in the material, so that strains can be controlled. The author found significant improvement in

---

[48] According to C. J. Warren [1994] of Alcoa, aluminum alloy C188 was created for this purpose.

formability in hemispherical punch stretching using this method, and suggests that aluminum is a good material for this method.

Another novel idea, mentioned earlier in passing, is to use a reconfigurable die. A single reconfigurable die could be used to form a number of parts. Die creation, modification, maintenance, and storage costs would be greatly reduced. Further, through analytical methods and, if necessary, in-process measurements, die shape is easily changed to compensate for springback. Such a die is being developed jointly by MIT, Northrop Grumman, and Cyril Bath in an ARPA-funded project.

8.3 PRECISION FABRICATION IN THE CONTEXT OF LEAN MANUFACTURING

Becoming leaner requires reducing all forms of waste. In the factory setting, the most significant forms are excessive inventory, excessive flow time, and excessive variation. Precision fabrication is most effective when it is in a lean production environment; stated another way, the changes proposed in this thesis are only a part of the changes needed to become leaner. According to the most current version of the LAI Factory Operations Lean Implementation Model, changes in the production environment can be grouped into four levels, as shown in the following diagram.

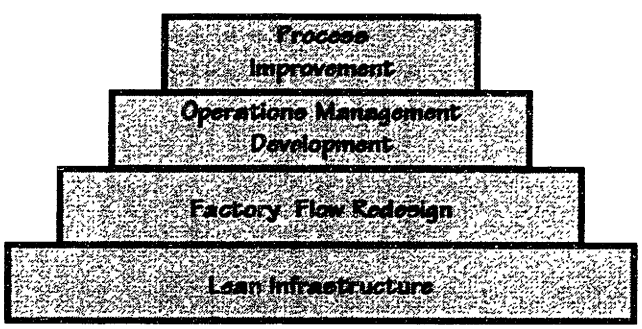

Figure 8.2 Factory Operations Lean Implementation Model structure

Process Improvement includes reducing variation, improving quality, and increasing flexibility and speed. Most of the work in this thesis has been in process improvement. Operations Management Development includes training workers and aligning their incentives, reallocating support resources, and implementing pull type production management systems. Factory Flow Redesign includes grouping products, standardizing processes, and redesigning factory layout into cells based on product flow. Lean Infrastructure includes identifying business goals and issues, benchmarking, identifying needed skills and training, and establishing cross-functional

linkages. The categories indicate a large number of improvements that should be made in order to create a lean production environment. One of these, factory flow redesign, is addressed next to show what changes may be needed.

Currently, the factory layout is organized by equipment type, not by material flow. A redesign of the factory floor according to material flow along with a drastic reduction in inventory is recommended for extrusion stretch forming. For example, a cell consisting of one or two stretch presses, heat treat, routing, and, if absolutely necessary, check and straighten could be created. Ideally, the heat treat operation could also be eliminated, as discussed above. Batches (much smaller in size than today) of material would flow through the cell without the significant delays generally found in aircraft fabrication. In addition to significantly reducing flow time, this would promote more frequent and more timely communication.

Lean assembly

As discussed already, precision fabrication is a requirement of precision assembly, a significant step towards becoming leaner in assembly by reducing or eliminating hard, inflexible assembly tooling. Even apart from contributing to precision assembly, the reduction or elimination of hand work to bring parts into contour in the check and straighten operation and the reduction or elimination of fitting, shimming, and rework in assembly will make a significant contribution to lean manufacturing.

8.3.2 Interaction between precision fabrication and design

Precision fabrication, precision assembly, and design of the aircraft are strongly tied to each other. Design of the assembly strategy relies heavily on the tolerances achievable in fabrication. Increased precision in fabricated parts will affect the design of the assembly process and ultimately the design of the assembly itself.

8.4 APPLICATION TO OTHER PROCESSES

The research presented in this thesis has application to other manufacturing processes as well, as shown in the following table and explained below.

	Stretch Forming		Forming (no CC)	Machining	General
	Sheet Metal	Extru-sions			
Approach Seven Step Engrg. & Statist.	✔ ✔	✔ ✔	✔ ✔	✔ ✔	✔ ✔
Analytical Model	✔	✔	✔		
Shop Floor Study Variation & Variation Sources	✔ ✔	✔ ✔	✔ ✔	✔ ✔	✔ ✔
Improvements Strain Control Settings	✔ ✔	✔ ✔	✔ ✔	✔	✔

Table 8.1 Applicability of approach, analysis, shop floor study, and improvements

The approach taken to precision improvement in this thesis was to enhance the standard seven step statistical approach to quality improvement with an analytical model of the stretch forming operation. The analytical model is part of a more typically engineering approach, but it greatly enhances the seven step approach by promoting understanding of the stretch forming operation and by revealing process sensitivities which are difficult determine on the shop floor. This combined approach is applicable to all manufacturing processes, and is most important for proactive, step improvement.

The analytical model developed in this thesis can be used to model not only stretch forming of sheet metal and extrusions, but most sheet metal and extrusion forming operations which do not involve compound contours or significant sliding.

While the results of the shop floor study are obviously specific to the stretch forming operation, the methodology used in the study is applicable to all processes. The significant operations within the process are first identified, generally from the experience of those on the shop floor. Then, the current variation is measured and measurements are made of the potentially significant sources of variation to determine those that actually are. If possible, their effect is quantified. The goal is to find the one or few sources of variation that have the most significant effect on the output.

Of the two recommended improvements—strain control and repeatably achieving optimized settings—the latter has wider applicability. Repeatably achieving optimized

settings is most important for manually controlled operations, where settings are likely to vary from one part or one lot to the next, but should be required for all operations. Strain control was demonstrated to be useful because: the operation is less sensitive to changes in strain than to changes in force, the operation is less sensitive to parameter changes under strain control, and strain measures what's actually going on in the material. While strain control may not be applicable to more than some other metal forming operations, these three points can be applied to all other operations.

8.5 Final word

This thesis started with the objective of reducing the amount of tooling in aircraft assembly through precision assembly, and ended with improving the precision of the detail parts that constitute an assembly. Both of these are part of the larger effort of becoming lean—reducing waste, improving material flow, reducing inventory, and improving quality. I hope this thesis has made a significant contribution to these goals, and that the reader will come away with some treasures and some new insight that will help him or her do better work and make his or her workplace a better place to work.

BIBLIOGRAPHY

The bibliography is divided into sections, the first of which is an alphabetical list of references cited in the thesis. The second section is a bibliography of references grouped according to topic; it includes the references cited in the thesis.

ALPHABETICAL LIST OF REFERENCES IN THESIS

Allen, Donald R., "Process Control in Stamping Lines," in *SAE Transactions*, v. 98, section 5, paper # 890343, Society of Automotive Engineers, Inc., Warrendale, PA, pp. 189-195, 1989.

Alting, Leo, *Manufacturing Engineering Processes*, English version edited by Boothroyd, Marcel Dekker, Inc., New York, 1982.

Aluminum Company of America (ALCOA), *Forming ALCOA Aluminum*, ALCOA, ALCOA Center, Pennsylvania, 1974.

Anderson, Lindsay Norman, *Assembly Process Development for Commercial Aircraft Using Computer-Aided Tolerance Analysis Tools*, S.M. Thesis, Materials Science and Engineering and Sloan School of Management, 1993.

Anonymous, "Closing the Bending Loop," in *Manufacturing Engineering*, April, 1995.

Aryshenskii, Yu. M., "Calculation of Technological Parameters of Simple Stretch-Wrap Forming," in *Izvestiya VUZ. Aviatsionnaya Tekhnika* [English Translation], v. 26, n. 2, 1983, pp. 16-20 [13-17].

ASTM, *Standard Test Methods of Tension Testing Wrought and Cast Aluminum- and Magnesium-Alloy Products*, Specification B557, American Society for Testing and Materials, 1994.

Augustine, Norman R ., *Augustine's Laws and Major System Development Programs*, second edition, American Institute of Aeronautics and Astronautics, Washington DC, 1983.

Baba, Akijiro and Yasuhisa Tozawa, "Effect of Tensile Force in Stretch-Forming Process on the Springback," in *Bulletin of the JSME* (Japan Society of Mechanical Engineers), v. 7, n. 28, 1964, pp. 835-843.

Barrie, Douglas, "Assembling the Future," in *Flight International*, 10-16 June, 1992, pp. 50-52.

Bartelson, Kevin D., *Analysis And Redesign Of The Production System Structure For 757 and 737 Aircraft Doors*, S.M. Thesis, Department of Mechanical Engineering and Management, Massachusetts Institute of Technology, 1993.

Bodunov, N. M., I. M. Zakirov, M. I. Lysov, and G. V. Druzhinin, "Calculation of Parameters at Shaping the Profiled Parts by Stretching With Tension and Radial Compression," in *Izvestiya VUZ. Aviatsionnaya Tekhnika* [English Translation], v. 37, n. 3, 1994a, pp. 60-65 [61-65].

Bodunov, N. M., I. M. Zakirov, M. I. Lysov, and G. V. Druzhinin, "Approximate Method for Calculating the Working Conditions of Profiled Part Bending Process," in

Izvestiya VUZ. Aviatsionnaya Tekhnika [English Translation], v. 37, n. 4, 1994b, pp. 93-97 [93-97].

Boeing, *Hardware Variability Control*, for internal use, Boeing Commercial Airplane Group, Wichita Division, 1994.

Braun, R. and R. Zanella, *Flexible Assembly Subsystems*, interim technical report, available from the Manufacturing Technology Directorate, Wright Research and Development Center, Air Force Systems Command, Wright-Patterson Air Force Base, Ohio, procurement instrument identification number F33615-84-C-5048, 1988.

Braun, R. and R. Zanella, *Flexible Assembly Subsystems*, phase I final report, available from the Manufacturing Technology Directorate, Wright Research and Development Center, Air Force Systems Command, Wright-Patterson Air Force Base, Ohio, procurement instrument identification number F33615-84-C-5048, 1986.

Coleman, Robert Mark, *Effects of Design, Manufacturing Processes, and Operations Management on the Assembly of Aircraft Composite Structure*, S.M. Thesis, Department of Aeronautics and Astronautics and Sloan School of Management, Massachusetts Institute of Technology, 1991.

Crandall, Stephen H., Norman H. Dahl, and Thomas J. Lardner, *An Introduction to the Mechanics of Solids*, second edition with SI units, McGraw-Hill, London, 1987

Cunningham, Timothy W., Ramakrishna Mantripragada, Don J. Lee, Anna C. Thornton, Daniel E. Whitney, "Definition, Analysis, and Planning of a Flexible Assembly Process," *Japan-U.S.A. Symposium on Flexible Automation*, 1996.

Cutler, John. *Understanding Aircraft Structures*, second edition, Blackwell Scientific Publications, Oxford, UK, 1992.

Davis, J. R. (editor), *ASM Specialty Handbook: Aluminum and Aluminum Alloys*, ASM International, Ohio, 1993.

Duncan, J. L. and J. E. Bird, "Die Forming Approximations for Aluminium Sheet," in *Sheet Metal Industries*, v. 55, n. 9, September, 1978, pp. 1015-1025.

El-Domiaty, Aly and A. H. Shabaik, "Bending of Work-Hardening Metals Under the Influence of Axial Load," in *Journal of Mechanical Working Technology*, v. 10, 1984, pp. 57-66.

El-Domiaty, Aly, "Stretch Forming of Beams of Non-Uniform Section," in *Journal of Materials Processing Technology*, v. 22, 1990, pp. 21-28.

El-Megharbel A., A. El-Domiaty, and M. Shaker, "Springback and Residual Stresses After Stretch Bending of Workhardening Sheet Metal," in *Journal of Materials Processing Technology*, v. 24, 1990, pp. 191-200.

Ewert, Lee R., Sumner B. Sargent, and Walter Leodolter, *US Patent Number 4,989,439*, February 5, 1991.

Finan, Jeffrey John, *System Dynamics Analysis Of An Ordering System Used For Commercial Aircraft Manufacture*, S.M. Thesis, Department of Aeronautics and Astronautics, and Sloan School of Management, Massachusetts Institute of Technology, 1993.

Gillespie, LaRoux K. (editor), *Troubleshooting Manufacturing Processes*, fourth edition, Society of Manufacturing Engineers, 1988.

Goodman, Harvey, "Assembly Cell Speeds Riveting," in *Tooling & Production*, December, 1990b, pp. 50-53.

Goodman, Harvey, "Flexible Tooling for Flexible Assembly," in *Automation*, September, 1990a, pp. 42-43.

Gordon, S. J., "Elimination of Customized Fixtures Through High-Performance 3D Vision," in *Flexible Assembly Systems—1989*, edited by D. P. Sathyadev, conference proceedings, The American Society of Mechancial Engineers, 1989, pp. 9-14.

Gordon, Steven, *Automated Assembly Using Feature Localization*, Ph.D. Thesis, Mechanical Engineering, Massachusetts Institute of Technology, 1987.

Guangnan, Chen, Shen Huan, Hu Shiguang, and Bernard Baudelet, "Roughening of the Free Surfaces of Metallic Sheets During Stretch Forming," in *Materials Science and Engineering*, A128, 1990, pp. 33-38.

Hatch, John E. (editor), *Aluminum: Properties and Physical Metallurgy*, published the American Society for Metals, Metals Park, Ohio, 1984.

Hawthorne, John, "From ASAT to Masterhead™," an *SME Technical Paper*, AD89-636, Society of Manufacturing Engineers, Dearborn, Michigan, 1989.

Hessami, M. A. and W. Y. D. Yuen, "Residual Stresses Induced by Stretch-Bending," in proceedings of the *Fourth International Conference on Manufacturing Engineering*, Brisbane, 1988, pp. 78-83.

Hill, R., The *Mathematical Theory of Plasticity*, Oxford University Press, Oxford, 1950.

Holt, R. A. and C. J. Warren, "C188 Laboratory Formability Testing: Preliminary Results and Analysis," Alcoa Technical Center private report, Aluminum Company of America, 1994.

Hooper, W. H. and W. M. MacFarlane, "Stretch Forming of Pre-Sculptured Gore Panels for the External Tank," in *Man's Presence in Space* from the 3rd Annual AIAA/GNOS Aerospace Technology Symposium, (A86-32931) 1985.

Hoppes, John, *Lean Manufacturing Practices in the Defense Aircraft Industry*, S.M. Thesis, Sloan School of Management, Massachusetts Institute of Technology, 1995.

Iizuka, Katsuhiro, Hidetaka Nakao, Kaoru Okuyama, Seiji Honda, and Minoru Noumaru, "The Development of Intelligent Body Assembly System," in *Japan/USA Symposium on Flexible Automation*, v. 2, 1992.

Itoh, Masters Thesis, Nagoya University, Japan, 1968.

Jackson, Paul (editor in chief), *Jane's All the World's Aircraft*, Jane's Information Group, Alexandria, VA, 1995.

Ju, Xiang, *Springback Under Combined Stretching and Bending in Sheet Metal Forming*, S.M. Thesis, Engineering Mechanics, Michigan Technological University, 1985.

Kandebo, Stanley W., "F/A-18E/F to Exploit Flexible Tooling," in *Aviation Week & Space Technology*, August 22, 1994, p. 53.

Keeler, S. P., "Statistical Deformation Control for SPQC Monitoring of Sheet Metal Forming," in *SAE Transactions*, paper # 850278, Society of Automotive Engineers, Inc., Warrendale, PA, 1985.

Kelley, Maryellen R. and Todd A. Watkins, "The Myth of the Specialized Military Contractor," in *Technology Review*, April, 1995, pp. 53-58.

Kirkwood, Brad L., *The Creation and Use of a Manufacturing Process Development Strategy in the Aerospace Industry*, S.M. Thesis, Department of Mechanical Engineering and Sloan School of Management, Massachusetts Institute of Technology, 1992.

Knight, Thomas Patrick, *Inventory Reduction in a Large Job Shop*, S.M. Thesis, Department of Mechanical Engineering and Sloan School of Management, Massachusetts Institute of Technology, 1992.

Kobayashi, Shiro, Soo-Ik Oh, and Taylan Altan, *Metal Forming and the Finite-Element Method*, Oxford University Press, New York, 1989.

Koonmen, James P., *Implementing Precision Assembly Techniques in the Commercial Aircraft Industry*, S.M. Thesis, Department of Aeronautics and Astronautics and Sloan School of Management, Massachusetts Institute of Technology, 1994.

Kudo, Hideaki, "Towards Net-Shape Forming," in *Journal of Materials Processing Technology*, v. 22, 1990, pp. 307-342.

Lange, Kurt (Editor), *Handbook of Metal Forming*, McGraw-Hill Book Company, New York, 1985.

Lee, Deishin, *Reduction of Variability in Aircraft Manufacturing Using Photogrammetry as an Inspection Tool*, S.M. Thesis, Mechanical Engineering and Sloan School of Management, Massachusetts Institute of Technology, 1992.

Lee, Deishin, *Reduction Of Variability in Aircraft Manufacturing Using Photogrammetry as an Inspection Tool*, S.M. Thesis, Department of Mechanical Engineering and Sloan School of Management, Massachusetts Institute of Technology, 1992.

Lundstrom, Mark E., *Inventory And Flowtime Reduction Through Integrating An Aerospace Manufacturing System*, S.M. Thesis, Department of Aeronautics and Astronautics and the Sloan School of Management, Massachusetts Institute of Technology, 1993.

Luxon, J. T., Parker, D. E., Plotkowski, P. D., *Lasers In Manufacturing*, IFS (Publications) Ltd., Bedford, UK, and Springer-Verlag, Berlin, 1987.

Lysov, M. I. and L. G. Komarova, "Calculation of Stress-Strain State in Stretch Forming of Sheet Parts With Differential Elongation," in *Izvestiya VUZ. Aviatsionnaya Tekhnika* [English Translation], v. 30, n. 2, 1987, pp. 55-60 [68-73].

Lysov, M. I., V. A. Gorbunov, and N. M. Bodunov, "On Determining the Load Parameters in Profile Shaping by the Stretch-Wrap Forming Method," in *Izvestiya VUZ. Aviatsionnaya Tekhnika* [English Translation], v. 28, n. 4, 1985, pp. 87-89 [84-86].

Lysov, M. I., V. A. Gorbunov, N. M. Bodunov, and G. V. Druzhinin, "An Analytical Method for Calculation of the Form Parameters in an Elastoplastic Bending With Distension of Profile-Shaped Articles," in *Izvestiya VUZ. Aviatsionnaya Tekhnika* [English Translation], v. 30, n. 3, 1987, pp. 42-47 [51-56].

Marschner, C. F., *Aircraft Assembly*, Pitman Publishing Corporation, New York, NY, 1942.

Maskow, Jürgen, "Airbus-Assembly Concepts to Improve Productivity and Flexibility in Aircraft Construction," in proceedings from the *15th Congress of the International Council of the Aeronautical Sciences*, v. 1, International Council of the Aeronautical Sciences, 1986, pp. 227-231.

McAfee, Andrew Paul, *On The Appropriate Level Of Automation For Advanced Structural Composites Manufacturing For Commercial Aerospace Applications*, S.M. Thesis, Department of Mechanical Engineering and Sloan School of Management, Massachusetts Institute of Technology, 1990.

Montgomery, Douglas C. *Introduction to Statistical Quality Control*, John Wiley & Sons, New York, 1985.

Moore, Harry and Donald Kibbey, *Manufacturing: Materials and Processes*, Richard D. Irwin, Inc., IL, 1965.

Mroz, Z., "On the Description of Anisotropic Workhardening," in *Journal of the Mechanics and Physics of Solids*, v. 15, 1967, pp. 163-175.

Norris, Jeff, sketches, cost analysis, and description, Vought proprietary, 1993.

Northrop Grumman, *Reconfigurable Tooling for Flexible Fabrication, 4th Quarterly & 2nd Annual Review*, Northrop Grumman Aircraft Division, Dallas, TX, 1996.

Oding, S. S., "Control of Shaping of Double-Curvature Skins on Stretch-Forming Equipment With Programmed Control. II," in *Izvestiya VUZ. Aviatsionnaya Tekhnika* [English Translation], v. 30, n. 4, 1987b, pp. 39-43 [44-48].

Oding, S. S., "Controlling the Formation of Double Curvature Skin Elements on a Program-Controlled Stretch Former. I," in *Izvestiya VUZ. Aviatsionnaya Tekhnika* [English Translation], v. 30, n. 3, 1987a, pp. 47-51 [57-61].

Olsen, Howard B., "A Flexible Robotic Work Cell fo the Assembly of Airframe Components," in *Proceedings: 1990 IEEE International Conference on Robotics and Automation*, v. 2, IEEE Computer Society Press, 1990, pp. 1278-1283.

Papazian, John, *Results of tensile test experiments on aluminum*, internal document, Northrop Grumman, 1991.

Parkinson, H., *Engineering and Aircraft Limits Fits and Tolerances*, Sir Isaac Pitman & Sons, LTD., London, 1942.

Parris, Andrew, *A Comparison of Manufacturing Process Control Strategies for Quality Improvement*, S.M. Thesis, Department of Mechanical Engineering, Massachusetts Institute of Technology, 1993.

Phadke, Madhav S., *Quality Engineering Using Robust Design*, P T R Prentice Hall, Englewood Cliffs, New Jersey, 1989.

Queener, D. A. and R. J. De Angelis, in *ASM Transactions Quarterly (American Society for Metals)*, 61, 1968, pp. 757-768.

Sa, Chung-Yeh, "Sensitivity of Sheet Metal Forming Parameters," in *SAE 1989 Transactions, Journal of Materials and Manufacturing*, section 5, v. 98, 1989.

Sekine, Yoshitada, Shinji Koyama, and Hidetoshi Imazu, "Nissan's New Production System: Intelligent Body Assembly System," in (*Journal of Materials and Manufacturing*) *SAE Transactions*, Section 5, v. 100, SAE, Warrendale, PA, 1991.

Shiba, Shoji, Alan Graham, and David Walden, *A New American TQM*, Productivity Press, Portland, Oregon, 1993.

Shingo, Shigeo. Zero Quality Control (Source Inspection and the Poka-yoke System), Productivity Press, Oregon, 1986.

Smith, Bruce, Paul Proctor, and Pierre Sparaco, "Airframers Pursue Lower Aircraft Costs," in *Aviation Week & Space Technology*, September 5, 1994, pp. 57-58.

Swift, H. W., "Plastic Bending Under Tension," in *Engineering*, v. 166, 1948, pp. 333-335 & 357-359.

Taylor, Wayne A., *Optimization and Variation Reduction in Quality*, McGraw-Hill, Inc., New York, 1991.

Thornton, Peter A. and Vito J. Colangelo, *Fundamentals of Engineering Materials*, Prentice-Hall, Inc., Englewood Cliffs, NJ, 1985.

Tozawa, Y., in *Journal of Mechanical Society* (Kikai Gakkai Shi), v. 68, n. 559, 1965, p. 1090 (in Japanese).

Tozawa, Y., "Dynamics of Springback," in *Journal of Japan Society for Technology of Plasticity* (*Sosei To Kako*), v. 18, n. 202, 1977, pp. 953-963 (in Japanese).

Tozawa, Y., "Plastic Deformation Behavior Under Conditions of Combined Stress," in *Mechanics of Sheet Metal Forming*, from the Symposium on Mechanics of Sheet Metal Forming, edited by Koistinen and Wang, Plenum Press, New York, 1978.

Tozawa, Yasuhisa, "Forming Technology for Raising the Accuracy of Sheet-Formed Products," in *Journal of Materials Processing Technology*, v. 22, 1990, pp. 343-351.

Treuting, R. G. And W. T. Read, Jr., "A Mechanical Determination of Biaxial Residual Stress in Sheet Metals," in *Journal of Applied Physics*, v. 22, 1951, pp. 130-134.

Udin, M. Nasim (editor), *Body Assembly & Manufacturing proceedings of the 1994 International Body Engineering Conference*, IBEC, Ltd. Publications, Warren, MI, 1994.

Ueda, Masanobu, Keii Ueno, and Masaro Kobayashi, "A Study of Springback in the Stretch Bending of Channels," in *Journal of Mechanical Working Technology*, v. 5, 1981, pp. 163-179.

Umehara, Yuji, "Technologies for the More Precise Press-Forming of Automobiles," in *Journal of Materials Processing Technology*, v. 22, 1990, pp. 239-256.

vanDer Muelen, Jacob A., *The Politics of Aircraft: Building and American Military Industry*, University Press of Kansas, 1991.

Wang, Chuanto, *Mechanics of Bending, Flanging, and Deep Drawing and a Computer-Aided Modeling System for Predictions of Strain, Fracture, Wrinkling and Springback in Sheet Metal Forming*, Ph.D. Thesis, Department of Industrial and Systems Engineering, Ohio State University, 1993.

Wenstrup, David J., *Material Identification and Tracking in Manufacturing*, S.M. Thesis, Department of Electrical Engineering and Sloan School of Management, Massachusetts Institute of Technology, 1991.

Wilson, D. V., "Aluminum Versus Steel in the Family Car—The Formability Factor," in *Journal of Mechanical Working Technology*, v. 16, 1988, pp. 257-277.

Womak, James P., Daniel T. Jones, and Daniel Roos *The Machine That Changed The World*, Rawson Associates, New York, 1990.

REFERENCES CITED IN THESIS PLUS OTHERS, GROUPED BY TOPIC

General

Allen, Donald R., "Process Control in Stamping Lines," in *SAE Transactions*, v. 98, section 5, paper # 890343, Society of Automotive Engineers, Inc., Warrendale, PA, pp. 189-195, 1989.

Alting, Leo, *Manufacturing Engineering Processes*, English version edited by Boothroyd, Marcel Dekker, Inc., New York, 1982.

Anonymous, "Closing the Bending Loop," in *Manufacturing Engineering*, April, 1995.

ASTM, *Standard Test Methods of Tension Testing Wrought and Cast Aluminum- and Magnesium-Alloy Products*, Specification B557, American Society for Testing and Materials, 1994.

Boeing, *Hardware Variability Control*, for internal use, Boeing Commercial Airplane Group, Wichita Division, 1994.

Cunningham, Timothy W., Ramakrishna Mantripragada, Don J. Lee, Anna C. Thornton, Daniel E. Whitney, "Definition, Analysis, and Planning of a Flexible Assembly Process," submitted for special session on *Assembly Modeling and Its Application for Concurrent Engineering*, 1996. [???]

Cutler, John. *Understanding Aircraft Structures*, second edition, Blackwell Scientific Publications, Oxford, UK, 1992.

Gillespie, LaRoux K. (editor), *Troubleshooting Manufacturing Processes*, fourth edition, Society of Manufacturing Engineers, 1988.

Hooper, W. H. and W. M. MacFarlane, "Stretch Forming of Pre-Sculptured Gore Panels for the External Tank," in *Man's Presence in Space* from the 3rd Annual AIAA/GNOS Aerospace Technology Symposium, (A86-32931) 1985.

Hoppes, John, *Lean Manufacturing Practices in the Defense Aircraft Industry*, S.M. Thesis, Sloan School of Management, Massachusetts Institute of Technology, 1995.

Kandebo, Stanley W., "F/A-18E/F to Exploit Flexible Tooling," in *Aviation Week & Space Technology*, August 22, 1994, p. 53.

Keeler, S. P., "Statistical Deformation Control for SPQC Monitoring of Sheet Metal Forming," in *SAE Transactions*, paper # 850278, Society of Automotive Engineers, Inc., Warrendale, PA, 1985.

Kelley, Maryellen R. and Todd A. Watkins, "The Myth of the Specialized Military Contractor," in *Technology Review*, April, 1995, pp. 53-58.

Kudo, Hideaki, "Towards Net-Shape Forming," in *Journal of Materials Processing Technology*, v. 22, 1990, pp. 307-342.

Luxon, J. T., Parker, D. E., Plotkowski, P. D., *Lasers In Manufacturing*, IFS (Publications) Ltd., Bedford, UK, and Springer-Verlag, Berlin, 1987.

Marschner, C. F., *Aircraft Assembly*, Pitman Publishing Corporation, New York, NY, 1942.

Moore, Harry and Donald Kibbey, *Manufacturing: Materials and Processes*, Richard D. Irwin, Inc., IL, 1965.

Norris, Jeff, sketches, cost analysis, and description, Vought proprietary, 1993.

Parkinson, H., *Engineering and Aircraft Limits Fits and Tolerances*, Sir Isaac Pitman & Sons, LTD., London, 1942.

Parris, Andrew, *A Comparison of Manufacturing Process Control Strategies for Quality Improvement*, S.M. Thesis, Department of Mechanical Engineering, Massachusetts Institute of Technology, 1993.

Sa, Chung-Yeh, "Sensitivity of Sheet Metal Forming Parameters," in *SAE 1989 Transactions, Journal of Materials and Manufacturing*, section 5, v. 98, 1989.

Smith, Bruce, Paul Proctor, and Pierre Sparaco, "Airframers Pursue Lower Aircraft Costs," in *Aviation Week & Space Technology*, September 5, 1994, pp. 57-58.

Tozawa, Yasuhisa, "Forming Technology for Raising the Accuracy of Sheet-Formed Products," in *Journal of Materials Processing Technology*, v. 22, 1990, pp. 343-351.

Udin, M. Nasim (editor), *Body Assembly & Manufacturing proceedings of the 1994 International Body Engineering Conference*, IBEC, Ltd. Publications, Warren, MI, 1994.

Umehara, Yuji, "Technologies for the More Precise Press-Forming of Automobiles," in *Journal of Materials Processing Technology*, v. 22, 1990, pp. 239-256.

vanDer Muelen, Jacob A., *The Politics of Aircraft: Building and American Military Industry*, University Press of Kansas, 1991.

Vision systems and flexible and automated assembly

Amirat, M. Y., J. Pontnau, and F. Artigue, "A Three-Dimensional Measurement System for Robot Applications," in *Journal of Intelligent and Robotic Systems*, v. 9, 1994, pp. 291-299.

Andreasen, M. Myrup, and Ahm, T., *Flexible Assembly Systems*, IFS Publications, UK, and Springer-Verlag, New York, 1988.

Atkins, D. E. and R. A. Volz, *Flexible Automatic Discrete Parts Assembly*, final report, available from the Manufacturing Technology Directorate, Wright Research and Development Center, Air Force Systems Command, Wright-Patterson Air Force Base, Ohio, report number WRDC-TR-89-8037, 1989.

Barrie, Douglas, "Assembling the Future," in *Flight International*, 10-16 June, 1992, pp. 50-52.

Braun, R. and R. Zanella, *Flexible Assembly Subsystems*, phase I final report, available from the Manufacturing Technology Directorate, Wright Research and Development Center, Air Force Systems Command, Wright-Patterson Air Force Base, Ohio, procurement instrument identification number F33615-84-C-5048, 1986.

Braun, R. and R. Zanella, *Flexible Assembly Subsystems*, interim technical report, available from the Manufacturing Technology Directorate, Wright Research and Development Center, Air Force Systems Command, Wright-Patterson Air Force Base, Ohio, procurement instrument identification number F33615-84-C-5048, 1988.

Brem, Lawrence and N. Nandhakumar, "A Machine Vision System for Enhancing Teleoperation of an Industrial Robot," in *Machine Vision and Applications*, v. 7, 1994, pp. 187-198.

Buitrago Barrientos, Jaime Humberto, *Design of Robot-Operated Modular and Adaptable Fixturing Systems*, S.M. Thesis, Mechanical Engineering, Massachusetts Institute of Technology, 1988.

Derby, S., "Precision Robotic Assembly Using The Clamp Robotic End Effector," in *Flexible Assembly Systems—1989*, edited by D. P. Sathyadev, conference proceedings, The American Society of Mechancial Engineers, 1989, pp. 43-7.

Fields, Antony Jonathan, *The Analysis and Design of a Flexible Robotic Fixturing and Drilling System*, S.M. Thesis, Mechanical Engineering, Massachusetts Institute of Technology, 1985.

Glascock, B., B. Sarh, O. Weingart, and K. Wright, *Flexible Assembly Subsystems*, final report, available from the Manufacturing Technology Directorate, Wright Research and Development Center, Air Force Systems Command, Wright-Patterson Air Force Base, Ohio, report number WRDC-TR-89-8033, 1989.

Goodman, Harvey, "Flexible Tooling for Flexible Assembly," in *Automation*, September, 1990a, pp. 42-43.

Goodman, Harvey, "Assembly Cell Speeds Riveting," in *Tooling & Production*, December, 1990b, pp. 50-53.

Gordon, Steven, *Automated Assembly Using Feature Localization*, Ph.D. Thesis, Mechanical Engineering, Massachusetts Institute of Technology, 1987.

Gordon, S. J., "Elimination of Customized Fixtures Through High-Performance 3D Vision," in *Flexible Assembly Systems—1989*, edited by D. P. Sathyadev, conference proceedings, The American Society of Mechancial Engineers, 1989, pp. 9-14.

Hawthorne, John, "From ASAT to Masterhead™," an *SME Technical Paper*, AD89-636, Society of Manufacturing Engineers, Dearborn, Michigan, 1989.

Iizuka, Katsuhiro, Hidetaka Nakao, Kaoru Okuyama, Seiji Honda, and Minoru Noumaru, "The Development of Intelligent Body Assembly System," in *Japan/USA Symposium on Flexible Automation*, v. 2, 1992.

Lee, Deishin, *Reduction of Variability in Aircraft Manufacturing Using Photogrammetry as an Inspection Tool*, S.M. Thesis, Mechanical Engineering and Sloan School of Management, Massachusetts Institute of Technology, 1992.

Lindsay, K., *Automated Airframe Assembly Program*, final report, available from the Manufacturing Technology Directorate, Wright Research and Development Center, Air Force Systems Command, Wright-Patterson Air Force Base, Ohio, report number WRDC-TR-92-8019, 1992.

Liou, F. W., Krishnamurthy, K., Mehta, M. B., Liang, H. T., and Chien, J. H., "Design Of A Flexible Fixture For Flexible Assembly—A Case Study," in *Flexible Assembly Systems—1989*, edited by D. P. Sathyadev, conference proceedings, The American Society of Mechancial Engineers, 1989, pp. 85-91.

Liu, Wing Shuen, *Computer-Aided Analysis of Reconfigurable Sheet Metal Fixturing System for Robotic Drilling*, S.M. Thesis, Mechanical Engineering, Massachusetts Institute of Technology, 1986.

Luxon, J. T., Parker, D. E., Plotkowski, P. D., *Lasers In Manufacturing*, IFS (Publications) Ltd., Bedford, UK, and Springer-Verlag, Berlin, 1987.

Olsen, Howard B., "A Flexible Robotic Work Cell fo the Assembly of Airframe Components," in *Proceedings: 1990 IEEE International Conference on Robotics and Automation*, v. 2, IEEE Computer Society Press, 1990, pp. 1278-1283.

Maskow, Jürgen, "Airbus-Assembly Concepts to Improve Productivity and Flexibility in Aircraft Construction," in proceedings from the *15th Congress of the International Council of the Aeronautical Sciences*, v. 1, International Council of the Aeronautical Sciences, 1986, pp. 227-231.

Sathyadev, D. P. (editor), *Flexible Assembly Systems*, conference proceedings, The American Society of Mechanical Engineers, 1989. (Note that this conference and the proceedings continued for at least two more years)

Sekine, Yoshitada, Shinji Koyama, and Hidetoshi Imazu, "Nissan's New Production System: Intelligent Body Assembly System," in (*Journal of Materials and Manufacturing*) *SAE Transactions*, Section 5, v. 100, SAE, Warrendale, PA, 1991.

Stauffer, Lt. Robert J., *Automated Assembly Center*, a program administered by the Manufacturing Technology Directorate at Wright Laboratory (AFMC), Wright Patterson AFB, document identification: N93-32123, 1993.

Vincze, M., J. P. Prenniger, and H. Gander, "A Laser Tracking System to Measure Position and Orientation of Robot End Effectors Under Motion," in *The International Journal of Robotics Research*, v. 13, n. 4, August, 1994, pp. 305-314.

Tolerances and tolerancing

Anderson, Lindsay Norman, *Assembly Process Development for Commercial Aircraft Using Computer-Aided Tolerance Analysis Tools*, S.M. Thesis, Materials Science and Engineering and Sloan School of Management, 1993.

Anonymous (Select Panel on Research Opportunities in Mechanical Tolerancing), *Research Needs and Technological Opportunities in Mechanical Tolerancing*, American Society of Mechanical Engineers, 1988.

Bjørke, Øyvind, *Computer-Aided Tolerancing*, second edition, American Society of Mechanical Engineers, 1989.

Buckingham, Earle, *Principles of Interchangeable Manufacturing*, second edition, The Industrial Press, New York, 1941.

Lean, TQM, and SPC books

Montgomery, Douglas C. *Introduction to Statistical Quality Control*, John Wiley & Sons, New York, 1985.

Phadke, Madhav S., *Quality Engineering Using Robust Design*, P T R Prentice Hall, Englewood Cliffs, New Jersey, 1989.

Shiba, Shoji, Alan Graham, and David Walden, *A New American TQM*, Productivity Press, Portland, Oregon, 1993.

Shingo, Shigeo. Zero Quality Control (Source Inspection and the Poka-yoke System), Productivity Press, Oregon, 1986.

Taylor, Wayne A., *Optimization and Variation Reduction in Quality*, McGraw-Hill, Inc., New York, 1991.

Womak, James P., Daniel T. Jones, and Daniel Roos *The Machine That Changed The World*, Rawson Associates, New York, 1990.

About aluminum and aluminum properties

Aluminum Company of America (ALCOA), *Forming ALCOA Aluminum*, ALCOA, ALCOA Center, Pennsylvania, 1974.

Davis, J. R. (editor), *ASM Specialty Handbook: Aluminum and Aluminum Alloys*, ASM International, Ohio, 1993.

Guangnan, Chen, Shen Huan, Hu Shiguang, and Bernard Baudelet, "Roughening of the Free Surfaces of Metallic Sheets During Stretch Forming," in *Materials Science and Engineering*, A128, 1990, pp. 33-38.

Hatch, John E. (editor), *Aluminum: Properties and Physical Metallurgy*, published the American Society for Metals, Metals Park, Ohio, 1984.

Holt, R. A. and C. J. Warren, "C188 Laboratory Formability Testing: Preliminary Results and Analysis," Alcoa Technical Center private report, Aluminum Company of America, 1994.

Lee, E. W. and W. E. Frazier, "The Effect of Stretch on the Microstructure and Mechanical Properties of 2090 Al-Li," in *Scripta METALLURGICA*, v. 22, 1988, pp. 53-57.

Northrop Grumman, *Reconfigurable Tooling for Flexible Fabrication, 4th Quarterly & 2nd Annual Review*, Northrop Grumman Aircraft Division, Dallas, TX, 1996.

Papazian, John, *Results of tensile test experiments on aluminum*, internal document, Northrop Grumman, 1991.

Thornton, Peter A. and Vito J. Colangelo, *Fundamentals of Engineering Materials*, Prentice-Hall, Inc., Englewood Cliffs, NJ, 1985.

Warren, C. J. and R. J. Rioja, "Forming Characteristics and Post-Formed Properties of Al-Li Alloys," in *Aluminum-Lithium Alloys: Proceedings of the Fifth International Aluminum-Lithium Conference*, v. 1, Materials and Component Engineering Publications, Birmingham, UK, 1989, pp. 417-429.

Wilson, D. V., "Aluminum Versus Steel in the Family Car—The Formability Factor," in *Journal of Mechanical Working Technology*, v. 16, 1988, pp. 257-277.

Selected MIT Theses on the aircraft industry

Anderson, Lindsay Norman, *Assembly Process Development for Commercial Aircraft Using Computer-Aided Tolerance Analysis Tools*, S.M. Thesis, Department of Materials Science and Engineering and Sloan School of Management, Massachusetts Institute of Technology, 1993.

Bartelson, Kevin D., *Analysis And Redesign Of The Production System Structure For 757 and 737 Aircraft Doors*, S.M. Thesis, Department of Mechanical Engineering and Management, Massachusetts Institute of Technology, 1993.

Behnen, Stephen W., *Achieving Competitive Advantage: an Aerospace Case Study*, S.M. Thesis, Sloan School of Management, Massachusetts Institute of Technology, 1987.

Coleman, Robert Mark, *Effects of Design, Manufacturing Processes, and Operations Management on the Assembly of Aircraft Composite Structure*, S.M. Thesis, Department of Aeronautics and Astronautics and Sloan School of Management, Massachusetts Institute of Technology, 1991.

Denktsis, Georgia F., *Part Cost Computer Modeling of Job Shops As A Function Of Manufacturing Parameters*, S.M. Thesis, Department of Aeronautics and Astronautics, Massachusetts Institute of Technology, 1990.

Field, John Douglas, *A Rule-Based Design System for Aircraft Engine Tooling*, S.M. Thesis, Department of Mechanical Engineering and Sloan School of Management, Massachusetts Institute of Technology, 1992.

Finan, Jeffrey John, *System Dynamics Analysis Of An Ordering System Used For Commercial Aircraft Manufacture*, S.M. Thesis, Department of Aeronautics and Astronautics, and Sloan School of Management, Massachusetts Institute of Technology, 1993.

Kirkwood, Brad L., *The Creation and Use of a Manufacturing Process Development Strategy in the Aerospace Industry*, S.M. Thesis, Department of

Mechanical Engineering and Sloan School of Management, Massachusetts Institute of Technology, 1992.

Knight, Thomas Patrick, *Inventory Reduction in a Large Job Shop*, S.M. Thesis, Department of Mechanical Engineering and Sloan School of Management, Massachusetts Institute of Technology, 1992.

Koonmen, James P., *Implementing Precision Assembly Techniques in the Commercial Aircraft Industry*, S.M. Thesis, Department of Aeronautics and Astronautics and Sloan School of Management, Massachusetts Institute of Technology, 1994.

Lee, Deishin, *Reduction Of Variability in Aircraft Manufacturing Using Photogrammetry as an Inspection Tool*, S.M. Thesis, Department of Mechanical Engineering and Sloan School of Management, Massachusetts Institute of Technology, 1992.

Lundstrom, Mark E., *Inventory And Flowtime Reduction Through Integrating An Aerospace Manufacturing System*, S.M. Thesis, Department of Aeronautics and Astronautics and the Sloan School of Management, Massachusetts Institute of Technology, 1993.

MacDuffie, John Paul, *Beyond Mass Production: Flexible Production Systems and Manufacturing Performance in the World Auto Industry*, Ph.D. Thesis, Sloan School of Management, Massachusetts Institute of Technology, 1991.

McAfee, Andrew Paul, *On The Appropriate Level Of Automation For Advanced Structural Composites Manufacturing For Commercial Aerospace Applications*, S.M. Thesis, Department of Mechanical Engineering and Sloan School of Management, Massachusetts Institute of Technology, 1990.

Raymond, Arthur James, *Applicability of Toyota Production System to Commercial Airplane Manufacturing*, S.M. Thesis, Department of Mechanical Engineering and Sloan School of Management, Massachusetts Institute of Technology, 1992.

Shanahan, Patrick Michael, *Manufacturing System Performance a Case Analysis of Boeing Sheet Metal Production*, S.M. Thesis, Department of Mechanical Engineering and Sloan School of Management, Massachusetts Institute of Technology, 1991.

Shipp, Christine Temple, *Cost Effective Use Of Advanced Composite Materials In Commercial Aircraft Manufacture*, S.M. Thesis, Department of Mechanical Engineering and Management, Massachusetts Institute of Technology, 1990.

Wenstrup, David J., *Material Identification and Tracking in Manufacturing*, S.M. Thesis, Department of Electrical Engineering and Sloan School of Management, Massachusetts Institute of Technology, 1991.

Whiting, Kathryn Lee, *Reducing the Flowtime of a Manufacturing Order Release Process*, S.M. Thesis, Department of Mechanical Engineering and Sloan School of Management, Massachusetts Institute of Technology, 1992.

Books on plastic deformation and metal forming

Alexander, J. M. and J. S. Gunasekera, *Strength of Materials Volume 2: Advanced Theory and Applications*, Ellis Horwood Limited, New York, 1991.

Altan, Taylan, Soo-Ik Oh, and Harold L. Gegel, *Metal Forming, Fundamentals and Applications*, American Society for Metals, Metals Park, Ohio, 1983.

American Society for Metals, *Cold Working of Metals* (from a seminar coordinated by M. Gensamer), American Society for Metals, Cleveland, Ohio, 1949.

Cook, Nathan H. *Manufacturing Analysis*, Addison-Wesley Publishing Company, Inc., Reading, Massachusetts, 1966.

Hibbeler, R. C., *Mechanics of Materials*, Macmillan Publishing Company, New York, 1991.

Hill, R., The *Mathematical Theory of Plasticity*, Oxford University Press, Oxford, 1950.

Lange, Kurt (Editor), *Handbook of Metal Forming*, McGraw-Hill Book Company, New York, 1985.

Kobayashi, Shiro, Soo-Ik Oh, and Taylan Altan, *Metal Forming and the Finite-Element Method*, Oxford University Press, New York, 1989.

Mansfield, E.H., *The Bending and Stretching of Plates*, second edition, Cambridge University Press, Cambridge, 1989.

Slater, R. A. C., *Engineering Plasticity*, John Wiley & Sons, New York, 1977.

Thomsen, Erich G., Charles T. Wang, and Shiro Kobayashi, *Mechanics of Plastic Deformation in Metal Processing*, The Macmillan Company, New York, 1965.

Timoshenko, S., *Strength of Materials, Part II, Advanced Theory and Problems*, third edition, D. Van Nostrand Company, Inc., Princeton, New Jersey, 1956.

Articles on mechanics of bending and stretch forming

Baba, Akijiro and Yasuhisa Tozawa, "Effect of Tensile Force in Stretch-Forming Process on the Springback," in *Bulletin of the JSME* (Japan Society of Mechanical Engineers), v. 7, n. 28, 1964, pp. 835-843.

Chu, Chin-Chan, "A Three-Dimensional Model of Anisotropic Hardening in Metals and its Application to the Analysis of Sheet Metal Formability," in *Journal of the Mechanics and Physics of Solids*, v. 32, n. 3, 1984, pp. 197-212.

Chu, Chin-Chan, "Elastic-Plastic Springback of Sheet Metals Subjected to Complex Plane Strain Bending Histories," in *International Journal of Solids and Structures*, v. 22, n. 10, 1986, pp. 1071-1081.

Chu, Chin-Chan, "The Effect of Restraining Force on Springback," in *International Journal of Solids Structures*, v. 27, n. 8, 1991, pp. 1035-1046.

Clairmont, Kerry J., *Precision Sheet Metal Fabrication of the Press Brake in Fabricating Sheet Metal Products*, Thesis, University of Wisconsin-Stout, 1972.

Dadras, P. and S. A. Majlessi, "Plastic Bending of Work Hardening Materials," in *Journal of Engineering for Industry, Transactions of the ASME*, v. 104, 1982, pp. 224-230.

Davies, R. G., C. C. Chu, and Y. C. Liu, "Recent Progress on the Understanding of Springback," in *Computer Modeling of Sheet Metal Forming Process; Theory, Verification and Application*, edited by N. -M. Wang and S. C. Tang, 1985, pp. 259-271.

Duncan, J. L. and J. E. Bird, "Die Forming Approximations for Aluminium Sheet," in *Sheet Metal Industries*, v. 55, n. 9, September, 1978, pp. 1015-1025.

El-Domiaty, Aly and A. H. Shabaik, "Bending of Work-Hardening Metals Under the Influence of Axial Load," in *Journal of Mechanical Working Technology*, v. 10, 1984, pp. 57-66.

El-Domiaty, Aly, "Stretch Forming of Beams of Non-Uniform Section," in *Journal of Materials Processing Technology*, v. 22, 1990, pp. 21-28.

El-Megharbel A., A. El-Domiaty, and M. Shaker, "Springback and Residual Stresses After Stretch Bending of Workhardening Sheet Metal," in *Journal of Materials Processing Technology*, v. 24, 1990, pp. 191-200.

Ewert, Lee R., Sumner B. Sargent, and Walter Leodolter, *US Patent Number 4,989,439*, February 5, 1991.

Gardiner, F. J., *Transactions of the American Society of Mechanical Engineers*, 79, 1957, pp. 1-7.

Hayward, Susan P. *Analysis of Dimensional Variance in Stretch Draw Forming*, S.M. Thesis, Michigan Technological University, 1992.

Hessami, M. A. and W. Y. D. Yuen, "Residual Stresses Induced by Stretch-Bending," in proceedings of the *Fourth International Conference on Manufacturing Engineering*, Brisbane, 1988, pp. 78-83.

Ingvarsson, Lars, "Cold-Forming Residual Stresses in Thin-Walled Structures," in *??*, 19??, pp. 575-587.

Ingvarsson, Lars, "Cold-Forming Residual Stresses, Effect on Buckling," in *Proceedings of the 3rd International Spec. Conference on Cold Formed Steel Structures (Research and Developments in Cold-Formed Steel Design)*, 1975, pp. 85-119.

Itoh, Masters Thesis, Nagoya University, Japan, 1968.

Johnson, W. and T. X. Yu, "On the Range of Applicability of Results for the Springback if an Elastic/Perfectly Plastic Rectangular Plate After Subjecting it to Biaxial Pure Bending—II," in *International Journal of Mechanical Science*, v. 23, n. 10, 1981, pp. 631-637.

Johnson, W. and T. X. Yu, "Springback After the Biaxial Elastic-Plastic Pure Bending of a Rectangular Plate—I," in *International Journal of Mechanical Science*, v. 23, n. 10, 1981, pp. 619-630.

Ju, Xiang, *Springback Under Combined Stretching and Bending in Sheet Metal Forming*, S.M. Thesis, Engineering Mechanics, Michigan Technological University, 1985.

Makinouchi, A., "Elastic-Plastic Stress Analysis of Bending and Hemming of Sheet Metal," in *Computer Modeling of Sheet Metal Forming Process; Theory, Verification and Application*, edited by N. -M. Wang and S. C. Tang, 1985, pp. 161-176.

Monfort, G. and A. Bragard, "A Simple Model of Shape Errors in Forming and its Application to the Reduction of Springback," in *Computer Modeling of Sheet Metal Forming Process; Theory, Verification and Application*, edited by N. -M. Wang and S. C. Tang, 1985, pp. 273-297.

Mroz, Z., "On the Description of Anisotropic Workhardening," in *Journal of the Mechanics and Physics of Solids*, v. 15, 1967, pp. 163-175.

Queener, D. A. and R. J. De Angelis, in *ASM Transactions Quarterly (American Society for Metals)*, 61, 1968, pp. 757-768.

Rolf, R. L. and E. P. Patrick, "Bending and Springback of Aluminum Alloy Sheet and Plate," in *Formability Topics—Metallic Materials, ASTM STP 647*, B. A. Niemeier, A. K. Schmeider, and J. R. Newby, editors, American Society for Testing and Materials, Philadelphia, PA, 1978, pp. 65-85.

Sanchez, Luis Rafael, *A General Computer Model for Plane Strain Sheet Forming Under Combined Bending and Pulling and Its Application to the Flow of Sheet Between Drawbeads*, Ph.D. Thesis, Michigan Technological University, 1987.

Schroeder, W., "Mechanics of Sheet-Metal Bending," in *Transactions of the American Society of Mechanical Engineers*, v. 65, 817-27, 1943.

Shaffer, B. W. and R. N. House, Jr., "The Elastic-Plastic Stress Distribution Within a Wide Curved Bar Subjected to Pure Bending," in *ASME Journal of Applied Mechanics*, v. 22, 1955, pp. 305-310.

Swift, H. W., "Plastic Bending Under Tension," in *Engineering*, v. 166, 1948, pp. 333-335 & 357-359.

Tozawa, Y., in *Journal of Mechanical Society* (Kikai Gakkai Shi), v. 68, n. 559, 1965, p. 1090 (in Japanese).

Tozawa, Y., "Dynamics of Springback," in *Journal of Japan Society for Technology of Plasticity* (*Sosei To Kako*), v. 18, n. 202, 1977, pp. 953-963 (in Japanese).

Tozawa, Y., "Plastic Deformation Behavior Under Conditions of Combined Stress," in *Mechanics of Sheet Metal Forming*, from the Symposium on Mechanics of Sheet Metal Forming, edited by Koistinen and Wang, Plenum Press, New York, 1978.

Tozawa, Yasuhisa, "Forming Technology for Raising the Accuracy of Sheet-Formed Products," in *Journal of Materials Processing Technology*, v. 22, 1990, pp. 343-351.

Treuting, R. G. And W. T. Read, Jr., "A Mechanical Determination of Biaxial Residual Stress in Sheet Metals," in *Journal of Applied Physics*, v. 22, 1951, pp. 130-134.

Ueda, Masanobu, Keii Ueno, and Masaro Kobayashi, "A Study of Springback in the Stretch Bending of Channels," in *Journal of Mechanical Working Technology*, v. 5, 1981, pp. 163-179.

Verguts, H. and R. Sowerby, "The Pure Plastic Bending of Laminated Sheet Metals," in *International Journal of Mechanical Science*, v. 17, 1975, pp. 31-51.

Wang, Chuanto, *Mechanics of Bending, Flanging, and Deep Drawing and a Computer-Aided Modeling System for Predictions of Strain, Fracture, Wrinkling and Springback in Sheet Metal Forming*, Ph.D. Thesis, Department of Industrial and Systems Engineering, Ohio State University, 1993.

Wenner, M. L., "On Work Hardening and Springback in Plane Strain Draw Forming," *Journal of Applied Metal Working*, v. 2, n. 4, 1983, pp. 277-287.

Woo, D. M. and J. Marshall, in *The Engineer (London)*, v. 208, pp. 135-136, 1959.

Xu, Y., L. C. Zhang, and T. X. Yu, "The Elastic-Plastic Pure Bending and Springback of L-Shaped Beams," in *International Journal of Mechanical Science*, v. 29, n. 6, 1987, pp. 524-433.

Yu, T. X. and W. Johnsen, "Influence of Axial Force on the Elastic-Plastic Bending and Springback of a Beam," in *Journal of Mechanical Working*, v. 6, 1982, pp. 5-21.

Yuen, W. Y. D., "Springback in the Stretch-Bending of Sheet Metal With Non-Uniform Deformation," in *Journal of Materials Processing*, v. 22, 1990, pp. 1-20.

Soviet articles on stretch forming

Aryshenskii, Yu. M., "Calculation of Technological Parameters of Simple Stretch-Wrap Forming," in *Izvestiya VUZ. Aviatsionnaya Tekhnika* [English Translation], v. 26, n. 2, 1983, pp. 16-20 [13-17].

Bodunov, N. M., I. M. Zakirov, M. I. Lysov, and G. V. Druzhinin, "Calculation of Parameters at Shaping the Profiled Parts by Stretching With Tension and Radial Compression," in *Izvestiya VUZ. Aviatsionnaya Tekhnika* [English Translation], v. 37, n. 3, 1994a, pp. 60-65 [61-65].

Bodunov, N. M., I. M. Zakirov, M. I. Lysov, and G. V. Druzhinin, "Approximate Method for Calculating the Working Conditions of Profiled Part Bending Process," in *Izvestiya VUZ. Aviatsionnaya Tekhnika* [English Translation], v. 37, n. 4, 1994b, pp. 93-97 [93-97].

Eliseev, V. V., "Calculation of Transitions in Stretch Forming," in *Izvestiya VUZ. Aviatsionnaya Tekhnika* [English Translation], v. 34, n. 2, 1991, pp. 108-111 [118-121].

Gorbunov, V. A. and N. M. Bodunov, "Determining the Stretch-Wrap Forming Process Load Parameters with Account for Geometric Nonlinearity," in *Izvestiya VUZ. Aviatsionnaya Tekhnika* [English Translation], v. 29, n. 1, 1986, pp. 90-93 [107-110].

Lysov, M. I., "Parametric Analysis of Thin-Walled Part Shaping Process by Plastic Stretching and Bending of a Blank With Account for the Geometric Non-Linearity," in *Izvestiya VUZ. Aviatsionnaya Tekhnika* [English Translation], v. 35, n. 1, 1992, pp. 71-77 [77-83].

Lysov, M. I., V. A. Gorbunov, and N. M. Bodunov, "On Determining the Load Parameters in Profile Shaping by the Stretch-Wrap Forming Method," in *Izvestiya VUZ. Aviatsionnaya Tekhnika* [English Translation], v. 28, n. 4, 1985, pp. 87-89 [84-86].

Lysov, M. I., V. A. Gorbunov, N. M. Bodunov, and G. V. Druzhinin, "An Analytical Method for Calculation of the Form Parameters in an Elastoplastic Bending

With Distension of Profile-Shaped Articles," in *Izvestiya VUZ. Aviatsionnaya Tekhnika* [English Translation], v. 30, n. 3, 1987, pp. 42-47 [51-56].

Lysov, M. I. and L. G. Komarova, "Calculation of Stress-Strain State in Stretch Forming of Sheet Parts With Differential Elongation," in *Izvestiya VUZ. Aviatsionnaya Tekhnika* [English Translation], v. 30, n. 2, 1987, pp. 55-60 [68-73].

Oding, S. S., "Controlling the Formation of Double Curvature Skin Elements on a Program-Controlled Stretch Former. I," in *Izvestiya VUZ. Aviatsionnaya Tekhnika* [English Translation], v. 30, n. 3, 1987a, pp. 47-51 [57-61].

Oding, S. S., "Control of Shaping of Double-Curvature Skins on Stretch-Forming Equipment With Programmed Control. II," in *Izvestiya VUZ. Aviatsionnaya Tekhnika* [English Translation], v. 30, n. 4, 1987b, pp. 39-43 [44-48].

Oding, S. S. and I. A. Alimenko, "Stretch-Wrap Forming of Multilayer Skins," in *Izvestiya VUZ. Aviatsionnaya Tekhnika* [English Translation], v. 29, n. 2, 1986, pp. 98-101 [119-123].

Oding, S. S. and L. A. Burdakova, "Shaping of Sign-Variable Curvature Skins by Stretch-Forming," in *Izvestiya VUZ. Aviatsionnaya Tekhnika* [English Translation], v. 34, n. 1, 1991, pp. 47-51 [56-61].

APPENDIX 1: HEAT TREAT BASICS AND TERMINOLOGY

The following brief tutorial is for those not familiar with aluminum heat treat and its associated terminology. The material here has been taken from Davis [1993]. Page numbers are referenced as well.

A1.1 WROUGHT ALUMINUM ALLOYS (3-4)

The first number in the alloy designation system for aluminum indicates the main alloying element. These different alloy families have different uses because of their differing properties. This is summarized in the following.

- 1*xxx* unalloyed composition
- 2*xxx* copper is principal alloying element; widely used in aircraft
- 3*xxx* manganese ...; general purpose
- 4*xxx* silicon ...; used in welding rods and brazing sheet
- 5*xxx* magnesium ...; used in marine environments
- 6*xxx* magnesium and silicon; common for architectural extrusions
- 7*xxx* zinc; high strength applications, especially aircraft
- 8*xxx* miscellaneous, including tin and lithium
- 9*xxx* reserved for future use

For example, the main alloying element in 2024 aluminum is copper, and it is one of the two alloys (the other is 7075) dealt with in this thesis.

A1.2 HEAT-TREATABLE AND NON-HEAT-TREATABLE ALLOYS (5)

Heat-treatable alloys are those that can be hardened (strengthened) by a controlled cycle of heating and cooling [including solution heat treatment, quenching, and precipitation (age) hardening]. Some alloys, usually in the 2*xxx*, 6*xxx*, and 7*xxx* series, are heat treatable. They can be further strengthened by cold working.

Non-heat-treatable alloys are hardenable by cold working, but not by heat treatment. The initial strength of these alloys, usually in the 1*xxx*, 3*xxx*, 4*xxx*, and 5*xxx* series, is provided by the hardening effect of their alloying systems.

Note that both 2024 and 7075 are heat-treatable.

A1.3 BASIC TEMPER DESIGNATIONS (19,24)

F, As Fabricated—this is applied to products shaped by cold working, hot working, or casting processes in which no special control over thermal conditions or strain hardening is employed. For wrought products, there are no mechanical property limits.

O, Annealed—O applies to wrought products that are annealed to obtain lowest-strength temper and to cast products that are annealed to improve ductility and dimensional stability. The O may be followed by a digit other than zero.

H, Strain Hardened—this indicates products that have been strengthened by strain hardening, with or without supplementary thermal treatment to produce some reduction in strength. The H is always followed by two or more digits, ...

W, Solution Heat-Treated—this is an unstable temper applicable only to alloys whose strength naturally (spontaneously) changes at room temperature over a duration of months or even years after solution heat treatment. The designation is specific only when the period of natural (i.e., room temperature) aging is indicated (for example, W 1/2h).

T, Solution Heat Treated—this applies to alloys whose strength is stable within a few weeks of solution heat treatment. The T is always followed by one or more digits, ...

A1.4 SYSTEM FOR HEAT-TREATABLE ALLOYS (29,30)

The W designation denotes an unstable temper, whereas the T designation denotes a stable temper other than F, O, or H. The T is followed by a numeral from 1 to 10, each numeral indicating a specific sequence of basic treatments.

- T1, Cooled from an Elevated-Temperature Shaping Process and Naturally Aged to a Substantially Stable Condition.
- T2, Cooled from an Elevated-Temperature Shaping Process, Cold-Worked, and Naturally Aged to a Substantially Stable Condition.
- T3, Solution Heat-Treated, Cold-Worked, and Naturally Aged to a Substantially Stable Condition.
- T4, Solution Heat-Treated and Naturally Aged to a Substantially Stable Condition.
- T5, Cooled from an Elevated-Temperature Shaping Process and Artificially Aged.
- T6, Solution Heat-Treated and Artificially Aged.
- T7, Solution Heat-Treated and Overaged or Stabilized.
- T8, Solution Heat-Treated, Cold Worked, and Artificially Aged.

- T9, Solution Heat-Treated, Artificially Aged, and Cold Worked.
- T10, Cooled from an Elevated-Temperature Shaping Process, Cold Worked, and Artificially Aged
- Tx51, Tx510, and Tx511 have undergone stress relief by stretching, and the last may also have undergone minor straightening.
- T42 and T62 indicate that the materials have been solution heat-treated from the O or F temper and naturally or artificially aged, to demonstrate response to heat treatment.

The tempers T3, T4, and T6 are common in aircraft parts. For example, many leading edges are formed out of 2024-T3 sheet.

A1.5 STRENGTHENING MECHANISM FOR HEAT-TREATABLE ALLOYS (34-36)

Heat treatment for precipitation strengthening—solution heat treatment at a high temperature to maximize solubility, followed by rapid cooling or quenching to a low temperature so obtain a solid solution supersaturated with both solute elements and vacancies, followed by natural or artificial aging. Electrical conductivity is also affected, which makes it a useful measure of heat treatment.

A1.6 WROUGHT PRODUCTS (59)

Aluminum wrought products are those aluminum products that have been subjected to plastic deformation by hot working and cold working processes, so as to transform cast aluminum ingot into desired product form.

APPENDIX 2: BENDING AND SPRINGBACK BASICS

This section of the appendix is given for those who are unfamiliar or rusty with the basics of the mechanics of solids and its application to bending and springback. More detailed sources such as Crandall et al [1987] are listed in the categorized bibliography.

A2.1 STRAIN FROM BENDING

Strain is a measure of the amount of stretch in a part. A common measure of strain is the change in length divided by the original length. For example, if a part originally 10" long is stretched to 11" long, the change in length is 1", and the strain is 10% (or 0.10). When the part is bent, the material above the midplane stretches as a function of the radius of curvature R and the distance from the midplane y. Based on simple geometry, the length of an arc is the product of the radius of the arc times the angle θ (called the bend angle here) that defines the arc; thus, the length of material, due to bending, is given by

$$l(y) = (R + y)\theta . \tag{A2.1}$$

This is shown in the following diagram.

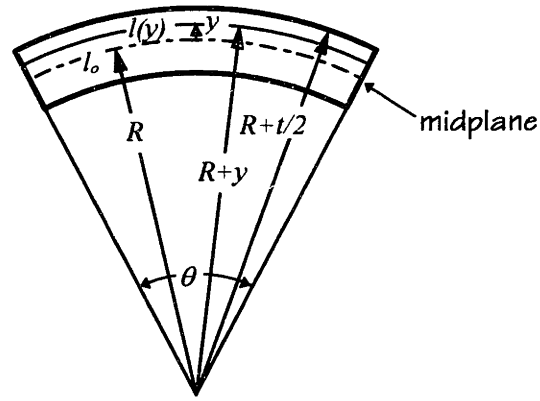

Figure A2.1 Bent part and radii of curvature, midplane, and bend angle

The length of the midplane is $l_o = R\theta$, and the length of the bent portion of the sheet at the top is $l(t/2) = (R + t/2)\theta$.

The engineering strain, e, (change in length over original length) is given by

$$e = \frac{l - l_o}{l_o} = \frac{(l_o + y\theta) - l_o}{l_o} = \frac{y\theta}{R\theta} = \frac{y}{R} . \tag{A2.2}$$

The above equation states that as the material is bent the strain in the material outside (inside) of the midplane increases (decreases) with increasing distance from the midplane and decreasing radius of curvature, the latter implying sharper bend. By definition, the relationship between engineering strain, e, and true strain, ε, is

$$\varepsilon = \ln(1+e)\,. \tag{A2.3}$$

True strain is often a better measure of strain for a variety of reasons, the most important of which is that it better represents the amount of stretch. For example, if a part is stretched a certain amount and then compressed back to the original dimension, the true strain will give a net strain of zero, while the engineering strain will not. Stress-strain relationships are generally determined for true strain, not engineering strain. Therefore, true strain should be used when performing analyses using a stress-strain curve. Due to the logarithm involved, this presents mathematical difficulties. However, if the strains are kept low, the engineering strain e can be used to approximate the true strain ε, and this approximation is often adequate. The following table demonstrates the relationship between ε and e for various values of e.

e	ε	Error ($\{e-\varepsilon\}/\varepsilon$)
0.01 (1%)	0.00995 (0.995%)	0.50%
0.05 (5%)	0.0488 (4.88%)	2.46%
0.10 (10%)	0.0953 (9.53%)	4.93%
0.50 (50%)	0.405 (40.5%)	23.4%

Table A2.1 Comparison of engineering and true strain

The error must be kept in mind when using e as an estimate of ε. Engineering strains less than 0.1 (10%) serve as good estimates of the true strain (at e = 10%, the true strain is overestimated by 5%). Engineering strain overestimates the true strain. When using strain to calculate stresses in the elastic range, the error in stress is quite small, since elastic strains are quite small. For example, at 0.2% strain, the actual stress is overestimated by only 0.1%. When using strain to calculate stresses in the plastic range, the error in stress is quite small due to the slow increase of stress. For example, at 5.0% strain, the actual stress is overestimated by only 0.5% (for a strain hardening exponent of n = 0.21). Therefore, the use of engineering strain as a surrogate for true strain when calculating stresses is acceptable because of the small magnitude of the

error introduced by this simplification. In all following calculations, e will be used as an approximation of ε. The symbol ε will be used.

A2.2 ELASTIC, PERFECTLY PLASTIC STRESS-STRAIN RELATIONSHIP

In order to calculate springback in bending, a model of the relationship between the stress σ and strain ε in the material is necessary. Stress is defined as a force divided by a unit area. For example, if a rod of 0.1" cross-sectional area is pulled at both ends with a force of 100 pounds, then the longitudinal stress is 100/0.1 = 1000 psi (pounds per square inch). A very simple stress-strain model is the *elastic, perfectly plastic* model. How the stress changes as a function of strain for this stress-strain relationship is shown in the following diagram.

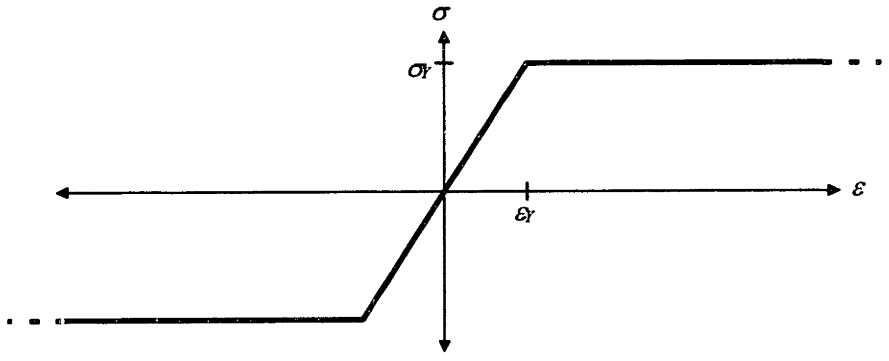

Figure A2.2 Diagram of elastic, perfectly plastic stress-strain relationship

Starting at zero strain, stress and strain are linearly proportional, i.e., $\sigma = E\varepsilon$ (E is called the elastic modulus or the modulus of elasticity and is the slope of the elastic portion of the stress-strain curve), up to the yield stress, σ_Y (which occurs at the strain ε_Y and is the stress at which plastic deformation begins); at larger strains, $\varepsilon > \varepsilon_Y$, the stress remains at the constant value of σ_Y. This is stated mathematically as

$$\begin{aligned} \sigma &= E\varepsilon \quad \text{for } |\varepsilon| \leq \varepsilon_Y, \\ \sigma &= \sigma_Y \quad \text{for } \varepsilon > \varepsilon_Y, \\ \sigma &= -\sigma_Y \quad \text{for } \varepsilon < -\varepsilon_Y. \end{aligned} \tag{A2.4}$$

If the material is strained into plastic tensile deformation and then released, the stresses will decrease along the slope of the elastic portion of the stress-strain curve. Initial development of equations for bending stresses and springback are performed with this elastic, perfectly plastic stress-strain relationship.

A2.3 MODELING PURE BENDING WITH AN ELASTIC, PERFECTLY PLASTIC MATERIAL

A2.3.1 Calculation of stresses and bending moment

Stresses can be calculated from the equations above, since the strain is a function of known variables. For an initial radius of curvature R_i, the moment required to bend the part can be calculated. The following diagram shows the lengthwise stresses and strains in the workpiece as a function of y, the distance from the midplane. The vertical axis is the thickness of the material, from the inside to the outside of the bend, while the horizontal axis is both the stress and the strain, appropriately scaled. The stress and strain are scaled so that the lines lie directly on top of one-another in the portion where they are parallel; they are drawn separately in order to show that they both exist.

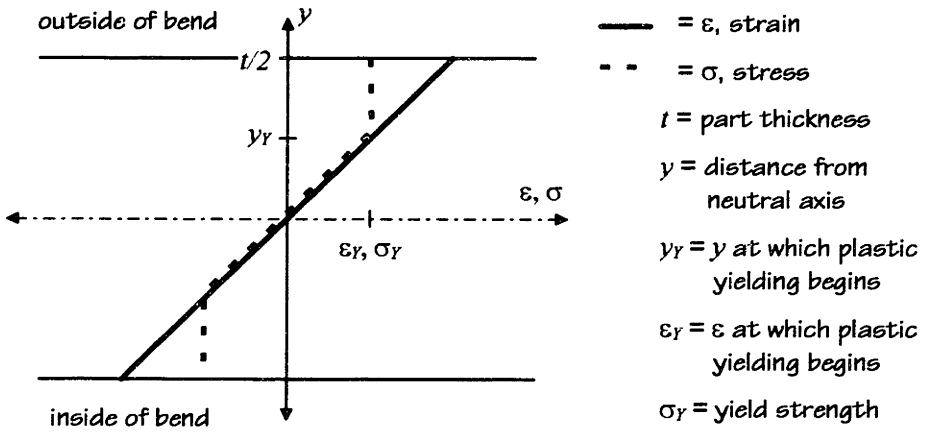

Figure A2.3 Stresses and strains within a bent part

The distance from the midplane, y_Y, at which plastic deformation begins is

$$y_Y = \frac{\sigma_Y R_i}{E}. \tag{A2.5}$$

Therefore, y_Y is a known function of the radius of curvature, yield strength, and elastic modulus. The bending moment on the sheet is given by the equation

$$M = \int_{-t/2}^{t/2} y\sigma dA = \int_{-t/2}^{t/2} y\sigma w dy, \tag{A2.6}$$

where w is the width of the sheet. The initial bending moment M_i is given by

$$M_i = \int_{-t/2}^{t/2} y\sigma w dy = 2w\int_0^{t/2} y\sigma dy = 2\left[\int_0^{y_Y} y\sigma dy + \int_{y_Y}^{t/2} y\sigma dy\right] = 2\left[\int_0^{y_Y} y\frac{Ey}{R_i}dy + \int_{y_Y}^{t/2} y\sigma_Y dy\right]$$
$$= 2w\left[\int_0^{y_Y} y^2\frac{E}{R_i}dy + \int_{y_Y}^{t/2} y\sigma_Y dy\right] = 2w\left[\left(\frac{E}{3R_i}y^3\right)\Big|_0^{y_Y} + \left(\frac{\sigma_Y}{2}y^2\right)\Big|_{y_Y}^{t/2}\right] \quad , \quad \text{(A2.7)}$$
$$= 2w\left[\left(\frac{E}{3R_i}{y_Y}^3\right) + \left(\frac{\sigma_Y}{2}\left(\left(\frac{t}{2}\right)^2 - {y_Y}^2\right)\right)\right]$$
$$= 2w\left[\left(\frac{E}{3R_i}\left(\frac{\sigma_Y R_i}{E}\right)^3\right) + \left(\frac{\sigma_Y}{2}\left(\left(\frac{t}{2}\right)^2 - \left(\frac{\sigma_Y R_i}{E}\right)^2\right)\right)\right]$$

which simplifies to

$$M_i = w\sigma_Y\left(\left(\frac{t}{2}\right)^2 - \frac{1}{3}\left(\frac{\sigma_Y R_i}{E}\right)^2\right). \quad \text{(A2.8)}$$

A2.3.2 Calculation of springback

Springback occurs because the final moment in the sheet M_f must be zero. Once the sheet is released, springback occurs as the material elastically deforms to bring the final moment to zero. Therefore,

$$M_f = \int_{-t/2}^{t/2} y\sigma w dy = 0. \quad \text{(A2.9)}$$

The final strain distribution (after springback) within the sheet is given by

$$\varepsilon_f = \frac{y}{R_f}, \quad \text{(A2.10)}$$

where R_f is the final radius of curvature. In the region of initial elastic deformation, $0 \le y \le y_Y$, the final stress is given by

$$\sigma_f = E\varepsilon_f = \frac{Ey}{R_f}. \quad \text{(A2.11)}$$

In the region of initial plastic deformation, $y_Y \le y \le t/2$, the final stress is given by

$$\sigma_f = \sigma_Y + E\left(\varepsilon_f - \varepsilon_i\right) = Ey\left(\frac{1}{R_f} - \frac{1}{R_i}\right) + \frac{Ey_Y}{R_i}. \quad \text{(A2.12)}$$

This is shown in the following diagram.

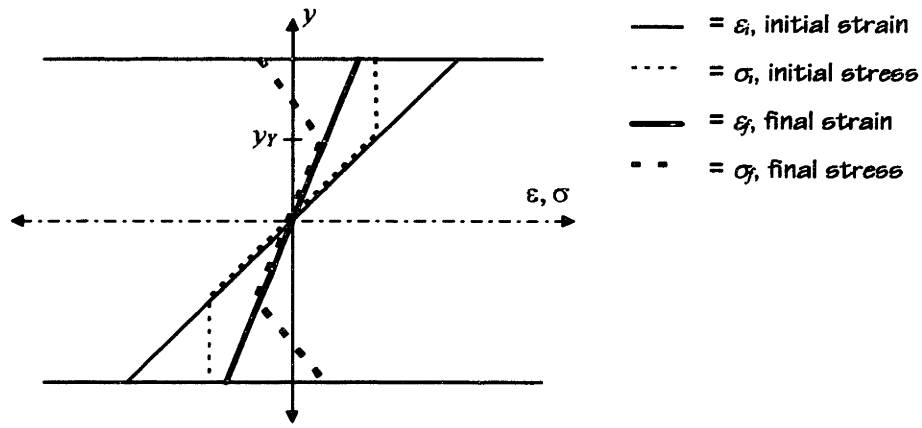

Figure A2.4 Stresses and strains in bent part after springback

The radius of curvature increases to reduce the magnitude of the strains, which cause the stresses to change. The radius of curvature increases until the moment generated by the internal stresses is zero. A measure of springback, R_i/R_f, the *springback ratio*, is the ratio of the initial radius of curvature over the final radius of curvature, R_i/R_f. Note that the term springback ratio can be somewhat misleading, because the smaller the ratio, the more springback there is, and the larger the ratio, the more springback there is. A springback ratio of 1 indicates no springback. In the stretch forming operation, the final radius of curvature is always larger than the original radius of curvature, so that the springback ratio is always less than one. The following diagram shows how the stress distribution changes as a result of springback when the springback ratio is 0.5. It shows the stress from the above diagram, but with the axes rearranged. Since the springback ratio is 0.5, the strain at each point is reduced by one half from the initial to final condition and the stress changes elastically in direct proportion to the change in strain. This gives the typical saw-tooth residual stress distribution shown.

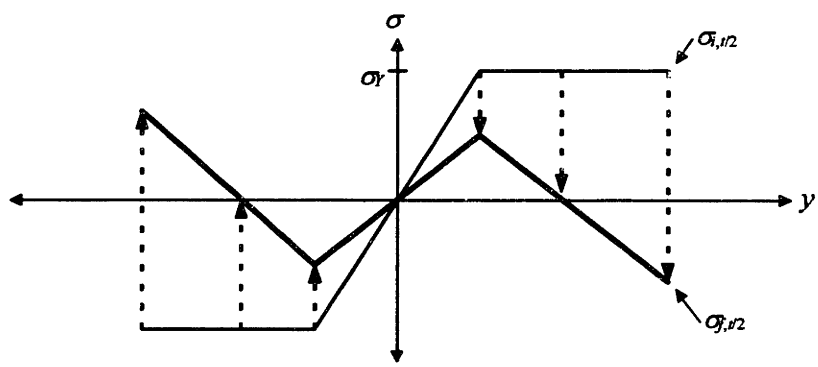

Figure A2.5 Changes in stress due to springback

The moment equation is used to determine the springback ratio that causes the final moment to be zero. Because the moment is symmetric about the midplane, it is simpler to limit the analysis to the upper half of the sheet. As well, since w is a non-zero constant, it can be dropped. This gives

$$M_f = 0 = \int_0^{t/2} y\sigma dy = \int_0^{y_Y} y\sigma dy + \int_{y_Y}^{t/2} y\sigma dy . \tag{A2.13}$$

Plugging the two final stress equations into the moment equation and integrating gives the standard springback equation for elastic, perfectly plastic material

$$\frac{R_i}{R_f} = 1 + \frac{1}{2}\left(\frac{y_Y}{t/2}\right)^3 - \frac{3}{2}\left(\frac{y_Y}{t/2}\right). \tag{A2.14}$$

Because the length of an arc is equal to the product of the radius and the enclosed angle, and the length of the bent portion of the sheet (arc length at the midplane) does not change in pure bending, so that

$$l_o = \theta_i R_i = \theta_f R_f \quad \Rightarrow \quad \frac{R_i}{R_f} = \frac{\theta_f}{\theta_i}. \tag{A2.15}$$

This permits statement of the springback equation in terms of initial and final angles:

$$\frac{\theta_f}{\theta_i} = \frac{R_i}{R_f} = 1 + \frac{1}{2}\left(\frac{y_Y}{t/2}\right)^3 - \frac{3}{2}\left(\frac{y_Y}{t/2}\right). \tag{A2.16}$$

With the material parameters explicitly stated, this is

$$\frac{\theta_f}{\theta_i} = \frac{R_i}{R_f} = 1 + \frac{1}{2}\left(\frac{\sigma_Y R_i/E}{t/2}\right)^3 - \frac{3}{2}\left(\frac{\sigma_Y R_i/E}{t/2}\right). \tag{A2.17}$$

A2.3.3 Findings from springback ratio equation

Some conclusions can be drawn from this equation—remembering that the stress-strain relationship is a simplified model:

- if all deformation is plastic (y_Y =0), there is no springback (R_i/R_f = 1);
- if all deformation is elastic ($y_Y \geq t/2$), there is total springback (R_i/R_f = 0);
- between the two limits, springback increases (R_i/R_f decreases) with decreasing plastic deformation (increasing y_Y);
- increasing thickness reduces springback (increases R_i/R_f).

Since

$$y_Y = \frac{\sigma_Y R_i}{E}, \tag{A2.18}$$

it can also be concluded that

- springback increases (R_i/R_f decreases) with increasing yield strength and initial radius of curvature and with decreasing elastic modulus.

The change in springback ratio as a function of the amount of plastic deformation normalized by the material thickness is shown in the following diagram.

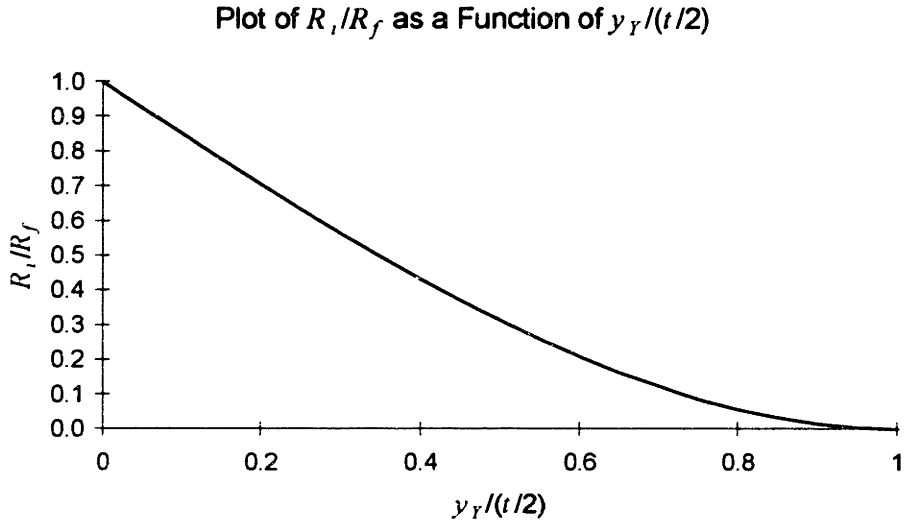

Figure A2.6 Springback ratio as a function of $y_Y/(t/2)$

A2.3.4 Example

In order to demonstrate use of the equation, consider the simple example of a piece of sheet metal t = 1.0 mm thick bent to an initial angle of θ_i = 90° with an initial radius of curvature of R_i = 5.0 mm. The yield strength is σ_Y = 50 MPa and the elastic modulus is E = 10,000 MPa. This gives y_Y = 50×5/10,000 = 0.025", and as a result

$$\frac{\theta_f}{\theta_i} = \frac{R_i}{R_f} = 1 + \frac{1}{2}\left(\frac{0.025}{0.5}\right)^3 - \frac{3}{2}\left(\frac{0.025}{0.5}\right) = 0.925. \tag{A2.19}$$

In this example, springback causes the final angle to be θ_f = 86.6°. If R_i were 10 mm, the springback ratio would be R_i/R_f = 0.851, and the final angle would be θ_f = 76.6°.

The maximum engineering strain in the workpiece is $e = (t/2)/R_i$ = 0.05/0.5 = 0.10, while the true strain is actually ε = 0.095. While this is an overestimation of about 5%, the

actual impact of the overestimation is much less than that because in an elastic, perfectly plastic material, the stress is constant after initial yielding.

A2.4 MODELING PURE BENDING WITH A POWER LAW MATERIAL

The pure bending analysis is now repeated using the power law stress-strain relationship. These equations represent the condition of stretch formed material before stretching, and the springback calculated is what would happen if material that is being stretch formed were released before stretching.

A2.4.1 Calculation of stresses and bending moment

The initial moment from bending alone is given by

$$M_i = \int_{-t/2}^{t/2} y\sigma_i w dy = 2\int_{0}^{t/2} y\sigma_i w dy, \tag{A2.20}$$

As before, this integral is broken into two distinct segments—below and above the point at which plastic deformation begins. For the power law stress-strain relationship, this is

$$\begin{aligned} \sigma_i &= E\varepsilon = E\frac{y}{R_i} && \text{for } \sigma_i < \sigma_Y \quad (\varepsilon < \varepsilon_Y) \\ \sigma_i &= K\varepsilon^n = K\left(\frac{y}{R_i}\right)^n && \text{for } \sigma_i > \sigma_Y \quad (\varepsilon > \varepsilon_Y) \end{aligned} \tag{A2.21}$$

This gives

$$M_i = 2\int_{0}^{y_Y} yE\frac{y}{R_i} w dy + 2\int_{y_Y}^{t/2} yK\left(\frac{y}{R_i}\right)^n w dy = 2w\left[\int_{0}^{y_Y} y^2 \frac{E}{R_i} dy + \int_{y_Y}^{t/2} y^{n+1}\frac{K}{R_i^n} dy\right], \tag{A2.22}$$

which in turn gives

$$M_i = 2w\left[\frac{E}{3R_i} {y_Y}^3 + \frac{K}{(n+2)R_i^n}\left(\left(\frac{t}{2}\right)^{n+2} - {y_Y}^{n+2}\right)\right], \tag{A2.23}$$

the equation for the moment in the material at the end of bending.

A2.4.2 Calculation of springback

To determine the springback ratio, the final moment is set to zero. As explained already, the material springs back from the fully bent shape to its final shape as the moment is removed. As the material springs back, the radius of curvature increases,

causing only elastic strain. The strain caused by springback is compressive on the top and compressive on the bottom. This elastic springback strain is given by

$$\varepsilon_{SB} = \frac{y}{R_f} - \frac{y}{R_i} = y\left(\frac{1}{R_f} - \frac{1}{R_i}\right) = \frac{y}{R_i}\left(\frac{R_i}{R_f} - 1\right), \tag{A2.24}$$

The final (residual) stress, σ_f, is given by

$$\sigma_f = \sigma_i + E\varepsilon_{SB} = \sigma_i + Ey\left(\frac{1}{R_f} - \frac{1}{R_i}\right) = \sigma_i + \frac{Ey}{R_i}\left(\frac{R_i}{R_f} - 1\right), \tag{A2.25}$$

so that the final moment equation becomes

$$0 = \int_{-t/2}^{t/2} y\left(\sigma_i + E\varepsilon_{SB}\right) w dy = 2\int_0^{t/2}\left[y\sigma_i + \frac{Ey^2}{R_i}\left(\frac{R_i}{R_f} - 1\right)\right] w dy, \tag{A2.26}$$

which simplifies to

$$\frac{M_i}{2wE} = -\int_0^{t/2} \frac{y^2}{R_i}\left(\frac{R_i}{R_f} - 1\right) dy, \tag{A2.27}$$

which is solved as follows

$$\frac{M_i}{2wE} = -\int_0^{t/2} \frac{y^2}{R_i}\left(\frac{R_i}{R_f} - 1\right) dy = -\frac{1}{R_i}\left(\frac{R_i}{R_f} - 1\right)\left(\frac{y^3}{3}\right)\Bigg|_0^{t/2} = -\frac{(t/2)^3}{3R_i}\left(\frac{R_i}{R_f} - 1\right). \tag{A2.28}$$

Plugging the equation for the initial moment M_i into the above equation gives

$$\frac{(t/2)^3}{3R_i}\left(\frac{R_i}{R_f} - 1\right) = -\frac{1}{E}\left[\frac{E}{3R_i} y_Y{}^3 + \frac{K}{(n+2)R_i{}^n}\left(\left(\frac{t}{2}\right)^{n+2} - y_Y{}^{n+2}\right)\right], \tag{A2.29}$$

which, after further manipulation, gives

$$\frac{R_i}{R_f} = 1 - \frac{3R_i}{(t/2)^3}\left[\frac{1}{3R_i} y_Y{}^3 + \frac{K}{E(n+2)R_i{}^n}\left(\left(\frac{t}{2}\right)^{n+2} - y_Y{}^{n+2}\right)\right], \tag{A2.30}$$

the equation for the springback ratio for bending of power law material. In terms of material parameters, this equation is

$$\frac{R_i}{R_f} = 1 - \frac{3R_i}{(t/2)^3}\left[\frac{1}{3R_i}\left(\frac{\sigma_Y R_i}{E}\right)^3 + \frac{K}{E(n+2)R_i{}^n}\left(\left(\frac{t}{2}\right)^{n+2} - \left(\frac{\sigma_Y R_i}{E}\right)^{n+2}\right)\right]. \tag{A2.31}$$

When n = 0 (and therefore $K = \sigma_Y$), the stress-strain curve becomes elastic, perfectly plastic, and the springback equation simplifies to the springback equation for elastic, perfectly plastic material.

The springback ratio can be used in determining the residual stress distribution in the material, to give

$$\sigma_f = \sigma_i + \frac{Ey}{R_i}\left(\frac{R_i}{R_f} - 1\right) = \begin{Bmatrix} E\dfrac{y}{R_f} & \text{for } |\varepsilon_i| < \varepsilon_Y \\ K\left(\dfrac{y}{R_i}\right)^n + \dfrac{Ey}{R_i}\left(\dfrac{R_i}{R_f} - 1\right) & \text{for } \varepsilon_i > \varepsilon_Y \\ -K\left(\dfrac{|y|}{R_i}\right)^n + \dfrac{Ey}{R_i}\left(\dfrac{R_i}{R_f} - 1\right) & \text{for } \varepsilon_i < -\varepsilon_Y \end{Bmatrix}, \quad \text{(A2.32)}$$

A2.4.3 Example

A 1.6 mm thick specimen is bent to an angle of θ_i = 90° with a radius of curvature of R_i = 10.0 mm. The springback ratio is

$$\frac{R_i}{R_f} = 1 - \frac{30}{0.8^3}\left[\frac{1}{30}\left(\frac{770}{68947}\right)^3 + \frac{320.9}{68947 \times 2.21 \times 10^{0.21}}\left(0.8^{2.21} - \left(\frac{770}{68947}\right)^{2.21}\right)\right]. \quad \text{(A2.33)}$$

$$\frac{R_i}{R_f} = 1 - 58.59\left[.033 \times 0.011^3 + 0.00130\left(0.8^{2.21} - 0.011^{2.21}\right)\right] = 0.953$$

The final radius of curvature is R_f = 10.0/0.953 = 10.49 mm, and the final angle is θ_f = 90×0.953 = 85.77°. The residual stresses are given by

$$\sigma_f = \begin{Bmatrix} \dfrac{68947y}{10.49} & \text{for } |y| < y_Y \quad \left(|y| < \dfrac{77 \times 10}{68947}\right) \\ 320.9\left(\dfrac{y}{10}\right)^{0.21} - \dfrac{68947y}{10} \times 0.047 & \text{for } y > y_Y \quad \left(\dfrac{77 \times 10}{68947} < y < \dfrac{16}{2}\right) \\ -320.9\left(\dfrac{-y}{10}\right)^{0.21} - \dfrac{68947y}{10} \times 0.047 & \text{for } y < -y_Y \quad \left(\dfrac{-16}{2} < y < \dfrac{-77 \times 10}{68947}\right) \end{Bmatrix}, \quad \text{(A2.34)}$$

and, finally,

$$\sigma_f = \begin{cases} 6571y & \text{for } |y| < y_Y \quad (|y| < 0.011) \\ 320.9\left(\frac{y}{10}\right)^{0.21} - 324y & \text{for } y > y_Y \quad (0.011 < y < 0.8) \\ -320.9\left(\frac{|y|}{10}\right)^{0.21} - 324y & \text{for } y < -y_Y \quad (-0.8 < y < -0.011) \end{cases}. \qquad \text{(A2.35)}$$

The initial and residual stresses for this part are shown in the following diagram along with the change in stress due to springback, called the springback stress.

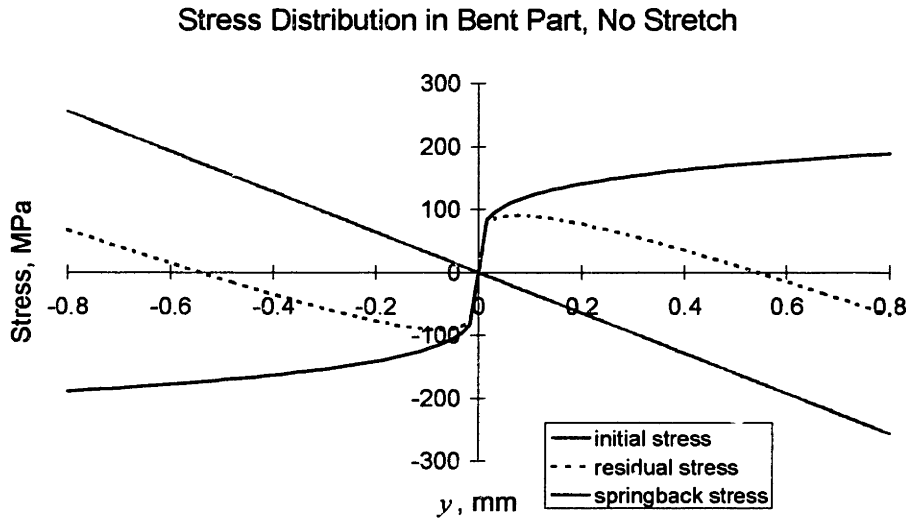

Figure A2.7 Initial and residual stress distributions in bent and released part

APPENDIX 3: PLANE STRAIN ADJUSTMENTS[49]

A3.1 PRELIMINARIES

The orientation used in this section is consistent with that used in Chapter 4. The y direction is the thickness direction, the z direction is the width direction, and the x direction is the length direction, the direction of stretch.

When bending and stretching sheet metal, it is assumed that the stresses in the thickness direction of the material are zero. Therefore, plane stress conditions exist with $\sigma_y = 0$.

In bending material which is *not* very wide, a phenomenon known as anticlastic curvature develops (bending an eraser provides a good example of this). In anticlastic curvature, the width of the top of the part decreases while the width of the bottom increases due to the lengthwise tensile and compressive strains developed in the top and bottom of the material. However, with sheet metal, which is thin and very wide, anticlastic curvature (strain in the width direction) is not possible, and so a plane strain condition is imposed, which requires that the strain in the width direction is zero ($\varepsilon_z = 0$). As well, this same plane strain condition generally also exists during stretching because, due to friction between the part and the die and the fact that both of the part's edges are gripped along the entire width, the width of the material is constrained. It would be possible to assume plane strain conditions for the bending and triaxial strain conditions for the stretching of the part, if it is determined that this better reflects what's actually happening. However, due to the added complexity, this task is not undertaken.

The part is assumed to have a linear elastic and power law plastic strain hardening stress-strain relationship. Hooke's law is used for elastic deformation, and von-Mises' equations and equivalent stresses and strains are used for plastic deformation.

Next, adjusted material properties for plane stress and plane strain conditions are developed.

---

[49] Thanks to Srihari Balasubramanian for his significant guidance and help given for the material in this sub-section.

A3.2 ELASTIC DEFORMATION

Hooke's Law for elastic deformation of isotropic material is given below.

$$\begin{aligned}\varepsilon_x &= \frac{1}{E}\left[\sigma_x - \nu\left(\sigma_y + \sigma_z\right)\right] \\ \varepsilon_y &= \frac{1}{E}\left[\sigma_y - \nu\left(\sigma_x + \sigma_z\right)\right] \\ \varepsilon_z &= \frac{1}{E}\left[\sigma_z - \nu\left(\sigma_x + \sigma_y\right)\right]\end{aligned} \tag{A3.1}$$

Due to the plane stress ($\sigma_y = 0$) and plane strain ($\varepsilon_z = 0$) assumptions, the above equations simplify to

$$\begin{aligned}\varepsilon_x &= \frac{1}{E}\left[\sigma_x - \nu\sigma_z\right] \\ \varepsilon_y &= \frac{-\nu}{E}\left[\sigma_x + \sigma_z\right], \\ 0 &= \frac{1}{E}\left[\sigma_z - \nu\sigma_x\right]\end{aligned} \tag{A3.2}$$

the last of which gives

$$\sigma_z = \nu\sigma_x. \tag{A3.3}$$

Plugging this into the first simplified equation gives

$$\varepsilon_x = \frac{1}{E}\left[\sigma_x - \nu^2\sigma_x\right] = \frac{\left(1-\nu^2\right)}{E}\sigma_x, \tag{A3.4}$$

which rearranges to give

$$\sigma_x = \frac{E}{\left(1-\nu^2\right)}\varepsilon_x. \tag{A3.5}$$

Recall that ε_x is the strain at a given point imposed by bending and stretching. Therefore, the elastic modulus under plane strain, plane stress conditions is increased from its triaxial strain, uniaxial stress conditions by the factor $1/(1-\nu^2)$, and the elastic bending moment is given by

$$M_{elastic} = \frac{2wE\left(t/2\right)^3}{3\left(1-\nu^2\right)R_i}. \tag{A3.6}$$

Further,

$$\varepsilon_y = \frac{-\nu}{E}\left[\sigma_x + \sigma_z\right] = \frac{-\nu(1+\nu)}{E}\sigma_x = \frac{-\nu(1+\nu)}{E}\frac{E}{\left(1-\nu^2\right)}\varepsilon_x, \tag{A3.7}$$

which simplifies to

$$\varepsilon_y = \frac{-\nu}{(1-\nu)}\varepsilon_x \tag{A3.8}$$

Since, for aluminum, $\nu \approx 0.3$ [Crandall et al, 1978], the above equations give

$$\sigma_x = \frac{E}{0.91}\varepsilon_x \quad \sigma_z = 0.3\sigma_x \quad \varepsilon_y = -\frac{3}{7}\varepsilon_x.$$

A3.3 PLASTIC DEFORMATION

The equivalent plastic stress and strain equation for the power law strain hardening plastic flow rule used is

$$\bar{\sigma} = K\bar{\varepsilon}^n. \tag{A3.9}$$

Plasticity equations for equivalent strain and equivalent stress are

$$\bar{\varepsilon} = \sqrt{\frac{2}{3}\left(\varepsilon_x{}^2 + \varepsilon_y{}^2 + \varepsilon_z{}^2\right)} \tag{A3.10}$$

and

$$\bar{\sigma} = \sqrt{\frac{1}{2}\left(\left(\sigma_x - \sigma_y\right)^2 + \left(\sigma_x - \sigma_z\right)^2 + \left(\sigma_z - \sigma_y\right)^2\right)}. \tag{A3.11}$$

In plastic deformation, incompressibility is assumed,[50] which gives

$$\varepsilon_x + \varepsilon_y + \varepsilon_z = 0. \tag{A3.12}$$

Since $\varepsilon_z = 0$, this gives

$$\varepsilon_y = -\varepsilon_x. \tag{A3.13}$$

Combined with Equation (A3.10), this gives

$$\bar{\varepsilon} = \sqrt{\frac{2}{3}\left(\varepsilon_x{}^2 + \varepsilon_x{}^2\right)} = \sqrt{\frac{4}{3}\varepsilon_x{}^2}, \tag{A3.14}$$

which gives the relationship between the equivalent strain and the strain in the x direction,

---

[50] While this assumption is more accurate at higher strains, it is used here in order to simplify things.

$$\bar{\varepsilon} = \frac{2}{\sqrt{3}}\varepsilon_x \tag{A3.15}$$

The flow rule dictates that

$$\frac{d\varepsilon_x}{\sigma'_{xx}} = \frac{d\varepsilon_y}{\sigma'_{yy}} = \frac{d\varepsilon_z}{\sigma'_{zz}} = \lambda \neq 0, \tag{A3.16}$$

in which the σ' indicates deviatoric stress. Since $\varepsilon_z = 0$, it must be true that $d\varepsilon_z = 0$, and therefore also $\sigma'_{zz} = 0$. This is written out as

$$\sigma'_{zz} = 0 = \sigma_z - \frac{1}{3}tr(\sigma_{ij}) = \sigma_z - \frac{1}{3}(\sigma_x + \sigma_y + \sigma_z) = -\frac{1}{3}\sigma_x - \frac{1}{3}\sigma_y + \frac{2}{3}\sigma_z. \tag{A3.17}$$

Since $\sigma_y = 0$, this gives

$$0 = -\frac{1}{3}\sigma_x + \frac{2}{3}\sigma_z, \tag{A3.18}$$

which simplifies to the relationship between stresses in the x and z directions

$$\sigma_z = \frac{1}{2}\sigma_x. \tag{A3.19}$$

Plugging this into Equation (A3.11), along with $\sigma_y = 0$, gives

$$\bar{\sigma} = \sqrt{\frac{1}{2}\left(\sigma_x{}^2 + \left(\frac{1}{2}\sigma_x\right)^2 + (-\sigma_x)^2\right)} = \sqrt{\frac{3}{4}\sigma_x{}^2}, \tag{A3.20}$$

which simplifies to give the relationship between the equivalent stress and the stress in the x direction,

$$\bar{\sigma} = \frac{\sqrt{3}}{2}\sigma_x. \tag{A3.21}$$

Combining the relations between the equivalent strains and stresses and the actual strains and stresses in the x direction into the power law hardening rule gives

$$\frac{\sqrt{3}}{2}\sigma_x = K\left(\frac{2}{\sqrt{3}}\varepsilon_x\right)^n, \tag{A3.22}$$

which rearranges to give

$$\sigma_x = \left(\frac{4}{3}\right)^{\frac{n+1}{2}} K\varepsilon_x{}^n. \tag{A3.23}$$

Equation (A3.23) indicates that it is still acceptable to use a power law strain hardening rule for plastic deformation, with modification to the constant K for plane strain and plane stress conditions. Similarly for elastic deformation, Equation (A3.5) shows that plane conditions can be modeled simply by appropriate scaling.

A3.4 COMBINING MODIFIED ELASTIC AND PLASTIC STRESS-STRAIN CURVE PARAMETERS

Combining the above results, the stress and strain curve in the x direction under plane strain and plane stress assumptions is given by

$$\sigma_x = \begin{Bmatrix} E'\varepsilon_x & |\varepsilon_x| \le \varepsilon'_Y \\ K'\varepsilon_x^{\,n} & \varepsilon_x > \varepsilon'_Y \\ -K'\varepsilon_x^{\,n} & \varepsilon_x < -\varepsilon'_Y \end{Bmatrix}, \tag{A3.24}$$

in which

$$E' = \frac{E}{\left(1-\nu^2\right)} \qquad \text{and} \qquad K' = \left(\frac{4}{3}\right)^{\frac{n+1}{2}} K, \tag{A3.25}$$

and ε'_Y is the strain at which plastic deformation begins; σ'_Y is the new yield strength. It is possible now to use von Mises plasticity criteria to determine ε'_Y. The method used by Queener and De Angelis [1968] results in a discontinuity in the stress-strain curve. However, it is possible to determine the yield point stress and strain by determining where the elastic and plastic portions of the curve meet. In this case, the value of ε'_Y is found by the following equation

$$\sigma'_Y = E'\varepsilon'_Y = K'\varepsilon'^{\,n}_Y. \tag{A3.26}$$

This gives

$$\varepsilon'^{\,1-n}_Y = \frac{K'}{E'} \quad \Rightarrow \quad \varepsilon'_Y = \left(\frac{K'}{E'}\right)^{\frac{1}{1-n}}, \tag{A3.27}$$

which, plugging in values for K' and E', gives

$$\varepsilon'_Y = \left(\frac{\left(1-\nu^2\right)K}{E}\left(\frac{4}{3}\right)^{\frac{n+1}{2}}\right)^{\frac{1}{1-n}}. \tag{A3.28}$$

The accompanying yield strength σ'_Y is $E\varepsilon'_Y$.

APPENDIX 4: CHEMICAL MILLING EQUATIONS

A4.1 DERIVATION OF EQUATIONS FOR EFFECT OF CHEM MILL, NO IPD MODEL

The equations to determine the effect of chem mill on springback and relaxation are now derived.

A4.1.1 Determining springback with chem mill

Since a single analytical equation was derived only for the No IPD model, a single equation is attempted only for this model. In order to model chem mill, the portion of material removed from the inside of the part is simply ignored (set to zero) in the final force and moment equations.[51] The physical reality corresponding to what is done mathematically would be to remove the chem milled material while the part is still on the die, just before the material is released. Since all strains are elastic, the order in which things are done is not important. Then the sheet, minus the removed material, is released and allowed to spring back and relax as before. The removed material is assumed to taken off of the entire width and length of the sheet.

In order to determine the springback, the final moment M_f and final net force F_f are set to zero. The lower limit of the integrals is now given by $-t_i = (-t/2) + t_{cm}$, in which t_{cm} is the thickness removed by chem mill. The two integrals that must be satisfied are

$$M_f = \int_{-t_i}^{t/2} y\sigma_f dA = 0 \tag{A4.1}$$

and

$$F_f = \int_{-t_i}^{t/2} \sigma_f dA = 0\,. \tag{A4.2}$$

The final stress distribution, which is assumed to be achieved by only elastic deformation, is given by

$$\sigma_f = \sigma_I + E\varepsilon_R + E\varepsilon_{SB}\,. \tag{A4.3}$$

Plugging this into the final moment equation gives

---

[51] This approach was suggested by professor Mary Boyce at MIT.

$$M_f = 0 = \int_{-t_i}^{t/2} y\left[K{\varepsilon_I}^n + E\varepsilon_R + E\varepsilon_{SB}\right]dA$$
$$= \int_{-t_i}^{t/2} y\left[K\left(\frac{y}{R_i} + \varepsilon_T\right)^n + E\varepsilon_R + y\frac{E}{R_i}\left(\frac{R_i}{R_f} - 1\right)\right]wdy \quad , \tag{A4.4}$$

which, after rearranging, gives

$$\int_{-t_i}^{t/2} yK\left(\frac{y}{R_i} + \varepsilon_T\right)^n wdy = -\int_{-t_i}^{t/2} y\left[E\varepsilon_R + y\frac{E}{R_i}\left(\frac{R_i}{R_f} - 1\right)\right]wdy \, . \tag{A4.5}$$

The left hand side is the equation for the intermediate moment, except that it is modified by the removal of material by chem mill. Solving by integration by parts, in the same manner as before, only with the adjusted lower limit, is shown below. Again, the assumption is made that the stretch is large enough that all of the intermediate stress is tensile plastic. In this case, for the left hand side,

$$M_{I,cm} = \int_{-t_i}^{t/2} yK\left(\frac{y}{R_i} + \varepsilon_T\right)^n wdy \, . \tag{A4.6}$$

Integration by parts,

$$\int udv = uv - \int vdu \, , \tag{A4.7}$$

in which

$$u = y; \quad dv = \left(\frac{y}{R_i} + \varepsilon_T\right)^n dy; \quad du = dy; \quad v = \frac{R_i}{n+1}\left(\frac{y}{R_i} + \varepsilon_T\right)^{n+1} \, , \tag{A4.8}$$

leads to

$$M_{I,cm} = Kw\left[\frac{yR_i}{n+1}\left(\frac{y}{R_i} + \varepsilon_T\right)^{n+1}\Bigg|_{-t_i}^{t/2} - \int_{-t_i}^{t/2} \frac{R_i}{n+1}\left(\frac{y}{R_i} + \varepsilon_T\right)^{n+1} dy\right]$$
$$= Kw\left[\frac{yR_i}{n+1}\left(\frac{y}{R_i} + \varepsilon_T\right)^{n+1} - \frac{{R_i}^2}{(n+1)(n+2)}\left(\frac{y}{R_i} + \varepsilon_T\right)^{n+2}\Bigg|_{-t_i}^{t/2}\right] \, , \tag{A4.9}$$
$$= \frac{KwR_i}{(n+1)}\left[y\left(\frac{y}{R_i} + \varepsilon_T\right)^{n+1} - \frac{R_i}{(n+2)}\left(\frac{y}{R_i} + \varepsilon_T\right)^{n+2}\Bigg|_{-t_i}^{t/2}\right.$$

which finally gives

$$M_{I,cm} = \frac{KwR_i}{(n+1)}\left[t/2\left(\frac{t/2}{R_i}+\varepsilon_T\right)^{n+1} + t_i\left(\frac{-t_i}{R_i}+\varepsilon_T\right)^{n+1} - \frac{R_i}{(n+2)}\left(\frac{t/2}{R_i}+\varepsilon_T\right)^{n+2} + \frac{R_i}{(n+2)}\left(\frac{-t_i}{R_i}+\varepsilon_T\right)^{n+2}\right]. \quad \text{(A4.10)}$$

for the left hand side of the equation. The right hand side of the moment equation is solved as follows

$$\begin{aligned} M_{I,cm} &= -\int_{-t_i}^{t/2}\left[E\varepsilon_R y + \frac{E}{R_i}\left(\frac{R_i}{R_f}-1\right)y^2\right]w dy \\ &= -w\left[\frac{E\varepsilon_R}{2}y^2 + \frac{E}{3R_i}\left(\frac{R_i}{R_f}-1\right)y^3\right]_{-t_i}^{t/2} \\ &= -w\left[\frac{E\varepsilon_R}{2}\left((t/2)^2 - {t_i}^2\right) + \frac{E}{3R_i}\left(\frac{R_i}{R_f}-1\right)\left((t/2)^3 + {t_i}^3\right)\right] \\ &= -\frac{wE\varepsilon_R}{2}\left((t/2)^2 - {t_i}^2\right) - \frac{wE}{3R_i}\left(\frac{R_i}{R_f}-1\right)\left((t/2)^3 + {t_i}^3\right) \end{aligned} \quad \text{(A4.11)}$$

Due to asymmetry, the elastic strain recovery, ε_R, does *not* drop out. The final force equilibrium equation is

$$F_{f,cm} = 0 = \int_{-t_i}^{t/2}\sigma_f dA = \int_{-t_i}^{t/2}\sigma_f w dy = \int_{-t_i}^{t/2}\left[K{\varepsilon_I}^n + E\varepsilon_R + E\varepsilon_{SB}\right]dy. \quad \text{(A4.12)}$$

The width w drops out because it is a constant. Integrating gives

$$\begin{aligned} 0 &= \int_{-t_i}^{t/2}\left[K{\varepsilon_I}^n + E\varepsilon_R + E\varepsilon_{SB}\right]dy = \int_{-t_i}^{t/2}\left[K\left(\frac{y}{R_i}+\varepsilon_T\right)^n + E\varepsilon_R + \frac{E}{R_i}\left(\frac{R_i}{R_f}-1\right)y\right]dy \\ &= \left[\frac{KR_i}{n+1}\left(\frac{y}{R_i}+\varepsilon_T\right)^{n+1} + E\varepsilon_R y + \frac{E}{R_i}\left(\frac{R_i}{R_f}-1\right)\frac{y^2}{2}\right]_{-t_i}^{t/2} \\ &= \frac{KR_i}{n+1}\left[\left(\frac{t/2}{R_i}+\varepsilon_T\right)^{n+1} - \left(\frac{-t_i}{R_i}+\varepsilon_T\right)^{n+1}\right] + E\varepsilon_R\left(t/2+t_i\right) \\ &\quad + \frac{E}{2R_i}\left(\frac{R_i}{R_f}-1\right)\left((t/2)^2 - {t_i}^2\right) \end{aligned} \quad \text{(A4.13)}$$

Note that, due to asymmetry, the springback no longer falls out. Rearranging gives

$$\varepsilon_R = -\frac{KR_i}{E(t/2+t_i)(n+1)}\left[\left(\frac{t/2}{R_i}+\varepsilon_T\right)^{n+1}-\left(\frac{-t_i}{R_i}+\varepsilon_T\right)^{n+1}\right] - \frac{1}{2(t/2+t_i)R_i}\left(\frac{R_i}{R_f}-1\right)\left((t/2)^2-t_i{}^2\right) \quad \text{(A4.14)}$$

Plugging this equation into the right hand side of the moment equation above gives

$$M_{I,cm} = \frac{wE}{2}\left((t/2)^2-t_i{}^2\right)\left\{\frac{KR_i}{E(t/2+t_i)(n+1)}\left[\left(\frac{t/2}{R_i}+\varepsilon_T\right)^{n+1}-\left(\frac{-t_i}{R_i}+\varepsilon_T\right)^{n+1}\right] + \frac{1}{2(t/2+t_i)R_i}\left(\frac{R_i}{R_f}-1\right)\left((t/2)^2-t_i{}^2\right)\right\} - \frac{wE}{3R_i}\left(\frac{R_i}{R_f}-1\right)\left((t/2)^3+t_i{}^3\right) \quad \text{(A4.15)}$$

Noting that

$$a^2-b^2=(a+b)(a-b) \quad \Rightarrow \quad \frac{(t/2)^2-t_i{}^2}{t/2+t_i}=t/2-t_i, \quad \text{(A4.16)}$$

the above equation can be simplified to

$$M_{I,cm} = \frac{wE}{2}(t/2-t_i)\left\{\frac{KR_i}{E(n+1)}\left[\left(\frac{t/2}{R_i}+\varepsilon_T\right)^{n+1}-\left(\frac{-t_i}{R_i}+\varepsilon_T\right)^{n+1}\right] + \frac{1}{2R_i}\left(\frac{R_i}{R_f}-1\right)\left((t/2)^2-t_i{}^2\right)\right\} - \frac{wE}{3R_i}\left(\frac{R_i}{R_f}-1\right)\left((t/2)^3+t_i{}^3\right) \quad \text{(A4.17)}$$

Collecting the springback terms gives

$$M_{I,cm} - \frac{wE}{2}(t/2-t_i)\left\{\frac{KR_i}{E(n+1)}\left[\left(\frac{t/2}{R_i}+\varepsilon_T\right)^{n+1}-\left(\frac{-t_i}{R_i}+\varepsilon_T\right)^{n+1}\right]\right\} = \left(\frac{R_i}{R_f}-1\right)\left[\frac{wE}{2}(t/2-t_i)\left\{\frac{1}{2R_i}\left((t/2)^2-t_i{}^2\right)\right\}-\frac{wE}{3R_i}\left((t/2)^3+t_i{}^3\right)\right] \quad \text{(A4.18)}$$

and further simplification gives

$$\frac{R_i}{R_f} = 1-\frac{\frac{M_{I,cm}R_i}{Ew}-\frac{KR_i{}^2(t/2-t_i)}{2E(n+1)}\left[\left(\frac{t/2}{R_i}+\varepsilon_T\right)^{n+1}-\left(\frac{-t_i}{R_i}+\varepsilon_T\right)^{n+1}\right]}{\frac{\left((t/2)^3+t_i{}^3\right)}{3}-\frac{(t/2-t_i)\left((t/2)^2-t_i{}^2\right)}{4}} \quad \text{(A4.19)}$$

Finally, combining this with the left hand side of the moment equation and simplifying gives

$$\frac{R_i}{R_f} = 1 - \frac{\frac{KR_i^2}{E(n+1)}\left[t/2\left(\frac{t/2}{R_i}+\varepsilon_T\right)^{n+1} + t_i\left(\frac{-t_i}{R_i}+\varepsilon_T\right)^{n+1}\right]}{\frac{\left((t/2)^3+t_i^3\right)}{3} - \frac{(t/2-t_i)\left((t/2)^2-t_i^2\right)}{4}}$$
$$+ \frac{\frac{KR_i^2}{E(n+1)}\left[\frac{R_i}{(n+2)}\left(\frac{t/2}{R_i}+\varepsilon_T\right)^{n+2} - \frac{R_i}{(n+2)}\left(\frac{-t_i}{R_i}+\varepsilon_T\right)^{n+2}\right]}{\frac{\left((t/2)^3+t_i^3\right)}{3} - \frac{(t/2-t_i)\left((t/2)^2-t_i^2\right)}{4}}, \qquad \text{(A4.20)}$$
$$+ \frac{\frac{KR_i^2(t/2-t_i)}{2E(n+1)}\left[\left(\frac{t/2}{R_i}+\varepsilon_T\right)^{n+1} - \left(\frac{-t_i}{R_i}+\varepsilon_T\right)^{n+1}\right]}{\frac{\left((t/2)^3+t_i^3\right)}{3} - \frac{(t/2-t_i)\left((t/2)^2-t_i^2\right)}{4}}$$

the final springback equation after chem mill.

The springback ratio obtained from this equation can be plugged into Equation (A4.14), the elastic relaxation equation, to determine ε_R.

A4.1.2 Final stress distribution

At this point, the final residual stress distribution in the part can be calculated from

$$\sigma_f = \sigma_I + E\varepsilon_R + E\varepsilon_{SB}. \qquad \text{(A4.21)}$$

APPENDIX 5: DETERMINATION OF MOMENT OF INERTIA

The moment of inertia of the entire cross-section is given by the sum of the individual moments of inertia relative to the midplane of the parts of the cross-section. Mathematically, this is stated as

$$I_{zz} = \sum_i I_{zz,i} + \left(\bar{y} - \bar{y}_i\right)^2 A_i \,, \tag{A5.1}$$

in which $I_{zz,i}$ is the moment of inertia of part i, $\bar{y}$ is the distance from the bottom of the midplane of the entire cross-section, $\bar{y}_i$ is the distance from the bottom of the cross-section to the midplane of part i, and A_i is the area of part i. If each part is rectangular in shape (which it generally can be approximated to be if it is not), then $I_{zz,i}$ is given by the equation

$$I_{zz,i} = \frac{1}{12} w_i {t_i}^3 \,, \tag{A5.2}$$

in which w_i is the width and t_i is the height of that rectangle. For example, an I-shaped cross-section extrusion can be broken up into three rectangular sections: the top horizontal portion, the bottom horizontal portion, and the vertical web in-between. Even though Z and square cross-sections do not fit exactly the model, they can both be modeled by finding the equivalent widths for the three sections vertically (if the widths are the same as that of an I cross-section part, they will be the same for this model).

APPENDIX 6: METRIC-ENGLISH UNITS CONVERSION TABLE

	English Units	Metric Units
Stress	1000 ksi	6.8947 MPa
	145.0 ksi	1 MPa
Distance	1 inch	25.4 mm
	0.0394 in	1 mm
Force	1000 lbs	4.4545 kN
	224.5 lbs	1 kN

Table A6.1 Conversion table between English and Metric units

THESIS PROCESSING SLIP

FIXED FIELD: ill _____ name _____

index _____ biblio _____

▶ COPIES (Archives) Aero Dewey (Eng) Hum

Lindgren Music Rotch Science

TITLE VARIES: ▶☐ _____

_____

_____

NAME VARIES: ▶☐ _____

_____

IMPRINT: (COPYRIGHT) _____

▶ COLLATION: 404p

_____

▶ ADD. DEGREE: _____ ▶ DEPT.: _____

SUPERVISORS: _____

_____

_____ _____

_____ _____

_____ _____

_____ _____

_____ _____

_____ _____

_____ _____

NOTES:

cat'r: date:

▶ DEPT: M.E. page: ▶ 5149

▶ YEAR: 1996 ▶ DEGREE: ~~M~~ Ph.D.

▶ NAME: PARRIS, Andrew

_____